Air-Cooled Heat Exchangers and Cooling Towers

Thermal-flow Performance Evaluation and Design

by

Detlev Gustav Kröger

A dissertation in fulfilment
of the requirements for the degree of
Doctor of Engineering
at the University of Stellenbosch

Promoter: Prof T.W. von Backström

University of Stellenbosch
December 2004

Declaration

I the undersigned declare that the work contained in this dissertation is my own original work and it has not previously in its entirety or in part been submitted at any university for a degree.

23 November 2004

D.G. Kroger **Date**

Air-Cooled Heat Exchangers and Cooling Towers

Thermal-flow Performance Evaluation and Design

Volume II

by

Detlev Gustav Kröger

Air-Cooled Heat Exchangers and Cooling Towers

Thermal-flow Performance Evaluation and Design

by

Detlev Gustav Kröger

A submission on research and development in fulfilment
of the requirements for the degree of
Doctor of Engineering
at the University of Stellenbosch

Promoter: Prof T.W. von Backström

University of Stellenbosch
November 2004

Declaration

I hereby certify that this submission is my own original work except where specifically acknowledged in the text.

Some of the research has been submitted in part as theses by co-workers but the text has not previously in its entirety or in part been submitted at any university for a degree.

23 November 2004

D.G. Kroger **Date**

Abstract

During the last 30 years I have been involved in the theory and practice of thermal engineering and in particular, in the areas of air-cooled heat exchangers and cooling towers for the power, refrigeration, process and petrochemical industries in South Africa and internationally. During this period, I have authored and co-authored more than 120 papers that were published in technical journals or presented at conferences nationally or internationally. Most of these papers are included in a manuscript entitled "Air-cooled Heat Exchangers and Cooling Towers", in which I present a systematic approach to the thermal performance evaluation and design of industrial air-cooled heat exchangers and cooling towers. This original publication also includes the relevant practice applicable to the design of cooling systems, based on my experience as a consultant to industry. Design offices throughout the world presently follow our design methods, or at least employ many of our research results. Our work has furthermore contributed to the development of improved cooling system designs (e.g. new dephlegmator header designs), components (e.g. single-row flattened finned tubes) and product improvement and quality control (e.g. performance testing and measurement of thermal contact resistance between fin and tube during production). Many of our research findings have found application in the modification of existing cooling systems. The manuscript has also been used as reference work during the presentation of short courses to practising engineers and consultants in industry and to engineering graduates at the University of Stellenbosch.

A two-volume edition of this manuscript was published by PennWell Corp., Tulsa, Oklahoma, USA in 2004.

Opsomming

Gedurende die laaste 30 jaar was ek betrokke by die teorie en praktyk van lugverkoelde warmte-oordraers en koeltorings vir die kragopwekkings-, verkoelings-, proses- en petro-chemiese-nywerhede in Suid-Afrika sowel as in die buiteland. Gedurende hierdie periode was ek outeur en mede-outeur van meer as 120 publikasies wat in tegniese tydskrifte, of by plaaslike of oorsese konferensies aangebied is. Die meeste van hierdie publikasies vorm deel van 'n manuskrip getiteld "Air-cooled Heat Exchangers and Cooling Towers" waarin ek 'n sistematiese benadering tot die bepaling van die termiese vermoë en ontwerp van industriële lugverkoelde warmteoordraers en koeltorings aanbied. Hierdie oorspronklike publikasie bevat ook die relevante praktyk wat van toepassing is op verkoelingsaanlegte. Ontwerpkantore wêreldwyd volg tans hierdie ontwerpsmetodes, of gebruik ten minste baie van ons navorsingsresultate. Ons werk het verder bygedra tot die ontwikkeling van verbeterde verkoelingsaanlegte (bv. nuwe deflegmatore), komponente (bv. enkelbuisry platvinbuise) en verbeterde produkte en kwaliteitskontrole (bv. toetsing van verkoelingsvermoë of termiese kontakweerstand tussen vin en buis gedurende produksie). Baie van ons bevindinge het toepassing gevind in die modifikasie van verkoelingsaanlegte. Die manuskrip is ook as verwysing gebruik gedurende die aanbieding van kort kursusse aan ingenieurs in die praktyk en aan nagraadse studente aan die Universiteit van Stellenbosch.

'n Twee-volume uitgawe van die manuskrip is deur PennWell Corp., Tulsa, Oklahome, VSA in 2004 gepubliseer.

Acknowledgements

This work is dedicated to my family and my students. I thank my wife Regine for her patience and support during the many hours I spent on my research activities. Without the inputs of my students, this contribution would not have been possible. They were always an inspiration for me and became a part of my family. I thank the university management for creating an environment that was conducive to research and development. Under the competent chairmanship of Professors P.A. Erens and T.W. von Backström it was possible for me to expand my laboratory facilities and research activities in the Department of Mechanical Engineering. For the development and outstanding operation of the laboratory, I and many a student, have to thank Mr C.J. Zietsman. Due to his hard word, initiative and professional approach, we were able to run sophisticated research projects and to conduct laboratory and plant tests for clients throughout the world.

Thanks also to Mr A. September for the many years of good work, my wonderful secretaries, the staff of the university workshop and my colleagues and friends in industry.

Although many organisations supported my research and development financially, a special word of thanks goes to the National Research Foundation (NRF) and the Water Research Commission (WRC).

AIR-COOLED HEAT EXCHANGERS AND COOLING TOWERS

THERMAL-FLOW PERFORMANCE EVALUATION AND DESIGN

VOLUME II

By Detlev G. Kröger

To my family and my students.

CONTENTS

Volume II

Preface

The objective of these volumes is to provide modern analytical and empirical tools for evaluation of the thermal-flow performance or design of air-cooled heat exchangers and cooling towers. People who can make use of this information include students, design engineers, manufacturers, contractors, planners, plant managers, and end users. They may be in the fields of air-conditioning, refrigeration, mining, processing, chemicals, petroleum, power generation, and many other industries. They will be able to prepare improved specifications and evaluate bids more critically with respect to thermal performance of new cooling systems. Possible improvements through retrofits of existing cooling units can be determined, and impacts of plant operations and environmental influences can be predicted. Reasons for poor performance will be better understood, and where necessary, a plant can be optimized to achieve the lowest life cycle cost.

The format and presentation of the subject matter has evolved from courses offered at universities and from industry-based research, development, and consultation over many years. Volume I consists of chapters 1 through 5; Volume II consists of chapters 6 through 10. The Table of Contents for the companion volumes is listed in Appendix D in each volume.

An attempt is made to maintain a meaningful compromise between empirical, analytical, and numerical methods of analysis to achieve a satisfactory solution without introducing an unnecessary degree of complexity or cost. In some cases, sophisticated numerical methods have to be used in order to obtain sufficient insight into aspects of a particular problem. Such programs and the related infrastructure and manpower may be expensive, so it is desirable to stress analytical or empirical methods where meaningful.

The reader is introduced systematically to the literature, theory, and practice relevant to the performance evaluation and design of industrial cooling systems. Problems of increasing complexity are presented. Many of the procedures and examples presented are not only of academic interest, but are applicable to actual systems, and have been tested in practice. The design engineer is supplied with an extensive and up-to-date source of information.

In order to be an informed planner or client, it is important to understand the factors that influence the type and thermal-flow design of any cooling system in order to prepare clear and detailed specifications. A lack of insight

and poor specifications often lead to serious misunderstandings between suppliers and clients and can result in significant increases in the ultimate cost of the plant.

The merits of a particular cooling system should be evaluated critically. Often this can only be done in a holistic and interdisciplinary approach. This approach takes into consideration the entire cycle or plant and its environment when an optimization exercise is performed.

For those interested in further reading, an extensive list of references is included at the end of every chapter.

In view of the iterative nature of solving most heat exchanger performance evaluation or thermal-flow design problems, computers are essential tools. An exception is simple first approximations.

In the numerical examples, values are often given to a large number of decimal places. These numbers are usually from the computer output and do not necessarily imply a corresponding degree of accuracy. However, increasingly improved designs are essential to reduce system costs in the design of large systems or where mass production is involved. In view of the increasing competition, access to computers and more reliable design information will lead to more refined and sophisticated designs. With a better understanding of the performance characteristics of a cooling system, control can be improved in different operating conditions. The worked problems not only show how to apply various equations but each problem forms a part of the learning process and introduces important additional information. The problems gradually lead up to more extensive and complex evaluations.

I am grateful to many friends and colleagues in both the academic and industrial worlds who directly or indirectly contributed to this work. However, this text would not have been written without the support and patience of my family and the valuable input of my graduate students.

List of Symbols

A	Area, m^2
ATD	Air travel distance, m
a	Coefficient; constant; length, m; surface area per unit volume, m^{-1}
B	Breadth, m
b	Exponent; constant; length, m; defined by Equation 3.3.4
C	Coefficient; heat capacity rate mc_p, W/K; C_{min}/C_{max}; cost
c	Concentration, kg/m^3
cp	Specific heat at constant pressure, J/kgK
cv	Specific heat at constant volume, J/kgK
D	Diffusion coefficient, m^2/s
$DALR$	Dry adiabatic lapse rate, K/m
d	Diameter, m
de	Equivalent or hydraulic diameter, m
E	Elastic modulus, N/m^2; energy, J
Ey	Characteristic pressure drop parameter, m^{-2}
e	Effectiveness
F	Force, N; fan; correction factor
f	Friction factor
G	Mass velocity, kg/sm^2
g	Gravitational acceleration, m/s^2; gap, m
H	Height, m
h	Heat transfer coefficient, W/m^2K
hD	Mass transfer coefficient defined by Equation 4.1.3, m/s
hd	Mass transfer coefficient defined by Equation 4.1.13, kg/m^2s
I	Insolation; Bessel function
i	Enthalpy, J/kg
i_{fg}	Latent heat, J/kg
J	Bessel function
K	Loss coefficient; incremental pressure drop number
k	Thermal conductivity, W/mK
L	Length, m
L_{hy}	Hydraulic entry length, (x/d_eRe)
M	Molecular weight, kg/mole; torque, Nm; mass, kg
m	Mass flow rate, kg/s

N	Revolutions per minute, minute^{-1}; NTU
NTU	Number of transfer units, UA/C_{min}
Ny	Characteristic heat transfer parameter, m^{-1}
n	Number; exponent
P	Pitch, m; power, W
Pe	Perimeter, m
p	Pressure, N/m^2
p_{cr}	Critical pressure, N/m^2
Q	Heat transfer rate, W
q	Heat flux, W/m^2
R	Gas constant, J/kgK; thermal resistance, m^{2}K/W
Ry	Characteristic flow parameter, m^{-1}
r	Radius, m; recirculation factor defined by Equation 8.4.1
s	Blade tip clearance, m
st	Yield or ultimate stress, N/m^2
T	Temperature, °C or K
Tu	Turbulence intensity
t	Thickness, m
U	Overall heat transfer coefficient, W/m^{2}K
u	Internal energy, J/kg
V	Volume flow rate, m^3/s; molecular volume; volume, m^3
v	Velocity, m/s
W	Work, J; width, m
w	Humidity ratio, kg water vapor/kg dry air
X	Mole fraction
x	Co-ordinate; elevation, m; distance, m; quality
Y	Defined by Equation 5.2.4
y	Co-ordinate
z	Co-ordinate; elevation, m; exponent

Greek Symbols

α	Thermal diffusivity, $k/\rho c_p$; thermal expansion coefficient; void fraction
α_e	Kinetic energy coefficient defined by Equation 1.4.5
α_m	Momentum velocity distribution correction factor defined by Equation 1.4.25
α_Q	Defined by Equation 9.2.9

β	Volume coefficient of expansion, K^{-1}; porosity
Γ	Flow rate per unit length, kg/sm
γ	c_p/c_v; as defined by Equation 3.4.39
Δ	Differential
δ	Boundary layer thickness, m; condensate film thickness, m
ε	Surface roughness, m; expansibility factor
η	Efficiency; degree of separation
θ	Angle, °; temperature differential, K; potential temperature, °C
κ	Von Karman constant
λ	Eigenvalue; defined by Equation 2.7.4; defined by Equation 4.4.19
μ	Dynamic viscosity, kg/ms
ν	Kinematic viscosity, m^2/s; Poisson's ratio
ξ	Temperature lapse rate, K/m
ρ	Density, kg/m^3
σ	Area ratio; surface tension, N/m
τ	Shear stress, N/m^2; time, s
φ	Potential function; angle, °; defined by Equation 3.2.21 or Equation 3.3.13; relative humidity defined by Equation 4.1.21; expansion factor defined by Equation 5.2.3; dimensionless temperature difference
ψ	Defined by Equation 2.7.5

Dimensionless Groups

Eu	Euler number, $\Delta p/(\rho v^2)$
Fr	Froude number, $v^2/(dg)$
Fr_D	Densimetric Froude number, $\rho v^2/(\Delta\rho dg)$
Gr	Grashof number, $g\rho^2L^3\beta\Delta T/\mu^2$ for a plate or $g\rho^2d^3\beta\Delta T/\mu^2$ for a tube
Gz	Graetz number, *RePrd/L* for a tube
Ku	Kutateladze number, $i_{fg}/(c_p\Delta T)$
j	Colburn j-factor, $StPr^{0.67}$
Le	Lewis number, $k/(\rho c_p D)$ or *Sc/Pr*
Lef	Lewis factor, $h/(c_p h_d)$
Me	Merkel number, $h_d a_{fi} L_{fi}/G_w$
Nu	Nusselt number, *hL/k* for a plate or *hd/k* for a tube
Oh	Ohnesorge number, $\mu/(\rho d\sigma)^{0.5}$

Pe	Péclet number, $RePr$
Pr	Prandtl number, $\mu c_p/k$
Re	Reynolds number, $\rho vL/\mu$ for a plate or $\rho vd/\mu$ for a tube
Sc	Schmidt number, $\mu/(\rho D)$
Sh	Sherwood number, $h_D L/D$ for a plate or $h_D d/D$ for a tube
St	Stanton number, $h/(\rho v c_p)$ or $Nu/(RePr)$

Subscripts

a	Air or based on air-side area
abs	Absolute
ac	Adiabatic cooling
acc	Acceleration
al	Aluminum
amm	Ammonia
av	Mixture of dry air and water vapor
app	Apparent; approach
b	Base; bundle; bend
c	Concentration; convection heat transfer; combining header; casing; contraction; cold; critical; condensate
cd	Conservative design
cf	Counterflow
cp	Constant properties
cr	Critical
ct	Cooling tower
ctc	Cooling tower contraction
cte	Cooling tower expansion
cu	Copper
cv	Control volume
D	Darcy; drag; drop; diffusion
d	Diameter; diagonal; drop; dynamic; dividing header; dry section; diffusion; mass transfer
do	Downstream
db	Drybulb
de	Drift or drop eliminator
ds	Steam duct

dif	Diffuser
e	Energy; expansion; effective; equivalent; evaporative
F	Fan
F/dif	Fan/diffuser
Fhe	Fan to heat exchanger distance
f	Fin; friction; fluid; factor
fi	Fill
fr	Frontal; face
fs	Fill support
g	Gas; ground
gen	Generator
H	Height
h	Hot; header; hub
he	Heat exchanger
i	Inlet; inside
isen	Isentropic
id	Ideal
iℓ	Inlet louver
iso	Isothermal
j	jet; junction
ℓ	Laminar; longitudinal; liquid; lateral; large
ℓm	Logarithmic mean
m	Mean; momentum; model; mass transfer; mixture
max	Maximum
min	Minimum
mo	Monin-Obukhov
n	Nozzle; normal
na	Noise attenuator
nu	Non-uniform
o	Outlet; outside; initial; oil; original
ob	Obstacle
P	Poppe
p	Constant pressure; production; plate; process fluid; passes; plume
pℓ	Plenum chamber
q	Constant heat flux
r	Root; row; radial co-ordinate; refrigerant; reference; recirculation; ratio
re	Effective root

rec	Recovery
red	Reducer
rz	Rain zone
s	Screen; steam; static; saturation; shell; support; superficial; steel; soil; scaling; spray
sc	Settling chamber; surface condenser
si	Inlet shroud
sp	Spray
ss	Supersaturated
T	Constant temperature; temperature; T-junction; test
ΔT	Constant temperature difference
t	Total; tube; tape; transversal; turbulent; transition; terminal; blade tip; fin tip
tp	Two-phase
tr	Tube row
ts	Tube cross section; tower support
tus	Wind tunnel upstream cross section
ud	Upstream and downstream
up	Upstream
v	Vapor
vc	Vena contracta
w	Water; wall; wind; walkway; wet section
wb	Wetbulb
wd	Water distribution system
x	Co-ordinate; quality
y	Co-ordinate
z	Co-ordinate; zinc
θ	Inclined; yawed
π	At 180°
∞	Infinite; free stream

6

Fans

6.0 Introduction

Different types of fans find application in air-cooled heat exchangers and evaporative coolers. These fans include axial flow, centrifugal flow, mixed flow, and crossflow. When selecting a fan for a particular application, the factors usually considered are:

- cost
- performance (stability of operation, ease of control, power consumption, flow range)
- mechanical arrangement (convenience of installation)
- self cleaning blade properties
- noise emission characteristics

The effective operation of fans in a system may be influenced by various structural and aerodynamic factors. Numerous books on the subject have been published including those by Berry, Jorgensen, Eck, Daly, Wallis, Osborne, and Bleier. Guides for the selection of appropriate fans in specific applications are also available, such as *A Guide to Fan Selection and Performance,*

Item No. 79037 from ESDU and Monroe's *Maximising Fan Performance*. In this chapter, characteristics are highlighted of axial flow fans (Fig. 6.0.1) having general application in air-cooled heat exchangers.

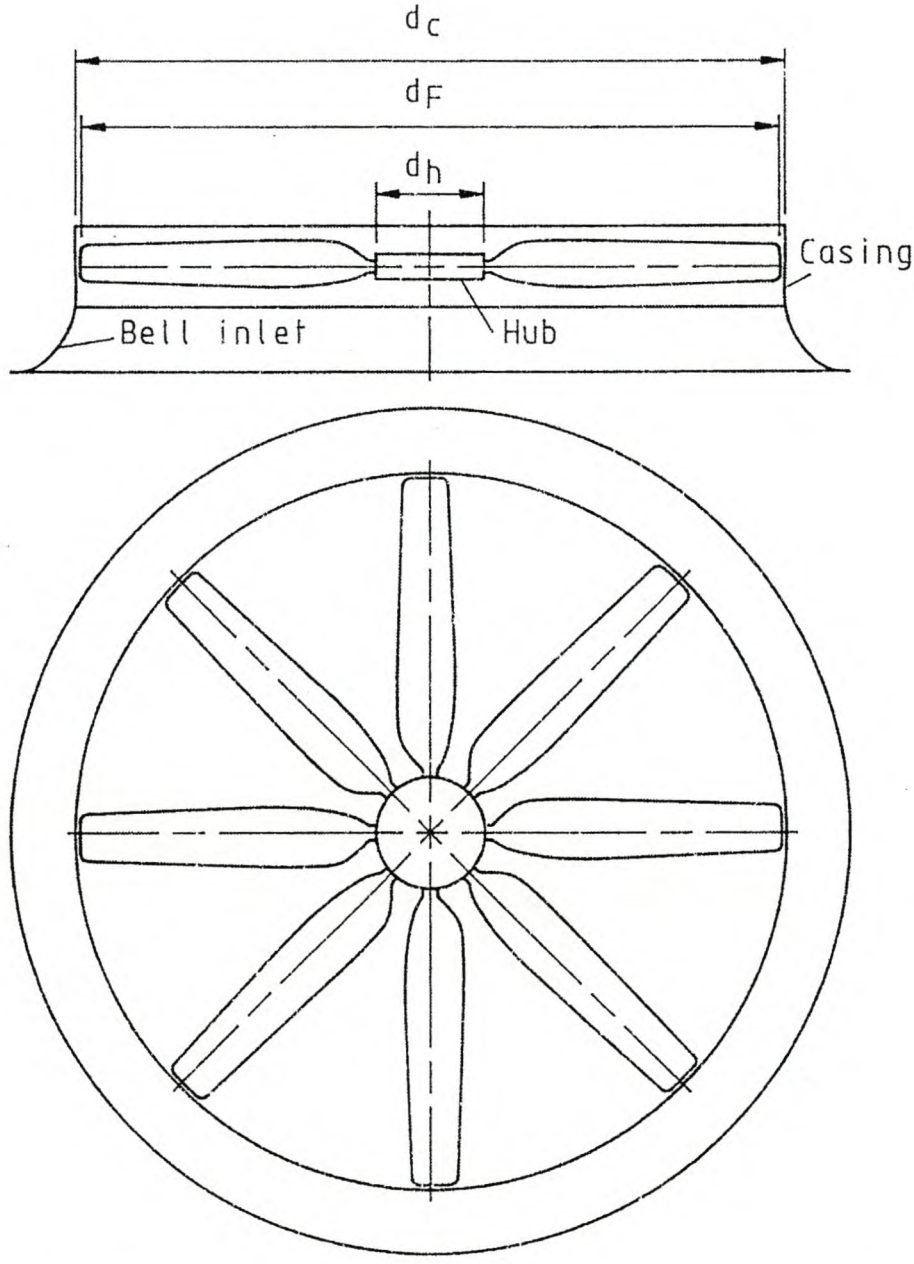

Fig. 6.0.1 Eight-Bladed Axial Flow Fan in Casing or Shroud with Bell-Type Inlet

Modern axial flow fans have extruded aluminum or molded fiberglass blades. By nature, extruded aluminum blades are always of uniform chord width although sections may be welded onto the extrusion, while molded fiberglass blades can have any shape desired.

One of the basic criteria for blade design is to produce as uniform an air flow as possible over the entire plane of the fan. As one moves from the tip of the blade to the hub, the tangential velocity decreases. In order to produce uniform airflow, the blade width and twist must increase. The air velocity vectors at the inboard sections of the blade may actually reverse direction. In a fan designed with a hub seal disc, this effect is reduced. An example in Figure 6.0.2 from Monroe illustrates performance differences due to blade shape and backflow. In the absence of a bell inlet, the fan performance is measurably reduced.

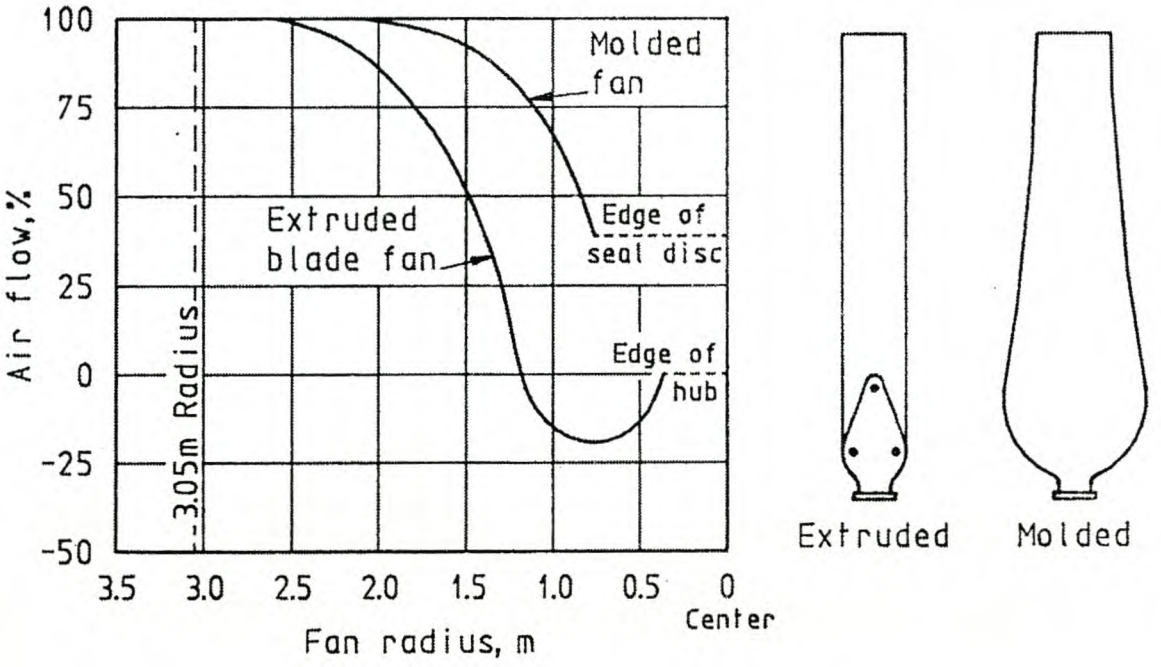

Fig. 6.0.2 Air Flow Distribution through Fan

Axial flow fans are usually provided with four to eight blades. Both the fan cost and the air volume supplied at a given fan speed increase as the number of blades increases. For a specified air volume flow rate, the rotational speed can be reduced with increasing numbers of blades. This has the effect of reducing noise and increasing efficiency, but cost also increases.

By minimizing system losses and introducing *low-noise fans*, noise levels can be significantly reduced according to Van der Speck. An example of a large low-noise fan is shown in Figure 6.0.3. In modern air-cooled condensers, increasing attention is being given to the reduction of noise levels according to authorities such as Smith and Romeister, Leitz, and a Staff

Report in *Modern Power Systems*. According to Häussermann, high efficiency, speed-controlled, sickle-bladed, axial flow fans reduce the power consumption and noise of air-cooled condensers in refrigeration and air-conditioning plants. In many vehicles, the radiator fan was found to be the major source of noise during certain driving conditions according to both Katte and Hebard and Tebby. By improving fan performance and control, significant reductions in noise levels are achievable.

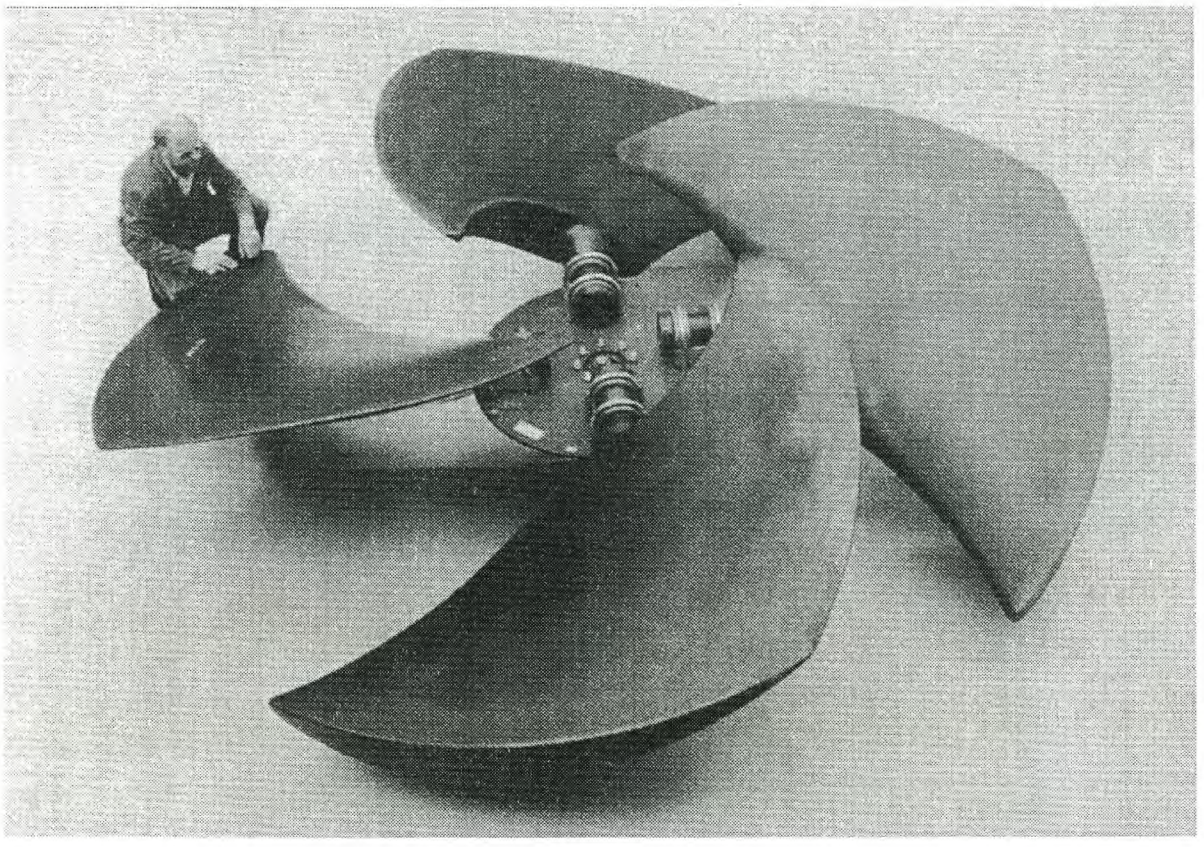

Fig. 6.0.3 Low-Noise Fan

6.1 Test Facilities and Procedures

The performance characteristics of fans are determined in test facilities that must comply with specifications set out in one of many codes or

standards. For axial flow fans, existing standards are related to a certain extent according to Roslyng. Examples of such standards include:

- ASME Test Code for Fans PTC 11-1946
- VDI-Richtlinien, Abname- und Leistungsversuche an Ventilatoren, VDI 2044
- AMCA Standard 210-74
- ASHRAE Standard 51-75
- ASME PTC 1
- British Standards Institution BS 848
- Deutsches Institut für Normung DIN 24163 Teil 1 and 2

According to Deeprose and Smith, the modern versions are more comprehensive and are regularly updated.

The International Organization for Standardization (ISO) has agreed to recognize four standard fan installation types:

- Installation Type A: free inlet, free outlet
- Installation Type B: free inlet, ducted outlet
- Installation Type C: ducted inlet, free outlet
- Installation Type D: ducted inlet, ducted outlet

Free inlet or outlet signifies the air enters or leaves the fan directly from or to the unobstructed free atmosphere. Type A installations have an exception—a partition in which the fan is mounted may support a pressure difference between the inlet and the outlet sides. Ducted inlet or outlet signifies the air enters or leaves the fan through a long straight duct of the same cross-sectional area and directly connects to the fan inlet or outlet.

Standardized airways designed for Type A installation tests may be adapted to provide tests for Type B, C, or D installations.

An example of a Type A test installation is shown in Figure 6.1.1. The air mass flow rate through this installation is determined by measuring the pressure in the wall of a calibrated inlet venturi nozzle or bellmouth (1).

The general expression for the mass flow rate through this type of nozzle is as follows:

$$m = C_n \varepsilon_n A_n \, (2 \, \rho_n \, \Delta p_n)^{0.5} \tag{6.1.1}$$

where

C_n = the flow coefficient

ε = the expansibility factor

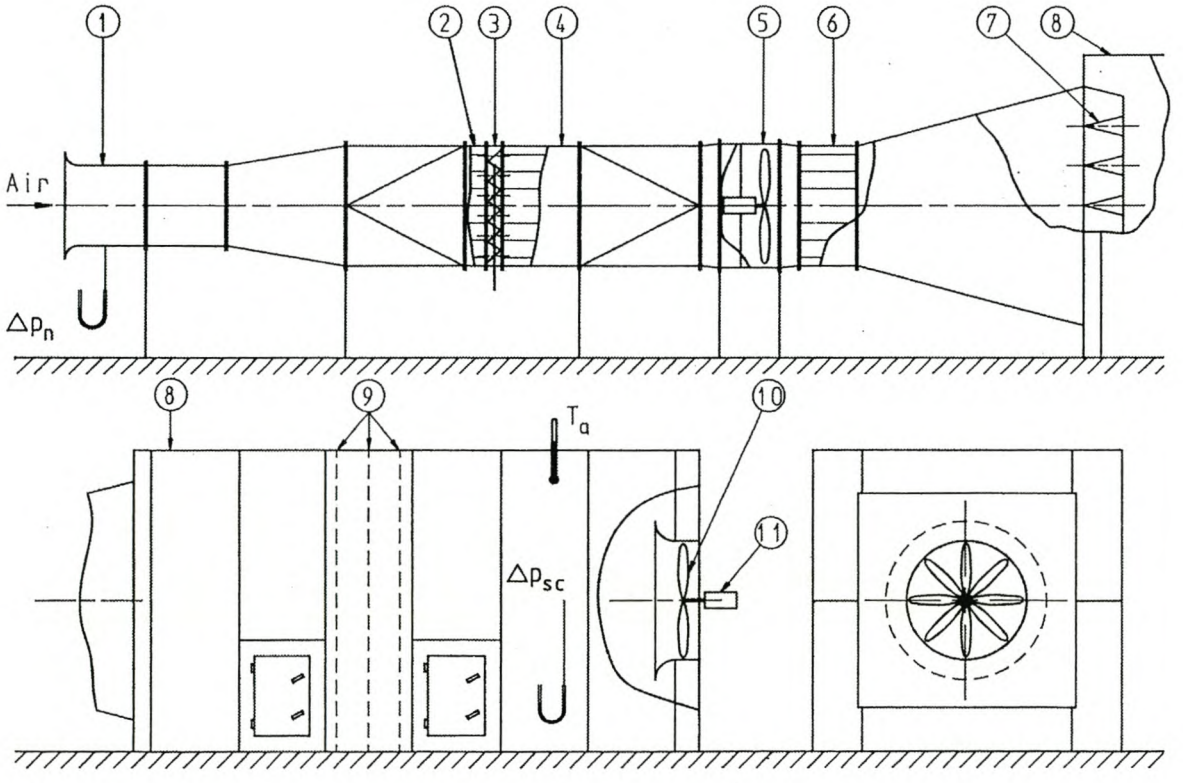

Fig. 6.1.1 Example of a Type A Test Installation

The product of $C_n\varepsilon_n$ for a particular nozzle can be determined experimentally by doing a velocity traverse with the aid of a pitot-static tube.

An adjustable louver flow control device (3) is preceded and followed by flow straighteners (2) and (4). The auxiliary fan (5) is installed to overcome the flow resistance of the test airways under certain operating conditions. Any swirl subsequent to the auxiliary fan is eliminated by the flow straighteners (6).

A set of flow guide vanes (7) ensures a relatively even flow distribution into the settling chamber (8). The wire screens (9) further improve the air flow through the settling chamber.

Temperature and static pressure measuring points are located after the screens to define fan inlet conditions. The static pressure differential, Δp_{sc}, is measured between the inside surface of the settling chamber wall and ambient conditions. The density of the air in the settling chamber, ρ_T ($_T$ refers to the fan test), can be determined from the perfect gas relation, i.e.,

$$\rho_T = (p_a + \Delta p_{sc})/RT_a \tag{6.1.2}$$

where

p_a = the ambient pressure

T_a = and the ambient temperature

The air volume flow rate through the test fan is thus

$$V_T = m/\rho_T \tag{6.1.3}$$

Although the air velocity in the settling chamber immediately upstream of the fan is small, it is not necessarily negligible, and the dynamic pressure associated with it may be determined from

$$p_{dT} = 0.5(m/A_{sc})^2/\rho_T \tag{6.1.4}$$

The fan is mounted in an appropriate casing or shroud at the outlet of the settling chamber. Details of the type of inlet employed during tests must

be specified. Care should be taken to avoid the presence of any obstruction that may significantly modify air flow immediately before or after the fan. The fan should be operated at a speed close to that specified. It may be driven by a variable speed electric or hydraulic drive. The torque, M_T, in the shaft at the impeller and the rotational speed, N_T (rpm), are monitored during testing. The power input to the fan can be determined with these values according to

$$P_{FT} = 2\,\pi\,M_T N_T/60 \tag{6.1.5}$$

For this test, fan static pressure is defined as

$$\Delta p_{FsT} = -\Delta p_{sc} - p_{dT} \tag{6.1.6}$$

In some cases, it may be preferable to present the fan pressure characteristics in terms of the fan total pressure, which is defined as the difference in total pressure at fan inlet and outlet for the Type A test, i.e.,

$$\Delta p_{FtT} = \Delta p_{FsT} + (m/A_c)^2/(2\rho_T) \tag{6.1.7}$$

where

A_c = the gross area at the outlet of the casing, without deduction for motor fairings or other obstructions

In some standards, Δp_{FtT} is based on the net outlet area according to the Institut für Normung DIN 24163, Teil 1.

Fan static efficiency is defined as

$$\eta_{FsT} = V_T \Delta p_{FsT} \,/\, P_{FT} \tag{6.1.8}$$

and fan total efficiency is defined as

$$\eta_{FtT} = V_T \Delta p_{FtT}/P_{FT} \tag{6.1.9}$$

The total efficiency is always larger than the static efficiency.

Examples of the other standardized test airways are shown in Figure 6.1.2. The installation type or types selected for testing a particular fan depends on the intended application of the fan. Although fans are sometimes installed in duct systems similar to one of the standard installation types, this is not always the case. If the fan system geometry deviates considerably from one of the standard installations, performance tests should be conducted on the system or a model.

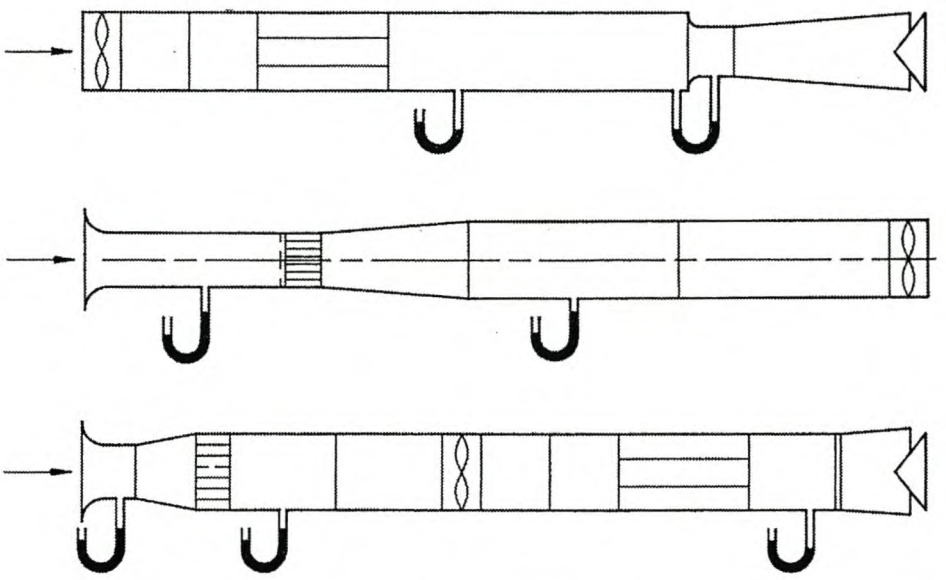

Fig. 6.1.2 Standardized Airways (a) Free Inlet, Ducted Outlet, Type B Installation,
(b) Ducted Inlet, Free Outlet, Type C Installation,
(c) Ducted Inlet, Ducted Outlet, Type D Installation

6.2 Presentation of Data and Results

Since it is usually impossible to carry out fan tests at exactly the speed or density specified, conversion rules, also known as *fan laws*, are used to determine the fan performance at the specified rotational speed, N, and the fan inlet density, ρ, i.e.,

Volume flow rate

$$\frac{V}{V_T} = \frac{N}{N_T} \tag{6.2.1}$$

Pressure

$$\frac{\Delta p_{Ft}}{\Delta p_{FtT}} = \frac{\Delta p_{Fs}}{\Delta p_{FsT}} = \frac{p_{Fd}}{p_{FdT}} = \left(\frac{N}{N_T}\right)^2 \left(\frac{\rho}{\rho_T}\right) \tag{6.2.2}$$

Power

$$\frac{P_F}{P_{FT}} = \left(\frac{N}{N_T}\right)^3 \left(\frac{\rho}{\rho_T}\right) \tag{6.2.3}$$

Efficiency

$$\eta_{Ft} = \eta_{FtT} \text{ and } \eta_{Fs} = \eta_{FsT} \tag{6.2.4}$$

The actual test results, or the results after conversion according to the previous rules, may be plotted as a series of test points against inlet volume flow. Rotational speeds are referred to a specified speed, N, and densities are referred to a specified density, ρ, which is usually chosen to be 1 kg/m^3 or 1.2 kg/m^3.

Adjustable duty fan characteristics are required for a fan having means for altering its performance due to variable pitch blades. A family of constant speed characteristics at 1.2 kg/m^3 inlet density is recommended and selected at suitable steps of adjustment. Efficiencies may be shown by means of smooth contours drawn through points of equal efficiency on the fan pressure characteristics. Figure 6.2.1 shows an example of fan static pressure characteristics of an 8-bladed axial flow fan installed in a 1542 mm diameter casing. Figure 6.0.1 shows this fan with a bell inlet.

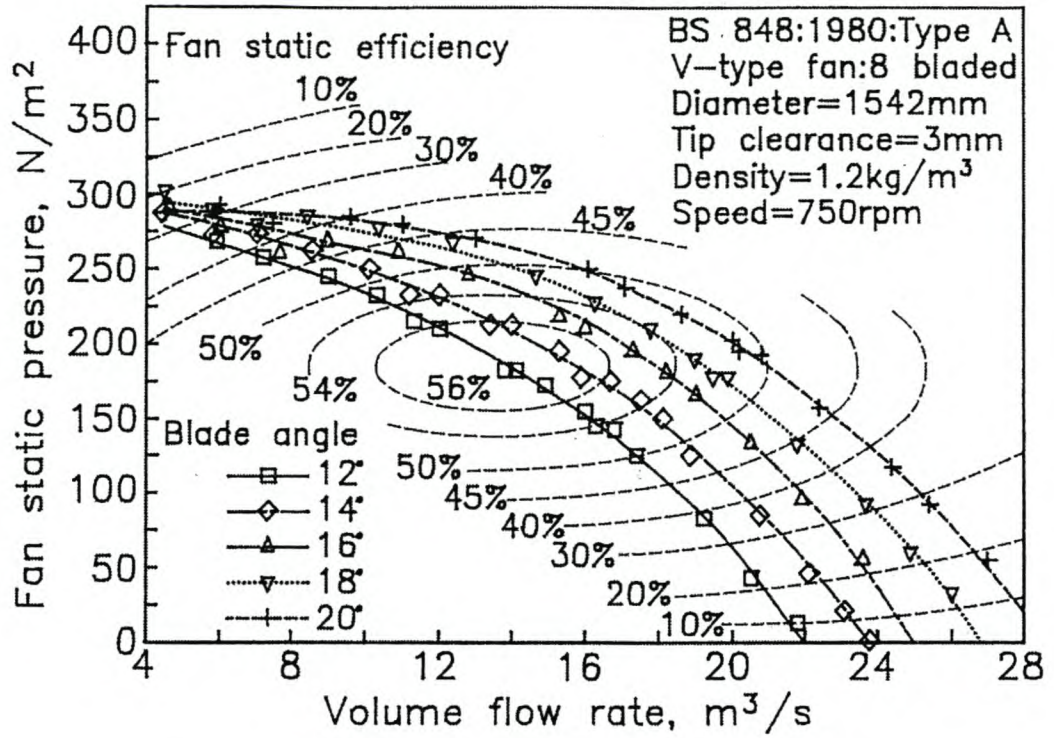

Fig. 6.2.1 Fan Static Pressure and Efficiency

The corresponding fan power and static efficiency is shown in Figures 6.2.2 and 6.2.3.

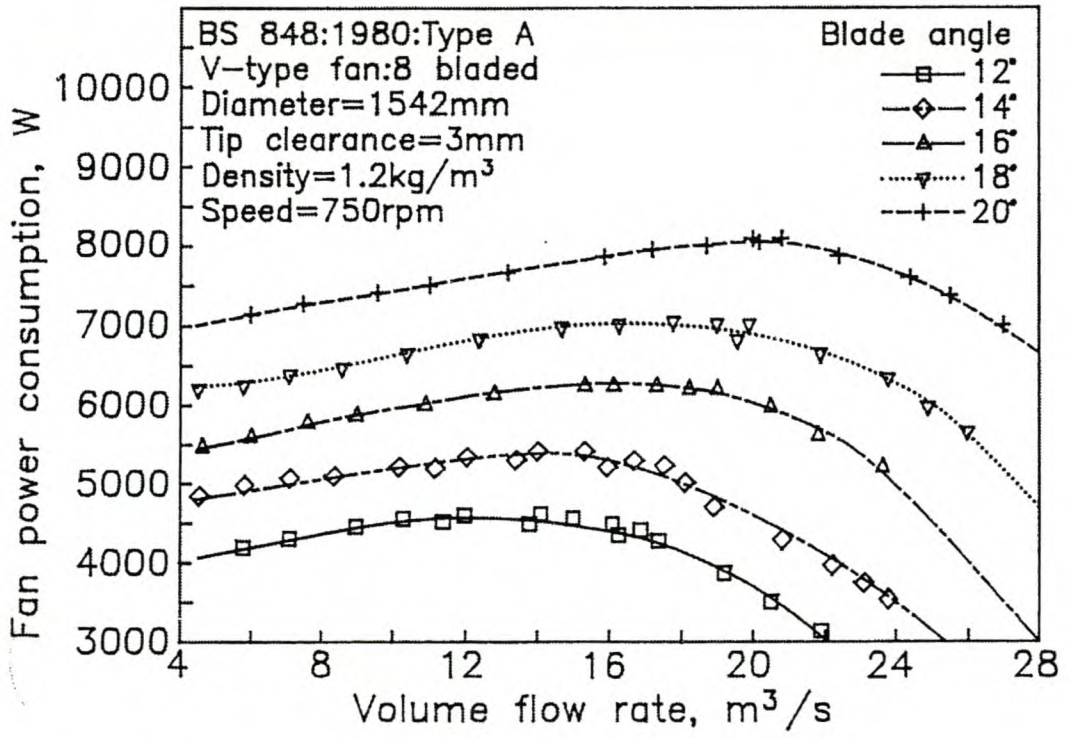

Fig. 6.2.2 Fan Power

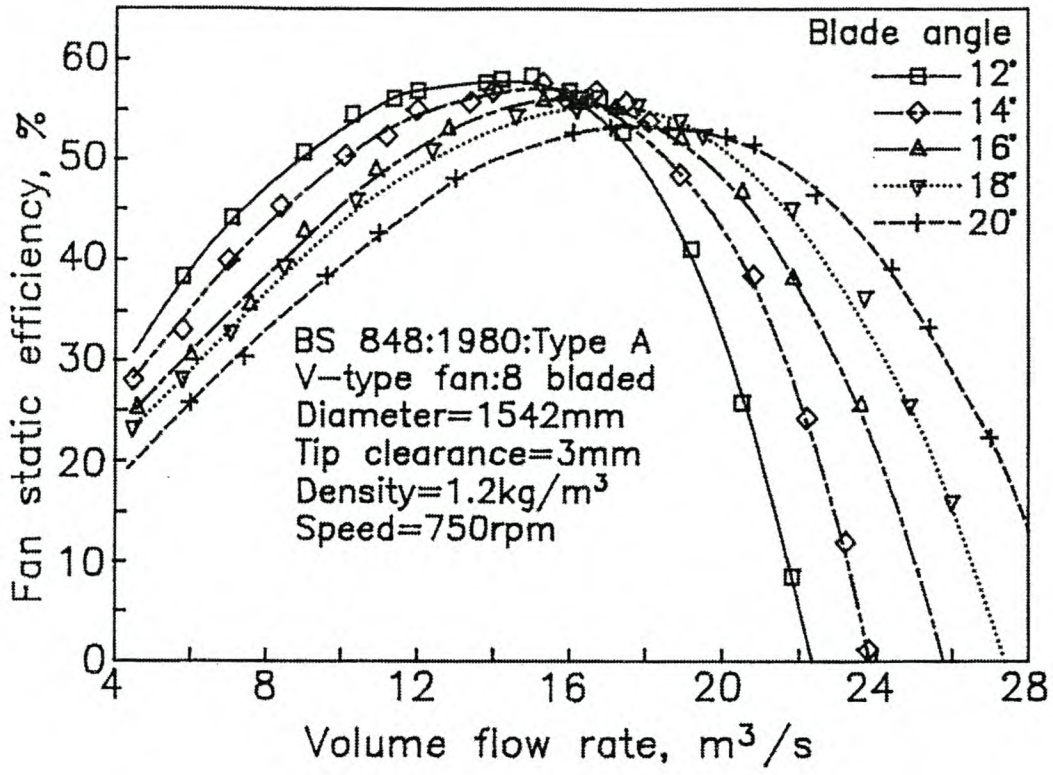

Fig. 6.2.3 Fan Static Efficiency

When presenting fan performance curves, it is important to specify the casing diameter or blade tip clearance in addition to details of the fan and casing inlet geometry, blade angle, type of test, reference density, and rotational speed.

Very large diameter axial flow fans find application in industry. Since suitable test facilities for such service fans are unavailable, geometrically similar smaller models are tested in standardized airways.

The following conversion rules may be applied to model test results to predict the performance of geometrically similar larger fans.

- Volume flow rate

$$\frac{V_\ell}{V} = \frac{N_\ell}{N}\left(\frac{d_{F\ell}}{d_F}\right)^3 \qquad (6.2.5)$$

- Pressure

$$\frac{\Delta p_{Ft\ell}}{\Delta p_{Ft}} = \frac{\Delta p_{Fs\ell}}{\Delta p_{Fs}} = \frac{p_{Fd\ell}}{p_{Fd}} = \left(\frac{N_\ell}{N}\right)^2 \left(\frac{d_{F\ell}}{d_F}\right)^2 \left(\frac{\rho_\ell}{\rho}\right) \tag{6.2.6}$$

- Power

$$\frac{p_{F\ell}}{p_F} = \left(\frac{N_\ell}{N}\right)^3 \left(\frac{d_{F\ell}}{d_F}\right)^5 \left(\frac{\rho_\ell}{\rho}\right) \tag{6.2.7}$$

- Efficiency

$$\eta_{Ft\ell} = \eta_{Ft} \text{ and } \eta_{Fs\ell} = \eta_{Fs} \tag{6.2.8}$$

Fans much larger than the test model may be expected to show a slight deviation from predicted performance under certain circumstances. However, according to most standards, no allowance for this scale effect should be made without other agreed-upon evidence between manufacturer and purchaser. Because the fan laws do not take into consideration frictional effects, there is a possibility of discrepancy in predicted performance of the larger fan. If the tip speed of the model and the larger fan is the same, the Reynolds number of the larger fan will also be greater due to its wider chord. Thus, the predicted larger fan pressure and air volume flow rate will be achieved at a slightly lower blade angle.

According to VDI standards, if the Reynolds number based on fan diameter of the test fan and that of a larger fan are different, the dependence of the frictional losses on this number should be considered. An approximate relation between the efficiencies of two such fans is

$$\eta_{F\ell} = 1 - 0.5(1 - \eta_F)\ [1 + (Re_F/Re_{F\ell})^{0.2}] \tag{6.2.9}$$

where

$Re_F = \rho v_t d_F/\mu$

v_t = the blade tip speed

Fan blade tip speeds of 60 m/s or less are recommended in areas where relatively low noise levels must be maintained.

The VDI standard gives the following conversion rule for tip clearance in fans of different diameters:

$$\frac{s_{F\ell}}{s_F} = \left(\frac{d_{F\ell}}{d_F}\right)^{0.8} \left(\frac{\Delta p_F}{\Delta p_{F\ell}}\right)^{0.1} \tag{6.2.10}$$

Example 6.2.1

Determine the fan static pressure, fan power, and fan static efficiency of an adjustable 8-bladed axial flow fan, called V-fan, shown in Figure 6.0.1. The V-fan was tested according to BS 848 installation Type A (Fig. 6.1.1).

Details of the test fan installation are as follows:

- Fan diameter: $d_F = 1.536$ m
- Fan casing diameter: $d_c = 1.542$ m
- Fan blade tip clearance: $s_F = 0.003$ m
- Fan blade angle: $\theta_F = 16^\circ$
- Bell mouth nozzle diameter: $d_n = 1.008$ m
- Bell mouth inlet coefficient: $C_n \varepsilon_n = 0.9802$
- Settling chamber cross-sectional area: $A_{sc} = 4\text{m} \times 4\text{m} = 16\text{m}^2$
- Ambient conditions:
  - Atmospheric pressure: $p_a = 100499.05$ N/m^2
  - Temperature: $T_a = 20^\circ$C
- Test data:
  - Fan torque: $M_T = 77.41$ Nm
  - Rotational speed: $N_T = 749$ rpm
  - Settling chamber pressure: $\Delta p_{sc} = -213.68$ N/m^2
  - Bell mouth inlet pressure differential: $\Delta p_n = 244.43$ N/m^2

All characteristics are to be referred to a reference density of $\rho = 1.2$ kg/m^3 and a rotational speed of $N = 750$ rpm.

Solution

From the perfect gas relation, it follows that the ambient air density is

$$\rho_a = p_a/RT_a = 100499.05/[287.08(273.15 + 20)] = 1.1942 \text{ kg/m}^3$$

According to Equation 6.1.1, the air mass flow rate through the fan is

$$m = 0.9802\ \pi(1.008)^2\ (2 \times 1.1942 \times 244.43)^{0.5}/4 = 18.9 \text{ kg/s}$$

In the settling chamber, the air density according to Equation 6.1.2 is

$$\rho_T = \rho_a\ (p_a + \Delta p_{sc})/p_a = 1.1942\ (100499.05 - 213.68)/100499.05 = 1.1917 \text{ kg/m}^3$$

With this value, it is possible to determine the air volume flow rate through the fan, i.e.,

$$V_T = m/\rho_T = 18.9/1.1917 = 15.86 \text{ m}^3/\text{s}$$

According to Equation 6.1.4, the dynamic pressure in the settling chamber is

$$p_{dT} = 0.5 \times (18.9)^2 / (1.1917 \times 16^2) = 0.585 \text{ N/m}^2$$

From Equation 6.1.6, the fan static pressure is

$$\Delta p_{FsT} = 213.68 - 0.585 = 213.1 \text{ N/m}^2$$

The power input to the fan is determined according to Equation 6.1.5.

$$P_{FT} = 2\pi \times 77.41 \times 749/60 = 6071.66 \text{ W}$$

The corresponding fan static efficiency follows from Equation 6.1.8.

$$\eta_{FsT} = 15.86 \times 213.1/6071.66 = 0.557 \text{ or } 55.7\%$$

To present the data graphically, convert the test results to the reference conditions specified.

According to Equation 6.2.1, the volume flow rate is

$$V = 15.86 \text{ x } 750/749 = 15.88 \text{ m}^3/\text{s}$$

while the converted fan static pressure follows from Equation 6.2.2

$$\Delta p_{Fs} = 213.1(750/749)^2 \ (1.2/1.1917) = 215.16\text{N/m}^2$$

The power input to the fan, according to Equation 6.2.3, is

$$P_F = 6071.66(750/749)^3 \ (1.2/1.1917) = 6138.5\text{W}$$

According to Equation 6.2.4, the fan static efficiency remains unchanged, thus

$$\eta_{Fs} = 0.557 \text{ or } 55.7\ \%$$

The actual performance characteristics of this fan are shown in Figure 6.2.1. The corresponding fan power and static efficiency curves are shown in Figures 6.2.2 and 6.2.3.

Note

Fan performance characteristics shown in Figures 6.2.1 to 6.2.3 can be predicted by means of computational methods according to Meyer and Kröger.

In most practical installations, the selected fan tends to operate near its point of maximum efficiency (Fig. 6.2.3) or preferably to the right of this point. It is also important not to operate a fan such that the blade-passing frequency or one of its dominant harmonics is close to the natural vibration frequency of a blade.

The maximum power input to the fan is required when the ambient air temperature is at its lowest and its density is high. In instances where blades are mechanically adjusted for summer and winter operation, the motor should be oversized by 15% according to Paikert. Smaller fans are usually driven by V-belts (30–40 kW), while various types of reduction gears are employed for higher driving powers.

In multifan cooling plants, energy may be saved under certain operating conditions or ambient conditions. Monroe and Fahlsing suggest shutting down individual fans in winter, changing blade angles either manually or automatically, or reducing the rotational speed. Variable speed motors are finding increasing application. In some cases, fans are driven by controllable hydraulic drives.

Example 6.2.2

Determine the performance characteristics of a scaled up version of the fan and casing described in Example 6.2.1. The fan diameter is 9.145 m, and it rotates at 125 rpm. The blade angles are set at 16°, and the density remains the same at 1.2 kg/m^3. If the fan efficiency is to remain unchanged, determine the casing diameter.

Solution

According to Equation 6.2.5, the air volume flow rate through this large fan is

$$V_\ell = 15.88 \text{ x } (125/750)\ (9.145/1.536)^3 = 558.6 \text{m}^3/\text{s}$$

At this volume flow rate, the corresponding fan static pressure given by Equation 6.2.6 is

$$\Delta p_{Fs\ell} = 215.16\ (125/750)^2\ (9.145/1.536)^2 = 211.9\ \text{N/m}^2$$

From Equation 6.2.7, it follows that

$$P_{F\ell} = 6138.5\ (125/750)^3\ (9.145/1.536)^5 = 212.6 \text{ x } 10^3\ \text{W}$$

The fan static efficiency is assumed to remain unchanged as stated by Equation 6.2.8, i.e., $\eta_{Fs} = 0.557$.

However, to retain this efficiency, the tip clearance of the fan must be scaled according to Equation 6.2.10.

$$s_{F\ell} = 0.003\ (9.145/1.536)^{0.8}\ (215.16/211.9)^{0.1} = 0.0125\ \text{m}$$

The casing diameter of the fan is thus

$$d_{c\ell} = 9.145 + 2 \text{ x } 0.0125 = 9.17\text{m}$$

By making similar calculations at other points, it is possible to obtain empirical performance correlations for design purposes, i.e.,

- Fan static pressure

$$\Delta p_{Fs\ell} = 320.0451719 - 0.2975215484 V_\ell + 6.351486 \text{ x } 10^{-4} V_\ell^2$$
$$- 8.14 \text{ x } 10^{-7} V_\ell^3, \text{N/m}^2$$

- Fan power

$$P_{F\ell} = 186645.2333 - 59.413863388 V_\ell + 0.476168398 V_\ell^2 - 5.08308 \times 10^{-4} V_\ell^3, \text{W}$$

- Fan static efficiency

$$\eta_{Fs\ell} = \Delta p_{Fs\ell} \, V_\ell / P_{F\ell}$$

These correlations are presented in Figure 6.2.4.

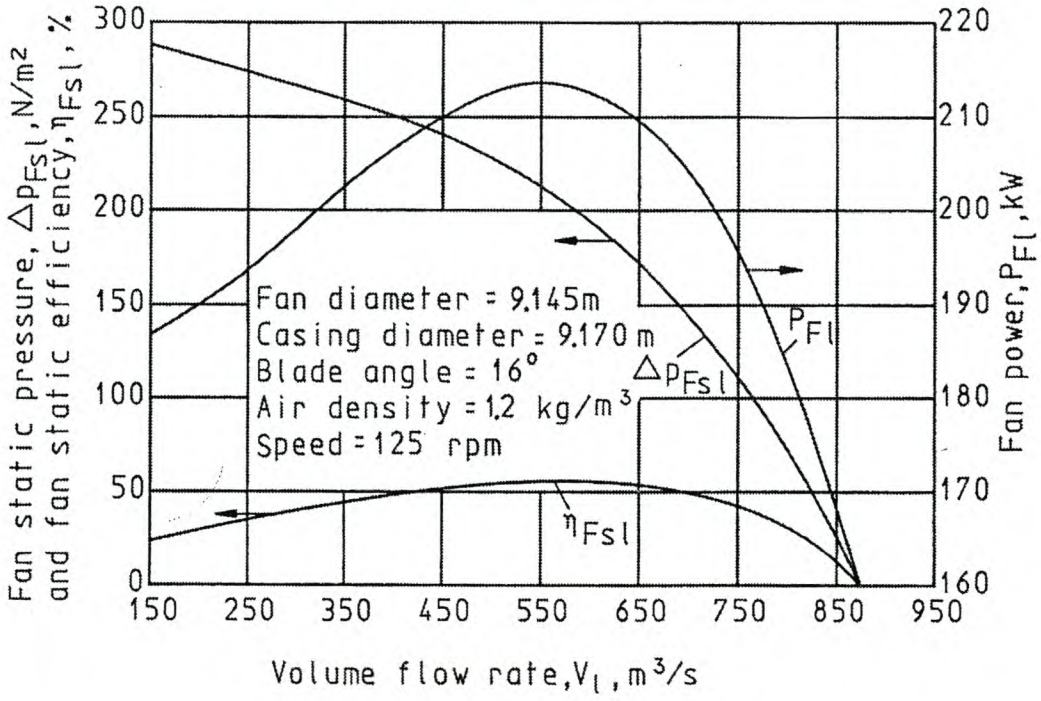

Fig. 6.2.4 Fan Performance Characteristics

6.3 Tip Clearance

An increase in the gap between the fan blade tip and the casing, also referred to as the fan blade tip clearance, s_F, results in a reduction of the fan efficiency according to Monroe, Wallis, and Venter and Kröger. This is due primarily to air leakage from the higher pressure fan outlet stream to the lower pressure inlet region around the tips of the fan blades. In practical

systems, a recommended difference between casing diameter and fan diameter is 0.5–1.0 % of the fan diameter or less, i.e.,

$$s_F/d_F \approx s_F/d_c = (d_c - d_F)/(2d_c) = 0.005 \text{ to } 0.01$$

In the petro-chemical industry, a radial clearance of 0.5% of the fan diameter or 19 mm between the fan tip and the casing, whichever is smaller, is recommended according to API Standard 661.

Ruden found there is a measurable reduction in pressure rise across the fan as the tip clearance increases.

According to Wallis, the loss in fan efficiency due to tip clearance can be expressed as

$$\text{Efficiency loss} = 2\left(\frac{\text{tip clearance}}{\text{blade span}} - 0.01\right) \qquad (6.3.1)$$

for a (tip clearance)/(blade span) ratio of more than 0.01.

Figure 6.3.1 shows the effect of increasing tip clearance on the fan static pressure for the V-fan. Venter and Kröger find both the fan pressure and the air volume flow rate through the fan decrease linearly with increasing tip clearance (Fig. 6.3.2). This is true in the region of maximum efficiency if the system loss coefficient is essentially constant throughout the practical operating range.

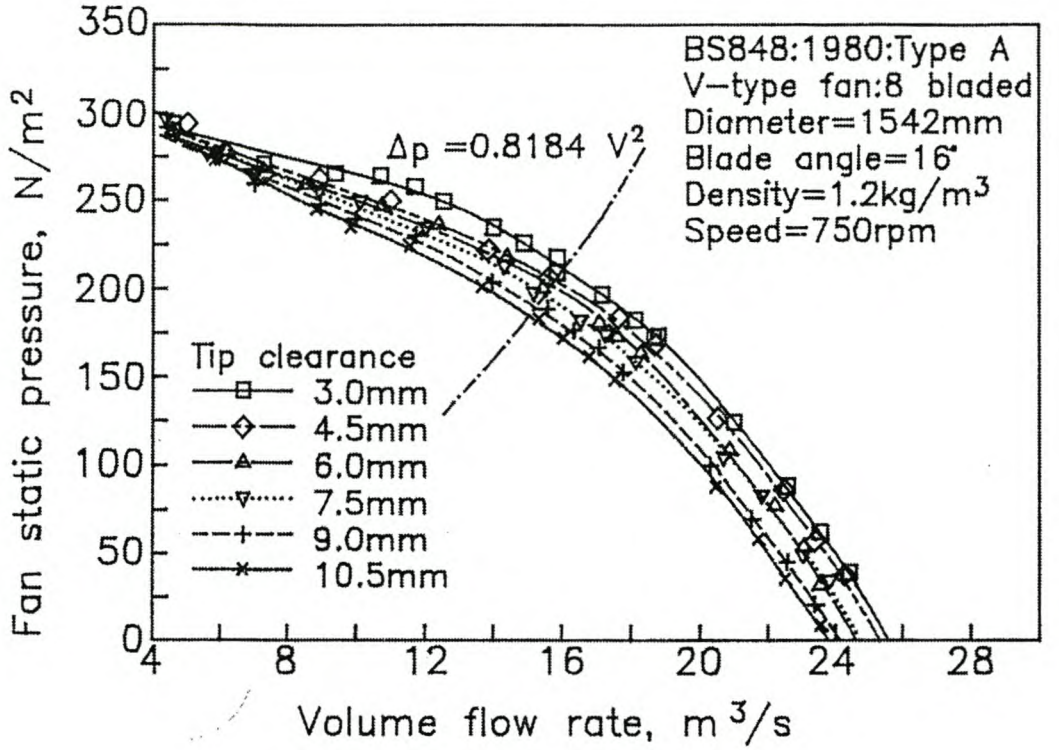

Fig. 6.3.1 Effect of Tip Clearance on Fan Pressure

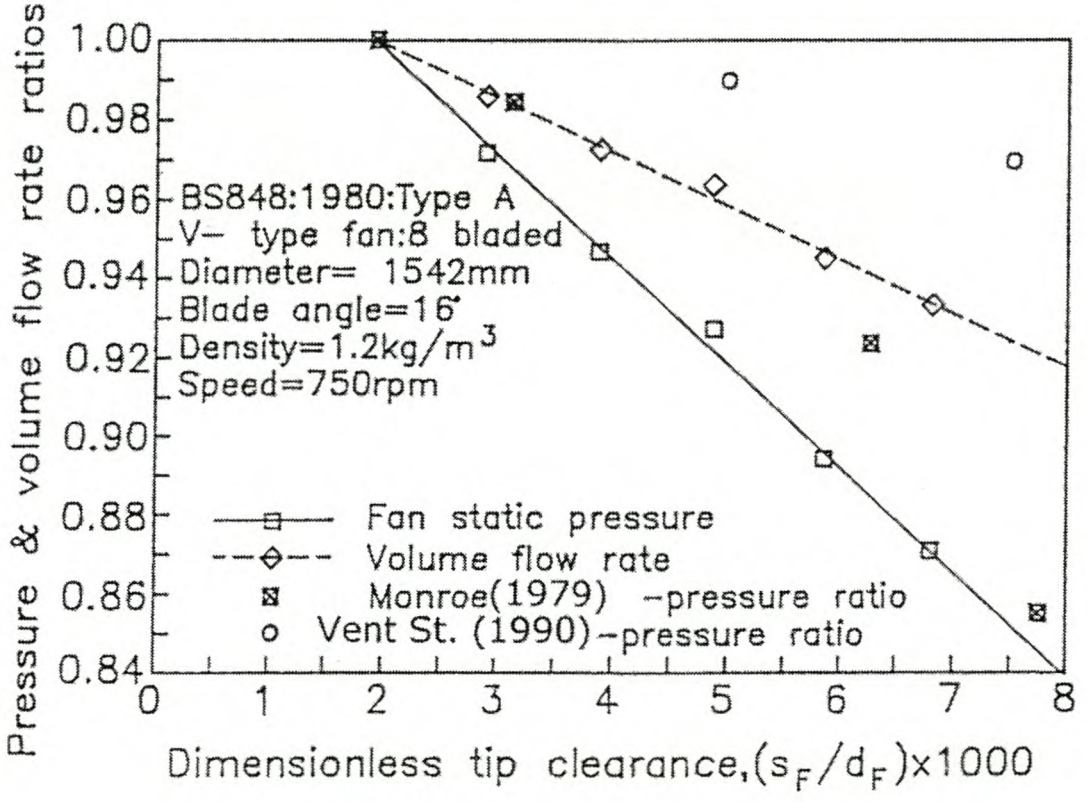

Fig. 6.3.2 Effect of Tip Clearance on Fan Performance

The data from Monroe is for a constant air volume flow rate through the fan. For a given installation, this form of presentation is not realistic since it does not reflect the actual trend in air flow as the tip clearance increases.

If the tip clearance in a practical installation differs from that employed during fan performance tests, its approximate influence can be determined by means of Equations 6.2.10, and 6.3.1 as well as the linear relations shown in Figure 6.3.2.

Noise levels rise with increasing tip clearance according to Hunnabal. In view of the demand for high efficiency and quiet operation, small tip clearances are desirable. The addition of aerodynamic winglets at the blade tips decrease vortex development and reduce noise.

According to Wallis, blade root clearance is relevant for adjustable pitch fans where the root clearance must be adequate to deal with large angular blade changes and possible hub dirt accumulation.

Reverse flow usually occurs in the vicinity of the hub of an axial flow fan according to Monroe. The magnitude of this phenomenon increases progressively with increasing system flow resistance. By designing the fan with profiled blades or locating a disc on the downstream side of the hub, this problem can be reduced. In some cases, a reduction in backflow and a corresponding small improvement in performance may also be achieved by retrofitting an existing fan with a disc.

6.4 Fan System

The interaction between the fan and the installation flow resistances, known as the *system* or *installation effect*, has been recognized and investigated by a number of authors including Nowakowski, Graham, Costelli, O'Connor, Woods-Ballard, Riera-Ubiergo and Charbonelle, McEwan, and Kröger and Woods-Ballard. In addition to the flow resistances, resultant flow distortions through the fan influence its performance and may lead to blade vibration and failure according to Staiger and Stetter. Available literature covers only a sector of the complete range of all applications in industry. Beard and Hay et al. explored the system effects associated with inlet shrouds and with the distance between radiator and fan in vehicle cooling systems. The system effect associated with elbows, diffusers, and contractions, both at the fan inlet and outlet, is examined by a number of

authors such as Daly, Deeprose and Smith, Roslyng, and Zaleki. Studies by Cory and Coward are relevant to the same range of fan applications. The effect of fan plenum chambers on the fan performance is presented by Lambert et al, Stone and Wen, Russell and Berryman, and Meyer and Kröger. In view of the complexity of the flow in some systems, it may be prudent to perform model tests on such systems.

Upstream and downstream obstacles

Venter and Kröger conducted experiments on the V-type fan described in the previous sections to determine the influence on performance of flow resistances located immediately upstream and downstream. The resistances included support structures, screens, and walkways. For a uniformly distributed resistance, their conclusions showed the "bulk method" described by Ventilatoren Stork Hengelo satisfactorily predicted effective pressure loss coefficients. Figures 6.4.1 and 6.4.2 show the loss coefficients based on the velocity through the fan for resistances created by obstacles located on the upstream or suction side and the downstream or discharge side of the fan. These coefficients are a function of the projected area of the obstacle, A_{ob}, and the distance, x, from the fan.

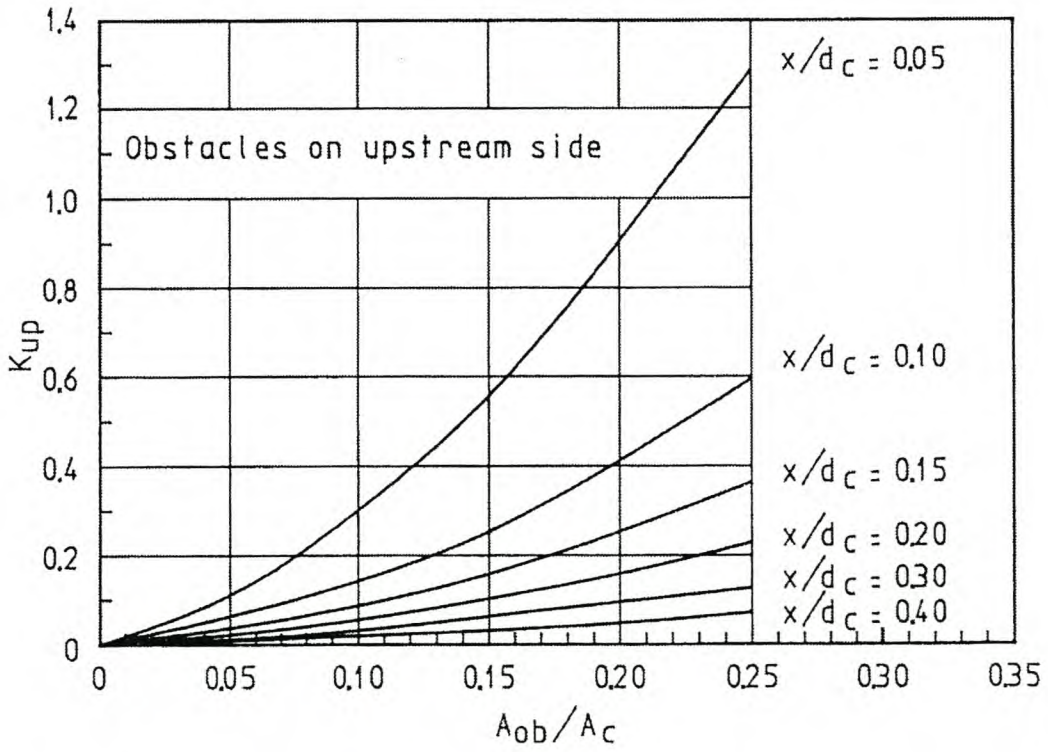

Fig. 6.4.1 Upstream Loss Coefficient Due to Obstacles

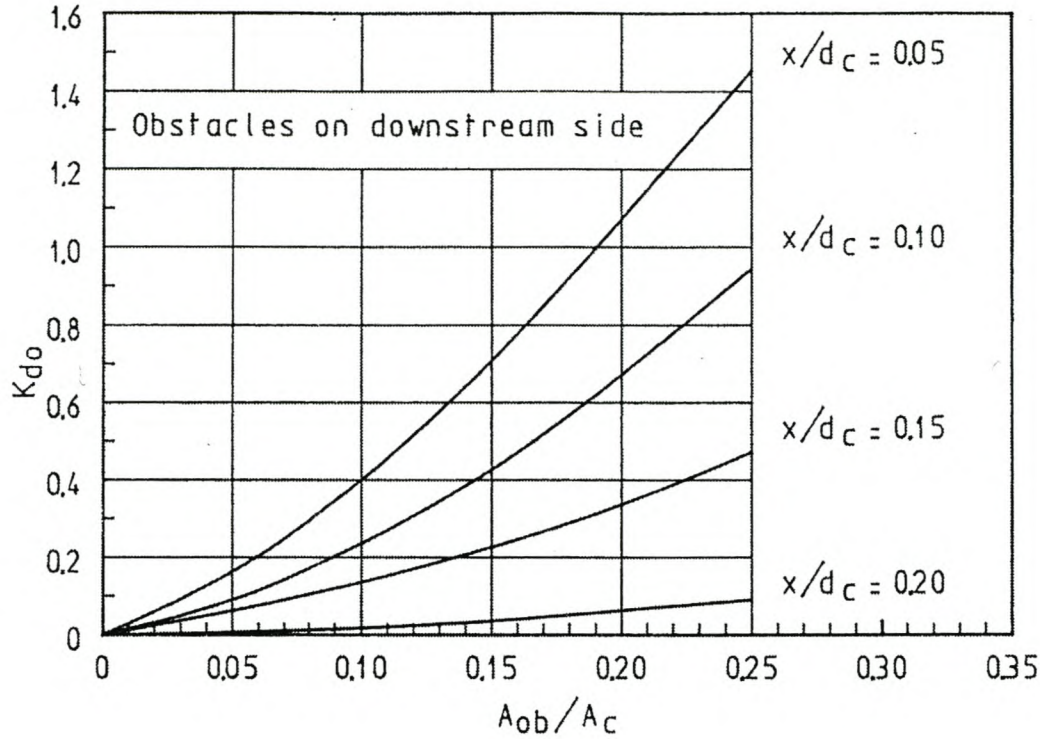

Fig. 6.4.2 Downstream Loss Coefficient Due to Obstacles

The upstream obstacle loss coefficient can be expressed as

$$K_{up} = 2\Delta p_{up}/(\rho v^2) = 2\rho\Delta p_{up}/(m_a/A_e)^2 = f\,(x/d_c, A_{ob}/\eta_\eta) \qquad (6.4.1)$$

where

$A_e = A_c - A_h$

A_c = the casing cross-sectional area

A_h = the hub cross-sectional area

The downstream loss coefficient can be expressed as

$$K_{do} = 2\Delta p_{do}/(\rho v^2) = 2\rho\Delta p_{do}/(m_a/A_e)^2 = f\,(x/d_c, A_{ob}/A_c) \qquad (6.4.2)$$

Plenum chamber

In induced draft exchangers, the *plenum chamber* or the *plenum* is the enclosed space between the drift eliminator or heat exchanger and the fan. It is also the enclosed space between the fan and the fill or heat exchanger in forced draft systems.

Examples of typical plenum chambers found in air-cooled heat exchangers used in the petro-chemical and process industries are shown in Figure 6.4.3. These are from API Standard 661.

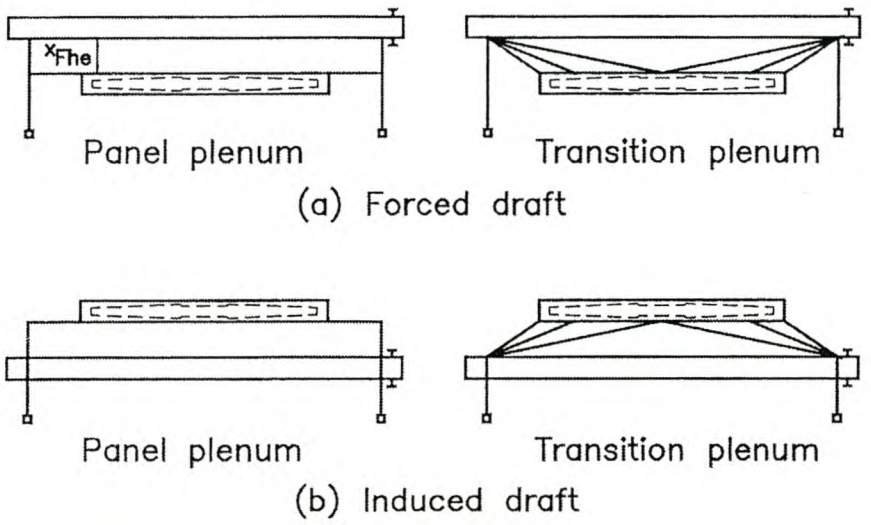

Fig. 6.4.3 Plenum Chambers

The complexity of the flow in a plenum chamber is illustrated by a few studies such as those by Turner, Berryman and Russell, and Russell and Berryman.

Figure 6.4.3(a) shows a forced-draft, air-cooled heat exchanger consisting of a fan, plenum chamber, and heat exchanger. In the absence of flow resistances other than those due to the heat exchanger, a conservative air volume flow rate, V_{cd}, through this heat-exchanger can be determined by finding the intersection between:

- the fan static pressure curve obtained in a Type A installation test
- the heat exchanger resistance curve obtained during tests under uniform normal flow conditions

Add to this the approximate loss due to the kinetic energy of the air leaving the heat exchanger uniformly, i.e.,

$$\Delta p_{Fs} = K_{he}\rho v_{hec}^2/2 + \rho v_{hec}^2/2 \qquad (6.4.3)$$

where

$v_{hec} = V_{cd}/A_{fr}$

A_{fr} = the frontal area of the heat exchanger.

The previously mentioned characteristics are shown in Figure 6.4.4.

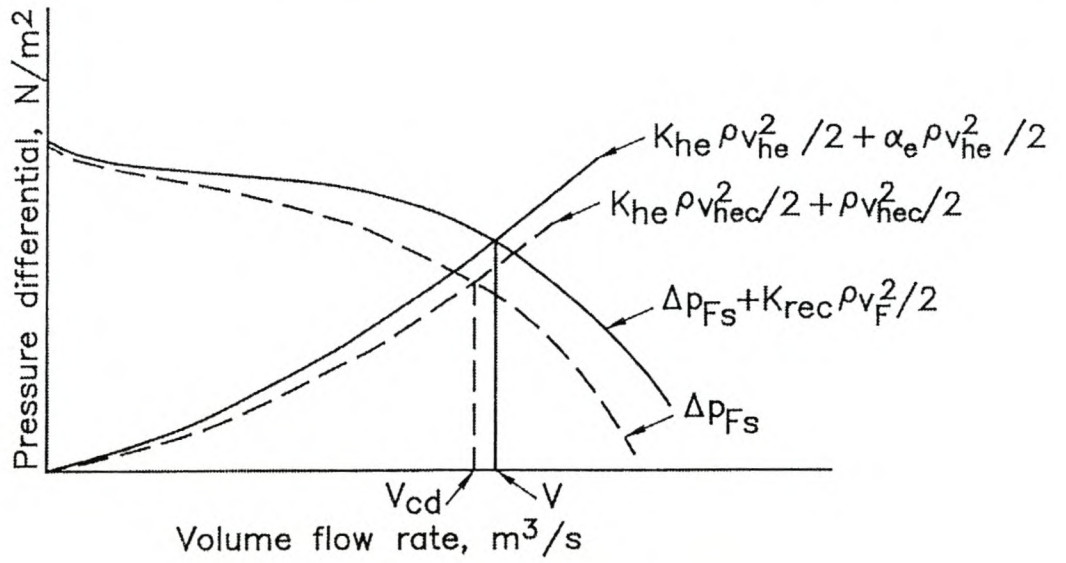

Fig. 6.4.4 Air-Cooled Heat Exchanger Air Volume Flow Rate

Usually, the air velocity distribution at the outlet of the heat exchanger is not uniform. This results in the flow losses on the right side of Equation 6.4.3 are more correctly expressed as

$$K_{he}\rho v_{he}^2/2 + \alpha_e\rho v_{he}^2/2$$

where

α_e = the kinetic energy velocity distribution correction factor defined by Equation 1.4.5.

In Equation 6.4.3, it is implied that all the kinetic energy of the air leaving the fan during an installation Type A test is dissipated in the plenum chamber. Meyer and Kröger show this is not the case. A kinetic energy recovery coefficient, K_{rec}, is defined by the following equation, which equates the more effective fan system performance characteristic to the more realistic losses, i.e.,

$$\Delta p_{Fs} + K_{rec}\,\rho v_F^2 / 2 = K_{he}\rho v_{he}^2 / 2 + \alpha_e\,\rho v_{he}^2 / 2 \qquad (6.4.4)$$

where

K_{rec} = the plenum recovery coefficient based on the mean air velocity through the fan

$v_{he} = V/A_{fr}$

Due to this recovery of kinetic energy, the net air volume flow rate, V, through the system is usually found to be more than the conservative design value, V_{cd}, shown in Figure 6.4.4.

Both the energy correction factor and the recovery coefficient depend on numerous geometric and operating variables.

Meyer and Kröger conducted forced-draft, air-cooled heat exchanger model tests employing various eight-bladed fans with the following characteristics:

- molded blades
- 1.25 m and 1.542 m diameter
- bell-type, inlet casing
- 960 rpm and 750 rpm operating speeds (at or near the point of maximum fan efficiency)

Their tests included heat exchangers made up of different types of industrial finned tube bundles. Bundle flow loss coefficients spanned the range $7 \leq K_{he} \leq 24$, while the ratio of the fan cross-sectional area to heat exchanger frontal area varied in the range $0.34 \leq A_c/A_{fr} \leq 0.599$. An example of their test results is shown in Figure 6.4.5 for the V-type fan, also referred to

as S-fan, together with a two-row, plate-finned heat exchanger bundle having a loss coefficient shown in Figure 5.6.8.

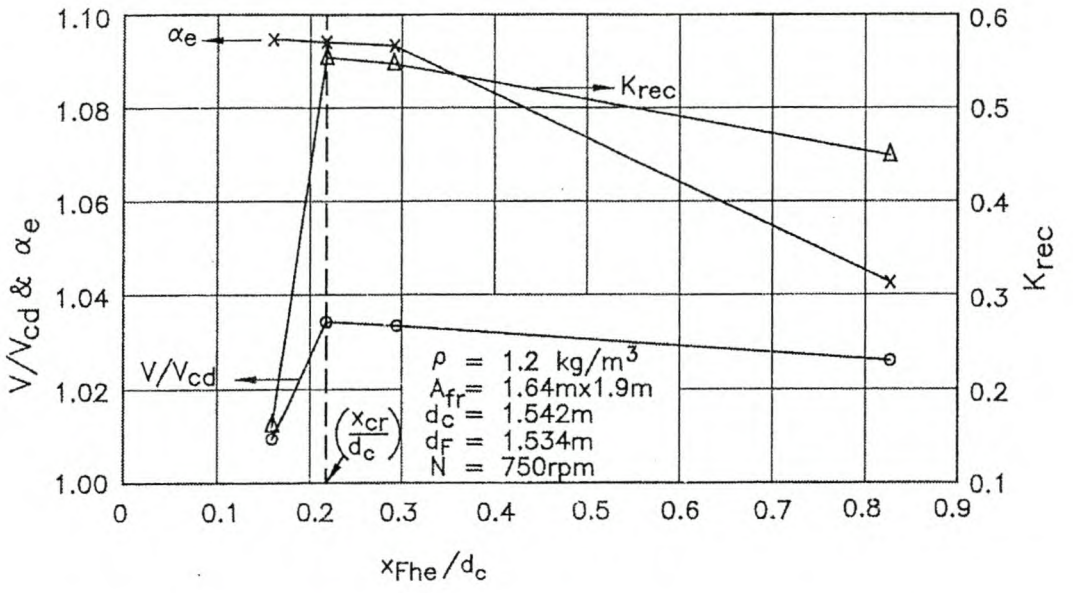

Fig. 6.4.5 Heat Exchanger Performance Characteristics

There was an abrupt drop in performance below a fan outlet to heat exchanger inlet distance of $x_{Fhe}/d_c = x_{cr}/d_c = 0.22$. If the outlet of the fan is flush with the plenum chamber wall,

$$x_{Fhe} = H_{p\ell}$$

where

$H_{p\ell}$ = the plenum height

Due to the recovery of kinetic energy, $V/V_{cd} > 1$ for $x_{Fhe} \geq x_{cr}$, despite the fact that $\alpha_e > 1$.

The critical distance between the outlet of the fan and the inlet to the heat exchanger is a complex function of different variables. The critical distance lies in the range $0.22 \leq x_{cr}/d_c \leq 0.32$ for the $15 \leq K_{he} \leq 24$ range of practical industrial air-cooled heat exchangers and $0.34 \leq A_c/A_{fr} \leq 0.599$ as well as different fan types. For all practical industrial forced draft air-cooled heat exchanger designs, a value of $x_{Fhe}/d_c \geq 0.3$ is recommended. In these

tests, the recovery coefficient was found to lie in the range of $0.2 \leq K_{rec} \leq 0.6$. For most designs, a conservative value of $K_{rec} = 0.3$ is recommended.

Where space is at a premium, $x_{Fhe}/d_c = 0.2$ is acceptable. The latter is important in certain smaller air-cooled heat exchangers, including refrigerant condensers and vehicle radiators (Fig. 6.4.8). In the case of vehicle cooling systems, Costelli et al. recommend $H_{p\ell}$ should not be less than 20% of a blower fan diameter and at least 10% of a suction fan diameter.

The kinetic energy velocity distribution correction factor measured by Meyer and Kröger at the critical distance between the fan and the heat exchanger during operation of the fan near its maximum efficiency is shown in Figure 6.4.6. The data can be correlated approximately by the following empirical relation:

$$\alpha_e = 1.6 - 0.48\, A_c/A_{fr} - 0.012\, K_{he} \qquad (6.4.5)$$

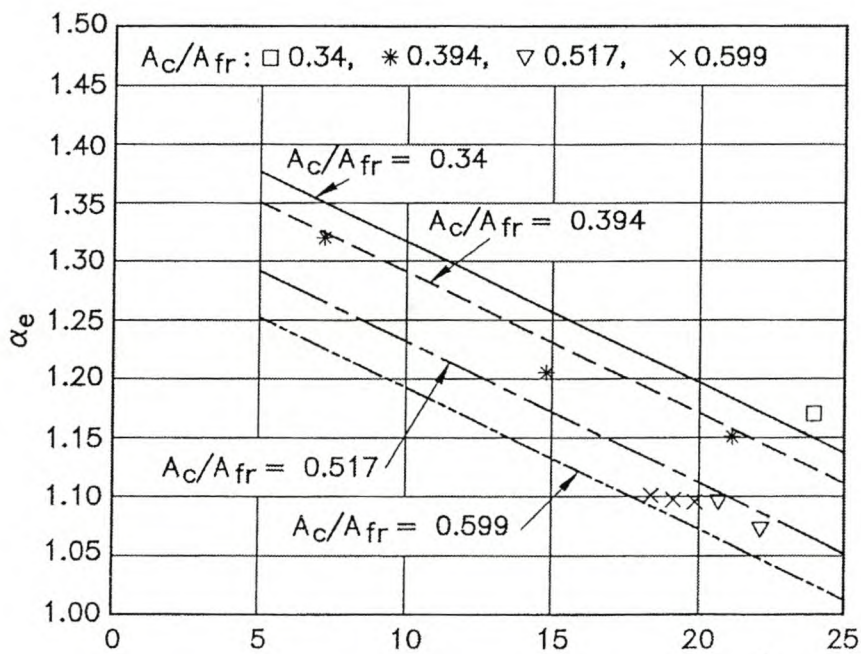

Fig. 6.4.6 Kinetic Energy Correction Factor

Equation 6.4.5 is applicable for

$$\alpha_e \geq 1$$

where

$K_{he} \geq 7$

$0.34 \leq A_c/A_{fr} \leq 0.599$

According to Paikert, fans are sized so the minimum value of the ratio A_c/A_{fr} = 0.4. Monroe suggests that A_c/A_{fr} shall not be less than 40% for induced draft units and 50% for forced draft units. Although a ratio as low as 30% for induced draft units is possible, the larger values are preferred.

For the A-frame configuration in Figure 1.2.3, no kinetic energy is recovered in the plenum. This figure has the following characteristics:

- an apex angle of approximately 60°
- an area ratio of $A_c/A_{fr} \approx 0.3$
- an open grid overhead walkway supports the fan

In the absence of the walkway, $K_{rec} \approx 0.3$. This result is obtained if losses through the A-frame are determined using Equation 5.6.19.

Shroud or casing

A well-rounded or bellmouth type inlet shroud or casing (Fig. 6.0.1) ensures good fan performance. Although other less costly shroud inlets are used in a variety of applications, they generally reduce performance. Examples of different inlet shrouds with their corresponding loss coefficients, K_{fsi}, are shown in Figure 6.4.7 from Ventilatoren Stork Hengelo V.960874.

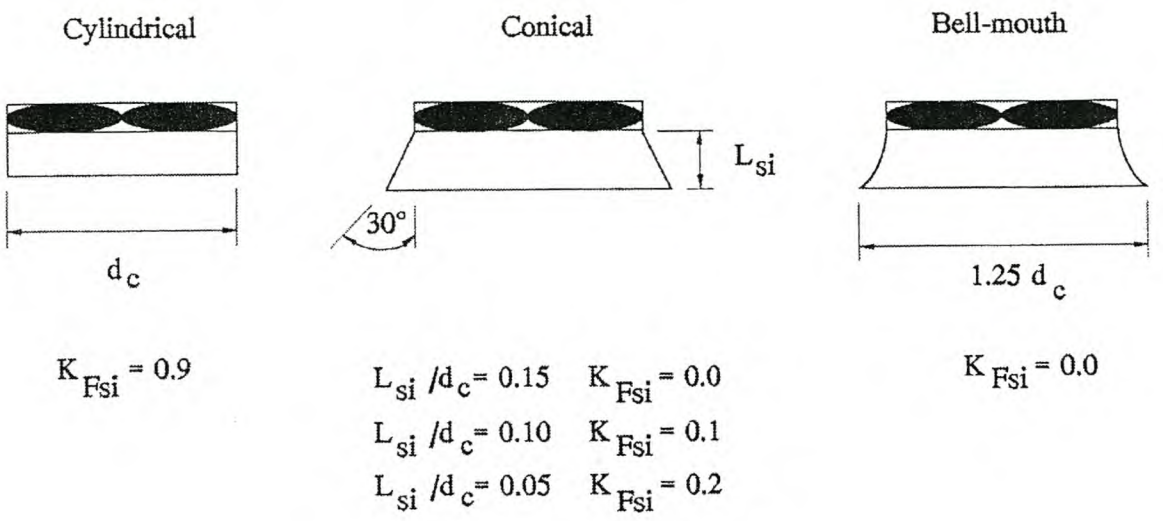

Fig. 6.4.7 Shroud or Casing Inlets

According to Duvenhage et al., if a given fan in an industrial heat exchanger is fitted with a conical or cylindrical inlet shroud, the flow rate will be about 3% or 5% less than if a bellmouth type inlet had been fitted.

For the cylindrical inlet, Duvenhage et al. show the optimum ratio of the shroud inlet length to fan diameter, $L_{si}/d_F \approx 0.16$. They also show there should be no cylindrical section between the outlet of the cone or bellmouth and the upstream side of the fan blades for conical and bellmouth inlets. Generally, the height of the fan casing should be at least a sixth the fan diameter for forced and induced draft designs.

In very short casings or shrouds, the position of the fan can be critical. The optimal position of the fan in different shrouds found in the automotive industry is shown in Figure 6.4.8 from U.S. Army AMCP-706-361. Hay and Taylor, Baransky, Chu, and Taylor and Chu recommended the fan be located such that two-thirds of the projected blade width (p.w.) of the fan is inside the shroud in case of suction. At the same time, two-thirds of the blade projection should be located outside the shroud when air is blown through the heat exchanger. The venturi type shroud provides the best fan efficiency when the fan tip clearance is 1.5% or less of the fan diameter.

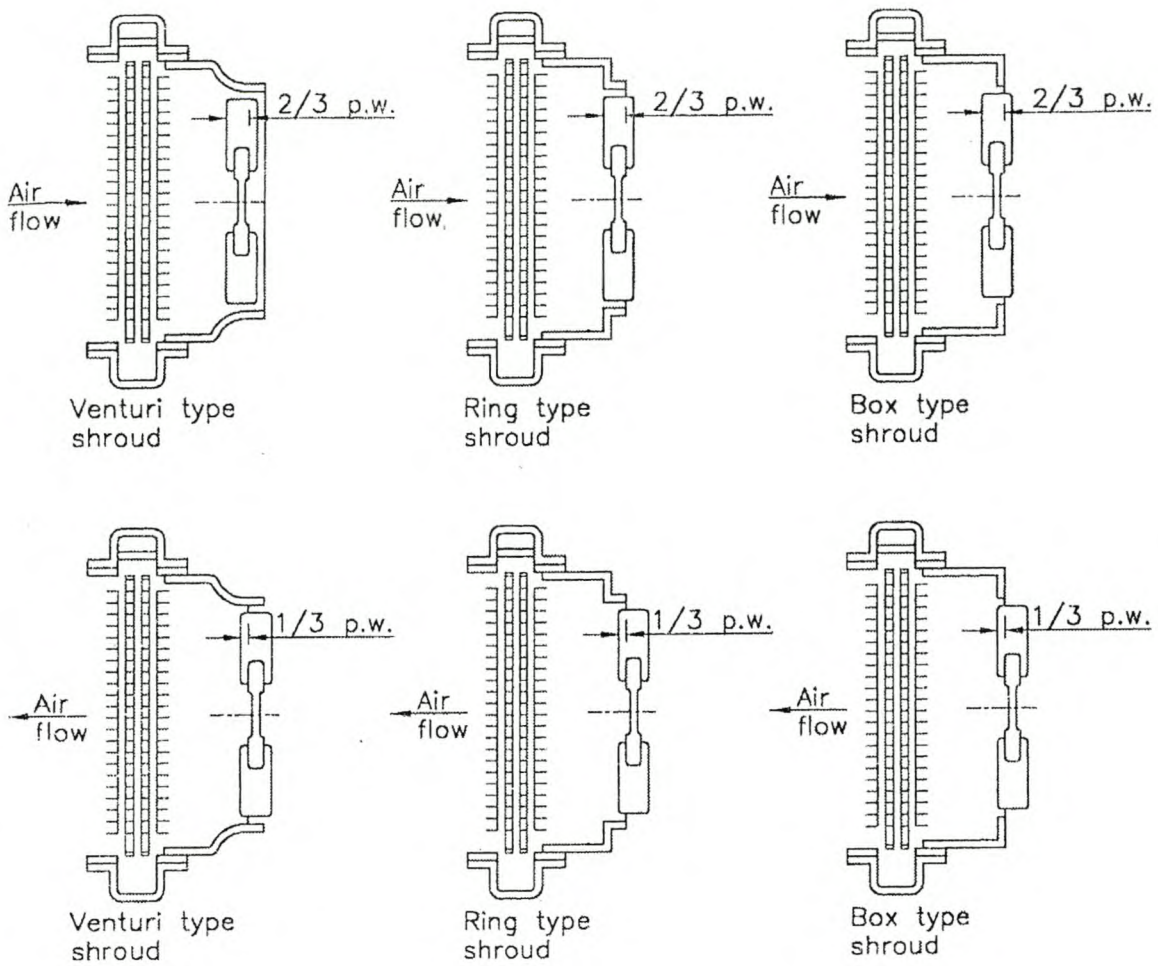

Fig. 6.4.8 Fan Shroud Types and Recommended Fan Positions

Diffuser

By installing a diffuser downstream of an axial flow fan, the air velocity and corresponding kinetic energy is reduced, and its static pressure is increased. The result is a net decrease in the power absorbed by the fan. Published diffuser efficiency data indicate peak values of 0.9 (Fig. 2.3.9).

The included angle of a practical diffuser lies in the range $12^\circ \leq 2\theta \leq 17^\circ$. An example of such a diffuser is shown in Figure 6.4.9. Depending on the cost structure, other geometries may be found to be more effective.

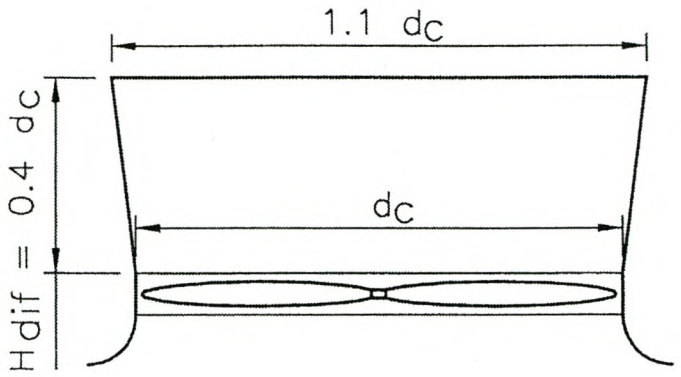

Fig. 6.4.9 Practical Fan Diffuser

For most engineering applications with symmetrical inlet flow conditions, Wallis recommends the use of a conservative diffuser efficiency of $\eta_{dif} = 0.8$.

Since the velocity distribution is not uniform at the outlet of the fan and the diffuser, the previous data can give approximate performance characteristics at best. Wherever possible, the fan should be tested together with the appropriate diffuser to give fan/diffuser performance characteristics that can be used for design purposes.

REFERENCES

Air Moving and Conditioning Association, "Laboratory Methods of Testing Fans for Rating Purposes," Air Moving and Conditioning Association Standard 210-274, 1974.

American Petroleum Institute , *Air-Cooled Heat Exchangers for General Refinery Services*, API Standard 661, American Petroleum Institute, Washington, 1978.

American Society of Heating Refrigerating and Air-Conditioning Engineers, "Laboratory Methods of Testing Fans for Rating Purposes," ASHRAE Standard 51-75, 1975.

American Society of Mechanical Engineers, *Performance Test Codes - General Instructions*, PTC 1, 1980.

American Society of Mechanical Engineers, *Test Code for Fans*, ASME PTC 11-1946, New York, 1946.

Baransky, B. R., *Designing the Engine Cooling Fan*, SAE 740691, Society of Automotive Engineers , 1974.

Barna, P. S, "Estimation of Scale Effects in Axial Flow Fans," *Aircraft Engineering*, November 1961.

Beard, R. A., *Truck Radiator Technology, Part II, Product Application Technology*, Heat Transfer Division, Covrad Ltd., Conventry, 1980.

Berry, H. C., *Flow and Fan-Principles of Moving Air through Ducts*, The Industrial Press, New York, 1954.

Berryman, R. J. and C. M. B. Russell, "Airflow in Air-Cooled Heat Exchangers," *Heat Transfer Engineering*, 8-4:40–44, 1987

Bleier, F. P., *Fan Handbook: Selection, Application and Design*, McGraw-Hill, New York, 1998.

British Standards Institution, *Fans for General Purposes, Part 1, Methods of Testing Performance*, BSI 848, 1980.

Chiou, J. P., *Engine Cooling System of Military Combat/Tactical Vehicles*, SAE 750030, Society of Automotive Engineers, 1975.

Cory, W. T. W., *Fan Performance Testing the Effects of the System*, British Hydromechanics Research Association, International Conference on Fan Design and Applications, Guildford, September 1982.

Costelli, A., P. Gabriele, and D. Giordanengo, *Experimental Analysis of the Air Circuit for Engine Cooling Systems*, SAE 800033, Society of Automotive Engineers, 1980.

Coward, C. W., "A Summary of Pressure Loss Values for Various Fan Inlet and Outlet Duct Fittings," American Society of Heating Refrigerating and Air Conditioning, *Transactions*, vol. 89, 1983.

Daly, B. B., *Interaction between the Fan and the System, Installation Effects in Ducted Fan Systems,* Institute of Mechanical Engineers, Conference Publication no. C110/84, 1–7, 1984.

Daly, B. B., *Woods Practical Guide to Fan Engineering,* Woods of Colchester Ltd., 1978.

Deeprose, W. M. and T. W. Smith, "The Usefulness of BS848 Part 1, 1980, in Establishing the Installed Performance of a Fan," Institute of Mechanical Engineers, Conference Publication, no. C115/84, 9–20, 1984.

Deutsche Norm, *Ventilatoren; Leistungsmessung, Normkennlinien,* DIN 24163, Teil 1 & 2, Deutsches Institut für Normung, Berlin, 1985.

Duvenhage, K., J. A. Vermeulen, C. J. Meyer, and D. G. Kröger, "Flow Distortions at the Fan Inlet of Forced-Draught Air-Cooled Heat Exchangers," *Applied Thermal Engineering,* 16-8/9:741–752, 1996.

Eck, B., *Fans—Design and Operation of Centrifugal, Axial Flow and Crossflow Fans,* Pergamon Press, 1973.

Engineering Sciences Data Unit, *A Guide to Fan Selection and Performance,* Item No. 79037, ESDU, London, 1980

Fahlsing, P. M., "Benefits of Variable Speed Drives Applied on Dry Condensing at the Wyodak Plant," *Proceedings,* American Society of Mechanical Engineers Joint Power Generation Conference, 28:463–471, Minneapolis, October 1995.

Graham, J. B., "Fan Selection and Application Considerations," *Proceedings,* Power Plant Fans Symposium—State of the Art, Indianapolis, October 1981.

Häussermann, G., "Erfahrungen beim Einsatz von geregelten Sichelventilatoren in der Kältetechnik, *Ki Luft- und Kältetechnik,* 1:18–23, 1996.

Hay, N. and S. R. G. Taylor, "The Effects of Vehicle Cooling Systems Geometry on Fan Performance," Conference on Fan Technology and Practice, Institution of Mechanical Engineers, 176–192, London, April 1972.

Hebard, P. J. and S. W. Tebby, "The Design and Optimisation of Engine Cooling Systems for Low Noise and Power Consumption," *Proceedings,* 15th Fédération Internationale des Sociétés des Techniques de l'Automobiles Conference, 1974.

Hunnabal, P. J., "Control of Tonal Noise Generation in Axial Flow Fans by Optimising Geometry of Fixed and Rotating Components," *Proceedings,* Institute of Noise Control Engineering Symposium, Centre Technique des Industries Mécaniques, Senlis, 475–482, September 1992.

Jorgensen, R., ed., *Fan Engineering,* Buffalo Forge Company, New York, 1961.

Kröger. D. G., "Fan Performance in Air-Cooled Steam Condensers," *Heat Recovery Systems and CHP,* 14-4:391–399, 1994.

Lambert, P. C., G. H. Cowan, and T. R. Bott, *Flow Characteristics in a Box-shaped Plenum Chamber Associated with an Air-Cooled Heat Exchanger,* United Kingdom Atomic Energy Authority, Harwell, 1972.

Leitz, R., "Operating Experience with an Air-Cooled Condenser System in a Combined Cycle Power Station in the U. K.," Paper, 9th International Association for Hydraulics Research Cooling Tower Symposium and Spraying Pond Symposium, Von Karman Institute, Brussels, September 1994.

McEwan, D. and W. R. Woods-Ballard, "Fan Connected Ductwork Fittings Installation Effects," Paper, Institution of Mechanical Engineers Seminar on Installation Effects in Fan Systems, London, September 1993.

Meyer, C. J. and D. G. Kröger, "Numerical Simulation of the Flow Field in the Vicinity of an Axial Flow Fan," *International Journal for Numerical Methods in Fluids*, 36:947–969, 2001.

Meyer, C. J. and D. G. Kröger, "Plenum Chamber Flow Losses in Forced Draught Air-Cooled Heat Exchangers," *Applied Thermal Engineering*, 18-9/10:875–893, 1998.

Modern Power Systems Staff Report, "Dry Cooling Solves GTCC Siting Problems," *Modern Power Systems*, 39–43, June 1993.

Monroe, R. C., "Improving Cooling Tower Fan System Efficiencies," *Combustion Magazine*, 50-11:20–26, May 1979.

Monroe, R. C., "Maximising Fan Performance, EPRI TR-108483 2113," *Proceedings*, Cooling Tower Technology Conference, 2.4–2.51, July 1997.

Monroe, R. C., "Minimizing Fan Energy Costs," *Chemical Engineering*, 141–142, May 1985a.

Monroe, R. C., "Minimizing Fan Energy Costs," *Chemical Engineering*, 57–59, June 1985b.

Nowakowski, J. K., "Pressure Losses in the Inlet and Outlet Channels of High-pressure Single-and Two-Stage Axial Flow Fans," *Proceedings*, Sixth Conference on Fluid Machinery, 760–769, Hungary, 1979.

O'Connor, J. F., "The System Effect on How It Changes Fan Performance," American Society of Heating Refrigerating and Air Conditioning, *Transactions*, vol. 89, 1983.

Osborne, W. C., *Fans*, Pergamon Press, New York, 1996.

Paikert, P., "Air-Cooled Heat Exchangers," *Handbook for Heat Exchanger Design*, Begell House, New York, 1983.

Riera-Ubiergo, J. A. and F. Charbonelle, "Installation Effects in Fan Systems," *Proceedings*, Institute of Mechanical Engineers European Conference. London, March 1990.

Roslyng, O., "Installation Effect on Axial Flow Fan Caused by Swirl and Non-Uniform Velocity Distribution," Institution of Mechanical Engineers, *Proceedings*, C114/84:21–28, 1984.

Ruden, P., "Investigation of Single Stage Axial Flow Fans," Technical Memorandum no. 1062, National Advisory Committee for Aeronautics, Washington, 1944.

Russell, C. M. B. and R. J. Berryman, "The Calculation of Pressure Losses in Air-Cooled Heat Exchanger Air Inlets and Plenum Chambers," *Heat Transfer Division*,

American Society of Mechanical Engineers Heat Transfer Division, 96:429–234, New York, 1988.

Smith, A. R. and D. Romeister, "Rye House 700 MW Combined Cycle Power Station," *Modern Power Systems*, 41–48, November 1993.

Staiger, M. and H. Stetter, "Aerodynamic Response of Axial Fan Bladings to Non-Uniform Inlet Flow Fields," Paper, Institution of Mechanical Engineers Seminar on Installation Effects in Fan Systems, London, September 1993.

Stone, R. D. and S. H. Wen, "Airflow Characteristics of Built-Up Fan Plenums and Performance of Airflow Correction Devices," American Society of Heating, Refrigeration and Air Conditioning Semi-annual Meeting, Chicago, January, 1973.

Taylor, D. O. and A. C. Chu, *Wind Tunnel Investigation of the Effects of Installation Parameters on Truck Cooling System Performance,* SAE-760832, Society of Automotive Engineers, 1976.

Turner, J. T., "The Aerodynamics of Forced Draught Air Cooled Heat Exchangers," International Symposium on Cooling Systems, British Hydromechanics Research Association Fluid Engineering, Cranfield, 1975.

U.S. Army Material Command, *Engineering Design Handbook, Military Vehicle Power Plant Cooling,* AMCP-706-361, Virginia, 1975.

Van der Speck, H. F., "Advanced Low Noise Cooling Fans," Paper, International Association for Hydraulics Research 9th Cooling Tower and Spraying Pond Symposium, von Karman Institute, Brussels, September 1994.

Venter, S. J. and D. G. Kröger, "The Effect of Tip Clearance on the Performance of an Axial Flow Fan," *Energy Conversion and Management*, 33-2:89–97, 1992.

Venter, S. J. and D. G. Kröger, "An Evaluation of Methods to Predict the System Effect Present in Air-Cooled Heat Exchangers," *Heat Recovery Systems and CHP*, 11-5:31–440, 1991.

Ventilatoren Stork Hengelo, *General Instructions for E-type Fans*, V.960874, Amsterdam, 1985.

Ventilatoren Stork Howden B.V., *Fan Performance Catalog*, Hengelo, Amsterdam, 1990.

Verein Deutscher Ingenieure, "VDI-Richtlinien, Abname-und Leistungs- versuche an Ventilatoren," *Dieselmotor*, AT2, vol. 8, 1971.

Wallis, R. A., *Axial Flow Fans and Ducts*, John Wiley and Sons, New York, 1983.

Woods Ballard, W. R., "Fans in Air Handling Units, Installation Effects in Fan Systems," *Proceedings*, Institute of Mechanical Engineers European Conference, London, March 1990.

Zaleki, T. H., "System Effect Factors for Axial Flow Fans, Installation Effects on Fan Systems," *Proceedings*, Institute of Mechanical Engineers European Conference, London, March 1990.

7

Natural Draft Cooling Towers

7.0 Introduction

Natural draft cooling towers are found in power and chemical plants throughout the world. Different shapes and types of structures exist, but their fundamental function is the same, i.e., to create the flow of air through the fill or bundles of finned tube heat exchangers by means of buoyancy effects.

The hyperbolic concrete tower, which is normally operated in the wet mode, is also effectively employed as a dry-cooling tower if designed specifically for this purpose. Other towers may be made of aluminum-clad steel or wood. The main dimensions of cooling towers are usually determined by

- performance
- structure, according to Niemann
- economic considerations, according to both Alomwooja et al. and Krings

At the same time, Grange asserts aerodynamic and thermal factors should not be ignored. In areas of the world where seismic activity is

prevalent, aluminum clad steel towers may be preferred. Cost structures may be such that this type of dry-cooling tower is cheaper than a concrete tower.

The performance of any natural draft cooling tower is influenced by the characteristics of the fill or the finned-tube, heat-exchanger bundles at the base of the tower, the tower geometry, and ambient conditions, such as temperature, pressure, winds, inversions, and precipitation according to Moore and Heberholz and Schulz. Furthermore, fouling reduces transfer coefficients and increases flow resistances. The result is a corresponding reduction in cooling tower performance. Where specific information on fouling is available, this can be incorporated directly in the design.

7.1 Dry-Cooling Tower

Consider the example of a hyperbolic, natural-draft, dry-cooling tower shown in Figure 7.1.1. The heat exchanger bundles are located horizontally at the inlet cross section of the tower. The density of the heated air inside the tower is less than the density of the atmosphere outside the tower. As a result, the pressure inside the tower is less than the external pressure at the same elevation. This pressure differential causes air to flow through the tower at a rate dependent on the various flow resistances encountered, the cooling tower dimensions, and the heat exchanger characteristics according to Buxmann, Moore and Hsieh, Moore, Montakhab, and Becker.

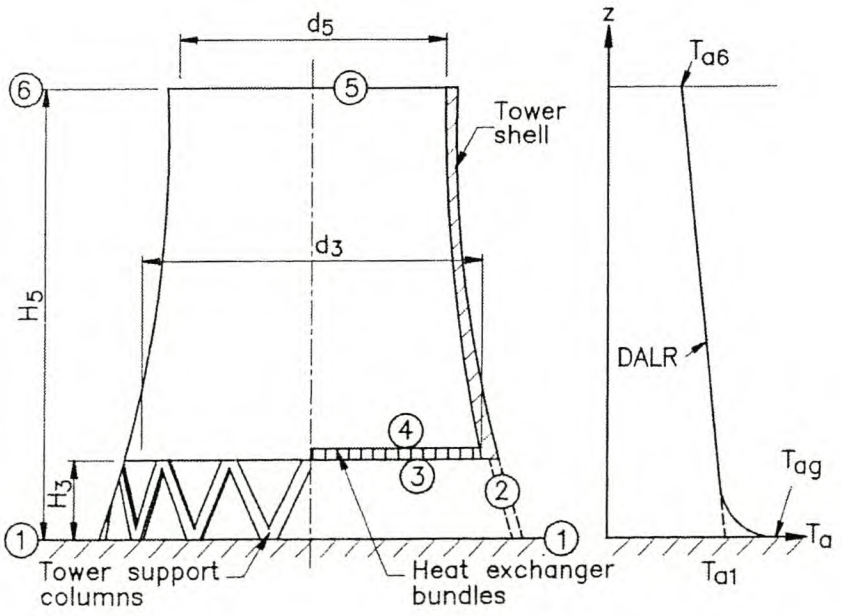

Fig. 7.1.1 Natural Draft Cooling Tower with Horizontal Heat Exchanger

Conradie and Kröger found both the energy and the draft equation must be satisfied in order to evaluate the performance characteristics of such a cooling tower. The following analysis has been found to give results that accurately predict the performance of large dry-cooling towers.

Ambient conditions influence the performance of the cooling tower. Figure 9.1.3 shows significant changes in temperature may occur near ground level during any 24-hour period. During a clear dry day, a temperature lapse rate of approximately -0.00975 Km^{-1}, also known as the *dry adiabatic lapse rate* (DALR), is often observed in the region of the *surface boundary layer* (SBL). Significant deviations do occur at ground level, which if not taken into consideration, may lead to erroneous design specifications or the incorrect interpretation of cooling tower acceptance test data. Other temperature distributions are discussed in chapter 9.

For this analysis, the specified ambient air temperature at any elevation, z, will be assumed to be as given by Equation 9.1.8, i.e.,

$$T_a = T_{a1}\text{-}0.00975\ z$$

where

T_{a1} = the temperature at ground level, obtained by extrapolating the measured DALR to that elevation

T_{a1} usually differs from the actual temperature

T_{ag} is measured at ground level (Fig. 7.1.1)

At elevation (6), which corresponds to the top of the cooling tower, the temperature of the ambient air is

$$T_{a6} = T_{a1}\text{-}0.00975\ Hz \tag{7.1.1}$$

The heat transfer characteristics of the heat exchangers in the cooling tower can be expressed according to Equations 3.5.6 and 3.5.16 as

$$Q = m_a c_{pa}(T_{a4}\text{-}T_{a3}) = m_w c_{pw}(T_{wi}\text{-}T_{wo}) \tag{7.1.2}$$

and

$$Q = \frac{UA\,F_T\,[(T_{wi} - T_{a4}) - (T_{wo} - T_{a3})]}{\ell n\,[(T_{wi} - T_{a4})/(T_{wo} - T_{a3})]} \qquad (7.1.3)$$

From Equations 1.4.2 and 1.4.8, the approximate inlet temperature to the heat exchanger located at an elevation H_3 above ground level is given by

$$T_{a3} = T_{a1} - (v_{a3}^2/2 + gH_3)/c_{pa}$$

For natural draft cooling towers,

$$v_{a3}^2/2 << g\,H_3$$

with the result that

$$T_{a3} \approx T_{a1} - gH_3/c_{pa} = T_{a1} - g(\gamma - 1)H_3/(\gamma R) = T_{a1} - 0.00975H_3 \qquad (7.1.4)$$

where

$g = 9.8 \text{m/s}^2$

$\gamma = 1.4$

$R = 287.08$ J/kgK

The approximate pressure differential between the outside and the inside of the tower at the mean heat exchanger elevation, that causes the air to flow through the tower, may be expressed in terms of the flow resistances according to Montakhab.

$$\Delta p_a \approx (\rho_{ao} - \rho_{ai})g[H_5 - (H_3 + H_4)/2] = \Sigma \text{ flow resistances} \qquad (7.1.5)$$

where ρ_{ao} and ρ_{ai} are respectively the densities outside and inside the tower at the elevation of the heat exchanger. This is also known as the draft equation.

Although this approximate relation is used frequently in cooling tower designs, it is inadequate in many cases. A more detailed approach is followed in the following analysis.

For dry air, use Equation 9.1.11 to find the pressure external to the tower at (6), i.e.,

$$p_{a6} = p_{a1}(1\text{-}0.00975\ H_5/T_{a1})^{3.5} \tag{7.1.6}$$

when $H_6 = H_5$ is the tower height.

The difference in pressure between (1) at ground level and (5) at the outlet of the tower may be expressed in terms of the losses experienced by the air stream as it flows through various resistances in the tower (Fig. 7.1.2).

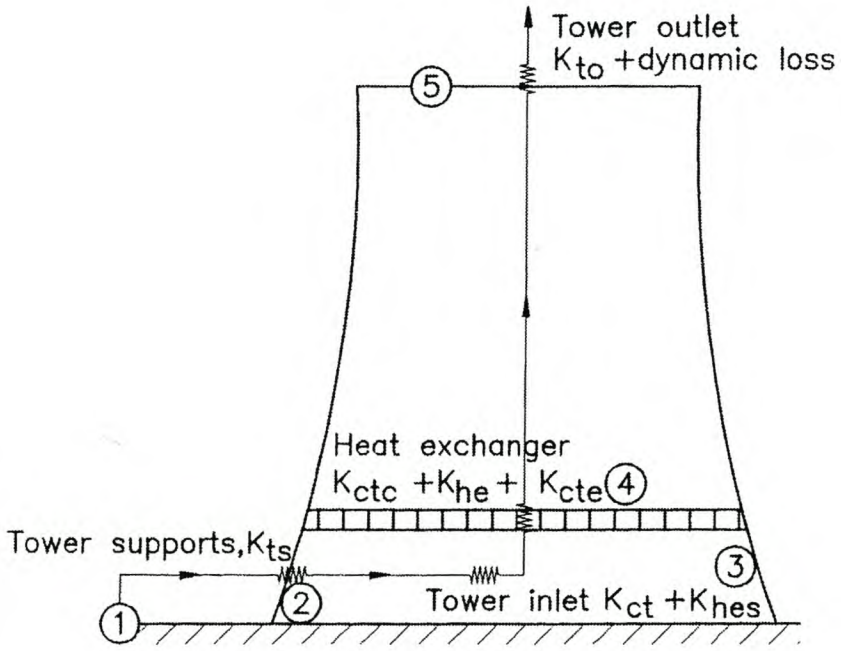

Fig. 7.1.2 Losses through Cooling Tower

The stagnant ambient air at (1) accelerates to flow through the tower supports at (2), where it experiences certain losses (K_{ts}) before flowing through the heat exchanger bundles from (3) to (4). Upstream of the heat exchanger, losses are experienced due to separation and redirection of the flow at the lower edge of the tower shell (K_{ct}), and the presence of the heat exchanger supports (K_{hes}). Contraction (K_{ctc}), form and frictional (K_{he}), and expansion (K_{cte}) losses are experienced across the heat exchanger. The flow is essentially isentropic from (4) to (5) with a further loss in kinetic energy at the outlet of the tower. The resultant total pressure difference is found by adding the resistances between (1) and (5).

$$p_{a1}-[p_{a5}+\alpha_{e5}(m_a/A_5)^2/(2\rho_{a5})]$$

$$= (K_{ts}+K_{ct}+K_{hes}+K_{ctc}+K_{he}+K_{cte})_{he}(m_a/A_{fr})^2/(2\rho a_{34})$$

$$+ p_{a1}[1-\{1-0.00975(H_3+H_4)/(2T_{a1})\}^{3.5}]$$

$$+ p_{a4}[1-\{1-0.00975(H_5-H_3/2-H_4/2)T_{a4}\}^{3.5}] \qquad (7.1.7)$$

where

m_a = the air mass flow rate through the tower

The subscript $_{he}$ implies all loss coefficients are referred to the frontal area of the heat exchanger and the mean density of the air flowing through it. This form of the equation is useful for comparing the relative magnitudes of the flow losses. The frontal area is the projection of the effective finned surface as viewed from the upstream side. Impeding flow through the heat exchanger with stiffening beams, straps, or other obstructions located up against the finned surface must be considered when evaluating the effective frontal area, A_{fr}. The last two terms on the right side of Equation 7.1.7 are analogous to Equation 7.1.6. They take into consideration static pressure differentials due to elevation between ground level and the mean heat exchanger elevation as well as the latter and the tower outlet.

Du Preez and Kröger studied the velocity and pressure distribution in the outlet plane of hyperbolic natural draft cooling towers. They found the velocity distribution is almost uniform for $1/Fr_D \leq 3$, i.e., $\alpha_{e5} \approx 1$ for dry-cooling towers where the heat exchangers are located in the cross section near the base of the tower. This was true even for wet counterflow towers where the flow through the fill may be more distorted due to its lower flow resistance. The mean pressure at the outlet plane was found to be slightly less than that of the ambient air at the same elevation, i.e.,

$$p_{a5} = p_{a6}+\Delta p_{a56} = p_{a6}+K_{to}(m_a/A_5)^2/(2\rho_{a5}) \qquad (7.1.8)$$

For a hyperbolic tower with a cylindrical outlet the loss coefficient is given by

$$K_{to} = \Delta p_{a56}/(\rho_{a5} v_{a5}^2/2) = 2\rho_{a5}\Delta p_{a56}/(m_a/A_5)^2$$

$$= -0.28 Fr_D^{-1} + 0.04 Fr_D^{-1.5} \qquad (7.1.9)$$

where

$Fr_D = (m_a/A_5)^2/[\rho_{a5}(\rho_{a6} - \rho_{a5})g d_5]$.

This equation is valid for

$$0.5 \leq d_5/d_3 \leq 0.85 \text{ and } 5 \leq K_{he} \leq 40$$

Using Equation 1.4.2, the temperature at the tower outlet can be approximated by

$$T_{a5} = T_{a4} + [(v_{a4}^2 - v_{a5}^2)/2 + g(H_4 - H_5)]/c_{pa} \approx T_{a4} + g(H_4 - H_5)/c_{pa}$$

$$= T_{a4} - g(\gamma - 1)(H_5 - H_4)/(\gamma R) = T_{a4} - 0.00975 (H_5 - H_4) \qquad (7.1.10)$$

since

$$(v_{a4}^2 - v_{a5}^2) << g(H_4 - H_5)$$

for natural draft cooling towers. From the perfect gas relation it follows that for

$$p_{a5} \approx p_{a6}$$

the density at the outlet of the tower is

$$\rho_{a5} = p_{a6}/[R\{T_{a4} - 0.00975 (H_5 - H_4)\}] \qquad (7.1.11)$$

where p_{a6} is obtained from Equation 7.1.6.

The density of the ambient air at elevation (6) follows from

$$\rho_{a6} = p_{a6}/RT_{a6} \tag{7.1.12}$$

where T_{a6} is given by Equation 7.1.1.

If dynamic effects are neglected, an approximate expression for p_{a4} may be obtained.

$$p_{a4} \approx p_{a1}\,[1 - 0.00975\,(H_3 + H_4)/(2T_{a1})]^{3.5}$$

$$- (K_{ts} + K_{ct} + K_{ctc} + K_{he} + K_{cte})_{he}\,(m_a/A_{fr})^2/(2\rho_{a34}) \tag{7.1.13}$$

Substitute Equations 7.1.6, 7.1.8, and 7.1.13 into Equation 7.1.7, and find with $\alpha_{e5} = 1$,

$$p_{a1}\,[\{1 - 0.00975\,(H_3 + H_4)/(2T_{a1})\}^{3.5}$$

$$\text{x}\ \{1 - 0.00975\,(H_5 - H_3/2 - H_4/2)/T_{a4}\}^{3.5} - (1 - 0.00975\,H_5/T_{a1})^{3.5}]$$

$$= (K_{ts} + K_{ct} + K_{hes} + K_{ctc} + K_{he} + K_{cte})_{he}\,(m_a/A_{fr})^2/(2\rho_{a34})$$

$$\text{x}\ [1 - 0.00975\,(H_5 - H_3/2 - H_4/2)/T_{a4}]^{3.5} + (1 + K_{to})(m_a/A_5)^2/(2\rho_{a5}) \tag{7.1.14}$$

This equation is known as the *draft equation* for a natural draft cooling tower where the heat exchangers are arranged horizontally in the base of the tower. If the heat exchangers are arranged in the form of A-frames or V-arrays, K_{he} is replaced by $K_{he\theta}$. The latter can be determined according to Equation 5.6.16.

In determining the density of the dry air after the heat exchanger, the specified pressure at ground level can be employed in the perfect gas relation, i.e.,

$$\rho_{a4} \approx p_{a1}/RT_{a4} \tag{7.1.15}$$

For all practical purposes,

$$\rho_{a3} \approx p_{a1}/RT_{a3} \tag{7.1.16}$$

The harmonic mean density of the dry air flowing through the heat exchanger follows from:

$$1/\rho_{a34} = 0.5(1/\rho_{a3} + 1/\rho_{a4}) = 0.5R(T_{a3} + T_{a4})/p_{a1} \tag{7.1.17}$$

The loss coefficient through the tower supports, K_{ts}, is based on the drag coefficient of the particular support geometry.

$$C_{Dts} = 2F_{Dts}/(\rho_{a1} v_{a2}^2 A_{ts}) \tag{7.1.18}$$

A list of drag coefficients for different geometries is given in section 2.5. Most concrete cooling tower supports have a square or rectangular cross-section. The construction of more rounded or streamlined shapes, having a lower flow resistance and causing less flow distortion at the inlet to the tower, may be justified in certain cases according to Martinez et al.

With Equation 7.1.18, the effective pressure drop across the tower supports is approximately

$$\Delta p_{ats} = n_{ts} F_{Dts}/A_2 = n_{ts} F_{Dts}/(\pi d_3 H_3) = \rho_{a1} v_{a2}^2 C_{Dts} L_{ts} d_{ts} n_{ts}/(2p d_3 H_3) \tag{7.1.19}$$

where

L_{ts} = the support length

d_{ts} = the effective diameter or width

n_{ts} = the number of tower supports

The corresponding loss coefficient based on the conditions at the tower supports (2) is

$$K_{ts} = 2\Delta\, p_{ats}/(\rho_{a1} v_{a2}^2) = C_{Dts} L_{ts} d_{ts} n_{ts}/(\pi\, d_3 H_3) \qquad (7.1.20)$$

For substitution into Equation 7.1.14, this loss coefficient is required to be based on conditions at the heat exchanger, i.e.,

$$K_{tshe} = 2\Delta p_{ats}\, \rho_{a34}/(m_a/A_{fr})^2 = \frac{C_{Dts} L_{ts}\, d_{ts}\, n_{ts}\, A_{fr}^2}{(\pi d_3 H_3)^3} \left(\frac{\rho_{a34}}{\rho_{a1}}\right) \qquad (7.1.21)$$

The air density and the velocity distribution through the supports is assumed to be uniform. This is not true in practice, and since the distance between the tower supports is finite, the previous approach tends to underestimate somewhat the magnitude of the loss coefficient.

Due to separation at the lower edge of the cooling tower shell and distorted inlet flow patterns, a cooling tower loss coefficient, K_{ct}, based on the tower cross-sectional area (3), can be defined to take these effects into consideration. Empirical equations for this coefficient are presented in section 7.3.

The cooling tower inlet loss coefficient referred to heat exchanger conditions is

$$K_{cthe} = K_{ct}(\rho_{a34}/\rho_{a3})(A_{fr}/A_3)^2 \qquad (7.1.22)$$

The heat exchanger support structure consists of pillars and beams that offer limited flow resistance. These resistances can be expressed in terms of a loss coefficient, K_{hes}.

Depending on the heat exchanger bundle arrangement in the cooling tower base, only a portion of the available area is effectively covered due to the rectangular shape of the bundles. This reduction in effective flow area results in contraction and subsequent expansion losses. These losses may be approximated by Equations 2.3.7 and 2.3.8 based on the effective reduced flow area, A_{e3},

$$K_{ctc} = 1\text{-}2/\sigma_c + 1/\sigma_c^2 \tag{7.1.23}$$

and

$$K_{cte} = (1\text{-}A_{e3}/A_3)^2 \tag{7.1.24}$$

The effective area, A_{e3}, corresponds to the frontal area of the heat exchanger bundles if they are installed horizontally. In the case of an array of A-frames, A_{e3} corresponds to the projected frontal area of the bundles. Because of the porous nature of the bundles, the actual contraction loss coefficient will be less than the value given by Equation 7.1.23. However, if the flow resistance of the heat exchanger support structure, K_{hes}, is not considered separately, this value is realistic.

Based on the conditions at the heat exchanger, the previous expressions become

$$K_{ctche} = (1\text{-}2/\sigma_c + 1/\sigma_c^2)(\rho_{a34}/\rho_{a3})(A_{fr}/A_{e3})^2 \tag{7.1.25}$$

and

$$K_{ctehe} = (1\text{-}A_{e3}/A_3)^2(\rho_{a34}/\rho_{a4})(A_{fr}/A_{e3})^2 \tag{7.1.26}$$

Similar equations may be deduced for a tower as shown in Figure 7.1.3, where the heat exchangers are arranged vertically around the circumference at the base of the tower. For a DALR, the mean inlet air temperature to the heat exchangers is

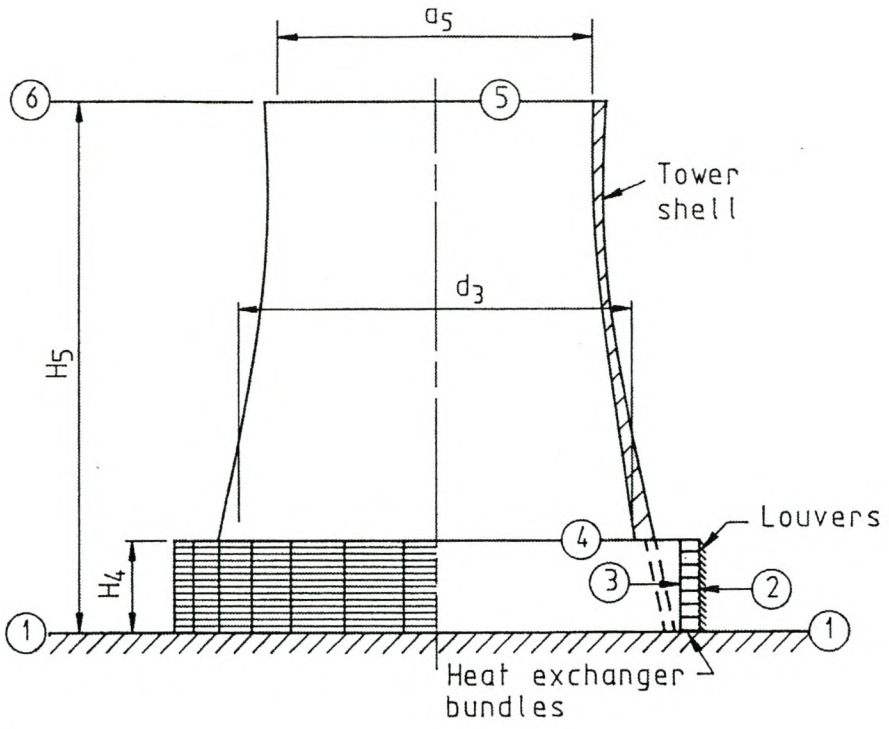

Fig. 7.1.3 Natural Draft Cooling Tower with Vertical Heat Exchangers

$$T_{a2} \approx T_{a1} - 0.00975\ H_4/2 \tag{7.1.27}$$

The relevant heat transfer equations are:

$$Q = m_a\ c_{pa}\ (T_{a3} - T_{a2}) = m_w\ c_{pw}(T_{wi} - T_{wo}) \tag{7.1.28}$$

and

$$Q = \frac{UA\ F_T\left[(T_{wi} - T_{a3}) - (T_{wo} - T_{a2})\right]}{\ell n\left[(T_{wi} - T_{a3})/(T_{wo} - T_{a2})\right]} \tag{7.1.29}$$

The corresponding draft equation for dry air is

$$p_{a1}\,[(1\text{-}0.00975\,H_4/2T_{a1})^{3.5}\,\{1\text{-}0.00975\,(H_5 - H_4/2)/T_{a3}\}^{3.5}$$

$$- (1.0.00975\,H_5/T_{a1})^{3.5}]$$

$$= (K_{i\ell} + K_{ctc} + K_{he} + K_{cte} + K_{ct})_{he}\,(m_a/A_{fr})^2/\,(2\rho_{a23})$$

$$\text{x}\,[1\text{-}0.00975\,(H_5 - H_4/2)/T_{a3}]^{3.5} + (K_{to} + a_{e5})(m_a/A_5)^2/(2\rho_{a5}) \qquad (7.1.30)$$

where

$K_{i\ell}$ = the inlet louver loss coefficient based on A_{fr}

The velocity distribution at the outlet of this type of tower is less uniform than cases where the heat exchangers are installed horizontally. A velocity distribution correction factor, α_{e5}, takes this effect into consideration. Du Preez and Kröger determined the value of α_{e5} numerically and proposed the following empirical relations:

$$a_{e5} = 1.004 + 5.8(d_5/d_3)9 + [0.007 + 0.043(d_5/d_3)^{2.5}]Fr_D^{-1.5} \qquad (7.1.31)$$

The tower outlet loss coefficient is correlated by

$$K_{to} = -0.129(Fr_D\,d_5/d_3)^{-1} + 0.0144(Fr_D\,d_5/d_3)^{-1.5} \qquad (7.1.32)$$

for

$1/Fr_D \leq 3$, $0.49 \leq d_5/d_3 \leq 0.69$ and $5 \leq K_{he} \leq 40$

If the heat exchanger bundles are arranged in the form of deltas or A-frames, K_{he} is replaced by $K_{he\theta}$. All loss coefficients are based on conditions at the heat exchanger.

The air density at the outlet of the tower is

$$\rho_{a5} = p_{a6}/[R\{T_{a3} + 0.00975(H_4/2 - H_5)\}] \qquad (7.1.33)$$

7.2 Wet-Cooling Tower

Consider the example of a hyperbolic, natural-draft, wet-cooling tower as shown in Fig. 7.2.1. The fill is located horizontally at the inlet cross section of the tower. The density of the warm moist air inside the tower is less than the density of the atmosphere outside the tower. Hence, the pressure inside the tower is less than the external pressure at the same elevation. This pressure differential causes air to flow through the tower at a rate that is dependent on

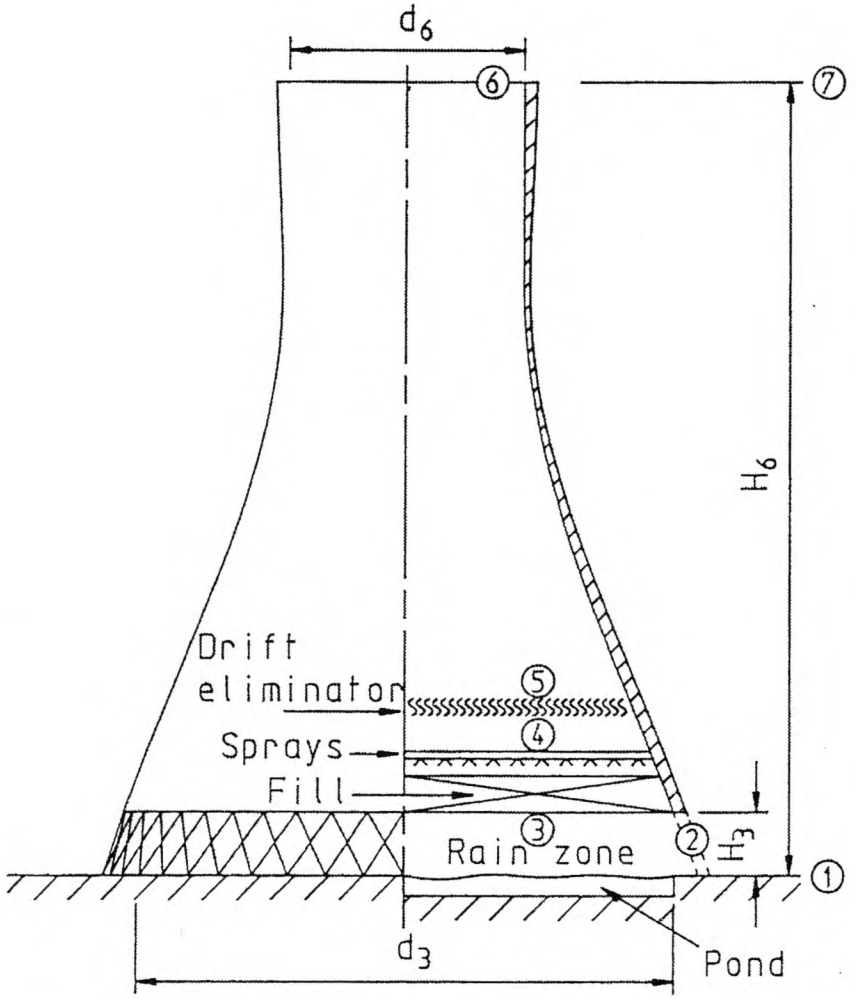

Fig. 7.2.1 Natural Draft Cooling Tower with Horizontal Fill

- the various flow resistances encountered
- the cooling tower dimensions
- the transfer characteristics of the spray, fill, and rain zones

Different approaches for evaluating the performance characteristics of such a cooling tower appear in the literature. Works by Merkel, Chilton, Lowe and Christie, Rish, Singham, Poppe, Zien, Mesarovic, Yadigaroglu and Pastor, Nahavandi et al., Nahavandi and Oellinger, Bourillot, Majumdar and Singhal, Sutherland, Majumdar et al., Johnson, Poppe and Rögener, and Mohiuddin and Kant describe various methods. In practice, the classical Merkel method or Poppe's more detailed method are most commonly employed in the performance evaluation of wet-cooling towers.

Two- and three-dimensional numerical models have been developed to determine the performance characteristics of wet-cooling towers. The two-dimensional models include:

- FACTS as described by Benton
- TEFERI from Bourillot
- VERA 2D by Majumdar et al.
- STAR from Caytan
- ETHER by Grange and others including Lees and Cooper
- TACT from Radosavljevic and Spalding (a three-dimensional model)

Even in the most sophisticated of these programs, use is made of empirical or experimental data. That is, fill performance characteristics and simplifying assumptions are made to avoid excessive complexity. For instance, the TEFERI model is a one-dimensional analysis in the case of a counterflow cooling tower. It assumes uniform fluid flow through the fill, and air properties are assumed constant over the draft height. The overall pressure loss coefficient in the cooling tower is assumed to be independent of the condition of operation. The rain zone is not described in the model.

The results obtained with the *multi-dimensional* numerical codes are not necessarily better than those obtained by the application of extended one-dimensional point models. This is attributable to the fact the multi-dimensional approach still employs empirical relations and makes numerous simplifying assumptions. Numerical methods are essential in cases where

- the air does not flow uniformly through the fill due to variable fill thickness

- the water distribution changes in the radial direction (according to Gösi) or is non-uniform
- plugging or other disturbances are present (according to Eldredge)

The following approach is similar to that applied to the dry-cooling tower in the previous section. A procedure is presented showing how the performance of a counterflow wet-cooling tower with a uniform thickness fill can be determined to a high degree of accuracy.

Neglecting the evaporation loss, which is 1–3% of the water mass flow rate, an energy balance for the wet-cooling tower shown in Figure 7.2.1. yields

$$Q = m_a \, (i_{ma5} - i_{ma1}) = m_w \, c_{pwm} \, (T_{wi} - T_{wo}) \qquad (7.2.1)$$

where

m_a = the dry air flow rate through the tower

m_w = water mass flow rate through the tower

i_{ma5} = the outlet enthalpy of the air flowing through the tower

i_{ma1} = inlet enthalpy of the air flowing through the tower

The specific heat of the water is evaluated at the mean water temperature. Equation 7.2.1 is analogous to Equation 7.1.2. However, in addition to Equation 7.2.1, a relation must be satisfied that expresses the heat transfer rate in terms of an overall transfer coefficient analogous to Equation 7.1.3 but is applicable to the wet-cooling tower.

Energy is transferred in three regions of the cooling tower shown in Figure 7.2.1, i.e., rain, fill, and spray zone.

In the rain zone of this particular tower, the transfer coefficient from Equation 4.6.12 can be expressed approximately as

$$\frac{h_{drz}\, a_{rz}\, H_3}{G_w} = 12\left(\frac{D_1}{v_{av3}\, d_d}\right)\left(\frac{H_3}{d_d}\right)\left(\frac{p_a 1}{R_v T_{a1}\, \rho_{wo}}\right) Sc_1^{0.33}\left[\ell n\left(\frac{w_{s1} + 0.622}{w_1 + 0.622}\right)\right.$$

$$\left./\,(w_{s1} - w_1)\right]\left[0.90757\ a_\rho \rho_{av1} - 30341.04\ a_\mu \mu_{av1} - 0.37564 + 4.04016\right.$$

$$\text{x}\left[\left\{0.55 + 41.7215(a_L\, d_d)^{0.80043}\right\}\left\{0.713 + 3.741(a_L\, H_3)^{-1.23456}\right\}\right.$$

$$\text{x}\left\{3.11\ \exp\left(0.15 a_v v_{av} 3\right) - 3.13\right\}\exp\left[\left\{5.3759\ \exp\ (-0.2092\ a_L H_3)\right\}\right.$$

$$\text{x}\ \ell n\left\{0.3719\ \exp\left(0.0019055 a_L d_i\right) + 0.55\right\}]]]$$

$$\text{x}\ \ell n\ \{0.3719\ \exp\ (0.0019055 a_L d_i) + 0.55\}]]] \qquad (7.2.2)$$

where

$a_\mu = 3.061 \text{ x } 10^{-6}\ (\rho_{wo}^4\, g^9 / \sigma_{wo})^{0.25}$

$a\rho = 998/\rho_{wo}$

$a_v = 73.298\ (g^5 \sigma_{wo}^3 / \rho_{wo}^3)^{0.25}$

$a_L = 6.122\ (g\ \sigma_{wo} / \rho_{wo})^{0.25}$

This equation is valid for:

- $0^\circ\text{C} \le T_{a1} \le 40^\circ\text{C}$
- $10^\circ\text{C} \le T_{wo} \le 40^\circ\text{C}$
- $0.927\ \text{kg/m}^3 \le \rho_{av1} \le 1.289\ \text{kg/m}^3$

- $992.3\ kg/m^3 \leq \rho_{wo} \leq 1000\ kg/m^3$
- $1.717 \times 10^{-5}\ kg/ms \leq \mu_{av1} \leq 1.92 \times 10^{-5}\ kg/ms$, $0.0696\ N/m \leq \sigma_{wo} \leq 0.0742\ N/m$
- $0.002\ m \leq d_d \leq 0.008\ m$
- $9.7\ m/s^2 \leq g \leq 10\ m/s^2$
- $30\ m \leq d_3/2 \leq 70\ m$
- $4\ m \leq H_3 \leq 12\ m$
- $0.0075 \leq v_{w3} \leq 0.003\ m/s$
- $1\ m/s \leq v_{av3} \leq 3\ m/s$

Equations 4.3.1, 4.3.3, or 4.3.4 describe the transfer characteristics of the fill. Equation 4.3.3 can be written for the entire fill height as

$$\frac{h_{dfi}\, a_{fi}\, L_{fi}}{G_w} = a_d\, L_{fi} G_w^{bd} G_a^{cd} \tag{7.2.3}$$

In the spray zone above the fill, the data of Lowe and Christie can be correlated to give

$$\frac{h_{dsp}\, a_{sp}\, L_{sp}}{G_w} = 0.2\ L_{sp} \left(\frac{G_a}{G_w}\right)^{0.5} \tag{7.2.4}$$

If the transfer characteristics of the fill were determined according to the Merkel method, the Merkel relation given by Equation 4.2.22 may now be applied to the entire region between the inlet of the rain zone and the outlet of the spray zone, i.e.,

$$\frac{h_{drz}\, a_{rz} H_3}{G_w} + \frac{h_{dfi}\, a_{fi}\, L_{fi}}{G_w} + \frac{h_{dsp}\, a_{sp}\, L_{sp}}{G_w} = \int_{T_{wo}}^{T_{wi}} \frac{c_{pw}\, d\, T_w}{(i_{masw} - i_{ma})} \tag{7.2.5}$$

To deduce the corresponding draft equation, consider the variation of pressure with elevation in the atmosphere external to the cooling tower, i.e.,

$$dp_a = -\rho_{av}\, g\, dz \tag{7.2.6}$$

As in the case of the dry-cooling tower, the ambient temperature distribution for a DALR (- 0.00975 K/m) will be assumed external to the tower.

$$T_a = T_{a1} - 0.00975\, z \tag{7.2.7}$$

where T_{a1} is found by extrapolating the DALR to ground level.

According to Equation A.3.1, the density of air containing water vapor is expressed as

$$\rho_{av} = (1 + w)\left[1 - w/(w + 0.62198)\right] p_a/(RT_a) \tag{7.2.8}$$

where

R = 287.08 J/kg K

Substitute Equations 7.2.7 and 7.2.8 into Equation 7.2.6, and integrate to find the difference in pressure between elevations (1) and (7) external to the tower for a constant humidity ratio, $w \approx w_1$.

$$p_{a1} - p_{a7} = p_{a1}\left[1-\left(1-0.00975\ H_6/T_{a1}\right)^{3.5(1+w_1)\{1-w_1/(w_1+0.62198)\}}\right] \tag{7.2.9}$$

where

$H_7 = H_6$

By following a similar procedure, an expression can be obtained for the static pressure difference between ground level and the mean fill height at $(H_3 + L_{fi}/2)$.

Rising moist air inside the tower is adiabatically cooled, causing vapor to condense and precipitate out of the rising air. The energy removed by this condensation process is available to heat the surrounding air. According to Equation 9.1.30, the lapse rate for this pseudo-adiabatic process is given by

$$\xi_{Ta5} = \frac{-(1+w_5)g\left[1+0.42216 \times 10^{-11} w_5^2 p_{a5} \exp(5406.1915/T_{a5}) i_e/\{(w_5+0.622)RT_{a5}\}\right]}{c_{pma} + 3.6693 \times 10^{-8} w_5^2 p_{a5} \exp(5406.1915/T_{a5})\, i_e/T_{a5}^2} \qquad (7.2.10)$$

where

$c_{pma} = c_{pa} + w_5 c_{pv}$

T_{a5} is in K

The specific heats in this equation are evaluated at

$$(T_{a5} + 273.15)/2 \text{ K and } i_e = i_{fgwo} - (c_{pw} - c_{pv})(T_{a5} - 273.15)$$

The difference in static pressure due to the column of saturated air between the mean fill elevation and the outlet of the tower for this temperature lapse rate can be evaluated with the aid of Equation 9.1.33.

$$p_{a34} - p_{a6} \approx p_{a5}\left[1-\left\{1+\xi_{Ta5}\left(H_6-H_3-L_{fi}/2\right)/T_{a5}\right\}^{-0.021233\,(1+w_5)/\{\xi_{Ta5}(w_5+0.622)\}}\right] \qquad (7.2.11)$$

The net pressure differential between the ambient air and the air inside the tower may be determined from these expressions to give the draft equation for a natural draft counterflow, wet-cooling tower, i.e.,

$$(p_{a1} - p_{a7}) - (p_{a1} - p_{a34}) - (p_{a34} - p_{a6}) - (p_{a6} - p_{a7}) \approx$$

$$- p_{a1}\left[1 - \{1 - 0.00975\,(H_3 + L_{fi}/2)/T_{a1}\}^{3.5(1+w_1)\{1-w_1/(w_1+0.62198)\}}\right]$$

$$- p_{a5}\left[1 - \left\{1 + \xi_{Ta5}\,(H_6 - H_3 - L_{fi}/2)/T_{a5}\right\}^{-0.021233(1+w5)/\{\xi_{Ta5}(w5+0.622)\}}\right]$$

$$- (p_{a6} - p_{a7})$$

$$= (K_{ts} + K_{i\ell})\,(m_{av2}/A_2)^2/(2\rho_{av2}) + K_{ct}\,(m_{av2}/A_3)^2$$

$$/(2\rho_{av2}) + (K_{rz} + K_{fs})(m_{av23}/A_{fr})^2$$

$$/(2\rho_{av23}) + K_{ctc}(m_{av3}/A_{fr})^2/(2\rho_{av3}) + K_{fi}(m_{av34}/A_{fr})^2/(2\rho_{av34})$$

$$+(K_{cte} + K_{sp} + K_{wd} + K_{de})(m_{av4}/A_{fr})^2$$

$$/(2\rho_{av4}) + a_{e6}\,(m_{av6}/A_6)^2/(2\rho_{av6})$$

To simplify this equation, assume:

- $m_{av2} \approx m_{av23} \approx m_{av1}$
- $m_{av4} \approx m_{av6} \approx m_{av5}$
- $m_{av34} \approx m_{av15}$
- $\rho_{av2} \approx \rho_{av3} \approx \rho_{av1}$
- $\rho_{av4} \approx \rho_{av5}$

such that

$$p_{a1}\left[1-(1-0.00975\ H_6/T_{a1})^{3.5\,(1+w_1)\,\{1-w_1/(w_1+0.62198)\}}\right]$$

$$-\,p_{a1}\left[1-\{1-0.00975\,(H_3+L_{fi}/2)/T_{a1}\}^{3.5\,(1+w_1)\{1-w_1/(w_1+0.62198)\}}\right]$$

$$-\,p_{a5}\left[1-\{1+\xi_{Ta5}\,(H_6-H_3-L_{fi}/2)/T_{a5}\}^{-0.021233(1+w_5)/\{\xi_{Ta5}(w_5+0.622)\}}\right]$$

$$-(p_{a6}-p_{a7})$$

$$=\left(K_{ts}+K_{i\ell}+K_{ct}+K_{rz}+K_{fs}+K_{ctc}+K_{fi}+K_{cte}+K_{sp}+K_{wd}+K_{de}\right)_{fi}$$

$$\text{x}\ \left(m_{av15}/A_{fr}\right)^2/\left(2\rho_{av15}\right)+a_{e6}\left(m_{av5}/A_6\right)^2/\left(2\rho_{av6}\right) \qquad (7.2.12)$$

The subscript $_{fi}$ implies all loss coefficients are referred to the frontal area of the fill and the mean density through the fill.

With the previous simplifying assumptions and the assumption that the dynamic term at elevation (5) is negligible, the effective value for p_{a5} for substitution into Equation 7.2.12 can be approximated by the following expression:

$$p_{a5}=p_{a1}\left[1-0.00975\left(H_3+L_{fi}/2\right)/T_{a1}\right]^{3.5(1+w_1)\{1-w_1/(w_1+0.62198)\}}$$

$$-\left(K_{ts}+K_{i\ell}+K_{ct}+K_{rz}+K_{fs}+K_{ctc}+K_{fi}+K_{cte}+K_{sp}+K_{wd}+K_{de}\right)_{fi}$$

$$\text{x}\ \left(m_{av15}/A_{fr}\right)^2/\left(2\rho_{av15}\right) \qquad (7.2.13)$$

According to Du Preez and Kröger, the difference in the mean pressure at the tower outlet and the ambient pressure at the same elevation is given by

$$p_{a6} - p_{a7} = \left(0.02\ Fr_D^{-1.5} - 0.14/Fr_D\right)\left(m_{av5}/A_6\right)^2/\rho_{av6} \qquad (7.2.14)$$

where

$$Fr_D = \left(m_{av5}/A_6\right)^2/\left[\rho_{av6}\left(\rho_{av7} - \rho_{av6}\right)g d_6\right]$$

Substitute Equations 7.2.13 and 7.2.14 into Equation 7.2.12, and re-arrange to find the final simplified form of the draft equation.

$$p_{a1}\left[\left\{1 - 0.00975\left(H_3 + L_{fi}/2\right)/T_{a1}\right\}^{3.5(1+w_1)\{1-w_1/(w_1+0.62198)\}}\right.$$

$$\times\left\{1 + \xi_{Ta5}\left(H_6 - H_3 - L_{fi}/2\right)/T_{a5}\right\}^{-0.021233(1+w_1)/\{\xi_{Ta5}(w_5+0.622)\}}$$

$$\left. - \left\{1 - 0.00975\ H_6/T_{a1}\right\}^{3.5(1+w_1)\{1-w_1/(w_1+0.62198)\}}\right]$$

$$- \left(0.02\ Fr_D^{-1.5} - 0.14/Fr_D\right)\left(m_{av5}/A_6\right)^2/\rho_{av6}$$

$$= \left(K_{ts} + K_{i\ell} + K_{ct} + K_{rz} + K_{fs} + K_{ctc} + K_{fi} + K_{cte} + K_{sp} + K_{wd} + K_{de}\right)_{fi}$$

$$\times \left(m_{av15}/A_{fr}\right)^2 / \left(2\rho_{av15}\right)$$

$$\times \left[1 + \xi_{Ta5}\left(H_6 - H_3 - L_{fi}/2\right)/T_{a5}\right]^{-0.021233(1+w_5)/\{\xi_{Ta5}(w_5+0.622)\}}$$

$$+ a_{e6}\left(m_{av5}/A_6\right)^2/\left(2\rho_{av6}\right) \qquad (7.2.15)$$

where

$_{fi}$ implies the loss coefficients are referred to the geometry and conditions through the fill.

The loss coefficient due to the tower supports, K_{ts}, may be determined according to Equation 7.1.21.

Louvers are often installed at the inlet of a cooling tower to prevent water from splashing outside the tower especially during windy periods. According to Kelly, the louver loss coefficient is $K_{i\ell} = 5$ for a crossflow tower, while Jorgenson states the value for this coefficient may vary between 2 and 5 based on the frontal area of the louver. A 30° louver with 80% or more open area can have a loss coefficient as low as 2, while the older types of louvers with a 45° angle can have a loss coefficient as high as 5. In addition to the flow resistance, louvers at the inlets of counterflow induced-draft and natural-draft towers (Fig. 1.1.6a) can distort the air-flow pattern at the inlet and through the fill. This reduces the performance of the towers. Other devices, such as windwalls in the rain zone or extended basins are generally preferred in counterflow towers.

The loss coefficient for inlet louvers based on experimental data may be given as an approximate constant value or be expressed in terms of a flow Reynolds number through the louvers as

$$K_{i\ell} = a_{i\ell} Re_{i\ell}^{b_{i\ell}} \tag{7.2.16}$$

or

$$K_{i\ell fi} = a_{i\ell} Re_{i\ell}^{b_{i\ell}} (\rho_{av15}/\rho_{av1}) \, (A_{fr} / A_2)^2 (m_{av1} / m_{av15})^2 \tag{7.2.17}$$

where

$_{fi}$ implies the coefficient is based on conditions through the fill

Expressions may be employed for the tower inlet loss coefficient, K_{ct}, for a counterflow cooling tower described in section 7.3.

From Equation 4.6.11, the loss coefficient through the rain zone can be expressed as

$$K_{rz} = 3\ a_v v_{w3}\ (H_3 / d_d)\left[0.2246 - 0.31467\ a_\rho \rho_{av1}\right.$$

$$+ 5263.04\ a_\mu \mu_{av1} + 0.775526 \times \{1.4824163 \exp(71.52\ a_L\ d_d)$$

$$- 0.91\}\{0.39064 \exp(0.010912 a_L d_i) - 0.17\} \times \{2.08915\ (a_v v_{av3})^{-1.3944}$$

$$\left. + 0.14\right\} \exp[\{0.8449\ \ell n\ (a_L d_3 / 2) - 2.312\}\{0.3724\ \ell n\ (a_v v_{av3})$$

$$\left. + 0.7263\}\ell n\{206.757\ (a_L H_3)^{-2.8344} + 0.43\}\right]\Big]$$

or, if referred to fill conditions,

$$K_{rzfi} = K_{rz}(\rho_{av15} / \rho_{av2}) \approx K_{rz}(\rho_{av15} / \rho_{av1})(m_{av1} / m_{av15})^2 \qquad (7.2.18)$$

Losses due to the fill support structure including pillars and crossbeams, K_{fs} may be expressed in terms of a drag coefficient or an approximate constant value. If the fill does not cover the entire cross-sectional area of the tower, a contraction loss should be considered. Equation 7.1.23 can be used for this purpose.

After the fill, an expansion loss given by Equation 7.1.24 may be relevant if the fill does not cover the entire tower cross section. The loss coefficient through the fill is given by either Equation 4.3.2 or Equation 4.3.5. Effects due to changes in momentum across the fill must also be taken into consideration as described in the note at the end of Example 4.3.1.

In the spray region above the fill, data presented by Cale suggests the loss coefficient may be expressed approximately as

$$K_{sp} \approx L_{sp}[0.4(G_w / G_a) + 1] \tag{7.2.19}$$

or, based on fill condition,

$$K_{spfi} \approx L_{sp}[0.4(G_w / G_a) + 1](\rho_{av15}/\rho_{av5})\,(m_{av5} / m_{av15})^2 \tag{7.2.20}$$

where

L_{sp} = the height of the spray zone

The spray should be distributed uniformly above the fill by a system of pipes fitted with spray nozzles. A typical value for the loss coefficient of such a system is

$$K_{wdfi} = 0.5(\rho_{av15}/\rho_{av5})(m_{av5}/m_{av15})^2$$

Losses through the drift or droplet eliminators located above the spray nozzles may be expressed as

$$K_{defi} = a_{de} Ry_{de}^{\,b_{de}}(\rho_{av15}/\rho_{av5})\,(m_{av5} / m_{av15})^2 \tag{7.2.21}$$

The values for a_{de} and b_{de} are obtained by fitting Equation 4.7.1 to test data as shown for typical drift eliminators in Figure 4.7.3.

It is important for the water to flow uniformly through the fill since non-uniform flow tends to reduce tower performance according to both Lees and Looper and Liffick and Cooper and may cause freezing during cold periods as stated in VGB-R 129P.

The approximate harmonic mean density in the fill is given by

$$\rho_{av34} \approx \rho_{av15} = 2/(1/\rho_{av1} + 1/\rho_{av5}) \tag{7.2.22}$$

where, according to the equations in appendix A,

$$\rho_{av1} = (1 + w_1)\left[1 - w_1/(w_1 + 0.62198)\right] p_{a1}/(RT_{a1}) \qquad (7.2.23)$$

and

$$\rho_{av5} = (1 + w_5)\left[1 - w_5/(w_5 + 0.62198)\right] p_{a5}/(RT_{a5}) \qquad (7.2.24)$$

If dynamic effects are neglected, the air temperature at the outlet of the tower is

$$T_{a6} \approx T_{a5} + \xi_{Ta5}(H_6 - H_3 - L_{fi} - L_{sp}) \qquad (7.2.25)$$

The corresponding mean pressure p_{a6} follows from Equation 7.2.14 where p_{a7} is given by Equation 7.2.9. With these values, find the density at (6)

$$\rho_{av6} = (1 + w_5)\left[1 - w_5/(w_5 + 0.62198)\right] p_{a6}/(RT_{a6}) \qquad (7.2.26)$$

Distortions in velocity distribution at the tower outlet are taken into consideration by the factor α_{e6}, which is equal to unity for a hyperbolic counterflow tower according to Du Preez.

The amount of water that is evaporated is given by

$$m_{we} = m_a(w_5 - w_1) \qquad (7.2.27)$$

In a comparative study, Grange shows the Merkel method (Merkel) may underestimate the amount of water that evaporates under certain conditions when compared to the Poppe approach (Poppe). However, this discrepancy decreases with increasing ambient temperatures.

In large, natural-draft, counterflow cooling towers, the fill is sometimes installed in annular layers, which increase in thickness with increasing radius (Fig. 7.2.2). Cooling air entering at the lower edge of the shell is not exposed to much of the rain zone and will tend to flow through a greater fill thickness or height than the air entering near ground level. The condition of the air leaving the fill should be more uniform than in the case of constant fill thickness. According to Lowe and Christie, other arrangements of packings are found in practice. Variations in fill density, spray nozzle pitch, or water flow rate through the fill may be considered to improve performance. Numerical methods are required to analyze the flow through such configurations.

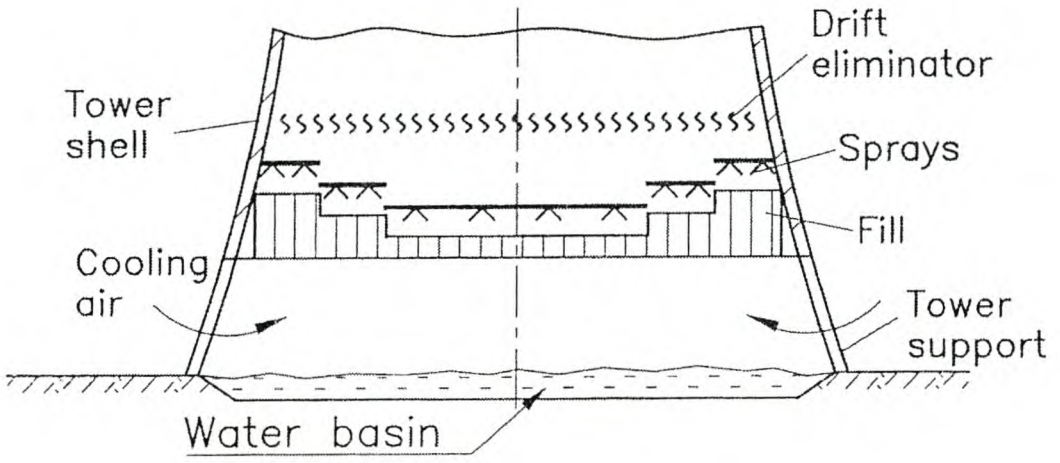

Fig. 7.2.2 Annular Variable Thickness Fill Installation

Another tower inlet configuration found in water-recovery, counterflow cooling towers is shown in Figure 7.2.3 from both Vogelsang and Hackeschmidt and Goldwirt et al.. The fill is of uniform thickness. Droplets leaving the fill are collected in plastic troughs located immediately below the fill before being returned to the condenser. This reduces the required water pumping power. In the absence of a rain zone, noise levels are significantly reduced, and the conditions of the air leaving the fill are relatively uniform.

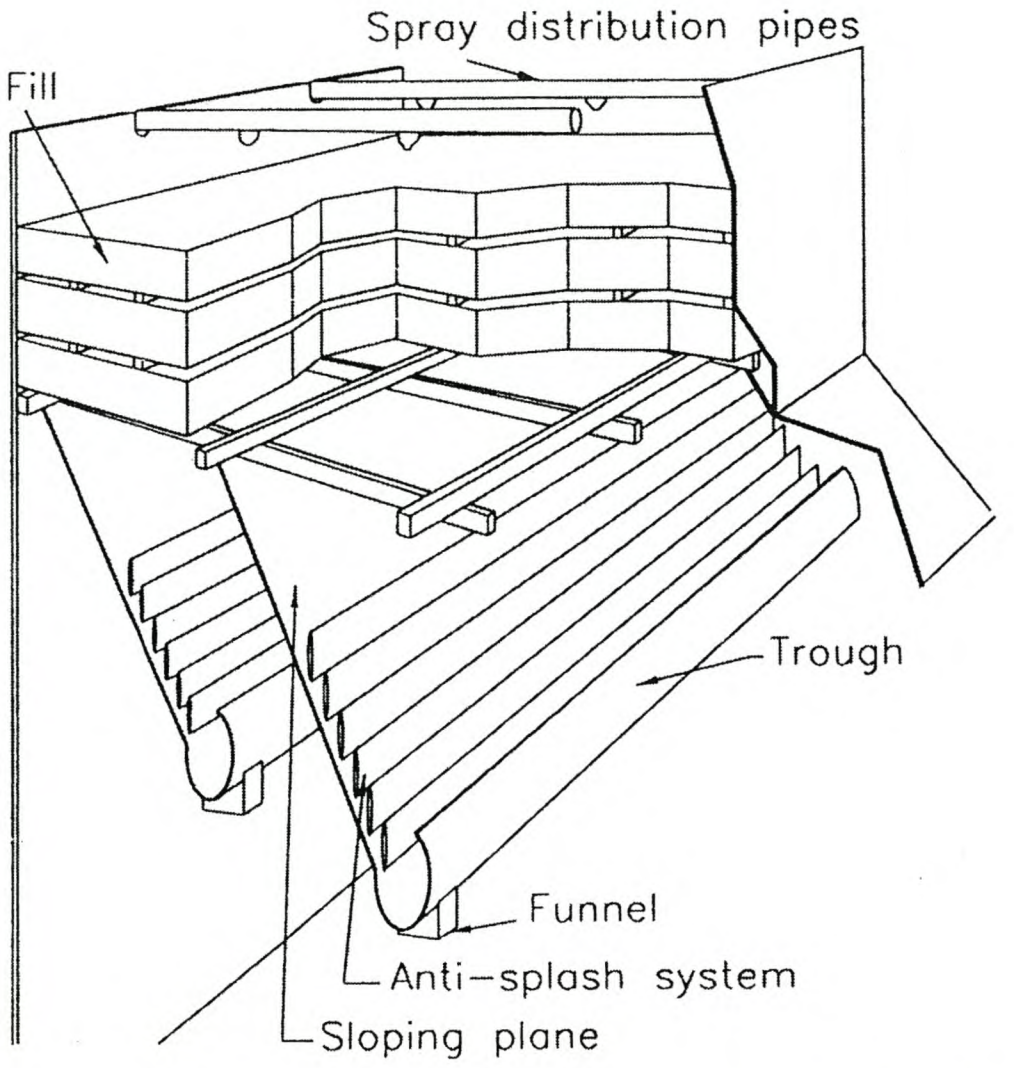

Fig. 7.2.3 Droplet Collecting Troughs in a Large Counterflow Cooling Tower

A similar analysis is applicable to a crossflow cooling tower. The transfer process can be modeled numerically (two-dimensional). An easier approach is to employ the effectiveness-NTU method described in section 4.4. As in the case of a counterflow tower, spray droplet size and maldistribution of flow can influence performance measurably according to Caytan and Franza.

Thermal performance acceptance tests for wet-cooling towers are described by various standards including the ASME PTC-23, British Standards Institution BS 4485, Deutsche Norm DIN 1947, and the Cooling Tower Institute Acceptance Test Code ATC-105.

7.3 Inlet Losses

As in the case of most duct inlets where flow losses occur due to separation or other disturbances, similar phenomena are observed at the inlets to natural-draft cooling towers. In the absence of any flow resistance caused by heat exchangers or fills in the inlet to the tower and if flow through such a tower can be maintained, flow separation will occur at the lintel or lower edge of the shell. The separation will form a vena contracta with a corresponding distorted inlet velocity distribution (Fig. 7.3.1a). A significant pressure difference will exist between a point inside the tower at the lower edge of the shell and the ambient stagnant conditions far from the tower.

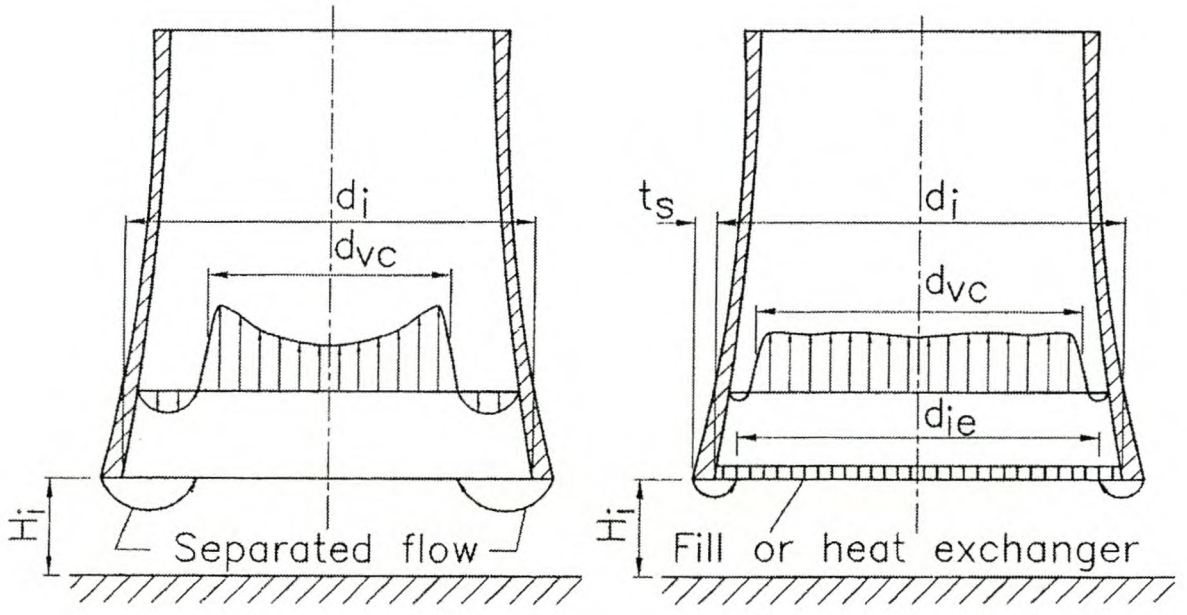

Fig. 7.3.1 Tower Inlet Flow Patterns (a) Empty Tower
(b) Tower with Horizontal Heat Exchanger or Fill

The tower static inlet loss coefficient may be defined as

$$K_{cts} = (p_a - p)/(\rho v^2/2) \qquad (7.3.1)$$

where

p_a = ambient stagnation pressure

p = static pressure inside the tower at the lower edge of the shell

v = mean velocity based on the horizontal cross-sectional flow area at the inlet

ρ = density based on ambient conditions

A number of experimental and theoretical studies have been conducted to determine the tower inlet losses in the absence of heat exchangers or fills for different inlet diameters, d_i, to height, H_i, ratios, and some of the results are shown in Figure 7.3.2.

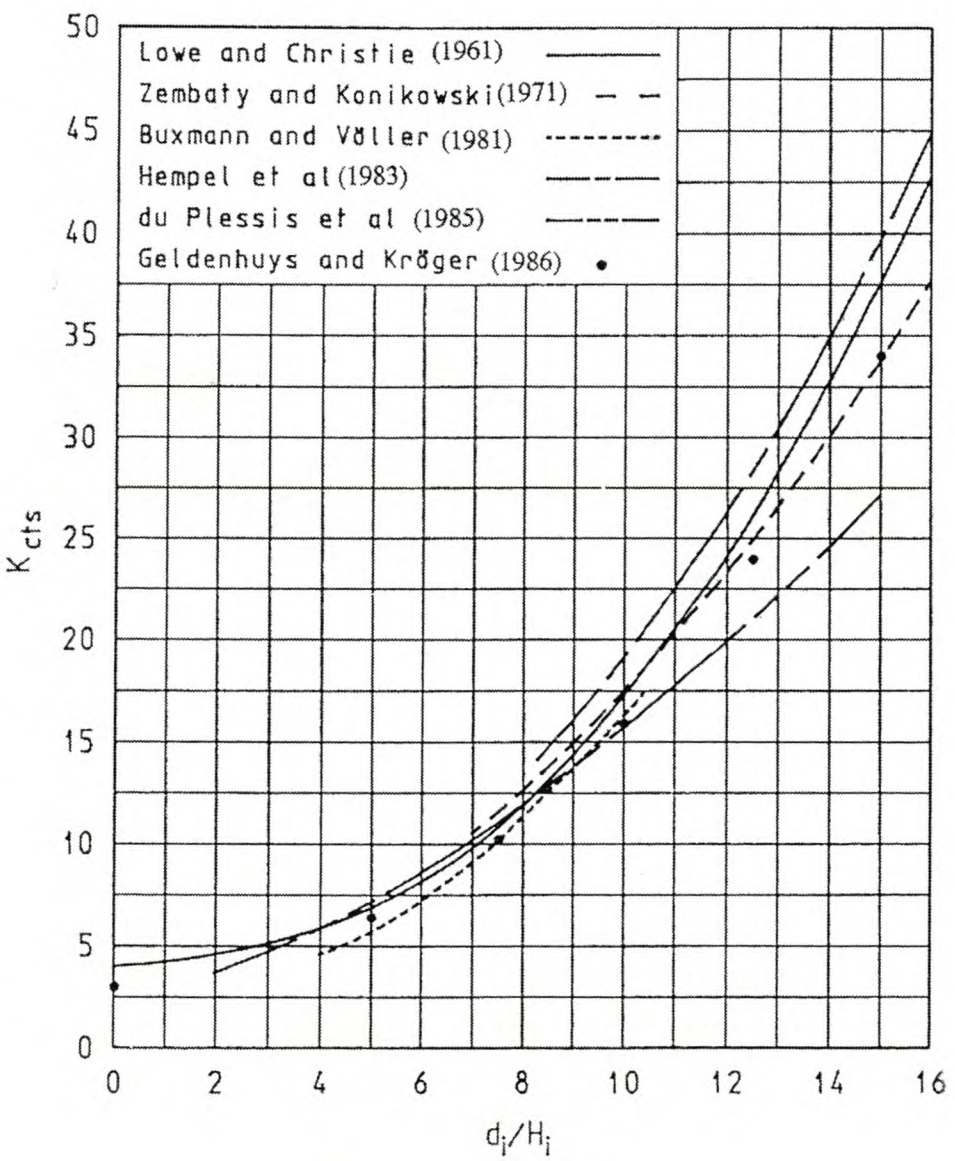

Fig. 7.3.2 Empty Tower Static Inlet Loss Coefficient

When a heat exchanger is installed horizontally in the tower, the velocity distribution tends to become more uniform (Fig. 7.3.1b), and a corresponding reduction in tower inlet loss is observed.

Most of the original studies on cooling tower losses were made with a view to the design of wet-cooling towers, such as those by Lowe and Christie, Vogelsang and Hackeschmidt, Zembaty and Konikowski, Garde, Moore and Garde, Buxmann and Völler, Hempel et al., Witte, Geldenhuys and Kröger, Du Preez and Kröger, and Terblanche and Kröger. However, a few of the more recent papers make specific reference to dry-cooling towers.

Terblanche and Kröger performed model tests to determine the tower loss coefficient as a function of the heat exchanger loss coefficient K_{he}. They expressed the loss coefficient in terms of the change in total pressure between the stagnant ambient air, p_a, far from the tower and in the plane of the vena contracta after the heat exchanger, i.e.,

$$K_{ct} = \frac{p_a/\rho - (p_{vc}/\rho_{vc} + \alpha_{evc} v_{vc}^2/2)}{v^2/2} - K_{he} \frac{\rho}{\rho_{he}} \left(\frac{A}{A_{fr}}\right)^2 \qquad (7.3.2)$$

where

A = inlet cross-sectional area of the tower

A_{fr} = total frontal area of the heat exchanger

ρ_{he} = harmonic mean density of the air flow

v_{vc} = mean velocity in the plane of the vena contracta

α_{evc} = kinetic energy coefficient

This equation is applicable to both the vertical and horizontal arrangements of heat exchanger bundles.

In horizontal arrangements where the velocity distribution may be relatively uniform over the tower cross section, Equation 7.3.2 can be simplified to read:

$$K_{ct} = \frac{p_a/\rho - (p_o/\rho_o + v_o^2/2)}{v^2/2} - K_{he}\frac{\rho}{\rho_{he}}\left(\frac{A}{A_{fr}}\right)^2 \qquad (7.3.3)$$

where

v_o = outlet air velocity based on the frontal area of the fill or the heat exchanger

If the heat exchanger is arranged in the form of A-frames or arrays of V-bundles, v_o is based on the projected frontal area. Subscript $_o$ refers to conditions after the heat exchanger.

A further simplification is possible for the case where the heat exchanger is installed such that it covers the entire inlet cross-section of the cooling tower, i.e.,

$$K_{ct} \approx \frac{(p_a/\rho - p_o/\rho_o)}{v^2/2} - 1 - K_{he}\left(\frac{\rho}{\rho_{he}}\right) \qquad (7.3.4)$$

The recommended loss coefficient for this layout is given by

$$K_{ct} = \left[100 - 18(d_i/H_i) + 0.94(d_i/H_i)^2\right]$$

$$\times\ K_{he}^{[-1.28 + 0.183(d_i/H_i) - 7.769 \times 10^{-3}(d_i/H_i)^2]} \qquad (7.3.5)$$

This equation is applicable in the following ranges:

- $10 \leq (d_i/H_i) \leq 15$
- $5 \leq K_{he} \leq 25$
- $t_s/d_i = 0.0045$

Equation 7.3.5 can also be applied in conjunction with Equation 7.3.2 where

$$\alpha_{evc} = 1.175$$

For higher values of K_{he}, the following equation is preferred according to Du Preez and Kröger:

$$K_{ct} = \left[-18.7 + 8.095\,(d_i / H_i) - 1.084\,(d_i / H_i)^2 + 0.0575\,(d_i / H_i)^3\right] \times K_{he}^{[0 - 165 - 0.035\,(d_i/H_i)]} \quad (7.3.6)$$

where

$19 < K_{he} < 50$

$5 < d_i/H_i < 15$

For dry-cooling towers, where

$K_{he} \geq 30$

$5 \leq d_i/H_i < 10$

the following simplified expression is recommended by Geldenhuys and Kröger:

$$K_{ct} = 0.072(d_i/H_i)^2 - 0.34(d_i/H_i) + 1.7 \quad (7.3.7)$$

Equations 7.3.6 and 7.3.7 are shown graphically in Figure 7.3.3.

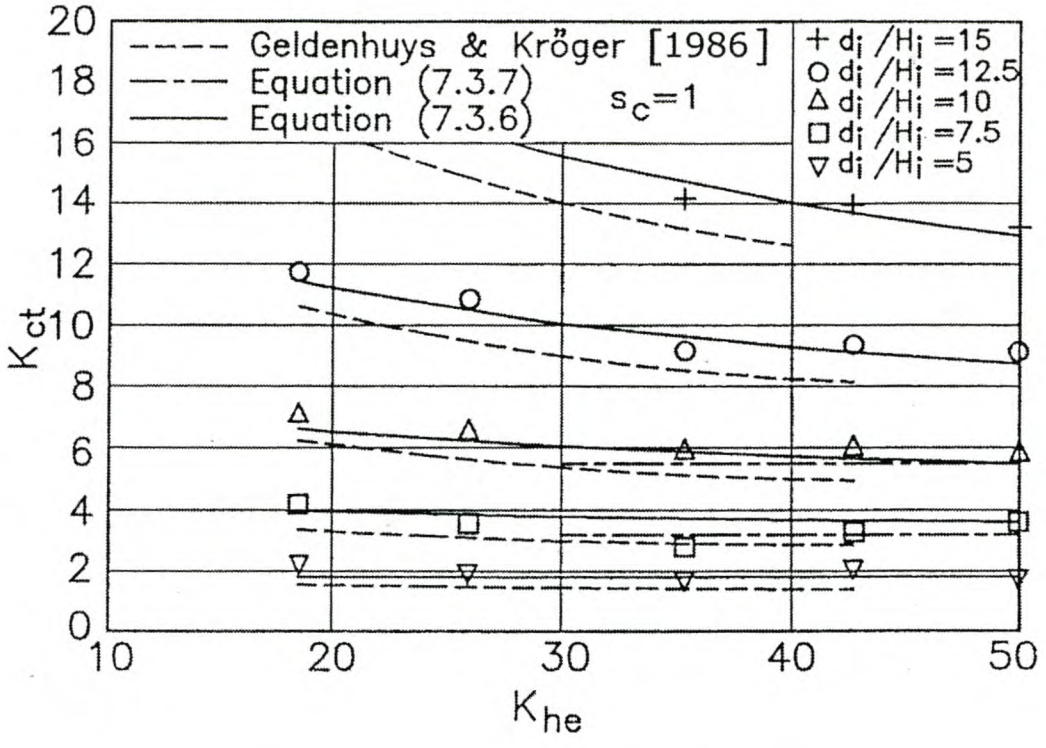

Fig. 7.3.3 Cooling Tower Loss Coefficient

The previous equations can also be applied with a contraction loss coefficient to towers in situations where the horizontally arranged rectangular heat exchangers:

- do not cover the entire cross-sectional area
- do not run continuously along the circumference at the base of the tower

Du Preez and Kröger have considered the geometry of situations where the heat exchanges do not run continuously along the circumference and define the following length ratio:

$$s_c = \frac{\text{Effective length of heat exchanger along tower circumference}}{\pi d_i} \qquad (7.3.8)$$

This ratio is less in a small tower than in a large tower as is shown in Figure 7.3.4 for the Grootvlei 6 and the Kendal towers.

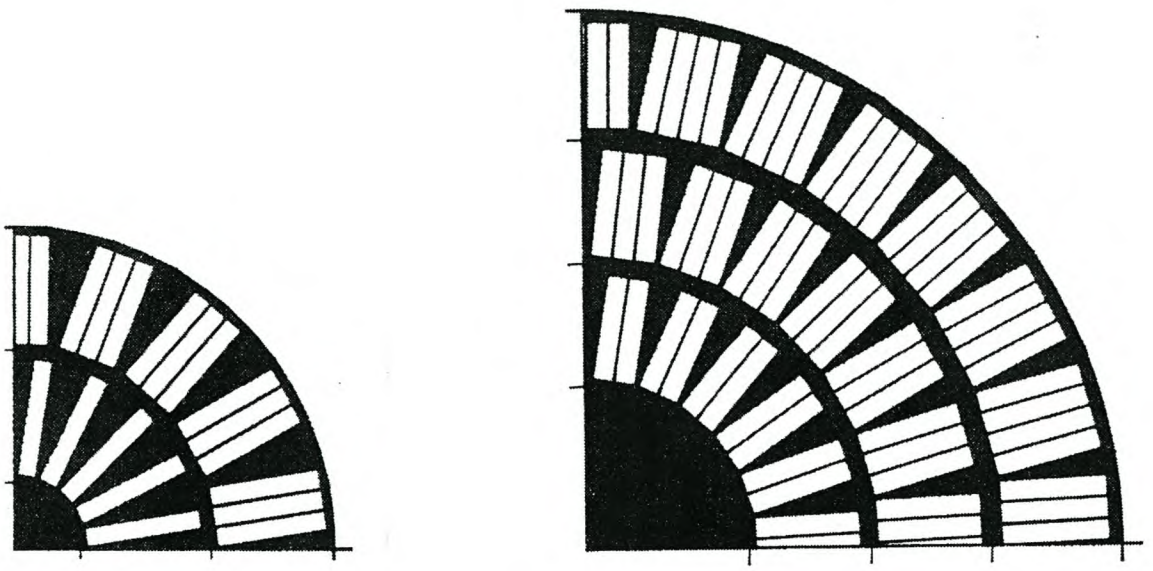

Fig. 7.3.4 Arrangement of Heat Exchangers in Tower Cross Section
(a) Grootvlei 6 (s_c = 0.62) (b) Kendal (s_c = 0.77)

Based on measured values, the following equation for K_{ct} as defined by Equation 7.3.3 is recommended for design purposes where the tower inlet cross section is not necessarily covered by heat exchanger bundles.

$$K_{ct} = [1.05 - 0.01(d_i / H_i)][1.6 - 0.29(d_i / H_i) + 0.072(d_i / H_i)^2] / s_c$$

$$+ (0.271 - 0.0115 K_{he} + 0.000124 K_{he}^2)(d_i / H_i)(1.66 - 6.325 s_c + 5.625 s_c^2) \quad (7.3.9)$$

where

$19 \leq K_{he} \leq 50$

$0.4 \leq s_c \leq 1$

$5 \leq d_i/H_i \leq 10$

This equation includes the contraction loss due to the reduction in flow area into the heat exchangers, but it does not include the expansion loss thereafter.

For s_c = 0.4 and d_i/H_i = 10, the flow into the cooling tower becomes unstable, and fluctuations in pressure are observed. However, Equation 7.3.9 can be applied since it gives conservative results under these conditions.

According to Terblanche and Kröger, it is possible to reduce the inlet loss coefficient by rounding off the inlet to the tower as shown in Figure 7.3.5.

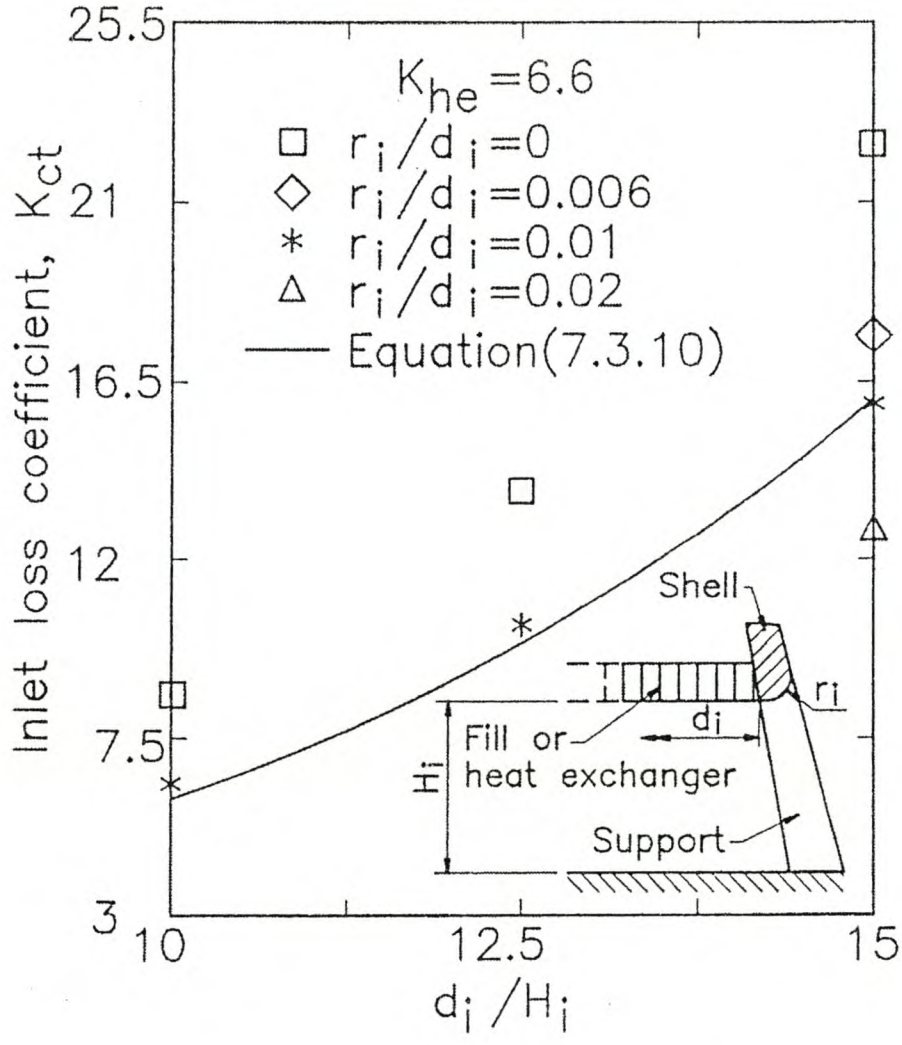

Fig. 7.3.5 Loss Coefficient with Rounded Tower Inlet

Rounded inlets are potentially most beneficial in the case of counterflow, wet-cooling towers where relatively large quantities of water have to be raised to the level of the spray nozzles located above the fill. This requires a significant amount of pumping power which can be reduced by lowering the fill and the corresponding tower inlet height. This leads to greater inlet

losses, which can be reduced by rounding off the inlet edge of the tower shell. In this case,

$$K_{ct} = 1.5 \exp(0.2\, d_i / H_i)\, K_{he}^{[-0.4645 + 0.02303\, d_i/H_i - 0.00095\, (d_i/H_i)^2]} \qquad (7.3.10)$$

in the ranges

- $10 \leq (d_i/H_i) \leq 15$
- $5 \leq K_{he} \leq 25$
- $r_i/d_i \approx 0.01$

This expression is applied approximately in conjunction with Equation 7.3.4 or with Equation 7.3.2 for $\alpha_{evc} = 1.1$.

Vauzanges and Ribier investigated the influence of the shape of the lintel and tower supports on the inlet losses. They concluded that radial elongated supports and a rounded lintel are advantageous in wet-cooling towers.

As shown in Figure 7.3.1, the degree of separation at the inlet of the tower is influenced by the characteristics of the heat exchanger. Geldenhuys and Kröger visually observed flow patterns in this region in their experimental sector model for $d_i/H_i = 7.5$ and different heat exchanger loss coefficients (Fig. 7.3.6).

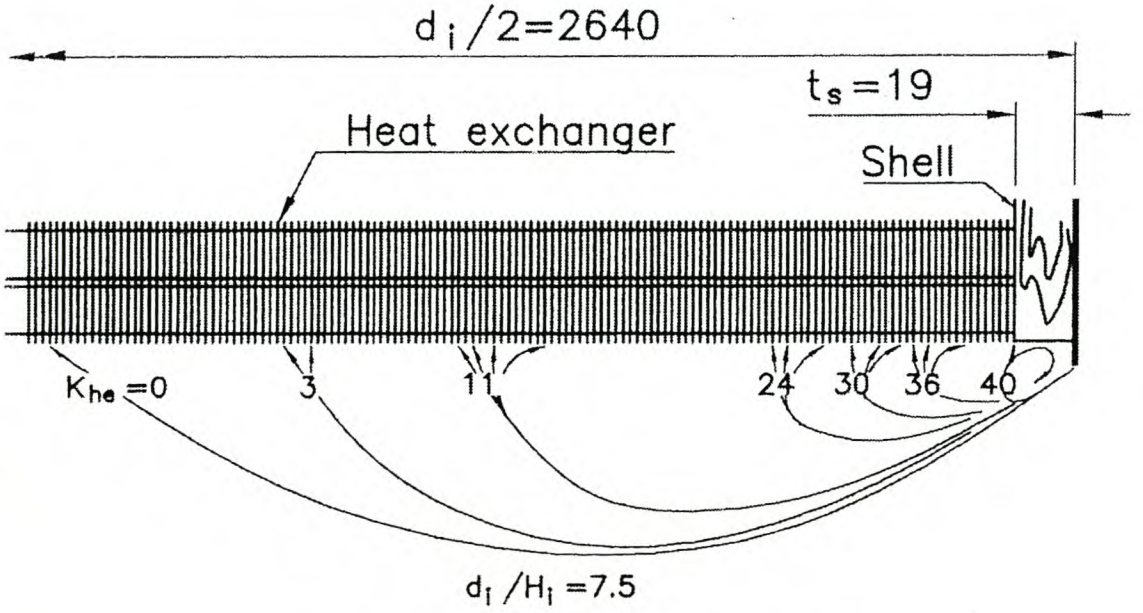

Fig. 7.3.6 Flow Patterns at Tower Inlet

Terblanche measured the velocity distribution through the heat exchanger and found various degrees of backflow occurring in the heat exchanger near the inlet of the tower. The ineffective region, region of backflow, increases as the heat exchanger loss coefficient decreases. For a dry-cooling tower where the loss coefficient is relatively high and the ratio d_i/H_i is relatively small, the ineffective area is usually negligible.

The effective approximate diameter of the fill or heat exchanger, d_{ie}, is given by

$$\frac{d_{ie}}{d_i + 2t_s} = 1.2549 - 0.21069\ \ell n\left(\frac{d_i + 2t_s}{H_i}\right) + \left[0.050673\ \ell n\left(\frac{d_i + 2t_s}{H_i}\right) - 0.052085\right]\ell n\ K_{he} \qquad (7.3.11)$$

where

t_s = the thickness of the square-edged (90°) shell at its base according to Oosthuizen

This equation is valid for

- $5.35 \leq (d_i + 2t_s)/H_i \leq 16$
- $3.6 \leq K_{he} \leq 49$
- $d_{ie}/d_i \leq 1$

By rounding off the inlet to a cooling tower shell, the reduction in effective frontal area can be reduced. The approximate effective diameter can be expressed as

$$\frac{d_{ie}}{d_i} = 1.27 - 0.16722\ \ell n\left(\frac{d_i}{H_i}\right) + \left[0.043653\ \ell n\left(\frac{d_i}{H_i}\right) - 0.062658\right]\ell n\ K_{he} \qquad (7.3.12)$$

This equation is valid for

- $5.35 \leq d_i/H_i \leq 16$
- $3.6 \leq K_{he} \leq 49$
- $r_i/d_i = 0.01$
- $d_{ie}/d_i \leq 1$

Terblanche and Kröger also studied the aerodynamic inlet losses obtained when the heat exchanger bundles are arranged vertically around the circumference of a dry-cooling tower. A prominent vena contracta was formed having an approximate kinetic energy coefficient of $\alpha_{evc} = 1.15$. The effective diameter of the vena contracta was a function of the d_i/H_i ratio (Fig. 7.3.7). To avoid further losses in the cooling tower itself, its diameter should be reduced from the inlet diameter to a value smaller than the diameter of the vena contracta.

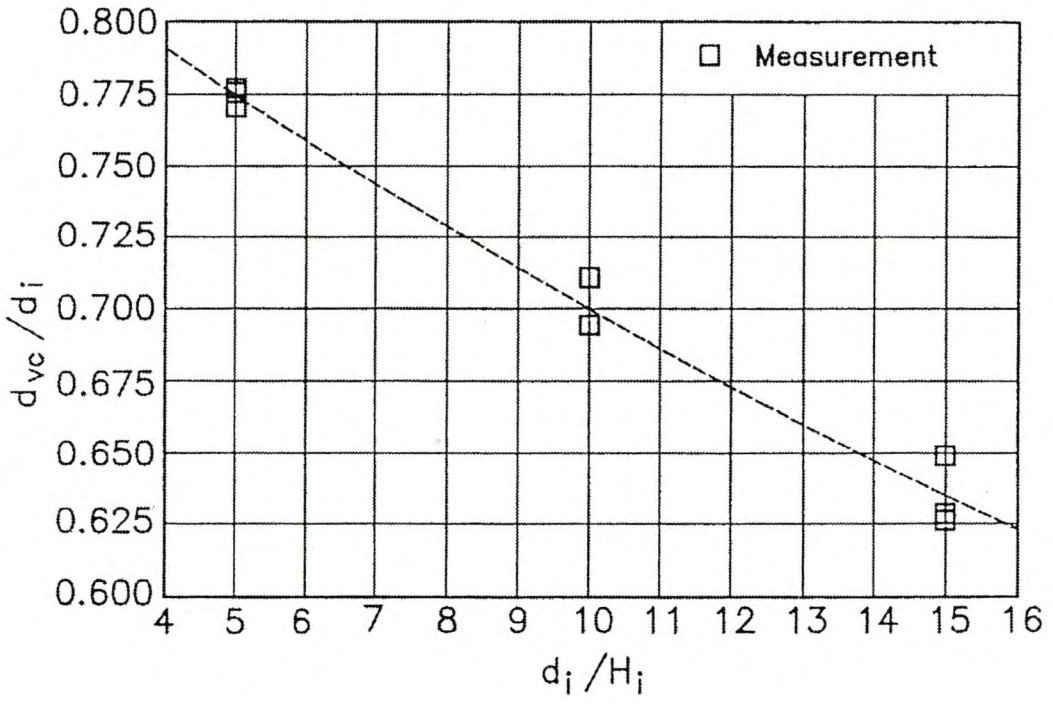

Fig. 7.3.7 Diameter of Vena Contracta

For this arrangement, the loss coefficient defined by Equation 7.3.2 is given by

$$K_{ct} = 2.21 - 0.42(d_i / H_i) + 0.091(d_i / H_i)^2 \qquad (7.3.13)$$

in the ranges

$5 \leq (d_i/H_i) \leq 15$

$5 \leq K_{he} \leq 40$

Equation 7.3.13 is independent of the heat exchanger flow resistance. No measurable reduction in loss coefficient is attained by rounding off the inlet to the heat exchangers. According to Markóczy, the flow through towers with this bundle arrangement is complex.

In a circular, counterflow, wet-cooling tower, De Villiers and De Villiers and Kröger show the type of fill and the rain zone have a measurable influence on the inlet loss coefficient. The presence of the rain zone reduces ineffective areas of the fill near the lower edge of the tower shell where separation of flow may occur and results in a more uniform air flow distribution through the fill.

In the case of an orthotropic fill, e.g., cellular film or fiber sheet fill, the inlet loss coefficient, K_{ct}, is the same as that for a dry-cooling tower.

For a counterflow cooling tower operating in the absence of a rain zone with an isotropic fill, e.g., splash or trickle type fill, the loss coefficient is

$$K_{ct(norz)} = 0.011266 \exp(0.093 d_i / H_i) K_{fi}^2$$

$$- 0.3105 \exp(0.1085 d_i / H_i) K_{fi} - 1.7522 + 4.5614 \exp(0.131 d_i / H_i)$$

$$+ \sinh^{-1}[\{(10970.2 \exp(-0.2442 K_{fi})$$

$$+ 1391.3) / (d_i / H_i - 15.7258) + 1205.54 \exp(-0.23 K_{fi})$$

$$+ 109.314\} \times \{2 r_i / d_i - 0.01942 / (d_i / H_i - 27.929) - 0.016866\}] \quad (7.3.14)$$

This is valid for

- $7.5 \leq d_i/H_i \leq 15$
- $5 \leq K_{fi} \leq 25$
- $0 \leq r_i/d_i \leq 0.02$

The presence of the rain zone tends to reduce the previously mentioned inlet loss coefficients by the same amount for both orthotropic or isotropic fills. By multiplying $K_{ct(norz)}$ by the following correction factor, the effective wet-cooling tower inlet loss coefficient is obtained.

$$C_{rz} = [0.2394 + 80.1\{0.0954/(d_i / H_i) + d_d\} \exp(0.395 G_w / G_a)$$

$$- 0.3195(G_w / G_a) - 966\{d_d / (d_i / H_i)\} \exp(0.686 G_w / G_a)]$$

$$\times (1 - 0.06825 G_w) K_{fi}^{0.09667} \exp\{8.7434(1/d_i - 0.01)\} \quad (7.3.15)$$

This correction factor is valid in these ranges:

- $7.5 \leq d_i/H_i \leq 20$
- $3 \leq d_d \leq 6\text{mm}$
- $1 \leq G_w \leq 3\ \text{kg/m}^2\text{s}$
- $1.2 \leq G_a \leq 3.6\ \text{kg/m}^2\text{s}$
- $80 \leq d_i \leq 120\ \text{m}$
- $5 \leq K_{fi} \leq 25$

where $G_a = \rho_a v_i$ and $G_w = \rho_w v_w$.

Example 7.3.1

Determine the heat rejection rate of a natural-draft, hyperbolic, concrete, dry-cooling tower shown in Figure 7.1.1, if m_w = 4390 kg/s and hot water enters at T_{wi} = 61.45 °C. The diameter of the upper section of the tower is constant.

Ambient conditions:

- Air temperature at ground level: T_{a1} = 15.6 °C (288.75 K)
- Wetbulb temperature at ground level: T_{wb} = 0°C (essentially dry air)
- Atmospheric pressure at ground level: p_{a1} = 84600 N/m^2
- Ambient temperature gradient: dT_a/dz = -0.00975 K/m from ground level

Cooling tower specifications:

- Tower height: H_5 = 120.0 m
- Tower inlet height: H_3 = 13.67 m
- Tower inlet diameter: d_3 = 82.958 m
- Tower outlet diameter (throat): d_5 = 58.0 m
- Number of tower supports: n_{ts} = 60
- Length of tower support: L_{ts} = 15.78 m

- Diameter of tower support: d_{ts} = 0.5 m
- Drag coefficient of support: C_{Dts} = 2.0
- Thickness of the square-edged (90°) shell at the inlet to the tower: t_s = 0.8 m

An extruded bi-metallic finned tube similar to that described in Example 5.4.2 is employed with performance characteristics shown in Figures 5.6.6. and 5.6.7. The bundles are arranged in the form of A-frames in a radial pattern (Fig. 1.2.15c).

Finned tube bundle specifications:

- Hydraulic diameter of tube: d_e = 0.0216 m
- Relative surface roughness: $\varepsilon/d_e = 5.24 \times 10^{-4}$
- Inside area of tube per unit length: A_{ti} = 0.0679 m
- Inside cross-sectional flow area: $A_{ts} = 3.664 \times 10^{-4}$ m^2
- Length of finned tube: L_t = 15.0 m
- Effective length of finned tube: L_{te} = 14.4 m (length of finned tube—ineffective length due to obstructions on air side)
- Number of tube rows: n_r = 4
- Number of tubes per bundle: n_{tb} = 154
- Number of water passes: n_{wp} = 2
- Number of bundles: n_b = 142
- Total effective frontal area of bundles: A_{fr} = 4625.3376 m^2
- Apex angle of A-frame: $2\theta = 61.5°$
- Ratio of minimum to free stream flow area: σ = 0.433
- Inlet contraction loss coefficient: K_{ci} = 0.05

Since the bundles do not cover the entire base of the tower, flow distortions due to downstream losses are reduced, and the characteristic heat transfer parameter for normal flow given in example 5.4.2 can be employed, i.e.,

$$Ny = 383.617313\, Ry^{0.523761}$$

Similarly, the loss coefficient for isothermal normal flow conditions listed in example 5.4.3 and shown in Figure 5.6.6 can be expressed as

$$K_{he} = 1383.94795\, Ry^{-0.332458}$$

The loss coefficient due to the heat exchanger supports, K_{hes}, is negligible.

Solution

This problem can only be solved by following an iterative procedure. As a first approximation, assume the cooling air leaving the heat exchanger is at a theoretical maximum temperature equal to the inlet water temperature, i.e., T_{a4} = 61.45°C (334.6K). This outlet air temperature will cause the maximum possible amount of air to flow through the tower.

According to Equation 7.1.15, the air density after the heat exchanger is

$$\rho_{a4} \approx 84600/(287.08 \times 334.6) = 0.88073\ \text{kg/m}^3$$

According to Equation 7.1.4, the air temperature before the heat exchanger is

$$T_{a3} \approx 288.75 - 0.00975 \times 13.67 = 288.6167\text{K}\ (15.4667^\circ\text{C})$$

From Equation 7.1.16, the density before the heat exchanger is

$$\rho_{a3} \approx 84600/(287.08 \times 288.62) = 1.02105\ \text{kg/m}^3$$

The mean density through the heat exchanger follows from Equation 7.1.17:

$$1/\rho_{a34} = 0.5(1/1.02105 + 1/0.88073) = 1.05741\ \text{m}^3/\text{kg}$$

or

$$\rho_{a34} = 0.94571\ \text{kg/m}^3$$

The arithmetic mean air temperature through the heat exchanger is

$$T_{a34} = 0.5(T_{a3} + T_{a4}) = 0.5(15.47 + 61.45) = 38.46^\circ\text{C}\ (311.61\text{K})$$

The dynamic viscosity of dry air at this temperature follows from Equation A.1.3:

$$\mu_{a34} = 1.9 \times 10^{-5} \text{ kg/sm}$$

The pressure at the top of the cooling tower $p_5 \approx p_6$ is obtained from Equation 7.1.6.

$$p_{a6} = p_{a1}(1 - 0.00975\ H_5 / T_{a1})^{3.5} = 84600(1 - 0.00975 \times 120/288.75)^{3.5}$$

$$= 83406.28 \text{ N/m}^2$$

With this value, the density of the air at the top of the tower can be determined from Equation 7.1.11.

$$\rho_{a5} = 83406.28/[287.08\{334.6 - 0.00975(120 - 15.61)\}] = 0.871 \text{ kg/m}^3$$

where, for the A-frame bundle arrangement, H_4 is approximately

$$H_4 = H_3 + \frac{A_{fr}}{n_b L_{te}} \cos\theta = 13.67 + \frac{46253376}{142 \times 14.4} \cos\left(\frac{61.5}{2}\right) = 15.61\text{m}$$

Neglect all flow resistances other than the loss due to the heat exchanger bundles under normal isothermal flow conditions to obtain explicitly an approximate initial value for the air mass flow rate through the cooling tower. In a dry-cooling tower, this resistance is usually larger than the sum of all other resistances listed in Equation 7.1.14. The approximate driving potential is given by Equation 7.1.5. If it is assumed that $H_3 \approx H_4$, find

$$K_{he}(m_a / A_{fr})^2 = 2\rho_{a34}(\rho_{a3} - \rho_{a4})\, g\, (H_5 - H_4)$$

$$= 2 \times 0.94571(1.02105 - 0.88073)9.8(120 - 15.61) = 271.541 \text{ kg}^2/\text{s}^2\text{m}^4$$

For normal flow through the specified heat exchanger,

$$K_{he} = 1383.94795(m_a/\mu_{a34} A_{fr})^{-0.332458} = 37.282(m_a/A_{fr})^{-0.332458}$$

thus

$$(m_a / A_{fr})^{1.667542} = 7.2827$$

or

$$m_a = (7.2827)^{0.59967} \text{ x } 4625.3376 = 15213.68 \text{ kg/s}$$

This flow rate will be considerably larger than the true flow rate due to the high air temperature assumed at the outlet of the heat exchanger. This results from high buoyancy and the fact that all resistances were neglected other than the heat exchanger under normal flow conditions. Also, the value of m_a will not satisfy Equations 3.5.6 and 3.5.16 for this particular heat exchanger.

If the more rigorous draft Equation 7.1.14 is used and the air mass flow rate is reduced in subsequent iterations, a value of the mass flow rate can be found that will satisfy the energy and the draft equations.

It will now be verified that a value of m_a = 10285.151 kg/s will satisfy the previous equations and will result in an air outlet temperature after the heat exchanger of

$$T_{a4} = 47.09708^{\circ}\text{C (320.24708K)}$$

and a water outlet temperature of

$$T_{wo} = 43.59495^{\circ}\text{C (316.74495 K).}$$

The mean air temperature through the heat exchanger under these conditions is

$$T_{a34} = 0.5(15.4667 + 47.09708) = 31.28189^{\circ}\text{C}$$

The properties of dry air at this temperature may be determined according to the equations given in appendix A.1, i.e.,

- Density: ρ_{a34} = 0.968004 kg/m^3
- Specific heat: c_{pa34} = 1007.1205 J/kgK
- Dynamic viscosity: μ_{a34} = 1.8672079 x 10^{-5} kg/ms
- Thermal conductivity: k_{a34} = 0.0265638 W/mK
- Prandtl number: Pr_{a34} = 0.7079204

According to Equation 3.5.6, the heat transfer to the air stream is

$$Q = 10285.151 \text{ x } 1007.1205 \text{ x } (47.09708 - 15.4667) = 327.639 \text{ x } 10^6 \text{ W}$$

The air-side characteristic flow parameter defined by Equation 5.4.11 is

$$Ry = \frac{m_a}{\mu_{a34} A_{fr}} = \frac{10285.151}{1.8672079 \text{ x } 10^{-5} \text{ x } 4625.3376} = 119089.803 \text{m}^{-1}$$

The corresponding heat transfer parameter for the heat exchanger specified is

$$Ny = 383.61731 \text{ x } (119089.803)^{0.523761} = 174760.525 \text{ m}^{-1}$$

This parameter is based on heat exchanger bundle tests in which a maximum number of finned tubes are installed in the bundle. In the actual cooling tower bundle, it is not practical to install half-tubes at the bundle ends, and a correction is made when determining the effective heat transfer coefficient according to Equation 5.4.13, i.e.,

$$h_{ae} A_a = k_{a34} \text{Pr}_{a34}^{0.333} A_{fr} Ny(n_{tb\ actual} / n_{tb\ maximum})$$

$$= 0.0265638 \text{ x } 0.7079204^{0.333} \text{ x } 4625.3374 \text{ x } 174760.525 \text{ x } [154/(154 + 2)]$$

$$= 18893738.37 \text{ W/K}$$

The arithmetic mean water temperature is

$$T_w = 0.5 \ (T_{wi} + T_{wo}) = 0.5 \ (61.45 + 43.59495) = 52.5224^{\circ}\text{C} \ (325.6724 \text{ K})$$

According to appendix A.4 the corresponding water properties are:

- Density: $\rho_w = 986.966 \text{ kg/m}^3$
- Specific heat: $c_{pw} = 4179.938 \text{ J/kgK}$
- Dynamic viscosity: $\mu_w = 5.216093 \text{ x } 10^{-4} \text{ kg/ms}$
- Thermal conductivity: $k_w = 0.645592 \text{ W/mK}$
- Prandtl number: $Pr_w = 3.377203$

According to Equation 3.5.6, the heat given off by the water stream is

$$Q = 4390 \text{ x } 4179.938 \text{ x } (61.45 - 43.59495) = 327.639 \text{ x } 10^6 \text{ W}$$

This value compares very well with the calculated value of the heat transferred to the air stream.

The Reynolds number for the water flowing inside the pipes is

$$Re_w = \frac{\rho_w v_w d_e}{\mu_w} = \frac{m_w n_{wp} d_e}{A_{ts} n_{tb} n_b \mu_w}$$

$$= \frac{4390 \text{ x } 2 \text{ x } 0.0216}{3.664 \text{ x } 10^{-4} \text{ x } 154 \text{ x } 142 \text{ x } 5.216093 \text{ x } 10^{-4}} = 45377.275$$

The corresponding average water velocity in the heat exchanger tubes is

$$v_w = \frac{m_w \ n_{wp}}{\rho_w \ A_{ts} \ n_{tb} \ n_b} = \frac{4390 \text{ x } 2}{986.966 \text{ x } 3.664 \text{ x } 10^{-4} \text{ x } 154 \text{ x } 142} = 1.11027 \text{ m/s}$$

The friction factor inside the tube is, according to Equation 2.2.14,

$$f_{Dw} = 0.3086/[\log_{10}\{6.9/45377.275 + (5.24 \text{ x } 10^{-4}/3.7)^{1.11}\}]^2 = 0.022698$$

The frictional pressure drop in the tubes is calculated by using Equation 2.2.2.

$$\Delta p_{fw} = f_{Dw} \frac{L_t n_{wp}}{d_e} \frac{\rho_w v_w^2}{2} = 0.022698 \frac{15 \text{ x } 2 \text{ x } 986.966 \text{ x } 1.11027^2}{0.0216 \text{ x } 2}$$

$$= 6948.76 \text{ W/m}^2$$

According to Equation 3.2.29, the heat transfer coefficient inside the tube is

$$h_w = \frac{0.645592 \text{ x } 0.022698 \text{ x } (45377.275 - 1000) \text{ x } 3.377203 \left[1 + (0.0216/14.4)^{0.67}\right]}{8 \text{ x } 0.0216 \left[1 + 12.7 (0.022698/8)^{0.5} \left(3.377203^{0.67} - 1\right)\right]}$$

$$= 6948.76 \text{ W/m}^2$$

The total surface area on the water side is

$$A_w = A_{ti} L_{te}\, n_{tb} n_b = 0.0679 \text{ x } 14.4 \text{ x } 154 \text{ x } 142 = 21381.6557 \text{ m}^2$$

where

L_{te} = effective finned tube length

It follows that:

$$UA = \left(\frac{1}{h_{ae}\ A_a} + \frac{1}{h_w\ A_w}\right)^{-1} = \left(\frac{1}{18893738.37} + \frac{1}{6948.76\ x\ 21381.6557}\right)^{-1}$$

$$= 16762169.05 \text{ W/K}$$

According to Equation 3.5.8, the logarithmic mean temperature difference is

$$\Delta T_{\ell m} = \frac{(61.45 - 47.09708) - (43.59495 - 15.4667)}{\ell n[(61.45 - 47.09708)/(43.59495 - 15.4667)]} = 20.474°\text{C}$$

According to Table B.8, the temperature correction factor for a two-pass, crossflow heat exchanger is given by

$$F_T = 1 - \sum_{i=1}^{4} \sum_{k=1}^{4} a_{i,k}\ (1 - \phi_3)^k\ \sin[2i \arctan(\phi_1 / \phi_2)]$$

where

$$\phi_1 = \frac{T_{wi} - T_{wo}}{T_{wi} - T_{ai}} = \frac{334.6 - 316.74495}{334.6 - 288.6167} = 0.38829$$

$$\varphi_2 = \frac{T_{ao} - T_{ai}}{T_{wi} - T_{ai}} = \frac{320.24708 - 288.6167}{334.6 - 288.6167} = 0.687866$$

$$\phi_3 = \frac{\phi_1 - \phi_2}{\ell n[(1 - \phi_2)/(1 - \phi_1)]} = \frac{0.38829 - 0.687866}{\ell n[(1 - 0.687866)/(1 - 0.38829)]} = 0.44525$$

The value of constants $a_{i,k}$ are, according to Table B.8, shown in Table 7.3.1.

$a_{i,k}$	i = 1	2	3	4
k = 1	-6.05×10^{-1}	2.31×10^{-2}	2.94×10^{-1}	1.98×10^{-2}
2	4.34×10^{0}	5.9×10^{-3}	-1.99×10^{0}	-3.05×10^{-1}
3	-9.72×10^{0}	-2.48×10^{-1}	4.32×10^{0}	8.97×10^{-1}
4	7.54×10^{0}	2.87×10^{-1}	-3.00×10^{0}	-7.31×10^{-1}

Table 7.3.1 Constants in Temperature Correction Equation from Table B.8

$$F_T = 1 - \sum_{i=1}^{4} \sum_{k=1}^{4} a_{i,k} (1 - 0.44525)^k \sin\left[2i \arctan \frac{038829}{0.687866}\right] = 0.9542649$$

The heat transfer rate may be determined according to Equation 3.5.16, i.e.,

$$Q = 16762169.05 \times 0.9542649 \times 20.474 = 327.49 \times 10^6 \text{ W}$$

This value compares well with the transfer rates calculated according to Equation 3.5.6.

To achieve these values, it was assumed that the entire air-side heat transfer surface is effective, i.e., air flow distortions due to separation at the lower edge of the tower shell are negligible. The correctness of this assumption will be confirmed.

To evaluate the draft Equation 7.1.14, the various loss coefficients have to be determined.

For non-isothermal flow through an array of A-frames, the heat exchanger loss coefficient is, according to Equation 5.6.16,

$$K_{he\theta} = K_{he} + \frac{2\rho_{a4}\,(1/\sin\rho_m - 1)}{(\rho_{a4} + \rho_{a3})}\left[\left(\frac{1}{\sin\theta_m}\right) + 2K_{ci}^{0.5}\right] + \frac{2\rho_{a3}\,K_d}{(\rho_{a4} + \rho_{a3})}$$

where

ρ_{a4} = the density of the air after the heat exchanger, i.e.,

$$\rho_{a4} \approx \frac{84600}{287.08 \times 320.24708} = 0.9202 \text{ kg/m}^3$$

According to Equation 7.1.17, the mean air density through the heat exchanger is

$$\rho_{a34} = 2/(1/1.02105 + 1/0.9202) = 0.968005 \text{ kg/m}^3$$

This value was previously obtained by evaluating ρ_{a34} at the arithmetic mean temperature through the heat exchanger.

The ratio of the minimum flow area to the free flow area is given as 0.433. This value may also be calculated according to values obtained in Example 5.4.2, i.e.,

$$\sigma = A_c/A_{fr} = 0.20719/0.4785 = 0.433$$

According to Equation 5.4.23 for non-isothermal normal flow,

$$K_{he} = \frac{1383.94795}{119089.803^{0.332458}} + \frac{2}{0.433^2}\left(\frac{1.02105 - 0.9202}{1.02105 + 0.9202}\right) = 28.9729$$

From Equation 5.6.13, it follows that the mean inlet flow angle is

$$\theta_m = 0.0019(61.5/2)^2 + 0.9133(61.5/2) - 3.1558 = 26.725^\circ$$

The downstream loss coefficient is found from Equation 5.6.10.

$$K_d = \exp\,[5.488405 - 0.2131209\,(61.5/2) + 3.533265 \times 10^{-3}\,(61.5/2)^2$$
$$- 0.2901016 \times 10^{-4}\,(61.5/2)^3] = 4.1886$$

Substitute these values into the expression for the bundle loss coefficient, and find

$$K_{he\theta} = 28.9729 + \left(\frac{2 \times 0.9202}{0.9202 + 1.02105}\right)\left(\frac{1}{\sin 26.725} - 1\right)$$

$$\times\left[\left(\frac{1}{\sin 26.725} - 1\right) + 2 \times 0.05^{0.5}\right] + \frac{2 \times 1.02105 \times 4.1886}{(0.9202 + 1.02105)} = 35.3175$$

As shown in Figure 5.6.6, this theoretically predicted value is higher than the measured loss coefficient under oblique flow conditions through the 4-row bundle. Since the base of the tower in this example is not completely covered by bundles, the

airstream leaving the bundles will experience average downstream losses that are less than predicted theoretically for arrays of V-bundles. With $K_{he\theta} = 35.3175$, the predicted performance of the tower will tend to be conservative.

Substitute this value of $K_{he\theta}$ into Equation 7.3.11, and find the effective diameter of the tower inlet, i.e.,

$$\frac{d_{3e}}{d_3 + 2t_s} = 1.2549 - 0.21069\ell n\left(\frac{82.958 + 2 \text{ x } 0.8}{13.67}\right)$$

$$+\left[0.050673\ \ell n\left(\frac{82.958 + 2\,x\,0.8}{13.67}\right)\right.$$

$$\left. - 0.052085\right]\ell n\ 35.3175 = 1.0145$$

Since d_{3e} cannot be greater than d_3, $d_{3e} = d_3$, i.e., the entire frontal area of the heat exchanger is effective as was previously assumed.

The loss coefficient through the tower supports based on conditions at the heat exchanger is determined according to Equation 7.1.21:

$$K_{tshe} = \frac{2 \text{ x } 15.78 \text{ x } 0.5 \text{ x } 60 \text{ x } (4625.3374)^2 \text{ x } 0.968005}{(\pi \text{ x } 82.958 \text{ x } 13.67)^3 \text{ x } 1.02105} = 0.42466$$

Since $K_{he\theta} > 30$, the tower inlet loss coefficient can be determined according to Equation 7.3.7. Substitute Equation 7.3.7 into Equation 7.1.22, and find, ignoring supports,

$$K_{cthe}\left[0.072\left(\frac{82.958}{13.67}\right)^2 - 0.34\left(\frac{82.958}{13.67}\right) + 1.7\right]\frac{0.968005}{1.02105}\left(\frac{4625.3374 \text{ x } 4}{\pi \text{ x } 82.958^2}\right)^2 = 1.5886$$

To determine the contraction and expansion losses, the effective reduced flow area at the tower inlet cross section is determined according to

$$A_{e3} = A_{fr} \sin \theta = 4625.3376 \text{ x } \sin (61.5/2) = 2364.903 \text{ m}^2$$

which gives a ratio of

$$A_{e3}/A_3 = 2364.903 \text{ x } 4/(\pi \text{ x } 82.958^2) = = 0.43753$$

The approximate contraction loss coefficient into the array of A-frames is obtained from Equation 7.1.23 with σ_c being determined according to Equation 2.3.10.

$$\sigma_c = 0.6144517 + 4.566493 \times 10^{-2} \times 0.43753 - 0.336651 \times 0.43753^2$$
$$+ 0.4082743 \times 0.43753^3 + 2.670410 \times 0.43753^4 - 5.963169 \times 0.43753^5$$
$$+ 3.558944 \times 0.43753^6 = 0.631397$$

Substitute this value in Equation 7.1.25, and find

$$K_{ctche} = (1 - 2/0.631397 + 1/0.631397^2)(0.968005/1.02105)(4625.3376/2364.903)^2$$
$$= 1.2359$$

The expansion loss coefficient follows from Equation 7.1.26:

$$K_{ctehe} = (1 - 0.43753)^2 \ (0.968005/0.9202) \ (4625.3376/2364.903)^2 = 1.27308$$

The pressure at the top of the cooling tower, $p_5 \approx p_6$, is obtained from Equation 7.1.6:

$$p_{a6} = 84600 \ (1 - 0.00975 \times 120/288.75)^{3.5} = 83406.283 \ N/m^2$$

With this value, the density of the air at the top of the tower can be determined from Equation 7.1.11.

$$\rho_{a5}=83406.283/[287.08\{320.24708–0.00975(120–15.61)\}]=0.910108 \ kg/m^3$$

Similarly, the ambient air density at the outlet height of the tower is determined from Equation 7.1.12.

$$\rho_{a6}= 83406.283/287.08[288.75 - 0.00975 \times 120]= 1.010269 \ kg/m^3$$

The tower outlet loss coefficient is calculated from Equation 7.1.9.

$$K_{to} = -0.28 \times 3.41913 + 0.04 \times 3.41913^{1.5} = -0.70446$$

where

$$Fr_D^{-1} = \frac{0.910108(1.010269 - 0.910108) \times 9.8 \times 58}{[10285.151 \times 4/(\pi \times 58^2)]^2} = 3.41913$$

Evaluate the left side of Equation 7.1.14.

$$84600\left[\{1-0.00975(13.67+15.61)/(2\text{ x }288.75)\}^{3.5}\right.$$

$$\text{x}\{1-0.00975(120-13.67/2-15.61/2)/320.24708\}^{3.5}$$

$$\left.-(1-0.00975\text{ x }120/288.75)^{3.5}\right]=103.070\text{ N/m}^2$$

Similarly for the right side,

$$(0.42466+1.5886+1.2359+35.3175+1.27308)(0.5/0.968005)$$

$$\text{x}\,(10285.151/4625.3374)^2\text{ x}\,[1-0.00975\,(120-13.67$$

$$/2-15.61/2)/320.24708]^{3.5}$$

$$+0.5\,(1-0.704466)\text{x}\left[10285.151\text{ x }4/(\pi\text{ x }58^2)\right]^2/0.910108=103.074\text{ N/m}^2$$

The values obtained for the two sides of Equation 7.1.14 are practically the same, which means the draft equation is satisfied. Note the heat exchanger loss coefficient of 35.3175 given in the previous relation is large compared to all other losses.

Example 7.3.2

Determine the heat rejection rate and the loss in cooling water due to evaporation in a hyperbolic, natural-draft, counterflow, wet-cooling tower shown in Figure 7.2.1.

- The water mass flow rate is m_w = 12500 kg/s.
- The water inlet temperature $T_{wi} = T_{w5}$ = 40°C (313.15 K).

The water and air flow distribution through the fill is assumed to be uniform. The inside diameter of the upper section of the tower is constant. The tower shell has a rounded inlet with r_i/d_3 = 0.02.

Ambient conditions:

- Air temperature at ground level: T_{a1} = 15.45 °C (288.6K)
- Wetbulb temperature at ground level: T_{wb} = 11.05 °C (284.2K)
- Atmospheric pressure: p_{a1} = 84100 N/m2
- Ambient temperature gradient: d_{Ta}/dz = – 0.00975 K/m from ground level

Cooling tower specifications:

- Tower height: H_6 = 147 m
- Tower inlet height: H_3 = 10 m
- Tower inlet diameter: d_3 = 104.5 m
- Tower outlet diameter: d_6 = 60.85 m
- Number of tower supports: n_{ts} = 72
- Length of tower supports: L_{ts} = 11.6 m
- Diameter of support: d_{ts} = 0.8 m
- Drag coefficient of tower support (round): C_{Dts} = 1.0
- Shell thickness (inlet): t_s = 1.0 m

Fill specifications:

The cooling tower is fitted with an expanded metal fill (L_{fi} = 2.504 m) described in Example 4.3.1 and for which the performance characteristics are:

Transfer coefficient

$$h_{dfi}\, a_{fi}/G_w = 0.25575\, G_w^{-0.094}\; G_a^{0.6023}$$

Loss coefficient

$$K_{fdm1} = 1.851\, G_w^{1.2752}\; G_a^{-1.0356}$$

These correlations are most reliable where the mean cooling water temperature

$$T_{wm} \approx 35^{\circ}\mathrm{C}$$

and the mean air temperature

$$T_{am} \approx 17.5^{\circ}\text{C}$$

The frontal area of the fill is

$$A_{fr} = 8300 \text{ m}^2$$

Other specifications:

- Depth of spray zone above fill: $L_{sp} = 0.5$ m
- Mean drop diameter in rain zone: $d_d = 0.0035$ m
- Loss coefficient for contraction and fill supports based on A_{fr}: $K_{fs} + K_{ctc} = 0.5$
- Loss coefficient for water distribution system: $K_{wd} = 0.5$
- Kinetic energy coefficient at cooling tower outlet: $\alpha_{e6} = 1.01$

The loss coefficient for the drift eliminator (type c) is given by Equation 4.7.2.

Solution

This problem can only be solved by following an iterative procedure to find a solution that will satisfy both the energy and the draft equations. The choice of an air-vapor mass flow rate through the fill of

$$m_{av15} = 16810.89 \text{ kg/s}$$

will satisfy these equations.

The corresponding pressure is

$$p_{a5} = 83937.7 \text{ N/m}^2$$

The air temperature is

$$T_{a5} = 26.4375^{\circ}\text{C or } 299.5875 \text{ K}$$

immediately after the drift or droplet eliminators.

The mean temperature of the recooled water in the basin or pond is

$$T_{wo} = 21.3885^{\circ}\text{C or } 294.5385 \text{ K.}$$

The pressure at the tower outlet is

$$p_{a6} = 82650.59 \text{ N/m}^2.$$

In the following numerical example, the correctness of these values will be confirmed.

At the specified air inlet drybulb temperature of

$$T_{a1} = 288.6 \text{ K}$$

and wetbulb temperature of

$$T_{wb} = 284.2 \text{ K}$$

find the following thermophysical properties employing the equations given in appendix A.

- Density of air-vapor using Equation A.3.1.

$$\rho_{av1} = 1.0101 \text{ kg/m}^3$$

- Humidity ratio of air using Equation A.3.5.

$$w_1 = 0.008127 \text{ kg/kg}$$

- Viscosity of the air vapor mixture using Equation A.3.3.

$$\mu_{av1} = 1.7857 \text{ x } 10^{-5} \text{ kg/ms}$$

The enthalpy of the inlet air is found using Equation A.3.6b with

$$c_{pa1} = 1006.44 \text{ J/kgK}$$

and

$$c_{pv1} = 1869.2 \text{ J/kgK}$$

being evaluated at

$$(T_{a1} + 273.15)/2 = (288.6 + 273.15)/2 = 280.875 \text{ K}$$

using Equations A.1.2 and A.2.2 respectively. The latent heat is found to be

$$i_{fgwo} = 2.5016 \text{ x } 10^6 \text{ J/kg K}$$

using Equation A.4.5 at 273.15 K.

With these values, find

$$i_{ma1} = 36114.71 \text{ J/kg dry air}$$

If the air is assumed to be saturated immediately after the drift or droplet eliminator, the wetbulb temperature at (5) will be equal to the given drybulb temperature T_{a5} = 299.5875 K at this elevation. The corresponding thermophysical properties at (5) can be determined using the equations given in appendix A.

The saturated vapor pressure according to Equation A.2.1 is

$$p_{v5} = 3448.436 \text{ N/m}^2$$

- Humidity ratio using Equation A.3.5

$$w_5 = 0.02679 \text{ kg/kg}$$

- Density of air-vapor using Equation A.3.1

$$\rho_{av5} = 0.96072 \text{ kg/m}^3$$

- Dynamic viscosity of air using Equation A.1.3

$$\mu_{a5} = 1.84 \times 10^{-5} \text{ kg/ms}$$

- Dynamic viscosity of vapor using Equation A.2.3

$$\mu_{v5} = 1.0033 \times 10^{-5} \text{ kg/ms}$$

- Dynamic viscosity of air-vapor using Equation A.3.3

$$\mu_{av5} = 1.81732 \times 10^{-5} \text{ kg/ms}$$

The enthalpy of the saturated air at (5) is found using Equation A.3.6b with

$$c_{pa5} = 1006.5517 \text{ J/kgK and } c_{pv5} = 1873.819 \text{ J/kgK}$$

being evaluated at

$$(T_{a5} + 273.15)/2 = (299.5875 + 273.15)/2 = 286.3688 \text{ K}$$

using Equations A.1.2 and A.2.2 respectively. With these values and

$$i_{fgwo} = 2.5016 \times 10^6 \text{ J/kg K}$$

find

$$i_{mas5} = 94947.3976 \text{ J/kg dry air.}$$

The approximate harmonic mean density of the air-vapor in the fill is given by Equation 7.2.22.

$$\rho_{av15} = 2/(1/\rho_{av1} + 1/\rho_{av5}) = 2/(1/1.0101 + 1/0.96072) = 0.9848 \text{ kg/m}^3$$

The dry air mass flow rate can be determined from the following relation:

$$m_{av15} = [m_a(1 + w_1) + m_a(1 + w_5)]/2$$

or

$$m_a = 2m_{av15}/(2 + w_1 + w_5)$$

$$= 2 \text{ x } 16810.89/(2 + 0.008127 + 0.02679) = 16522.464 \text{ kg/s}$$

The respective air-vapor mass flow rates upstream and downstream of the fill are

$$m_{av1} = m_a(1 + w_1) = 16522.464(1 + 0.008127) = 16656.742 \text{ kg/s}$$

and

$$m_{av5} = m_a(1 + w_5) = 16522.464(1 + 0.02679) = 16965.046 \text{ kg/s}$$

The corresponding mass velocities are

$$G_{av15} = m_{av15}/A_{fr} = 16810.89/8300 = 2.02541 \text{ kg/m}^2\text{s}$$

$$G_a = m_a/A_{fr} = 16522.464/8300 = 1.99066 \text{ kg/m}^2\text{s}$$

$$G_{av1} = m_{av1}/A_{fr} = 16656.742/8300 = 2.00684 \text{ kg/m}^2\text{s}$$

$$G_{av5} = m_{av5}/A_{fr} = 16965.046/8300 = 2.04398 \text{ kg/m}^2\text{s}$$

According to Equation A.4.2, the specific heat of water is

$$c_{pwm} = 4178.32 \text{ J/kg}$$

at the mean water temperature of

$$(T_{wi} + T_{wo})/2 = (313.15 + 294.5385)/2 = 303.8443 \text{ K}$$

At the mean outlet temperature of the water $T_{wo} = 294.5385$ K, find

Density of water using Equation A.4.1

$$\rho_{wo} = 997.867 \text{ kg/m}^3$$

Surface tension using Equation A.4.7

$$\sigma_{wo} = 0.07256 \text{ N/m}$$

Based on the frontal area of the fill, the mass velocity for the water is

$$G_w = m_w/A_{fr} = 12500/8300 = 1.50602 \text{ kg/m}^2\text{s}$$

The specified loss coefficient due to the fill support structure and the contraction loss into the fill is referred to the mean density through the fill, i.e.,

$$K_{fsfi} + K_{ctcfi} = 0.5(\rho_{av15}/\rho_{av1})(m_{av1}/m_{av15})^2$$
$$= 0.5(0.9848/1.0101)(16656.742/16810.89)^2 = 0.47857$$

According to the specified fill loss coefficient

$$K_{fdm} = 1.851\ L_{fi}\ G_w^{1.2752}\ G_a^{-1.0356} = 1.851 \text{ x } 2.504 \text{ x } 1.50602^{1.2752} \text{ x } 1.99066^{-1.0356}$$

$$= 3.82976$$

From the note at the end of Example 4.3.1, it follows that the actual fill loss coefficient applicable to the cooling tower is given by

$$K_{fi} = K_{fdm} + \left(G_{av5}^2/\rho_{av5} - G_{av1}^2/\rho_{av1}\right)/\left(G_{av15}^2/\rho_{av15}\right)$$

$$= 3.82976 + \left(2.04398^2/0.96072 - 2.00684^2/1.0101\right)/\left(2.02541^2/0.9848\right)$$

$$= 3.91657$$

The expansion loss coefficient after the fill follows from Equation 7.1.26.

$$K_{ctefi} = (1 - A_{fr}/A_3)^2(\rho_{av15}/\rho_{av5})(m_{av5}/m_{av15})^2$$

$$= \left[1 - 8300 \text{ x } 4/(\pi \text{ x } 104.5^2)\right]^2(0.9848/0.96072)(16965.046/16810.89)^2$$

$$= 0.001087$$

The loss through the spray zone above the fill is given by Equation 7.2.20.

$$K_{spfi} = L_{sp}\left[0.4\left(G_w / G_a\right)+1\right]\left(\rho_{av15} / \rho_{av5}\right)\left(m_{av5} / m_{av15}\right)^2$$

$$= 0.5\left[0.4\left(1.50602 / 1.99066\right)+1\right]\left(0.9848 / 0.96072\right)\left(16965.046 / 16810.89\right)^2$$

$$= 0.679934$$

For the water distribution system, it follows from the specified loss coefficient that

$$K_{wdfi} = 0.5\left(\rho_{av15} / \rho_{av5}\right)\left(m_{av5} / m_{av15}\right)^2$$

$$= 0.5\left(0.9848 / 0.96072\right)\left(16965.046 / 16810.89\right)^2 = 0.521975$$

From Equation 4.7.2, the loss coefficient for the specified type c drift eliminator based on fill conditions is

$$K_{defi} = 27.4892\ Ry^{-0.14247}\left(\rho_{av15} / \rho_{av5}\right)\left(m_{av5} / m_{av15}\right)^2$$

$$= 27.4892\left[m_{av5} / \left(\mu_{av5}\ A_{fr}\right)\right]^{-0.14247}\left(\rho_{av15} / \rho_{av5}\right)\left(m_{av5} / m_{av15}\right)^2$$

$$= 27.4892\left[16965.046 / \left(1.81732 \times 10^{-5} \times 8300\right)\right]^{-0.14247}$$

$$\times\ \left(0.9848 / 0.96072\right)\left(16965.046 / 16810.89\right)^2 = 5.472924$$

The sum of these loss coefficients in the vicinity of the fill is

$$\left[K_{fs} + K_{ctc} + K_{fi} + K_{cte} + K_{sp} + K_{wd} + K_{de}\right]_{fi} = 0.47857 + 3.91657$$

$$+ 0.001087 + 0.679934 + 0.521975 + 5.472924 = 11.07106$$

Substitute the sum of these coefficients (the effective fill resistance) into Equation 7.3.12, and find the effective fill diameter in the absence of a rain zone.

$$d_{3e} = d_3\left[1.27 - 0.16722\,\ell n\left(d_3 / H_3\right) + \{0.043653\,\ell n\left(d_3 / H_3\right) - 0.062658\}\right.$$

$$\left. \text{x } \ell n\left(K_{fs} + K_{ctc} + K_{fi} + K_{cte} + K_{sp} + K_{wd} + K_{de}\right)_{fi}\right]$$

$$= 104.5\left[1.27 - 0.16722\,\ell n\left(104.5 / 10\right) + \{0.043653\,\ell n\left(104.5 / 10\right)\right.$$

$$\left. - 0.062658\}\,\ell n\left(11.07106\right)\right] = 101.7\,\text{m}$$

The corresponding effective frontal area is

$$A_{fre} = \pi d_{e3}^{\,2} / 4 = \pi \text{ x } 101.7^2 / 4 = 8123.3\,\text{m}^2$$

According to De Villiers, the air flow pattern at the inlet to a counterflow wet-cooling tower is measurably influenced by the droplets in the rain zone particularly near the lower edge of the shell. A three-dimensional, computational, fluid dynamics simulation of the tower shows the "dead" or ineffective fill volume in the presence of a rain zone is about four times smaller than in the case of no rain zone. For all practical purposes, it may be assumed

$$A_{fre} = A_{fr} = 8300\text{m}^2$$

The transfer coefficients can be determined with the previous values. To find the transfer coefficient in the rain zone, use Equation 7.2.2. The *a* coefficients in the equation for the rain zone transfer and pressure drop are as follows:

$$a_\mu = 3.061 \text{ x } 10^{-6} \left[\rho_{wo}^4 \; g^9 \; / \; s_{wo}\right]^{0.25} = 3.061$$

$$\text{x } 10^{-6}\left[997.867^4 \text{ x } 9.8^9 \; / \; 0.07256\right]^{0.25} = 1.0000$$

$$a_\eta = 998.0 \; / \; \rho_{wo} = 998.0 \; / \; 997.867 = 1.0001$$

$$a_v = 73.298 \left[g^5 \; \sigma_{wo}^3 \; / \; \rho_{wo}^3 \right]^{0.25} = 73.298 \left[9.8^5 \text{ x } 0.07256^3 / 997.867^3\right]^{0.25} = 1.0008$$

$$a_L = 6.122 \left[g \; \sigma_{wo} \; / \; \rho_{wo}\right]^{0.25} = 6.122 \left[9.8 \text{ x } 0.07256 \; / \; 997.867\right]^{0.25} = 1.0003$$

Other quantities required to evaluate the rain zone transfer coefficient are:

- The humidity ratio of saturated air at T_{w1} using Equation A.3.5

$$w_{s1} = 0.019515 \text{ kg/kg}$$

- Diffusion coefficient at inlet conditions using Equation 4.1.2

$$D_1 = 2.29972 \text{ x } 10^{-5} \text{ m}^2/\text{s}$$

The Schmidt number is

$$Sc_1 = \mu_{av1}/(\rho_{av1} D_1) = 1.7857 \text{ x } 10^{-5}/(1.0101 \text{ x } 2.29972 \text{ x } 10^{-5}) = 0.7687$$

and the air-vapor velocity before the fill is

$$v_{av3} = m_{av1}/(\rho_{av1} A_{fr}) = 16656.742/(1.0101 \text{ x } 8300) = 1.9867 \text{ m/s}$$

With these values find

$$\frac{h_{drz}\, a_{rz}\, H_3}{G_w} = 12\left(\frac{D_1}{v_{av\,3}\, d_d}\right)\left(\frac{H_3}{d_d}\right)\left(\frac{p_{a1}}{R_v T_{a1}\eta_{wo}}\right) Sc_1^{0.33}\left[\ell n\left(\frac{w_{s1}+0.622}{w_1+0.622}\right)/(w_{s1}-w_1)\right]$$

$$\text{x}\left[0.90757\ a_\rho \rho_{av\,1} - 30341\ .04\, a_\mu \mu_{av\,1} - 0.37564\ + 4.04016\left[\{0.55 + 41.7215\right.\right.$$

$$\text{x}\left(a_L d_d\right)^{0.80043}\}\{0.713 + 3.741\left(a_L H_3\right)^{-1.23456}\}\{3.11\exp\left(0.15\, a_v v_{av\,3}\right) - 3.13\}$$

$$\left.\left.\text{x}\exp\left[\{5.3759\ \exp\left(-0.2092\ a_L H_3\right)\}\ell n\{0.3719\ \exp\left(0.0019055\ a_L d_3\right) + 0.55\}\right]\right]\right]$$

$$= 12\left(\frac{2.29972\ \text{x}\,10^{-5}}{1.9867\ \text{x}\ 0.0035}\right)\left(\frac{10}{0.0035}\right)\left(\frac{84100}{461.52\ \text{x}\ 288.6\ \text{x}\ 997.867}\right)0.7687^{\,0.33}$$

$$\text{x}\left[\ell n\left(\frac{0.019515\ + 0.622}{0.008127\ + 0.622}\right)/(0.019515\ - 0.008127)\right]\left[0.90757\ \text{x}\ 1.0001\right.$$

$$\text{x}\ 1.0101 - 30341\ .04\ \text{x}\ 1.7857\ \text{x}\ 10^{-5} - 0.37564\ + 4.04016\left[\{0.55 + 41.7215\right.$$

$$\left(1.0003\ \text{x}\ 0.0035\right)^{0.80043}\}\ \text{x}\ \{0.713 + 3.741\left(1.0003\ \text{x}\ 10\right)^{-1.23456}\}\{3.11\exp\left(0.15\right.$$

$$\text{x}\ 1.0008\ \text{x}\ 1.9867\ ) - 3.13\}\ \text{x}\ \exp\left[\{5.3759\ \exp\left(-0.2092\ \text{x}\ 1.0003\right.\right.$$

$$\left.\left.\text{x}\ 10)\}\ell n\{0.3719\ \exp\left(0.0019055\ \text{x}\ 1.0003\ \text{x}\ 104.5\right) + 0.55\}\right]\right] = 0.414391$$

The Merkel number applicable to the fill is specified, i.e.,

$$h_{dfi}\ a_{fi}\ L_{fi}\ /\ G_w = 0.25575\, L_{fi}\ G_w^{-0.094}\ G_a^{0.6023}$$

$$= 0.25575\ \text{x}\ 2.504\ \text{x}\, 1.50602^{-0.094}\ \text{x}\, 1.99066^{0.6023}$$

$$= 0.93287$$

Since the air in this particular cooling tower flows effectively through the entire fill frontal area, G_a is employed in the Merkel equation.

The transfer coefficient in the spray zone is given by Equation 7.2.4.

$$h_{dsp}\ a_{sp}\ L_{sp}\ /\ G_w = 0.2\ L_{sp}\ (G_a\ /\ G_w)^{0.5}$$

$$= 0.2 \text{ x } 0.5\,(1.99066 / 1.50602)^{0.5} = 0.11497$$

Since most of the heat and mass transfer usually occurs in the fill, it is important to follow the same procedure used to determine the fill transfer characteristics to evaluate its performance in the cooling tower. It follows from Equation 7.2.5 that

$$\frac{h_{drz}\ a_{rz}\ H_3}{G_w} + \frac{h_{dfi}\ a_{fi}\ L_{fi}}{G_w} + \frac{h_{dsp}\ a_{sp}\ L_{sp}}{G_w} = 0.414391$$

$$+ 0.93287 + 0.11497 = 1.46223$$

$$= \int_{T_{wo}}^{T_{wi}} \frac{c_{pw}\ dT_w}{(i_{masw} - i_{ma})}$$

If the four-point form of the Chebyshev integral is applied to this relation, the integral on the right side can be expressed as

$$\int_{T_{wo}}^{T_{wi}} \frac{c_{pw}\,dT_w}{(i_{masw} - i_{ma})} \approx \frac{c_{pwm}\,(T_{wi} - T_{wo})}{4}\left(\frac{1}{\Delta i_{(1)}} + \frac{1}{\Delta i_{(2)}} + \frac{1}{\Delta i_{(3)}} + \frac{1}{\Delta i_{(4)}}\right)$$

The enthalpy differentials are dependent on the following intermediate temperatures:

$T_{w(1)} = T_{wo} + 0.1(313.15 - T_{wo}) = 294.5385 + 0.1(313.15 - 294.5385) = 296.3997$ K

$T_{w(2)} = T_{wo} + 0.4(313.15 - T_{wo}) = 294.5385 + 0.4(313.15 - 294.5385) = 301.9831$ K

$T_{w(3)} = T_{wo} + 0.6(313.15 - T_{wo}) = 294.5385 + 0.6(313.15 - 294.5385) = 305.7054$ K

$T_{w(4)} = T_{wo} + 0.9(313.15 - T_{wo}) = 294.5385 + 0.9(313.15 - 294.5385) = 311.2888$ K

The bracketed subscript numbers refer to the intervals in the Chebyshev integral and should not be confused with the numbers indicating various positions in the cooling tower.

To find the corresponding increments in enthalpy, determine the enthalpy of saturated air at $T_{w(1)}$ = 296.3997 K. The relevant specific heats of air and water vapor respectively are evaluated at

$$(T_{w(1)} + 273.15)/2 = (296.3997 + 273.15)/2 = 284.7749 \text{ K}$$

- Specific heat of air according to Equation A.1.2

$$c_{pa(1)} = 1006.516 \text{ J/kg K}$$

- Specific heat of water vapor according to Equation A.2.2

$$c_{pv(1)} = 1872.471 \text{ J/kg K}$$

The pressure of saturated water vapor at $T_{w(1)}$ follows from Equation A.2.1, and the corresponding humidity ratio evaluated at $(p_{a1} + p_{a5})/2$ follows from Equation A.3.5.

- Pressure of the water vapor: $p_{vs(1)} = 2850.961 \text{ N/m}^2$
- Humidity ratio: $w_{s(1)} = 0.02196$ kg/kg

With these values, determine the enthalpy of saturated air at $T_{w(1)}$ using Equation A.3.6b

$$i_{masw(1)} = c_{pa(1)} (T_{w(1)} - 273.15) + w_{s(1)}[i_{fgwo} + c_{pv(1)} (T_{w(1)} - 273.15)]$$

$$= 1006.516 (296.3997 - 273.15) + 0.02196 [2.5106 \times 10^6 + 1872.471 (296.3997$$

$$- 273.15)] = 79291.462 \text{ J/kg dry air}$$

The enthalpy of the air at $T_{w(1)}$ can be determined by applying Equation 4.2.21, i.e.,

$$i_{ma(1)} = m_w \; c_{pwm} \; (T_{w(1)} - T_{wo}) / \; m_a + i_{ma1}$$

$$= 12500 \text{ x } 4178.32(296.3997 - 294.5385)/ 16522.464 + 36114.71$$

$$= 41997.996 \text{ J/kg dry air}$$

With these values, find the difference in enthalpy

$$\Delta i_{(1)} = i_{masw(1)} - i_{ma(1)} = 79291.462 - 41997.996 = 37293.465 \text{ J/kg dry air}$$

Repeat the procedure in the case of the other three intermediate temperatures, and find

$$\Delta i_{(2)} = 48550.99 \text{ J/kg dry air}$$

$$\Delta i_{(3)} = 60726.83 \text{ J/kg dry air}$$

$$\Delta i_{(4)} = 88227.85 \text{ J/kg dry air}$$

Substitute these values into the approximate expression for the integral, and find

$$\int_{T_{wo}}^{T_{wi}} \frac{c_{pw} dT_w}{(i_{masw} - i_{ma})} \approx \frac{c_{pwm} \; (T_{wi} - T_{wo})}{4} \left(\frac{1}{\Delta i_{(1)}} + \frac{1}{\Delta i_{(2)}} + \frac{1}{\Delta i_{(3)}} + \frac{1}{\Delta i_{(4)}} \right)$$

$$= \frac{4178.32(313.15 - 294.5385)}{4} \left(\frac{1}{37293.465} + \frac{1}{48550.99} + \frac{1}{60726.83} + \frac{1}{88227.85} \right)$$

$$= 1.4622266$$

This value is almost identical to the value obtained by adding the transfer coefficients in the three wet zones, which means the water outlet temperature, T_{wo} = 294.5385 K is correct.

According to Equation 7.2.1, the heat rejected by the cooling tower is given by

$$Q = m_w c_{pwm} (T_{wi} - T_{wo}) = 12500 \text{ x } 4178.32(313.15 - 294.5385) = 972.06 \text{ MW}$$

The correctness of the temperature of the saturated air leaving the spray zone, T_{a5}, can be confirmed from the relation

$$Q = m_a (i_{ma5} - i_{ma1})$$

To find the enthalpy of the saturated air at (5), determine the specific heat of air and water vapor at

$$(T_{a5} + 273.15)/2 = (299.5875 + 273.15)/2 = 286.3688 \text{ K}$$

according to Equations A.1.2 and A.2.2.

With the value of w_5 already known, use Equation A.3.6b to find

$$i_{ma5} = 94947.398 \text{ J/kg dry air}$$

Thus

$$Q = 16522.464 (94947.398 - 36114.71) = 972.06 \text{ MW}$$

The values of Q are in agreement, which means the value for T_{a5} is correct.

Finally, the draft equation is evaluated. To do this, the remaining loss coefficients must be determined.

The loss coefficient due to the tower supports referred to the fill follows from Equation 7.1.21.

$$K_{tsfi} = \left[C_{dts} \; L_{ts} \; d_{ts} \; n_{ts} \; A_{fr}^2 / (\pi \; d_3 \; H_3)^3\right] (\rho_{av15} / \rho_{av1}) (m_{av1} / m_{av15})^2$$

$$= \left[1 \text{x } 11.6 \text{ x } 0.8 \text{ x } 72 \text{ x } 8300^2 / (\pi \text{ x } 104.5 \text{ x } 10)^3\right](0.9848$$

$$/ 1.0101)(16656.742 \; / 16810.89)^2 = 1.245124$$

The inlet loss coefficient for a circular cooling tower with splash type isotropic fill operating in the absence of a rain zone and based on fill conditions can be determined according to Equation 7.3.14. This is applicable if the inlet is rounded with

- $r_i/d_3 = 0.02$
- $10 \leq d_i/H_i = d_3/H_3 = 104.5/10 = 10.45 \leq 15$

The sum of the loss coefficients in the vicinity of the fill (effective fill loss coefficient = 11.07106) also falls within the range of the applicability of the equation, i.e., $5 \leq K_{fi} \leq 25$.

$$K_{ctfi(norz)} = [\,0.011266\exp(0.093 d_3/H_3)11.07106^2 - 0.3105\exp(0.1085 d_3$$

$$/H_3)11.07106 - 1.7522 + 4.5614\exp(0.131 d_3/H_3)$$

$$+\sinh^{-1}[\{(10970.2\exp(-0.2442 \text{ x } 11.07106) + 1391.3)/(d_3/H_3 - 15.7258)$$

$$+1205.54\exp(-0.23 \text{ x } 11.07106) + 109.314\}\{2r_i/d_3 - 0.01942/(d_3/H_3$$

$$- 27.929) - 0.016866\}]] \text{ x } (\rho_{av15}/\rho_{av1})(m_{av1}/m_{av15})^2(4A_{fr}/\pi d_3^2)^2$$

$$=[\,0.011266\exp(0.093 \text{ x } 104.5/10)11.07106^2 - 0.3105\exp(0.1085$$

$$\text{x } 104.5/10)11.07106 - 1.7522 + 4.5614\exp(0.131 \text{ x } 104.5/10)$$

$$+ \sinh^{-1}[\,\{(10970.2\exp(-0.2442 \text{ x } 11.07106) + 1391.3)/(104.5/10$$

$$- 15.7258) + 1205.54\exp(-0.23 \text{ x } 11.07106) + 109.314\}\{2 \text{ x } 0.02$$

$$- 0.01942/(104.5/10 - 27.929) - 0.016866\}]\,](0.9848/1.0101)$$

$$\text{x } (16656.742/16810.89)^2(4 \text{ x } 8300/\pi \text{ x } 104.5^2)^2 = 6.15664$$

This value must be multiplied by the correction factor C_{rz} given by Equation 7.3.15 to obtain the correct inlet loss coefficient in the presence of a rain zone. Present values fall in the range of applicability of Equation 7.3.15.

$$C_{rz} = [0.2394 + 80.1\{0.0954/(d_3/H_3) + d_d\}\exp(0.395 G_w/G_a) - 0.3195(G_w/G_a)$$

$$-966\{d_d/(d_3/H_3)\}\exp(0.686 G_w/G_a)](1 - 0.06825 G_w)11.07106^{0.09667}$$

$$\text{x } \exp\{8.7434(1/d_3 - 0.01)\} = [0.2394 + 80.1\{0.0954/(104.5/10) + 0.0035\}$$

$$\text{x } \exp(0.395 \text{ x } 1.50602/1.99066) - 0.3195(1.50602/1.99066)$$

$$-966\{0.0035/(104.5/10)\}\exp(0.686 \text{ x } 1.50602/1.99066)](1 - 0.06825$$

$$\text{x } 1.50602)11.071^{0.09667} \exp\{8.7434(1/104.5 - 0.01)\} = 0.92348$$

Thus

$$K_{ctfi} = C_{rz}\, K_{ctfi(norz)} = 0.92348 \text{ x } 6.15664 = 5.686$$

With Equation 7.2.18, find the loss coefficient for the rain zone referred to fill conditions.

$$K_{rzfi} = 3a_v v_{w3}(H_3/d_d)[0.2246 - 0.31467 a_\rho \rho_{av1} + 5263.04 a_\mu \mu_{av1}$$

$$+0.775526\{1.4824163\exp(71.52 a_L d_d) - 0.91\}$$

$$\text{x } \{0.39064\exp(0.010912 a_L d_3) - 0.17\}\{2.0892(a_v v_{av3})^{-1.3944} + 0.14\}$$

$$\text{x } \exp[\{0.8449\ell n(a_L d_3/2) - 2.312\}\{0.3724\ell n(a_v v_{av3}) + 0.7263\}$$

$$\text{x } \ell n\{206.757(a_L H_3)^{-2.8344} + 0.43\}]](\rho_{av15}/\rho_{av1})(m_{av1}/m_{av15})^2(4A_{fr}/\pi d_3^2)^2$$

With the values of the a coefficients identical to those employed in the mass transfer coefficient equation and with $v_{w3} = G_w/\rho_{wo} = 1.50602/997.867 = 0.001509$ m/s, the value of the coefficient is found to be

$$K_{rzfi} = 3 \text{ x } 1.0008 \text{ x } 0.001509\,(10/0.0035)[0.2246 - 0.31467 \text{ x } 1.0001$$

$$\text{x } 1.0101 + 5263.04 \text{ x } 1.0000 \text{ x } 1.7857 \text{ x } 10^{-5} + 0.775526\{1.4824163 \exp(71.52$$

$$\text{x } 1.0003 \text{ x } 0.0035) - 0.91\} \text{ x } \{0.39064 \exp(0.010912 \text{ x } 1.0003 \text{ x } 104.5)$$

$$- 0.17\}\{2.0892\,(1.0008 \text{ x } 1.9867)^{-1.3944} + 0.14\} \exp[\{0.8449\,\ell n(1.0003$$

$$\text{x } 104.52) - 2.312\}\{0.3724 \ell n(1.0008 \text{ x } 1.9867) + 0.7263\}$$

$$\text{x } \ell n\{206.757(1.0003 \text{ x } 10)^{-2.8344} + 0.43\}]](0.9484$$

$$/1.0101)(16656.742/16810.89)^2 \text{ x } (4 \text{ x } 8300/\pi \text{ x } 104.5^2)^2 = 6.474$$

At this stage, it is possible to confirm the value of p_{a5} according to Equation 7.2.13.

$$p_{a5} = p_{a1}\left[1 - 0.00975\frac{(H_3 + L_{fi}/2)}{T_{a1}}\right]^{3.5(1 + w_1)\{1 - w_1/(w_1 + 0.62198)\}}$$

$$- (K_{ts} + K_{ct} + K_{rz} + K_{fs} + K_{ctc} + K_{fi} + K_{cte} + K_{sp} + K_{wd} + K_{de})_{fi}$$

$$\text{x } (m_{av15} / A_{fr})^2 / (2\rho_{av15})$$

$$= 84100\left[1 - \frac{0.00975(10 + 2.504/2)}{288.6}\right]3.5(1 + 0.008127)\{1 - 0.008127$$

$$/(0.008127 + 0.62198)\} - (1.245124 + 5.686 + 0.47857$$

$$+ 3.91657 + 0.001087 + 0.679934 + 0.521975 + 5.472924$$

$$+ 6.474)(16810.89/8300)^2/(2 \text{ x } 0.9848) = 83937.7 \text{ N/m}^2$$

This value is in agreement with that used in previous calculations in this example.

To find the temperature lapse rate inside the tower, the specific heat of water is evaluated at (299.5875 + 273.15)/2 = 286.369 K. According to Equation A.4.2, find

$$c_{pw} = 4192.593 \text{ J/kg K}$$

Using the previously obtained values for the specific heat of dry air and water vapor at this temperature, find, from Equation 7.2.10,

$$\xi_T = -(1 + w_5)g\left[1 + 0.42216 \text{ x } 10^{-11} w_5^2 p_{a5} \exp(5406.1915/T_{a5})\right.$$

$$\text{x}\left\{i_{fgwo} - (c_{pw} - c_{pv})(T_{a5} - 273.15)\right\}/\{(w_5 + 0.622)RT_{a5}\}\Big]$$

$$/\left[(c_{pa5} + w_5 c_{pv5}) + 3.6693\text{x}10^{-8} w_5^2 p_{a5} \exp(5406.1915/T_{a5})\right.$$

$$\text{x}\left\{i_{fgwo} - (c_{pw} - c_{pv})(T_{a5} - 273.15)\right\}/T_{a5}^2\Big]$$

$$= -(1 + 0.02679)9.8\left[1 + 0.42216\text{x}10^{-11} \text{x } 0.02679^2 \text{ x } 83937.7\right.$$

$$\text{x } \exp(5406.1915/299.5875)\left\{2.5016\text{x}10^6 - (4192.593 - 1873.819)\right.$$

$$\text{x } (299.5875 - 273.15)\}/\{(0.02679 + 0.622)287.08\text{x}299.5875\}\Big]$$

$$/\left[1056.75 + 3.6693\text{x}10^{-8} \text{ x } 0.02679^2 \text{ x } 83937.7 \exp(5406.1915/299.5875)\right.$$

$$\text{x}\left\{2.5016\text{x}10^6 - (4192.593 - 1873.819)(299.5875 - 273.15)\right\}/299.5875^2\Big]$$

$$= -0.00342 \text{ K/m}$$

To find the pressure difference (p_{a6} - p_{a7}) given by Equation 7.2.14, the air properties and corresponding Froude number must be determined at the outlet of the tower. Using the lapse rate obtained previously and assuming it to be constant over the height of the cooling tower, the air temperature at (6) may be determined.

The corresponding density of the air-vapor mixture at this temperature is, according to Equation A.3.1,

$$T_{a6} = T_{a5} + \xi_{T_{a5}}(H_6 - H_3 - L_{fi} - L_{sp}) = 299.5875 - 0.00342\,(147 - 10 - 2.504 - 0.5)$$

$$= 299.12\ \text{K}$$

The corresponding density of the air-vapor mixture at this temperature is according to equation (A.3.1)

$$\rho_{av6} = (1 + w_5)[1 - w_5 / (w_5 + 0.62198)]\, p_{a6} / (RT_{a6})$$

$$= (1 + 0.02679)\,[1 - 0.02679/(0.02679 + 0.62198)]$$

$$\text{x } 82650.59 / (287.08 \text{ x } 299.12) = 0.947\ \text{kg/m}^3$$

The ambient temperature at elevation (7) follows from Equation 7.2.7 with $H_7 = H_6$.

$$T_{a7} = T_{a1} - 0.00975H_6 = 288.6 - 0.00975 \text{ x } 147 = 287.167\ \text{K}$$

The pressure at (7) may be determined from Equation 7.2.9.

$$p_{a7} = p_{a1}\left[1 - 0.00975H_6 / T_{a1}\right]^{3.5(1+w_1)\{1-w_1/(w_1+0.62198)\}}$$

$$= 84100\left[1 - 0.00975 \text{x } 147/288.6\right]^{3.5(1+0.008127)\{1-0.008127/(0.008127+0.62198)\}}$$

$$= 82654.268\ \text{N/m}^2$$

According to Equation A.3.1, the corresponding density of the ambient air at elevation (7), assuming a uniform ambient humidity ratio w_1, is

$$\rho_{av7} = (1 + w_1)[1 - w_1 / (w_1 + 0.62198)]p_{a7} / (RT_{a7})$$

$$= (1 + 8.127 \times 10^{-3})[1 - 8.127 \times 10^{-3} / (8.127 \times 10^{-3} + 0.62198)]$$

$$\times 82654.268 / (287.08 \times 287.167) = 0.9977 \text{ kg/m}^3$$

With no cold inflow, these values yield

$$Fr_D = (m_{av5} / A_6)^2 / [\rho_{av6}(\rho_{av7} - \rho_{av6})gd_6]$$

$$= [16965.046 / (0.25 \times \pi \times 60.85^2)]^2 / [0.947\,(0.9977 - 0.947)\,9.8 \times 60.85] = 1.189$$

Substitute this expression for Fr_D into Equation 7.2.14, and find p_{a6}.

$$p_{a6} = p_{a7} + [0.02\, Fr_D^{-1.5} - 0.14 / Fr_D](m_{av5} / A_6)^2 / \rho_{av6}$$

$$= 82654.268 + [0.02 \times 1.189^{-1.5} - 0.14 / 1.189]$$

$$\times [16965.046 / (0.25 \times \pi \times 60.85^2)]^2 / 0.947 = 82650.59 \text{ N/m}^2$$

This is in agreement with the value given initially.

The draft Equation 7.2.15 may now be solved using the previous values. Upon substitution, the left side of the equation yields,

$$p_{a1}\left[\left\{1 - 0.00975\left(H_3 + L_{fi}/2\right)/T_{a1}\right\}^{3.5(1+w_1)\{1-w_1/(w_1+0.62198)\}}\right.$$

$$\text{x}\left\{1+\xi_{Ta5}\left(H_6 - H_3 - L_{fi}/2\right)/T_{a5}\right\}^{-0.02123(1+w_5)/\{\xi_{Ta5}(w_5+0.622)\}}$$

$$\left.-\left\{1 - 0.00975\ H_6/T_{a1}\right\}^{3.5(1+w_1)\{1-w_1/(w_1+0.62198)\}}\right]$$

$$-\left(0.02\ Fr_D^{-1.5} - 0.14/Fr_D\right)\left(m_{av5}/A_6\right)^2/\rho_{av6}$$

$$= 84100\left[\left\{1 - 0.00975(10 + 2.504/2)/288.6\right\}^{3.5(1+0.008127)\left\{1-\frac{0.008127}{(0.008127+0.62198)}\right\}}\right.$$

$$\text{x}\left\{1+0.00342(147-10-2.504/2)/299.5875\right\}^{-0.02123(1+0.02679)/\{-0.00342(0.02679+0.622)\}}$$

$$\left.-\left\{1 - 0.00975\ 147/288.6\right\}^{3.5(1+0.008127)\left\{1-\frac{0.008127}{(0.008127+0.62198)}\right\}}\right] - (0.02$$

$$\text{x}\,1.189^{-1.5} - 0.14/1.189\left)\left[16965.046/\left(\pi \text{x}\, 0.25 \text{x}\, 60.86^2\right)\right]^2/0.947 = 68.43\ \text{N/m}^2\right.$$

The value on the right side of Equation 7.2.15 is

$$\left(K_{ts} + K_{ct} + K_{rz} + K_{fs} + K_{ctc} + K_{fi} + K_{cte} + K_{sp} + K_{wd} + K_{de}\right)_{fi}$$

$$\text{x}\ \left(m_{av15}/A_{fr}\right)^2/\left(2\rho_{av15}\right)\left[1+\xi_{Ta5}\left(H_6 - H_3 - L_{fi}/2\right)\right.$$

$$\left./T_{a5}\right]^{-0.021233\ (1+w_5)/\{\xi_{Ta5}(w_5+0.622)\}} + a_{e6}\ \left(m_{av5}/A_6\right)^2/\left(2\rho_{av6}\right)$$

$$= (1.245124 + 5.686 + 6.474 + 0.47857 + 3.91657 + 0.001087 + 0.679934$$

$$+0.521975 + 5.472924)(16810.89/8300)^2/(2\text{x}\,0.9848)\left[1 - 0.00342(147 - 10\right.$$

$$\left.-2.504/2)\ /299.5875\right]^{-0.021233(1+0.02679)/[-0.00342(0.02679+0.622)]}$$

$$+1.01\left[16965.046/\left(\pi \text{x}\ 0.25\ \text{x}\ 60.85^2\right)\right]^2/(2\ \text{x}\ 0.947) = 68.36\ \text{N/m}^2$$

Since the value of the right side of Equation 7.2.15 is essentially the same as the left side, the chosen air-vapor mass flow rate is correct.

The amount of water lost due to evaporation is given by

$$m_{w(evap)} = m_a\,(w_5 - w_1) = 16522.464\,(0.02679 - 0.008127) = 308.304 \text{ kg/s}$$

Note

If the fill performance characteristics are available, the performance of the cooling tower described in example 7.3.2 can be determined at other operating conditions, and the results can be presented graphically (Fig. 7.3.8). In practice, the performance of the previously mentioned cooling tower is easily found at the prescribed conditions by following the arrows shown.

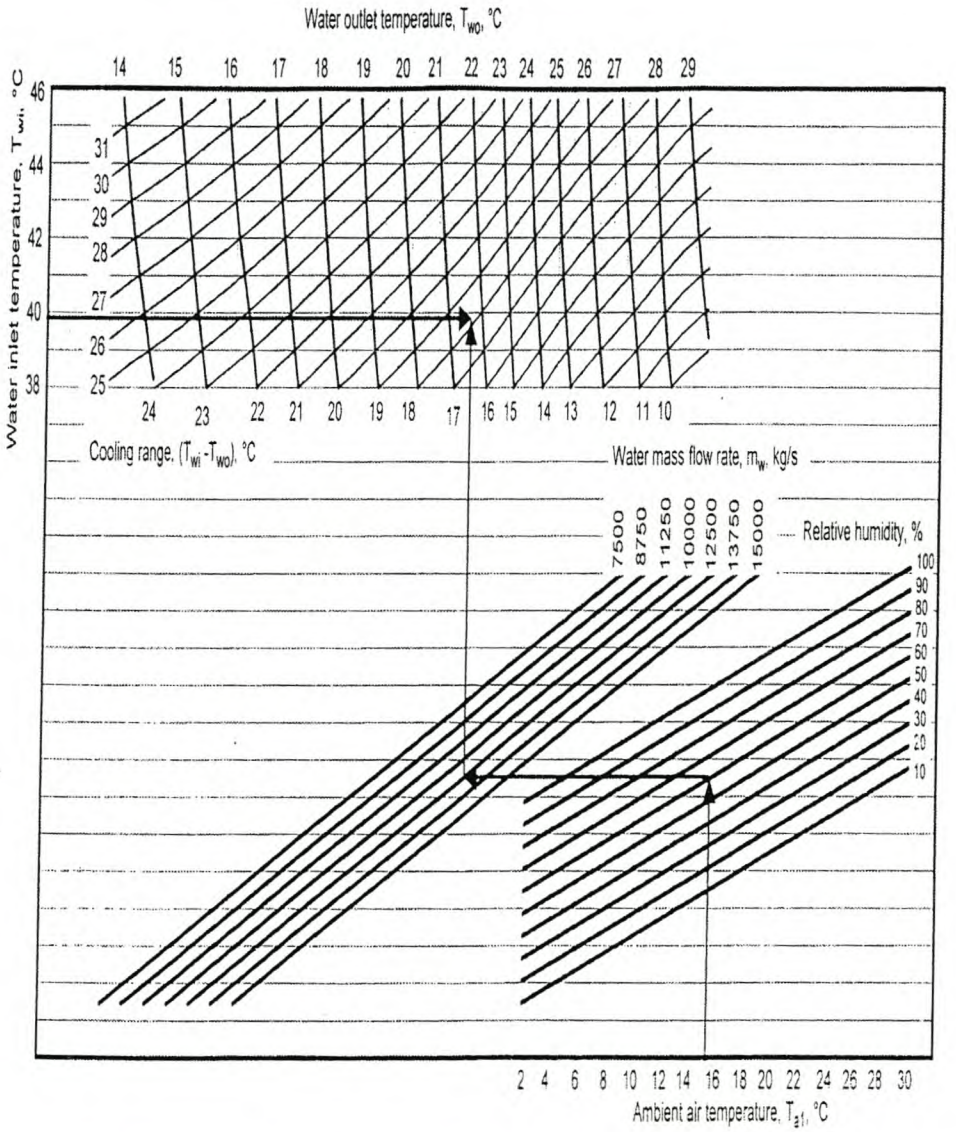

Fig. 7.3.8 Cooling Tower Performance Characteristics

Example 7.3.3

If the air mass flow rate through the cooling tower described in Example 7.3.2 is

$$m_a = 15975.21 \text{ kg/s}$$

and the water outlet temperature

$$T_{wo} = 294.618 \text{ K}$$

at the specified inlet conditions, determine the heat rejection rate employing the effectiveness-NTU method described in section 4.4.

The Merkel number of the 2.504 m thick expanded metal fill evaluated in the procedure described in Example 4.4.1 is correlated by the following relation

$$h_{dfi} \quad a_{fi} \quad L_{fi}/G_w = 0.6333\, G_w^{-0.0864}\, G_a^{0.5951}$$

Solution

To apply the effectiveness-NTU method, determine the enthalpy of saturated air at the inlet water temperature $T_{wi} = 313.15$ K. Find the specific heat of air and water vapor at

$$(T_{wi} + 273.15) / 2 = (313.15 + 273.15)/2 = 293.15 \text{ K}$$

using Equations A.1.2 and A.2.2 respectively, i.e.,

$$c_{pa} = 1006.729 \text{ J/kg and } c_{pv} = 1879.672 \text{ J/kg}$$

According to Equation A.3.5, the humidity ratio of saturated air at 313.15 K is

$$w_s = 0.060198 \text{ kg/kg dry air}$$

With these values, according to Equation A.3.6b, the enthalpy of the air is

$$i_{maswi} = 1006.729\ (313.15 - 273.15)$$

$$+ 0.060198\ [2.5016 \times 10^6 + 1879.672(313.15 - 273.15)]$$

$$= 195386.577 \text{ J/kg dry air}$$

The enthalpies of saturated air at the water outlet temperature

$$T_{wo} = 294.618 \text{ K}$$

and mean water temperature of

$$(T_{wi} + T_{wo})\ /2 = (313.15 + 294.618)/2 = 303.884\ \text{K}$$

have values of

$$i_{maswo} = 71512.827\ \text{J/kg dry air}$$

and

$$i_{maswm} = 119893.775\ \text{J/kg dry air}$$

Using Equation 4.4.14, the approximate gradient of the saturated air enthalpy-temperature curve is

$$\frac{di_{masw}}{dT_w} = \frac{i_{maswi} - i_{maswo}}{T_{wi} - T_{wo}} = \frac{195386.577 - 71512.827}{313.15 - 294.618} = 6684.316\ \text{J/K}$$

Determine the specific heat of water at 303.884 K according to Equation A.4.2, i.e.,

$$c_{pwm} = 4178.307\ \text{J/kg K.}$$

With these values find the capacity rate

$$C_{emin} = \frac{m_w\ c_{pwm}}{(\ di_{masw}/\ dT_w\ )} = \frac{12500\ \text{x}\ 4178.307}{6684.316} = 7813.64\ \text{kg/s}$$

while

$$C_{emax} = m_a = 15975.21\ \text{kg/s}$$

The evaporative capacity ratio is thus

$$C_e = C_{emin}/C_{emax} = 7813.64/15975.21 = 0.48911$$

According to Equation 4.4.19,

$$\lambda = (71512.827 + 195386.577 - 2\ \text{x}\ 119893.775)/4 = 6777.964$$

With this correction factor, find the maximum heat transfer rate given by Equation 4.4.20.

$$Q_{max} = 7813.64\ (195386.577 - 6777.964 - 36114.71) = 1.191532\ \text{x}\ 10^9\ \text{W}$$

To find NTU_e given by Equation 4.4.10, the value of the effective transfer coefficient $h_d aL/G_w$ must be determined. With

$$m_{av1} = m_a\ (1 + w_1) = 15975.21\ (1 + 0.008127) = 16105.03\ \text{kg/s}$$

find

$$v_{av3} = m_{av1}/(\rho_{av1} A_{fr}) = 16105.04/(1.0101 \times 8300) = 1.921\ \text{m/s}$$

Using Equation A.4.1, the density of water at $T_{wo} = 294.618$ is

$$\rho_{wo} = 997.85\ \text{kg/m}^3$$

With these values and the information given in Example 7.3.2, use Equation 7.2.2 to determine the Merkel number in the rain zone for

$$G_a = m_a/A_{fr} = 15975.21/8300 = 1.925\ \text{kg/sm}^2$$

$$\frac{h_{drz} a_{rz} H_3}{G_w} = 0.412$$

The fill Merkel number is found to be

$$\frac{h_{dfi}\, a_{fi}\, L_{fi}}{G_w} = 0.903$$

The Merkel number for the spray zone is, according to Equation 7.2.3,

$$\frac{h_{dsp}\ \ a_{sp}\ \ L_{sp}}{G_w} = 0.113$$

Thus

$$\frac{h_d aL}{G_w} = \frac{h_{drz} a_{rz} H_3}{G_w} + \frac{h_{dfi} a_{fi} L_{fi}}{G_w} + \frac{h_{dsp} a_{sp} L_{sp}}{G_w} = 0.412 + 0.903 + 0.113 = 1.428$$

According to Equation 4.4.10,

$$NTU_e = \frac{h_d A\ (di_{masw}/dT_w)}{m_w c_{pwm}} = \left(\frac{h_d aL}{G_w}\right)\left(\frac{di_{masw}/dT_w}{m_w c_{pwm}}\right) m_w$$

$$= \left(\frac{h_d aL}{G_w}\right)\frac{m_w}{C_{e\min}} = \frac{1.428 \times 12500}{7813.64} = 2.284$$

Using Equation 4.4.18, the effectiveness for a counterflow cooling tower is

$$e_e = \frac{1-\exp[-2.284(1-0.48911)]}{1-0.48911\exp[-2.284(1-0.48911)]} = 0.812367$$

With this value, find the actual heat transfer rate

$$Q = e_e Q_{max} = 0.812367 \text{ x } 1.191532 \text{ x } 10^6 = 967 \text{ MW}$$

7.4 Cold Inflow

A natural draft cooling tower contains a mass of slowly moving air that is slightly buoyant relative to the surrounding air. If it were not for the upward motion of the air, an instability would exist with cold outside air spilling into the tower at its upper edge. According to Ernst, Ernst and Wurz and Baer, the inflow of cold air into the top of a natural-draft cooling tower is not uncommon, especially in wet towers where the air velocity is low. Significant performance degradation is observed under these conditions. Premature flow separation in the tower results in an effective narrowing of the exit flow area of the tower according to both Rühl and Moore. In a certain range of wind speeds, air inflow may be periodic. Typical flow patterns are shown in Figure 7.4.1.

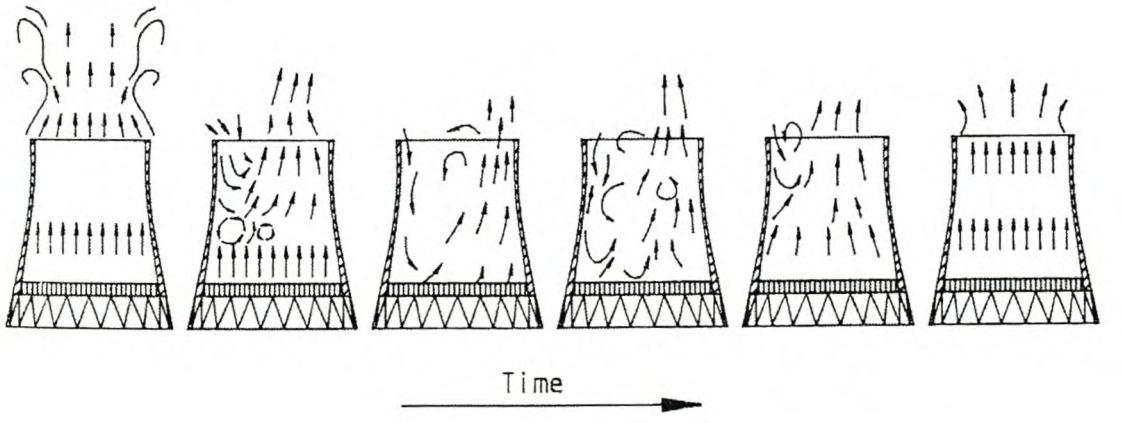

Fig. 7.4.1 Periodic Cold Inflow into Cooling Tower

Jörg and Scorer experimentally predicted the critical velocity needed for the onset of cold air inflow. Their test results were limited to relatively low Reynolds numbers and were obtained by using an inverted cylindrical vessel submerged in water. A salt water solution was injected at the top of the vessel, and the solution descended to the bottom of the vessel due to a combination of buoyancy and inertia forces. They visualized the inflow of the exterior fluid near the rim using a dye injection technique. The following empirical formula, which relates the buoyancy force, $(\rho_a - \rho)\, g/\rho$, and the eddy stress force, v^2/L_{tb}, is based on their experimental observations.

$$(\rho_a - \rho) g L_{tb} / (\rho v^2) = 8 \times 10^{-4} \qquad (7.4.1)$$

L_{tb} is defined as υ/v, a turbulent boundary layer length scale. This length scale was chosen since it was believed the length scale of a turbulent shear flow is more important than the dimension of the tower outlet.

Other researchers express their findings in terms of the densimetric Froude number based on the tower outlet diameter, i.e.,

$$1/Fr_D = (\rho_a - \rho) g d / (\rho v^2) \qquad (7.4.2)$$

where

ρ_a = the density of the ambient air at the elevation of the tower outlet

ρ = the density of the air leaving the tower

Lucas and Buchlin studied the problem of cold air inflow into a vertical heated tube. To test Equation 7.4.2, measurements were made to determine the dependence of the bulk buoyancy and the velocity, v, on the inlet loss coefficient for different heat inputs and d/H ratios. As the loss coefficient through the tower increases, the flow tends to become more unstable. These observations are supported by Richter who suspected when $1/Fr_D$ is increased, the plume tends to become increasingly more unstable.

According to Richter, small disturbances may cause flow instabilities in cooling towers resulting in cold air inflow for $1/Fr_D$ of greater than 3.05 as defined by Equation 7.4.2. This latter value is in fair agreement with a value of 2.8 subsequently proposed by Moore. Cold inflow is entrained by the plume for $3.05 < 1/Fr_D < 6$ while penetration to the packing or heat exchanger elevation occurs at $1/Fr_D > 7$.

Grange analyzed the flow in a natural draft cooling tower and obtained an expression for the inside shape of the shell, which ensures that cold inflow does not occur in the upper part of the tower. Although it is not essential that the shell have this shape, it is important the outlet diameter of the tower, d_o, does not exceed a prescribed value. For a turbulent mixing coefficient of 0.1 find

$$\frac{d_o}{d_i} = \left[1 + \frac{2}{Fr_D}\left(\frac{d_i}{d_o}\right)^5 \left(\frac{H_d}{d_i}\right)\right]^{-0.25} + 0.2\left(\frac{H_d}{d_i}\right) \qquad (7.4.3)$$

where

d_i = the tower inlet diameter

H_d = the effective draft height

From this equation it follows that the maximum tower outlet diameter and the stability of the natural draft depends not only on the densimetric Froude number at the outlet of the tower but also on the ratios H_d/d_i and d_i/d_o.

The assumption of a turbulent mixing coefficient of 0.1 in Equation 7.4.3 tends to be conservative. Values of mixing coefficients of up to 0.17 are possible, and this would increase the coefficient of the second term on the right side of Equation 7.4.3 to 0.34.

Equation 7.4.3 can be rewritten to give the densimetric Froude number in terms of the cooling tower dimensions.

$$Fr_D = 2\left(\frac{d_i}{d_o}\right)^5 \left(\frac{H_d}{d_i}\right)\left[\left(\frac{d_o}{d_i} - 0.2\,\frac{H_d}{d_i}\right)^{-4} - 1\right]^{-1} \qquad (7.4.4)$$

The critical densimetric Froude number for a given tower can be determined from this equation.

The value of $1/Fr_D$ may be reduced, and the outlet velocity in the boundary layer is accelerated by having a cylindrical or a convergent rather than a divergent tower outlet (Fig. 7.4.2). Since dynamic losses increase with a reduction in outlet area, convergence should not be excessive.

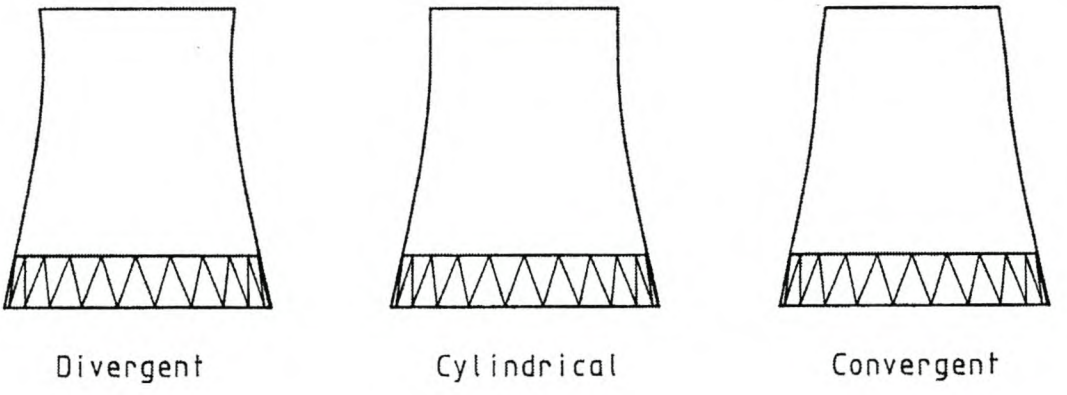

Fig. 7.4.2 Different Cooling Tower Outlet Shapes

Based on an approximate analysis, Moore suggests a ratio of draft height to tower diameter of unity or even less may be possible without cold inflow occurring. This is conditional on the upper third of the tower converging slightly and vigorous flow mixing and turbulence being promoted near the wall at the outlet.

It has been demonstrated that the problem of cold inflow can largely be overcome in a cooling tower having a converging outlet. However, model tests suggest the benefit of this geometry is limited to conditions at low wind speeds (Fig. 7.4.3) according to Ruscheweyh.

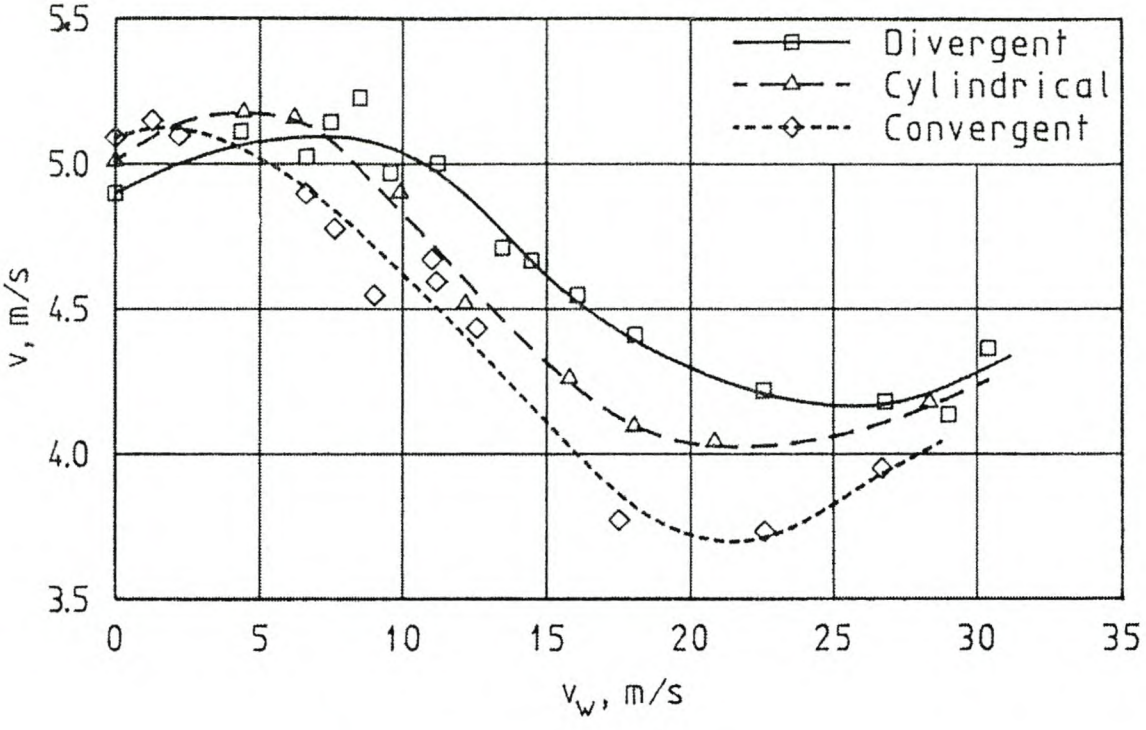

Fig. 7.4.3 Air Velocity at Smallest Cross Section in Tower
as Function of Wind Velocity for Different Tower Outlet Shapes

The flow at the outlet becomes more stable for the other shapes as the wind speed increases. Since the dynamic losses are less than those for the converging shape under these conditions, their relative performance is better. The cylindrical shape appears to offer a good, cost-effective compromise solution according to Tesche.

In some cooling towers, a reinforcing ring projecting inward at the outlet of the tower tends to trip the boundary layer and reduce the tendency for cold inflow to occur.

Where the heat exchangers or the fill are located vertically around the base of the tower, the flow pattern inside the tower can be very complex. A more conservative approach compared to the horizontal arrangement should be followed. Existing dry-cooling towers with horizontal fill or heat exchanger arrangements typically have ratios of tower outlet to base diameters of approximately 0.6. Those with vertical arrangements have ratios of 0.5 to 0.55 as shown in Figure 7.4.4 from Szabó to avoid cold inflow and to reduce wind effects and flow losses in the tower itself.

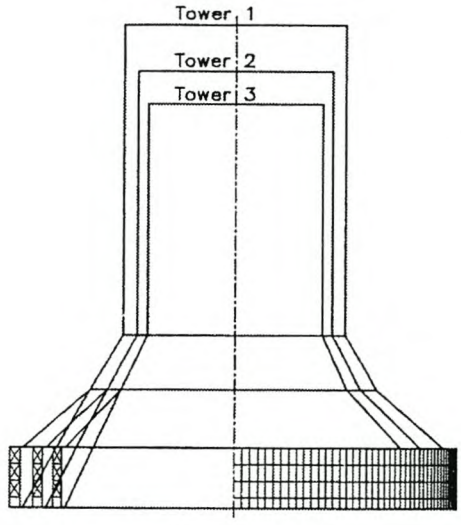

	Tower 1	Tower 2	Tower 3
Inlet temperature difference, (T_{wi} - T_{ai})	26°C	29°C	32°C
Tower height	146 m	132 m	122 m
Base diameter	127 m	114 m	103 m
Outlet diameter	62.5 m	59 m	57 m
Number of 15 m high deltas	156	140	126

Figure 7.4.4 Dry-Cooling Tower Geometries

Example 7.4.1

Will cold inflow occur in the tower analyzed in Example 7.3.1?

Solution

The value of $1/Fr_D = 3.41913$ found at the outlet of the tower is larger than the limit of 3.05 suggested by Richter or 2.8 proposed by Moore for no cold inflow.

According to Equation 7.4.4, the critical densimetric Froude number for the particular tower is

$$Fr_D = 2\left(\frac{d_3}{d_5}\right)^5 \left(\frac{H_5 - H_3}{d_3}\right)\left[\left\{\frac{d_5}{d_3} - \frac{0.2\,(H_5 - H_3)}{d_3}\right\}^{-4} - 1\right]^{-1}$$

$$= 2\left(\frac{82.958}{58}\right)^5 \left(\frac{120.0 - 13.67}{82.958}\right)\left[\left\{\frac{58}{82.958} - \frac{0.2\,(120.0 - 13.67)}{82.958}\right\}^{-4} - 1\right]^{-1}$$

$$= 0.61354$$

or

$$1/Fr_D = 1.629885$$

This value suggests cold inflow will occur in the particular cooling tower. However, this value is conservative in view of the low turbulent mixing coefficient assumed.

References

Alomwooja, K. T., P. L. Gould, and I. Furzer, "Optimization of Large Cooling Towers," *Proceedings*, Second International Symposium on Natural Draught Cooling Towers, Ruhr-Universität, 413– 429, Bochum, September 1984.

American Society of Mechanical Engineers, *ASME-PTC23 Cooling Tower Test Code*, American Society of Mechanical Engineers, New York, 1986.

Baer, E., "Einfluss des Windes Auf die Strömung im Kamin eines Naturzugkühlturmes," Doctoral thesis, Universität Karlsruhe, 1978.

Becker, N., "Druckverlust und Wärmeübertragung von Rippenrohrbündeln für Naturzug-trockenkühltürme, Doctoral thesis, R-W Technische Hochschule Aachen, 1984.

Benton, D. J., *A Numerical Solution of Heat Transfer in Evaporative Cooling Towers*, Tennessee Valley Authority Report WR 28-1-900-110, 1983.

Bourillot, C., *TEFERI, Numerical Model for Calculating the Performance of an Evaporative Cooling Tower*, CS-3212-SR, Electric Power Research Institute Report, August 1983.

Bouton, F., "Design Studies for Natural Draught Dry Towers," Société Hydrotechnique de France Conference, Paris, 1978.

British Standards Institution, *Water Cooling Towers: Part 2. Methods for Performance Testing*, BS 4485, BSI, 1988.

Buxmann, J. and G. Völler, "Die Bedeutung des Eintrittsdruck-verlustes beim Naturzug-Trockenkühlturm," *Brennstoff-Wärme-Kraft*, 33-7/8:313–316, 1981.

Buxmann, J., "Berechnung der Kennfelder von Trockenkühlern," *Brennstoff-Wärme-Kraft*, 26-10:421–428, 1974.

Cale, S. A., *Development of Evaporative Cooling Packing, Commission of European Communities*, Report EUR 7709 EN, Luxembourg, 1982.

Caytan, Y. and L. Franza, "Method for Dimensioning Crossflow Cooling Towers," *Proceedings*, International Cooling Tower Conference, Report GS-6317, Electric Power Research Institute, Palo Alto, 1989.

Caytan, Y., "Numerical Simulation of the Operation of Natural Draft Cooling Towers," Fifth International Conference on Numerical Methods in Thermal Problems, Montreal, June 1987.

Chilton, H., "Performance of Natural-draught Water Cooling Towers," *Proceedings*, Institution of Electrical Engineers, 99-71:440–456, 1952.

Conradie, A. E. and D. C. Kröger, "Performance Evaluation of Dry-Cooling Systems for Power Plant Applications," *Applied Thermal Engineering*, 16-3:219–232, 1996.

Cooling Tower Institute, *Cooling Tower Institute Acceptance Test Code ATC-105*, CTI, Houston, 1986.

Cooling Tower Institute, *Cooling Tower Test Code CTI-ATC 105*, CTI, Houston, 1997.

De Villiers, E. and D. G. Kröger, "Inlet Losses in Counterflow Wet-Cooling Towers," *Proceedings*, American Society of Mechanical Engineers International Joint Power Generation Conference, vol. 2, PWR, 34:601–606, 1999.

De Villiers, E., "Heat , Mass and Momentum Transfer in the Rain Zone of a Cooling Tower," Master's thesis, Department of Mechanical Engineering, University of Stellenbosh, 1998.

Deutsche Norm, *DIN 1947, Wärmetechnische Abnahmemessungen an Nasskühltürmen,* VDI-Kühlturmregeln, Berlin, 1989.

Du Plessis, J. P., M. R. Collins, and D. G. Kröger, "Numerical Modelling of Air Flow in Confined Tapered Duct Inlets," *Proceedings*, 11th International Association for Mathematics and Computers World Congress on System Simulation and Scientific Computation, vol. 1, 1985

Du Preez, A. F. and Kröger D. G., "The Influence of a Buoyant Plume on the Performance of a Natural Draft Cooling Tower," 9th International Association for Hydraulics Research Cooling Tower and Spraying Pond Symposium, Brussels, 1994.

Du Preez, F. and D. G. Kröger, "Experimental Evaluation of Aerodynamic Inlet Losses in Natural Draft Cooling Towers," *Proceedings*, Sixth International Association for Hydraulic Research Cooling Tower Workshop, Pisa, 1988.

Eldredge, T. V., "Cooling Tower Modeling with Computational Fluid Dynamics, EPRI TR-108483 2113," *Proceedings*, Cooling Tower Technology Conference, 1.49–1.60, July 1997.

Ernst, G. and D. Wurz, *Untersuchung zur Schwadenströmung in den Kronen von Naturzugkühltürmen*, Verein Deutscher Ingenieure Kühlturmseminar, Düsseldorf, 1977.

Ernst, G., "Cooling Towers, Design and Plume Behaviour," Seminar of International Centre for Heat and Mass Transfer, Dubrovnik, 1975.

Garde, M. A., "Experimental Evaluations of Entrance Losses of Flared Natural Draft Cooling Towers," Master of Science thesis, Cornell University, 1981.

Geldenhuys, J. D. and D. G. Kröger, "Aerodynamic Inlet Losses in Natural Draft Cooling Towers," *Proceedings*, Fifth International Association for Hydraulic Research Cooling Tower Workshop, Monterey, 1986.

Goldwirt, F., M. Ghuzel, and P. Lemoine, Hydraulics Works Study of Golfech Cooling Towers, *Proceedings*, Electric Power Research Institute Report GS-6317, International Cooling Tower Conference, April 1989.

Gösi, P., "Practical Conclusions from Cooling Tower Model Studies," *Proceedings*, Fifth International Association for Hydraulic Research Cooling Tower Workshop, Monterey, 1986.

Grange, J. L., "A Computer Code for Particular Operating Conditions of Wet Cooling Towers," Seventh International Association for Hydraulic Research Cooling Tower and Spraying Pond Symposium, Leningrad, 1990.

Grange, J. L., "Calculating the Evaporated Water Flow in a Wet Cooling Tower," Paper, Ninth International Association for Hydraulic Research Cooling Tower and Spraying Pond Symposium, von Karman Institute, Brussels, September 1994.

Grange, J. L., "The Shape of Natural Draft Cooling Towers," Paper, Eighth International Association for Hydraulic Research Cooling Tower and Spraying Pond Symposium, Karlsruhe, October 1992.

Heberholz, P. and S. Schulz, "The Influence of Atmospheric Precipitation on the Operation of a Natural Draught Indirect-contact Cooling Tower," *German Chemical Engineering*, 2-1:352–360, 1979.

Hempel, D. C., K. Stephan, and G. Hesse, "Strömungswiderstand, Geschwindigkeitsverteilung und Optimale Höhe für den Lufteintritt in Naturzug-Kühltürmen," *Brennstoff-Wärme-Kraft*, 35-11:470–477, 1983.

Johnson, B. M., ed., *Cooling Tower Performance Prediction and Improvement, Applications Guide,* EPRI Report GS-6370 vol. 1, Electric Power Research Institute, Palo Alto, 1989.

Johnson, B. M., ed., *Cooling Tower Performance Prediction and Improvement, Knowledge Base,* EPRI Report GS-6370 vol. 2, Electric Power Research Institute, Palo Alto, 1989.

Jörg, O. and R. S. Scorer, "An Experimental Study of Cold Inflow into Chimneys," *Atmospheric Environment*, vol. 1, 645, 1967.

Jorgensen, R., *Fan Engineering*, Buffalo Forge Co., Buffalo, 1961.

Kelly, N. W., *Kelly's Handbook of Crossflow Cooling Tower Performance*, N. W. Kelly and Associates, Kansas City, Missouri, 1976.

Krings, W., "Economical Calculation for the Optimal Design of General Shells of Revolution for Natural Draft Cooling Towers by means of Membrane Theory," *Proceedings*, Second International Symposium on Natural Draught Cooling Towers, Ruhr-Universität, 440–455, Bochum, September 1984.

Lees, U. A. and J. W. Cooper, " 'Cost Effective' Thermal Performance Upgrade of the Callaway Plant Cooling Tower," Paper, Electric Power Research Institute Cooling Towers and Advanced Cooling Systems Conference, St. Petersburg Beach, August 1994.

Liffick, G. W. and J. W. Cooper, "Thermal Performance Upgrade of the Arkansas Nuclear One Cooling Tower: A 'Root Cause' Analysis Approach," *Proceedings*, American Power Conference, 57-2:1357–1362, 1995.

Liu, B. M., "Numerical Prediction for the Performance of a Natural-draft Cooling Tower with Comparison to the Field Test Data," *Proceedings*, Tenth International Heat Transfer Conference, 7:309–314, Brighton, 1994.

Lowe, H. J. and D. G. Christie, *Heat Transfer and Pressure Drop Data on Cooling Tower Packings, and Model Studies of the Resistance of Natural Draught*

Towers to Airflow, International Development in Heat Transfer, Part V, American Society of Mechanical Engineers, New York, 1961.

Lucas, M. J. and J. M. Buchlin, "A Study of Cold Air Inflow into a Vertical Heated Tube," Paper, Fifth International Association for Hydraulic Research Cooling Tower Workshop, Monterey, 1986.

Majumdar, A. K. and A. K. Singhal, *VERA2D: Program for 2-D Analysis of Flow, Heat, and Mass Transfer in Evaporative Cooling Towers*, Report CS-2923, Electric Power Research Institute, March 1983.

Majumdar, A. K., A. K. Singhal, and T. Mukerjee, *VERA2D-84: A Computer Program for Two-dimensional Analysis of Flow, Heat and Mass Transfer in Evaporative Cooling Towers*, Report CS-4073, vols. 1 & 2, Electric Power Research Institute, 1985.

Majumdar, A. K., A. K. Singhal, and D. B. Spalding, "Numerical Modelling of Wet Cooling Towers," Transactions of the American Society of Mechanical Engineers, *Journal of Heat Transfer*, 105:728–743, November 1983.

Markóczy, E. and E. Stämpfli, "Experimentelle Untersuchung des Einflusses atmosphärischer Umgebungsbedingungen auf das Betriebsverhalten von Naturzug-Trockenkühltürmen," *EIR-Bericht*, no. 324, Würenlingen, 1977.

Merkel, F., "Verdunstungskühlung," *Verein Deutscher Ingenieure-Zeitschrift*, 70:123–128, 1926.

Mesarovic, M. M., "Ararat—A Computer Code for Thermal Design of Cooling Towers," *Nuclear Engineering and Design*, 24:57–70, North Holland Pub. Co., 1973.

Mohiuddin, A. K. M. and K. Kant, "Knowledge Base for the Systematic Design of Wet Cooling Towers: Parts I and II," *International Journal of Refrigeration*, 9-1:43–60, 1996.

Montakhab, A., *Waste Heat Disposal to Air with Mechanical and Natural Draft-Some Analytical Design Considerations*, No. 78-WA/HT-17, American Society of Mechanical Engineers, 1978.

Montakhab, A., "Waste Heat Disposal to Air with Mechanical and Natural Draft-Some Analytical Design Considerations," *Journal of Engineering for Power*, 102-3:719-727, July 1980.

Moore, F. K., "Dry Cooling Towers," *Advances in Heat Transfer*, vol. 12, ed. T. F. Irvine and J. P. Hartnett, Academic Press, 1976a.

Moore, F. K., "Analysis of Large Dry Cooling Towers with Power-law Heat Exchange Performance," Transactions of the American Society of Mechanical Engineers, *Journal of Heat Transfer*, 345–352, 1976b.

Moore, F. K., "Analysis of Large Dry Cooling Towers with Spine-Fin Heat Exchange Performance," Transactions of the American Society of Mechanical Engineers, *Journal of Heat Transfer*, 345–352, 1975.

Moore, F. K., "Cold Inflow and its Implications for Dry Tower Design," Second Conference on Waste Heat Management and Utilization, Miami, 1978a.

Moore, F. K., "Effects of Aerodynamic Losses on the Performance of Large Dry Cooling Towers," Paper 78-WA/HT-18, American Society of Mechanical Engineers Winter Annual Meeting, 1978b.

Moore, F. K. and M. A. Garde, "Aerodynamic Losses of Highly Flared Natural Draft Cooling Towers," Third Waste Heat Management and Utilization Conference, Miami, 1981.

Moore, F. K. and T. Hsieh, "Concurrent Reduction of Draft Height and Heat-Exchange Area for Large Dry Cooling Towers," Transactions of the American Society of Mechanical Engineers, *Journal of Heat Transfer,* 279-285, 1974.

Nahavandi, A. M. and J. J. Oellinger, "An Improved Model for the Analysis of Evaporative Counterflow Cooling Towers," *Nuclear Engineering and Design*, vol. 40, North Holland Pub. Co., 1977.

Nahavandi, N., R. M. Kershah, and B. J. Serico, "The Effect of Evaporation Losses in the Analysis of Counterflow Cooling Towers," *Nuclear Engineering and Design*, 32:29–36, North Holland Pub. Co., 1975.

Niemann, H. J., "Ein Windlastkonzept für Naturzug Kühltürme," *Technische Mitteilungen 70*, 493–499, 1977.

Oosthuizen, P. C., "Performance Characteristics of Hybrid Cooling Towers," Master's thesis, Department of Engineering, University of Stellenbosch, Stellenbosch, 1995.

Poppe, M., "Wärme und Stoffübertragung bei der Verdunstungskühlung in Gegen-und Kreuzstrom," Doctoral thesis, Technische Universität, Hannover, 1972.

Poppe, M. and H. Rögener, "Berechnung von Rückkühlwerken," *VDI-Wärmeatlas*, Mi1–Mi15, Verein Deustche Ingenieure-Verlag Düsseldorf, 1991.

Radosavljevic, D. and D. B. Spalding, "Simultaneous Prediction of Internal and External Aerodynamic and Thermal Flow Fields of a Natural Draft Cooling Tower in a Cross-wind," Sixth International Association for Hydraulic Research Cooling Tower Workshop, Pisa, 1988.

Richter, E., "Untersuchung der Strömungsvorgänge am Austritt von Naturzugkühltürmen und deren Einfluss auf die Kühlwirkung," Doctoral thesis, Technische Universität, Dresden, 1969.

Rish, R. F., "The Design of a Natural Draught Cooling Tower," *Proceedings*, 2nd International Heat Transfer Conference, Colorado, 1961.

Rühl, H., "Convergent Configuration of the Top of Larger Cooling Towers Together with an Upward Spray Water Distribution," VGB Congress, Copenhagen, 1977.

Ruscheweyh, H., "Modelluntersuchung zum Einfluss der Kühlturm-kronenform auf das Zugverhalten grosser Naturzugkühltürme unter Querwindeinfluss," *Brennstoff- Wärme- Kraft*, 34-7:361–369, 1982.

Singham, J. R , *The Thermal Performance of Natural Draught Cooling Towers: 1) Analysis of Test Data; 2) Design and Optimisation; 3) Prediction of Performance*, Report ED/R/1, Imperial College of Science and Technology, London, April 1967.

Sutherland, J. W., "Analysis of Mechanical-draught Counterflow Air/water Cooling Towers," Transactions of the American Society of Mechanical Engineers, *Journal of Heat Transfer*, vol. 105, August 1983.

Szabó, Z., *Why Use the "Heller System"? Circuitry Characteristics and Special Features*, EGI Contracting and Engineering, Hungary, March 1991.

Terblanche, J. E. and D. G. Kröger, "Experimental Evaluation of the Aerodynamic Inlet Losses in Cooling Towers," *South African Institute of Mechanical Engineers Research and Development Journal*, 10-2:41–44, 1994.

Terblanche, J. E., "Inlaatverliese by Koeltorings," Master's thesis, Department of Engineering, University of Stellenbosch, 1993.

Tesche, W., "Untersuchungen zur optimalen Schalenkontur grosser Naturzugkühltürme," *VGB- Kraftwerkstechnik*, 9-64:825–829, 1984.

Vauzanges, M. and G. Ribier, "Variation of the Head Losses in the Air Inlets of Natural Draft Cooling Towers with the shape of the Lintel and Shell Supports," *Proceedings*, Fifth International Association for Hydraulic Research Cooling Tower Workshop, Monterey, 1986.

Vereinigung der Grosskaftwerksbetreiber E.V., *VGB—Empfehlung über den Winterbetrieb von Kraftwerks-Nasskühltürmen*, VGB-R 129P, Essen, 1988.

Vogelsang, E. and M. Hackeschmidt, "Experimentelle Untersuchungen über die Ungleichförmigkeit der Strömung in Verdunstungskühlern," *Luft- und Kältetechnik*, 7:306–318, 1968.

Witte, R., "Das Betriebsverhalten atmosphärisch beeinflusster Trocken-kühltürme," *Fortschritt-Bericht VDI-Zeitschrit*, Reihe 6, no. 132, Verein Deutscher Ingenieure Verlag, Düsseldorf, 1983.

Yadigaroglu, G. and E. J. Pastor, *An Investigation of the Accuracy of the Merkel Equation for Evaporative Cooling Tower Calculations*, 74-HT-59, American Society of Mechanical Engineers 1974.

Zembaty, W. and T. Konikowski, "Untersuchung über den aerodynamischen Widerstand von Kühltürmen," *Brennstoff- Wärme-Kraft*, 23-10:441–445, 1971.

Zien, H. B., "Problems of Airflow Through Large Natural Draft Cooling Towers," Paper, National Science Foundation, 72–75, April 1972.

8

Mechanical Draft Coolers

8.0 Introduction

Many different types of mechanical draft coolers or heat exchangers are found in a wide spectrum of industries. Some examples are shown in Chapter 1. Air may be blown or drawn through the heat exchanger by a fan. The former configuration is referred to as a *forced-draft* system while the latter is called an *induced-draft* system. Despite the poor cooling properties of air, it is available in unlimited quantities throughout the year. No costs are incurred for its procurement, and there is no disposal problem or significant impact on the environment.

Operating temperatures, fan accessibility, process specifications, ambient conditions, fouling, and other practical considerations will influence the ultimate system design. Although fouling effects are not specifically included in the performance evaluations described in this chapter, its effect on the heat transfer and mass transfer rates and the flow resistance can be incorporated readily in any analysis.

To design small air-cooled heat exchangers or to evaluate the performance characteristics of a particular unit, relatively simple but approximate methods may be adequate. A number of authors have reported on these methods and

include Russell and Bos, Brown et al., Zanker, Paikert, Shaikh, McKetta, and Hewitt et al. However, these methods are usually less acceptable in the case of mass produced or large, specialized, and expensive systems.

The performance of air-cooled heat exchangers may be determined according to different standards from authorities such as Rose et al., the American Institute of Chemical Engineers, Verein Deutscher Ingenieure, and ASME PTC 30-1991.

Examples of mechanical draft cooling towers are shown in Figures 1.1.3, 1.1.4, and 1.1.5.

8.1 Air-Cooled Heat Exchangers and Cooling Towers

Air-cooled heat exchangers found in refinery and petro-chemical plants may consist of bundles made up of headers 2–3 m wide, finned tubes 8–12 m long, and frames. The majority of finned tubes are composed of tubes ranging from 19–51 mm in diameter. The fins usually range from 300–450 fins/m. The fin heights range from 6–19 mm. Approximately 80% of the tubes have an outside diameter of 25.4 mm and have 350–450 fins/m of 16 mm fin height. More than 90% of the fins are made of aluminum, and the remainder may be either copper, steel, stainless steel, or galvanized steel. Type-L and type-G fins find the greatest number of applications.

The number of rows of finned tubes usually ranges from 3–6 rows. A typical bay is made up of one or more tube bundles served by two or more fans complete with structure, plenum, and other attendant equipment according to both Shipes and Mukherjee. Fans normally range from 1.8–4.1 m in diameter and may have from 3–6 blades. However, 4–6 blades are most common. A large heat exchanger may consist of a bank of many of these bays. To facilitate the procurement and manufacture of air-cooled heat exchangers for refinery service, use publications such as the American Petroleum Institute Standard 661 and complementary specifications available from Rose, Wilson, and Cowan. These provide purchase specifications and other practical aspects of heat exchangers.

The Air-Cooled Heat Exchanger Manufacturer Association (ACHEMA) recommends a standard to assist those who specify, design, purchase, install, and maintain air-cooled heat exchangers. Using the standards helps

professionals obtain the necessary information for proper and safe selection and application.

Consider the example of a forced-draft air-cooled heat exchanger unit shown in Figure 8.1.1.

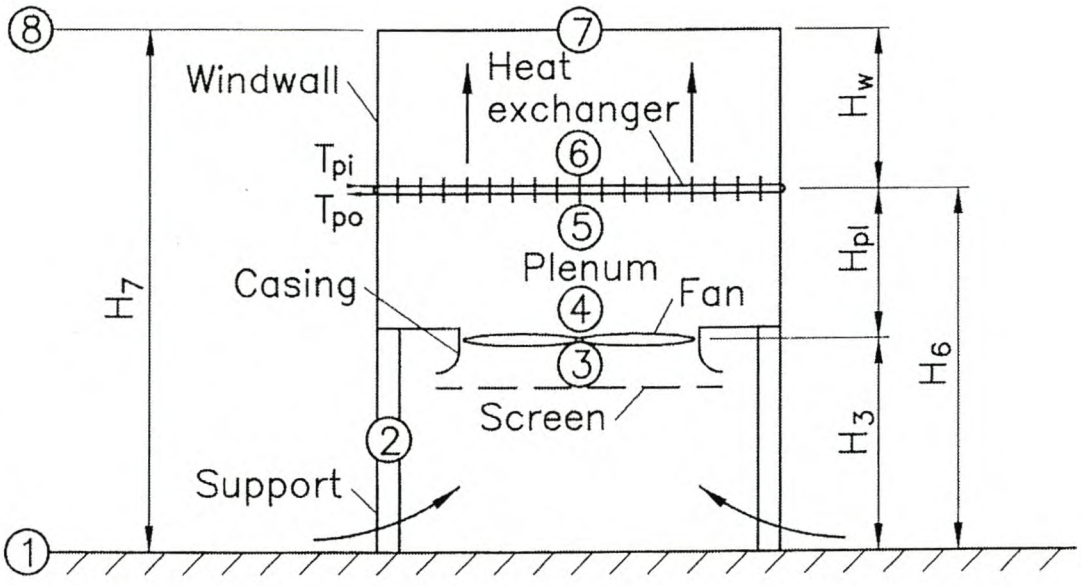

Fig. 8.1.1 Forced-Draft Air-Cooled Heat Exchanger

The heat exchanger consists of bundles of finned tubes located horizontally above the fans. A hot process fluid enters the tubes at a temperature, T_{pi}, while cooler ambient air flows across the finned surfaces. A windwall of height, H_w, may be installed to reduce the recirculation of hot plume air.

The amount of heat transferred to the air stream from the process fluid can be expressed as

$$Q = m_a c_{pa}(T_{a6}-T_{a5}) = m_p c_{pp}(T_{pi}-T_{po}) \qquad (8.1.1)$$

where

$_p$ = process fluid

The heat transfer rate may also be expressed in terms of the effectiveness of the heat exchanger, i.e.,

$$Q = eC_{\min}(T_{pi} - T_{a5}) \tag{8.1.2}$$

where

$C_{\min}$ = the smaller of $m_a c_{pa}$ and $m_p c_{pp}$

e = effectiveness, and depends on the geometry and flow patterns of the fluids through the heat exchanger

For an air-cooled condenser, the effectiveness is given by Equation 3.5.22, while the values for single-pass, cross-flow heat exchangers are listed in Table 3.5.1. For an air-cooled heat exchanger having four or more tube passes in counterflow, the effectiveness for double pipe counterflow may be employed. The more general Equation 3.5.23 can be applied where there are n_p identical passes.

The effectiveness will be influenced by the upstream turbulence of the air and the maldistribution of the fluids. In a well-designed, forced-draft, industrial, air-cooled heat exchanger, the reduction in effectiveness due to maldistribution of the flow on the air side is relatively small. This was shown in section 5.10, and it is counteracted to some extent by heat transfer enhancement due to increased upstream turbulence as discussed in section 5.9.

Upon substitution of Equation 1.4.8 into Equation 1.4.2 and applying the latter between sections (1) and (5), find the approximate inlet air temperature to the heat exchanger.

$$T_{a5} = T_{a1} + P_F/(m_a c_{pa1}) - gH_5/c_{pa1}$$

$$= T_{a1} + P_F/(m_a c_{pa1}) - 0.00975 H_5 \tag{8.1.3}$$

In this equation, it is assumed the kinetic energy of the air entering the heat exchanger is negligible and the mean heat exchanger height above ground level is $H_5 \approx H_6$.

In practice, the draft equation for an air-cooled heat exchanger is sometimes obtained by matching only the fan performance curve and the flow characteristics through the heat exchanger bundles. The thermophysical properties of the air are evaluated at ambient ground level conditions. Although this may give useful values in some cases, serious errors have been incurred in other designs. Increasing competitiveness and high system costs generally justify the more detailed analysis which follows.

A suitable fan must deliver a cooling air flow rate efficiently to guarantee the desired heat transfer rate. In order to achieve this, a series of flow resistances must be overcome.

Stagnant ambient air at (1) accelerates and flows across the heat exchanger supports at (2) before reaching the fan at section (3), where upstream obstacles such as structural supports or a screen or mesh guard may be located. After leaving the fan at (4) where further downstream obstacles may be located, the flow experiences losses in the plenum before entering the heat exchanger bundle at (5) and exiting at (6).

Apply the relevant relations and Equation 2.3.2 across the consecutive flow resistances. Upon addition, find an expression for the pressure difference between sections (1) and (7). This was done in the case of a cooling tower for a DALR.

$$p_{a1} - p_{a7} = p_{a1}\left[1 - (1 - 0.00975\,H_6 / T_{a1})^{3.5}\right] + K_{ts}(m_a / A_2)^2 / (2\rho_{a2})$$

$$+ K_{Fsi}(m_a / A_c)^2 / (2\rho_{a3}) + K_{up}(m_a / A_3)^2 / (2\rho_{a3}) - \left[\Delta p_{Fs} + \alpha_{eF}(m_a / A_c)^2\right.$$

$$\left. / (2\rho_{a4})\right] + K_{pl}(m_a / A_c)^2 / (2\rho_{a4}) + K_{do}(m_a / A_4)^2 / (2\rho_{a4}) + K_{he}(m_a / A_{fr})^2$$

$$/ (2\rho_{a56}) + p_{a6}\left[1 - \{1 - 0.00975(H_7 - H_6) / T_{a6}\}^{3.5}\right] + \alpha_{e7}(m_a / A_{fr})^2 / (2\rho_{a7})$$

(8.1.4)

where

the velocity is replaced by the air mass flow rate and the corresponding flow area.

Effects of inlet flow distortions on fan performance, see section 8.3, are neglected in Equation 8.1.4.

According to Equation 7.1.20, the loss coefficient due to the heat exchanger supports can be expressed as

$$K_{ts} = C_{Dts} L_{ts} d_{ts} n_{ts} / A_2 \tag{8.1.5}$$

The shape of the fan shroud inlet is taken into consideration by K_{Fsi} for which values are given in section 6.4.3. Details for evaluating the upstream and downstream loss coefficients, K_{up} and K_{do}, are given in section 6.4.1. These loss coefficients are based on the area

$$A_3 = A_4 = A_e = A_c - A_h$$

where

A_c = fan casing area

A_h = hub cross-sectional area

Fan performance characteristics incorporated in the Δp_{Fs} term are obtained from standard installation tests. However, not one of these installations is truly representative of the air-cooled heat exchanger configuration shown in Figure 8.1.1. Tests conducted on air-cooled heat exchanger systems suggest a part of the kinetic energy at the outlet of the fan is lost in the plenum chamber. This loss can be expressed in terms of a plenum loss coefficient, K_{pl}. It is convenient to combine the fan and the plenum characteristics as follows:

$$-\left[\Delta p_{Fs} + \alpha_{eF}(m_a/A_c)^2/(2\rho_{a4})\right] + K_{pl}(m_a/A_c)^2/(2\rho_{a4}) \approx -\left[K_{Fs} + (\alpha_{eF} - K_{pl})\right]$$

$$x\,(m_a/A_c)^2/(2\rho_{a3}) = -(K_{Fs} + K_{rec})(m_a/A_c)^2/(2\rho_{a3}) \tag{8.1.6}$$

where

α_{eF} = the kinetic energy velocity distribution correction factor at the outlet of the fan

The fan static pressure rise coefficient is defined as

$$K_{Fs} = 2\Delta p_{Fs} \rho_{a3} / (m_a / A_c)^2 \qquad (8.1.7)$$

where

A_c = the fan casing cross-sectional area

Δp_{Fs} = fan static pressure obtained from tests conducted in a type A installation

The plenum recovery coefficient is

$$K_{rec} = (\alpha_{eF} - K_{pl}).$$

The heat exchanger loss coefficient, K_{he}, expressed in Equations 5.4.22 and 5.4.23 is obtained experimentally or can be determined with the aid of empirical equations such as those given in section 5.5.2 for circular finned tubes.

If the ambient air far from the heat exchanger is dry and the temperature distribution is according to the DALR, the difference in pressure between (1) and (8) follows from Equation 9.1.11.

$$(p_{a1} - p_{a8}) = (p_{a1} - p_{a7}) = (p_{a1} - p_{a6}) + (p_{a6} - p_{a7})$$

$$\approx p_{a1} \left[1 - (1 - 0.00975\, H_6 / T_{a1})^{3.5}\right]$$

$$+ p_{a6} \left[1 - \{1 - 0.00975 (H_7 - H_6) / T_a 1\}^{3.5}\right] \qquad (8.1.8)$$

where

ambient air temperature at elevation (6) is assumed to be approximately equal to T_{a1}

Although the air temperature distribution near ground level generally deviates considerably from the DALR, the error introduced by this assumption in Equation 8.1.8 is small for relatively high heat exchangers.

Substitute Equation 8.1.8 into Equation 8.1.4, and use Equation 8.1.6 to find the draft equation for the forced-draft, air-cooled heat exchanger shown in Figure 8.1.1.

$$p_{a6}\left[\{1-0.00975(H_7-H_6)/T_{a6}\}^{3.5}-\{1-0.00975(H_7-H_6)/T_{a1}\}^{3.5}\right]$$

$$\approx p_{a1}\left[\{1-0.00975(H_7-H_6)/T_{a6}\}^{3.5}-\{1-0.00975(H_7-H_6)/T_{a1}\}^{3.5}\right]$$

$$= K_{ts}(m_a/A_2)^2/(2\rho_{a1}) + K_{Fsi}(m_a/A_c)^2/(2\rho_{a3}) + K_{up}(m_a/A_e)^2/(2\rho_{a3})$$

$$-(K_{Fs}+K_{rec})(m_a/A_c)^2/(2\rho_{a3}) + K_{do}(m_a/A_e)^2/(2\rho_{a3})$$

$$+K_{he}(m_a/A_{fr})^2/(2\rho_{a56}) + \alpha_{e6}(m_a/A_{fr})^2/(2\rho_{a6}) \qquad (8.1.9)$$

where the following assumptions are made:

$p_{a6} \approx p_{a1}$ on the left side of Equation 8.1.9

$H_8 = H_7$

$\rho_{a2} \approx \rho_{a1}$

$\rho_{a4} \approx \rho_{a3}$

$\rho_{a7} \approx \rho_{a6}$

frictional losses between (6) and (7) are negligible

the kinetic energy factor $\alpha_{e6} \approx \alpha_{e7}$

For a DALR, the approximate air temperature at section (3) is

$$T_{a3} = T_{a1} - 0.00975\,H_3 - \alpha_{eF} v_F^2/(2\,c_{pa}) \approx T_{a1} - 0.00975\,H_3 - v_F^2/(2\,c_{pa})$$

$$\approx T_a 1 - 0.00975\,H_3 \approx T_{a1} \qquad (8.1.10)$$

The second and third terms on the right side of this equation are both orders of magnitude smaller than the absolute temperature. Since the velocity correction factor α_{eF} through the fan is usually not known, the kinetic energy at (3) is neglected in Equation 8.1.10. However, its value may be of the same order or greater than that of the second term on the right side of the equation.

The corresponding approximate density of the air at this elevation is

$$\rho_{a3} \approx p_{a1}/(RT_{a3}) \qquad (8.1.11)$$

The approximate density of the air immediately before the heat exchanger is

$$\rho_{a5} \approx p_{a1}/(RT_{a5}) \qquad (8.1.12)$$

A similar equation gives the density of the air immediately after the heat exchanger at a temperature T_{a6}.

The harmonic mean density through the heat exchanger is given by

$$\rho_{a56} \approx 2p_{a1}/[R(T_{a5} + T_{a6})] \qquad (8.1.13)$$

In the previous equations, the thermophysical properties for dry air are usually employed since the influence of water vapor is negligible.

Although the terms on the left side of Equation 8.1.9 are often relatively small, they may become important where the system operates at low fan speeds or in a natural convection mode with windwalls.

By following the previous procedure, the energy and draft equations can be deduced for an induced-draft, air-cooled heat exchanger fitted with a diffuser (Fig. 8.1.2).

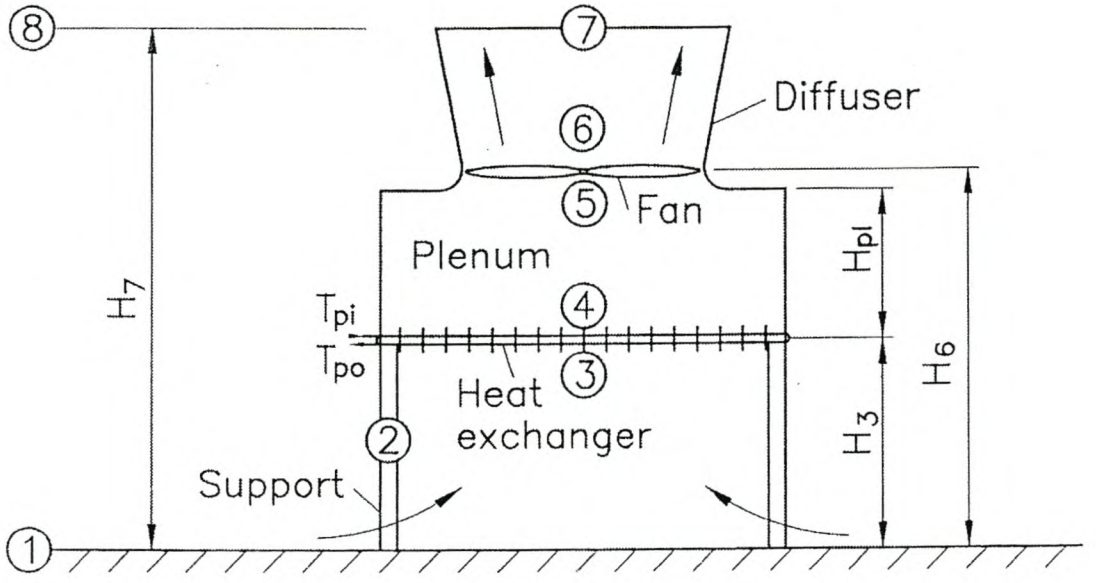

Fig. 8.1.2 Induced-Draft Air-Cooled Heat Exchanger

The heat transfer rate is

$$Q = m_a c_{pa}(T_{a4} - T_{a3}) = m_p c_{pp}(T_{pi} - T_{po}) \tag{8.1.14}$$

or

$$Q = e\, C_{min}(T_{pi} - T_{a3}) \tag{8.1.15}$$

where

$$T_{a3} = T_{a1} - 0.00975 H_3 - v_{a3}^2 / (2 c_{pa}) \approx T_{a1} - 0.00975 H_3 \tag{8.1.16}$$

In an induced-draft heat exchanger, the usual air flow through the heat exchanger is uniform and upstream turbulence is low.

The draft equation is given by

$$p_{a1}\left[\{1-0.00975(H_7-H_4)/T_{a4}\}^{3.5}-\{1-0.00975(H_7-H_4)/T_{a1}\}^{3.5}\right]$$

$$= K_{ts}(m_a/A_2)^2/(2\rho_{a1})+K_{ct}(m_a/A_{fr})^2/(2\rho_{a1})+K_{he}(m_a/A_{fr})^2/(2\rho_{a34})$$

$$+K_{pl}(m_a/A_c)^2/(2\rho_{a4})+K_{up}(m_a/A_e)^2/(2\rho_{a4})-(K_{Fs}+\alpha_{eF})(m_a/A_c)^2/(2\rho_{a4})$$

$$+K_{do}(m_a/A_e)^2/(2\rho_{a4})+K_{dif}(m_a/A_c)^2/(2\rho_{a4})+\alpha_{e7}(m_a/A_7)^2/(2\rho_{a4})$$

$$= K_{ts}(m_a/A_2)^2/(2\rho_{a1})+K_{ct}(m_a/A_{fr})^2/(2\rho_{a1})+K_{he}(m_a/A_{fr})^2/(2\rho_{a34})$$

$$+K_{pl}(m_a/A_c)^2/(2\rho_{a4})+K_{up}(m_a/A_e)^2/(2\rho_{a4})-K_{Fs}(m_a/A_c)^2/(2\rho_{a4})$$

$$+K_{do}(m_a/A_e)^2/(2\rho_{a4})+K_{dif}(m_a/A_c)^2/(2\rho_{a4})+\alpha_{eF}(1/A_7-1/A_c^2)m_a^2/(2\rho_{a4}) \quad (8.1.17)$$

where

K_{dif} = the diffuser loss coefficient

K_{ct} = the inlet loss coefficient (see section 8.3)

$H_8 = H_7$

$H_4 \approx H_3$

$\rho_{a2} \approx \rho_{a1}$

$\rho_{a7} \approx \rho_{a6} \approx \rho_{a5} \approx \rho_{a4}$.

$\alpha_{e7} \approx \alpha_{eF}$ for a short diffuser

Also,

$$\rho_{a34} \approx 2p_{a1}/[R(T_{a3}+T_{a4})] \tag{8.1.18}$$

Since α_{eF} is not known usually, it is helpful if the performance characteristics of the fan/diffuser unit $K_{F/dif}$ are available. In this case, three terms in Equation 8.1.17 can be replaced by

$$-K_{F/dif}(m_a/A_c)^2/(2\rho_{a4}) = -K_{Fs}(m_a/A_c)^2/(2\rho_{a4}) + K_{dif}(m_a/A_c)^2/(2\rho_{a4})$$

$$+\alpha_{eF}(1/A_7^2 - 1/A_c^2)m_a^2/(2\rho_{a4}) \tag{8.1.19}$$

When the fans moving the air across the tube bank are shut off, the heat exchanger will operate in a natural convection heat transfer mode. The heat exchanger structure, including the tube bundles, plenum chamber, and diffuser or stack will cause some draft. This results in a corresponding amount of cooling. However, the weak draft is very sensitive to even the lightest winds.

Example 8.1.1

A forced-draft, air-cooled heat exchanger bank at a petro-chemical plant consists of bays having two fans (Figs. 1.2.1 and 8.1.3). The process fluid enters the heat exchanger at

- Temperature: T_{pi} = 152 °C
- Flow rate: m_p = 30.55 kg/s,

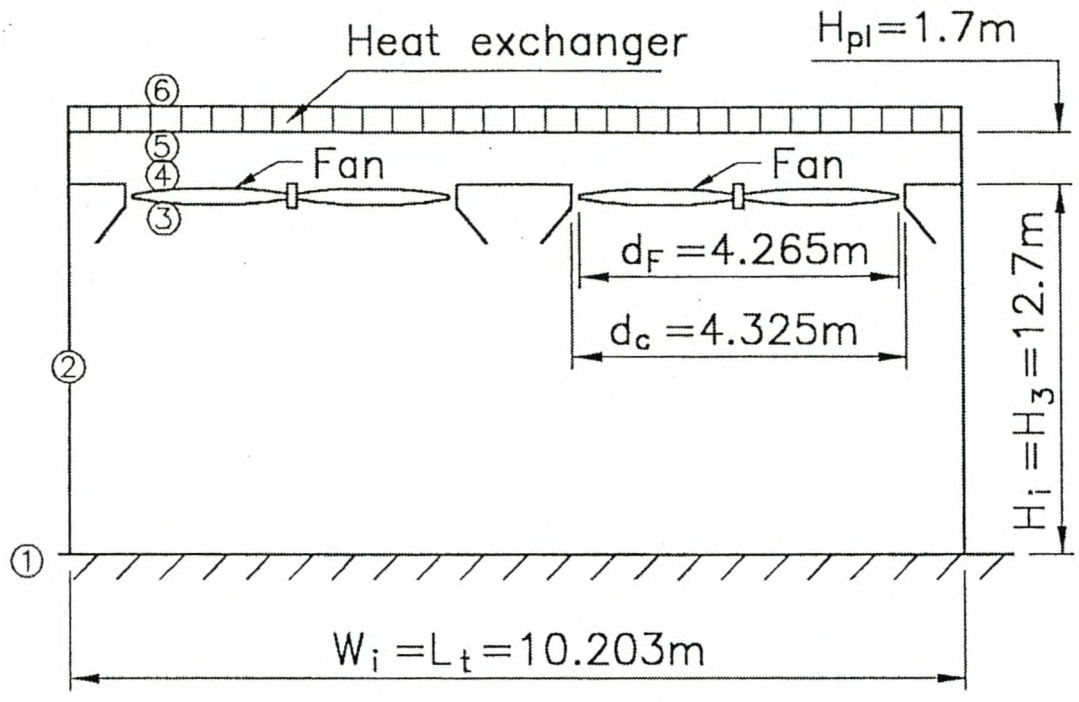

Fig. 8.1.3 Air-Cooled Heat Exchanger Bay

Determine the heat rejected by such a bay and the shaft power required by each fan, if the following details are specified:

Ambient conditions:

- Air temperature at ground level: T_{a1} = 28°C (301.15 K)
- Atmospheric pressure at ground level: p_{a1} = 101325 N/m^2
- The ambient temperature gradient: - 0.00975 K/m from ground level.

It may be assumed the air is dry.

Process fluid data:

- Specific heat: c_{pp} = 3960 J/kg K
- Thermal conductivity: k_p = 0.09125 W/m K
- Dynamic viscosity: μ_p = 0.00172 kg/ms
- Prandtl number: Pr_p = 74.643

It may be assumed these properties do not change significantly with temperature across the cooling range. The process fluid flows inside finned tubes where its heat transfer coefficient, which includes fouling effects, is h_p = 1208 W/m^2 K.

Finned tube bundle specifications:

- Heat exchanger tubes arranged in a triangular pattern
- Finned tubes: type G
- Aluminum fins
- Diameter: 57.15 mm
- Number of bundles: $n_b = 2$
- Effective frontal area of one bundle: A_{fr} = 35.96 m^2
- Effective length of finned tube: L_t = 10.203 m
- Inside diameter of tube: d_i = 0.0211 m
- Area ratio: $\sigma = A_c/A_{fr}$ = 0.511 (A_c = minimum flow area through finned tube bundle)
- Number of tube rows: $n_r = 6$
- Number of tubes per row: $n_{tr} = 55$
- Number of tube passes (process fluid mixes between passes): $n_p = 2$

The characteristic heat transfer parameter is determined experimentally for a bundle and is given by

$$N_y = 834.8044\, Ry^{0.49353}$$

This correlation was obtained for a very low turbulence intensity in the upstream air. Due to upstream turbulence in the forced-draft air-cooled heat exchanger, the heat transfer rate is assumed to be improved by 1%.

The isothermal loss coefficient through the bundle is

$$K_{he} = 588.653\, Ry^{-0.2931}$$

Fan installation:

- Bays: 2 fans with conical inlet shrouds
- Fans: $n_F = 2$
- Fan diameter: d_F = 4.265 m
- Fan casing diameter: d_c = 4.325 m
- Fan rotational speed: N_F = 265 rpm
- Fan hub diameter: d_h = 1.524 m

- Plenum height: $H_{p\ell} = 1.7$ m
- Height of fan platform above ground level: $H_3 = 12.7$ m
- Upstream loss coefficient (based on A_e): $K_{up} = 0.1$
- Downstream loss coefficient (based on A_e): $K_{do} = 0.15$
- Conical shroud inlet loss coefficient: $K_{Fsi} = 0.07$
- Heat exchanger support loss coefficient: $K_{ts} = 1.5$ (based on frontal area of heat exchanger)
- No windwall

The performance characteristics of a 4.265 m diameter fan mounted in a 4.325 m diameter casing with a bellmouth type inlet and tested according to BS 848 in a type A installation are specified at a reference air density of

$$\rho_r = 1 \text{ kg/m}^3 \text{ and } N_{Fr} = 216 \text{ rpm}$$

Fan static pressure:

$$\Delta p_{Fsr} = 140.2243 + 0.8776\, V_{Fr} - 0.014\, V_{Fr}^2 + 1.5075 \times 10^{-5}\, V_{Fr}^3, N/m^2$$

Fan shaft power:

$$P_{Fr} = 31.6268 - 0.9904\, V_{Fr} + 0.019\, V_{Fr}^2 - 1.4427 \times 10^{-4}\, V_{Fr}^3$$

$$+ 3.7075 \times 10^{-7}\, V_{Fr}^4, \text{kW}$$

Losses due to separation at the inlet to the fan platform can be neglected.

Solution

This problem is solved by following an iterative procedure. The energy Equations 8.1.1 and 8.1.2 as well as the draft Equation 8.1.9 must be satisfied simultaneously. These equations are satisfied for a total air mass flow rate of m_a = 306.934 kg/s through the bay.

At this flow rate, the temperature of the air entering the heat exchanger is T_{a5} = 301.218 K, and its outlet temperature is T_{a6} = 341.547 K. The corresponding air densities at these temperatures and a pressure of p_{a1} = 101325 N/m^2 are, according to Equation 8.1.12,

$$\rho_{a5} = 1.1717 \text{ kg/m}^3$$

and

$$\rho_{a6} = 1.0334 \text{ kg/m}^3$$

The mean density of the air through the heat exchanger is, according to Equation 8.1.13,

$$\rho_{a56} = 2 \text{ x } 101325/[287.08(301.218 + 341.547)] = 1.0982 \text{ kg/m}^3$$

Using the equations given in Appendix A, the thermophysical properties of the air flowing through the heat exchanger are evaluated at the arithmetic mean temperature, i.e.,

$$T_{am} = (T_{a5} + T_{a6})/2 = (301.218 + 341.547)/2 = 321.383 \text{ K}$$

- Specific heat: c_{pam} = 1007.9284 J/kg K using Equation A.1.2
- Dynamic viscosity: $\mu_{am} = 1.944 \text{ x } 10^{-5}$ kg/ms using Equation A.1.3
- Thermal conductivity: k_{am} = 0.0279 W/mK using Equation A.1.4
- Prandtl number: Pr_{am} = 0.7023

The total effective frontal area of the heat exchanger in the bay is given by

$$A_{frt} = n_b A_{fr} = 2 \text{ x } 35.96 = 71.92 \text{ m}^2$$

Find the characteristic flow parameter

$$Ry = m_a/(\mu_{am} A_{frt}) = 306.934/(1.944 \text{ x } 10^{-5} \text{ x } 71.92) = 219533 \text{ m}^{-1}$$

According to the specified relation, the corresponding heat transfer parameter is

$$Ny = 834.8044 \text{ x } 219533^{0.49353} = 361223 \text{ m}^{-1}$$

It follows from Equation 5.4.13 that

$$h_{ae} A_a = Nyk_{am} A_{frt} Pr_{am}^{0.333} = 361223 \text{ x } 0.0279 \text{ x } 71.92 \text{ x } 0.7023^{0.333}$$

$$= 644349 \, W/K$$

The total inside surface area of the tubes exposed to the process fluid can be expressed as

$$A_p = n_{tr} n_r L_t n_b \pi d_i = 55 \text{ x } 6 \text{ x } 10.203 \text{ x } 2 \text{ x } \pi \text{ x } 0.0211 = 446.38 \text{ m}^2$$

With the previous values, find the overall heat transfer coefficient.

$$UA = \left(\frac{1}{h_{ae}A_a} + \frac{1}{h_pA_p}\right)^{-1} = \left(\frac{1}{644349} + \frac{1}{1208 \text{ x } 446.38}\right)^{-1} = 293560 \text{ W/K}$$

To find the number of transfer units,

$$C_{min} = m_pc_{pp} = 30.55 \text{ x } 3960 = 120978 \text{ W/K} < C_{max}$$

$$= m_ac_{pam} = 306.934 \text{ x } 1007.9284 = 309368 \text{ W/K}$$

such that

$$NTU = \frac{UA}{C_{min}} = \frac{293560}{120978} = 2.4266$$

There are two tube-side passes, with each pass having

$$NTU_p = N_p = NTU/2 = 2.4266/2 = 1.213$$

The heat capacity ratio is

$$C = C_{min}/C_{max} = 120978/309368 = 0.391$$

If both the air stream and the process fluid are unmixed in each pass, then the effectiveness per pass, according to Table 3.5.1, is given by

$$e_p = 1 - \exp\left[N_p^{0.22}\left\{\exp\left(-CN_p^{0.78}\right) - 1\right\}/C\right]$$

$$= 1 - \exp\left[1.213^{0.22}\left\{\exp\left(-0.391 \text{ x } 1.213^{0.78}\right) - 1\right\}/0.391\right] = 0.6227$$

With this value, the effectiveness of the entire heat exchanger follows from Equation 3.5.23 where process fluid mixing occurs between passes.

$$e = \left[\left\{(1 - 0.6227 \text{ x } 0.391)/(1 - 0.6227)\right\}^2 - 1\right] / \left[\left\{(1 - 0.6227 \text{ x } 0.391)/(1 - 0.6227)\right\}^2 - 0.391\right] = 0.8322$$

According to Equation 8.1.2, the rate of heat transfer is

$$Q = e\, C_{min}(T_{pi} - T_{a5}) = 0.8322 \times 120978\,[152 - (301.218 - 273.15)] = 12.477\ \text{MW}$$

The heat transfer rate can also be determined from Equation 8.1.1, i.e.,

$$Q = 306.934 \times 1007.9284\,(341.547 - 301.218) = 12.477\ \text{MW}$$

These two values for the heat transfer rate are in agreement.

To determine whether the draft equation is satisfied, the fan performance has to be evaluated.

According to Equation 8.1.16, the approximate air temperature at the fan inlet is

$$T_{a3} \approx 301.15 - 0.00975 \times 12.7 = 301.026\ \text{K}$$

At this temperature and the specified atmospheric pressure at ground level, find $\rho_{a3} = 1.172\ \text{kg/m}^3$ and $c_{pa3} = 1006.99\ \text{J/kgK}$ using Equations 8.1.11 and A.1.2 respectively.

The actual air volume flow rate through each fan is

$$V = m_a / (n_F \rho_{a3}) = 306.934 / (2 \times 1.172) = 130.9\ m^3/s$$

Since the actual air density and the rotational speed of the fan are not the same as the reference conditions for which fan performance characteristics were specified, the relevant fan laws given in section 6.2 are employed.

According to Equation 6.2.1,

$$V_{Fr} = V(N_{Fr}/N_F) = 130.9 \times 216/265 = 106.7\ \text{m}^3/\text{s}$$

At this flow rate, the reference fan static pressure is given by

$$\Delta p_{Fsr} = 140.2243 + 0.8776 \times 106.7 - 0.014 \times 106.7^2 + 1.5075 \times 10^{-5} \times 106.7^3$$

$$= 92.788\ N/m^2$$

The actual change in fan static pressure expressed by Equation 6.2.2 is

$$\Delta p_{Fs} = \Delta p_{Fsr}\,(N_F/N_{Fr})^2\,(\rho_{a3}/\rho_r) = 92.788\,(265/216)^2\,(1.172/1) = 163.75\ N/m^2$$

At the reference condition, the fan shaft power is

$$P_{Fr} = 31.6268 - 0.9904 \times 106.7 + 0.019 \times 106.7^2 - 1.4427 \times 10^{-4} \times 106.7^3$$

$$+ 3.7075 \times 10^{-7} \times 106.7^4 = 15.06 \text{ kW}$$

The actual fan shaft power follows from Equation 6.2.3, i.e.,

$$P_F = P_{Fr}(N_F / N_{Fr})^3(\rho_{a3} / \rho_r) = 15.06(265 / 216)^3(1.1725 / 1) = 32.61 \text{ kW}$$

With this value, it is possible to determine the approximate temperature of the air immediately upstream of the heat exchanger according to Equation 8.1.3.

$$T_{a5} \approx T_{a1} + P_F/(m_a c_{pa3}/2) - 0.00975(H_3 + H_{p1})$$

$$= 301.15 + 2 \times 32\,610/(306.934 \times 1006.99) - 0.00975 \times (12.7 + 1.7) = 301.2 \text{ K}$$

This value is essentially the one given initially.

The fan static pressure rise coefficient follows from Equation 8.1.7, i.e.,

$$K_{Fs} = 2\Delta p_{Fs} \rho_{a3} / (m_a / A_c)^2 = 2 \times 163.75 \times 1.172 / [306.934 \times 2 / (\pi \times 4.325^2)]^2$$

$$= 3.52$$

For non-isothermal flow, it follows from Equation 5.4.23 that the heat exchanger loss coefficient in this case is given by

$$K_{he} = 588.653\, Ry^{-0.2931} + \frac{2(\rho_{a5} + \rho_{a6})}{\sigma^2(\rho_{a5} + \rho_{a6})}$$

$$= 588.653 \times 219\,533^{-0.2931} + \frac{2(1.1717 - 1.0334)}{0.511^2(1.1717 + 1.0334)} = 16.486$$

According to section 6.4.2, the recommended plenum recovery factor K_{rec} = 0.3 for $15 \leq K_{he} \leq 24$. Furthermore, for $H_{p\ell}/d_c$ = 1.7/4.325 = 0.393 > 0.3, the

corresponding heat exchanger outlet kinetic energy correction factor is, according to Equation 6.4.5,

$$\alpha_{e6} = 1.6 - 0.48 \text{ x} \pi \text{ x } 4.325^2 / (4 \text{ x } 35.96) - 0.012 \text{ x } 16.486 = 1.2061$$

Using Equation 5.10.1, the heat exchanger effectiveness due to maldistribution of the air-side flow is

$$e_{nu} \approx 1.05 - 0.05 \text{ x } 1.2061 = 0.99$$

Since it was specified that the heat transfer rate is enhanced by 1% due to upstream turbulence, the reduction of 1% due to maldistribution is effectively counteracted.

The upstream and downstream loss coefficients, K_{up} and K_{do}, are based on the effective fan area.

$$A_e = A_c - A_h = \pi (d_c^2 - d_h^2)/4 = \pi (4.325^2 - 1.524^2)/4 = 12.8672\, m^2$$

Since no windwall is provided, $H_6 = H_7$, and the left side of draft Equation 8.1.9 is equal to 0. The terms on the right side of the equation give

$$K_{ts}(m_a/A_{frt})^2/(2\rho_{a3}) + K_{Fsi}[m_a/(2A_c)]^2/(2\rho_{a3}) + K_{up}[m_a/(2A_e)]^2/(2\rho_{a3})$$

$$-(K_{Fs} + K_{rec})[m_a/(2A_c)]^2/(2\rho_{a3}) + K_{do}[m_a/(2A_e)]^2/(2\rho_{a3})$$

$$+ K_{he}(m_a/A_{frt})^2/(2\rho_{a56}) + \alpha_{e6}(m_a/A_{frt})^2/(2\rho_{a6})$$

$$= 1.5(306.934/71.92)^2/(2 \text{ x } 1.172) + 0.07[306.934 \text{ x } 4/(2 \text{ x } \pi \text{ x } 4.325^2)]^2$$

$$/(2 \text{ x } 1.172) + 0.1[306.934/(2 \text{ x } 12.8672)]^2/(2 \text{ x } 1.172) - (3.52 + 0.3)$$

$$\text{x } [306.934 \text{ x } 4/(2 \text{ x } \pi \text{ x } 4.325^2)]^2/(2 \text{ x } 1.172) + 0.15[306.934/(2 \text{ x } 12.8672)]^2$$

$$/(2 \text{ x } 1.172) + 16.486(306.934/71.92)^2/(2 \text{ x } 1.0982) + 1.2061(306.934/71.92)^2$$

$$/(2 \text{ x } 1.0334) = -0.4 \text{ N/m}^2$$

This value is close to zero, and the draft equation is thus satisfied.

Note

The fan shaft power is found to be P_F = 32.61 kW at the specified design point. Power requirements at start-up and during operation at lower ambient air temperature will be higher than this value.

Example 8.1.2

An induced-draft air-cooled heat exchanger bank at a petro-chemical plant consists of bays having two fans as shown in Figures 1.2.2 and 8.1.4. The process fluid characteristics and other specifications are as given in Example 8.1.1 except for the following:

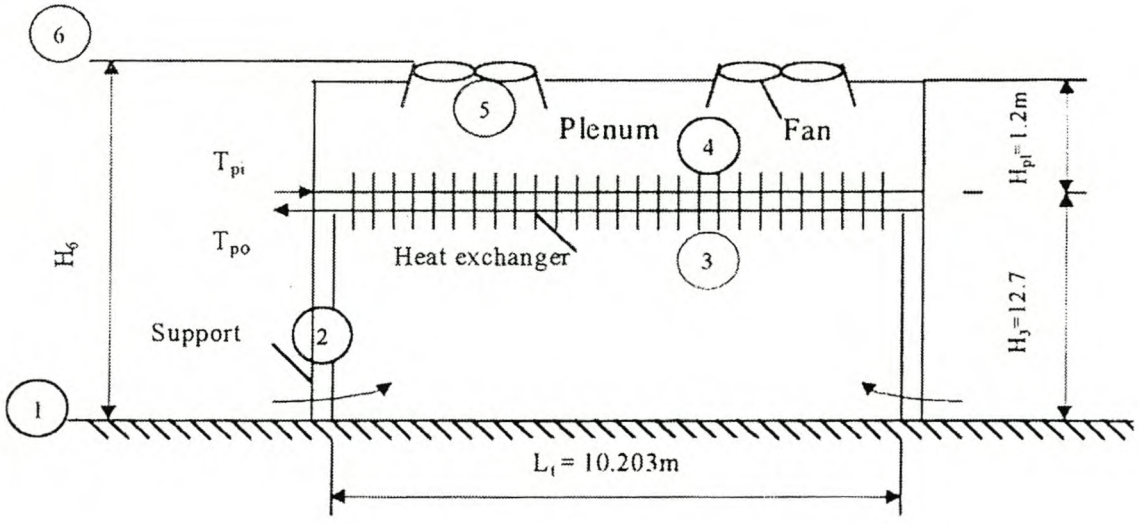

Fig. 8.1.4 Air-Cooled Heat Exchanger Bay

- Height of heat exchanger above ground level: H_3 = 12.7 m
- Height of plenum chamber: H_{pl} = 1.2 m
- Height of fans above ground level: H_6 = 13.9 m
- Fan rotational speed: N_F = 291 rpm

Assume the plenum and inlet losses are negligible ($K_{pl} = 0$, $K_{ct} = 0$) and the velocity distribution through the heat exchanger is uniform.

Determine the heat rejected by such a bay and the shaft power required by each fan.

Solution

The energy and draft equations, i.e., Equations 8.1.14, 8.1.15, and Equation 8.1.17 are satisfied for a total air-mass flow rate through the bay of

$$m_a = 304.4515 \text{ kg/s}$$

At this flow rate, the temperature of the air entering the heat exchanger is

$$T_{a3} = 301.026\text{K } (27.876\ ^\circ\text{C})$$

and the outlet temperature is

$$T_{a4} = 341.6884 \text{ K } (68.5384^\circ\text{C})$$

The corresponding air densities at these temperatures and at a pressure of p_{a1} = 101325 N/m^2 are, according to Equation A.1.1, approximately

$$\rho_{a3} = 1.1725 \text{ kg/m}^3$$

$$\rho_{a4} = 1.03296 \text{ kg/m}^3$$

According to the equations given in Appendix A, the thermophysical properties of the air flowing through the heat exchanger are evaluated at the arithmetic mean temperature

$$T_{am} = (T_{a3} + T_{a4})/2 = (301.026 + 341.6884)/2 = 321.3572 \text{ K}$$

- Density: $\rho_{am} = \rho_{a34} = 1.09831$ kg/m^3 using Equation A.1.1
- Specific heat: $c_{pam} = 1007.927$ J/kgK using Equation A.1.2
- Dynamic viscosity: $\mu_{am} = 1.944 \times 10^{-5}$ kg/ms using Equation A.1.3
- Thermal conductivity: $k_{am} = 0.027859$ W/mK using Equation A.1.4
- Prandtl number: $Pr_{am} = 0.7033$

With the total effective frontal area of the heat exchanger in the bay A_{frt} = 71.92 m^2, find the characteristic flow parameter

$$Ry = m_a/(\mu_{am} A_{frt}) = 304.4515/(1.944 \times 10^{-5} \times 71.92) = 217757.03 \text{ m}^{-1}$$

For the specified relation, the corresponding heat transfer parameter is

$$Ny = 834.8044 \times 217757.03^{0.49353} = 359777.615 \text{ m}^{-1}$$

It follows from Equation 5.4.13 that

$$h_{ae}A_a = Nyk_{am}\,A_{frt}\mathrm{Pr}_{\mathrm{am}}^{0.333}$$

$$= 359777.615 \times 0.027859 \times 71.92 \times 0.7033^{0.333} = 641131.576 \text{ W/K}$$

For a total inside surface area of the tubes A_p = 446.38 m^2, find the overall heat transfer coefficient

$$UA = \left(\frac{1}{h_{ae}A_a} + \frac{1}{h_pA_p}\right) = \left(\frac{1}{641128.55} + \frac{1}{1208 \times 446.38}\right)^{-1} = 292890.21 \text{ W/K}$$

To find the number of transfer units,

$$C_{\min} = 120978 \text{ W/K} < C_{\max} = m_a\,c_{pam} = 304.4515 \times 1007.927 = 306864.89 \text{ W/K}$$

such that

$$NTU = \frac{UA}{C_{min}} = \frac{292890.21}{120978} = 2.421$$

For each tube pass,

$$N_p = NTU/2 = 2.421/2 = 1.2105$$

and

$$C = C_{\min}/C_{\max} = 120978/306864.89 = 0.3942$$

such that the effectiveness becomes

$$e_p = 1 - \exp\left[N_p^{0.22}\left\{\exp\left(-CN_p^{0.78}\right) - 1\right\}/C\right]$$

$$= 1 - \exp\left[1.2105^{0.22}\left\{\exp\left(-0.3942 \times 1.2105^{0.78}\right) - 1\right\}/0.3942\right] = 0.6214$$

According to Equation 3.5.23, the effectiveness of the entire heat exchanger is

$$e = [\{(1 - 0.6214 \times 0.3942) / (1 - 0.6214)\}^2 - 1] / [\{(1 - 0.6214 \times 0.3942) / (1 - 0.6214)\}^2 - 0.3942] = 0.83093$$

The rate of heat transfer is given by Equation 8.1.15.

$$Q = 0.83093 \times 120978\,(152 - 27.876) = 12.477 \text{ MW}$$

The heat transfer rate can also be determined from Equation 8.1.14.

$$Q = 304.4514 \times 1007.927(68.5384 - 27.876) = 12.477 \text{ MW}$$

The two values for the heat transfer rate are in agreement.

To determine whether the draft equation is satisfied, the fan performance has to be evaluated.

The actual air volume flow rate through each fan is

$$V = m_a/(n_F\ \rho_{a5}) \approx m_a/(n_F\ \rho_{a4}) = 304.4515/(2 \times 1.03296) = 147.368\ m^3/s$$

Since the actual density and rotational speed of the fan are not the same as the reference conditions for which the performance characteristics were specified, the relevant fan laws given in section 6.2 are employed.

According to Equation 6.2.1,

$$V_{Fr} = V(N_{Fr}/N_F) = 147.367 \times 216/291 = 109.387\ m^3/s$$

At this flow rate the reference fan static pressure is given by

$$\Delta p_{Fsr} = 140.2243 + 0.8776 \times 109.387 - 0.014 \times 109.387^2 + 1.5075 \times 10^{-5} \times 109.387^3 = 88.436\ N/m^2$$

The actual change in fan static pressure expressed by Equation 6.2.2 is

$$\Delta p_{Fs} = \Delta p_{Fr}(N_F/N_{Fr})^2\ (\rho_{a4}/\rho_r) = 88.436(291/216)^2(1.03296/1) = 165.8032\ N/m^2$$

At the reference condition, the fan shaft power is

$$P_{Fr} = 31.6268 - 0.9904 \times 109.387 + 0.019 \times 109.387^2 - 1.4427 \times 10^{-4} \times 109.387^3 + 3.7075 \times 10^{-7} \times 109.387^4 = 14.885\ kW$$

The actual fan shaft power follows from Equation 6.2.3, i.e.,

$$P_F = P_{Fr}(N_F/N_{Fr})^3\ (\rho_{a4}/\rho_r) = 14.885(291/216)^3\ (1.03296/1) = 37.597\ kW$$

The fan static pressure rise coefficient follows from Equation 8.1.7, i.e.,

$$K_{Fs} = 2\Delta p_{Fs}\ \rho_{a4}/(m_a/A_c)^2$$

$$= 2 \times 165.8032 \times 1.03296/[304.4515 \times 2/(\pi \times 4.325^2)]^2 = 3.1905$$

From Equation 5.4.23, the heat exchanger loss coefficient for non-isothermal flow in this case is given by

$$K_{he} = 588.653 \text{ x } 217757.03^{-0.2931} + 2(1.1725 - 1.03296) / [0.511^2 (1.1725 + 1.03296)]$$

$$= 16.528$$

Upon simplifying the draft Equation 8.1.17, find

$$p_a 1 \, [\{1 - 0.00975 \, (H_6 - H_3) / \, T_{a4}\}^{3.5} - \{1 - 0.00975 \, (H_6 - H_3) / \, T_{a1}\}^{3.5}]$$

$$= K_{ts} \, (m_a / A_{frt})^2 / \, (2\rho_{a1}) + K_{he} \, (m_a / A_{frt})^2 / \, (2\rho_{a34}) - K_{Fs} \, [m_a / (2A_c)]^2 / \, (2\rho_{a4})$$

$$+ K_{do} \, [m_a / (2A_e)]^2 / (2\rho_{a4}) + K_{up} \, [m_a / (2A_e)]^2 / (2\rho_{a4}) + K_{Fsi} \, [m_a / (2A_c)]^2 / (2\rho_{a4})$$

Evaluate the left side of this equation.

$$101325 \, [\{1 - 0.00975 \, (13.9 - 12.7) / 341.6884\}^{3.5} - \{1 - 0.00975 \, (13.9 - 12.7)$$

$$/ \, 301.15\}^{3.5}] = 1.6345 \text{ N/m}^2$$

The value of the right side of the equation is

$$1.5(304.4515 / 71.92)^2 / (2 \text{ x } 1.172) + 16.528 \, (\, 304.4515 / 71.92)^2$$

$$/ \, (2 \text{ x } 1.09831) - 3.1905 \, [304.4515 \text{ x } 2 / (\pi \text{ x } 4.325^2 \,)]^2$$

$$/ \, (2 \text{ x } 1.03296) + (0.1 + 0.15) \, [304.4515 / (2 \text{ x } 12.8672) \,]^2$$

$$/(2 \text{ x } 1.03296) + 0.07 \, [304.4515 \text{ x } /(\pi \text{ x } 4.325^2 \,)]^2 / (2 \text{ x } 1.03296) = 1.072 \text{ N/m}^2$$

Since the values of the two sides of the equation are approximately the same, the draft equation is satisfied.

Note

The heat transfer rate achieved in the induced-draft, air-cooled heat exchanger shown in Figure 8.1.4 is the same as the forced-draft unit shown in Figure 8.1.3. However, the fan-shaft power required to achieve this in the induced-draft unit is 35.597 kW or 15% higher than the 32.61 kW required for the forced-draft unit.

Example 8.1.3

Hot water is flowing at

- Rate: m_w = 1000 kg/s
- Temperature: T_{wi} = 44 °C (317.15 K)

It is to be cooled to T_{wo} = 30.44 °C (303.59 K). This is to be achieved at

- Ambient air temperature: T_{a1} = 33.5 °C (306.65 K)
- Wetbulb temperature: T_{wb} = 25 °C (298.15 K)
- Atmospheric pressure: p_{a1} = 101000 N/m^2
- Measured at: 5.5 m above ground level

Show that the induced-draft, crossflow, mechanical-draft cooling tower shown in Figure 8.1.5 will achieve the required cooling under the specified conditions. Since changes in absolute pressure are small, all thermophysical properties can be evaluated at p_{a1}, and buoyancy effects can be ignored. It is assumed the flow distribution of air and water is uniform. Determine the fan power required.

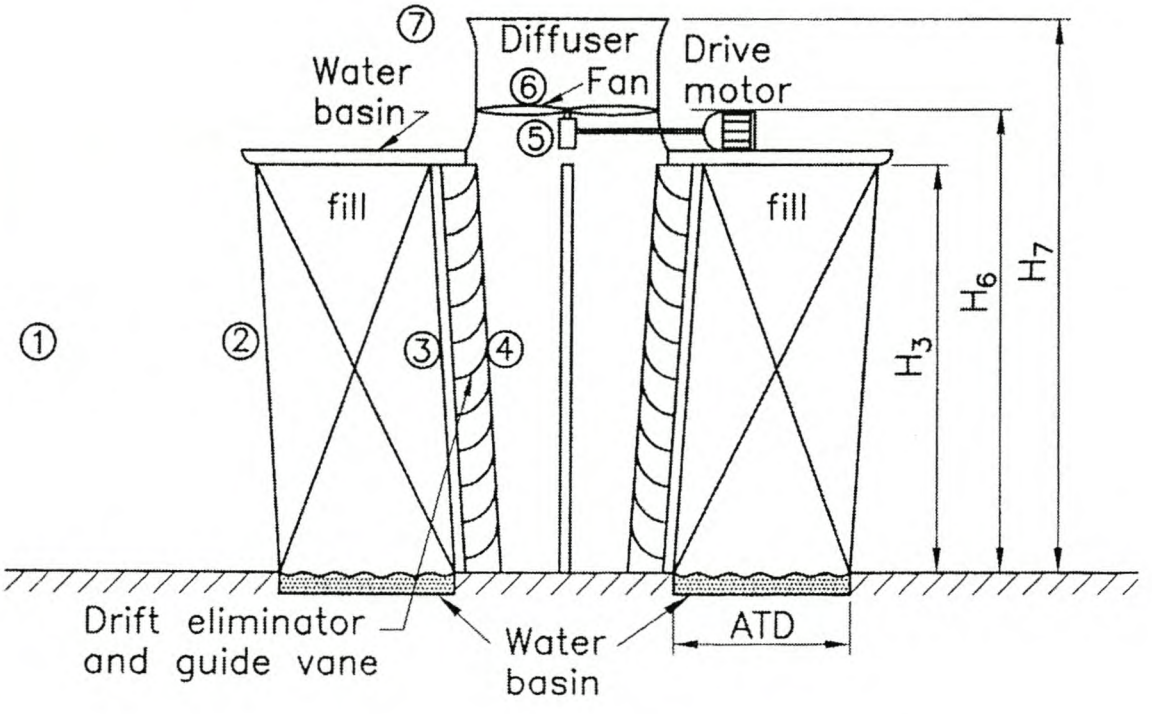

Fig. 8.1.5 Induced-Draft Crossflow Cooling Tower

Cooling tower specifications:

- Inlet height (fill height): H_3 = 11 m
- Inlet width (fill width): W_3 = 11 m
- Fill depth (air travel distance): ATD = 4.57 m
- Height of fan: H_6 = 12 m
- Diffuser outlet height: H_7 = 15 m

Fill performance characteristics:

- Fill material (Fig. 4.3.3a): Heavy-duty, Doron V-bar, 101.6 x 203.2, employed in the wet section
- Transfer coefficient per meter of fill height: Found in Table 4.3.2(a)

$$h_d a_{fi} / G_w = 0.268 (G_w / G_a)^{-0.56}$$

- Loss coefficient per meter of ATD: Found in Table 4.3.2(a)

$$K_{fi1} = 0.751\, G_w^{0.66}\, G_a^{-0.73}$$

- Loss coefficient of the fill support based on conditions through the fill: $K_{fs} = 0.5$
- Downstream and drift eliminator losses based on downstream conditions: $K_{de} = 3$

The drift eliminator in this case also acts as a guide vane and directs the entering air upwards such that losses between the drift eliminators and the fan inlet are small.

Fan/diffuser dimensions and performance characteristics:

- Fan diameter: d_F = 9.5 m
- Fan casing diameter: d_c = 9.5265 m
- Fan rotational speed: N_F = 118 rpm
- Height of diffuser: H_{dif} = 3 m
- Fan upstream and downstream loss coefficient: K_{ud} = 0.5 based on casing cross-sectional area

The performance characteristics are specified at a reference air density of

$$\rho = 1.2 \text{ kg/m}^3$$

and

$$N_{F/dif} = 120 \text{ rpm}$$

and tested according to BS 848 in a type A installation.

- Fan diameter: 9.5 m
- Casing mounting: 9.5265 m diameter
- Inlet: Bellmouth type
- Diffuser height attached at outlet: 3 m

Fan/diffuser static pressure:

$$\Delta p_{F/difs} = 299.903 + 40.0071 \text{ x } 10^{-3} V_{F/dif} - 96.5087 \text{ x } 10^{-6} V_{F/dif}^2$$

$$- 152.2243 \text{ x } 10^{-9} V_{F/dif}^3, \text{ N/m}^2$$

Fan/diffuser power consumption:

$$P_{F/dif} = 203302.6779 - 58.3775 V_{F/dif} + 458.7692 \text{ x } 10^{-3} V_{F/dif}^2$$

$$- 405.2315 \text{ x } 10^{-6} V_{F/dif}^3, \text{ W}$$

Solution

This problem is solved by following an iterative procedure and initially assuming some value for the air-mass flow rate. A solution is obtained at a dry air-mass flow rate

$$m_a = 982.15 \text{ kg/s}$$

The following calculations confirm the correctness of this flow rate.

The effectiveness-NTU method described in section 4.4 will be employed to analyze this crossflow evaporative cooling system. To apply this method, find the enthalpy of the air entering the fill at

- T_{a1} = 33.5°C (306.65K)
- T_{wb} = 25 °C (298.15 K)
- p_{a1} = 101000 N/m^2

Evaluate the specific heat of dry air and water vapor at a mean temperature of

$$(273.15 + 306.65)/2 = 289.9 \text{ K}$$

according to Equations A.1.2 and A.2.2, to give

$$c_{pa} = 1006.6 \text{ J/kg K}$$

and

$$c_{pv} = 1876.8 \text{ J/kg K}$$

Using Equation A.2.1, the partial vapor pressure at 298.15 K is

$$p_{vwb} = 3166.7 \text{ N/m}^2$$

With these values, find the corresponding humidity ratio using Equation A.3.5, i.e.,

$$w_1 = \frac{2501.6 - 2.3263(298.15 - 273.15)}{2501.6 + 1.8577(306.65 - 273.15) - 4.184(298.15 - 273.15)}$$

$$\text{x}\left[\frac{0.62509 \text{ x } 3166.7}{101000 - 1.005 \text{ x } 3166.7}\right] - \frac{1.00416(306.65 - 298.15)}{2501.6 + 1.8577(306.65 - 273.15) - 4.184(298.15 - 273.15)}$$

$$= 0.016635 \text{ kg/kg dry air}$$

Substitute the previous values into Equation A.3.6(b), and find the enthalpy of the inlet air

$$i_{ma1} = 76384.5 \text{ J/kg dry air}$$

Similarly, find the enthalpy of saturated air at the water inlet temperature

$$T_{wi} = 317.15 \text{ K, i.e., } i_{maswi} = 204395.5 \text{ J/kg dry air}$$

at the water outlet temperature

$$T_{wo} = 303.59 \text{ K, i.e., } i_{maswo} = 102640.4 \text{ J/kg dry air}$$

and at the mean water temperature

$$T_{wm} = (317.15 + 303.59)/2 = 310.37 \text{ K, i.e., } i_{maswm} = 145357.7 \text{ J/kg dry air}$$

Using Equation 4.4.14, the gradient of the enthalpy-temperature curve can be expressed as

$$\frac{di_{masw}}{dT_w} = \frac{i_{maswi} - i_{maswo}}{T_{wi} - T_{wo}} = \frac{204395.5 - 102640.4}{317.15 - 303.59} = 7504 \text{ J/kg K}$$

With this value and the mean specific heat of water evaluated according to Equation A.4.2 at

$$T_{wm} = 310.37 \text{ K}, \text{ i.e., } c_{pwm} = 4176.8 \text{ J/kg K}$$

find the following capacity rates:

$$C_{\text{emin}} = \frac{m_w c_{pwm}}{di_{masw} / dT_w} = \frac{1000 \text{ x } 4176.8}{7504} = 556.6 \text{ kg/s}$$

$$< C_{\text{emax}} = m_a = 982.15 \text{ kg/s}$$

such that

$$C_e = C_{\text{emin}}/C_{\text{emax}} = 556.6/982.15 = 0.567$$

According to Equation 4.4.19, find

$$\lambda = (102640.4 + 204395.5 - 2 \text{ x } 145357.7)/4 = 4080 \text{ J/kg dry air}$$

It follows from Equation 4.4.20 that the maximum rate of enthalpy transfer is

$$Q_{\text{max}} = C_{\text{emin}} (i_{maswi} - \lambda - i_{mai}) = 556.6 \ (204395.5 - 4080 - 76384.5)$$
$$= 69 \text{ x } 106 \text{ W}$$

The transfer coefficient per unit ATD is specified as

$$\frac{h_d a_{fi}}{G_w} = \frac{h_d A}{m_w (ATD)} = \frac{2 h_d a_{fi} H_3 W_3 (ATD)}{m_w (ATD)} = 0.268 \left(\frac{G_w}{G_a} \right)^{-0.56}$$

where

A = the total wetted surface area in the fill

$G_w = m_w/[2(ATD)W_3] = 1000/(2 \text{ x } 4.57 \text{ x } 11) = 9.946 \text{ kg/sm}^2$

$G_a = m_a/(2H_3W_3) = 982.15/(2 \text{ x } 11 \text{ x } 11) = 4.058 \text{ kg/sm}^2$

With these values, find

$$h_d a_{fi}/G_w = 0.268(9.946/4.045)^{-0.56} = 0.162 \text{ m}^{-1}$$

According to Equation 4.4.10,

$$NTU_e = \frac{h_d A (di_{masw}/dT_w)}{m_w c_{pw}} = \frac{h_d a_{fi}}{G_w} \frac{m_w H_3}{C_{emin}} = 0.162 \text{ x } 1000 \text{ x } 11 / 556.6$$

$$= 3.2$$

For both streams unmixed, it follows from Table 3.5.1 that the effectiveness can be expressed as

$$e_e = 1 - \exp\left[3.2^{0.22} \left\{\exp\left(-0.567 \text{ x } 3.2^{0.78}\right) - 1\right\} / 0.567\right] = 0.82$$

to give a heat transfer rate of

$$Q = e_e Q_{max} = 0.82 \text{ x } 69 \text{ x } 106 = 56.6 \text{ x } 10^6 \text{ W}$$

The original Doron V-bar transfer characteristics were obtained by employing the Merkel method. Ideally, the same method should have been used to determine the performance of the present tower. In that case, the heat transfer rate would have been 56 x 10^6 W.

The outlet temperature of the water follows from Equation 4.4.12, i.e.,

$$Q = m_w c_{pwm} (T_{wi} - T_{wo})$$

or

$$T_{wo} = T_{wi} - Q/(m_w c_{pwm}) = 317.15 - 56.6 \text{ x } 10^6/(1000 \text{ x } 4176.8)$$

$$= 303.59 \text{ K or } 30.44 \text{ }^\circ\text{C}$$

Furthermore,

$$m_w c_{pwm} (T_{wi} - T_{wo}) = m_a (i_{ma3} - i_{ma1})$$

or the enthalpy of the air after the fill is

$$i_{ma3} = (m_w/m_a)\, c_{pwm}\, (T_{wi} - T_{wo}) + i_{ma1}$$

$$= (1000/982.15)\ 4176.8\ (317.15 - 303.59) + 76384.5$$

$$= 134051 \text{ J/kg}$$

Since the analysis assumes the air leaving the fill is saturated, i.e., $i_{ma3} = i_{mas3}$, the corresponding air temperature can be determined with the aid of Equation A.3.6(b) by following an iterative procedure.

Assume the temperature is T_{a3} = 308.77 K, and determine the specific heats of dry air and water vapor according to Equations A.1.2 and A.2.2 at

$$(T_{a3} + 273.15)/2 = (308.77 + 273.15)/2 = 290.96 \text{ K}$$

Find the partial pressure of saturated water vapor at 308.77 K using Equation A.2.1, i.e.,

$$p_{v3} = 5820 \text{ N/m}^2$$

while the corresponding humidity ratio is found from Equation A.3.5, i.e.,

$$w_3 = 0.038235 \text{ kg/kg dry air}$$

With these values, find the enthalpy of saturated outlet air according to Equation A.3.6(b).

$$i_{mas3} = 1006.667(308.77 - 273.15) + 0.038235\left[2.5016 \text{ x } 10^6\right.$$

$$\left. + 1877.759\,(308.77 - 273.15)\right] = 134063 \text{ J/kg}$$

Since this value is essentially the same as that obtained for i_{ma3}, the assumed corresponding air temperature T_{a3} = 308.77 K is correct.

In addition to satisfying the energy equation, the draft equation must also be satisfied. To determine the various loss coefficients, find the air-vapor mass flow rate entering the fill.

$$m_{av2} = m_{av1} = m_a(1 + w_1) = 982.15(1 + 0.016635) = 998.49 \text{ kg/s}$$

The corresponding density follows from Equation A.3.1, i.e.,

$$\rho_{av2} = \rho_{av1} = (1 + 0.016635)\left[1 - 0.016635 / (0.016635 + 0.62198)\right]$$

$$\text{x } 101000 / (287.08 \text{ x } 306.65) = 1.136 \text{ kg} / m^3$$

The corresponding free stream air-vapor velocity is thus

$$v_{av1} = \frac{m_a(1 + w_1)}{\rho_{av1} A_{fr}} = \frac{982.15\,(1 + 0.016635)}{1.136 \text{ x } 11 \text{ x } 11 \text{ x } 2} = 3.632 \, m/s$$

After the fill, the air-vapor density is, according to Equation A.3.1,

$$\rho_{av3} = (1+0.038235)\left[1-0.038235/(0.038235+0.62198)\right]101000$$

$$/\,(287.08 \times 308.77) = 1.1145\,\text{kg}/\text{m}^3$$

The air-vapor mass flow rate after the fill is

$$m_{av3} = m_a(1 + w_3) = 982.15(1 + 0.038235) = 1019.7 \text{ kg/s}$$

The corresponding free stream velocity is

$$v_{av3} = \frac{m_{av3}}{\rho_{av3}\, A_{fr}} = \frac{1019.7}{1.1145 \times 11 \times 11 \times 2} = 3.781\, m/s$$

The mean harmonic air-vapor density across the fill is

$$\rho_{av13} = 2\left[\frac{1}{\rho_{av1}} + \frac{1}{\rho_{av3}}\right]^{-1} = 2\left[\frac{1}{1.136} + \frac{1}{1.1145}\right]^{-1} = 1.125\,\text{kg}/m^3$$

The mean air-vapor, mass-flow rate through the fill is

$$m_{av13} = \frac{m_a(2 + w_1 + w_3)}{2} = \frac{982.15\,(2+0.016635+0.038235)}{2} = 1009.1\,\text{kg}/s$$

The corresponding mean velocity is

$$v_{av13} = \frac{m_{av13}}{\rho_{av13}\, A_{fr}} = \frac{1009.1}{1.125 \times 11 \times 11 \times 2} = 3.706\, m/s$$

The note following Example 4.3.1 shows the effective loss coefficient across the fill is given by

$$K_{fi} = K_{fi1} \text{ x } ATD + (\rho_{av3}\ v_{av3}^2\ /2 - \rho_{av1}\ v_{av1}^2\ /2)/(\rho_{av13}\ v_{av13}^2\ /2)$$

$$= 0.751 \text{x } 4.57 \text{ x } 9.946^{0.66}\ 4.058^{-0.73} + (1.1145 \text{ x } 3.781^2 / 2 - 1.136 \text{ x } 3.632^2 / 2)$$

$$/ (1.125 \text{x } 3.706^2 / 2) = 5.68$$

The downstream loss coefficient based on fill conditions is

$$K_{defi} = 3 \left(\frac{\rho_{av13}}{\rho_{av3}} \right) \left(\frac{m_{av3}}{m_{av13}} \right)^2 = 3 \left(\frac{1.125}{1.1145} \right) \left(\frac{1019.7}{1009.1} \right)^2 = 3.09$$

The mean air-vapor velocity through the fan can be approximated by the following expression

$$v_{Fav} = \frac{4\, m_{av3}}{\rho_{av3}\ \pi\ d_c^2} = \frac{4 \text{ x } 1019.7}{1.1145 \text{ x } \pi \text{ x } 9.5265^2} = 12.837 \text{ m/s}$$

If buoyancy effects are neglected, the draft equation for this induced-draft heat exchanger can be approximated by

$$0 = (K_{fs} + K_{fi} + K_{defi})\, \rho_{av13}\ v_{av13}^2\ /2 + (K_{ud} - K_{F/difs})\, \rho_{av3}\ v_{Fav}^2 / 2$$

$$= (0.5 + 5.68 + 3.09)\, 1.125 \text{ x } 3.706^2 / 2 + (0.5 - K_{F/difs})\, 1.1145 \text{ x } 12.837^2 / 2$$

or

$$K_{F/difs} = 1.2799$$

The corresponding required fan/diffuser static pressure is

$$\Delta p_{F/difs} = K_{F/difs}\, \rho_{av3}\, v_{Fav}^2 / 2 = 1.2799 \text{ x } 1.1145 \text{ x } 12.837^2 / 2 = 117.5 \text{ N/m}^2$$

The air volume flow rate through the fan is

$$V_F = \frac{m_{av3}}{\rho_{av3}} = \frac{1019.7}{1.1145} = 914.94\ m^3/s$$

The corresponding flow through the fan at a rotational speed of 120 rpm is, according to Equation 6.2.1,

$$V_{F/dif} = V_F\left(\frac{N_{F/dif}}{N_F}\right) = 914.94 \text{ x } \frac{120}{118} = 930.45\ m^3/s$$

At this volume flow rate, the fan/diffuser static pressure is, according to the specified expression,

$$\Delta p_{F/difs} = 299.903 + 40.0071 \text{ x } 10^{-3} \text{ x } 930.45 - 96.5087 \text{ x } 10^{-6} \text{ x } 930.45^2$$

$$- 152.2243 \text{ x } 10^{-9} \text{ x } 930.45^3 = 130.9 \text{ N/m}^2$$

According to Equation 6.2.2, the fan static pressure at 118 rpm and an air density of 1.12 kg/m^3 is

$$\Delta p_{Fs} = \Delta p_{F/difs}\left(\frac{N_F}{N_{F/difs}}\right)^2\left(\frac{\rho_{av3}}{\rho}\right) = 130.9 \text{ x } \left(\frac{118}{120}\right)^2\left(\frac{1.1145}{1.2}\right) = 117.5 \text{ N/m}^2$$

The fan will achieve the required pressure differential at the prescribed flow rate.

The fan shaft power required at reference conditions is given by

$$P_{F/dif} = 203302.6779 - 58.3775 \text{ x } 930.45 + 458.7692 \text{ x } 10^{-3} \text{ x } 930.45^2$$

$$- 405.2315 \text{ x } 10^{-6} \text{ x } 930.45^3 = 219.73 \text{ kW}$$

The actual fan power follows from Equation 6.2.3, i.e.,

$$P_F = P_{F/dif}\left(\frac{N_F}{N_{F/dif}}\right)^3\left(\frac{\rho_{av3}}{\rho}\right) = 219.73 \text{ x } \left(\frac{118}{120}\right)^3\left(\frac{1.1145}{1.2}\right) = 194 \text{ kW}$$

Air-cooled condenser

Single-pass, air-cooled condensers are sloped at least 1 in 50 to the horizontal from inlet to outlet in order to assist drainage. Air-cooled steam condensers in power plants usually consist of arrays of A-frame heat exchanger units according to Conradie and Kröger. Consider the example of a forced-draft, air-cooled steam condenser shown in Figure 8.1.6. In this configuration, the heat exchanger is arranged in the form of a delta or A-frame to

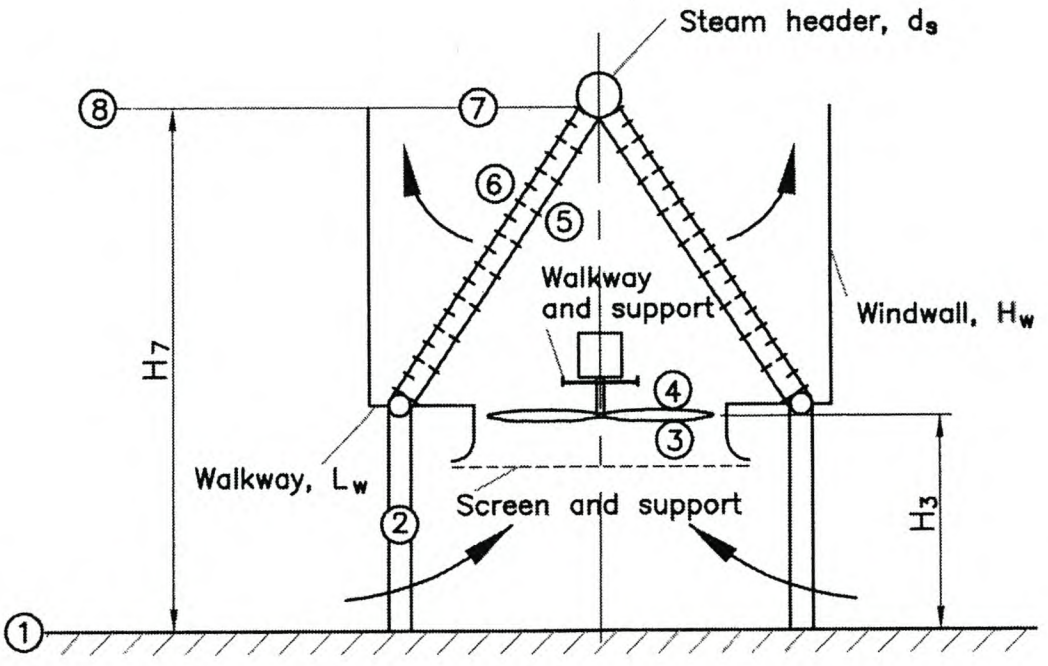

Fig. 8.1.6 Air-Cooled Condenser Unit

- drain condensate effectively
- reduce distribution steam duct lengths
- minimize the required ground surface area

A windwall is provided to reduce recirculation of the hot plume air.

The heat transfer characteristics of the air-cooled condenser can be expressed as

$$Q = m_a c_{pa}(T_{a6} - T_{a5}) = m_c i_{fg} \qquad (8.1.20)$$

where subcooling of the condensate is neglected, and

m_c = the condensate mass flow rate
i_{fg} = the latent heat
T_{a5} = the temperature as given by Equation 8.1.3

In a practical air-cooled condenser, the fin pitch may change in consecutive tube rows according to Conradie and Kröger. If the performance data is available for individual finned tube rows, the energy equation for n_r tube rows is written as

$$Q = \sum_{i=1}^{n_r} m_a c_{pa(i)} (T_{ao(i)} - T_{ai(i)}) = \sum_{i=1}^{n_r} m_{c(i)} i_{fg} \tag{8.1.21}$$

The effectiveness of each tube row is, according to Equation 3.5.22,

$$e_{(i)} = 1 - \exp\left[-U_{(i)} A_{(i)} / (m_a c_{pa(i)})\right] \tag{8.1.22}$$

With this expression, the heat transfer rate becomes

$$Q = \sum_{i=1}^{n_r} e_{(i)} m_a c_{pa(i)} (T_s - T_{ai(i)}) \tag{8.1.23}$$

The draft equation is deduced in the same manner as the forced-draft, air-cooled heat exchanger described previously, but takes into consideration additional losses due to the inclined flow approaching and leaving the bundles according to Kröger.

Considering all flow losses through the heat exchanger, find the difference in pressure between (1) and (7).

$$p_{a1} - p_{a7} = p_{a1}\left[1-(1-0.00975\,H_6/T_{a1})^{3.5}\right]+K_{ts}(m_a/A_2)^2/(2\rho_{a2})$$

$$+K_{up}(m_a/A_e)^2/(2\rho_{a3})-\left[\Delta p_{Fs}+\alpha_{eF}(m_a/A_c)^2/(2\rho_{a4})\right]$$

$$+K_{pl}(m_a/A_c)^2/(2\rho_{a4})+K_{do}(m_a/A_e)^2/(2\rho_{a4})+K_{\theta t}(m_a/A_{fr})^2/(2\rho_{a56})$$

$$+p_{a6}\left[1-\{1-0.00975(H_7-H_6)/T_{a6}\}^{3.5}\right] \qquad (8.1.24)$$

where

$K_{\theta t}$, given by Equation 5.6.19, includes losses across the heat exchanger and kinetic energy losses at the outlet elevation (7)

According to section 6.4.2, $K_{p\ell} = \alpha_{eF}$ for this configuration, and it follows from Equation 8.1.6 that

$$-\left[\Delta p_{Fs}+\alpha_{eF}(m_a/A_c)^2/(2\rho_{a4})\right]+K_{pl}(m_a/A_c)^2/(2\rho_{a4})$$

$$\approx -K_{Fs}(m_a/A_c)^2/(2\rho_{a3}) \qquad (8.1.25)$$

For a DALR far from the heat exchanger, the pressure difference between (1) and (8) is given by Equation 8.1.8.

Substitute Equation 8.1.8 into Equation 8.1.24, and use Equation 8.1.25 to find the draft equation for the air-cooled condenser shown in Figure 8.1.6.

$$p_{a1}\left[\{1-0.00975(H_7-H_6)/T_{a6}\}^{3.5}-\{1-0.00975(H_7-H_6)/T_{a1}\}^{3.5}\right]$$

$$=K_{ts}(m_a/A_2)^2/(2\rho_{a1})+K_{up}(m_a/A_e)^2/(2\rho_{a3})-K_{Fs}(m_a/A_c)^2/(2\rho_{a3})$$

$$+K_{do}(m_a/A_e)^2/(2\rho_{a3})+K_{et}(m_a/A_{fr})^2/(2\rho_{a56}) \qquad (8.1.26)$$

where

$K_{\theta t}$, given by Equation 5.6.19, includes losses across the heat exchanger and kinetic energy losses at the outlet elevation (7)

$H_8 = H_7$

$\rho_{a2} \approx \rho_{a1}$

$\rho_{a4} \approx \rho_{a3}$

$\rho_{a7} \approx \rho_{a6}$

$p_{a6} \approx p_{a1}$

The values of T_{a3}, ρ_{a3}, ρ_{a6} and ρ_{a56} are determined according to Equations 8.1.10, 8.1.11, and 8.1.13 respectively.

Example 8.1.4

Determine the heat that is rejected and the fan power consumption for a forced-draft steam condenser shown in Figure 8.1.6.

Ambient conditions:

- Air temperature at ground level: T_{a1} = 15.6 °C (288.75K)
- Wetbulb temperature at ground level: T_{wb} = 0 °C (essentially dry air).
- Atmospheric pressure at ground level: p_{a1} = 84,600 N/m^2
- Ambient temperature gradient: -0.00975 K/m from ground level

Steam conditions:

- Saturated steam supply temperature: T_v = 60°C
- Steam quality at condenser bundle inlet: x = 1
- Diameter of steam header: d_s = 1.25 m
- Total mean steam ducting loss coefficient: K_{sd} = 2.5, based on the steam velocity at inlet to first tube row

Finned tube bundle specifications:

The condenser consists of two rows of staggered, plate-finned, flattened tubes (Fig. 5.6.9). Each row has different performance characteristics. Approximately the same amount of steam condenses in each row to ensure noncondensables are not trapped in the condenser.

- Hydraulic diameter of tube: $d_e = 0.02975$ m
- Inside area of tube per unit length: $A_{ti} = 0.21341$ m
- Inside cross-sectional tube flow area: $A_{ts} = 0.00159$ m^2
- Length of finned tube: $L_t = 9.5$ m
- Inside height of tube: $H_t = 0.097$ m
- Inside width of tube: $W_t = 0.017$ m
- Number of tube rows: $n_r = 2$
- Number of tubes per bundle (first row): $n_{tb(1)} = 57$
- Number of tubes per bundle (second row): $n_{tb(2)} = 58$
- Number of steam passes: $n_{vp} = 1$
- Number of bundles: $n_b = 8$
- Effective frontal area of one bundle (second row): $A_{fr} = 27.55$ m^2
- Apex angle of A-frame: $2\theta = 60^\circ$
- Ratio of minimum to free stream flow area through finned tube bundle: $\sigma = 0.48$
- Ratio of minimum to free stream flow area at inlet to finned tube bundle: $\sigma_{21} = 0.875$
- Steam-side tube inlet loss coefficient: $K_c = 0.6$

The characteristic heat transfer parameter for normal flow through the first row of tubes, determined experimentally, is given by the following empirical relation:

$$Ny_{(1)} = 366.007945\ \mathrm{Ry}^{0.433256}$$

For the second row,

$$Ny_{(2)} = 360.588007\ \mathrm{Ry}^{0.470373}$$

According to the data shown in Figure 5.6.9, the heat transfer coefficient for inclined plate-finned tubes may be somewhat higher than under conditions of normal flow during testing. However, the more conservative normal flow correlations will be retained for this example to make provision for distortions in the entering flow pattern. Potentially small enhancements in heat transfer due to the turbulence in the wake of the fan may be assumed to be canceled by some maldistribution of the air flow through the heat exchanger.

The loss coefficient across the entire bundle under normal isothermal flow conditions is given as

$$K_{he} = 4177.08481\,Ry^{-0.4392686}$$

Fan installation specifications:

- Axial flow fan: 8 blades at an angle of 16°
- Fan diameter: d_F = 9.145 m
- Fan casing diameter: d_c = 9.170 m
- Fan hub diameter: d_h = 1.4 m
- Rotational speed: N = 125 rpm
- Efficiency of fan drive system: η_{Fd} = 0.9
- Inlet screen distance from fan blade (upstream): x_{si} = 1.3 m
- Support beam distance from fan blade (upstream): x_{bi} = 1.34 m
- Support beam distance from blade (downstream): x_{bo} = 0.53 m
- Walkway distance from fan blade (downstream): x_{so} = 1.0 m
- Ratio of inlet screen area to fan casing area: σ_{si} = 0.125
- Ratio of support beam area to fan casing area (upstream): σ_{bi} = 0.15
- Ratio of support beam area to fan casing area (downstream): σ_{bo} = 0.05
- Ratio of walkway area to fan casing area: σ_{so} = 0.1
- Height of fan above ground level: H_3 = 25 m
- Height of windwalls: H_w = 8.27 m
- Width of walkway between heat exchanger bundle and windwall: L_w = 0.2 m
- Heat exchanger inlet support loss coefficient: K_{ts} = 1.5, based on frontal area of heat exchanger

The fan has the performance characteristics given in Example 6.2.2. According to Example 6.2.2, the fan performance characteristics at a reference density of 1.2 kg/m^3 (Fig. 6.2.4) can be approximated by the following correlations:

Fan static pressure:

$$\Delta p_{Fs} = 320.0451719 - 0.2975215484\,V + 6.351486 \times 10^{-4}\,V^2 - 8.14 \times 10^{-7}\,V^3, \text{ N/m}^2$$

Fan power:

$$P_F = 186645.2333 - 59.413863388\,V + 0.476168398\,V^2 - 5.08308 \times 10^{-4}\,V^3, \text{ W}$$

Effects of flow separation at the inlet to the fan platform and recirculation of hot plume air can be ignored.

Solution

This problem is solved by following an iterative procedure. The relevant energy and draft equations will be satisfied at an air mass flow rate of m_a = 604.483 kg/s. At this flow rate, the inlet air temperature to the first tube row is found to be

$$T_{ai(1)} = 15.614\ ^{\circ}\text{C}\ (288.764\ \text{K})$$

The mean outlet air temperature after the first tube row is

$$T_{ao(1)} = 33.324^{\circ}\text{C}\ (306.474\ \text{K})$$

This is also the mean inlet air temperature to the second tube row.

The mean outlet temperature after the second tube row is

$$T_{ao(2)} = 47.858\ ^{\circ}\text{C}\ (321.008\ \text{K})$$

The steam velocity at the inlet to the first tube row is

$$v_{vi(1)} = 49.419\ m/s$$

and the corresponding density is

$$\rho_{vi(1)} = 0.127461\ \text{kg}/m^3$$

For the second tube row,

$$v_{vi(2)} = 39.882\ m/s$$

These results were obtained with the aid of the following equations. The density of the air immediately upstream of the heat exchanger bundles is, according to the gas law,

$$\rho_{a5} \approx p_{a1}/(RT_{ai(1)}) = 84600/(287.08 \times 288.764) = 1.0205\ \text{kg}/m^3$$

Neglecting pressure changes through the heat exchanger, the air density after the bundles is

$$\rho_{a6} \approx 84600/(287.08 \times 321.008) = 0.9180\ \text{kg/m}^3$$

The mean air temperature through the first row of finned tubes is

$$T_{a(1)} = (15.614 + 33.324)/2 = 24.469\ ^{\circ}C\ (297.619\ K)$$

The corresponding properties for dry air may be determined according to the equations given in Appendix A.1

- Density: $\rho_{a(1)} = 0.9902\ kg/m^3$ using Equation A.1.1
- Specific heat: $c_{pa(1)} = 1006.8701\ J/kgK$ using Equation A.1.2
- Dynamic viscosity: $\mu_{a(1)} = 1.836 \times 10^{-5}\ kg/ms$ using Equation A.1.3
- Thermal conductivity: $k_{a(1)} = 0.0260369\ W/mK$ using Equation A.1.4
- Prandtl number: $Pr_{a(1)} = 0.7100$

The mean air temperature through the second row of tubes is

$$T_{a(2)} = (33.324 + 47.858)/2 = 40.591^{\circ}C\ (313.741K)$$

The corresponding air properties are:

- Density: $\rho_{a(2)} = 0.9393\ kg/m^3$ using Equation A.1.1
- Specific heat: $c_{pa(2)} = 1007.5319\ J/kgK$ using Equation A.1.2
- Dynamic viscosity: $\mu_{a(2)} = 1.91 \times 10^{-5}\ kg/ms$ using Equation A.1.3
- Thermal conductivity: $k_{a(2)} = 0.0272786\ W/mK$ using Equation A.1.4
- Prandtl number: $Pr_{a(2)} = 0.7053$

The rate of heat transfer to the air flowing through the first tube row is given by

$$Q_{a(1)} = m_a c_{pa(1)} (T_{ao(1)} - T_{ai(1)})$$

$$= 604.483 \times 1006.8701 (33.324 - 15.614) = 10.779 \times 10^6\ W$$

Similarly, through the second tube row,

$$Q_{a(2)} = m_a c_{pa(2)} (T_{ao(2)} - T_{ao(1)})$$

$$= 604.483 \times 1007.5319 (47.858 - 33.324) = 8.850 \times 10^6\ W$$

According to Equation 8.1.21, the total heat transfer rate is

$$Q_a = Q_{a(1)} + Q_{a(2)} = 19.629 \times 10^6\ W$$

The air-side characteristic flow parameter for the first tube row, $Ry_{(1)}$, takes into consideration the reduced effective frontal area caused by the smaller number of tubes. The bundle side walls are assumed to be shaped to avoid any air bypass. According to Equation 5.4.11, this parameter is

$$Ry_{(1)} = m_a / \left[\mu_{a(1)} A_{fr} n_{tb(1)} / n_{tb(2)} \right]$$

$$= 604.483 / (1.836 \times 10^{-5} \times 8 \times 27.55 \times 57 / 58) = 152011.58 \text{ m}^{-1}$$

The corresponding heat transfer parameter is based on the given specifications

$$Ny_{(1)} = 366.007945 \, Ry^{0.433256} = 366.007945 \times 152011.58^{0.433256} = 64356.19 \text{ m}^{-1}$$

The corresponding effective heat transfer coefficient is found from

$$h_{ae(1)} A_{a(1)} = k_{a(1)} Pr_{a(1)}^{0.333} A_{fr} Ny_{(1)} n_{tb(1)} / n_{tb(2)}$$

$$= 0.0260369 \, (0.7100)^{0.333} \times 8 \times 27.55 \times 64356.19 \, (57/58)$$

$$= 323778.97 \text{ W/K}$$

Due to the loss coefficient, K_{sd} = 2.5, specified for the steam duct system, a pressure drop will occur between the inlet to the steam duct and the condenser tubes. The pressure drop is given by

$$\Delta p_{sd} = K_{sd} \rho_{vi(1)} v_{vi(1)}^2 / 2 = 2.5 \, \rho_{vi(1)} v_{vi(1)}^2 / 2$$

As the steam enters the finned tubes from the header, a further contraction loss occurs as given by Equation 3.4.60, i.e.,

$$\Delta p_i = \left(1 - \sigma^2 + K_c\right) \rho_{vi(1)} v_{vi(1)}^2 / 2$$

The approximate area contraction ratio for the flattened tube is given by

$$\sigma = W_t / P_t = W_t L_t n_{tb(2)} / A_{fr}$$

where

W_t = the inside width of the tube

For the specified inside cross-sectional tube flow area

$$A_{ts} = 0.00159 \text{ m}^2$$

and the corresponding height

$$H_t = 0.097 \text{ m}$$

find the inside width of the tube from

$$A_{ts} = \pi W_t^2/4 + (H_t - W_t)W_t$$

or

$$0.00159 = \pi W_t^2/4 + (0.097 - W_t)W_t$$

The result is

$$W_t = 0.017 \text{ m}$$

Upon substitution of this and other specified values in the previous expression for the inlet pressure drop, find

$$\Delta p_i = \left[1 - (0.017 \text{ x } 9.5 \text{ x } 58/27.55)^2 + 0.6\right] \rho_{vi} v_{vi(1)}^2/2$$

$$= 1.4844 \, \rho_{vi(1)} v_{vi(1)}^2/2$$

The drop in pressure between the inlet to the steam supply duct and a point just inside the inlet to the condenser tubes is given by

$$\Delta p_{sd} + \Delta p_i = (2.5 + 1.4844)\, 0.127461 \text{ x } 49.419^2/2 = 620.15202 \text{ N/m}^2$$

The mean saturation pressure of the steam at the inlet to the steam duct is 19925.113 N/m^2. Inside the inlet of the first row of finned tubes, the steam pressure is

$$(19925.113 - 620.15202) = 19304.971 \text{ N/m}^2$$

The saturation temperature corresponding to this pressure can be determined according to Equation 3.4.65, i.e.,

$$T_{vi} = 5149.6889682 / \ell n(1.020472843 \text{ x } 10^{11}/19304.971) - 273.15 = 59.505 \text{ °C}$$

This will also be the approximate inlet vapor temperature in the second row of tubes if the rate of condensation is similar to that of the first row.

Using Appendix A.2, the thermophysical properties of saturated steam at this temperature are:

- Density: $\rho_{vi} = 0.1274605$ kg/m^3 using Equation A.2.5
- Specific heat: $c_{pvi} = 1926.064$ J/kgK using Equation A.2.2
- Dynamic viscosity: $\mu_{vi} = 1.1066802 \times 10^{-5}$ kg/ms using Equation A.2.3
- Thermal conductivity: $k_{vi} = 2.1002853 \times 10^{-2}$ W/mK using Equation A.2.4

Due to the pressure changes along the finned tube, the condensation process will not take place at a constant steam temperature.

The mean static pressure in the flattened tube can be determined according to Equation 3.4.64. For this equation, find with $\rho_{vi(1)} = \rho_{vi}$,

$$Re_{vi(1)} = \rho_{vi} v_{vi(1)} d_e/\mu_{vi} = 0.1274605 \times 49.419 \times 0.02975/(1.1066802 \times 10^{-5}) = 16933.18$$

$$Re_{vn(1)} = Re_{vi(1)}\ W_t/(2L_t) = 16933.18 \times 0.017/(2 \times 9.5) = 15.151$$

$$a_{1(1)} = 1.0649 + 1.041 \times 10^{-3}\ Re_{vn(1)} - 2.011 \times 10^{-7}\ Re^3_{vn(1)}$$

$$= 1.0649 + 1.041 \times 10^{-3} \times 15.151 - 2.011 \times 10^{-7} \times 15.151^3 = 1.079973$$

$$a_{2(1)} = 290.1479 + 59.3153\ Re_{vn(1)} + 1.5995 \times 10^{-2}\ Re^3_{vn(1)}$$

$$= 290.1479 + 59.3153 \times 15.151 + 1.5995 \times 10^{-2} \times 15.151^3 = 1244.446$$

Substitute these values in Equation 3.4.64, and find

$$p_{vm(1)} = 19304.971 - \frac{0.1582 \times (1.1066802 \times 10^{-5})^2 \times 9.5}{0.1274605 \times 0.02975^3 \times 16933.18}$$

$$\times \left(0.267 \times 1.079973 \times 16933.18^{2.75} + 0.364 \times 1244.44 \times 16933.18^{1.75}\right)$$

$$+ 2 \times 0.1274605 \times 49.419^2 / 3 = 19078.1\ \text{N/m}^2$$

The corresponding mean steam temperature is, according to Equation 3.4.65,

$$T_{vm(1)} = 5149.6889682/\ell n(1.020472843 \times 10^{11}/19078.1) - 273.15 = 59.251\ ^\circ\text{C}$$

The thermophysical properties of the condensate in the first tube row are evaluated at 59.251 °C using Appendix A.4:

- Density: $\rho_{c(1)} = 983.60925$ kg/m^3 using Equation A.4.1
- Specific heat: $c_{pc(1)} = 4183.616$ J/kgK using Equation A.4.2
- Dynamic viscosity: $\mu_{c(1)} = 4.685 \times 10^{-4}$ kg/ms using Equation A.4.3
- Thermal conductivity: $k_{c(1)} = 0.65246$ W/mK using Equation A.4.4
- Latent heat of vaporization: $i_{fg(1)} = 2.360282 \times 10^6$ J/kg using Equation A.4.5

The condensate flow rate out of the first tube row is

$$m_{c(1)} = Q_{a(1)}/i_{fg(1)} = 10.779 \times 10^6 / 2.360282 \times 10^6 = 4.567 \text{ kg/s}$$

All steam entering the tube is assumed to be condensed. Due to the relatively high velocity at the inlet to the tube, shear stresses acting on the condensate film have a strong influence on its development. Gravity control becomes more important further from the inlet, and the condensation heat transfer coefficient given by Equation 3.4.23 is applicable over the greater part of the tube.

$$h_c = 0.9245\left[\frac{L_t\, k_{c(1)}^3\, \rho_{c(1)}^3\, g \cos(90° - \theta)\, i_{fg(1)}}{\mu_{c(1)}\, m_a\, c_{pa(1)} (T_{vm} - T_{ai})\left[1 - \exp\{-U_{c(1)}\, H_t\, L_t/(m_a\, c_{pa(1)})\}\right]}\right]^{0.333}$$

In the first tube row, the inside tube area exposed to the condensing steam is

$$A_{c(1)} = n_{tb(1)}\, n_b\, A_{ti}\, L_t = 57 \times 8 \times 0.21341 \times 9.5 = 924.4921 \text{ m}^2$$

The effective height over which condensation takes place inside the tube is $Ht \approx 0.097$ m. By neglecting the thermal resistance of the condensate film, the approximate overall heat transfer coefficient based on the condensing surface area can be expressed as

$$U_{c(1)} H_t L_t = h_{ae(1)}\, A_{a(1)}/(2 \times n_{tb(1)} \times n_b) = 323778.97/(2 \times 57 \times 8) = 355.0208 \text{ W/K}$$

The corresponding air-mass flow rate flowing on one side of a finned tube is

$$m_a/(2 \times n_{tb(1)} \times n_b) = 604.483/(2 \times 57 \times 8) = 0.66281 \text{ kg/s}$$

Substitute the previous values in Equation 3.4.23, and find the mean condensation heat transfer coefficient.

$$h_{c(1)} = 0.9245\left[\frac{0.65246^3 \times 983.60925^2 \times 9.8 \times \cos 60° \times 2.360282 \times 10^6 \times 9.5}{4.685 \times 10^{-4} \times 0.66281 \times 1006.8701 (59.251 - 15.614)}\right]^{0.333}$$

$$\times \left[1 - \exp\{-355.0208/(0.66281 \times 1006.8701)\}\right]^{-0.333} = 16063.319 \text{ W/m}^2\text{K}$$

Thus, the overall heat transfer coefficient for the first tube row is given by

$$UA_{(1)} = \left[\frac{1}{(h_{ae}A_a)_{(1)}} + \frac{1}{(h_c A_c)_{(1)}}\right]^{-1}$$

$$= [(1/323778.97) + 1/(16063.319 \text{ x } 924.4921)]^{-1}$$

$$= \left[308.853 \text{ x } 10^{-8} + 6.734 \text{ x } 10^{-8}\right]^{-1} = 316870.343 \text{ W/K}$$

The thermal resistance of the condensate film is small compared to the overall resistance, i.e., 6.734/(308.853 + 6.734) = 0.0213 or 2.13%.

According to Equation 8.1.22, the effectiveness for the first row of condenser tubes may be expressed as

$$e_{(1)} = 1 - \exp\left[-UA_{(1)}/(m_a c_{pa(1)})\right] = 1 - \exp\left[-316870.343/(604.483 \text{ x } 1006.8701)\right]$$

$$= 0.40585$$

From Equation 8.1.23, it follows that the heat transfer rate for one row is

$$Q_{a(1)} = m_a c_{pa(1)} (T_v - T_{ai(1)})\, e_{(1)}$$

$$= 604.483 \text{ x } 1006.8701 (59.251 - 15.614) \text{ x } 0.40585 = 10.780 \text{ x } 10^6 \text{ W}$$

This compares well with the previous value of 10.779 MW.

The previous procedure is followed to determine conditions in the second tube row with an inlet steam velocity of $v_{vi(2)}$ = 39.882 m/s and other thermo-physical steam properties approximately the same as those in the first tube row. Find

$$Ry_{(2)} = 604.483/(1.91 \text{ x } 10^{-5} \text{ x } 8 \text{ x } 27.55) = 143622.41 \text{ m}^{-1}$$

$$Ny_{(2)} = 360.588 \text{ x } 143622.41^{0.47037} = 96120.02 \text{ m}^{-1}$$

$$h_{ae(2)}A_{a(2)} = 0.0272786 \text{ x } 0.7053^{0.333} \text{ x } 8 \text{ x } 27.55 \text{ x } 96120.02 = 514410.53 \text{ W/K}$$

$$Re_{vi(2)} = 0.1274605 \text{ x } 39.882 \text{ x } 0.02975/(1.1066802 \text{ x } 10^{-5}) = 13665.27$$

$$Re_{vn(2)} = 13665.27 \text{ x } 0.017/(2 \text{ x } 9.5) = 12.227$$

$$a_{1(2)} = 1.077261$$

$$a_{2(2)} = 1044.622$$

With these values, the mean steam pressure in row 2 is determined, according to Equation 3.4.64, as

$$p_{vm(2)} = 19304.971 - \frac{0.1582 \text{ x } (1.1066802 \text{ x } 10^{-5})^2 \text{ x } 9.5}{0.1274605 \text{ x } 0.02975^3 \text{ x } 13665.27}$$

$$\text{x } \left(0.267 \text{ x } 1.077261 \text{ x } 13665.27^{2.75} + 0.364 \text{ x } 1044.622 \text{ x } 13665.27^{1.75}\right)$$

$$+ 2 \text{ x } 0.1274605 \text{ x } 39.882^2 / 3 = 19308 \text{ N/m}^2$$

Using Equation 3.4.65, the corresponding saturation steam temperature is

$$T_{vm(2)} = 5149.6889682/\ell n(1.020472843 \text{ x } 10^{11}/19308) - 273.15 = 59.322 \text{ °C}$$

The pressure drop in the different tube rows is usually not identical. The result is that steam backflow will occur. To avoid this and the corresponding accumulation of noncondensables, a dephlegmator is usually installed after the condenser.

The thermophysical properties of the condensate at 59.322 °C are:

- Density: $\rho_{c(2)} = 983.57208$ kg/m^3 using Equation A.4.1
- Specific heat: $c_{pc(2)} = 4183.660$ J/kgK using Equation A.4.2
- Dynamic viscosity: $\mu_{c(2)} = 4.679 \text{ x } 10^{-4}$ kg/ms using Equation A.4.3
- Thermal conductivity: $k_{c(2)} = 0.65253$ W/m K using Equation A.4.4
- Latent heat of vaporization: $i_{fg(2)} = 2.360109 \text{ x } 10^6$ J/kg using Equation A.4.5
- The condensate flow rate for the second tube row is:

$$m_{c(2)} = Q_{a(2)}/i_{fg(2)} = 8.850 \text{ x } 10^6/(2.360109 \text{ x } 10^6) = 3.75 \text{ kg/s}$$

- The effective condensation heat transfer area on the inside of the tubes is:

$$A_{c(2)} = A_{c(1)} \text{ x } 58/57 = 924.4921 \text{ x } 58/57 = 940.7113 \text{ m}^2$$

- The approximate overall heat transfer coefficient based on this area is:

$$U_{c(2)} H_t L_t = h_{ae(2)} A_{a(2)}/(2 \text{ x } n_{tb(2)} \text{ x } n_b) = 514410.53/(2 \text{ x } 8 \text{ x } 58) = 554.3217 \text{ W/K}$$

- The corresponding air mass flow rate flowing on one side of a finned tube is:

$$m_a/(2 \text{ x } n_{tb(2)} \text{ x } n_b) = 604.483/(2 \text{ x } 58 \text{ x } 8) = 0.6514 \text{ kg/s}$$

- The condensation heat transfer coefficient follows from Equation 3.4.23:

$$h_{c(2)} = 0.9245\left[\frac{0.65253^3 \text{ x } 983.57208^2 \text{ x } 9.8 \text{ x } \cos 60^\circ \text{ x } 2.360109 \text{ x } 10^6 \text{ x } 9.5}{0.4679 \text{ x } 10^{-3} \text{ x } 0.6514 \text{ x } 1007.5319(59.322 - 33.324)}\right]^{0.333}$$

$$\text{x } [1 - \exp\{-554.3217/(0.6514 \text{ x } 1007.5319)\}]^{-0.333} = 17240.447 \text{ W/m}^2\text{K}$$

- The actual overall heat transfer coefficient for the second tube row is given by:

$$UA_{(2)} = [1/514410.53 + 1/(17240.447 \text{ x } 940.7114)]^{-1} = 498596.091 \text{ W/K}$$

According to Equation 8.1.22, the effectiveness for the second row is

$$e_{(2)} = 1 - \exp[-498596.091/(604.483 \text{ x } 1007.5313)] = 0.55898$$

The heat transfer rate is given by

$$Q_{a(2)} = 604.483 \text{ x } 1007.5313 \text{ (} 59.322 - 33.324) \text{ x } 0.55898 = 8.8507 \text{ x } 10^6 \text{ W}$$

This compares well with the previous value of $Q_{a(2)} = 8.850 \text{ x } 10^6$ W.

Evaluation of the draft equation. To evaluate the draft equation, the fan operating point must be determined. According to Equation 8.1.10, the approximate air temperature at the fan suction side is

$$T_{a3} \approx T_{a1} - 0.00975 H_3 = 15.6 - 0.00975 \text{ x } 25 = 15.3563^\circ\text{C} (288.5063 \text{ K})$$

and the corresponding air density is

$$\rho_{a3} = 84600/(287.08 \text{ x } 288.5063) = 1.0214 \text{ kg/m}^3$$

The specific heat of the air is

$$c_{pa3} = 1006.474 \text{ J/kgK}$$

and the volume flow rate through the fan is

$$V = m_a/\rho_{a3} = 604.483/1.0214 = 591.796 \text{ m}^3/\text{s}$$

This volume flow rate is more than the 573.148 m^3/s at the point of maximum fan efficiency. Thus, the fan will operate effectively.

According to the empirical third order correlation specified for the fan static pressure in terms of the volume flow rate at the reference air density of 1.2 kg/m^3, find

$$\Delta p_{Fs(1.2)} = 320.0451719 - 0.2975215484 \times 591.796 + 6.351486 \times 10^{-4} \times 591.796^2$$

$$-8.14 \times 10^{-7} \times 591 - 796^3 = 197 - 7169 \text{ N/m}^2$$

According to Equation 6.2.2, the fan static pressure across this fan operating at a density of 1.0214 kg/m^3 is

$$\Delta p_{Fs} = 197.7169 \ (1.0214/1.2) = 168.290 \text{ N/m}^2$$

The corresponding fan coefficient defined by Equation 8.1.7 is

$$K_{Fs} = 2\Delta p_{Fs} \rho_{a3} (A_c/m_a)^2 = 2 \times 168.290 \times 1.0214$$

$$[\pi \times 9.170^2/(4 \times 604.483)]^2 = 4.1037$$

The required fan shaft power at an air density of ρ_{a3} = 1.0214 kg/m^3 follows from the density-corrected specified fan power curve, i.e.,

$$P_F = (1.0214/1.2)(186645.2333 - 59.413863388 \times 591.796$$

$$+ 0.476168398 \times 591.796^2 - 5.08308 \times 10^{-4} \times 591.796^3) = 181.238 \times 10^3 \text{ W}$$

According to Equation 8.1.3, find the approximate temperature of the air before it enters the heat exchanger.

$$T_{a5} = T_{ai(1)} = T_{a1} + P_f/(m_a \ c_{pa}) - 0.00975 \ H_5$$

where

$$H_5 = H_3 + 0.5 \ L_{st} \cos \theta = 25 + 0.5 \times 9.5 \cos 30^\circ = 29.1136 \text{ m}$$

Thus

$$T_{a5} = 15.6 + 181.194 \times 10^3/(604.42 \times 1006.474) - 0.00975 \times 29.1136 = 15.614 \ ^\circ\text{C}$$

The electrical power input to the fan is determined as follows:

$$P_e = P_F/\eta_{Fd} = 181.238/0.9 = 201.376 \times 10^3 \text{W}$$

The loss coefficient due to the fan safety screen, the support beams at both the fan suction and discharge sides, and the walkway above the fan are determined by employing the bulk method described in section 6.4.1. The bulk method relates the pressure loss coefficient to the total resistance area exposed to flow and to the distance between the flow resistance and the fan rotor.

By employing the area ratios and dimensionless distances shown in Figures 6.4.1 and 6.4.2, the loss coefficients can be obtained directly from the curves.

For the fan safety screen,

$$x_{si}/d_c = 0.142$$

and

$$A_{si}/A_c = \sigma_{si} = 0.125.$$

From Figure 6.4.1,

$$K_{si} = 0.1317$$

For the fan safety screen support beams,

$$x_{bi}/d_c = 0.146$$

and

$$A_{bi}/A_c = \sigma_{bi} = 0.15$$

From Figure 6.4.1,

$$K_{bi} = 0.16523$$

Thus, the total loss coefficient for flow obstacles at the fan suction or upstream side is

$$K_{up} = 0.1317 + 0.16523 = 0.29693$$

The total loss coefficient for flow obstacles at the fan discharge or downstream side, e.g., walkway and support beams, is obtained from Figure 6.4.2 and found to be

$$K_{do} = K_{so} + K_{bo} = 0.2324 + 0.1584 = 0.3908$$

The sum of the upstream and downstream losses is thus

$$K_{up} + K_{do} = 0.29693 + 0.3908 = 0.68773$$

The heat exchanger loss coefficient under normal isothermal flow conditions is specified, i.e.,

$$K_{he} = 4177.08481\ \mathrm{Ry}^{-0.4392686}$$

The characteristic flow number, *Ry*, is evaluated by using the mean dynamic viscosity μ_{a56}. At the mean air temperature through the heat exchanger,

$$T_{a56} = 0.5(15.614 + 47.858) = 31.736\ ^{\circ}C\ (304.886\ K)$$

Find the dynamic viscosity of the air stream $\mu_{a56} = 1.869287 \times 10^{-5}$ kg/ms. The corresponding characteristic flow number, based on the minimum frontal area, is

$$Ry = m_a/(A_{fr}\ \mu_{a56}\ n_{tb(1)}/n_{tb(2)}) = 604.483/(8 \times 27.55 \times 1.869287 \times 10^{-5} \times 57/58)$$

$$= 149296.5\ m^{-1}$$

Thus

$$K_{he} = 4177.08481(149296.5)^{-0.4392686} = 22.290$$

According to Equation 2.3.10, the contraction coefficient is

$$\sigma_c = 0.6144517 + 0.04566493 \times 0.875 - 0.336651 \times 0875^2 + 0.4082743 \times$$

$$0.875^3 + 2.672041 \times 0.875^4 - 5.963169 \times 0.875^5 + 3.558944 \times 0.875^6 = 0.77515$$

According to Equation 5.6.20, the entrance contraction loss coefficient is

$$K_c = \left[\frac{1}{0.875}\left(\frac{1}{0.77515} - 1\right)\right]^2 = 0.1099$$

The effective mean inlet flow angle is obtained from Equation 5.6.13 as

$$\theta_m = 0.0019 \times 30^2 + 0.9133 \times 30 - 3.1558 = 25.95315^{\circ}$$

The downstream loss coefficient, K_d, consists of the turning and jetting losses as well as the kinetic energy loss to the atmosphere. According to Equations 5.6.21 and 5.6.22, find the jetting loss

$$K_{dj} = [\{-2.8919(0.2/9.5) + 2.9329(0.2/9.5)^2\}$$

$$\times \{\sin 30^{\circ} - 1.25/(2 \times 9.5) + 0.2/9.5\}^{-1}$$

$$\times [1 - 0.5 \times 1.25/\{9.5(\sin 30^{\circ} + 0.2/9.5)\}]^{-1} \times (28/30)^{0.4}$$

$$+ \{\exp(2.36987 + 5.8601 \times 10^{-2} \times 30 - 3.3797 \times 10^{-3} \times 30^2)$$

$$\times (1 - 0.5 \times 1.25/(9.5\ (\sin 30^{\circ} + 0.2/9.5))\}^{0.5}$$

$$\times \{1 + 0.2/9.5 \times \sin 30^{\circ})\}^{-1}]^2 = 1.955121$$

and the outlet loss coefficient

$$K_o = [\{-2.89188 \times 0.2/9.5 + 2.93291(0.2/9.5)^2\}$$

$$\times[1 - 0.5 \times 1.25/\{9.5(\sin 30^\circ + 0.2/9.5)\}]^3 + 1.9874$$

$$-3.02783\{0.5 \times 1.25/9.5(\sin 30^\circ + 0.2/9.5)\}$$

$$+ 2.0817\{0.5 \times 1.25/9.5(\sin 30^\circ + 0.2/9.5)\}^2]$$

$$\times \{\sin 30^\circ - 1.25/(2 \times 9.5) + 0.2/9.5\}^{-2} = 7.70772$$

Thus,

$$K_d = 1.955121 + 7.70772 = 9.662841$$

Substitute these values into Equation 5.6.19, and find

$$K_{\theta t} = 22.290 + [2/(0.48)^2]\ (1.0205 - 0.9180)/(1.0205 + 0.9180)$$

$$+ (1/\sin 25.95315^\circ - 1)\ (1/\sin 25.95315^\circ - 1 + 2 \times 0.1099^{0.5})$$

$$\times 2 \times 0.9180/(1.0205 + 0.9180) + 9.662841 \times 2 \times 1.0205/(1.0205 + 0.9180)$$

$$= 35.2920$$

The harmonic mean density through the bundle is

$$\rho_{a56} = 2/(1/\rho_{a5} + 1/\rho_{a6}) = 2/(1/1.0205 + 1/0.9180) = 0.9666 \text{ kg/m}^3$$

Furthermore

$$A_c = \pi \times 9.17^2/4 = 66.0433 \text{ m}^2$$

and

$$A_e = \pi \times (9.17^2 - 1.4^2)/4 = 64.5039 \text{ m}^2$$

The value of the left side of Equation 8.1.26 is

$$84600\ [(1 - 0.00975 \times 0.5 \times \cos 30^\circ \times 9.5/321.008)^{3.5}$$

$$- (1 - 0.00975 \times 0.5 \times \cos 30^\circ \times 9.5/288.75)^{3.5}] = 4.1317 \text{ N/m}^2$$

The value of the right side of Equation 8.1.26 is

$$\frac{1.5}{2 \times 1.0205}\left(\frac{604.483}{8 \times 27.55}\right)^2 + \frac{0.68773}{2 \times 1.0214}\left(\frac{604.483}{64.5039}\right)^2 - \frac{4.1037}{2 \times 1.0214}\left(\frac{604.483}{66.0433}\right)^2$$

$$+ \frac{35.2920}{2 \times 0.9666}\left(\frac{604.483}{8 \times 27.55}\right)^2 = 4.1266 \text{ N/m}^2$$

The agreement between the two sides of the draft equation is good, i.e., the draft equation is satisfied.

8.2 Noncondensables

The effectiveness of an air-cooled vapor condenser is reduced if noncondensable gases are present during the condensation process. In steam condensers, atmospheric air leaking into the low-pressure portion of the steam-cycle equipment and gases from chemicals used for treatment of boiler feedwater tend to accumulate in the condenser. Trapped noncondensables

- reduce performance
- promote metal corrosion
- cause freezing of the condensate in winter

Figure 8.2.1 illustrates trapping of noncondensables in more detail. This simple steam condenser has just two rows of tubes and undivided manifolds or headers.

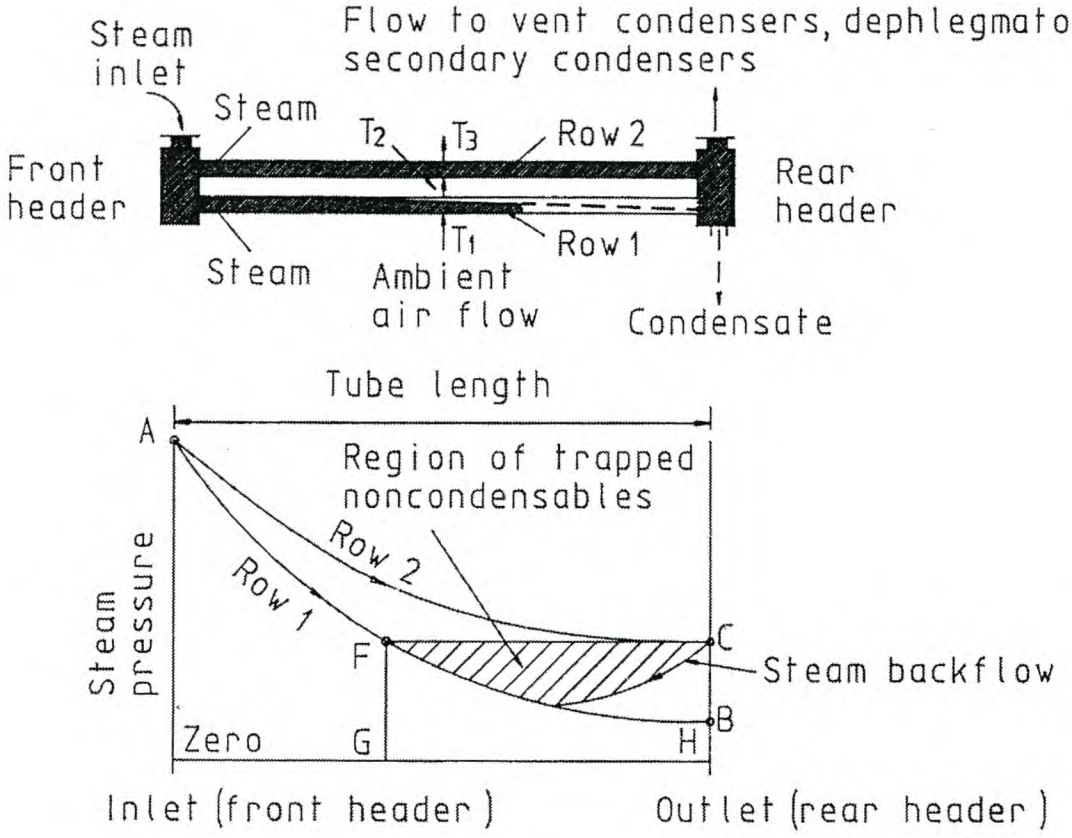

Fig. 8.2.1 Trapping of Noncondensable Gases in an Air-Cooled Condenser

The second row condenses less steam than the first, and, therefore, has a lower steam pressure drop. This occurs because the first row of tubes is exposed to the lower ambient inlet air temperature while the second row is contacted by preheated air. The pressure in the outlet header equals the inlet header pressure minus the pressure drop in the second tube row. Thus, the pressure in the outlet header exceeds the pressure that would have existed at the outlet of the first tube row if the higher rate of condensation had occurred along its entire length. Instead, steam from the outlet header tends to flow into the outlet end of the first tube row and traps noncondensables in these tubes (Fig. 8.2.1).

A number of investigators have studied the process of condensation in a multi-tube-row, air-cooled heat exchanger such as Forgó, Rozenman and Pundyk, Berg and Berg, Schrey and Kern, Breber et al., Schrey, and Fabbri.

To overcome the problem of noncondensable gases in multi-row air-cooled condensers, some designs add a dephlegmator or deaerator. These secondary reflux condensers are added in series to increase the steam flow in the main condenser and create a net flow of steam out of every tube (Fig. 8.2.2).

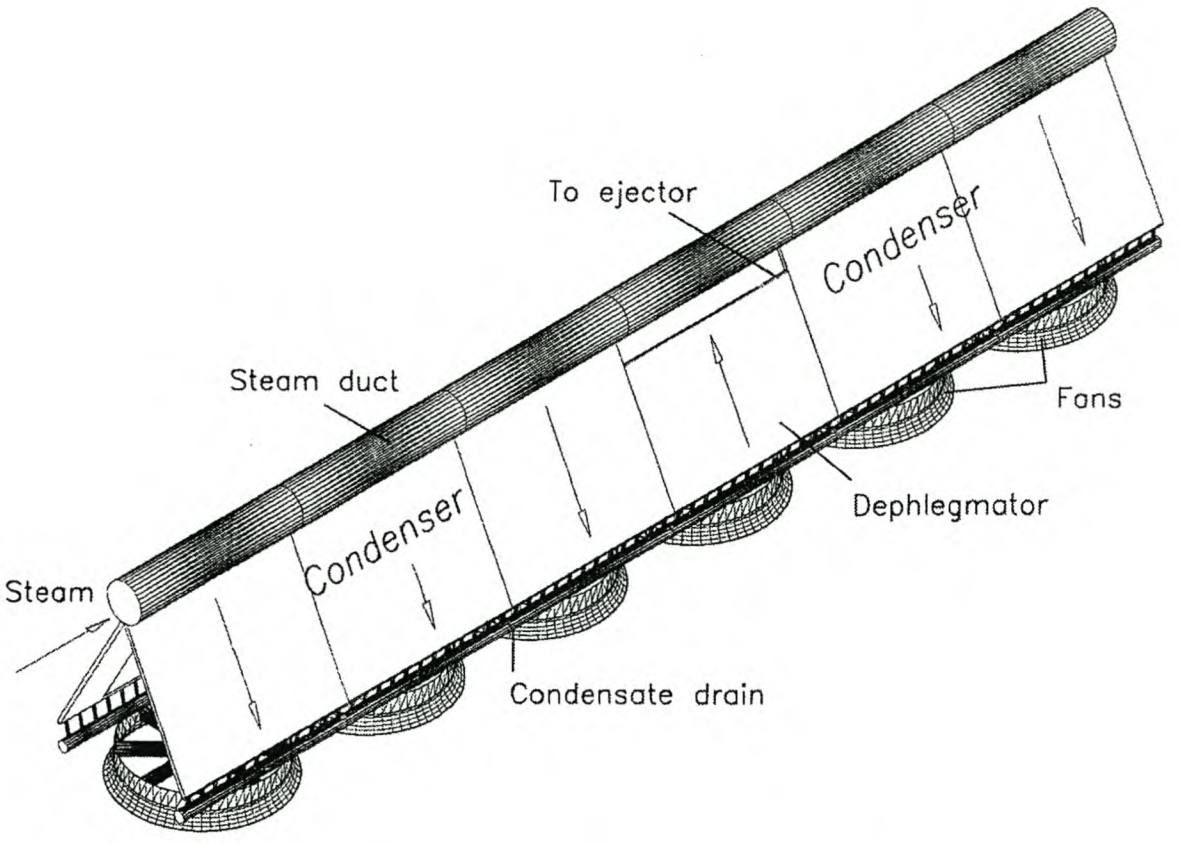

Fig. 8.2.2 Condenser with Dephlegmator

The effectiveness of this concept may be further improved by changing the fin height or fin pitch in consecutive tube rows to achieve a more balanced drop in steam pressure. Despite this improvement, freezing has been experienced at some plants under extremely low ambient temperature in the past. The reflux condenser or dephlegmator is particularly prone to freezing due to possible flooding or other liquid holdup. By employing variable speed motors and modern control systems, the dangers of freezing are greatly reduced according to Fahlsing.

Figure 8.2.3 shows a steam condenser in which each bundle has its own main and vent section. The horizontal tubes have a two-pass arrangement and are interposed to minimize steam pressure differences in the outlet headers and at the connection to the steam-jet air ejector. Rows 1 and 4 of the main condenser connect to rows 2 and 3 of the vent condenser, and rows 2 and 3 connect to vent rows 1 and 4.

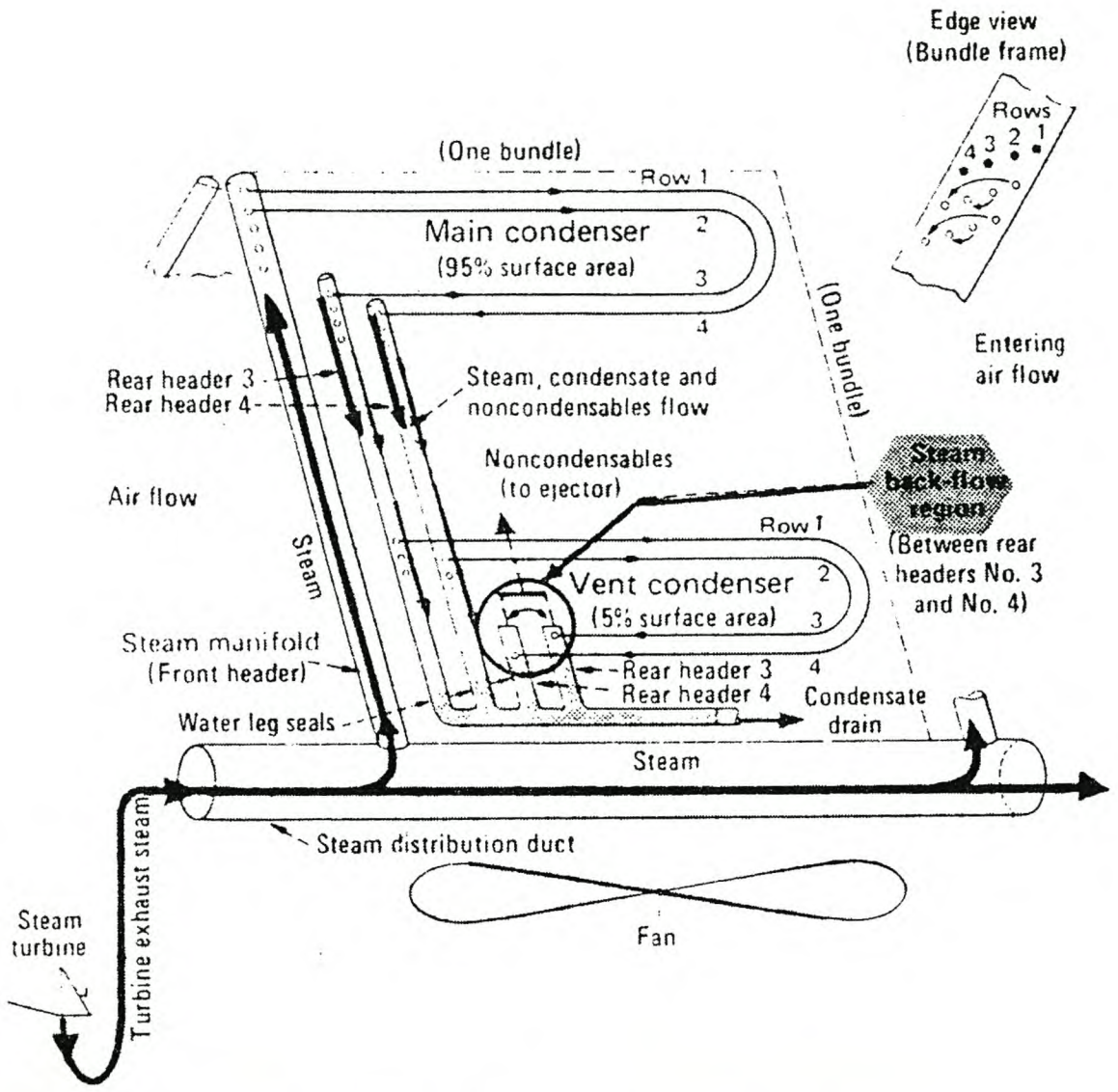

Fig. 8.2.3 Main and Vent Condenser Unit

According to Larinoff et al., steam backflow and trapping of gases may occur in specific regions of the previously described arrangements under certain operating conditions.

They describe a condenser in which the tube rows are connected to a common steam inlet header by individual outlet headers, vent tubes, and ejectors as shown in Figure 8.2.4. The vent tubes are installed in the heated portion of the air stream to avoid freezing. Other refinements to remove noncondensables have also been proposed by Larinoff.

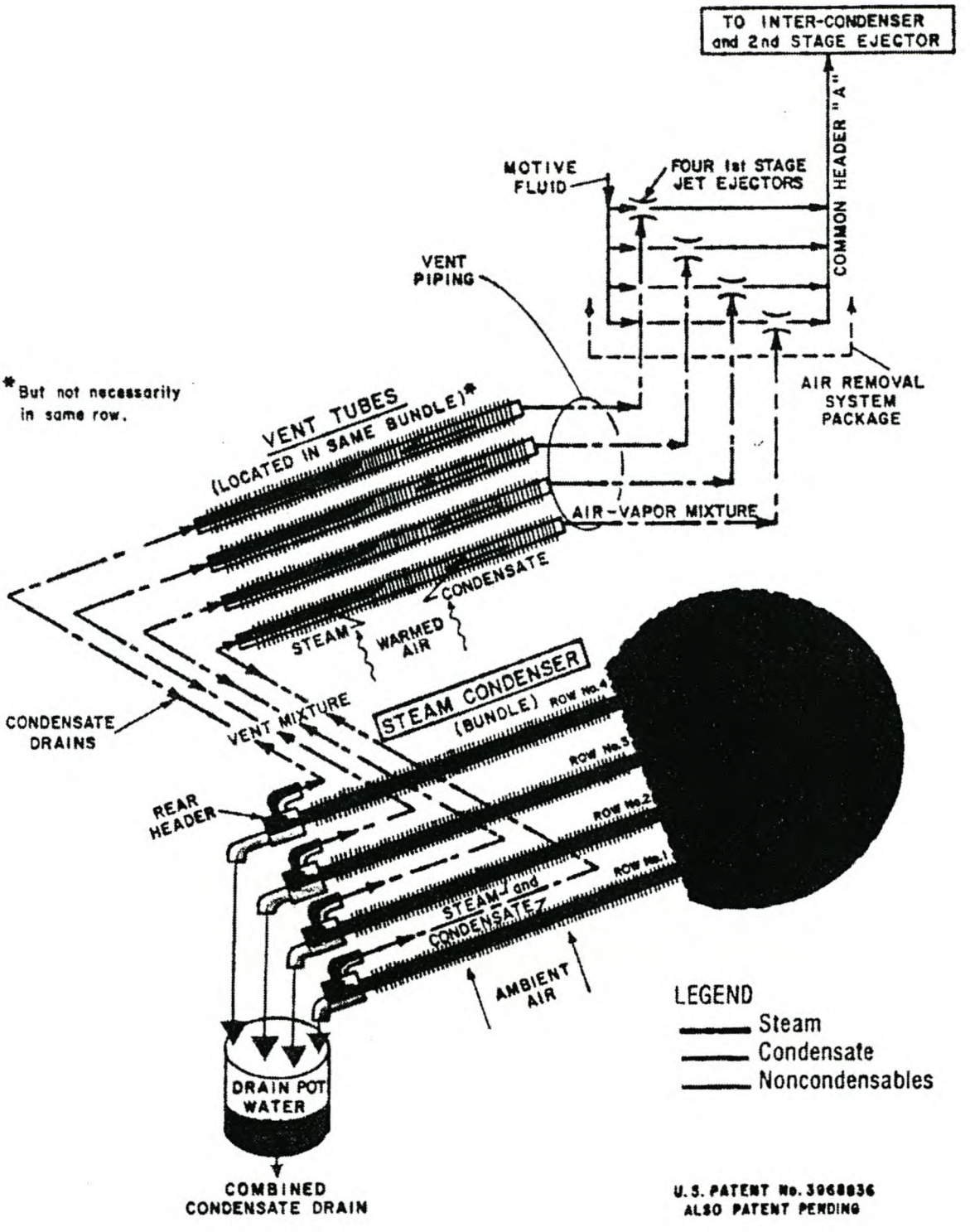

Fig. 8.2.4 Stacked Single Row Condensers

The multi-row effect is eliminated in modern condensers consisting of bundles having only one row of finned tubes. Due to possible maldistribution of air or steam flow, de-aeration of the single-row condenser cannot be ignored according to Schrey.

During reflux condensation, a downflowing condensate film is formed, i.e., countercurrent flow exists when a vapor enters a vertical or inclined tube at the bottom and condenses uniformly on the inner surface. Experimental studies on reflux condensation in vertical tubes show the transition from counterflow to co-current upflow can differ markedly from that for adiabatic gas-liquid flow illustrated in Figure 2.7.6. These studies are reported by authors such as Banerjee et al., Girard and Chang, Obinelo et al., and Reuter and Kröger. During condensation, the vapor flow rate decreases in the direction of the flow compared to adiabatic flow where it remains constant. Upward transport of condensate into regions of lower vapor velocities leads to:

- condensate accumulation
- subsequent formation of a liquid plug in the single-phase region

This is accompanied by a sharp rise in pressure drop across the ends of the tube. At sufficiently high condensation rates, the liquid plug is ejected at the top of the tube. The formation and subsequent ejection of a liquid plug can be cyclic in nature. The formation of a condensate plug is less likely to occur in inclined flattened ducts. The sharp rise in pressure drop tends to be due to an accumulation and entrainment of liquid near the lower inlet of the duct.

The particular condition where a sharp rise in pressure drop occurs in reflux condensers, frequently referred to as *flooding*, was observed by a number of researchers. These include English et al., Diehl and Koppany, Russel, Banerjee et al., Fürst, Girard and Chang, Obinelo et al., Reuter, Reuter and Kröger, and Schoenfeld and Kröger.

For values of $a_4\ Fr_{D\ell}^{0.6}\ Oh^{0.2}<11$ commonly found in air-cooled reflux steam condensers, Equation 2.7.11 can be simplified by expressing the exponential function in terms of a power series and neglecting higher order terms of $a_4\ Fr_{D\ell}^{0.6}\ Oh^{0.2}$ according to Schoenfeld and Kröger. The resulting equation for predicting the flooding gas velocity becomes

$$Fr_{Dg} \approx a_3\left(1-a_4\, Fr_{D\ell}^{0.6}\, Oh^{0.2}\right)\approx a_3 \tag{8.2.1}$$

To avoid reduced performance of a reflux condenser or dephlegmator, it is important to ensure flooding will not occur under any operating condition.

Unacceptably high pressure drops have been observed in practical power plant dephlegmators according to Zapke and Kröger. In some cases, they were found to be due to condensate entrainment in the lower header and not due to flooding in the finned tubes according to Smit.

Example 8.2.1

Dry saturated steam enters the square-edged (90°) inlet of a flattened air-cooled reflux condenser tube with the following specifications:

- Steam temperature: 50°C
- Length: L = 8 m
- Incline: $\varphi = 60°$ with the horizontal as shown in Figure 8.2.5.
- Inside height of the tube: H = 97 mm
- Width: W = 17 mm
- Steam condensation rate is uniform: 1.049 x 10^{-3} kg/s per meter length of tube
- All condensed steam flows back down the tube and leaves it at its lower end

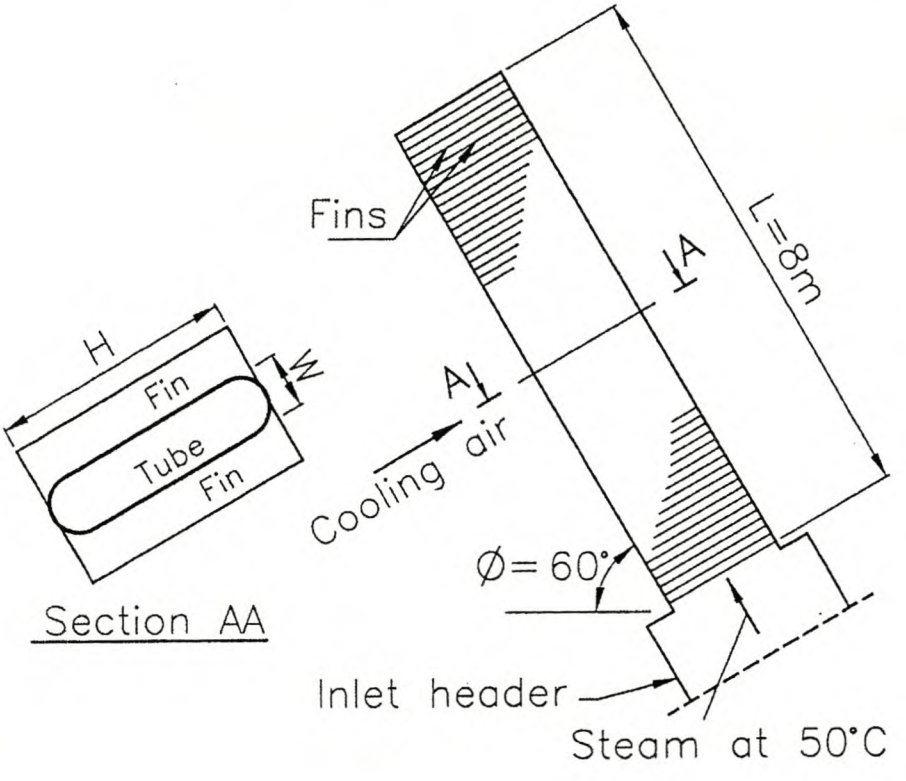

Fig. 8.2.5 Inclined Flattened Tube Condenser

Determine the speed of the steam where flooding will occur at the lower end, and compare it with the actual speed of the steam entering the flattened tube at that point.

Solution

Evaluate $a_4\ Fr_{D\ell}^{0.6}\ Oh^{0.2}$ in Equation 8.2.1.

The cross-sectional flow area of the duct is

$$A_{ts} = (H - W)W + \pi\ W^2/4 = (0.097 - 0.017)0.017 + \pi \times 0.017^2/4 = 1.587 \times 10^{-3}\ m^2$$

The corresponding equivalent diameter is

$$d_e = 4A_{ts}/[2(H - W/2) + \pi\ W] = 4 \times 0.001587/[2 \times (0.097 - 0.017/2) + \pi \times 0.017]$$

$$= 0.02755\ \text{m}$$

The steam mass flow rate entering the duct is the product of the specified condensate rate per unit length and the tube length

$$m = 1.049 \times 10^{-3} \times 8 = 8.392 \times 10^{-3}\ \text{kg/s}$$

From Equation A.2.5 in Appendix A, the density of dry saturated steam (vapor or gas) at 50°C (323.15 K) is

$$\rho_v = \rho_g = -4.062329056 + 0.10277044 \times 323.15 - 9.76300388 \times 10^{-4} \times 323.15^2$$

$$+ 4.475240795 \times 10^{-6} \times 323.15^3 - 1.004596894 \times 10^{-8} \times 323.15^4$$

$$+ 8.9154895 \times 10^{-12} \times 323.15^5 = 0.083\ \text{kg/m}^3$$

The corresponding density of water or liquid follows from Equation A.4.1.

$$\rho_w = \rho_\ell = (1.49343 \times 10^{-3} - 3.7164 \times 10^{-6} \times 323.15 + 7.09782 \times 10^{-9} \times 323.15^2$$

$$- 1.90321 \times 10^{-20} \times 323.15^6)^{-1} = 988.13\ \text{kg/m}^3$$

The liquid viscosity is, according to Equation A.4.3,

$$\mu_w = \mu_\ell = 2.414 \times 10^{-5} \times 10^{247.8/(323.15-140)} = 5.442 \times 10^{-4} \text{ kg/ms}$$

and the surface tension follows from Equation A.4.7

$$\sigma = 5.148103 \times 10^{-2} + 3.998714 \times 10^{-4} \times 323.15 - 1.4721869 \times 10^{-6} \times 323.15^2$$

$$+ 1.21405335 \times 10^{-9} \times 323.15^3 = 0.06793 \text{ N/m}$$

For a duct inclination of $\varphi = 60°$,

$$a_3 = 0.4952$$

$$a_4 = 27.7615$$

With these values, find

$$a_4 Fr_{D\ell}^{0.6} Oh^{0.2} = 27.7615\left[(8.392/1.587)^2/\{9.8 \times 0.02755 \times 988.13(988.13 - 0.083)\}\right]^{0.6}$$

$$\times \left[0.0005442/(988.13 \times 0.02755 \times 0.06793)^{0.5}\right]^{0.2} = 0.0239$$

Since this value is much smaller than unity, Equation 8.2.1 can be employed to determine the approximate gas or vapor speed where flooding occurs

$$v_{gs} \approx \left[a_3(\rho_\ell - \rho_g) gH/\rho_g\right]^{0.5} = \left[0.4952(988.13 - 0.083)9.8 \times 0.097/0.083\right]^{0.5} = 74.9 \text{ m/s}$$

From Equation 2.7.9, the actual steam speed at the duct inlet is

$$v_{gs} = 8.392 \times 10^{-3}/(0.083 \times 0.001587) = 63.71 \text{ m/s}$$

which means that flooding will not occur.

8.3 Inlet Losses

Large air-cooled heat exchangers may consist of one or more fan units. Where many fan units are required, these are usually arranged in long banks consisting of one or more rows of fans. Due to flow distortion and separation of the cooling air stream at the inlet to the banks, losses occur and result in a reduction of the heat exchanger effectiveness.

The flow through a forced convection system may be reduced considerably if the fan or fans are located too close to ground level. It is good practice to ensure the approach air velocity at the entrance to a fan (Fig. 8.3.1a) is no more than half the velocity through the fan throat, i.e., $v_{app} < 0.5\ v_F$ or $H_i > 0.5\ d_F$ according to Monroe.

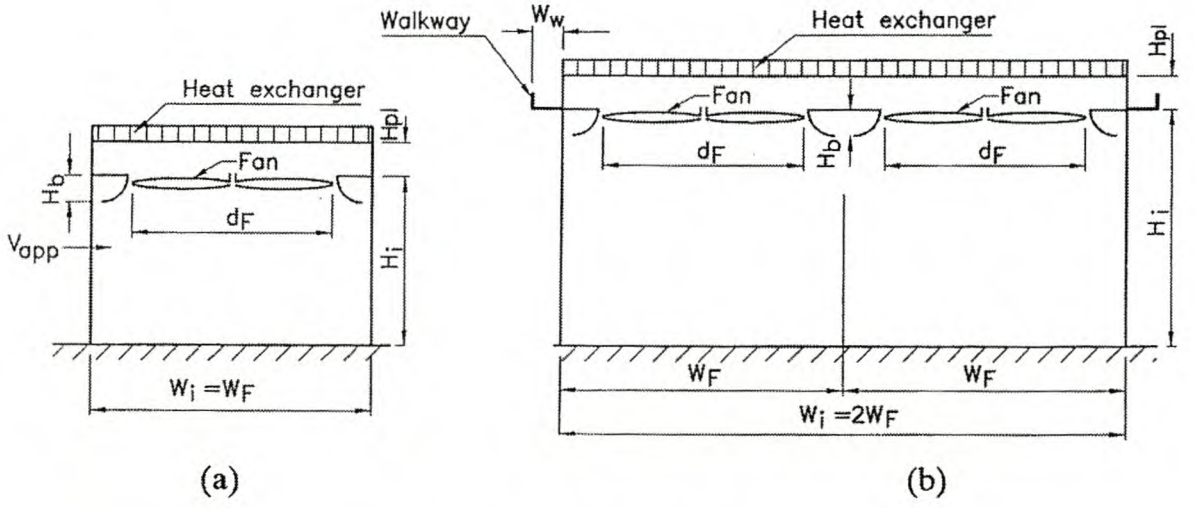

Fig. 8.3.1 Forced-Draft Air-Cooled Heat Exchangers (a) (b)

The height of the fan inlets should be at least one fan diameter, i.e., $H_i \geq d_F$, above ground level. This applies to the forced-draft units shown in Fig. 8.3.1b and to the underside of the bundle for induced-draft units for two rows of fans. To avoid excessive flow distortions and losses, consider the position of the air-cooled heat exchanger relative to buildings or other heat exchangers according to Rose et al.

A few studies have been conducted to quantify the effect of flow disturbances at the inlet to the heat exchanger on the performance of the fans in forced-draft systems according to Russell and Peachey, and Salta and Kröger.

Salta and Kröger report the results of tests conducted on models of two-dimensional, single- and multi-row, six-bladed fan units located at different heights above ground level. Figure 8.3.2 show the reduction they found in air volume flow rate through the heat exchanger as the fan platform height, H_i, was reduced. This applied to units consisting of one or more fan rows where the fans operated near maximum efficiency. Their findings are applicable to units where:

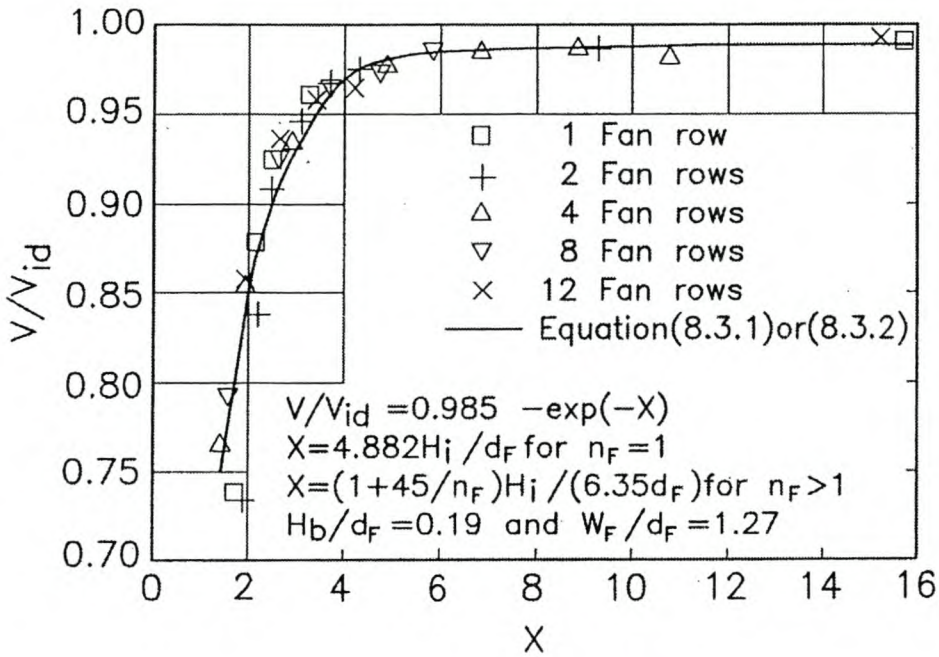

Fig. 8.3.2 Reduction in Air Volume Flow Rate

- ratio of the rounded-inlet bell height to fan diameter $H_b/d_F = 0.19$
- ratio of the fan pitch to fan diameter $W_F/d_F = 1.27$
- no walkway exists along the edge of the fan platform

For a long single row of fans, the ratio of the air volume flow rate through the heat exchanger compared to the ideal flow rate (Fig. 8.3.2), i.e., the sum of flows for individual freestanding fan units with undisturbed inlet conditions, can be correlated by the following equation

$$V/V_{id} = 0.985 - \exp(-X) \qquad (8.3.1)$$

where

$X = 4.882\ H_i/d_F$

For two-dimensional heat exchangers consisting of two or more long rows of fans, the following equation is applicable

$$V/V_{id} = 0.985 - \exp(-X) \tag{8.3.2}$$

where

$X = (1 + 45/n_F)H_i/(6.35\ d_F)$

n_F = the number of fan rows

The correctness of these correlations was confirmed numerically. It was also shown they are only slightly dependent on the shape of the fan inlet shroud, according to Duvenhage, Vermeulen, Meyer, and Kröger.

Experiments show the performance of the fans along the edge of the platform are most significantly affected. Upon reducing the platform height in a four-row heat exchanger with two fans on either side of the symmetry line, the flow through the individual rows is reduced (Fig. 8.3.3).

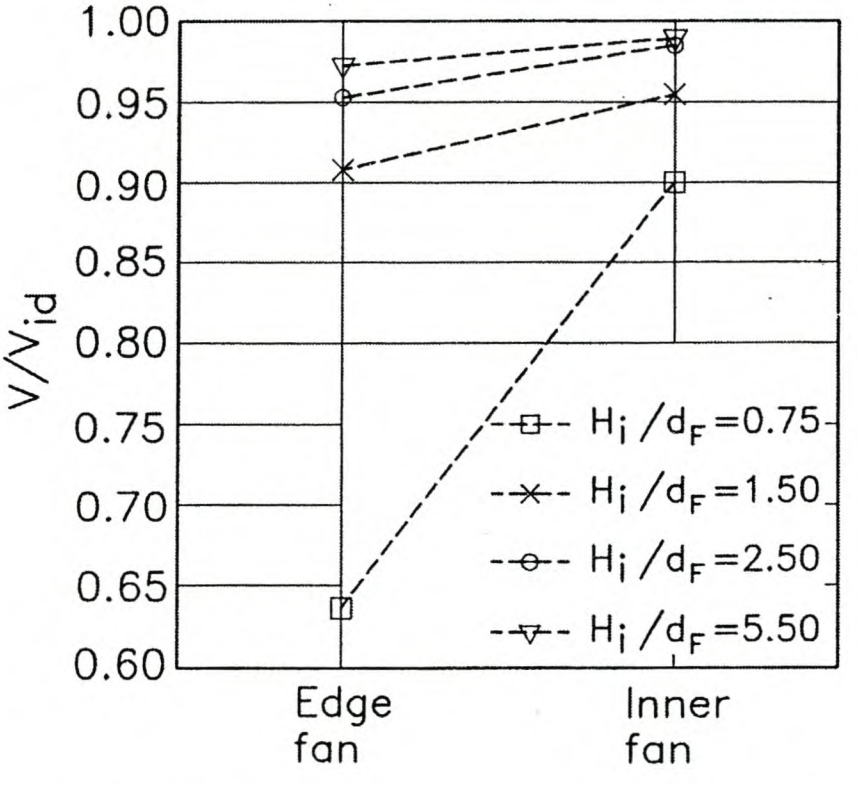

Fig. 8.3.3 Reduction in Air Volume Flow Rate through Individual Fan Rows in a Four-Fan-Row Heat Exchanger

If an unperforated walkway is affixed along the edge of the fan platform (Fig. 8.3.1b) for the heat exchanger geometry specified previously, the air-flow rate through the heat exchanger can be improved (Fig. 8.3.4) for a four-fan-row heat exchanger. The same trend can be achieved if the fan platform is extended along the edge.

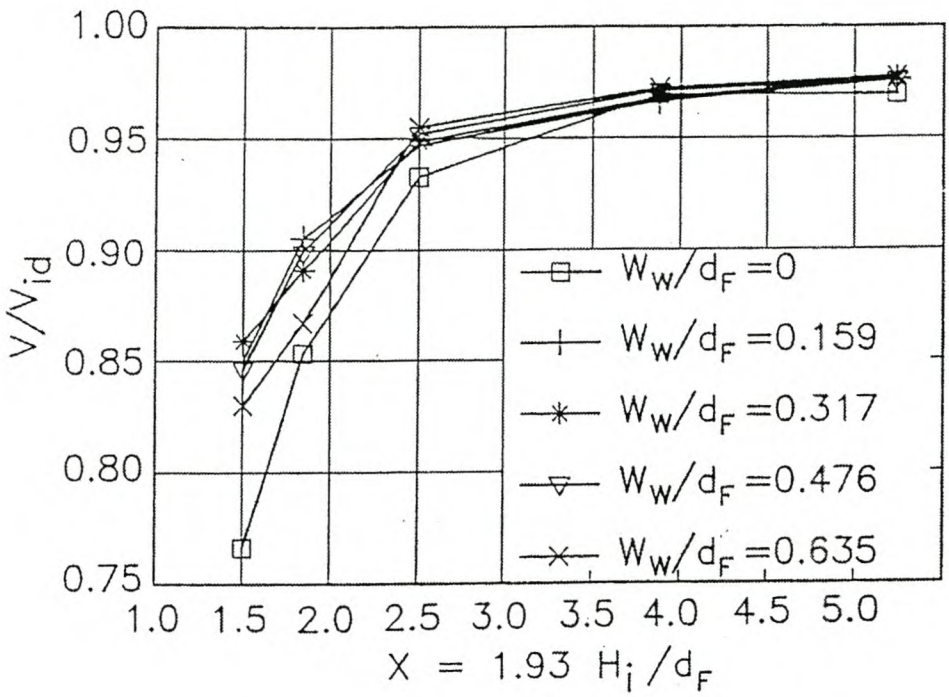

Fig. 8.3.4 Influence of Walkway on Volume Flow Rate through a Four-Fan-Row Heat Exchanger

The increased flow is due primarily to the improvement of flow through the fans along the edge of the four-fan-row heat exchanger (Fig. 8.3.5).

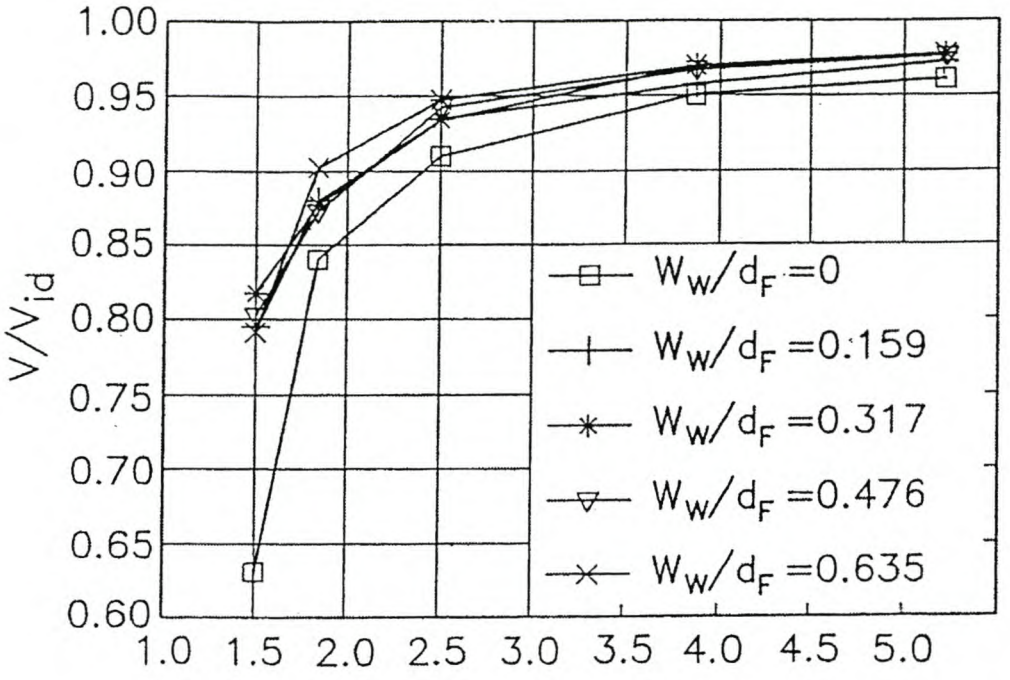

Fig. 8.3.5 Effect of Walkway Width on the Flow through Edge Fan in a Four-Fan-Row Heat Exchanger

In an induced-draft air-cooled heat exchanger (Fig. 8.1.2), inlet flow losses and possible reductions in effective heat exchanger width, $W_{ie} \leq W_i$, due to separated flow must be considered when determining the system flow resistance. If the heat exchanger loss coefficient is small, inlet losses and the maldistribution of flow caused by the distorted inlet conditions may reduce the effectiveness of the heat exchanger. This is the case in natural draft cooling towers.

Terblanche and Kröger performed isothermal model tests to determine the loss coefficient at the inlet to a horizontal, two-dimensional, induced-draft, air-cooled heat exchanger. According to Equation 7.3.4, the approximate loss coefficient can be expressed as

$$K_{ct} = \frac{\left(p_a/\rho - p_o/\rho_o\right)}{v^2/2} - 1 - K_{he}\left(\frac{\rho}{\rho_{he}}\right) \qquad (8.3.3)$$

The results of the experiments performed by Terblanche and Kröger are shown in Figure 8.3.6 and are compared to the following empirical correlation.

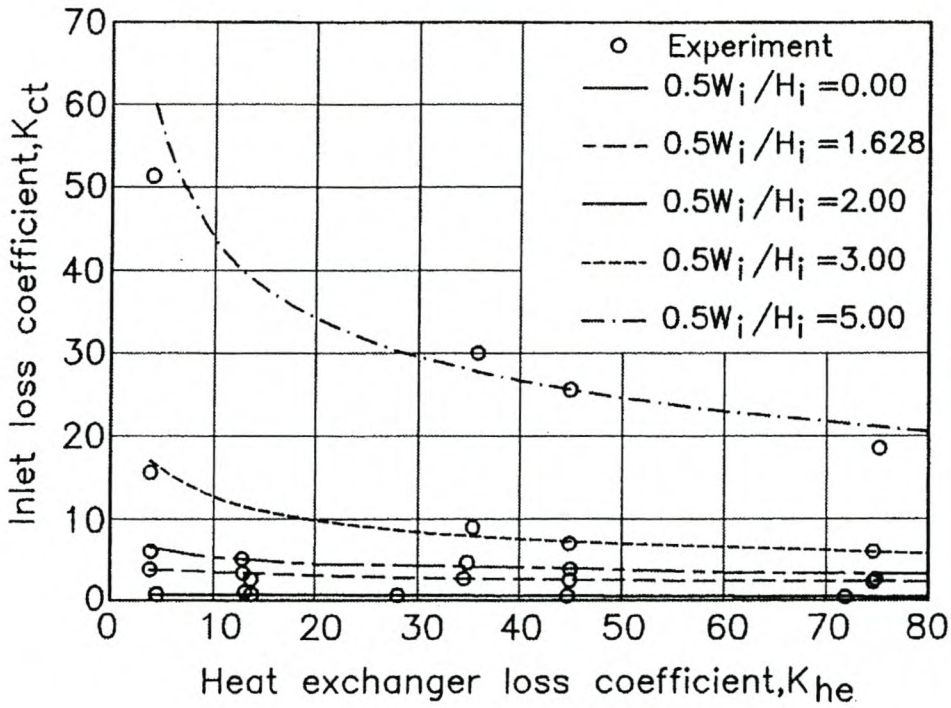

Fig. 8.3.6 Inlet Loss Coefficients in a Two-Dimensional Induced-Draft Unit

$$K_{ct} = \left[1.1 + 1.1\,(0.5\,W_i / H_i)^3 - 0.05\,(0.5\,W_i / H_i)\exp(0.5\,W_i / H_i)\right]$$

$$\times\, K_{he}^{\left[-0.29 + 0.079\cos\{(180/\pi)(0.5\,W_i/H_i)\} + 0.102\sin\{(180/\pi)(0.5\,W_i/H_i)\}\right]} \qquad (8.3.4)$$

for

$0 \le (0.5W_i/H_i) \le 5$

$4 \le K_{he} \le 80.$

W_i = the width of the heat exchanger (Fig. 8.3.7)

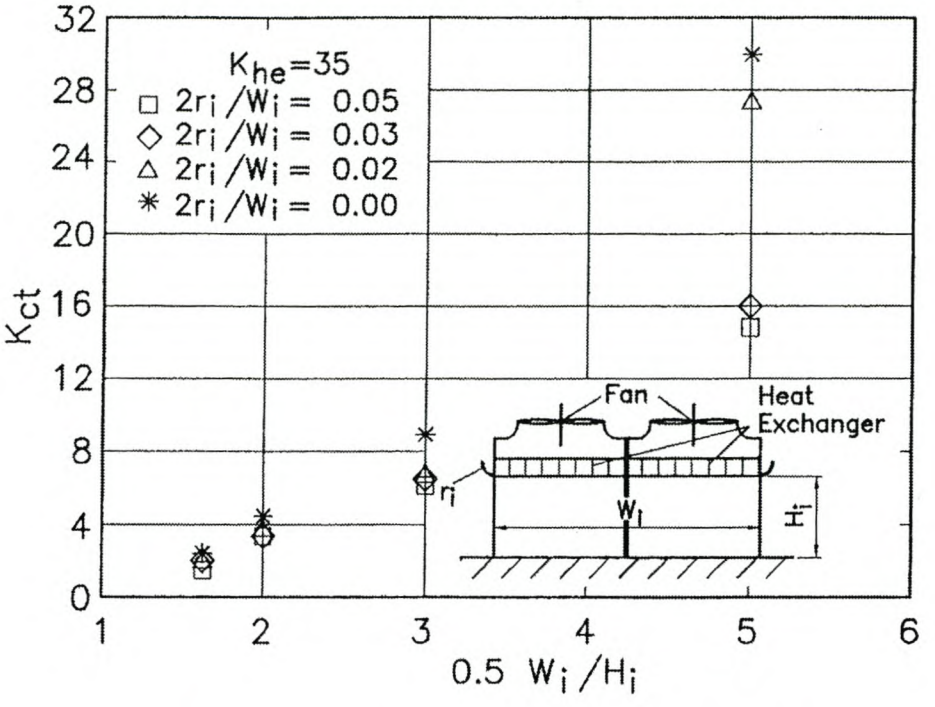

Fig. 8.3.7 Effect of Rounded Inlets on the Value of Kct

The effective width of the heat exchanger, $W_{ie} \leq W_i$, having a frame or plenum wall thickness, t_s, can be determined using the following equation according to Oosthuizen:

$$\frac{W_{ie}}{W_i + 2t_s} = 0.9366 - 0.12786\,\ell n\left(\frac{W_i + 2t_s}{H_i}\right) + 0.073\,\ell n\,K_{he} \qquad (8.3.5)$$

This equation is valid for

- $5 \leq (W_i + 2t_s)/H_i \leq 16.13$
- $2.5 \leq K_{he} \leq 20.2$

By rounding off the inlet to the unit, the inlet loss coefficient can be reduced as shown in Figure 8.3.7.

For a rounded inlet with r_i/W_i = 0.014, the effective width of the heat exchanger or fill is given by the following empirical relation:

$$W_{ie} / W_i = 1.0487 - 0.17408 \ell n (W_i / H_i) + 0.09 \ell n K_{he} \tag{8.3.6}$$

This equation is valid for

- $5 \leq W_i/H_i \leq 16.13$
- $2.5 \leq K_{he} \leq 20.2$

In a well-designed air-cooled heat exchanger or cooling tower, the value of W_{ie}/W_i should be equal to unity. If this is not the case, matters can be improved by rounding off the inlet or increasing the inlet height, H_i.

De Villiers and Kröger state for an orthotropically-packed, e.g., cellular film or fiber sheet type fill, induced-draft, rectangular, wet-cooling tower the inlet loss coefficients for induced-draft air-cooled heat exchangers are applicable.

For an isotropically-packed, e.g., splash or trickle type fill, induced-draft, rectangular, wet-cooling tower, the inlet loss coefficient is

$$K_{ct} = 0.2339 + (3.919 \times 10^{-3} K_{fi}^2 - 6.84 \times 10^{-2} K_{fi} + 2.5267)$$

$$\times \exp [W_i \{0.5143 - 0.1803 \exp (0.0163 K_{fi})\} / H_i]$$

$$- \sinh^{-1} [2.77 \exp (0.958 W_i / H_i) \exp \{10^{-2} K_{fi} (2.457 - 1.015 W_i / H_i)\}$$

$$\times (r_{ir} / W_i - 0.013028)] \tag{8.3.7}$$

where

r_i = the radius of the inlet rounding

Equation 8.3.7 is valid for

- $5 \leq K_{fi} \leq 25$
- $0 \leq r_{ir} / W_i \leq 0.025$
- $1 \leq W_i / H_i \leq 7.5$

The small reduction in inlet loss coefficient due to the rain zone should be ignored in both the previous cases.

Example 8.3.1

An air-cooled heat-exchanger bank at a petro-chemical plant consists of six adjacent bays. Each bay is 7.05 m broad and results in a bank length of 6 x 7.05 = 42.3 m as described in Example 8.1.1. Determine the heat rejected by the heat-exchanger bank if losses due to separation of the flow at the inlet edge of the fan platform are considered.

Solution

The reduction in air volume flow rate through the heat exchanger due to inlet losses is given by Equation 8.3.2 where, for a bank consisting of two fan rows,

$$X = (1 + 45/2)\ 12.7/(6.35 \times 4.265) = 11.02$$

Substitute this value into Equation 8.3.2, and find

$$V/V_{id} = 0.985 - \exp(-11.02) = 0.985$$

Thus, the approximate heat rejected by the heat exchanger bank is

$$Q_{6i} = 6(V/V_{id})Q = 6 \times 0.985 \times 12.477 = 73.739 \text{ MW}$$

Example 8.3.2

A large, free-standing, air-cooled steam condenser consists of 18 fan units described in Example 8.1.3 and arranged in three rows of six units each. The fan platform is located 25 m above ground level and is surrounded by a 8.27 m high windwall (Fig. 8.3.8). Determine the approximate mean reduced amount of heat rejected per condenser unit due to inlet flow distortions and compare it to the value obtained in example 8.3.1.

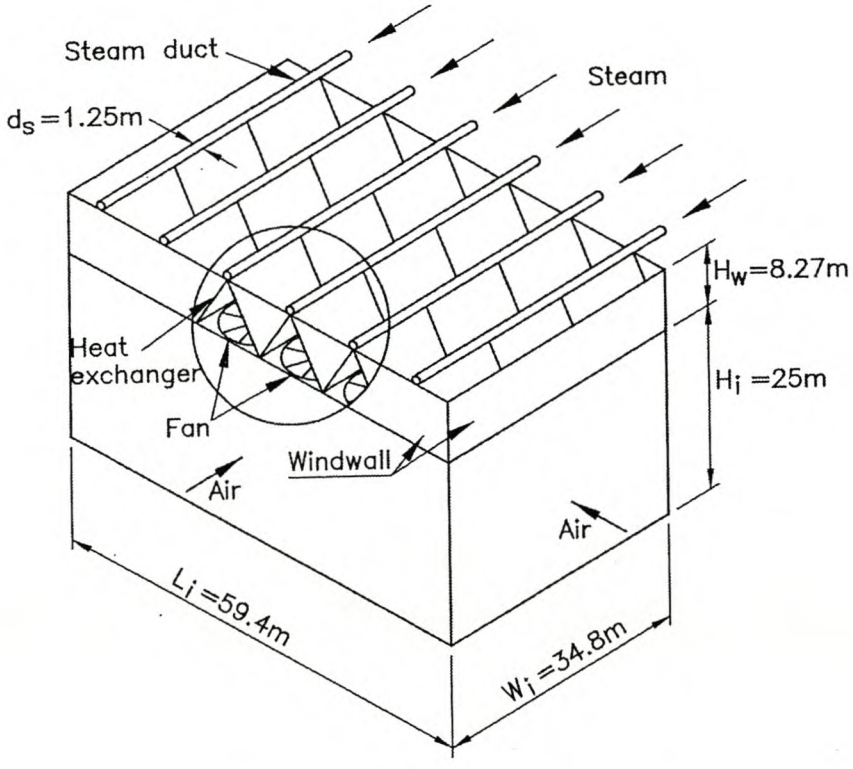

Fig. 8.3.8 Air-Cooled Steam Condenser

Solution

For purposes of analysis, the air-cooled condenser shown in Figure 8.3.8 may be considered to have inlet airflow characteristics similar to those found in a two-

dimensional, three-fan-row heat exchanger. According to Equation 8.3.2, the mean reduced air-volume flow rate due to inlet losses is given by

$$V/V_{id} = [0.985 - \exp\{-(1+45/n_F)H_i/(6.35 \text{ x } d_F)\}]$$

$$= [0.985 - \exp\{-(1+45/3)\,25/(6.35 \text{ x } 9.145)\}] = 0.98398$$

Due to this reduced air-volume flow rate, there will be a corresponding reduction in heat transfer rate. For this relatively small reduction in volume flow rate, the approximate heat transfer rate per fan unit can be determined as follows:

$$Q_i \approx Q_a\,(V/V_{id}) = 19.63 \text{ x } 10^6 \text{ x } 0.98398 = 19.316 \text{ x } 10^6 \text{ W}$$

For the condenser consisting of 18 fans, the heat rejection rate is

$$Q_{18i} = 18\,Q_i = 18 \text{ x } 19.316 = 347.68 \text{ x } 10^6 \text{ W}$$

Example 8.3.3

Show that hot water at a temperature of T_{wi} = 41.5° (314.65 K) and flowing at a rate of m_w = 412 kg/s can be cooled to T_{wo} = 30.3177 °C (303.4677 K) in an induced-draft wet-cooling tower (Fig. 8.3.9). What is the rate of evaporation?

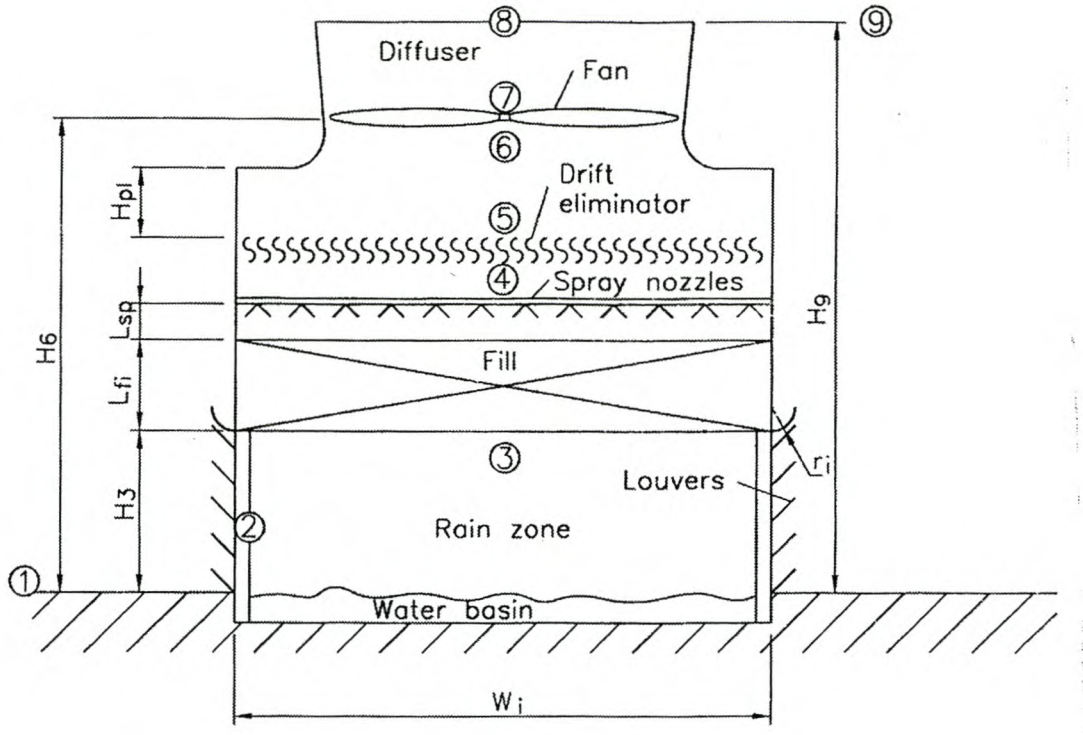

Fig. 8.3.9 Induced-Draft Wet-Cooling Tower

Ambient conditions:

- Atmospheric pressure at ground level: p_{a1} = 101,325 N/m^2
- Air temperature at ground level: T_{a1} = 33.5 °C (306.65 K)
- Wetbulb temperature at ground level: T_{wb} = 25°C (298.15K)

Cooling tower specifications:

- Tower height: H_9 = 12.5 m
- Fan height: H_6 = 9.5 m
- Tower inlet height: H_3 = 4 m
- Tower inlet width: W_i = 12 m
- Tower breadth or length: B_i = 12 m
- Fill height: L_{fi} = 1.878 m
- Height of spray zone: L_{sp} = 0.5 m
- Inlet rounding: r_i = 0.025 W_i, m
- Plenum chamber height: H_{pl} = 2.4 m

Fill specifications:

- Transfer coefficient (Merkel method with Chebyshev integration)

$$h_{dfi}\, a_{fi} / G_w = 0.2692\, G_w^{-0.094}\, G_a^{0.6023}$$

- Loss coefficient

$$K_{fdm1} = 1.9277\, G_w^{1.2752}\, G_a^{-1.0356}$$

- Frontal area of the fill

$$A_{fr} = B_i \text{ x } W_i = 144 \text{ m}^2$$

Other specifications:

- Mean drop diameter in rain zone: d_d = 0.0035 m
- Loss coefficient for inlet louvers: K_{il} = 2.5
- Loss coefficient for fill support and contraction: $K_{fs} + K_{ctc}$ = 0.5
- Loss coefficient for water distribution system: K_{wd} = 0.5
- Fan upstream losses: K_{up} = 0.52
- Loss coefficient for the drift eliminator (type c): given by Equation 4.7.2

Fan/diffuser with rounded inlet dimensions and performance characteristics:

- Fan diameter: d_F = 8 m
- Fan rotational speed: N_F = 120 rpm
- Test fan diameter: d_{Fr} = 1.536 m
- Reference rotational speed: N_{Fr} = 750 rpm
- Reference air density: ρ_r = 1.2 kg/m^3

Fan/diffuser static pressure (model test fan at reference conditions):

$$\Delta p_{F/dif} = 320.85 - 6.9604\, V_{F/dif} + 0.31373\, V_{F/dif}^2 - 0.021393\, V_{F/dif}^3, N/\text{m}^2$$

Fan shaft power:

$$P_{F/dif} = 4245.1 - 64.134\, V_{F/dif} + 17.586\, V_{F/dif}^2 - 0.71079\, V_{F/dif}^3, W$$

- Ignore blade tip clearance effects during scale-up

Solution

Solve this problem by following an iterative procedure to satisfy both the energy and draft equations. The choice of an air-vapor mass flow rate of

$$m_{av15} = 442.1426 \text{ kg/s}$$

through the fill will satisfy these equations. This gives the following results:

- corresponding pressure: $p_{a5} = 101{,}170.6 \text{ N/m}^2$
- air temperature: $T_{a5} = 306.7645 \text{ K}$
- exit water temperature: $T_{wo} = 303.4677 \text{ K}$

At the specified air inlet drybulb temperature of $T_{a1} = 306.65$ K, wetbulb temperature of $T_{wb} = 298.15$ K, and atmospheric pressure at ground level $p_{a1} = 101{,}325 \text{ N/m}^2$, find the following thermophysical properties employing the equations given in Appendix A.

- Density of air-vapor: $\rho_{av1} = 1.1397 \text{ kg/m}^3$ using Equation A.3.1
- Humidity ratio of inlet air: $w_1 = 0.016569$ kg/kg dry air using Equation A.3.5
- Viscosity of the air-vapor mixture: $\mu_{av1} = 1.85928 \times 10^{-5}$ kg/ms using Equation A.3.3

The enthalpy of the inlet air, i_{ma1}, is found, according to Equation A.3.6b, with

$$c_{pa1} = 1006.64 \text{ J/kgK}$$

$$c_{pv1} = 1876.84 \text{ J/kgK}$$

evaluated at

$$(T_{a1} + 273.15)/2 = (306.65 + 273.15)/2 = 289.9 \text{ K}$$

according to Equations A.1.2 and A.2.2 respectively. The latent heat is found to be

$$i_{fgwo} = 2.5016 \times 10^6 \text{ J/kg}$$

according to Equation A.4.5 at 273.15K. With these values find $i_{ma1} = 76213.73$ J/kg dry air.

If the air is assumed to be saturated immediately after the drift eliminator, the wetbulb temperature at (5) will be equal to the given drybulb temperature $T_{a5} = 306.7645$ K at this elevation. The corresponding thermophysical properties at (5) can be determined according to the equations given in Appendix A.

- Saturated vapor pressure: p_{v5} = 5206.305 N/m^2 using Equation A.2.1
- Humidity ratio: w_5 = 0.033922 kg/kg using Equation A.3.5
- Density of air-vapor: ρ_{av5} = 1.12634 kg/m^3 using Equation A.3.1
- Dynamic viscosity of air: μ_{a5} = 1.8779 x 10^{-5} kg/ms using Equation A.1.3
- Dynamic viscosity of vapor: μ_{v5} = 1.0254 x 10^{-5} kg/ms using Equation A.2.3
- Dynamic viscosity of air-vapor: μ_{av5} = 1.84273 x 10^{-5} kg/ms using Equation A.3.3

The enthalpy of the air, i_{mas5}, is found, according to Equation A.3.6b, with

$$c_{pa5} = 1006.64 \text{ J/kgK}$$

and

$$c_{pv5} = 1876.887 \text{ J/kgK}$$

being evaluated at

$$(T_{a5} + 273.15)/2 = (306.7645 + 273.15)/2 = 289.9573 \text{ K}$$

according to Equations A.1.2 and A.2.2 respectively.

The latent heat is found to be

$$i_{fgwo} = 2.5016 \text{ x } 10^6 \text{ J/kg}$$

according to Equation A.4.5 at 273.15 K. With these values find

$$i_{mas5} = 120836.9 \text{ J/kg dry air}$$

The approximate harmonic mean density of the air-vapor in the fill is given by Equation 7.2.22.

$$\rho_{av15} = \frac{2}{1/\rho_{av1} + 1/\rho_{av5}} = \frac{2}{1/1.1397 + 1/1.12634} = 1.132982 \text{ kg/m}^3$$

The dry air mass flow rate can be determined from the following relation:

$$m_{av15} = [m_a(1 + w_1) + m_a(1 + w_5)]/2$$

or

$$m_a = 2\, m_{av15}/(2 + w_1 + w_5) = 2(442.1426)/(2 + 0.016569 + 0.033922)$$

$$= 431.2545 \text{ kg/s}$$

The respective air-vapor mass flow rates upstream and downstream of the fill are

$$m_{av1} = m_a(1 + w_1) = 431.2545(1 + 0.016569) = 438.4 \text{ kg/s}$$

and

$$m_{av5} = m_a(1 + w_5) = 431.2545(1 + 0.033922) = 445.8834 \text{ kg/s}$$

The corresponding mass velocities are:

$$G_{av15} = m_{av15}/A_{fr} = 442.1426/144 = 3.070429 \text{ kg/m}^2\text{s}$$

$$G_a = m_a/A_{fr} = 431.2545/144 = 2.994823 \text{ kg/m}^2\text{s}$$

$$G_{av1} = m_{av1}/A_{fr} = 438.4/144 = 3.044444 \text{ kg/m}^2\text{s}$$

$$G_{av5} = m_{av5}/A_{fr} = 445.8834/144 = 3.096413 \text{ kg/m}^2\text{s}$$

According to Equation A.4.2, the specific heat of water c_{pwm} = 4176.992 J/kg at the mean water temperature of

$$(T_{wi} + T_{wo})/2 = (341.65 + 303.4677)/2 = 309.0589 \text{ K}$$

At the outlet temperature of the water, T_{wo} = 303.4677 K, find

Density of water: ρ_{wo} = 995.6046 kg/m^3 using Equation A.4.1

Surface tension: σ_{wo} = 0.0711808 N/m using Equation A.4.7

The mass velocity for the water based on the frontal area of the fill is:

$$G_w = m_w/A_{fr} = 412/144 = 2.86111 \text{ kg/m}^2\text{s}$$

The transfer coefficients can be determined with the previous values. To find the transfer coefficient in the rain zone, use Equation 4.6.15. The *a* coefficients appearing in the equation for the rain zone transfer and pressure drop coefficients are as follows:

$$a_\mu = 3.061 \text{ x } 10^{-6}\left(\rho_{wo}^4 g^9 / \sigma_{wo}\right)^{0.25} = 3.061 \text{ x } 10^{-6}\left(995.6046 \text{ x } 9.8^9 / 0.0711808\right)^{0.25}$$

$$= 1.0026$$

Other quantities required to evaluate the rain zone transfer coefficient are:

- $a_\rho = 998/\rho_{wo} = 998/995.6046 = 1.0024$
- $a_v = 73.298\left(g^5\sigma^3_{wo}/\rho^3_{wo}\right)^{0.25} = 73.298(9.8^5 \text{ x } 0.0711808^3/995.6046)^{0.25} = 0.9882$
- $a_L = 6.122(g\sigma_{wo}/\rho_{wo})^{0.25} = 6.122(9.8 \text{ x } 0.0711808/995.6046)^{0.25} = 0.996$
- The humidity ratio of saturated air at T_{wo} : w_{s1} = 0.027848 kg/kg using Equation A.3.5
- Diffusion coefficient at inlet conditions: D_1 = 2.09061 x 10^{-5}m^2/s using Equation 4.1.2
- The Schmidt number is

$$Sc_1 = \mu_{av1}/(\rho_{av1}/D_1) = 1.85928 \text{ x } 10^{-5}/(1.1397 \text{ x } 2.09061 \text{ x } 10^{-5}) = 0.7803$$

- The air-vapor velocity before the fill

$$v_{av3} = m_{av1}/(\rho_{av1} A_{fr}) = 438.4/(1.1397 \text{ x} 144) = 2.67127 \text{ m/s}$$

With these values, use Equation 4.6.15 to find

$$\frac{h_{drz} a_{rz} H_3}{G_w} = 3.6\left(\frac{D_1}{v_{av3}\, d_d}\right)\left(\frac{H_3}{d_d}\right)\left(\frac{p_{a1}}{\rho_{wo} R_v T_{av1}}\right) Sc_1^{0.33}\left[\ell n\left(\frac{w_{sl}+0.622}{w_1+0.622}\right)/(w_s - w)\right]$$

$$\text{x } [4.68851 a_\rho \rho_{av1} - 187128.7 a_\mu \mu_{av1} - 2.29322$$

$$+ 22.4121 \{0.350396(a_v v_{av3})^{1.38046} + 0.09\}\{1.60934 (a_L H_3)^{-1.12083} + 0.66\}$$

$$\text{x } \{34.6765 (a_L d_d)^{0.732448} + 0.45\}$$

$$\text{x exp } \{7.7389 \exp(-0.399827 a_L H_3)\, \ell n \{0.087498 \exp(0.026619 a_L W_i) + 0.85\}\}]$$

$$= 3.6\left(\frac{2.09061 \text{ x } 10^{-5}}{2.67127 \text{ x } 0.0035}\right)\left(\frac{12}{0.0035}\right)\left(\frac{101325}{995.6046 \text{ x } 461.52 \text{ x } 306.65}\right)$$

$$\text{x } 0.7803^{0.33}\left[\ell n\left(\frac{0.027848 + 0.622}{0.016569 + 0.622}\right)/(0.027848 - 0.016569)\right]$$

$$\text{x } [\, 4.68851 \text{ x } 1.0024 \text{ x } 1.1397 - 187128.7 \text{ x } 1.0026 \text{ x } 1.85928 \text{ x } 10^{-5} - 2.29322$$

$$+ 22.4121\{0.350396(0.9882 \times 2.67127)^{1.38046} + 0.09\}$$

$$\times \{1.60934(0.996 \times 4)^{-1.12083} + 0.66\}\{34.6765(0.996 \times 0.0035)^{0.732448} + 0.45\}$$

$$\times \exp\{7.7389 \exp(-0.399827 \times 0.996 \times 4)\ell n\{0.087498 \exp(0.026619 \times 0.996 \times 12)$$

$$+ 0.85\}\}] = 0.2851664$$

The Merkel number applicable to the fill is specified, i.e.,

$$\frac{h_{dfi}\, a_{fi}\, L_{fi}}{G_w} = 0.2692 L_{fi} G_w^{-0.094} G_a^{0.6023}$$

$$= 0.2692 \times 1.878 \times 2.86111^{-0.094} \times 2.994823^{0.6023} = 0.8866959$$

The transfer coefficient in the spray zone is given by Lowe and Christie:

$$\frac{h_{dsp}\, a_{sp}\, L_{sp}}{G_w} = 0.2 L_{sp} \left(\frac{G_a}{G_w}\right)^{0.5} = 0.2 \times 0.5 \left(\frac{2.994823}{2.86111}\right)^{0.5} = 0.10231$$

The total transfer characteristic of the cooling tower is

$$Me = \frac{h_{drz}\, a_{rz}\, H_3}{G_w} + \frac{h_{dfi}\, a_{fi}\, L_{fi}}{G_w} + \frac{h_{dsp}\, a_{sp}\, L_{sp}}{G_w}$$

$$= 0.2851664 + 0.8866959 + 0.10231 = 1.274172$$

According to Equation 4.2.22, the Merkel number, M_e, is

$$Me = \int_{T_{wo}}^{T_{wi}} \frac{c_{pw}\, dT_w}{(i_{masw} - i_{ma})}$$

If the four point Chebyshev integral is applied to this relation, the integral can be expressed as

$$Me = \int_{T_{wo}}^{T_{wi}} \frac{c_{pw}\, dT_w}{(i_{masw} - i_{ma})} \approx \frac{c_{pwm}\,(T_{wi} - T_{wo})}{4}\left(\frac{1}{\Delta i_{(1)}} + \frac{1}{\Delta i_{(2)}} + \frac{1}{\Delta i_{(3)}} + \frac{1}{\Delta i_{(4)}}\right)$$

The enthalpy differentials are dependent on the following intermediate temperatures:

$$T_{w(1)} = T_{wo} + 0.1(314.65 - T_{wo}) = 303.4677 + 0.1(314.65 - 303.4677) = 304.5859 \text{ K}$$

$$T_{w(2)} = T_{wo} + 0.4(314.65 - T_{wo}) = 303.4677 + 0.4(341.65 - 303.4677) = 307.9406 \text{ K}$$

$$T_{w(3)} = T_{wo} + 0.6(314.65 - T_{wo}) = 303.4677 + 0.6(314.65 - 303.4677) = 310.1711 \text{ K}$$

$$T_{w(4)} = T_{wo} + 0.9(314.65 - T_{wo}) = 303.4677 + 0.9(314.65 - 303.4677) = 313.5318 \text{ K}$$

The bracketed subscript numbers refer to the intervals in the Chebyshev integral and should not be confused with the numbers indicating various positions in the cooling tower.

To find the corresponding increments in enthalpy, determine the enthalpy of saturated air at $T_{w(1)}$ = 304.5859 K. The relevant specific heats of air and water vapor are evaluated at

$$(T_{w(1)} + 273.15)/2 = (304.5859 + 273.15)/2 = 288.868 \text{ K}$$

- Specific heat of air: $c_{pa(1)}$ = 1006.612 J/kg K using Equation A.1.2
- Specific heat of water vapor: $c_{pv(1)}$ = 1875.95 J/kg K using Equation A.2.2

The pressure of saturated water at $T_{w(1)}$ follows from Equation A.2.1, and the humidity ratio evaluated at p_{a15} follows from Equation A.3.5.

- $p_{a15} = (p_{a1} + p_{a5})/2 = (101325 + 101170.6)/2 = 101247.8$ N/m^2
- Pressure of the water vapor: $p_{vs(1)} = 4605.056$ N/m2 using Equation A.2.1
- Humidity ratio: $w_{s(1)} = 0.02979283$ kg/kg using Equation A.3.5

With these values, determine the enthalpy of saturated air at $T_{w(1)}$ according to Equation A.3.6b

$$i_{masw(1)} = c_{pa(1)}(T_{w(1)} - 273.15) + w_{s(1)}\left[i_{fgwo} + c_{pv(1)}(T_{w(1)} - 273.15)\right]$$

$$= 1006.612(304.5859 - 273.15) + 0.02979283\left[2.5016 \times 10^{6}\right.$$

$$\left. + 1875.95(304.5859 - 273.15)\right] = 107930.4 \text{ J/kg}$$

The enthalpy of the air at $T_{w(1)}$ can be determined by applying Equation 4.2.21, i.e.,

$$i_{ma(1)} = m_w c_{pwm}(T_{w(1)} - T_{wo}) / m_a + i_{ma1}$$

$$= 412 \times 4176.992\,(304.5859 - 303.4677) / 431.2545 + 76213.73 = 80676.0 \text{ J/kg}$$

With these values, find the difference in enthalpy

$$\Delta i_{(1)} = i_{masw(1)} - i_{ma(1)} = 107930.4 - 80676.0 = 27254.42 \text{ J/kg dry air}$$

Repeat the procedure for the other three intermediate temperatures, and find

$$\Delta i_{(2)} = 31490.49 \text{ J/kg dry air}$$

$$\Delta i_{(3)} = 40692.23 \text{ J/kg dry air}$$

$$\Delta i_{(4)} = 53759.63 \text{ J/kg dry air}$$

Substitute these values into the approximate expression for the integral, and find

$$Me = \int_{T_{wo}}^{T_{wi}} \frac{c_{pw}\, dT_w}{(i_{masw} - i_{ma})} \approx \frac{c_{pwm}(T_{wi} - T_{wo})}{4}\left(\frac{1}{\Delta i_{(1)}} + \frac{1}{\Delta i_{(2)}} + \frac{1}{\Delta i_{(3)}} + \frac{1}{\Delta i_{(4)}}\right)$$

$$= \frac{4176.992(314.65 - 303.4677)}{4}\left(\frac{1}{27254.42} + \frac{1}{34190.49} + \frac{1}{40692.23} + \frac{1}{53759.63}\right)$$

$$= 1.274150$$

This value is almost identical to the value obtained by adding the transfer coefficients in the three wet zones, which means the water outlet temperature, T_{wo} = 303.4677 K is correct.

According to Equation 7.2.1, the heat rejected by the cooling tower is given by

$$Q = m_w\, c_{pwm}\, (T_{wi} - T_{wo}) = 412 \text{ x } 4176.992\,(314.65 - 303.4677) = 19.243874 \text{ MW}$$

The correctness of the temperature of the saturated air leaving the spray zone, T_{a5}, can be confirmed from the relation

$$Q = m_a (i_{mas5} - i_{ma1})$$

The enthalpies i_{mas5} and i_{ma1} are already known, thus

$$Q = 431.2545\ (120836.9 - 76213.73) = 19.243942 \text{ MW}$$

The values of Q are in agreement, which means the value for T_{a5} is correct.

The specified loss coefficient due to the louvers is referred to the mean conditions through the fill, i.e.,

$$K_{ilfi} = K_{il}\left(\frac{\rho_{av15}}{\rho_{av1}}\right)\left(\frac{W_i B_i}{2 H_3 W_i}\right)\left(\frac{m_{av1}}{m_{av15}}\right)^2 = 2.5\left(\frac{1.132982}{1.1397}\right)\left(\frac{12 \text{ x } 12}{2 \text{ x } 4 \text{ x } 12}\right)\left(\frac{438.4}{442.1426}\right)^2$$

$$= 5.497609$$

With Equation 4.6.13, find the loss coefficient for the rain zone with

$$v_{w3} = \frac{G_w}{\rho_{wo}} = \frac{2.86111}{995.6046} = 2.873743 \text{ x } 10^{-3} \text{ m/s}$$

$$K_{rz} = 1.5 a_v v_{w3} (H_3 / d_d) [0.219164 - 0.30487 a_\rho \rho_{av1} + 8278.7 a_\mu \mu_{av1}$$

$$+ 0.954153 \{0.328467 \exp (135.7638 a_L d_d) + 0.47\}$$

$$\text{x} \{26.28482 (a_L H_3)^{-2.95729} + 0.56\} \exp \{\ell n (0.204814 \exp (0.066518 a_L W_i) + 0.21)$$

$$\text{x} (3.9186 \exp (-0.3 a_L H_3)) (0.31095 \ell n (a_L d_d) + 2.63745)\}$$

$$\text{x} \{2.177546 (a_v v_{av3})^{-1.46541} + 0.21\}]$$

$$= 1.5 \text{ x } 0.9882 \text{ x } 2.873743 \text{ x } 10^{-3} (4 / 0.0035)$$

$$\text{x} [0.219164 - 0.30487 \text{ x } 1.0024 \text{ x } 1.1397 + 8278.7 \text{ x } 1.0026 \text{ x } 1.85928 \text{ x } 10^{-5}$$

$$+ 0.954153 \{0.328467 \exp (135.7638 \text{ x } 0.996 \text{ x } 0.0035) + 0.47\}$$

$$\text{x} \{26.28482 (0.996 \text{ x } 4)^{-2.95729} + 0.56\} \exp \{\ell n (0.204814 \exp (0.066518 \text{ x } 0.996 \text{ x } 12)$$

$$+ 0.21) \text{ x } (3.9186 \exp (-0.3 \text{ x } 0.996 \text{ x } 4)) (0.31095 \ell n (0.996 \text{ x } 0.0035)$$

$$+ 2.63745)\} \text{ x } \{2.177546 (0.9882 \text{ x } 2.67127)^{-1.46541} + 0.21\}]$$

$$= 2.072855$$

The rain zone loss coefficient referred to fill conditions is

$$K_{rzfi} = K_{rz}\left(\frac{\rho_{av15}}{\rho_{av1}}\right)\left(\frac{m_{av1}}{m_{av15}}\right)^2 = 2.072855\left(\frac{1.132982}{1.1397}\right)\left(\frac{438.4}{442.1426}\right)^2 = 2.025911$$

The specified loss coefficient of the support structure of the fill is referred to the mean conditions through the fill, i.e.,

$$K_{fsfi} = K_{fs}\left(\frac{\rho_{av15}}{\rho_{av1}}\right)\left(\frac{m_{av1}}{m_{av15}}\right)^2 = 0.5\left(\frac{1.132982}{1.1397}\right)\left(\frac{438.4}{442.1426}\right)^2 = 0.4886764$$

According to the specified fill loss coefficient,

$$K_{fdm} = 1.9277\, L_{fi}\, G_w^{1.2752}\, G_a^{-1.0356}$$

$$= 1.9277 \text{ x } 1.878 \text{ x } (2.86111)^{1.2752}(2.994823)^{-1.0356} = 4.411997$$

From the note at the end of Example 4.3.1, the actual fill loss coefficient applicable to the cooling tower is given by

$$K_{fi} = K_{fdm} + \left(\frac{G_{av5}^2}{\rho_{av5}} - \frac{G_{av1}^2}{\rho_{av1}}\right) / \left(\frac{G_{av15}^2}{\rho_{av15}}\right)$$

$$= 4.441997 + \left(\frac{3.096413^2}{1.12634} - \frac{3.044444^2}{1.1397}\right) / \left(\frac{3.070429^2}{1.132982}\right) = 4.487634$$

The loss through the spray zone above the fill referred to the mean conditions through the fill is given by Equation 7.2.20.

$$K_{spfi} = L_{sp}\left[0.4\left(\frac{G_w}{G_a}\right)+1\right]\left(\frac{\rho_{av15}}{\rho_{av5}}\right)\left(\frac{m_{av5}}{m_{av15}}\right)^2$$

$$= 0.5\left[0.4\left(\frac{2.86111}{2.994823}\right)+1\right]\left(\frac{1.132982}{1.12634}\right)\left(\frac{445.8834}{442.1426}\right)^2 = 0.706958$$

The specified loss coefficient due to the water distribution system is referred to the mean conditions through the fill, i.e.,

$$K_{wdfi} = K_{wd}\left(\frac{\rho_{av15}}{\rho_{av5}}\right)\left(\frac{m_{av5}}{m_{av15}}\right)^2 = 0.5\left(\frac{1.132982}{1.12634}\right)\left(\frac{445.8834}{442.1426}\right)^2 = 0.5114949$$

From Equation 4.7.2, the loss coefficient for the specified type c drift eliminator based on fill conditions is

$$K_{defi} = 27.4829\,Ry^{-0.14247}\left(\frac{\rho_{av15}}{\rho_{av5}}\right)\left(\frac{m_{av5}}{m_{av15}}\right)^2$$

$$= 27.4892\left(\frac{445.8834}{1.84273 \times 10^{-5} \times 144}\right)^{-0.14247}\left(\frac{1.132982}{1.12634}\right)\left(\frac{445.8834}{442.1426}\right)^2 = 5.0649$$

The inlet loss coefficient in isotropically-packed, induced-draft, rectangular towers is, according to Equation 8.3.7,

$$K_{ct(norz)} = 0.2339 + \left(3.919 \times 10^{-3} K_{fie}^2 - 6.84 \times 10^{-2} K_{fie} + 2.5267\right)$$

$$\times \exp\left[W_i\{0.5143 - 0.1803\exp(0.0163 K_{fi})\}/H_3\right]$$

$$- \sinh^{-1}\left[2.77\exp\left(0.958\frac{W_i}{H_3}\right)\exp\left\{K_{fie}\left(2.457 - 1.015\frac{W_i}{H_3}\right)\times 10^{-2}\right\}\left(\frac{r_i}{W_i} - 0.013028\right)\right]$$

$$= 0.2339 + \left(3.919 \times 10^{-3} \times 11.25966^2 - 6.840 \times 10^{-2} \times 11.25966 + 2.5267\right)$$

$$\times \exp\left[12 \times 0.5143 - 0.1803\exp\left(0.0163 \times 11.25966\right)/4\right]$$

$$- \sinh^{-1}\left[2.77\exp\left(0.958\frac{12}{4}\right)\exp\left[11.25966\left(2.457 - 1.015\frac{12}{4}\right)\times 10^{-2}\right]\right.$$

$$\left.\times\left(0.3/12 - 0.103028\right)\right] = 5.212728$$

where

K_{fie} = the effective loss coefficient in the vicinity of the fill, i.e.,

$$K_{fie} = K_{fsfi} + K_{fi} + K_{spfi} + K_{wdfi} + K_{defi}$$

$$= 0.4886764 + 4.487634 + 0.706958 + 0.5114949 + 5.0649 = 11.25966$$

De Villiers and Kröger state it becomes acceptable to ignore the inlet loss correction factor in cases where $W_i/H_3 \leq 3$. In this case, $W_i/H_3 = 3$, which means that

$$K_{ct} = K_{ct(norz)}$$

Referred to the mean conditions through the fill, the inlet loss coefficient becomes

$$K_{ctfi} = K_{ct}\left(\frac{\rho_{av15}}{\rho_{av1}}\right)\left(\frac{m_{av5}}{m_{av15}}\right)^2 = 5.212728\left(\frac{1.132982}{1.1397}\right)\left(\frac{438.4}{442.1426}\right)^2 = 5.094674$$

The specified fan upstream loss coefficient is referred to the mean conditions through the fill, i.e.,

$$K_{upfi} = K_{up}\left(\frac{\rho_{av15}}{\rho_{av5}}\right)\left(\frac{m_{av5}}{m_{av15}}\right)^2\left(\frac{A_{fr}}{A_c}\right)^2 = 0.5\left(\frac{1.132982}{1.12634}\right)\left(\frac{445.8834}{442.1426}\right)^2\left(\frac{144 \text{ x } 4}{\pi \text{ x } 8^2}\right)^2$$

$$= 4.36576$$

The actual air volume flow rate through the fan is

$$V_F = m_{av5} / \rho_{av5} = 445.8834 / 1.12634 = 395.8676\, m^3/s$$

Since the actual air density and the rotational speed of the fan are not the same as the reference conditions for which fan performance characteristics were specified, the relevant fan laws given in section 6.2 are employed.

According to Equation 6.2.5,

$$V_{F/dif} = V_F\left(\frac{N_{Fr}}{N_F}\right)\left(\frac{d_{Fr}}{d_F}\right)^3 = 395.8676\left(\frac{750}{120}\right)\left(\frac{1.536}{8}\right)^3 = 17.51192\, m^3/s$$

At this flow rate, the fan static reference pressure difference is given by the specified relation

$$\Delta p_{F/dif} = 320.85 - 6.9604\, V_{F/dif} + 0.31373\, V_{F/dif}^2 - 0.021393\, V_{F/dif}^3$$

$$= 320.85 - 6.9604\ (17.51192) + 0.31373(17.51192)^2 - 0.021393(17.51192)^3$$

$$= 180.2833\ \text{N/m}^2$$

The actual fan static pressure difference expressed by Equation 6.2.6 is

$$\Delta p_{Fs} = \Delta p_{F/difs} \left(\frac{N_F}{N_{Fr}}\right)^2 \left(\frac{d_F}{d_{Fr}}\right)^2 \left(\frac{\rho_{av6}}{\rho_r}\right) = 180.2833 \left(\frac{120}{750}\right)^2 \left(\frac{8}{1.536}\right)^2 \left(\frac{1.12634}{1.2}\right)$$

$$= 117.5123\ \text{N/m}^2$$

At the reference condition, the test fan shaft power is

$$P_{F/dif} = 4245.1 - 64.134\, V_{F/dif} + 17.586\, V_{F/dif}^2 - 0.71079\, V_{F/dif}^3$$

$$= 4245.1 - 64.134 \text{ x } 17.1192 + 17.586 \text{ x } 17.51922^2 - 0.71079 \text{ x } 17.51922^3$$

$$= 4697.863\ \text{W}$$

The actual fan shaft power follows from Equation 6.2.7:

$$P_F = P_{F/dif} \left(\frac{N_F}{N_{Fr}}\right)^3 \left(\frac{d_F}{d_{Fr}}\right)^5 \left(\frac{\rho_{av6}}{\rho_r}\right) = 4697.863 \left(\frac{120}{750}\right)^3 \left(\frac{8}{1.536}\right)^5 \left(\frac{1.12634}{1.2}\right)$$

$$= 69222.04\ \text{W}$$

The static-pressure rise coefficient of the fan follows from Equation 8.1.7, i.e.,

$$K_{F/difs} = \frac{2\Delta p_{Fs}\, \rho_{av6}}{\left[4\, m_{av5} / (\pi\, d_c^2)\right]^2} = \frac{2 \text{ x } 117.5123 \text{ x } 1.12634}{\left[4 \text{ x } 445.8834 / (\pi \text{ x } 8^2)\right]^2} = 3.364199$$

At this stage, it is possible to confirm the value of p_{a5} according to

$$p_{a5} = p_{a1}\left[1-\frac{0.00975(H_3+L_{fi}/2)}{T_{a1}}\right]^{3.5(1+w_1)\left(1-\frac{w_1}{w_1+0.622}\right)}$$

$$(K_{ilfi}+K_{rzfi}+K_{fsfi}+K_{fi}+K_{spfi}+K_{wdfi}+K_{defi}+K_{ctfi})\,(m_{av15}/A_{fr})^2/(2\,\rho_{av15})$$

$$= 101325\left[1-\frac{0.009754\,(4+1.878/2)}{306.65}\right]^{3.5(1+0.016569)\left(1-\frac{0.016569}{0.016569+0.622}\right)}$$

$$-\,(5.497609 + 2.025911 + 0.4886764 + 4.487634 + 0.7069580 + 0.5114949 + 5.0649$$

$$+ 5.212728)\,(442.1426)^2/(2 \times 1.132982) = 101170.6\ \text{N/m}^2$$

This is in agreement with the value used in previous calculations in this example.

It is assumed the condition of the air at the inlet of the fan is equal to conditions at the outlet of the fill, i.e.,

$$T_{a6} = T_{a5},\ p_{a6} = p_{a5}$$

and

$$\rho_{av6} = \rho_{av5} = 1.12634\ \text{kg/m}^3$$

Ignoring pressure differences due to the gravity field, the draft equation can be expressed as

$$(K_{ilfi}+K_{rzfi}+K_{fsfi}+K_{fi}+K_{spfi}+K_{wdfi}+K_{defi}+K_{ctfi}+K_{upfi})(m_{av15}/A_{fr})^2/(2\,\rho_{av15})$$

$$-K_{fs}\,(m_{av5}/A_c)^2/(2\rho_{av6})=0$$

The terms on the left side of the equation give

$$(K_{ilfi}+K_{rzfi}+K_{fsfi}+K_{fi}+K_{spfi}+K_{wdfi}+K_{defi}+K_{ctfi}+K_{upfi})(m_{av15}/A_{fr})^2/(2\,\rho_{av15})$$

$$-K_{fs}\,(m_{av5}/A_c)^2/(2\rho_{av6}) = (5.798609+2.025911+0.4886764+4.487634+0.7069580$$

$$+0.5114949+5.0649+5.212728+4.36576)(442.1426/144)^2/(2 \times 1.132982)$$

$$-3.634199\left[(445.8834 \times 4)/(\pi \times 8^2)\right]^2/(2 \times 1.12634) = -0.00482$$

This value is close to zero, and the draft equation is satisfied.

The amount of water lost due to evaporation is given by

$$m_{w(evap)} = (m_{av5} - m_{av1}) = (445.8834 - 438.4) = 7.4834 \text{ kg/s}$$

or

$$m_{w(evap)} = m_a(w_5 - w_1) = 431.2545(0.033922 - 0.016569) = 7.48343 \text{ kg/s}$$

8.4 Recirculation

Heated plume air may recirculate in an air-cooled heat exchanger and reduce the cooling effectiveness of the system. Figure 8.4.1 depicts a cross section of an air-cooled heat exchanger. In the absence of wind, the buoyant jet or plume rises vertically above the heat exchanger. However, a part of the warm plume air may be drawn back into the inlet of the tower. This phenomenon is known as *recirculation*.

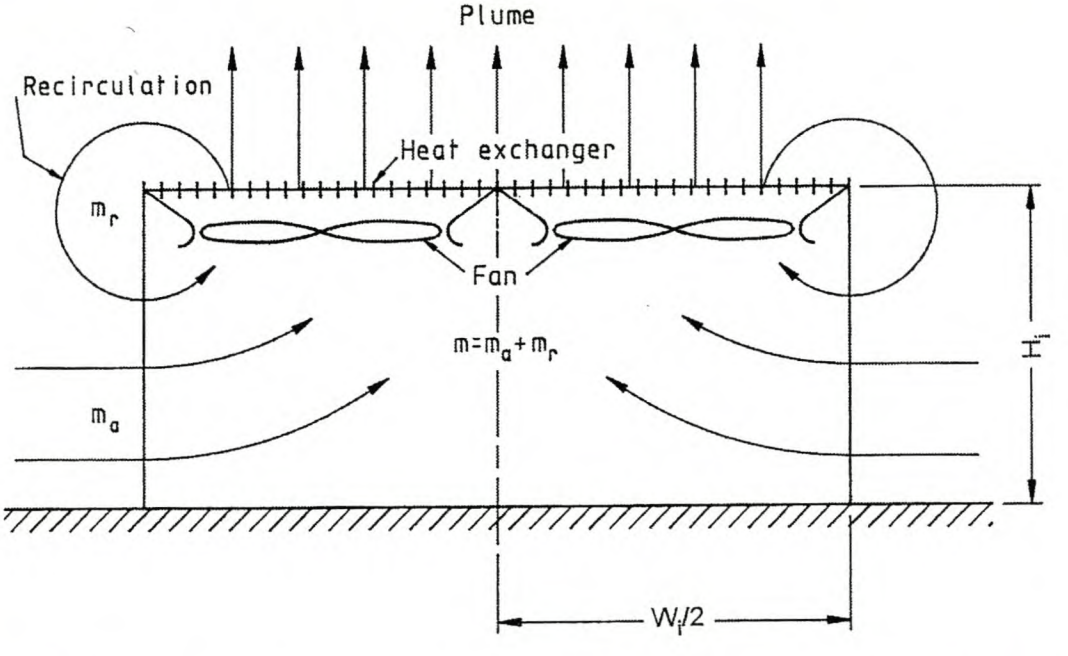

Fig. 8.4.1 Air-Flow Pattern about Forced-Draft Air-Cooled Heat Exchanger

Plume recirculation is usually a variable phenomenon influenced by many factors including:

- heat exchanger configuration
- heat exchanger orientation
- surrounding structures
- prevailing weather conditions

Because of higher discharge velocities, recirculation is usually less in induced-draft than in forced-draft designs.

Lichtenstein defines a recirculation factor as

$$r = m_r/(m_a + m_r) = m_r/m \tag{8.4.1}$$

where

m_r = the recirculating air mass flow rate

m_a = the ambient air flow rate into the heat exchanger

The results of numerous studies on recirculation appear in the literature; however, most are experimental investigations performed on heat exchangers having specific geometries and operating under prescribed conditions, e.g., Kennedy and Fordyce or Slawson and Sullivan. Gunter and Shipes define certain recirculation flow limits and present the results of field tests performed on air-cooled heat exchangers. Problems associated with solving recirculating flow patterns numerically have been reported in EPRI Report CS-1665. Kröger et al. investigated the problem analytically, experimentally, and numerically. They recommended a specific equation with which the performance effectiveness of two-dimensional, mechanical-draft heat exchangers experiencing recirculation can be predicted. This is reported in papers by Kröger; Du Toit and Kröger, and Duvenhage and Kröger.

Recirculation analysis

Consider half a two-dimensional, mechanical-draft, air-cooled heat exchanger in which recirculation occurs. For purposes of analysis, the heat exchanger is represented by a straight line at an elevation H_i above ground level (Fig. 8.4.2a).

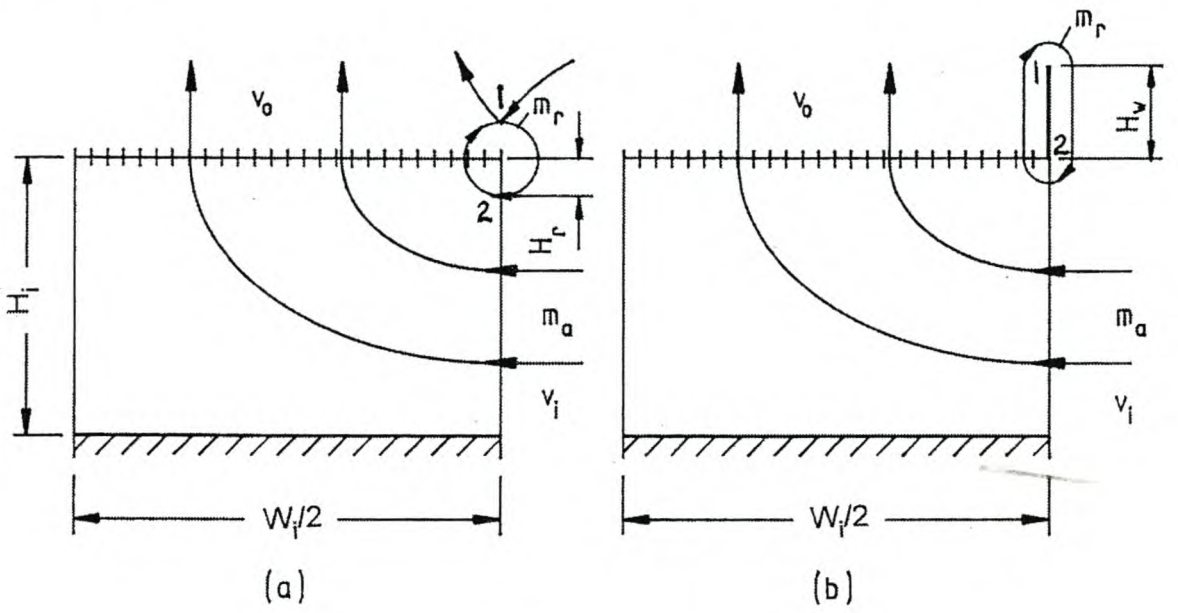

Fig. 8.4.2 Flow Pattern about Heat Exchanger (a) (b)

The velocity of the air entering the heat exchanger along its periphery is assumed to be in the horizontal direction with a mean value, v_i. The actual inlet velocity is highest at the edge of the fan platform and decreases towards ground level. The outlet velocity, v_o, is assumed to be uniform and vertical.

Consider the streamline at the outlet of the heat exchanger that diverges from the plume at (1) and forms the outer boundary of the recirculating air stream. This streamline will enter the platform at (2), some distance, H_r, below the heat exchanger. For purposes of analysis, it is assumed the elevation of (1) is approximately H_r above the heat exchanger. If viscous effects, mixing, and heat transfer to the ambient air are neglected, Bernoulli's equation can be applied between (1) and (2) to give

$$p_1 + \rho_o v_1^2/2 + \rho_o g(H_i + H_r) = p_2 + \rho_o v_2^2/2 + \rho_o g(H_i - H_r) \qquad (8.4.2)$$

It is reasonable to assume the total pressure at (1) is approximately equal to the stagnation pressure of the ambient air at that elevation, i.e.,

$$p_1 + \rho_o v_1^2/2 = p_{a1} \tag{8.4.3}$$

At (2), the static pressure can be expressed as

$$p_2 = p_{a2} - \rho_a v_2^2/2 \tag{8.4.4}$$

For the ambient air far from the heat exchanger,

$$p_{a1} + 2\rho_a g H_r = p_{a2} \tag{8.4.5}$$

Substitute Equations 8.4.3, 8.4.4, and 8.4.5 in Equation 8.4.2, and find

$$H_r = v_2^2/4g \tag{8.4.6}$$

In practice, the velocity at the inlet at elevation H_i is equal to zero because of viscous effects. However, the velocity gradient in this immediate region is very steep, and the velocity peaks at a value higher than the mean inlet velocity. Examples of numerically determined inlet velocity distributions for different outlet velocities and heat exchanger geometries are shown in Figure 8.4.3 according to Duvenhage and Kröger. Since most of the recirculation occurs in this region, the velocity v_2 is of importance but difficult to quantify analytically. For $W_i/(2H_i) \leq 1$, it is assumed v_2 can be replaced by the mean inlet velocity, v_i, in Equation 8.4.6. Thus,

$$H_r \approx v_i^2/4g \tag{8.4.7}$$

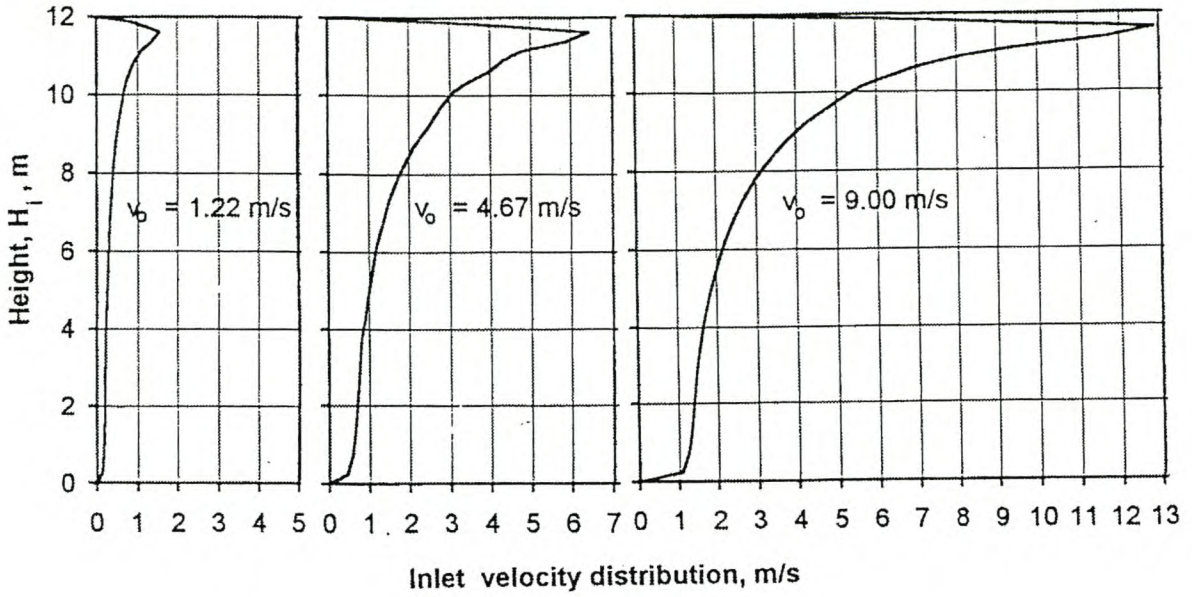

Fig. 8.4.3 Two-Dimensional Inlet Velocity Distribution for $W_i/2$ = 5.1 m

According to the equation of mass conservation, the flow per unit depth of the tower can be expressed as

$$\rho_o H_r v_i + \rho_a (H_i - H_r) v_i = \rho_o v_o W_i / 2$$

or

$$v_i \approx \rho_o v_o W_i / (2 \rho_a H_i) \tag{8.4.8}$$

if the amount of recirculation is small.

According to Equations 8.4.1 and 8.4.8, the recirculation factor is

$$r = \frac{m_r}{m} = \frac{2 \rho_o v_i H_r}{\rho_o v_o W_i} = \frac{\rho_o H_r}{\rho_a H_i} \tag{8.4.9}$$

Substitute Equations 8.4.7 and 8.4.8 in Equation 8.4.9, and find

$$r = \frac{1}{16} \left(\frac{\rho_o W_i}{\rho_a H_i} \right)^3 \frac{v_o^2}{g W_i} = \frac{1}{32} \left(\frac{\rho_o W_i}{\rho_a H_i} \right)^3 Fr \tag{8.4.10}$$

where

$Fr = 2v_o^2/(g\ W_i)12$ = the Froude number based on the width of the heat exchanger

In Figure 8.4.2(b), the approximate influence of a windwall or deep plenum can be determined by considering flow conditions between the top of the windwall, $H_i + H_w$, and elevation, H_i. Consider the extreme case when H_w is so large, $H_w = H_{wo}$, that no recirculation takes place and the ambient air velocity near the top of the windwall is zero. In this particular case, the static pressure at the tower exit is essentially equal to the ambient stagnation pressure. With these assumptions, apply Bernoulli's equation between the tower outlet at the top of the windwall and the elevation, H_i.

$$p_{a1} + \rho_o v_o^2/2 + \rho_o g H_{wo} = p_{a2} \tag{8.4.11}$$

However,

$$p_{a2} - p_{a1} = \rho_a g H_{wo} \tag{8.4.12}$$

Substitute Equation 8.4.12 into Equation 8.4.11, and find

$$H_{wo} = \rho_o v_o^2/[2(\rho_a - \rho_o)g] \tag{8.4.13}$$

Assume the recirculation decreases linearly with increasing windwall height. Equation 8.4.10 may be extended as follows:

$$r = \frac{1}{32}\left(\frac{\rho_o W_i}{\rho_a H_i}\right)^3 Fr\left(1 - a\frac{H_w}{H_{wo}}\right) \tag{8.4.14}$$

Since the recirculation is assumed to be essentially zero at $H_w = H_{wo}$, find a = 1. Substitute Equation 8.4.13 in Equation 8.4.14, and find

$$r = \frac{1}{16}\left(\frac{\rho_o W_i}{\rho_a H_i}\right)^3 \frac{v_o^2}{g W_i}\left[1 - 2\frac{(\rho_a - \rho_o) g H_w}{\rho_o v_o^2}\right]$$

$$= \frac{1}{32}\left(\frac{\rho_o W_i}{\rho_a H_i}\right)^3 Fr\left[1 - \frac{2}{Fr_{Dw}}\right] \qquad (8.4.15)$$

where

$Fr_{Dw} = \rho_o v_o^2 / [(\rho_a - \rho_o) g H_w]$ = the densimetric Froude number based on the windwall height

It is important to determine the effectiveness of the system when recirculation occurs. In this case, effectiveness is defined as

$$e_r = \frac{\text{heat transfer with recirculation}}{\text{heat transfer with no recirculation}} = \frac{Q_r}{Q} \qquad (8.4.16)$$

The interrelation between the recirculation and the effectiveness is complex in a real heat exchanger. However, two extremes can be evaluated analytically:

- no mixing
- perfect mixing

No mixing. The warm recirculating air does not mix at all with the cold ambient inflow and results in a temperature distribution shown in Figure 8.4.4(a). The recirculating stream assumes the temperature of the heat exchanger fluid, T_{he}.

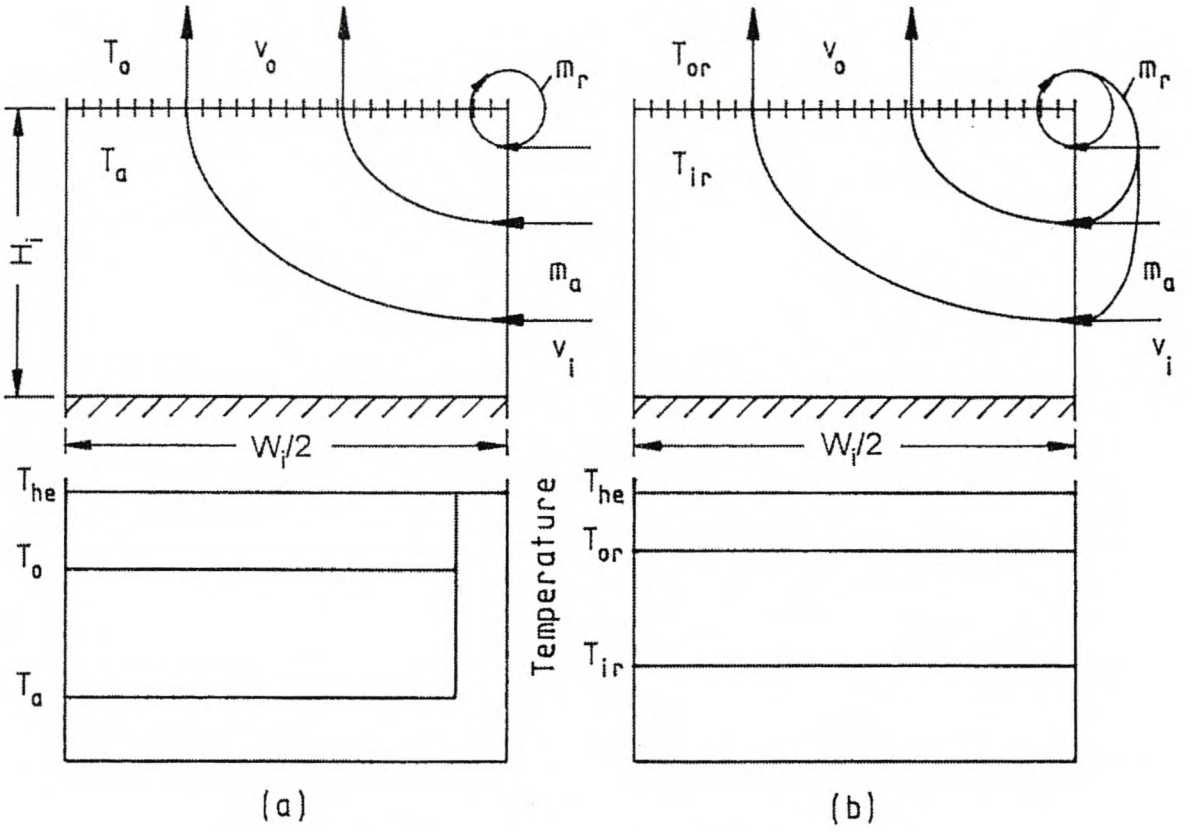

Fig. 8.4.4 Recirculation Flow Patterns (a) (b)

In effect, this means the part of the heat exchanger where recirculation occurs transfers no heat. The actual heat transfer rate is given by

$$Q_r = m_a c_p (T_o - T_a) \tag{8.4.17}$$

resulting in an effectiveness due to recirculation of

$$e_r = \frac{m_a c_p (T_o - T_a)}{(m_a + m_r) c_p (T_o - T_a)} = \frac{(m - m_r)}{m} = 1 - r \tag{8.4.18}$$

Substitute Equation 8.4.15 into Equation 8.4.18 and find

$$e_r = 1 - \frac{1}{16} \left(\frac{\rho_o W_i}{\rho_a H_i} \right)^3 \frac{v_o^2}{g W_i} \left[1 - 2 \frac{(\rho_a - \rho_o) g H_w}{\rho_o v_o^2} \right] \tag{8.4.19}$$

Perfect mixing. The recirculating air mixes perfectly with the inflowing ambient air and results in a uniform increase in both the effective inlet air temperature and the outlet air temperature (Fig. 8.4.4b).

For purposes of illustration, assume the temperature of the heat exchanger, T_{he}, is constant. It follows from Equation 3.5.22 that the effectiveness under cross-flow conditions is

$$e = \frac{mc_p(T_{or} - T_{ir})}{mc_p(T_{he} - T_{ir})} = \frac{(T_{or} - T_{ir})}{(T_{he} - T_{ir})} = 1 - \exp(-UA/mc_p) \tag{8.4.20}$$

or

$$T_{or} = T_{he} - (T_{he} - T_{ir})\exp(-UA/mc_p) \tag{8.4.21}$$

The enthalpy entering the heat exchanger is

$$mc_p T_{ir} = m_a c_p T_a + m_r c_p T_{or}$$

or

$$T_{ir} = \frac{(m - m_r)T_a}{m} + \frac{m_r T_{or}}{m} = (1 - r)T_a + r T_{or} \tag{8.4.22}$$

Substitute Equation 8.4.22 into Equation 8.4.21, and find

$$T_{or} = T_{he} - [T_{he} - (1 - r)T_a - r T_{or}]\exp(-UA/mc_p)$$

$$= \frac{T_{he} - [T_{he} - (1 - r)T_a]\exp(-UA/mc_p)}{1 - r\exp(-UA/mc_p)} \tag{8.4.23}$$

In this case, the effectiveness due to recirculation is given by

$$e_r = \frac{mc_p(T_{or} - T_{ir})}{mc_p(T_o - T_a)} = \frac{T_{or} - T_{ir}}{T_o - T_a}$$

From Equations 8.4.22 and 8.4.23, substitute the values of T_{ir} and T_{or} in this equation to find the effectiveness of the heat exchanger.

$$e_r = \frac{(1-r)}{(T_{or}-T_{ar})}\left[\frac{T_{he}-\{T_{he}-(1-r)T_a\}\exp(-UA/mc_p)}{1-r\exp(-UA/mc_p)}-T_a\right] \quad (8.4.24)$$

In practice, the effectiveness will be some value between that given by Equation 8.4.18 and Equation 8.4.24. Actual measurements conducted on air-cooled heat exchangers appear to suggest relatively little mixing occurs. This tendency is confirmed by numerical analysis of the problem according to Kröger as well as Duvenhage and Kröger.

Duvenhage and Kröger solved the recirculation problem numerically and correlated their results over a wide range of operating conditions and heat exchanger geometries by means of the following empirical equation:

$$e_r = 1-\left[0.006027\,(2H_i/W_i)^{-1.1352}\,(2H_w/W_i)^{-0.44641}\,Fr_D^{0.755515}\right] \quad (8.4.25)$$

This equation is valid in the ranges

- $0.49 \le 2H_i/W_i \le 2.75$
- $0.049 \le 2H_w/W_i \le 0.79$
- $0.175 \le F_{rD} \le 14.3$

where

$$Fr_D = 2\,\rho_a\,v_o^2/[(\rho_a-\rho_o)\,gW_i]$$

In this equation, H_w represents the effective height above the inlet to the fan platform and includes the plenum height in addition to any windwall height.

Equation 8.4.25 is shown graphically in Figure 8.4.5. For values of $2Hi/Wi \ge Fr_D^{0.265}$, Equation 8.4.19 is in good agreement with Equation 8.4.25.

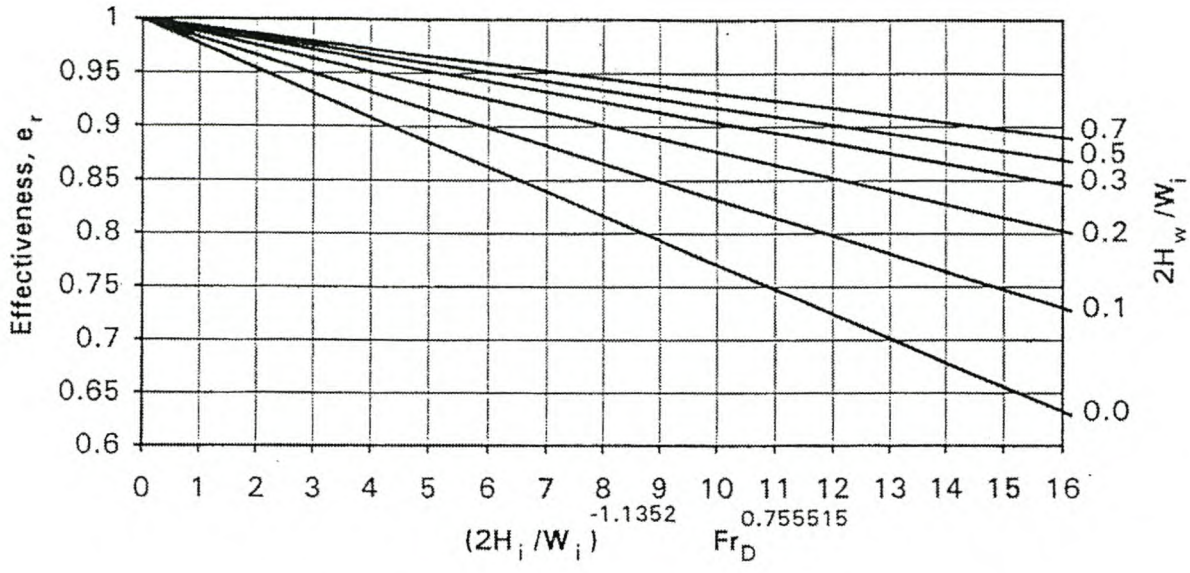

Fig. 8.4.5 Heat Exchanger Effectiveness

Example 8.4.1

Consider the air-cooled heat exchanger described in Example 8.3.1, and determine the reduced heat rejection rate if plume air recirculation is taken into consideration.

Solution

Find the effectiveness of the heat exchanger due to recirculation according to Equation 8.4.25.

The approximate velocity of the hot plume air leaving the heat exchanger may be expressed as

$$v_{a6} = m_a(V/V_{id})/(\rho_{a6} A_{frt}) = 306.934 \text{ x } 0.985/(1.0334 \text{ x } 71.92) = 4.0678 \text{ m/s}$$

According to Equation A.1.1, the density of the ambient air is

$$\rho_{a1} = 101325/(287.08 \text{ x } 301.15) = 1.172 \text{ kg/m}^3$$

With these values, find an approximate densimetric Froude number with $W_i \approx L_t$.

$$Fr_D = \frac{2\rho_{a1} v_{a6}^2}{(\rho_{a1} - \rho_{a6}) g L_t} = \frac{2 \text{ x } 1.172 \text{ x } 4.0678^2}{(1.172 - 1.0334) 9.8 \text{ x } 10.203} = 2.7987$$

Substitute this value in Equation 8.4.25, and find

$$e_r = 1 - \left[0.006027 \, (2 \text{ x } 12.7 / 10.203)^{-1.1352} \, (2 \text{ x } 1.7 / 10.203)^{-0.44641} \, 2.7987^{0.755515}\right]$$

$$= 0.9924$$

The heat rejected by the bank is

$$Q_{6ir} = e_r Q_{6i} = 0.9924 \text{ x } 73.739 = 73.179 \text{ MW}$$

Example 8.4.2

Consider the air-cooled condenser described in Example 8.3.2, and determine the approximate heat rejected if the influence of hot plume air recirculation is taken into consideration.

Solution

Considering hot plume air recirculation, the effectiveness of the air-cooled condenser can be determined according to Equation 8.4.25. In this equation, the relevant width of the particular configuration having three fan rows, $n_{Fr} = 3$, is given by:

$$W_i = n_{Fr} \left(\frac{A_{fr}}{L_t}\right) \left(\frac{n_b}{2}\right) = \frac{3 \text{ x } 27.55 \text{ x } 8}{9.5 \text{ x } 2} = 34.8 \text{ m}$$

- the length of the condenser (6 fan units)

$$L_i = 6 \text{ x } 2 \, (L_t \sin\theta + L_w) = 6 \text{ x } 2 \, (9.5 \text{ x } \sin 30^\circ + 0.2) = 59.4 \text{ m}$$

- the approximate mean outlet velocity of the hot plume air leaving the heat exchanger (18 fan units)

$$v_o \approx 18\, m_a (V/V_{id}) / (W_i L_i \rho_{a6}) = 18 \times 604.483 \times 0.98398 / (34.8 \times 59.4 \times 0.918)$$

$$= 5.642 \text{ m/s}$$

With these values, find the densimetric Froude number.

$$Fr_D = 2\, \rho_{a3} v_o^2 / [(\rho_{a3} - \rho_{a6}) g W_i] = 2 \times 1.0214 \times 5.642^2 / [(1.0214 - 0.918) 9.8 \times 34.8]$$

$$= 1.844$$

Substitute these values in Equation 8.4.25 to find the effectiveness of the heat exchanger.

$$e_r = 1 - [0.006027\, (2 \times 25 / 34.8)^{-1.1352} (2 \times 8.27 / 34.8)^{-0.44641} 1.844^{0.755515}]$$

$$= 0.99139$$

By taking into consideration the reduction in heat rejection ability due to hot plume air recirculation, the rate of heat transfer from 18 fan units is

$$Q_{18\,ir} = e_r Q_{18\,i} = 0.99139 \times 347.68 = 344.686 \times 10^6 \text{ W}$$

Measuring recirculation

In the absence of windwalls, recirculation can be significant and result in a corresponding reduction in heat transfer effectiveness. As shown in Figure 8.4.6, smoke generated at the lower end outlet of an A-frame type, forced-draft, air-cooled heat exchanger without windwalls is drawn directly downwards into the low pressure region created by the fans.

Fig. 8.4.6 Plume Air Recirculating in Air-Cooled Steam Condenser

The results of recirculation tests conducted at the Matimba power plant are reported by Conradie and Kröger. They measured the vertical temperature distribution of the air entering the heat exchanger and observed a relatively higher temperature in the vicinity of the fan platform. As shown by the smoke trail in Figure 8.4.7, recirculation of the plume air occurs in this region. Because of the approximately 10 m high windwall surrounding the

array of A-frame heat exchanger bundles, a reduction in effectiveness of less that 1% is experienced under normal operating conditions in the absence of wind. The effectiveness can be determined according to Equation 8.4.25.

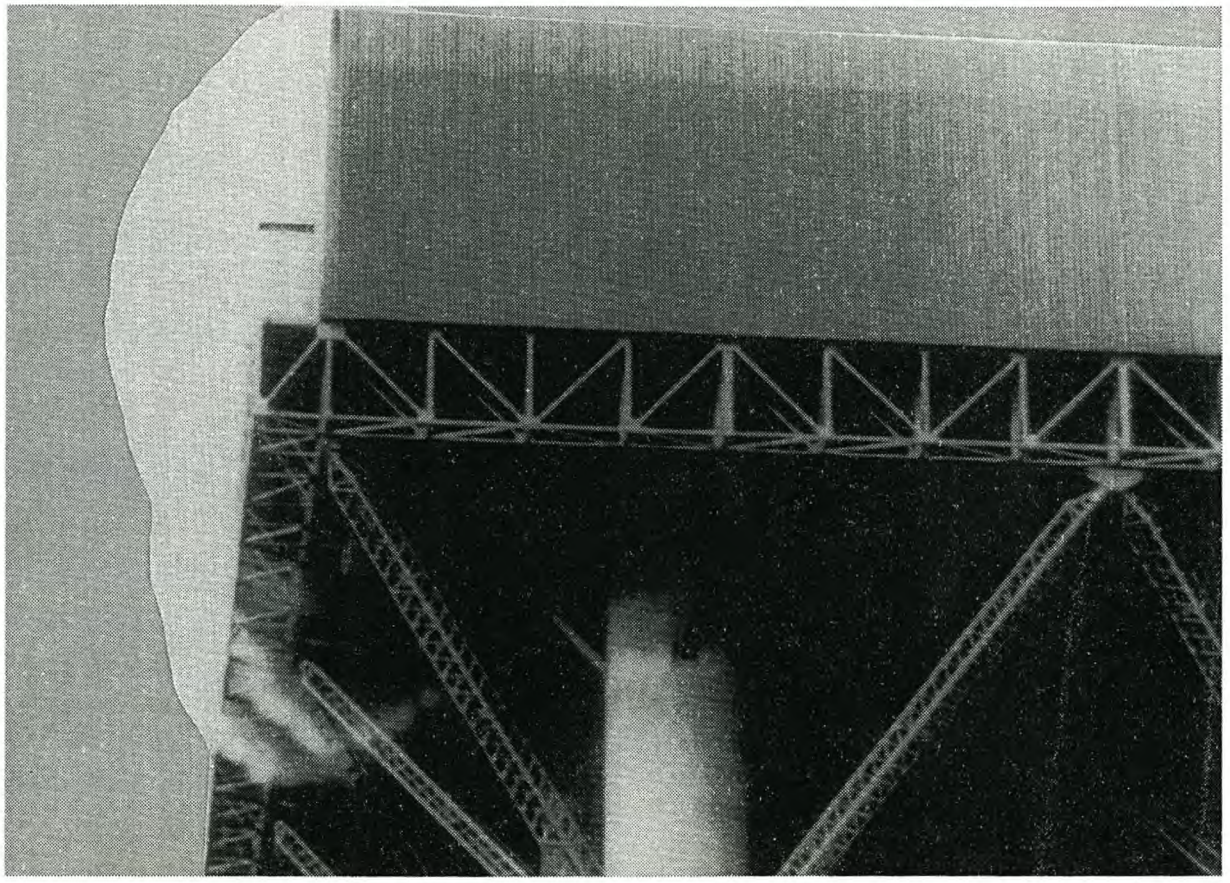

Fig. 8.4.7 Visualization of Recirculation with Smoke at the Matimba Power Plant

Generally, less recirculation occurs in induced-draft cooling systems because of the relatively high fan outlet velocity and height of diffuser—if one is present.

In numerous situations, a minimum tube wall temperature must be maintained. For example, air temperature control is essential to avoid plugging in the following instances:

- during cooling of heavy crude stocks with high pour points
- where a danger of solidification fouling exists due to the deposition of ammonium salts when the tube wall temperatures fall below 70 °C in an overhead condenser for a sour water stripper

In such situations, recirculation is employed in a system incorporating automatically controlled louvers that allow more or less of the hot plume air to mix with the ambient cooling air (Fig. 8.4.8). Other arrangements are also possible according to Rubin.

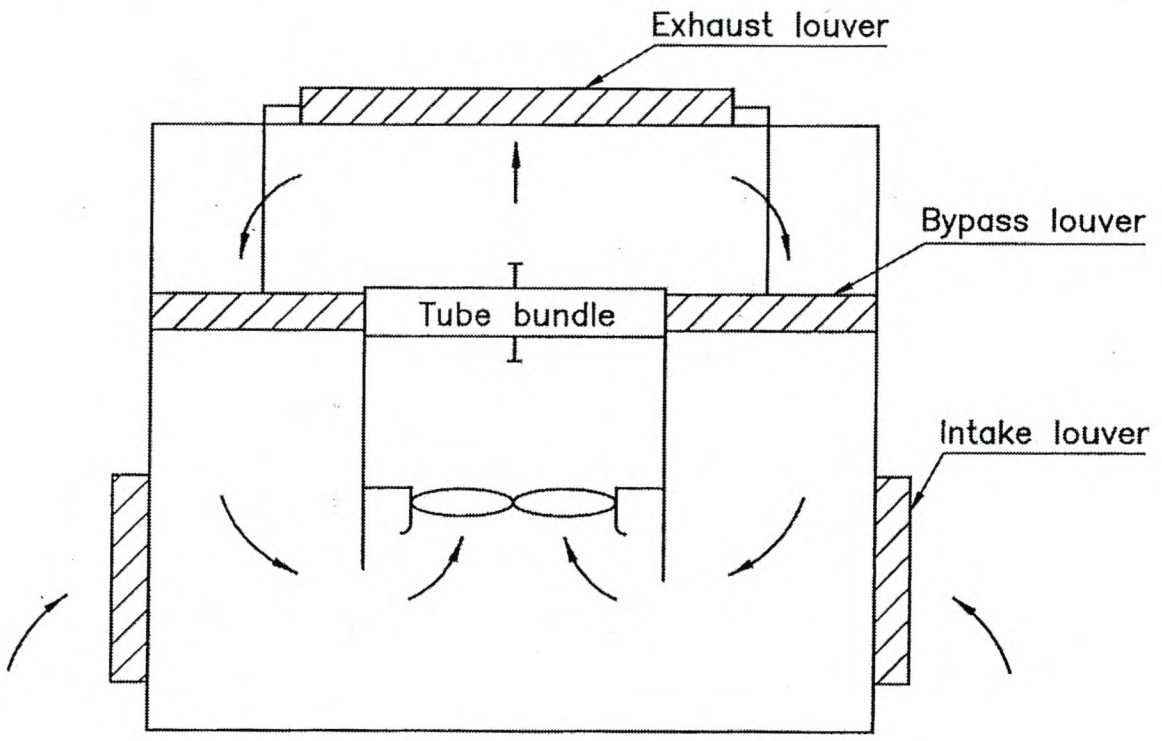

Fig. 8.4.8 Louver Controlled Plume Air Recirculation in Air-Cooled Heat Exchanger

Steam coils located immediately below the tube bundles may be required to preheat the air during startup in winter.

References

Air-Cooled Heat Exchanger Manufacturers Association, *Standard for Air-Cooled Heat Exchangers*, Air-Cooled Heat Exchanger Manufacturers Association, New York, 1986.

American Institute of Chemical Engineers, *Air-Cooled Heat Exchangers, A Guide to Performance Evaluation,* American Institute of Chemical Engineers, New York, 1978.

American Petroleum Institute, *Air-Cooled Heat Exchangers for General Refinery Services*, API Standard 661, American Petroleum Institute, Washington, 1992.

American Society of Mechanical Engineers, *Air-Cooled Heat Exchangers Performance Test Codes*, PTC 30-1991, American Society of Mechanical Engineers, New York, 1991.

Banerjee, S., J. S. Chang, R. Girard, and V. S. Krishnan, "Reflux Condensation and Transition to Natural Circulation in a Vertical U-tube," *Journal of Heat Transfer*, 105:719–727, 1983.

Berg, W. F. and J. L. Berg , *Flow Patterns for Isothermal Condensation in One Pass Air Cooled Heat Exchangers,* Paper 79-WA/HT-5, American Society of Mechanical Engineers, 1979.

Breber, G., J., W. Palen, and J. Taborek, "Study on Noncondensable Vapor Accumulation in Air-Cooled Condensers," *Proceedings*, Seventh International Heat Transfer Conference, 6:263–268, 1982.

Brown, R., V. Ganapathy, and J. Glass, "Design of Air-Cooled Exchangers," *Chemical Engineering*, 85-7:106–125, 1978.

Conradie, A. E. and D. G. Kröger, "Performance Evaluation of Dry-Cooling Systems for Power Plant Applications," *Applied Thermal Engineering*. 16-3:219–232, 1996.

Conradie, A. E. and D. G. Kröger, "Plume Recirculation in Air-Cooled Heat Exchangers," Paper 89-HT-11, Joint American Society of Mechanical Engineers and American Institute of Chemical Engineers National Heat Transfer Conference, Philadelphia, August 1989.

De Villiers, E. and D. G. Kröger, "Inlet Losses in Counterflow Wet-Cooling Towers," *Proceedings*, International Joint Power Generation Conference, vol. 2, PWR 34:601–606, 1999.

De Villiers, E. and D. G. Kröger, "Inlet Losses in Counterflow Wet-Cooling Towers," *Journal of Engineering for Gas Turbines and Power*, American Society of Mechanical Engineers, 123-2:460–464, April 2001.

Diehl, J. E. and C. R. Koppany, "Flooding Velocity Correlation for Gas-liquid Counterflow in Vertical Tubes," Chemical Engineering Progress Symposium Series, 65–92, 77–83, 1969.

Du Toit, C. G. and D. G. Kröger, "Modelling of the Recirculation in Mechanical-draught Heat Exchangers," *South African Institute of Mechanical Engineers R and D Journal*, 9-1:2–8, 1993.

Du Toit, C. G. and Kröger, D. G., "Numerical Modelling of Recirculation in Mechanical-draught Heat Exchangers," *Proceedings*, First International Center for Heat and Mass Transfer Numerical Heat Transfer Conference and Software Show, Guildford, 1991.

Duvenhage, K. and D. G. Kröger, "Plume Recirculation in Mechanical-Draft Air-Cooled Heat Exchangers," *Heat Transfer Engineering*, 16-4:42–49, 1995.

Duvenhage, K., J. A. Vermeulen, C. J. Meyer, and D. G. Kröger, "Flow Distortions at the Fan Inlet of Forced-draught Air-Cooled Heat Exchangers," *Applied Thermal Engineering*, 16-8/9:741–752, 1996.

Electrical Power Research Institute, *Investigation of Numerical Modeling Techniques for Recirculation Flows, Report CS-1665, Parts 1 and 2*, EPRI, 1981.

English, K. G., W. T. Jones, R. C. Spillers, and V. Orr, "Flooding in a Vertical Updraft Partial Condenser," *Chemical Engineering Progress*, 59-7:51–53, 1963.

Fabbri, G., "Analysis of the Noncondensable Contaminant Accumulation in Single-Pass Air-Cooled Condensers," *Heat Transfer Engineering*, 18-2:50–60, 1997.

Fahlsing, P. M., "Benefits of Variable Speed Drives Applied on Dry Condensing at the Wyodak Plant," *Proceedings*, American Society of

Mechanical Engineers Joint Power Generation Conference, PWR-28:463–471, October 1995.

Forgó, L., "Die Ursachen für schlechte Wärmeübertragung in Rohrbündel-Wärmeaustauschern bei kondensierendem Dampf," *Brennstoff-Wärme-Kraft*, 19-1:20–23, 1967.

Fürst, J., "Kondensation in geneigten ovalen Rohren," *Fortschritt-Berichte Verein Deutscher Ingenieure*, 19–36, Verein Deutscher Ingenieure Verlag, Düsseldorf, 1989.

Girard, R. and J. S. Chang, "Reflux Condensation Phenomena in Single Vertical Tubes," *International Journal of Heat Mass Transfer*, 35-9:2203–2218, 1992.

Gunter, A. Y. and K. V. Shipes, "Hot Air Recirculation by Air Coolers," *Chemical Engineering Progress*, 68-2:49–58, February 1972.

Hewitt, G. F., G. L. Shires, and T. R. Bott, *Process Heat Transfer*, CRC Press, London, 1994.

Kennedy, J. F. and H. Fordyce, "Plume Recirculation and Interference in Mechanical-Draft Cooling Towers," *Proceedings*, Cooling Tower Environment Symposium, University of Maryland, Baltimore, 58–87, 1974.

Kröger, D. G., "Fan Performance in Air-Cooled Steam Condensers," *Heat Recovery Systems CHP*, 14-4:391–399, 1994.

Kröger, D. G., "Fan Performance in Air-Cooled Steam Condensers," *Proceedings*, American Society of Mechanical Engineers International Joint Power Generation Conference, PWR-28:133–148, Minneapolis, October 1995.

Kröger, D. G., "Recirculation in Air-Cooled Mechanical Draught Heat Exchangers," *South African Mining World*, 65–69, November 1988.

Kröger, D. G., "Reduction in Performance Due to Recirculation in Mechanical Draft Cooling Towers," *Heat Transfer Engineering*, 10-4:37–43, 1989.

Larinoff, M. W., "Bundle Design Protects Air-Cooled Condenser from Freezing," *Power Engineering*, 33–35, February 1990.

Larinoff, M. W., W. E. Moles, and R. Reichhelm, "Design and Specification of Air-Cooled Steam Condensers," *Chemical Engineering*, 86–94, 1978.

Lichtenstein, J., "Recirculation in Cooling Towers," American Society of Mechanical Engineering Power Division Meeting, Atlanta, 1037–1042, 1951.

McKetta, J. J., *Heat Transfer Design Methods*, Marcel Dekker, Inc., New York, 1992.

Monroe, R. C., "Improving Cooling Tower Fan System Efficiencies," *Combustion Magazine*, 50-11:20–26, May 1979.

Mukherjee, R., "Effectively Designing Air-Cooled Heat Exchangers," *Chemical Engineering Progress*, 26–47, February 1997.

Obinelo, I. F., G. F. Round, and J. S. Chang, "Condensation Enhancement by Steam Pulsation in a Reflux Condenser," *International Journal of Heat and Fluid Flow*, 15–1, 1994.

Oosthuizen, P. C., "Performance Characteristics of Hybrid Cooling Towers," Master's thesis Department of Engineering, University of Stellenbosch, Stellenbosch, 1995.

Paikert, P., *Air-Cooled Heat Exchangers, Heat Exchanger Design Handbook*, ed. E. Schlünder et al., Verein Deutscher Ingenieure-Verlag, Düsseldorf, 1983.

Reuter, H. C. R. and D. G. Kröger, "Pressure Change and Flooding in Vertical and Inclined Tubes During Reflux Condensation of Steam," *Proceedings*, 9th International Symposium on Transport Phenomena in Thermal-Fluids Engineering (ISTP-9), 2:727–732, Singapore, June 1996.

Reuter, H. C. R., "Flow Modes and Pressure Change in an Inclined Tube During Reflux Condensation of Steam," Master's thesis, Department of Engineering, University of Stellenbosch, South Africa, 1994.

Rose, J. C., D. J. Wilson, and G. H. Cowan, *The Performance of Air-Cooled Heat Exchangers, Part II. Air-Cooled Heat Exchanger Performance Specification, AERE - R7450*, Heat Transfer and Fluid Flow Service, Harwell, 1973.

Rozenman, T. and Pundyk, J., "Effect of Unequal Heat Loads on the Performance of Air Cooled Condensers," American Institute of Chemical Engineers Symposium Series, 70-138:178–184, 1974.

Rubin, F. L., "Winterizing Air Cooled Heat Exchangers," *Hydrocarbon Processing*, 147–149, October 1980.

Russel, C. M. B., *Condensation of Steam in a Long Reflux Tube, Heat Transfer and Fluid Flow Service,* Association of Environment and Resource Economists, Harwell and National Engineering Laboratory, Harwell, United Kingdom, July 1980.

Russell, C. M. B. and W. H. Bos, "The Economic Design of Air Coolers," *Proceedings*, Conference on Air Coolers, Institution of Mechanical Engineers, 14–40, London, 1970.

Russell, C. M. B. and J. Peachey, "Air Flow Effects on Fan Performance in Air Cooled Heat Exchangers," Paper B3, *Proceedings*, International Conference on Fan Design and Applications, 79–90, Guildford, England, 1982.

Salta, C. A. and D. G. Kröger, "Effect of Inlet Flow Distortions on Fan Performance in Forced Draught Air-Cooled Heat Exchangers," *Heat Recovery Systems and CHP*, 15-6:555–561, 1995.

Schoenfeld, P. and D. G. Kröger, "Flooding During Reflux Condensation of Steam in an Inclined Elliptical Tube," *Proceedings*, International Conference and Exhibit, Heat Exchangers for Sustainable Development, Instituto Superior Técnico, Lisbon, 107–115, June 1998.

Schoenfeld, P. and D. G. Kröger, "Flooding During Reflux Condensation of Steam in an Inclined Elliptical Tube," *South African Institute of Mechanical Engineers R&D Journal,* 16:1–8, 2000.

Schrey, H. G. and J. Kern, "Zum Rohrreiheneffekt bei Gasbeaufschlagten Kondensatoren," *International Journal of Heat and Mass Transfer*, 24:335–342, 1981.

Schrey, H. G., "Operational Considerations for Air-Cooled Steam Condensers with One or Higher Numbers of Tube Rows," Paper, Ninth International Association for Hydraulic Research Cooling Tower and Spraying Pond Symposium, von Karman Institute, Brussels, September 1994.

Schrey, H. G., "Zur Bestimmung des Leistungsverhaltens bei Mehrreihigen, luft-bzw. gasgekühlten Kondensatoren mit Inerten," *Wärme – und Stoffübertragung*, 18-3:185–191, 1984.

Shaikh, N. M., "Estimate Air-Cooler Size," *Chemical Engineering*, 90-25:65–68, 1983.

Shipes, K. V., *Mechanical Design of Air-Cooled Heat Exchangers, Heat Exchanger Design Handbook,* ed. E. V. Schlünder, et al., Verein Deutscher Ingenieure-Verlag, Düsseldorf, 1983.

Slawson, P. R. and H. F. Sullivan, "Model Studies on the Design and Arrangement of Forced-Draft Cooling Towers to Minimize Recirculation and Interference," *Proceedings*, Conference on Waste Heat Management and Utilization, 235–244, 1981.

Smit, L., "Flow Distribution, Pressure Drop, Flooding and Entrainment in an Air-Cooled Reflux Steam Condenser," *South African Institute of Mechanical Engineers Research and Development Journal,* 17-3:58–61, 2001.

Terblanche, J. E. and D. G. Kröger, "Experimental Evaluation of the Aerodynamic Inlet Losses in Cooling Towers," *South African Institute of Mechanical Engineers Research and Development Journal,* 10-2:41–44, 1994.

Verein Deutscher Ingenieure, *VDI 2049: Wärmetechnische Abnahme – und Leistungsversuche an Trockenkühltürmen*, VDI, Düsseldorf, 1981.

Zanker, A., "Taking the Drudgery out of Designing Air-Cooled Heat Exchangers," *Machine Design*, 158–165, December 1979.

Zapke, A. and D. G. Kröger, "Vapor-Condensate Interactions during Counterflow in Inclined Reflux Condensers," HTD-342, American Society of Mechanical Engineers National Heat Transfer Conference, 4:157–162, Baltimore, 1997.

9

Meteorological Effects

9.0 Introduction

The performance of all air-cooled heat exchangers and cooling towers are affected by changes in ambient conditions. Changes in temperature, humidity, winds, inversions, rain, snow, hail, and solar radiation all influence the performance of air-cooled heat exchangers and cooling towers to a greater or lesser extent. The influences of winds and inversions are described in detail in the following sections. Rain tends to reduce the drybulb temperature nearly to wetbulb values. Some wetting of finned surfaces may occur in dry systems, and this has a beneficial influence on performance. In natural-draft cooling towers, cooling of the air in the tower and a reduction of the draft due to the falling droplets will have a detrimental effect on performance according to Heberholz and Schulz. Generally, the effects on performance due to rain and snow are small.

During periods of very low ambient temperatures, frozen cooling water can lead to serious structural and performance problems. Different devices and procedures are employed to avoid freezing according to Fabre, Michell, and Drew. In areas where hailstorms occur, protective screens are installed above finned surfaces. A maximum solar radiation of about 1 kW/m^2 may strike the heat transfer surface for a short period during the day. This will reduce the rate of heat rejection in some installations. According to Nouri-

Borujerdi, the draft and corresponding heat rejection rate of an aluminum-clad, natural-draft, dry-cooling tower is not affected to any degree when the tower shell is exposed to solar radiation.

According to Barbaud, the most stringent heat exchanger specifications concerning the integrity and performance under different meteorological and seismic conditions are found in the nuclear industry .

When designing a large industrial cooling system, ambient conditions must be considered. For instance, the orientation of the cooling system or even the entire plant may be determined by the direction of the prevailing winds.

9.1 Atmosphere

The atmosphere is a mixture of gases of which oxygen and nitrogen are the main constituents. It also contains small amounts of water vapor and other gases, including carbon dioxide, hydrogen, helium, and the rare inert gases argon, krypton, neon, etc. The properties of the constituents varies little across the range of altitudes involved in conventional aerodynamics, and the atmosphere may be regarded as a homogeneous gas of uniform composition.

Consider a small parcel of air that may be moved up or down in the atmospheric pressure field. If this process is adiabatic, i.e., no heat is transferred to the parcel by either conduction or radiation, it will experience a change in temperature as a result of the change in pressure.

The pressure gradient in a gravity field is given by

$$dp / dz = - \rho g \tag{9.1.1}$$

For an isentropic process

$$p / \rho^{\gamma} = \text{constant} \tag{9.1.2}$$

The air density may be expressed through the perfect gas law as

$$\rho = p / RT \tag{9.1.3}$$

Substitute Equation 9.1.3 in Equation 9.1.2 and differentiate with respect to altitude to find

$$\frac{(1-\gamma)}{\gamma p}\frac{dp}{dz}+\frac{1}{\mathrm{T}}\frac{dT}{dz}=0 \tag{9.1.4}$$

By combining the Equations 9.1.1, 9.1.3, and 9.1.4, the temperature gradient may be expressed as

$$\frac{dT}{dz} = -\frac{g(\gamma-1)}{\gamma R} \tag{9.1.5}$$

The gravitational acceleration, g, is a function of both latitude and altitude. However, changes in g are so small that the influence on the performance of an air-cooled heat exchanger or cooling tower is negligible.

For dry air with $\gamma = c_p/c_v = 1.4$ and $R = 287.08$ J/kg K, find $g = 9.8$ m/s^2

$$\frac{dT}{dz} = -0.00975\ \mathrm{K/m} \tag{9.1.6}$$

This temperature gradient is known as the dry adiabatic lapse rate (DALR).

Upon integration of Equation 9.1.5, find

$$T = T_1 - g(\gamma-1)z/(\gamma R) \tag{9.1.7}$$

where

T_1 = the temperature at ground level

For dry air this equation reduces to

$$T = T_1 - 0.00975z \tag{9.1.8}$$

From Equations 9.1.1 and 9.1.3, it follows that:

$$\frac{dp}{p} = -\frac{g\,dz}{RT} \tag{9.1.9}$$

Substitute Equation 9.1.7 into Equation 9.1.9, and integrate between ground level and an elevation z.

$$p = p_1[1 - g(\gamma - 1)z/(\gamma RT_1)]^{\gamma/(\gamma-1)} \tag{9.1.10}$$

For dry air with $g = 9.8$ m/s^2, Equation 9.1.10 becomes

$$p = p_1(1 - 0.00975z/T_1)^{3.5} \tag{9.1.11}$$

To find the temperature and pressure distribution for air containing water vapor, consider the density given by Equation A.3.1.

$$\rho_{av} = (1 + w)\,[1 - w/(w + 0.62198)]p_{abs}/(287.08T)$$

$$\approx 0.622(1 + w)p/[(w + 0.622)RT] \tag{9.1.12}$$

Substitute this density in Equation 9.1.2, and with γ replaced by γ_{av}, differentiate with respect to altitude to find the temperature gradient:

$$\frac{dT}{dz} = -\left(\frac{1-\gamma_{av}}{\gamma_{av}}\right)\frac{T}{p}\,\frac{dp}{dz} \tag{9.1.13}$$

Using Equation 9.1.1, $dp/dz = -\rho_{av}g$. Substitute this relation together with Equation 9.1.12 in Equation 9.1.13, and find

$$\frac{dT}{dz} = -\frac{0.622\,R_{av}\,g(1+w)}{c_{pav}R(w+0.622)} \tag{9.1.14}$$

where

$\gamma_{av} = c_{pav}/c_{vav}$

$c_{pav} - c_{vav} = R_{av}$

Substitute the following in Equation 9.1.14

$$R_{av} = R + wR_v = R(1 + wR_v/R) = R(1 + 461.52w/287.08) = R(1 + w/0.622)$$

$$c_{pav} = c_{pa} + wc_{pv} \approx 1006(1 + 1.9w)$$

and find

$$\frac{dT}{dz} = -\frac{g(1+w)}{1006(1+1.9w)} = -\frac{0.00975(1+w)}{(1+1.9w)} \qquad (9.1.15)$$

Integrate and find

$$T = T_1 - 0.00975(1 + w)z/(1 + 1.9w) \qquad (9.1.16)$$

Substitute Equations 9.1.12 and 9.1.16 into the relation $dp/dz = -\rho_{av}g$, and find upon integration

$$p = p_1\left[1 - \frac{0.00975(1+w)z}{(1+1.9w)T_1}\right]^{2.1778(1+1.9w)/(w+0.622)} \qquad (9.1.17)$$

When a parcel of moist air is raised in a gravitational field, adiabatic cooling takes place until the air reaches the point of saturation according to Seinfeld. Upon a further rise in elevation, cooling will cause vapor to condense and precipitate. The energy removed from the vapor during this condensation process is available to heat the surrounding air. The heating that takes place during the precipitation is a pseudoadiabatic process.

Consider a parcel of saturated air rising through a height, dz. The mass of the air constituent is M_a. The amount of condensate formed

during this change in elevation is dM_w. According to the first law of thermodynamics, find

$$M_a\,(i_{ma} + di_{ma}) + (M_w + dM_w)\,c_{pw}\,(T + dT - 273.15)$$

$$+ M_a\,(1 + w_s + dw_s)\,g\,(z + dz) + (M_w + dM_w)\,g\,(z + dz)$$

$$= M_a i_{ma} + M_{wCpw}(T - 273.15) + M_a(1 + w_s)gz + M_w gz \quad (9.1.18)$$

where, according to Equation A.3.6b,

$i_{ma} = c_{pa}(\mathrm{T} - 273.15) + w_s\,[i_{fgwo} + c_{pv}(T - 273.15)]$

$di_{ma} = c_{pa}dT + dw_s[i_{fgwo} + c_{pv}(T - 273.15)] + w_s c_{pv}dT$

i_{fgwo} = latent heat of water at 273.15K

When second order terms are neglected, Equation 9.1.18 reduces to

$$M_a(c_{pa} + w_s c_{pv})\,dT + M_a dw_s\,[i_{fgwo} + c_{pv}(T - 273.15)] + M_w c_{pw}dT + dM_w c_{pw}$$

$$\mathrm{x}\,(T - 273.15) + M_a(1 + w_s)gdz + M_a\,dw_s gz + M_w gdz + dM_w gz = 0 \quad (9.1.19)$$

According to the conservation of mass

$$dM_w = -\,M_a dw_s \quad (9.1.20)$$

For most practical cases, $M_w << M_a$. Substitute Equation 9.1.20 into Equation 9.1.19 to find

$$\frac{dT}{dz} = \xi_T = \frac{-(1+w_s)g}{c_{pma} + \left[i_{fgwo} - (c_{pw} - c_{pv})(T - 273.15)\right] dw_s/dT} \quad (9.1.21)$$

where

$c_{pma} = c_{pa} + w_s\, c_{pv}$

specific heats are evaluated at $(T + 273.15)/2$

According to Equation 4.1.12, the humidity ratio can be expressed as

$$w_s = 0.622\, p_{vs}/(p - p_{vs}) \tag{9.1.22}$$

where

p = the measured atmospheric pressure

The saturation pressure of water vapor is an exponential function of temperature and can be determined using Equation A.2.1 or more simply in the range 273.15 K to 313.15 K (0° to 40°C)

$$p_{vs} \approx 2.368745 \times 10^{11} \exp(-5406.1915/T) \tag{9.1.23}$$

where

T is in Kelvin

Differentiate Equation 9.1.22, and find

$$\frac{dw_s}{dT} = \frac{0.622\left[p(dp_{vs}/dT) - p_{vs}(dp/dT)\right]}{(p - p_{vs})^2} \tag{9.1.24}$$

Upon differentiation of Equation 9.1.23, find

$$dp_{vs}/dT = 5406.1915\, p_{vs}/T^2 \tag{9.1.25}$$

With Equation 9.1.1, find

$$dp/dT = (dp/dz)(dz/dT) = (dp/dz)/(dT/dz) = -\rho_{avw}g/(dT/dz) \quad (9.1.26)$$

The air may contain a mist of water droplets, and the density of saturated air is given by

$$\rho_{avw} = (1+w_s)\left[1-w_s/(w_s+0.62198)\right] p/RT + (w_{sc} - w_s)\, p_a/RT \quad (9.1.27)$$

where

w_{sc} = the humidity ratio of the saturated air where condensation commences

For most practical cooling tower designs,

$$(w_{sc} - w_s)p_a/RT << (1 + w_s)[1 - w_s/(w_s + 0.62198)]p/RT$$

with the result that Equation 9.1.27 can be simplified to give

$$\rho_{avw} \approx 0.622(1 + w_s)p/[(w_s + 0.622)RT] \quad (9.1.28)$$

Substitute Equations 9.1.22, 9.1.23, 9.1.25, 9.1.26, and 9.1.28 into Equation 9.1.24, and find

$$\frac{dw_s}{dT} = \frac{0.67872 \times 10^{-11} w_s^2\, p \exp(5406.1915/T)}{T}$$

$$\times \left[\frac{5406.1915}{T} + \frac{0.622g(1+w_s)/(w_s+0.622)}{R(dT/dz)}\right] \quad (9.1.29)$$

Substitute Equation 9.1.29 in Equation 9.1.21, and find

$$\frac{dw_s}{dT} = \xi_T =$$

$$\frac{-(1+w_s)g\left[1+0.42216\text{x}10^{-11}w_s^2 p\exp(5406.1915/T)i_e/\{(w_s+0.622)RT\}\right]}{c_{pma}+3.6693\text{x}10^{-8}w_s^2 p\exp(5406.1915/T)i_e/T_2} \tag{9.1.30}$$

where

$i_e = i_{fgwo}$ - $(c_{pw} - c_{pv})(T - 273.15)$

This temperature gradient is less than the dry adiabatic lapse rate.

Analytical integration of Equation 9.1.30 is not possible. However, it can be shown that the temperature gradient determined at a particular pressure and temperature hardly changes at higher elevations. This is true where both the pressure and the temperature will be lower, i.e., the temperature gradient is approximately constant, or

$$T = T_{sc} + \xi_T z_s \tag{9.1.31}$$

Substitute Equations 9.1.28 and 9.1.31 into the relation $dp/dz = -\rho_{avw}g$, and find

$$\frac{dp}{dz} = \frac{-0.622g(1+w_s)p}{R(w_s+0.622)\,(T_{sc}+\xi_T z_s)} \tag{9.1.32}$$

Upon integration, find the approximate pressure above the elevation where the air initially becomes saturated and condensation commences.

$$p_s \approx p_{sc}\left(1+\xi_T z_s/T_{sc}\right)^{-0.021233(1+w_{sc})/[\xi_T(w_{sc}+0.622)]} \tag{9.1.33}$$

Investigation has shown the atmosphere consists of two distinct contiguous regions. The lower of these regions is called the *troposphere*, and the temperature within the troposphere decreases linearly with height. The upper region is the *stratosphere* where the temperature remains almost constant with height. The supposed boundary between the two regions is termed the *tropopause*. A sharp distinction does not exist between the two, but one region merges gradually into the other. Nevertheless, this distinction represents a useful convention for the purposes of calculation. An International Standard Atmosphere (ISA) has been defined and is intended to approximate the atmospheric conditions prevailing for most of the year in temperate latitudes. The parameters are:

- a mean sea level pressure of 101,325 N/m^2
- a temperature of 15°C
- a mean lapse rate of 0.0065 K/m to a height of 11 km

These values are shown in Figure 9.1.1, which also shows the characteristics of two other agreed-upon standard atmospheres intended to represent the most extreme conditions likely to be encountered on earth. With this model of the atmosphere, it is possible to find an approximation of required physical characteristics at any altitude.

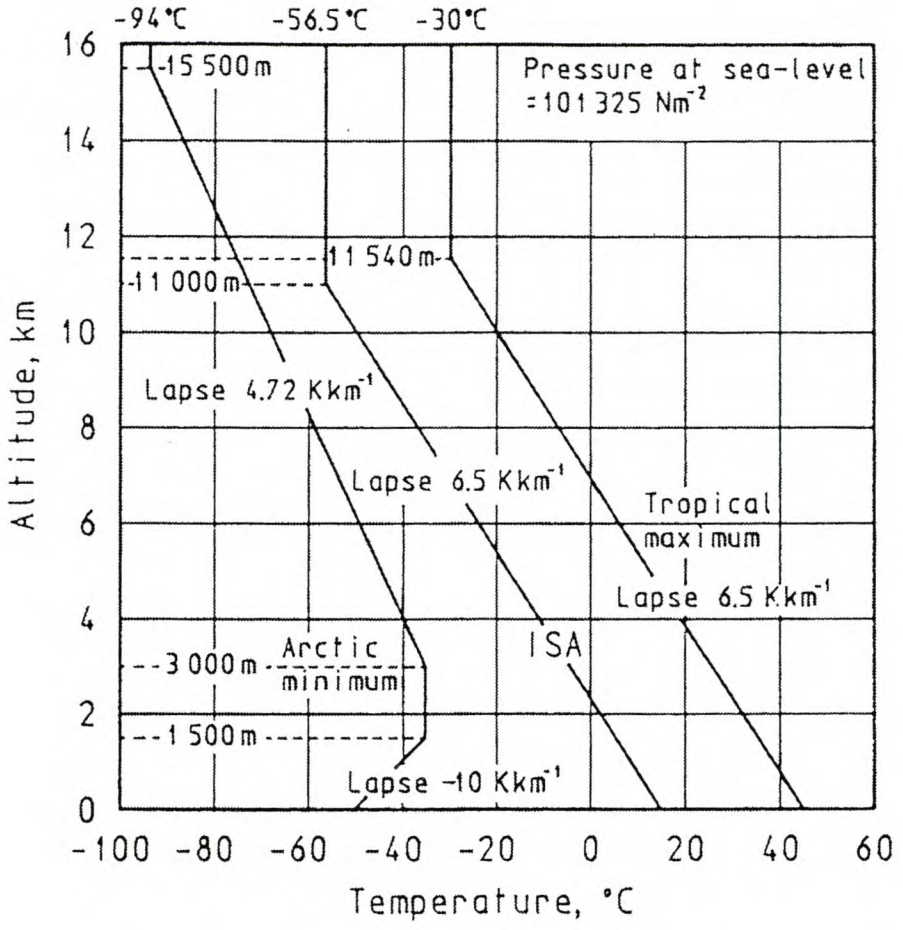

Fig. 9.1.1 Variation of Temperature with Height in the International Standard, Tropical Maximum and Arctic Minimum Atmosphere

The ISA lapse rate is lower than that given by Equation 9.1.6 due to the absorption of solar radiation by the atmospheric gases, especially carbon dioxide and water vapor. According to the former, the variation of temperature with altitude in the troposphere is

$$T = T_o - z\, dT / dz = 288.15 - 0.0065\, z \tag{9.1.34}$$

According to this lapse, the ISA troposphere obeys a law of the form

$$p / \rho^{1.235} = \text{constant} \tag{9.1.35}$$

With the exponent equal to 1.235, it can be shown, as in the case of Equation 9.1.10, the atmospheric pressure at elevation z above sea level is

$$p = p_1 \left[1 - 9.8(1.235 - 1) z / (1.235 \text{ x } 287.08 T_1)\right]^{1.235/(1.235-1)}$$

$$= p_1 \left[1 - 6.5 \text{ x } 10^{-3} \, z / T_1\right]^{5.255} \qquad (9.1.36)$$

where

$g = 9.8$ m/s^2

$R = 287.08$ J/kgK

For the ISA lapse rate with a temperature of T_1 = 15°C or 288.15 K at sea level, the pressure at any elevation up to 11,000 m is given by

$$p = p_1 \left(1 - 2.25577 \text{ x} 10^{-5} \, z\right)^{5.255} \qquad (9.1.37)$$

The lower 1–2 km of the troposphere is usually called the *planetary boundary layer* (PBL) after Lettau. It is also called the *friction layer*. This boundary layer is characterized by large vertical gradients in the wind velocity, air temperature, and humidity. Transport through the planetary boundary layer is accomplished by eddy diffusion, and the physical state of the boundary layer depends on the surface fluxes of momentum, heat, and moisture.

Significant diurnal variations in air temperature near the surface may be experienced due to radiative heating and cooling of the surface (Fig. 9.1.2). In the afternoon, the sun heats the ground to a temperature well above the mean air temperature, resulting in a net heat flux from the surface to the atmosphere. Convectively unstable conditions may be experienced where the temperature drops more sharply than predicted by the DALR. As the sun sets, the ground begins to cool by radiation—assuming a clear sky. The surface temperature may drop below the mean air temperature, and the net heat flux is reversed. This causes heat to flow from the few lowest meters of the atmosphere to the soil, and a surface temperature inversion may be formed. Cooling continues throughout the night, and the inversion layer

thickens to its maximum value at about sunrise. As morning progresses, greater amounts of solar radiation heat the ground, and a transition profile may be encountered. With sufficient heating, the unstable afternoon profile is established once again.

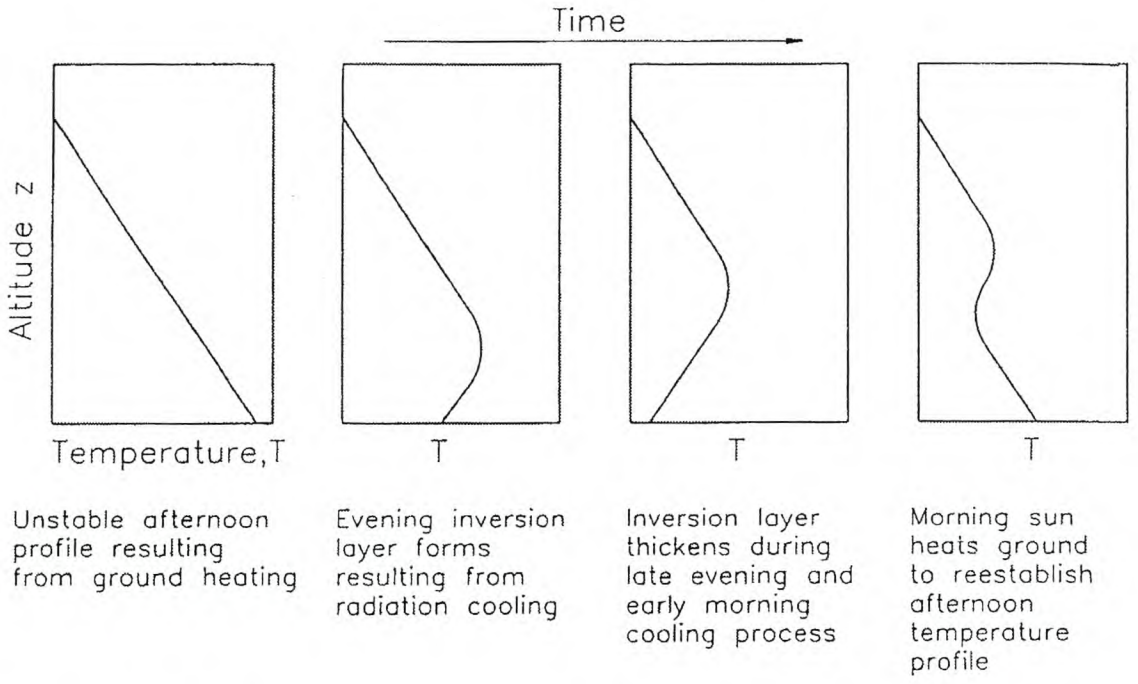

Fig. 9.1.2 Typical Diurnal Variation of Atmospheric Temperature Profile

An example of hourly temperature data measured at eight different heights on a 96 m weather mast over a period of 24 hours is listed in Table 9.1.1 and shown in Figure 9.1.3. The vertical temperature gradients obviously depend on local weather conditions. Clouds reflect much of the earth's radiation loss back to the surface, thereby raising the surface temperature substantially, even to the extent where the formation of an inversion is suppressed. Furthermore, the turbulence associated with wind will enhance mixing in the atmospheric boundary layer, and a much subdued temperature profile will result. Golder stated that wind velocities above 8 m/s will invariably result in a neutral or adiabatic atmosphere.

Alt.	Time					
m	12h00	13h00	14h00	15h00	16h00	17h00
96	28.15	29.61	29.79	30.35	30.91	30.31
65	28.43	29.90	30.20	30.72	31.41	30.73
40	28.65	30.36	30.53	31.23	31.89	30.93
20	29.04	30.52	30.81	31.42	31.88	31.04
10	29.55	31.07	31.27	31.95	32.01	31.20
5	30.21	31.59	31.92	32.46	32.45	31.53
2	30.88	32.21	32.57	33.01	32.75	31.69
1	31.45	32.90	33.10	33.63	33.32	31.94
	18h00	19h00	20h00	21h00	22h00	23h00
96	28.26	27.44	27.08	26.74	25.95	24.38
65	28.34	27.35	26.62	26.33	25.43	23.80
40	27.82	26.25	23.46	22.61	22.36	22.03
20	27.40	24.26	21.68	20.41	19.69	19.10
10	26.54	21.99	20.07	18.40	17.57	16.45
5	25.82	20.46	18.03	15.87	15.90	14.39
2	24.63	18.13	15.27	13.53	14.44	12.87
1	23.36	16.19	13.81	12.35	12.85	11.72
	00h00	01h00	02h00	03h00	04h00	05h00
96	24.90	23.36	22.41	21.55	22.12	23.11
65	24.74	22.57	20.99	18.80	20.62	20.85
40	22.71	20.50	18.90	16.11	18.07	17.19
20	18.97	16.63	15.96	15.58	15.51	14.43
10	14.80	11.48	13.78	10.81	10.83	11.16
5	11.81	10.50	11.38	9.30	8.70	9.12
2	10.65	9.85	9.81	8.40	7.94	8.24
1	9.86	9.17	8.95	7.66	7.44	7.62
	06h00	07h00	08h00	09h00	10h00	11h00
96	22.42	20.48	20.79	20.16	22.99	26.48
65	19.77	17.34	17.32	18.63	23.30	26.69
40	15.34	14.80	15.35	18.58	23.85	26.94
20	14.18	13.38	14.52	18.77	24.05	27.29
10	11.13	10.50	12.18	18.77	24.40	27.72
5	8.57	8.33	10.95	18.82	24.65	28.20
2	7.35	6.72	10.92	19.00	25.06	28.73
1	6.54	5.49	10.18	19.67	25.57	29.12

Table 9.1.1 Hourly Temperatures in °C at Different Elevations

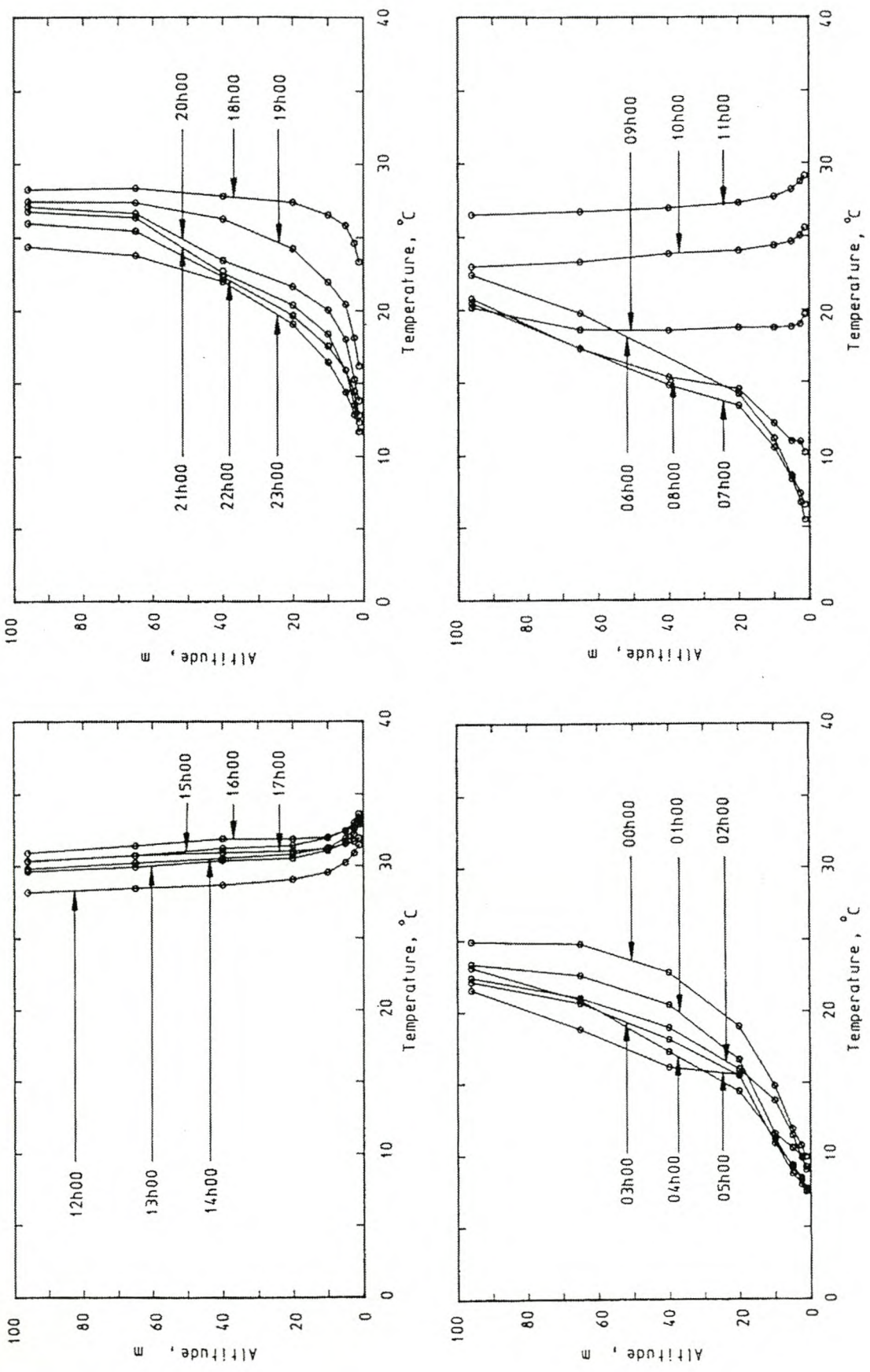

Fig. 9.1.3 Hourly Temperatures in °C at Different Elevations

The lowest 10% of the planetary boundary layer, often referred to as the *constant flux layer* or *surface boundary layer* (SBL), usually exhibits little, if any, change with height in the vertical fluxes of momentum, heat, and water vapor. Dimensional analysis of the mean wind and temperature profiles in the constant flux layer, well above the aerodynamic roughness elements, is well treated in textbooks, for example Seinfeld. Values for the surface roughness corresponding to particular surface geometries are listed in Table 9.1.2.

Surface configuration	Roughness length [m]
Urban areas:	
Central business district	8.000000
High density residential	4.500000
Low density residential	2.000000
Rolling relief:	
Coastal bush	1.000000
Open savanna	0.800000
Full grown root crops	0.250000
Shrubs	0.150000
Flat relief, vegetated:	
Uncut grass	0.070000
Crop stubble	0.020000
Snow and short grass	0.002000
Flat relief, unvegetated:	
Natural snow (temporary)	0.001000
Bare sand	0.000400
Open sea	0.000200
Water	0.000100
Snow (permanent)	0.000050
Mud flats and ice	0.000001

Table 9.1.2 Roughness Lengths for Various Surfaces

When the surface layer is non-neutral, the similarity theory of Monin and Obukhov suggests the vertical fluxes of momentum and heat in the surface layer may be expressed respectively by

$$\frac{dv}{dz} = \frac{v_s}{\kappa z}\varphi_m\left(\frac{z}{L_{mo}}\right) \tag{9.1.38}$$

and

$$\frac{d\theta}{dz} = \frac{\theta_s}{\kappa z}\varphi_h\left(\frac{z}{L_{mo}}\right) \tag{9.1.39}$$

where

κ = the von Karman constant (η = 0.4)

θ = the potential temperature, that is, the temperature a parcel of air will attain if it were brought adiabatically to a standard pressure at the earth's surface

φ_m = momentum in the constant flux layer

φ_h = heat transfer in the constant flux layer

The functions φ_m and φ_h depend on the thermal stability of the layer. Some values for φ_m and φ_h corresponding to various stability classes are listed in Table 9.1.3.

Limits	Momentum, ϕ_m	Heat, ϕ_h
$-\infty \le z/L_{mo} < -10$	$(1 - 16z/L_{mo})^{-0.25}$	$(1 - 16z/L_{mo})^{-0.5}$
$-10 \le z/L_{mo} < 0$	$(1 - 16z/L_{mo})^{-0.333}$	$(1 - 16z/L_{mo})^{-0.5}$
$0 \le z/L_{mo} < 0.3$	$(1 + 6z/L_{mo})$	$(1 + 6z/L_{mo})$
$0.3 \le z/L_{mo} \le 10$	$(1 + 22.8z/L_{mo})^{-0.5}$	$(1 + 22.8z/L_{mo})^{0.5}$

Table 9.1.3 A Summary of the Functions ϕ_m and ϕ_h for the Surface Boundary Layer

The scaling velocity, v_s, is defined as

$$v_s = \tau/\rho \tag{9.1.40}$$

where

τ = shear stress at the surface

The scaling temperature, θ_s, is defined as

$$\theta_s = - q/(\rho c_p \kappa v_s) \tag{9.1.41}$$

where

q = sensible heat flux

One way of establishing the stability class of the atmosphere is to use Monin and Obukhov's scaling length, L_{mo}, which may be interpreted as the height at which the magnitudes of mechanical and thermal production of turbulence are equal. The Monin-Obukhov length is defined in terms of the turbulent fluxes as follows :

$$L_{mo} = T_m v_s^2 /(g \kappa^2 \theta_s) \tag{9.1.42}$$

where

T_m = the mean temperature of the layer under consideration

The atmospheric stability is divided into classes based on the Monin-Obukhov length as follows :

$$L_{mo}^{-1} \begin{cases} < 0 & ; \text{unstable} \\ = 0 & ; \text{neutral} \\ > 0 & ; \text{stable} \end{cases}$$

To solve Equation 9.1.39, the surface temperature is required. This task is performed by considering an energy balance for a thin slab at the surface (Fig. 9.1.4). All fluxes directed towards the surface are taken as negative. It is assumed the earth's albedo, α, is known and constant and the soil is void of any moisture. Evaporation and condensation of moisture are ignored in the energy balance. If no information on the local albedo is available, Baer suggests an average value $\alpha = 0.25$.

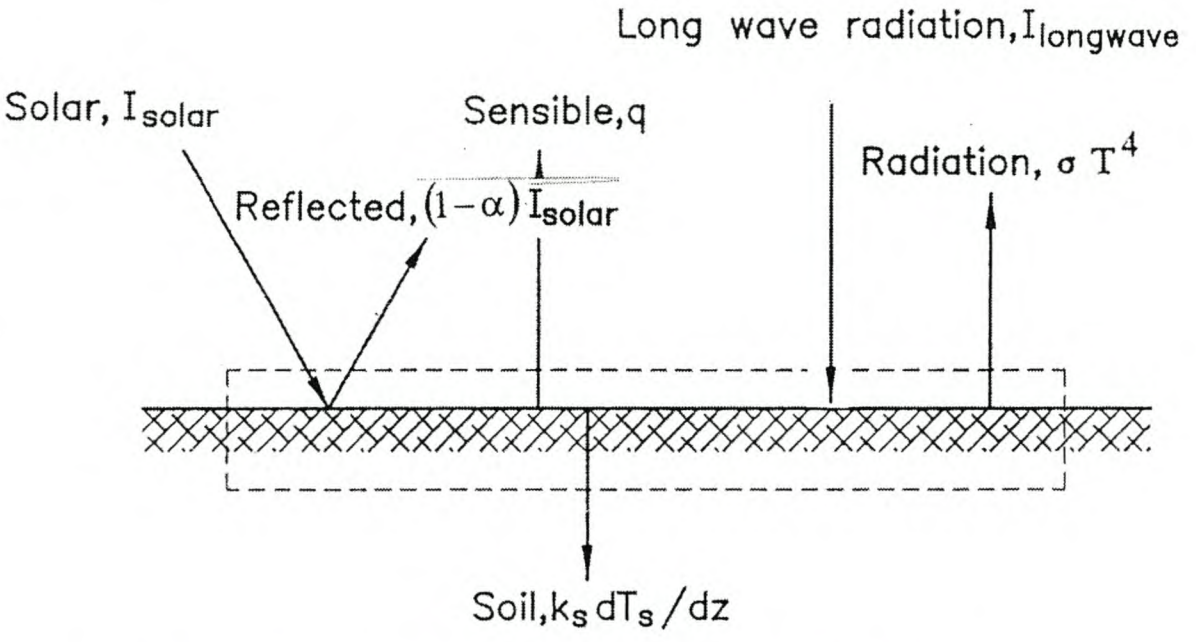

Fig. 9.1.4 Control Volume for Energy Balance at the Earth's Surface

In the absence of evaporation or condensation at the surface, the energy balance yields

$$q + \sigma T^4 + k_s \, dT_s / dz - (1 - \alpha) I_{solar} - I_{longwave} = 0 \qquad (9.1.43)$$

The heat flux to or from the soil is approximately 10% of the net radiation flux to the atmosphere according to De Bruin and Holtslag. However, this simplification is no real substitute for the true value of the soil heat flux since heat transfer in the soil is by virtue of conduction, which is easy to calculate.

The outer part of the atmospheric boundary layer is called the *Ekman layer*. The Swedish mathematician Ekman was the first to solve the simplified Navier-Stokes equations for wind and temperature in this layer by assuming a constant eddy diffusion coefficient. The behavior of the Ekman layer is complicated and difficult to predict. Numerous experimental studies by researchers such as Buchlin and Olivari have shown empirical power law profiles to be applicable in quite a wide range of atmospheric conditions. The velocity profile is then given by

$$v_w = v_{wc} + (v_{wr} - v_{wc}) [(z - z_c)/(z_r - z_c)]^b \qquad (9.1.44)$$

where

v_{wr} = reference velocity selected for the particular application

z_r = reference height selected for the particular application

z_c = height of the constant flux layer

The planetary boundary layer thickness is selected often as the reference height, and the geostrophic wind is selected as the corresponding reference velocity. Although the *1/7 power law* is quoted frequently for neutral conditions, the value of the exponent *b* generally increases with increasing stability and surface roughness. Gee proposed

$$b = 0.143 + 0.244\, L_{mo}^{-1} + 0.22\, L_{mo}^{-2} \qquad (9.1.45)$$

On windy days or nights, particularly with thick clouds, the PBL is completely turbulent, and its depth is determined by wind speed and surface roughness. The wind profile can be expressed as

$$v_w / v_{wr} = (z / z_r)^b \qquad (9.1.46)$$

According to Panofsky and Dutton, the exponent *b* can be approximated by the following relation

$$b = 1 / \ell n(z / z_o) \qquad (9.1.47)$$

The same procedure is also applicable in the evaluation of the temperature profile in this layer. The temperature in the upper atmosphere will not change significantly during the span of a few days, and it is assumed the temperature gradient conforms to the International Standard Atmosphere. If no temperature readings in the upper atmosphere are available, one may assume the ISA holds for the remainder of the atmospheric boundary layer from which it is possible to estimate the temperature at the top of the Ekman layer.

The most significant variations in temperature appear in the lower 100 m of the PBL or SBL. In general, the approximate temperature distribution in the SBL can be expressed by the following relation:

$$\frac{T - T_o}{T_r - T_o} = \left(\frac{z}{z_r}\right)^{b_T} \tag{9.1.48}$$

where

T_o = temperature near ground level

T_r = reference temperature measured at the reference height

z_r = the reference height

In the case of an inversion, the reference height may correspond to a temperature near the point where the inversion ends, i.e., where $dT/dz = 0$. The data at these two elevations may also be employed to determine the constants in the simple relation

$$T = az^{b_T} \tag{9.1.49}$$

The pressure at any elevation in an inversion may be determined by substituting Equations 9.1.49 and 9.1.3 in Equation 9.1.1.

$$dp/dz = -pg/\left(aRz^{b_T}\right)$$

Upon integration of this equation, find

$$p = p_o \exp\left[-gz^{(1-b_T)}/\{aR(1-b_T)\}\right] \tag{9.1.50}$$

Example 9.1.1

Consider the inversion at 06h00 shown in Figure 9.1.3. According to Table 9.1.1, the temperature measured 1 m above ground level is 6.54 °C or 279.69 K, and the temperature at 96 m is 22.42 °C or 295.57 K. Obtain an expression for the temperature distribution according to Equation 9.1.49 and the pressure at any elevation in the inversion in terms of the pressure p_o at ground level.

Solution

For the given temperatures, find the constants

$$a = 279.69$$

and

$$b_T = 0.0121$$

in Equation 9.1.49 such that

$$T = 279.69\ z^{0.0121}$$

According to Equation 9.1.50

$$p = p_o \exp\left[-9.8z^{(1-0.0121)}/\{279.69 \text{x } 287.08(1-0.0121)\}\right]$$

$$= p_o \exp\left(-1.2355 \text{x} 10^{-4} z^{0.9879}\right)$$

9.2 Effect of Wind on Cooling Towers

Measurements performed on natural draft cooling towers subject to crosswinds indicate a rise in water temperature with increasing wind speed for a given heat rejection rate. This is illustrated in the literature by authors such as Preussag, Christopher and Forster, Van der Walt, West, Sheer and Kuball, Markòczy and Stämpfli, Baer, Dibelius and Eberhof, Olivari and Thiry,

Bourillot et al., Grange and Lecoeuvre, Trage and Hintzen, Caytan and Fabre, Du Preez and Kröger, Wei, Zhang, Liu, Du and Meng. Studies on dry-cooling towers show similar trends to those found in wet towers. In a dry tower, the rise in outlet water temperature or change in the difference between this temperature and that of the ambient air entering the tower, i.e., the change in approach temperature, may be expressed as:

$$\Delta T_{wo} = \Delta (T_{wo} - T_{ai}) = (T_{wo} - T_{ai})_w - (T_{wo} - T_{ai}) \qquad (9.2.1)$$

where

the first term on the right side of the equation = temperature difference during windy conditions

the second term = the difference in temperature in the absence of wind

Soon after the dry-cooling towers at Rugeley and Ibbenbüren were commissioned, their performance was reported to be measurably reduced during windy periods according to Preussag, Christopher, and Forster. Markòczy and Stämpfli report the results of measurements performed at the Gagarin, also known as Visonta or Màtra, power plant in Hungary. The trend of their data is similar to that observed at Rugeley up to wind speeds of 6 m/s. Above this value, the two sets of data diverge as shown in Figure 9.2.1. Measurements conducted by Van der Walt et al. on the Grootvlei 5 tower where the heat exchanger bundles are arranged horizontally in a rectangular pattern of A-frames suggest this layout is less sensitive to wind. Markòczy argues that the greater temperature difference in the Grootvlei towers ensures a better flow through the bundles and the towers appear to be less affected by the wind. Approximate correlations of wind data for different dry-cooling towers are shown in Figure 9.2.2 from Trage and Hintzen. The curve for Grootvlei 6 appears to be unrealistically low, and results are more likely to follow the dashed curve.

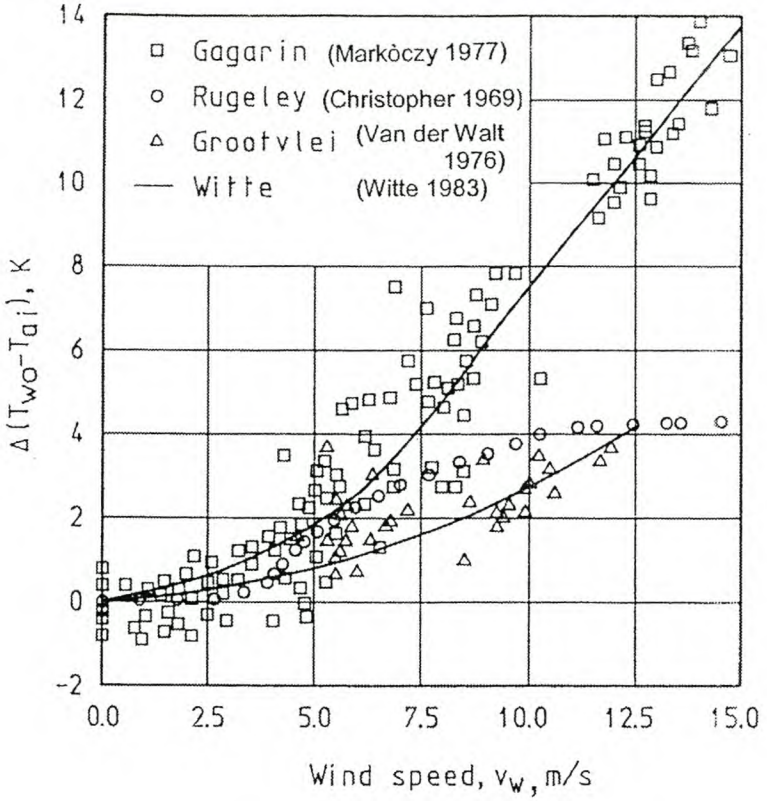

Fig. 9.2.1 Rise in Cooling Water Temperature due to Wind
Measured Approximately 10 m above Ground Level

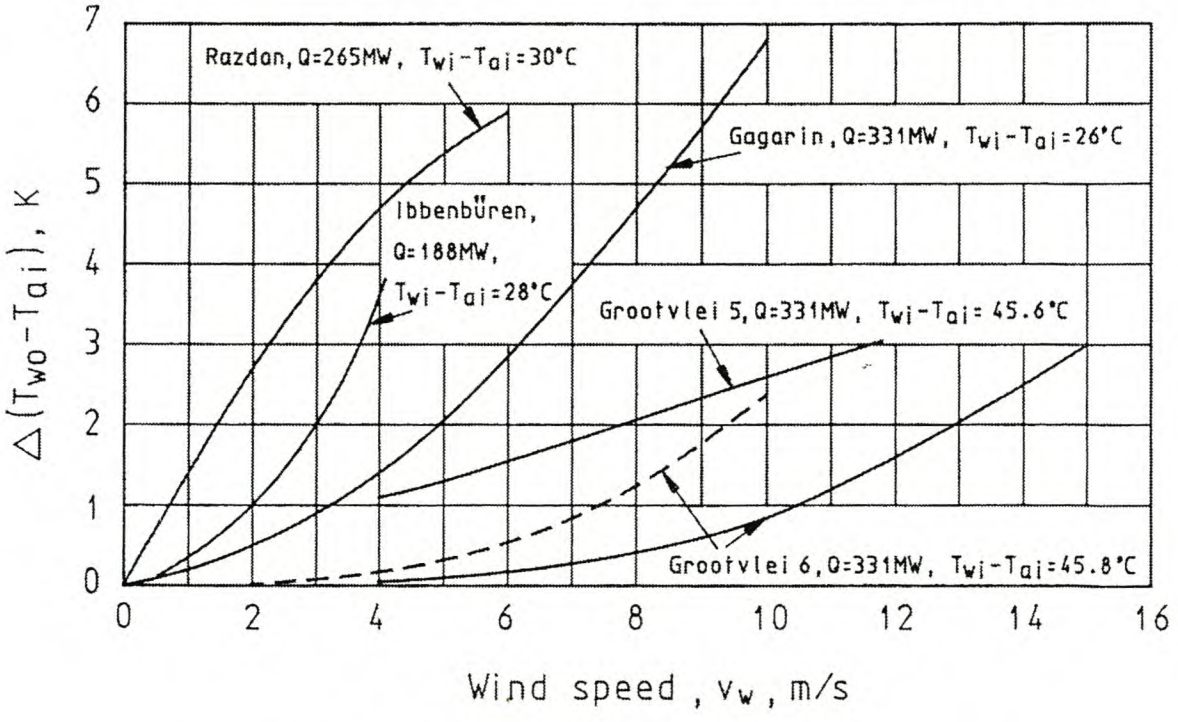

Fig. 9.2.2 Rise in Cooling Water Temperature due to Wind
Measured Approximately 10 m above Ground Level (Dry Towers)

Performance tests conducted on three towers at the Shahid Rajai power plant, suggest these towers are less sensitive to winds compared to other towers having vertical heat exchanger bundles according to Plánky and Sztrilich. The reason for this lower sensitivity is ascribed to the fact that these towers are higher and achieve a better draft and higher outlet air velocity. The effective flow resistance through the bundles is higher due to a reduced apex angle.

Wet towers with horizontal fills are also less sensitive to winds than crossflow towers. The change in temperature difference between the water outlet temperature and the wetbulb temperature of the entering ambient air, T_{wb}, for different wet towers is shown in Figure 9.2.3 according to Caytan and Fabre. According to Grange and Simon, all are counterflow towers except for Saint Laurent and Emile Huchet, which are crossflow towers. All wind speeds were measured at an elevation of 11 m above ground level.

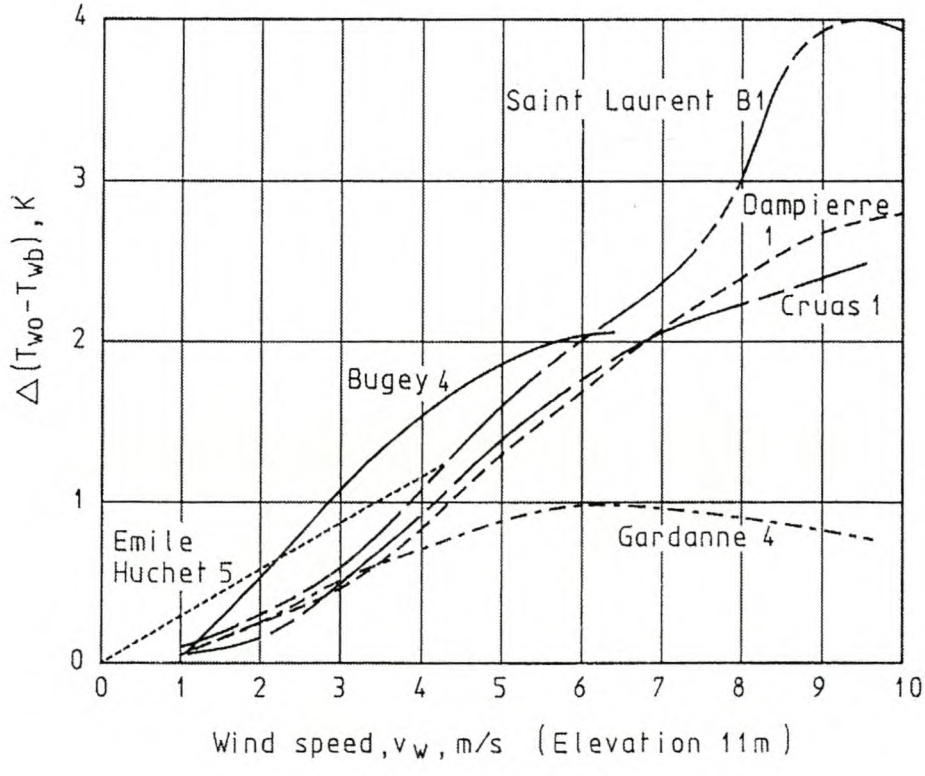

Fig, 9.2.3 Rise in Cooling-Water Temperature due to Wind (Wet Towers)

Generally, the scatter in the available test data may be due to a number of factors including:

- cold air inflow at low wind speeds
- variations in wind speed
- variations in wind direction
- variations in wind profile (according to Moore)
- inversions
- changes in ambient temperature
- changes in heat dissipated (according to Markòczy and Stämpfli)

Due to the variations in wind velocity, it is important to know the wind velocity distribution as well as the position and the height above ground level where the wind velocity was measured during any test. The closer to ground level the wind velocity is measured, the more sensitive the cooling tower will appear to be to a crosswind. Van der Walt et al. measured the wind velocity with a cup-type anemometer at the inlet height of the tower, and for the Grootvlei 6 tower it was measured 7.5 m above ground level. Markòczy only states the atmospheric conditions were obtained from a meteorologic station 500 m from the tower, but does not mention at which height the wind velocity was measured. He also states that the position of the cooling tower on which the measurements were performed was such that wind approaching from the prevailing wind direction was not disturbed by structures or obstacles. Caytan and Fabre, who published results of measurements performed on wet towers, used the wind velocity as measured at an elevation of 11 m as reference. Grange and Simon, who performed measurements on the Saint-Laurent wet tower, based his observations on the wind velocity 140 m above ground level obtained from a weather mast erected 200 m from the tower. Bourillot et al. used the wind velocity measured at the tower outlet elevation as reference. No details are given concerning the wind profiles. These would be different for the various tower sites.

The results of numerous model tests have been reported by authors such as Olivari and Thiry, Russell et al., Leene, Chaboseau, Ruscheweyh, Buxmann, and Völler. A few attempts have been made to predict the influence of winds on the performance of cooling towers by Witte, Völler, Buxmann, Du Preez and Kröger, and Wei et al. For a small-scale model, it is usually impossible to satisfy both the densimetric Froude number and the Reynolds number. In the past , model tests were based either on Froude's similarity or on isothermal tests

approximating Reynolds' similarity. Each of the techniques offer some advantage, but because all the dimensional groups are not satisfied in either of the approximations, each technique has its limitations.

Bourillot et al., Buchlin and Olivari, Grange and Simon, Ruscheweyh, and Sabaton et al. performed tests based on Froude's similarity. This was achieved by doing non-isothermal tests. Buchlin said these models allowed a realistic simulation of the possible interaction between the inlet and outlet thermal and aerodynamic phenomena. Fluid velocities obtained in these models are very low, and special measuring techniques usually have to be used. Consequently, the Reynolds numbers are approximately three orders of magnitude lower than those for a full-scale tower, which may result in erroneous results. Bourillot et al. observed large velocity fluctuations, and tests were repeated several times to eliminate random errors. Although heating models can be of value for comparative surveys of different tower shapes according to Ruscheweyh, it is still difficult to forecast the wind influence for a specific tower due to uncertainties in the measurements.

If the densimetric Froude number is neglected, isothermal tests may be performed according to Bouton, Russell et al, Bourillot et al., Leene, Chaboseau, Buxmann, Völler, Blanquet et al., and Vauzanges and Ribier. The natural draft phenomenon is not represented in these tests, and the tower draft is achieved by sucking or blowing a fluid through the model. Although the Reynolds numbers obtained in these tests are much higher than those found in non-isothermal models, they are still much lower than those found in full-scale towers. The advantage of this test method is that the main fluid velocity inside the tower can be determined easily because the fluid is forced through the model. The measurements performed on these models are accurate and stable, and both Bourillot et al. and Buchlin and Olivari obtained good reproducibility.

Witte et al. suggests the wind effect on the performance of a dry-cooling tower may be predicted by employing the external pressure distribution near the base of the cooling tower shell.

When a fluid flows across a cylinder, the static pressure varies circumferentially. A corresponding static pressure coefficient is defined as

$$C_p = (p_\theta - p_\infty) / (\rho_\infty v_\infty^2 / 2) \qquad (9.2.2)$$

where

p_θ = the local static pressure

the other variables refer to ambient conditions far from the cylinder

According to the potential flow theory, the distribution of this coefficient is shown in Figure 9.2.4.

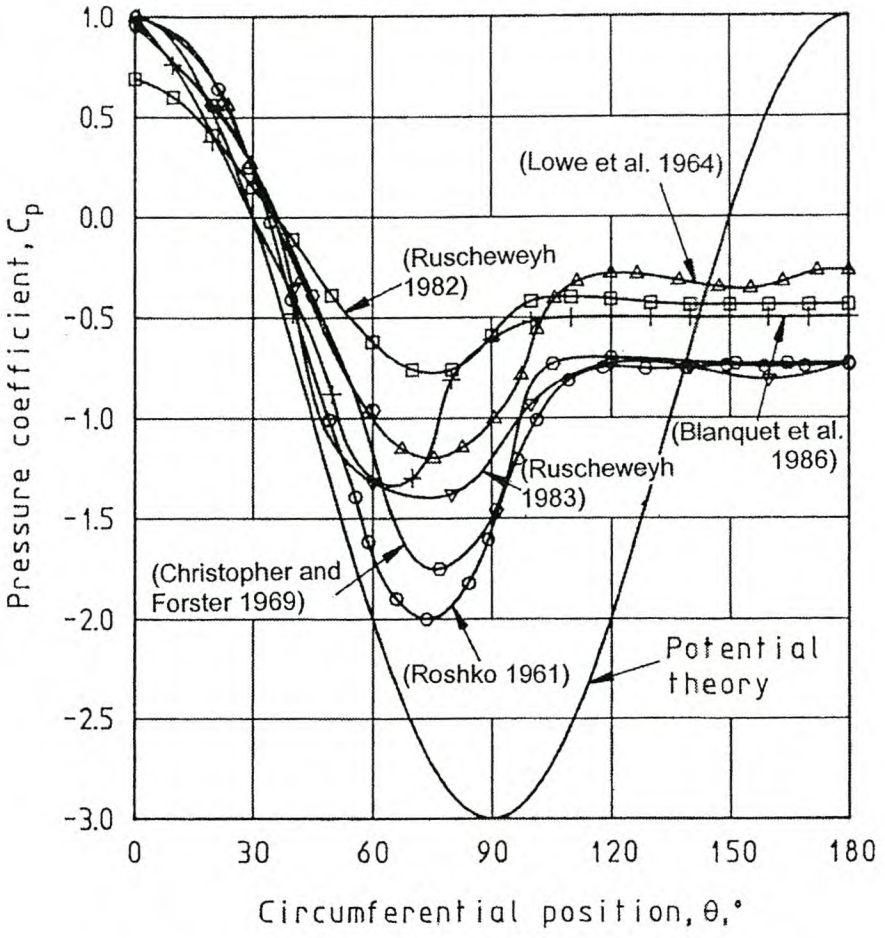

Fig. 9.2.4 Pressure Distribution about Cooling Tower

Actual pressure measurements performed on model towers at or near the lower edge of the shell or lintel are also shown in Figure 9.2.4. Roshko measured the pressure distribution about a cylinder at a Reynolds number of 8.4×10^6. His results are compared to the potential flow theory shown in Figure 9.2.4. Lowe, Christopher, and Ruscheweyh measured the pressure distribution near the inlet of a cooling tower model in a wind tunnel. Heat exchanger bundles were arranged horizontally in the inlet cross section of the tower in the tests conducted by Ruscheweyh, while vertical arrangements were tested in the other two cases. Some pressure distribution measurements about actual cooling towers have been reported by authors such as Ruscheweyh, Blanquet et al., Sun, and Gu.

To analyze the problem, the tower is divided circumferentially into an arbitrary number of sectors. The cooling tower energy and draft equations are applied to each sector. The ambient pressure is modified for each sector by introducing the corresponding local pressure coefficient. Finally, the contribution of all sectors are added to give the heat rejected by the tower.

At the point where the wind strikes the tower normally—the *stagnation point,* the pressure coefficient has a maximum value, and the total pressure at this point is greater than the ambient pressure. According to Witte, more cooling air will tend to flow through heat exchangers located at this point than at other locations. According to Markoczy and Stämpfli, this is true for towers with heat exchanger bundles arranged vertically around the base of the tower. However, it does not apply to horizontally installed bundles where the tower inlet air flow pattern is such that less air flows through the bundles located near the upwind side stagnation point according to Völler and Du Preez. Witte ignores any wind profile, the influence of wind induced air flow distortions through bundles arranged vertically in the form of deltas around the base of the tower (Fig. 1.2.15a), and effects at the outlet of the tower. However, his method satisfactorily predicts the reduction in performance due to wind in the Gagarin tower (Fig. 9.2.1). When his analysis was applied to the horizontally arranged bundles in the Grootvlei 5 tower, it was fortuitous that it predicted the trend of the data shown in Figure 9.2.1.

Buxmann and Völler performed isothermal model tests to determine the effect of different tower outlet shapes and the arrangement of the heat exchanger bundles on the performance characteristics of the cooling tower in the presence of wind. To quantify the influence of wind on the air mass flow rate through the tower, Buxmann defined pressure coefficients for the inlet, C_{pi}, and outlet, C_{po}, in terms of the static pressure difference between the throat of the tower and the ambient, i.e.,

$$C_{pi}, C_{po} = (\Delta p_w - \Delta p)/(\rho_w v_w^2/2) \qquad (9.2.3)$$

where

Δp_w = the static pressure difference with wind

Δp = the static pressure difference in the absence of any wind

the mean, air-mass, flow rate through the tower is the same in both cases

Their tests were all conducted for the same d_i/H_i ratio and, except for the vertical arrangement of the heat exchangers, a fixed value of heat exchanger loss coefficient. A uniform wind velocity distribution was maintained, and it was assumed this was representative of the mean value of a typical wind profile. The velocity distribution through the heat exchanger was measured in the presence of a crosswind, and a corresponding air-side heat transfer coefficient correction factor was defined to take into consideration the reduction in heat transfer due to the flow distortion.

By employing the results of these measurements, Völler evaluated the influence of winds on the performance of different cooling towers. Satisfactory agreement was found between the predicted and measured values for the Grootvlei 5 tower according to Van der Walt et al. The measured reduction in performance of the Rugeley tower reported by Christopher and Forster was underpredicted.

Du Preez and DuPreez and Kröger performed tests similar to those of Völler, but they extended the investigation to include:

- effects due to the conical inlet section of the tower
- a range of heat exchanger flow resistances
- different inlet diameter to height ratios, d_i/H_i
- effects due to tower supports
- wind velocity distribution
- different flow rates through the tower

The influence of the distorted air flow distribution through the heat exchanger was treated more rigorously. However, their tests were limited to cases where the heat exchanger bundles were arranged horizontally and covered the entire inlet cross-sectional area of the cooling tower. This arrangement is not typical of any practical cooling tower where bundles are usually installed in the form of A-frames or deltas covering only a part of the total available cross section.

Due to the influence of the different parameters on the value of the inlet pressure coefficient, it is not possible to find a simple correlation for C_{pi}. The following relation holds for cylindrical tower supports if it is accepted that the influence of the tower supports, the form of the wind profile, and the

taper angle of the tower shell on the value of C_{pi} vary linearly between the values for which the tests were done:

$$C_{pi} = \left[-0.57 + 0.0503 \left(\frac{v_{wo}}{v_m}\right)^{0.8} \left(\frac{d_i}{H_i}\right)^{-0.64} - 1.2/\exp\left(2.4 \left(\frac{v_{wo}}{v_m}\right)\left(\frac{d_i}{H_i}\right)^{-0.8}\right)\right]$$

$$\text{x}\left[1 - \left\{\frac{0.0067}{\exp(0.2\,K_{he})}\right\}\left\{40 - 6\left(\frac{v_{wo}}{v_m}\right)\left(\frac{d_i}{H_i}\right)^{-0.8}\right\}\right]$$

$$+\left[\left[-0.6 + 0.01\left(\frac{d_i}{H_i}\right) + 0.054\left\{-0.65 + 0.06\left(\frac{d_i}{H_i}\right) + 0.1\,K_{he}\right.\right.\right.$$

$$\left.\left.\left.\text{x}\left(0.23 - 0.039\left(\frac{d_i}{H_i}\right) + 0.001\left(\frac{d_i}{H_i}\right)^2\right)\right\}\left(24 - \frac{v_{wo}}{v_m}\right)\right]\right.$$

$$\left.+\sin\left\{\left(\frac{v_{wo}}{v_m}\right)/\left(1 + \frac{0.17\,v_{wo}}{v_m}\right)\right\}/\exp\left\{\frac{v_{wo}}{7\,v_m} + 0.2\left(15 - \frac{d_i}{H_i}\right) + \frac{K_{he}}{20}\right\}\right]$$

$$\text{x}\,(1 - 0.978\,K_{tse})\{1 - (0.003\,\text{x}\,2\theta_c + 2b + 0.027\,\text{x}\,2\theta_c\,\text{x}\,b)\} \qquad (9.2.4)$$

for

$5 \le d_i/H_i \le 15$

$0 \le K_{he} \le 30$

$0 \le v_{wo}/v \le 24$

$0 \le b \le 0.2$

$0 \le 2\theta_c \le 24^\circ$

$0 \le K_{tse} \le 1.02$

The wind velocity, v_{wo}, in Equation 9.2.4 refers to the wind velocity at the top of the cooling tower. K_{he} is the value of the loss coefficient of the heat exchangers obtained at an arbitrary Ry value of 2×10^5. The mean free-stream velocity through the heat exchanger is v_m. The effective loss coefficient of the tower supports, K_{tse}, is defined as the sum of the K_{ts} values of the different rings of supports based on the circumferential inlet area of the cooling tower including tower supports. Furthermore, b is the value of the exponent in the power law used to approximate the wind profile defined by Equation 9.1.46.

As the loss coefficient for the tower supports, K_{tse}, approaches a value of 1.02, the second term in Equation 9.2.4 becomes zero. This implies that, under these conditions, C_{pi} is independent of the wind profile and the contraction angle of the cooling tower shell. The range of applicability of the equation can be extended to values of $K_{he} > 30$ if K_{tse} approaches its upper limit.

The wind effect at the outlet of a cooling tower has been studied by a number of investigators such as Eck, Dibelius, Bourillot et al., Buchlin and Olivari, Chaboseau, Ruscheweyh, Buxmann, and Völler.

A qualitative picture of the flow pattern at the outlet of the cooling tower in the presence of a crosswind is shown in Figure 9.2.5.

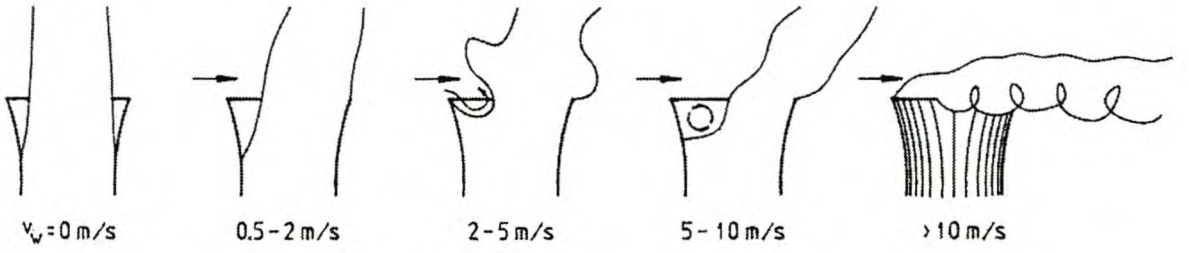

Fig. 9.2.5 Flow Patterns at Outlet of Cooling Tower for Different Wind Speeds

According to Du Preez and Kröger, the pressure coefficient at the outlet of a cooling tower is given by the following empirical relation:

$$C_{po} = -0.405 + 1.07\left(\frac{v_{wo}}{v_m}\right)^{-1}\left(\frac{A_o}{A_t}\right)^{-1.65} + 1.8\log_{10}\left[\left(\frac{v_{wo}}{2.7v_m}\right)\left(\frac{A_o}{A_t}\right)^{1.65}\right]$$

$$\times\left[\left(\frac{v_{wo}}{v_m}\right)\left(\frac{A_o}{A_t}\right)^{1.65}\right]^{-2} + \left[-1.04 + 1.702\left(\frac{A_o}{A_t}\right) - 0.662\left(\frac{A_o}{A_t}\right)^2\right]\left(\frac{v_{wo}}{v_m}\right)^{-0.7} \quad (9.2.5)$$

for

$1.8 \leq v_{wo}/v_m \leq 24$ if $A_o/A_t = 1$

$1.8 \leq v_{wo}/v_o \leq 12$ if $A_o/A_t \neq 1$

$0.893 \leq A_o/A_t \leq 1.232$

where

A_o = the tower outlet cross-sectional area

A_t = the throat area

This equation considers not only cylindrical outlets but also converging and diverging geometries. Experimental inlet and outlet pressure coefficients for particular operating and geometric conditions are compared graphically in Figure 9.2.6 using Equations 9.2.4 and 9.2.5 respectively.

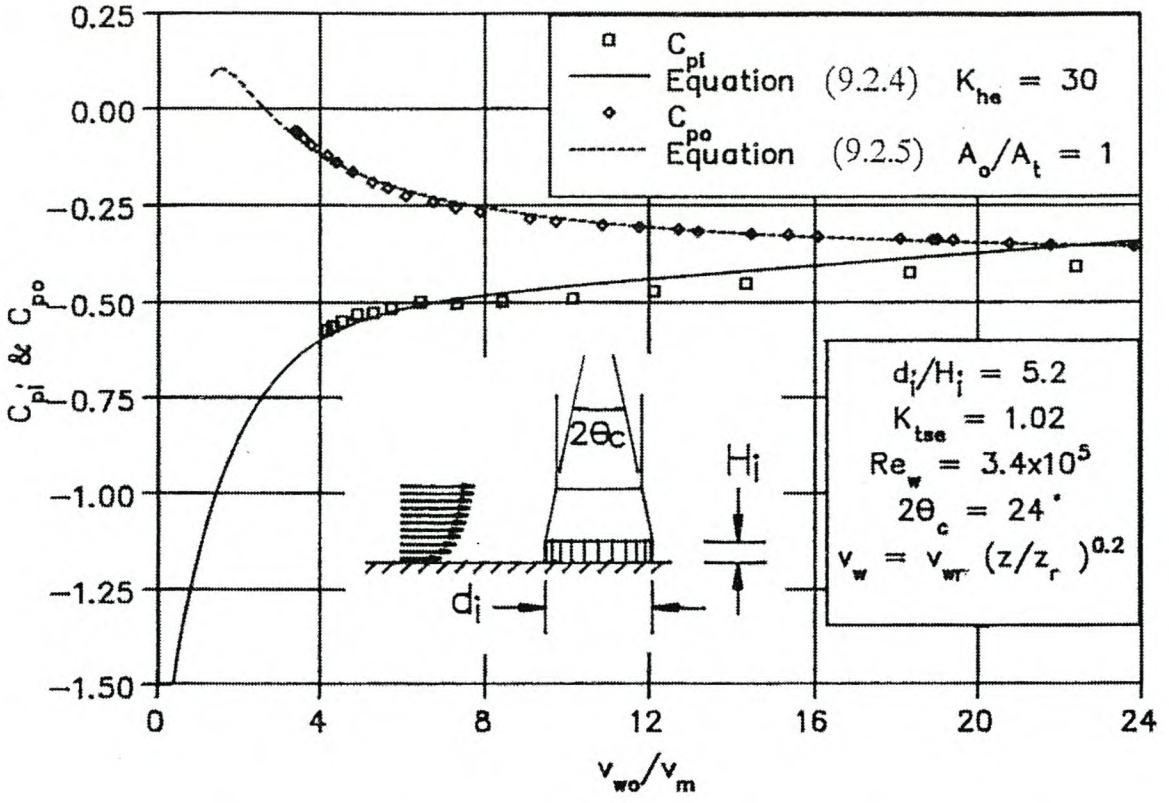

Fig. 9.2.6 Inlet and Outlet Pressure Coefficients according to Du Preez

Taking into consideration the pressure coefficients at the inlet and the outlet of the cooling tower, the draft Equation 7.1.14 is extended by Du Preez as follows:

$$p_{a1}\left[\{1-0.00975\,(H_3+H_4)/(2T_{a1})\}^{3.5}\{1-0.00975\,(H_5-H_3/2-H_4/2)/T_{a4}\}^{3.5}\right.$$

$$\left.-(1-0.00975\,H_5/T_{a1})^{3.5}\right]-C_{po}\,\rho_{w6}\,v_{w6}^2/2$$

$$+0.5\,C_{pi}\,\rho_{w6}\,v_{w6}^2\{1-0.00975\,(H_5-H_3/2-H_4/2)/T_{a4}\}^{3.5}$$

$$=(K_{ts}+K_{ct}+K_{he})_{he}\,(m_a/A_{fr})^2/(2\rho_{a34})[1-0.00975\,(H_5-H_3/2-H_4/2)/T_{a4}]^{3.5}$$

$$+(m_a/A_5)^2/(2\,\rho_{a5}) \qquad (9.2.6)$$

For a uniform air flow rate through a crossflow, finned-tube heat exchanger with two or more tube passes (essentially counterflow) as commonly found in a dry-cooling tower, the approximate heat transfer rate can be expressed in terms of the relevant effectiveness, e, listed in Table 3.5.1, i.e.,

$$Q \approx e\rho\, v_m \;\; A_{fr} \;\; c_p \left(T_{wi} - T_{ai}\right) \tag{9.2.7}$$

where

v_m = mean upstream air velocity

temperatures refer to inlet water and air values respectively

A crosswind distorts the velocity distribution through the heat exchanger according to Völler. As the wind increases, the flow through the heat exchanger becomes increasingly non-uniform with the maximum air speed at the lee side of the tower. On the upstream side, the air flow through the heat exchanger decreases due to flow separation at the inlet edge of the shell. Note that reverse flow may occur. An example of the velocity distribution observed in a model cooling tower is shown in Figure 9.2.7.

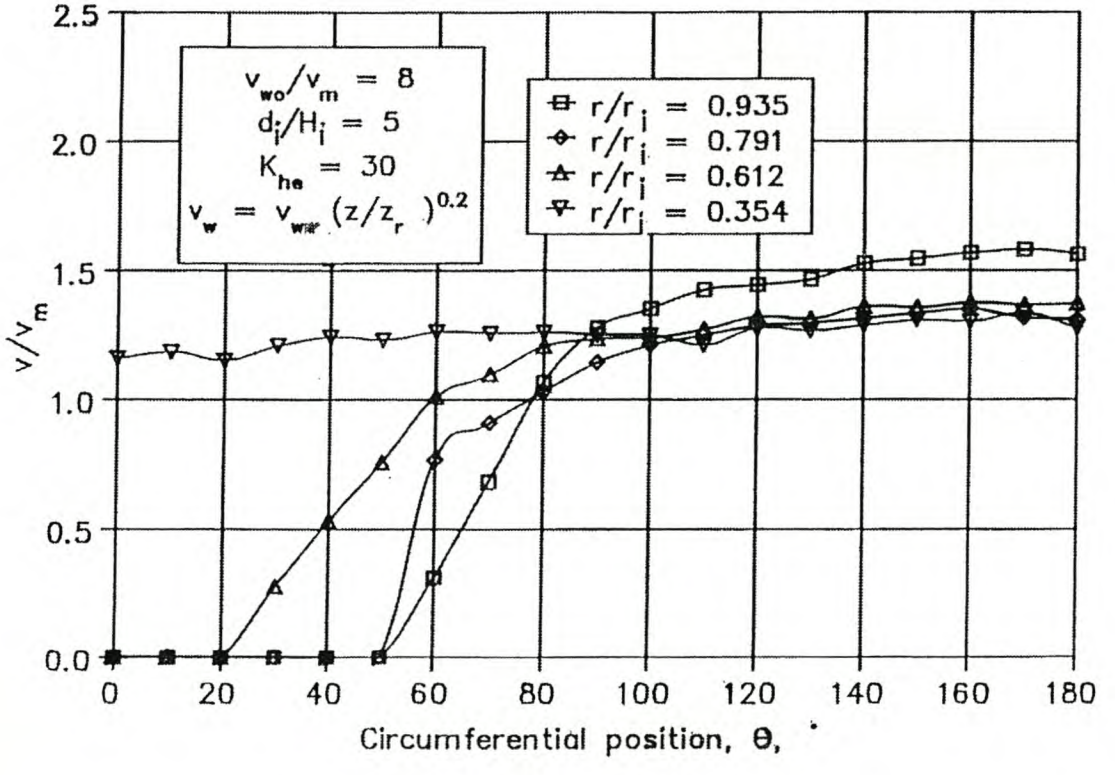

Fig. 9.2.7 Velocity Distribution through Heat Exchanger inside Cooling Tower according to Du Preez

The distorted or maldistributed air flow pattern through the heat exchangers reduces the effective heat transfer rate, which can be expressed in terms of a correction factor, i.e.,

$$Q_e = \alpha_Q \, Q \tag{9.2.8}$$

where

$$\alpha_Q = \int_{A_{fr}} \rho \, v \, c_p \, e \, d \, A_{fr} \, / \, (\rho \, v_m \, A_{fr} \, c_p \, e) \tag{9.2.9}$$

In an air-cooled heat exchanger, the effectiveness, e, is a function of UA and

$$UA \propto Ry^{b_{UA}}$$

where

$b_{UA} \approx 0.45$ for dry-cooling towers

The following empirical relation for α_Q is based on experimentally obtained data:

$$\alpha_Q = \left[1 - \frac{\left(\frac{v_{wo}}{v_m}\right)^{3.6} \exp\left(-\frac{v_{wo}}{3.75 v_m}\right) v_m^{0.576}}{3561} \right]$$

$$\times \left[0.98 + 0.02 \left\{ \exp\left(5.2 - \frac{d_i}{H_i}\right) + \exp\left(-\frac{v_{wo}}{v_m}\right) \right\} \right]$$

$$- (1.5 - 0.05 K_{he}) \left[\left\{ 0.013 - 0.0048 \left(\frac{d_i}{H_i}\right) + 0.000302 \left(\frac{d_i}{H_i}\right)^2 \right\} \right.$$

$$+ \left(\frac{v_{wo}}{v_m}\right) \left\{ 0.0134 - 0.00129 \left(\frac{d_i}{H_i}\right) + 0.000038 \left(\frac{d_i}{H_i}\right)^2 \right\}$$

$$\left. + \left\{ 0.0035 + 0.00206 \left(\frac{d_i}{H_i}\right) - 0.000085 \left(\frac{d_i}{H_i}\right)^2 \right\} \sin\left(\frac{v_{wo}}{1.9 v_m}\right) \right]$$

$$- \left(0.0053 - \frac{K_{he}}{9182}\right) (11.26 - 25.64 b_{UA}) \left(\frac{v_{wo}}{v_m}\right) \tag{9.2.10}$$

for

$5.2 \leq d_i/H_i \leq 15$

$10 \leq K_{he} \leq 30$

$0 \leq v_{wo}/v_m \leq 12$

$0 \leq b \leq 0.2$

$0 \leq K_{tse} \leq 1.02$

$0.4 \leq b_{UA} \leq 0.5$

$1 \leq v_m \leq 4$ m/s

If $\alpha_Q > 1$ in the previous equation, a value of $\alpha_Q = 1$ is assumed.

To determine the operating point of a dry-cooling tower subject to crosswinds, the density of the air in the cooling tower must be known. Since the temperature distribution of the air leaving the heat exchanger is not uniform and the degree of mixing in the tower is unknown, the mean density cannot be evaluated accurately.

One extreme would be to assume the air just above the heat exchangers is perfectly mixed. A mass mean air temperature would be used to calculate the tower draft, i.e.,

$$T_{a4} = Q_e/(m_a c_{pa34}) + T_{a3} \tag{9.2.11}$$

The other extreme would be to assume no mixing occurs. In this case, the lowest air temperature associated with the maximum air velocity through the heat exchanger would be employed to determine the draft. Based on experimental results, the maximum velocity through the heat exchanger can be expressed as

$$\frac{v_{max}}{v_m} = 1.014 - 0.0095\left(\frac{d_i}{H_i}\right) + 0.0014\left(\frac{d_i}{H_i}\right)^2$$

$$+\left\{-0.1265 + 0.0509\left(\frac{d_i}{H_i}\right) - 0.00245\left(\frac{d_i}{H_i}\right)^2\right\}\left(\frac{v_{wo}}{v_m}\right)(1 - 0.26\,b)$$

$$+\left[-0.362 + 0.0865\left(\frac{d_i}{H_i}\right) - 0.00321\left(\frac{d_i}{H_i}\right)^2\right.$$

$$\left.+\left\{0.288 - 0.0572\left(\frac{d_i}{H_i}\right) + 0.00242\left(\frac{d_i}{H_i}\right)^2\right\}\left(\frac{v_{wo}}{v_m}\right)\right](1.5 - 0.05\,K_{he}) \qquad (9.2.12)$$

for

$5.2 \leq d_i/H_i \leq 15$

$10 \leq K_{he} \leq 30$

$0 \leq v_{wo}/v_m \leq 12$

$0 \leq b \leq 0.2$

$0 \leq K_{tse} \leq 1.02$

This approach would give the more pessimistic tower performance. The actual operating point of a cooling tower will be at a point between the two extreme values obtained by the previous methods.

With these equations, it can be shown that the wind effect on the performance of a particular cooling tower (Example 9.2.1) decreases as shown in Figure 9.2.8. The tower height is increased while the heat rejection rate and other geometric parameters remain unchanged according to Du Preez. This is in agreement with similar findings published by Moore.

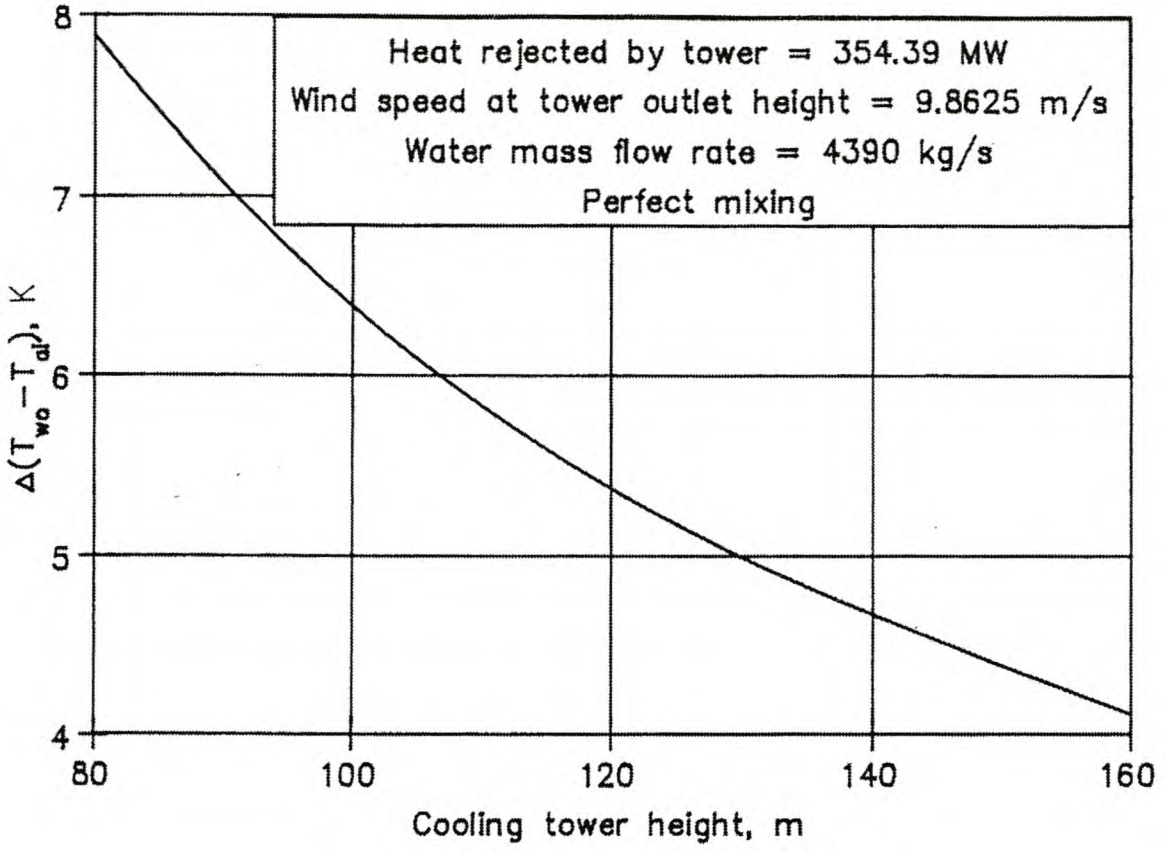

Fig. 9.2.8 Change in Approach Temperature with Cooling Tower Height

The previous empirical equations are based on experimental results, and the applicability is limited. More useful results can only be obtained by conducting tests in larger and more detailed models or by resorting to extensive numerical analysis of the problem such as those by Radosavljevic and Spalding, Du Preez, and Du Preez and Kröger.

Du Preez and Kröger studied the influence different tower supports have on performance during windy periods. They found that radially elongated supports have a beneficial effect under these conditions. This confirmed the experimental findings of Vauzanges and Ribier.

By employing a numerical approach, the effect of the heat exchanger arrangement and windbreak walls on the performance of natural-draft dry-cooling towers was investigated by Du Preez and Kröger. Body-fitted co-ordinates, which almost coincide with polar co-ordinates, are used to define the shape of a three-dimensional dry-cooling tower 165 m high with an inlet height of 24.5 m and an inlet diameter of 144.5 m. At the inlet of the

computational domain, a non-uniform wind velocity distribution was specified with the value of the exponent in Equation 9.1.46, i.e., b = 0.16. As a first approximation, finned tube heat exchanger bundles were simulated horizontally (no A-frame) over the entire inlet cross section of the tower.

The results of the calculations are given by curve 1 in Figure 9.2.9. The experimental results, obtained for a model cooling tower similar to that used in the numerical procedure, are shown by curve 2 in Figure 9.2.9. Good agreement between the results predicted by the two methods is obtained for high wind velocities, and the numerical procedure becomes more optimistic at lower wind speeds. The flow field about the tower is shown in Figure 9.2.10 for a wind speed of 12 m/s at the top of the tower.

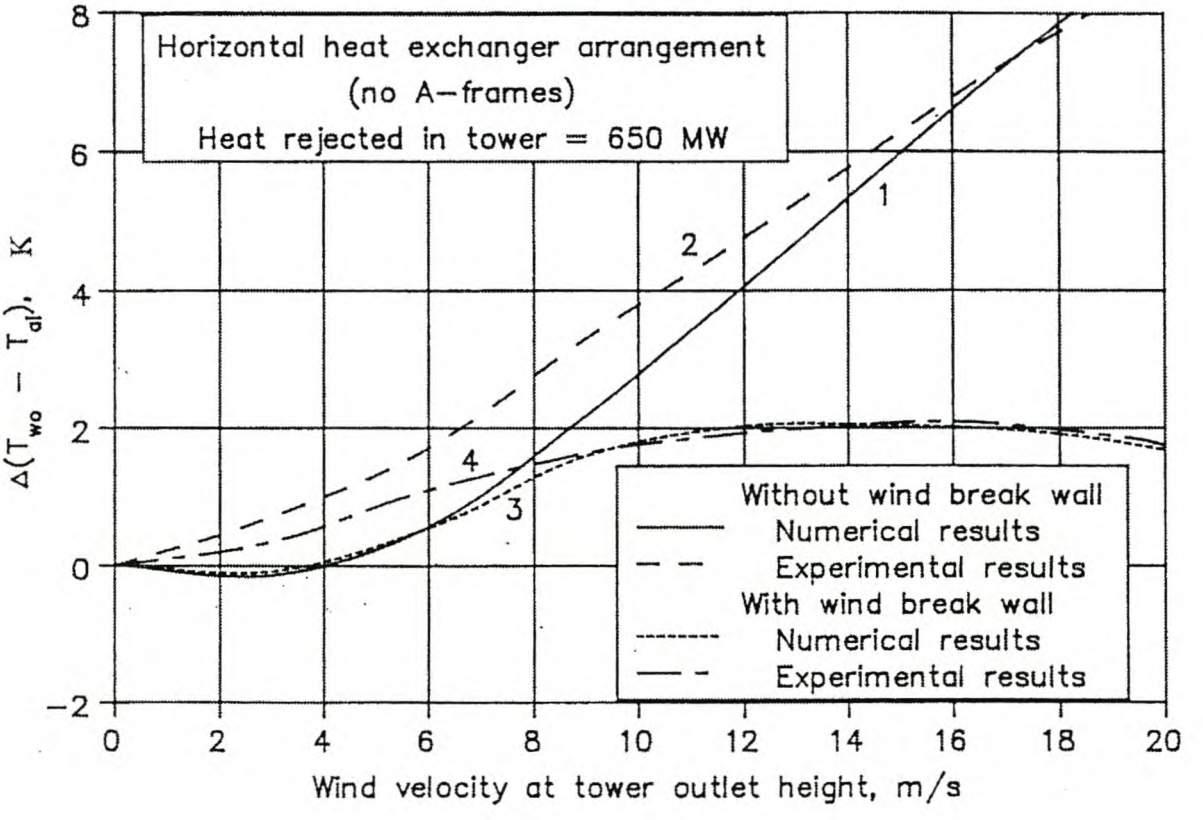

Fig. 9.2.9 Effect of Windbreak Wall on Tower Performance

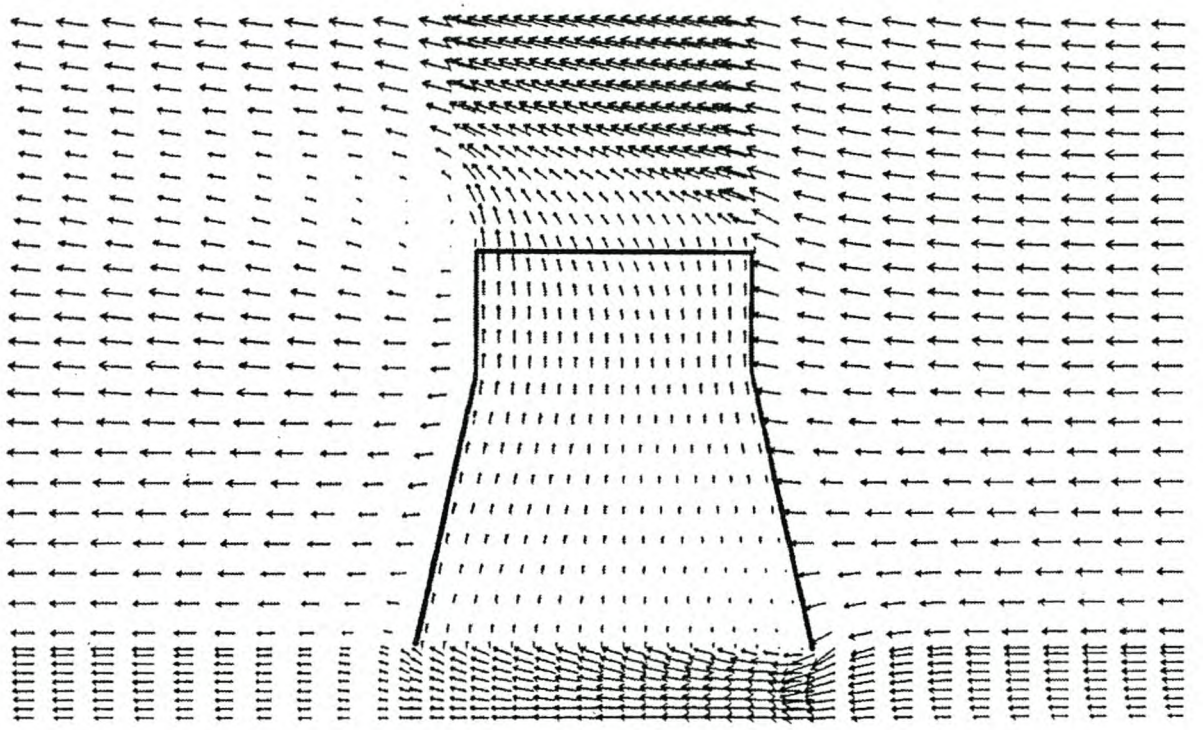

Fig. 9.2.10 Flow Field about Cooling Tower

The reduction in cooling tower performance during windy periods is mainly due to inlet effects. By installing windbreaks of two perpendicular porous walls in the form of a cross under the heat exchangers, this effect can be significantly reduced (Fig. 9.2.9) for the particular example. The loss coefficient of the porous wall is correlated by

$$K_{wall} = 2\Delta p/\rho v^2 = 37.39\ v^{-0.5232} \qquad (9.2.13)$$

where

Δp = difference in pressure across the wall

v = mean air velocity through the wall

Of course, the addition of windbreak walls will increase the initial costs of a tower. However, further calculations show the heights of these walls do not necessarily have to be equal to the inlet height of the tower to produce the best results. Figure 9.2.11 shows the relative increase in the heat rejection rate of the cooling tower as a function of the windbreak wall height and

different wall resistances—different porosities. The performance of the tower increases continuously as the height of the wall increases up to a wall height of approximately one-third of the inlet height of the tower. Further increases in the wall height yield no significant improvements. A slight reduction in the heat rejection rate of the tower is observed when the height of the wall approaches the inlet height of the tower. The latter trend is due to a deterioration of the velocity distribution through the heat exchangers shown by Figure 9.2.12.

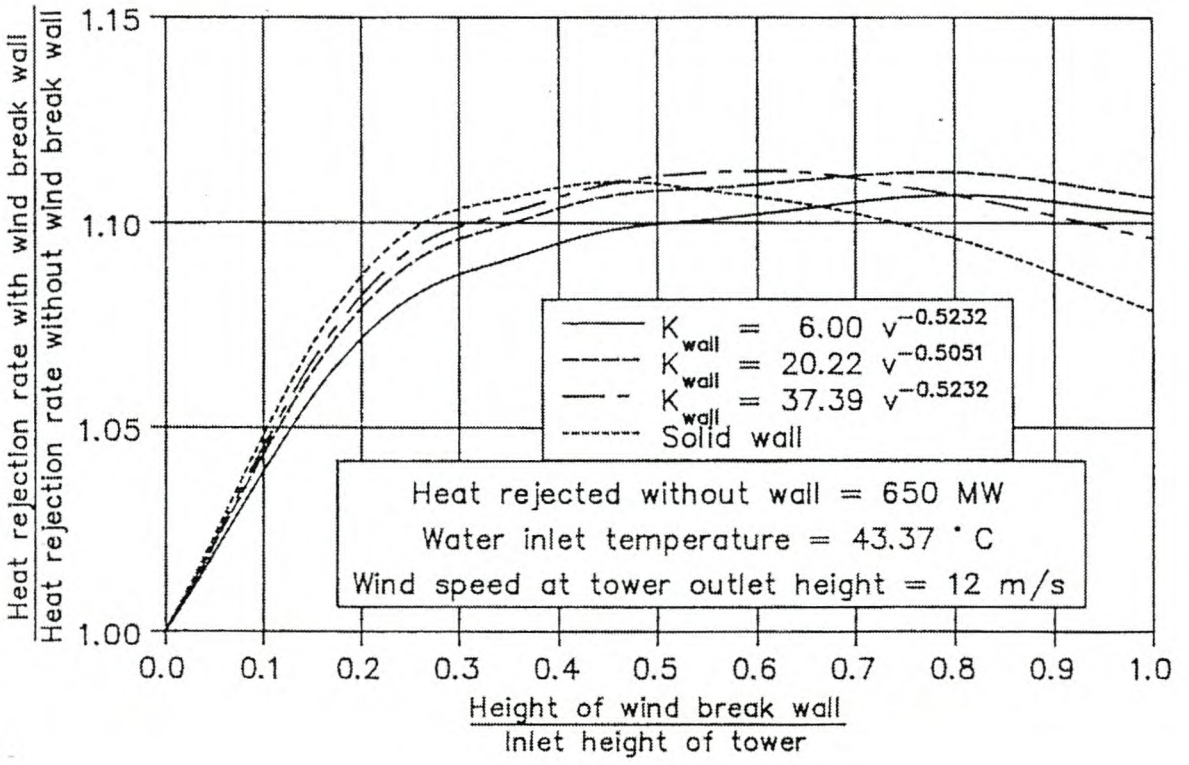

Fig. 9.2.11 Relative Change in the Heat Rejection Rate of a Tower as a Function of the Wall Height

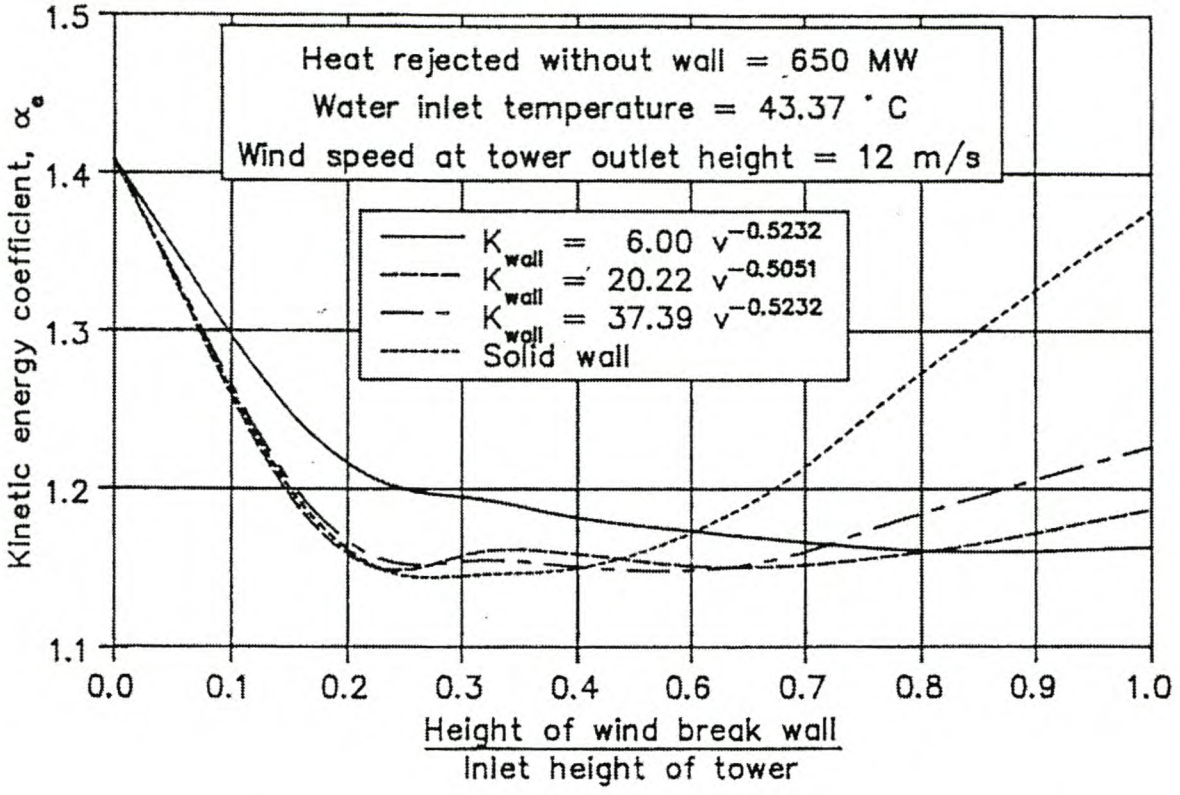

Fig. 9.2.12 Kinetic Energy Coefficient as a Function of the Wall Height

The heat exchanger layout in Figure 1.2.15(c) incorporating a central cylinder is also found to be less sensitive to wind when compared to the horizontal arrangement.

Du Preez and Kröger note the tower becomes less sensitive to winds as the heat rejection rate increases in a tower with heat exchangers arranged in A-frame forms and a radial pattern. This is due to a reduction in the effectiveness of the A-frame heat exchangers caused by distorted inlet air flow patterns. Curve 2 in Figure 9.2.13 shows the wind effect on a tower with similar dimensions to that described in the previous figure, but in this case, the heat exchangers are arranged radially in the horizontal inlet cross section of the tower.

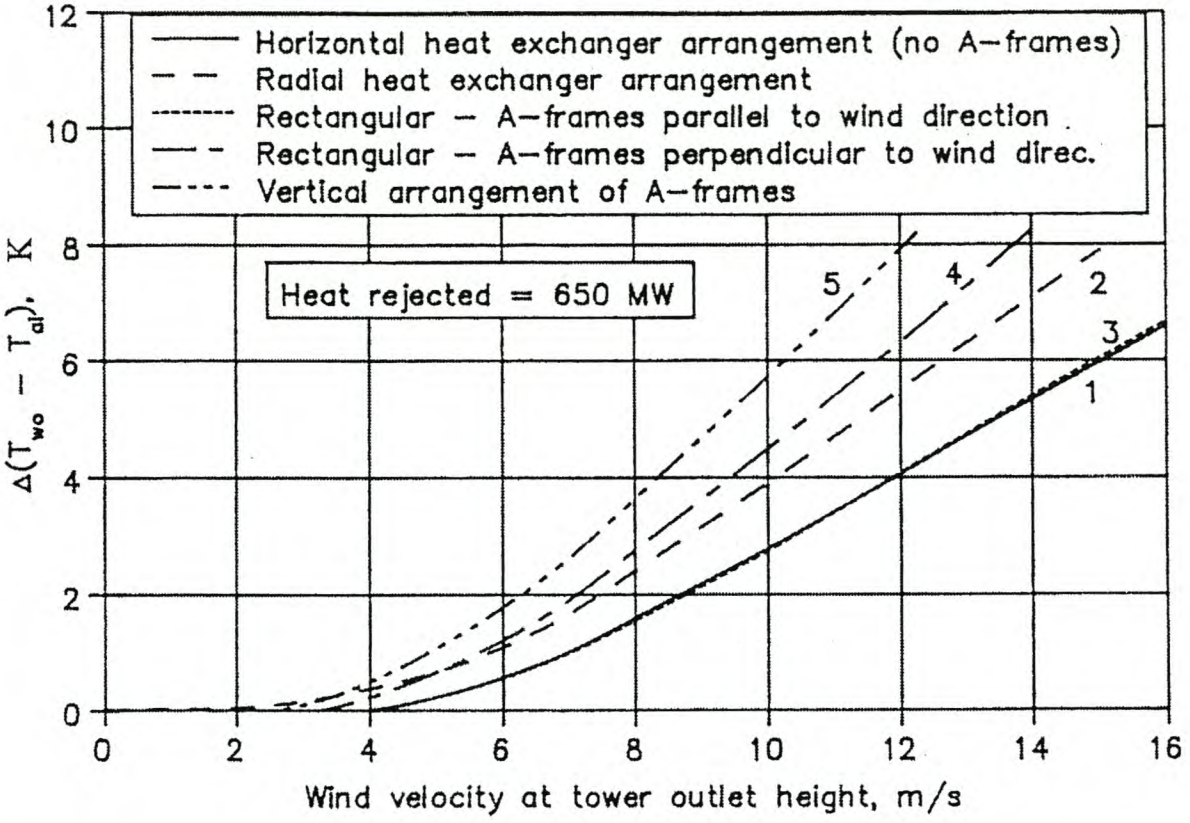

Fig. 9.2.13 Wind Effect on Tower with Different Heat Exchanger Arrangements

The tower dimensions, heat exchanger characteristics, and heat exchanger arrangement used in the numerical analysis correspond to that of the Kendal tower. Thus, the wind effect indicated by curve 2 in Figure 9.2.13 allows direct comparison with full scale measurements. In the Kendal tower, the finned tube heat exchangers are arranged radially in the form of A-frames with an apex angle of 60° in the horizontal inlet cross section. The wind velocity and temperature distribution was measured on a 96 m high weather mast 700 m from the tower. Air and water temperatures as well as the water flow rate through the tower were measured at the same time. The numerical prediction agrees favorably with the full scale measurements shown by curve 1 in Figure 9.2.14 from Du Preez and Kröger.

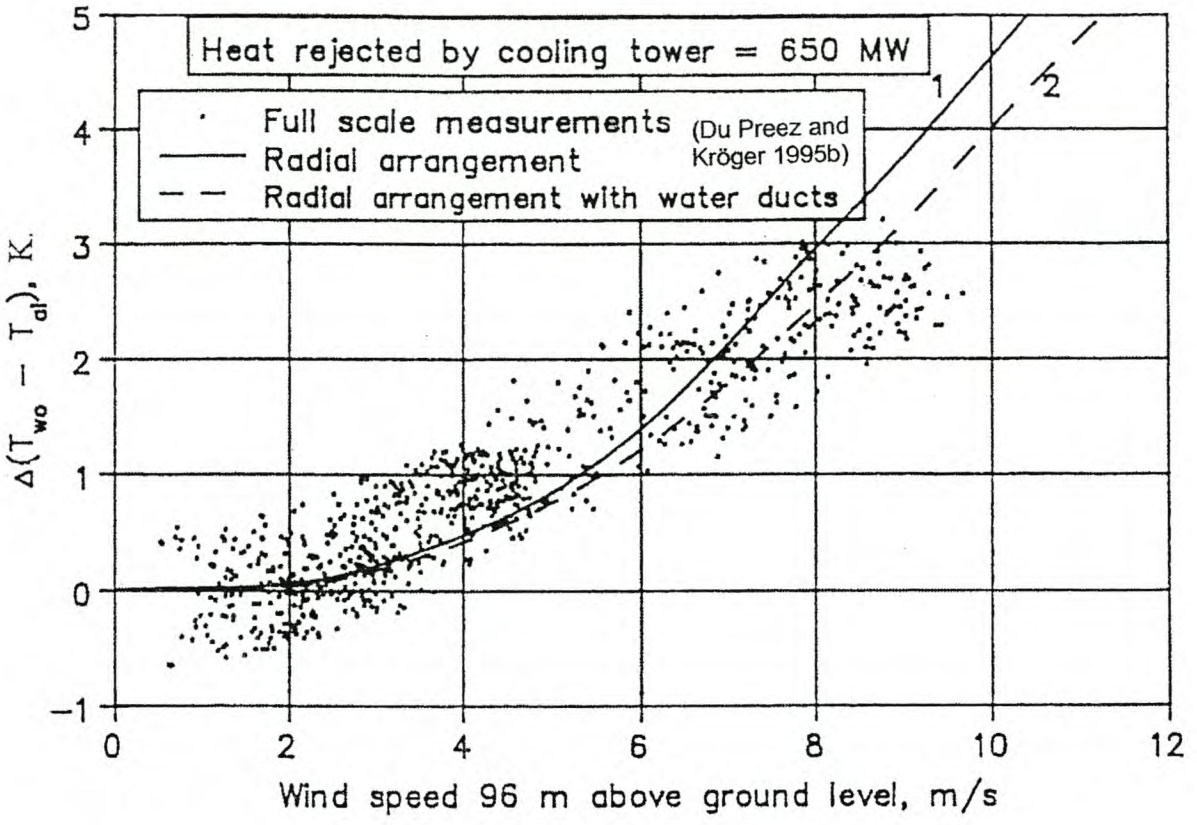

Fig. 9.2.14 Wind Effect on Kendal Tower

Water ducts and one or two storage tanks are usually located at the base of most dry-cooling towers. These act as windbreaks. For example, the water ducts in the Kendal tower are approximately 3 m in diameter, i.e., roughly one eighth of the inlet height of the tower. The effect of these ducts on the performance of the tower during windy periods is shown by curve 2 in Figure 9.2.14. This curve corresponds more closely with the full scale measurements, especially at higher wind speeds. If a 5 m high windbreak wall were installed on top of these ducts and increase the effective height to one-third the inlet height of the tower, a significant reduction in the wind effect can be expected when the wind blows perpendicular to the windbreak.

If A-frame heat exchangers are arranged in a horizontal rectangular pattern, the wind direction has a measurable effect on the tower performance. If the A-frames are positioned parallel to the wind direction, the effect of the A-frame is minimized with the wind influence on the tower correspondingly less as shown by curve 3 in Figure 9.2.13. Conversely, the tower performance deteriorates if the A-frames are positioned perpendicular to the wind direction as shown by curve 4.

Du Preez and Kröger found the wind effect on a tower with a vertical heat exchanger arrangement is higher than the predicted influence on a similar tower with a horizontal arrangement as shown by curve 5 in Figure 9.2.13. The latter trend is in direct agreement with full-scale observations. The adverse effect of wind on the mean mass flow rate through a tower with a vertical heat exchanger arrangement can be reduced by installing appropriate wind protecting devices around the tower inlet as suggested by Leene.

Factors affecting the performance of cooling towers during windy periods may thus be summarized as follows:

- Wind speed.
- Velocity distribution of approaching wind
- Heat rejected by cooling tower
- Mean air velocity through heat exchanger or fill
- Degree of mixing of air after heat exchanger or fill
- Transfer characteristics of heat exchanger or fill
- Loss coefficient of heat exchanger or fill
- Location and arrangement of heat exchanger or fill
- Height of cooling tower
- Ratio of inlet diameter to tower height, d_i/H_i
- Inlet taper and shape of shell
- Loss coefficient of tower supports
- Shape of tower supports
- Obstacles and structures in or near tower inlet

Example 9.2.1

Consider a cooling tower similar to the one described in Example 7.3.1 with a reduced tower inlet diameter of $d_3 = 78.3233$ m. The heat exchanger bundles are arranged horizontally rather than A-frame array and cover the entire inlet cross section of the tower. There are no obstructions on the air side of the heat exchangers, with the result that $L_{te} = L_t = 15$ m. The taper of the tower at the inlet is $2\theta_c = 20°$.

If the ambient conditions are similar to those specified in Example 7.3.1, determine the heat rejected by this tower and the corresponding water inlet and outlet temperatures.

Solution

By following the same procedure in Example 7.3.1, find

$$Q = 354.39 \times 10^6 \text{W}$$

where

water inlet temperature is $T_{wi} = 61.45^\circ\text{C}$

water outlet temperature is $T_{wo} = 42.136^\circ\text{C}$

Example 9.2.2

Determine the change in outlet water temperature given by Equation 9.2.1 for the cooling tower described in Example 9.2.1 if

- wind is 6 m/s
- elevation is 10 m above ground level

The wind velocity distribution is described by the power law with an exponent of $b = 0.2$ and

$$UA \; \alpha \; Ry^{0.46}$$

Employ the empirical Equations 9.2.4 to 9.2.12, and assume perfect mixing of the air occurs in the tower. The heat rejected by the tower is to remain unchanged, i.e.,

$$Q = Q_e = 354.39 \times 10^6 \text{ W}$$

Solution

A solution is obtained by following an iterative procedure similar to that described in Example 7.3.1. The following values are found to satisfy the energy and draft equations.

- Water inlet temperature: T_{wi} = 66.82794 °C
- Water outlet temperature: T_{wo} = 47.52647 °C
- Air mass flow rate: m_a = 10171.213 kg/s
- Air outlet temperature to satisfy energy equation: T_{a4} = 51.5887 °C
- Air outlet temperature to satisfy draft equation: T_{a4} = 50.059 °C
- Air temperature before the heat exchanger: T_{a3} = 15.4667°C
- Air density before the heat exchanger: ρ_{a3} = 1.02105 kg/m^3
- Mean air temperature through the heat exchanger:

$$T_{a34} = 0.5\ (T_{a3} + T_{a4}) = 0.5\ (15.4667 + 51.5887) = 33.5277°C$$

The following properties of dry air at this temperature are determined according to Appendix A:

- Density: ρ_{a34} = 0.960916 kg/m^3 using Equation A.1.1
- Specific heat: c_{pa34} = 1007.213 J/kgK using Equation A.1.2
- Dynamic viscosity: μ_{a34} = 1.8774805x10^{-5} kg/sm using Equation A.1.3
- Thermal conductivity: k_{a34} = 0.02673676 W/mK using Equation A.1.4
- Prandtl number: Pr_{a34} = 0.707274

Using Equation 9.2.11, if the air above the heat exchanger is perfectly mixed, the mass mean air temperature above the heat exchanger is given by:

$$T_{a4} = Q_e/(m_a c_{pa34}) + T_{a3} = 354.39 \times 10^6/(10171.213 \times 1007.213) + 15.4667 = 50.059\ °C$$

Using Equation 7.1.15, the density of the air corresponding to this temperature is

$$\rho_{a4} \approx 84600 / [287.08\ (273.15 + 50.059)] = 0.911766\ kg/m^3$$

Thus, using Equation 7.1.17, the harmonic mean density of the air through the heat exchanger is

$$\rho_{a34} = 2/(1/1.02105 + 1/0.911766) = 0.963318\ kg/m^3$$

According to the power law given by Equation 9.1.33, the wind velocity at the top of the cooling tower is

$$v_{w6} = v_{wr}\ (z / z_r)^{0.2} = 6(120 / 10)^{0.2} = 9.86251\ m/s$$

The mean air velocity based on the inlet cross-sectional area of the tower and the mean air density through the heat exchanger is given by:

$$v_m = 4\,m_a / \left(\pi\,\rho_{a34}\,d_3^{\,2}\right) = 4 \text{ x } 10171.213 / \left(\pi \text{ x } 0.963318 \text{ x } 78.3233^2\right) = 2.19145 \text{ m/s}$$

The ratio of the wind velocity at the outlet of the tower to the mean velocity is

$$v_{w6}/v_m = 9.86251 \;/\; 2.19145 = 4.50045$$

The loss coefficient for the specified heat exchanger can be determined at $Ry = 2 \text{ x } 10^5$, i.e.,

$$K_{he} = 1383.94795\; Ry^{-0.332458} = 1383.94795 \text{ x } (2 \text{ x } 10^5)^{-0.332458} = 23.91938$$

Substitute the previous relevant values into Equation 9.2.10, and find

$$\alpha_Q = \left[1 - (4.50045)^{3.6} \exp(-4.50045/3.75) 2.19145^{0.576} / 3561\right]$$

$$\text{x}\left[0.98 + 0.02\left\{\exp(5.2 - (78.3233/13.67)) + \exp(-4.50045)\right\}\right]$$

$$-(1.5 - 0.05 \text{ x } 23.91938)\left[\left\{0.013 - 0.0048 \text{ x } 78.3233/13.67\right.\right.$$

$$\left.\left. + 0.000302\,(78.3233/13.67)^2\right\}\right.$$

$$+ 4.50045\left\{0.0134 - 0.00129 \text{ x } 78.3233/13.67 + 0.000038\,(78.3233/13.67)^2\right\}$$

$$\left. + \left\{0.0035 + 0.00206(78.3233/13.67) - 0.000085\,(78.3233/13.67)^2\right\}\sin(4.50045/1.9)\right]$$

$$-(0.0053 - 23.91938/9182)(11.26 - 25.64 \text{ x } 0.46)\,4.50045 = 0.957662$$

The effective heat transfer rate given by Equation 9.2.8 is

$$Q_e = \alpha_Q\, m_a\, c_{pa34}\, (T_{a4} - T_{a3})$$

$$= 0.957662 \text{ x } 10171.213 \text{ x } 1007.213\ (51.5887 - 15.4667) = 354.39 \text{x} 10^6 \text{ W}$$

The air-side characteristic flow parameter defined by Equation 5.4.11 is

$$Ry = 10171.213 / (1.8774805 \times 10^{-5} \times \pi \times 78.3233^2/4) = 112441.11 \text{ m}^{-1}$$

The corresponding heat transfer parameter is

$$Ny = 383.61731 \times 112441.11^{0.523761} = 169580.452 \text{ m}^{-1}$$

Using Equation 5.4.13, find the effective heat transfer coefficient

$$h_{ae} A_a = 0.02673676 \times 0.707274^{0.333} \times 4818.06 \times 169580.452 \times 154/156$$
$$= 19216115.3 \text{ W/K}$$

The mean water temperature is

$$T_w = 0.5 (T_{wi} + T_{wo}) = 0.5 (66.82794 + 47.52647) = 57.1772 \text{ }^\circ\text{C}$$

At this temperature, the following properties of water are obtained according to the equations listed in Appendix A:

- Specific heat: c_{pw} = 4182.36 J/kgK using Equation A.4.2
- Dynamic viscosity: μ_w = 4.8384425x10^{-4} kg/sm using Equation A.4.3
- Thermal conductivity: k_w = 0.6504133 W/mK using Equation A.4.4
- Prandtl number: Pr_w = 3.111269

According to Equation 3.5.6, the heat given off by the hot water stream is

$$Q = 4390 \times 4182.36 \times (66.82794 - 47.52647) = 355.38 \times 10^6 \text{ W}$$

The Reynolds number for the water flowing inside the pipes is:

$$\text{Re}_w = m_w n_{wp} d_e / (A_{ts} n_{tb} n_b \mu_w)$$

$$= 4390 \times 2 \times 0.0216 / (3.664 \times 10^{-4} \times 154 \times 142 \times 4.8384425 \times 10^{-4}) = 48919.07$$

Using Equation 2.2.14, the friction factor inside the tube is

$$f_{Dw} = 0.3086 / \left[\log_{10}\left\{6.9/48919.07 + (5.24 \times 10^{-4}/3.7)^{1.11}\right\}\right]^2 = 0.0224$$

From Equation 3.2.29, it follows that

$$h_w = \frac{0.6504133 \text{ x } 0.0224 \text{ x } (48919.07 - 1000) \text{ x } 3.111269 \text{ x } \left[1+(0.0216/15)^{0.67}\right]}{8 \text{ x } 0.0216 \left[1+12.7\,(0.0224/8)^{0.5}\,(3.111269^{0.67}-1)\right]}$$

$$= 7209.95 \text{ W/m}^2$$

The total water-side area is given by

$$A_w = A_{ti}\, L_t\, n_{tb}\, n_b = 0.0679 \text{ x } 15 \text{ x } 154 \text{ x } 142 = 22272.558 \text{ m}^2$$

It follows that

$$UA = \left[\frac{1}{h_{ae}\, A_a} + \frac{1}{h_w\ \ A_w}\right]^{-1} = \left[\frac{1}{19216115.3} + \frac{1}{7209.95 \text{ x } 22272.558}\right]^{-1}$$

$$= 17162395.7 \text{ W/K}$$

The logarithmic mean temperature difference follows from Equation 3.5.8:

$$\Delta T_{\ell m} = \frac{(66.82794 - 51.5889) - (47.52647 - 15.4667)}{\ell n\left[(66.82794 - 51.5889) / (47.52649 - 15.4667)\right]} = 22.6165\,^{\circ}\text{C}$$

From Table B.8 in Appendix B, the crossflow correction factor is

$$F_T = 0.953369$$

From Equation 3.5.16 and with $\alpha_Q = 0.957662$, it follows that

$$Q = 17162395.7 \text{ x } 0.953369 \text{ x } 22.6165 \text{ x } 0.957662 = 354.39 \text{ x } 10^6 \text{ W}$$

This heat transfer rate is in agreement with the values obtained for the air and water streams respectively.

To determine the draft, various loss coefficients have to be evaluated.

For non-isothermal normal flow through the horizontal heat exchanger, it follows from Equation 5.4.23 that

$$K_{he} = 1383.94795 \text{ x } 112441.11^{-0.332458} + \frac{2}{(0.433^2)}\left(\frac{1.02105 - 0.911766}{1.02105 + 0.911766}\right)$$

$$= 29.56985$$

The tower inlet loss coefficient is found by substituting Equation 7.3.7 into Equation 7.1.22 to give

$$K_{cthe} = \left[0.072\left(\frac{78.3233}{13.67}\right)^2 - 0.34\left(\frac{78.3233}{13.67}\right) + 1.7\right]\left(\frac{0.963318}{1.02105}\right)\left(\frac{4818.06 \text{ x } 4}{\pi \text{ x } 78.3233^2}\right)^2$$

$$= 1.99595$$

The loss coefficient for the tower supports follows from Equation 7.1.21, i.e.,

$$K_{tshe} = \frac{2 \text{ x } 15.78 \text{ x } 0.5 \text{ x } 60 \text{ x } 4818.06^2 \text{ x } 0.963318}{(\pi \text{ x } 78.3233 \text{ x } 13.67)^3 \text{ x } 1.02105} = 0.54522$$

At the top of the cooling tower, the atmospheric pressure is given by Equation 7.1.6.

$$p_{a6} = 84600\ (1 - 0.00975 \text{ x } 120/288.75)^{3.5} = 83406.28 \text{ N/m}^2$$

For the horizontal bundle layout,

$$H_4 \approx H_3 = 13.67 \text{ m}$$

with the result that the air density at the top of the tower using Equation 7.1.11 is

$$\rho_{a5} = 83406.28 / [287.08\ \{323.209 - 0.00975\ (120 - 13.67)\}] = 0.90179 \text{ kg/m}^3$$

Similarly, the density of the ambient air at an elevation corresponding to the tower outlet given by Equation 7.1.12 is

$$\rho_{a6} = 83406.28 / [287.08\ (288.75 - 0.00975 \text{ x } 120)] = 1.010269 \text{ kg/m}^3$$

The ratio of the wind speed to the mean air velocity at the outlet of the tower is

$$v_{w5}/v_{a5} = \pi\, v_{w6}\, \rho_{a5}\, d^2{}_5 /(4m_a) = \pi \text{ x } 9.86251 \text{ x } 0.90179 \text{ x } 58^2 / (4 \text{ x } 10171.213)$$

$$= 2.31028$$

The outlet pressure coefficient for a cylindrical tower top section is given by Equation 9.2.5, i.e.,

$$C_{po} = -0.405 + \frac{1.07}{2.31028} + 1.8 \log_{10}\left(\frac{2.31028}{2.7}\right) / 2.31028^2 = 0.035316$$

The inlet pressure coefficient is given by Equation 9.2.4.

$$C_{pi} = \left[-0.57 + 0.0503 \text{ x } 4.50045^{0.8}\left(\frac{78.3233}{13.67}\right)^{-0.64}\right.$$

$$\left. -1.2/\exp\left\{2.4 \text{ x } 4.50045 \text{ x } \left(\frac{78.3233}{13.67}\right)^{-0.8}\right\}\right]$$

$$\text{x}\left[1 - \left\{\frac{0.0067}{\exp(0.2 \text{ x } 23.91938)}\right\}\left\{40 - 6 \text{ x } 4.50045\left(\frac{78.3233}{13.67}\right)^{-0.8}\right\}\right]$$

$$+\left[\left[-0.6 + 0.01\left(\frac{78.3233}{13.67}\right) + 0.054\left\{-0.65 + 0.06\left(\frac{78.3233}{13.67}\right) + 0.1 \text{ x } 23.91938\right.\right.$$

$$\left.\left. \text{x}\left(0.23 - 0.039\left(\frac{78.3233}{13.67}\right) + 0.001\left(\frac{78.3233}{13.67}\right)^2\right)\right\}(24 - 4.50045)\right]$$

$$+ \sin\{4.50045/(1 + 0.17 \text{ x } 4.50045)\}/\exp\{4.50045/7$$

$$+ 0.2\,(15 - 78.3233/13.67) + 23.91938/20\}]$$

$$\text{x}\,(1 - 0.978 \text{ x } 1.0)\,\{1 - (0.003 \text{ x } 20 + 2 \text{ x } 0.2 + 0.027 \text{ x } 20 \text{ x } 0.2)\} = -0.60406$$

With this value, evaluate the left side of the draft Equation 9.2.6.

$$84600\ [\{1 - 0.00975\ (13.67 + 13.67)/(2 \times 288.75)\}^{3.5}$$

$$\times \{1 - 0.00975\ (120 - 13.67/2 - 13.67/2)/323.209\}^{3.5} - (1 - 0.00975 \times 120 / 288.75)^{3.5}]$$

$$- 0.035316 \times 1.010269 \times 9.86251^2/2 - 0.5 \times 0.60406 \times 1.010269 \times 9.86251^2$$

$$\{1 - 0.00975\ (120 - 13.67/2 - 13.67/2)/323.209\}^{3.5} = 81.60\ N/m^2$$

For the right side of the equation, find

$$(0.54522 + 1.99595 + 29.56985)(10171.213/4818.06)^2/(2 \times 0.963318)$$

$$\times [1 - 0.00975\ (120 - 13.67/2 - 13.67/2)/323.209]^{3.5}$$

$$+ [10171.213 \times 4/(\pi \times 58^2)]^2/(2 \times 0.90179) = 81.66\ N/m^2$$

Because the values obtained for the left and right sides of the draft equation are practically the same, the draft equation is satisfied.

To maintain the same heat rejection rate, the change in the difference between the outlet water temperature and the entering ambient air under the specified wind conditions is

$$\Delta T_{wo} = (47.52647 - 15.6) - (42.136 - 15.6) = 5.39047\ ^\circ C$$

Example 9.2.3

Repeat example 9.2.2, but assume there is no mixing of the air above the heat exchangers. Assume the static pressure gradient above the heat exchangers is due to the hydrostatic pressure gradient of the coldest air leaving the heat exchanger. Find the change in outlet water temperature if the heat rejected by the tower remains unchanged, i.e.,

$$Q = 354.39 \times 10^6 W$$

Solution

By following an iterative procedure, find that the following values satisfy the energy and the draft equation.

- Water inlet temperature: T_{wi} = 68.2888 °C
- Water outlet temperature: T_{wo} = 48.9912 °C
- Air mass flow rate: m_a = 9756.793 kg/s
- Air outlet temperature to satisfy energy equation: T_{a4} = 53.21745 °C
- Air outlet temperature to satisfy draft equation: T_{a4} = 47.58163 °C

By repeating the calculation as in Example 9.2.2, find:

- the mean air inlet velocity v_{a34} = 2.093648 m/s
- the relative wind velocity v_{w5}/v_{a34} = 4.710681

By applying Equation 9.2.12, the ratio of the maximum air velocity to the mean inlet velocity is obtained, i.e.,

$$\frac{v_{max}}{v_{a34}} = 1.014 - 0.0095\left(\frac{78.3233}{13.67}\right) + 0.0014\left(\frac{78.3233}{13.67}\right)^2$$

$$+\left\{-0.1265 + 0.0509\left(\frac{78.3233}{13.67}\right) - 0.00245\left(\frac{78.3233}{13.67}\right)^2\right\} 4.710681\,(1 - 0.26 \times 0.2)$$

$$+\left[-0.362 + 0.0865\left(\frac{78.3233}{13.67}\right) - 0.00321\left(\frac{78.3233}{13.67}\right)^2\right.$$

$$\left.+\left\{0.288 - 0.0572\left(\frac{78.3233}{13.67}\right) + 0.00242\left(\frac{78.3233}{13.67}\right)^2\right\} 4.710681\right]$$

$$\times\,(1.5 - 0.5 \times 23.91938) = 1.44926$$

The maximum air velocity above the heat exchanger is

$$v_{max} = 1.44926 \times 2.093648 = 3.03424 \text{ m/s}$$

This is employed to determine the minimum air temperature above the heat exchanger. The characteristics of the heat exchanger are such that this temperature is found to be 47.58163 °C at a water inlet temperature of 68.2888 °C.

By following the procedure in example 9.2.2, find

$$\Delta T_w = (48.9912 - 15.6) - (42.136 - 15.6) = 6.8552\ ^\circ C$$

The performance characteristics for this particular cooling tower are shown in Figure 9.2.15 for different wind speeds. Du Preez finds a numerical solution of the problem tends to be optimistic at low wind speeds, but better agreement is obtained at higher wind speeds. Experimental and numerical results tend to be less reliable at high wind speeds. Excellent agreement is obtained in the case of no wind.

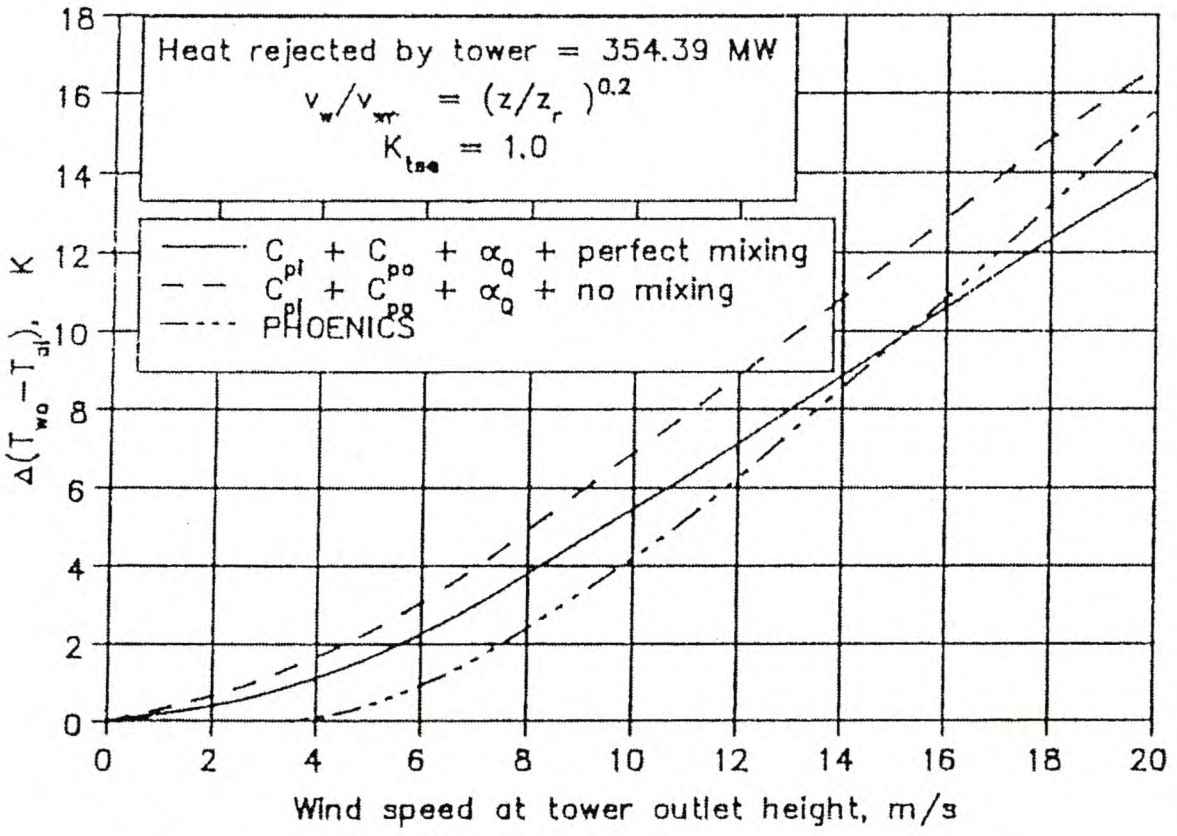

Fig. 9.2.15 Comparison of Predicted Cooling Tower Performance Characteristics

9.3 Effect of Wind on Air-Cooled Heat Exchangers

In general, winds have a negative effect on the performance of mechanical draft heat exchangers. Plume air recirculation tends to increase, while fan performance is usually reduced during windy periods.

Laboratory studies and field tests have shown the output of dry-cooled power stations may be significantly reduced by winds. As shown in Figure 9.3.1, the wind speed and direction significantly influences the turbine output at the Wydok power plant according to Schulenberg.

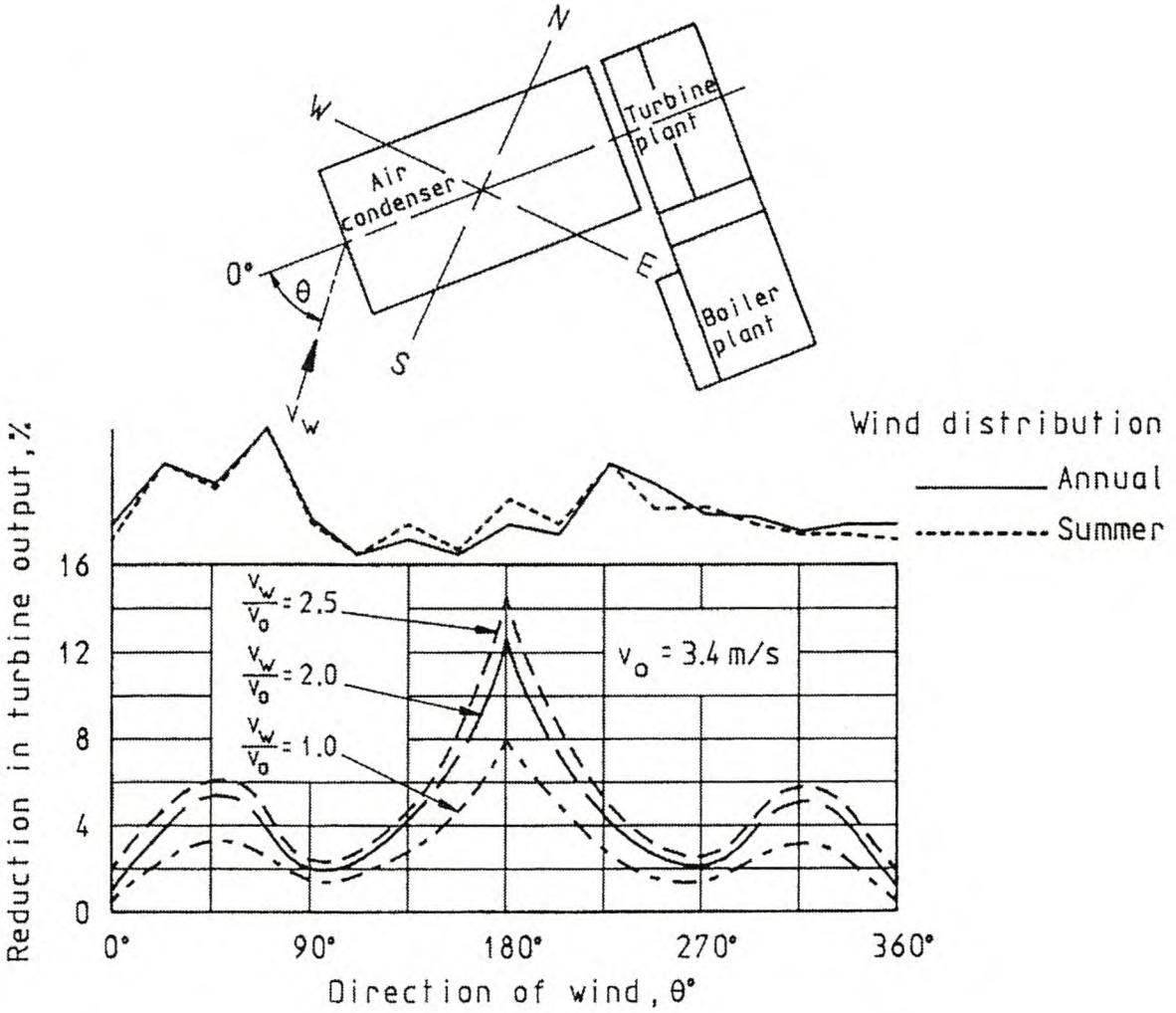

Fig. 9.3.1 Reduction in Turbine Output due to Wind at the Wyodak Power Plant

Before the 160 MWe power plant at Utrillas in Spain was built, extensive model tests were conducted. The tests used a scale of 1:150 to determine the optimum position of the air-cooled condenser and power plant orientation and also considered local wind patterns. The results of the tests are shown in Figure 9.3.2.

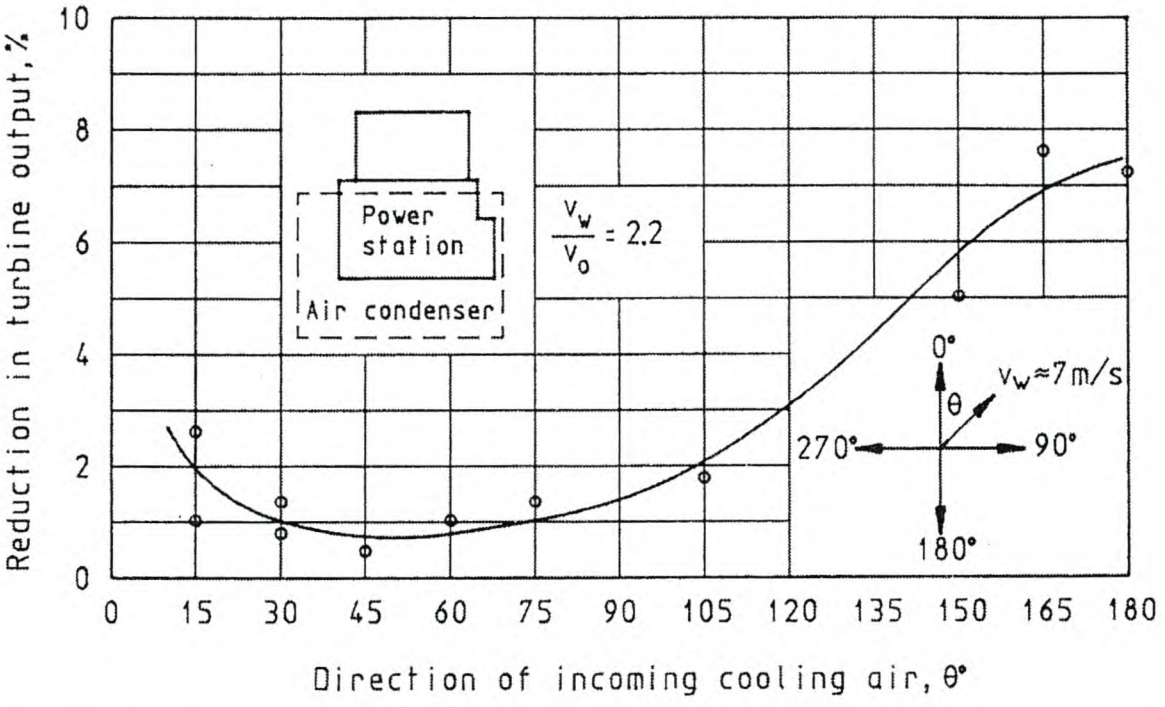

Fig. 9.3.2 Reduction in Turbine Output at the Utrillas Power Plant due to Wind

Goldschagg reports turbine performance at the Matimba power plant was reduced measurably during certain windy periods, and occasional turbine trips had occurred under extremely gusty conditions. After extensive experimental and numerical investigations, modifications to the windwalls and cladding were implemented (Fig. 9.3.3). Due to the improved air flow pattern into the air-cooled condenser during periods of westerly winds, no further trips were experienced and performance was significantly improved. This has been reported by Goldschagg, Vogt, du Toit, Thiart and Kröger, and Goldschagg.

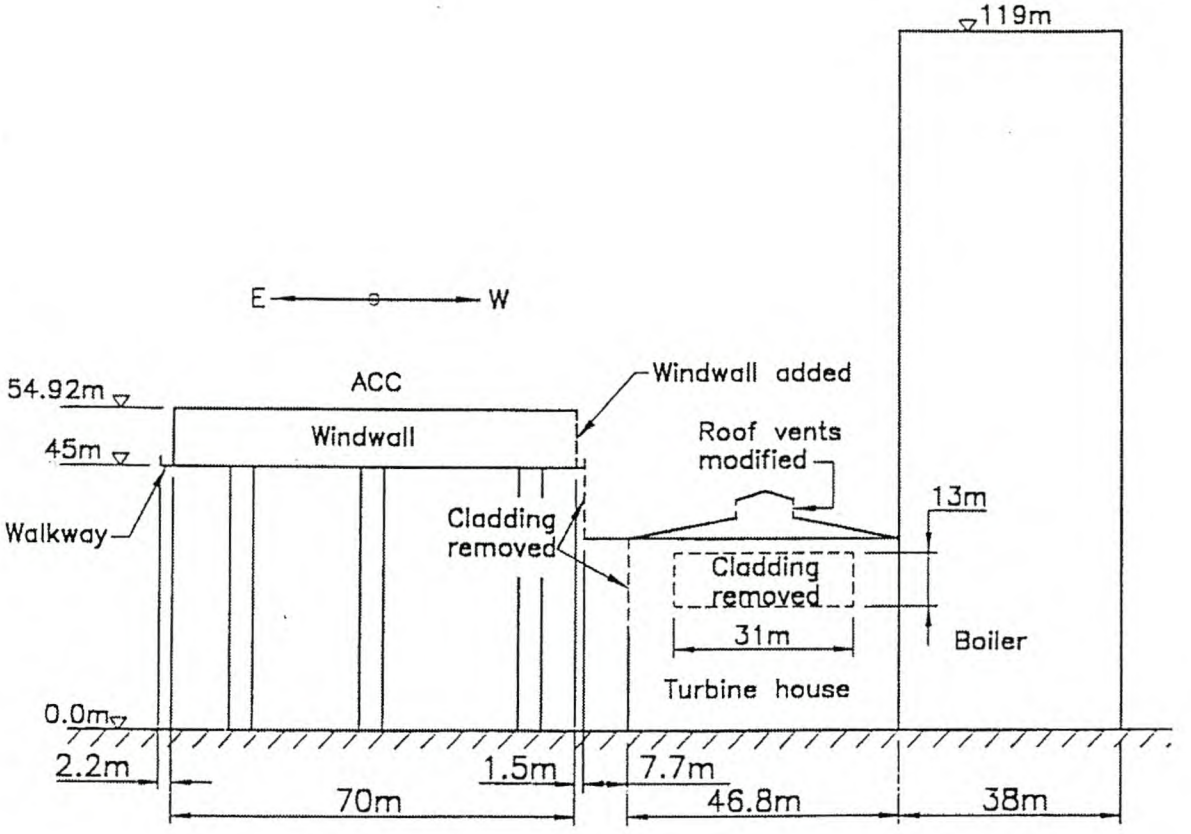

Fig. 9.3.3 Modifications at the Matimba Power Plant

From the case studies listed above, it is clear the interaction between the air-cooled heat exchanger and adjacent buildings or structures can significantly complicate flow patterns and reduce plant performance.

Kennedy and Fordyce report the results of model studies to determine the characteristics of downwind temperature distribution, recirculation, and interference, i.e., ingestion of an adjacent tower's effluent plume.

Slawson and Sullivan conducted experiments in a water flume to measure recirculation and interference for two conceptual configurations of forced-draft, dry-cooling towers. They studied both a rectangular array and a multiple round tower arrangement. The objective of the study was to investigate and make recommendations on the design and arrangement of cooling towers. Their goal was to provide optimum ambient air distribution to the heat transfer surfaces. Optimum air distribution is maintained by minimizing recirculation and interference. Recirculation and interference measurements of 40–70% were found to exist for the rectangular array concept, and values of 20–30% were measured for the round tower arrangement.

Field tests conducted by the Cooling Tower Institute (CTI) on induced mechanical draft cooling towers, clearly show a measurable increase of plume recirculation with an increase in wind speed when the wind blows in the longitudinal direction of the cooling tower bank. The results of numerous other experimental studies on recirculation have been reported by various researchers including Gunter and Shipes, Kennedy and Fordyce, Onishi and Trent, Slawson and Sullivan, and Ribier.

In addition to the effect of recirculation, the performance of the fans, especially in forced draft systems, are influenced during windy periods due to inlet air flow distortions.

Duvenhage and Kröger numerically modeled the air flow patterns about and through an air-cooled heat exchanger during windy conditions taking into consideration the coupled effects of both recirculation and fan performance. They considered a long heat exchanger bank shown in Figure 9.3.4 consisting of bays. Each bay had two 6-blade, 4.31 m diameter fans. The heat exchanger is subjected to winds blowing across or parallel to the longitudinal axis and having a velocity distribution given by Equation 9.1.46 with $b = 0.2$ as recommended by VDI 2049, i.e.,

$$v_w = v_{wr}(z / z_r)^{0.2}$$

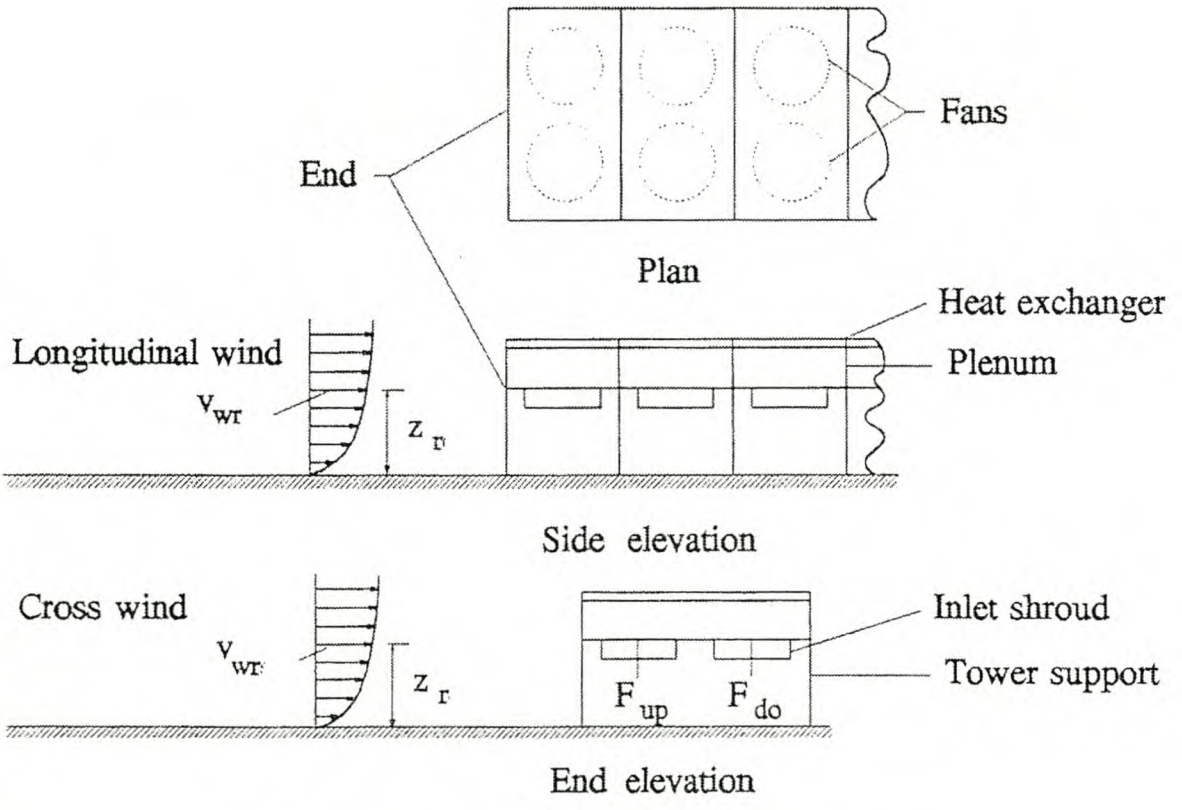

Fig. 9.3.4 Schematic of Air-Cooled Heat Exchanger

A more detailed cross section of the bay is shown in Figure 9.3.5. Each bay has

- an effective bundle frontal area of 7.07 m x 10.2 m = 72.12 m^2
- a tube bundle height of 0.72 m.

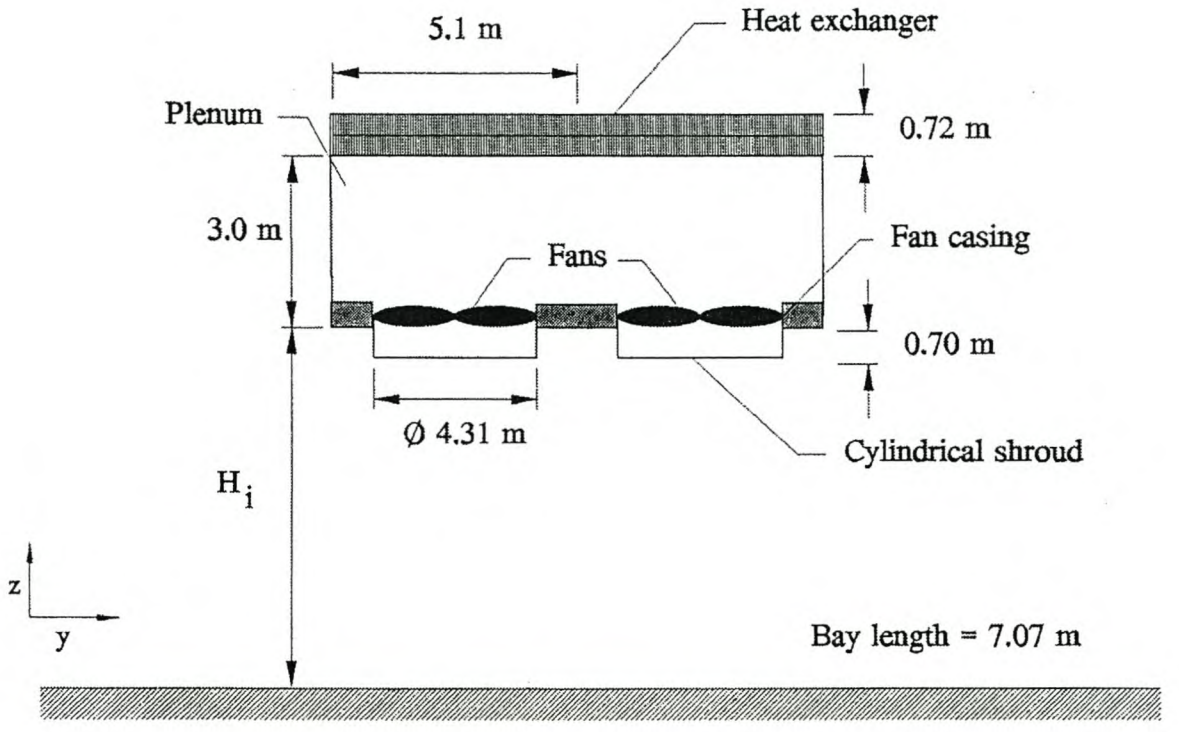

Fig. 9.3.5 Details of Bay Geometry

The fans have cylindrical inlet shrouds. The fan platform or inlet height H_i = 5.7 m, and the plenum chamber is 3 m high. With increasing wind speed, the air volume flow rate through the upwind fans, F_{up}, is reduced due to flow distortions. The flow through the downwind fans, F_{do}, may actually increase slightly (Fig.9.3.6) due to the increased kinetic energy in the air stream. However, the air-cooled heat exchanger performance is reduced due to a net decrease in mean air-volume flow rate through the fans, F_m, during windy periods.

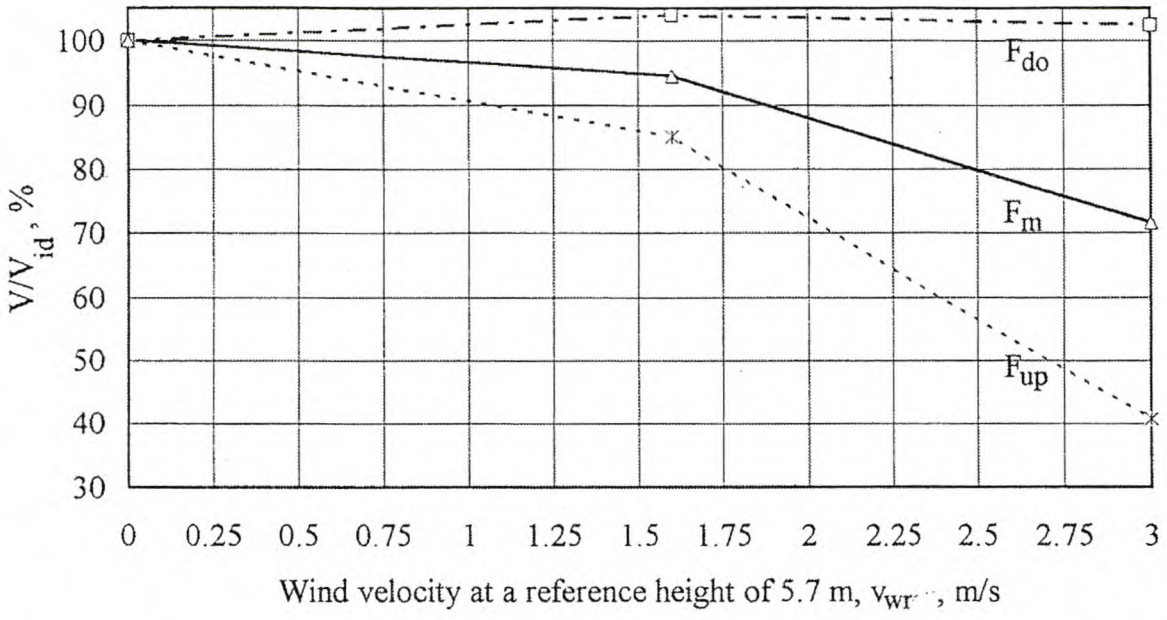

Fig. 9.3.6 Fan Air Flow Rate during Crosswinds for an Inlet Height Hi = 5.7 m

The influence on performance of recirculating hot plume air in this installation is relatively small. As shown in Figure 9.3.7, the effectiveness of the heat exchanger actually increases slightly for a light wind when compared to windless conditions. This is because the recirculation at the downwind side of the heat exchanger is eliminated. At higher wind speeds, recirculation gradually increases. This trend is in agreement with results observed by Du Toit et al.

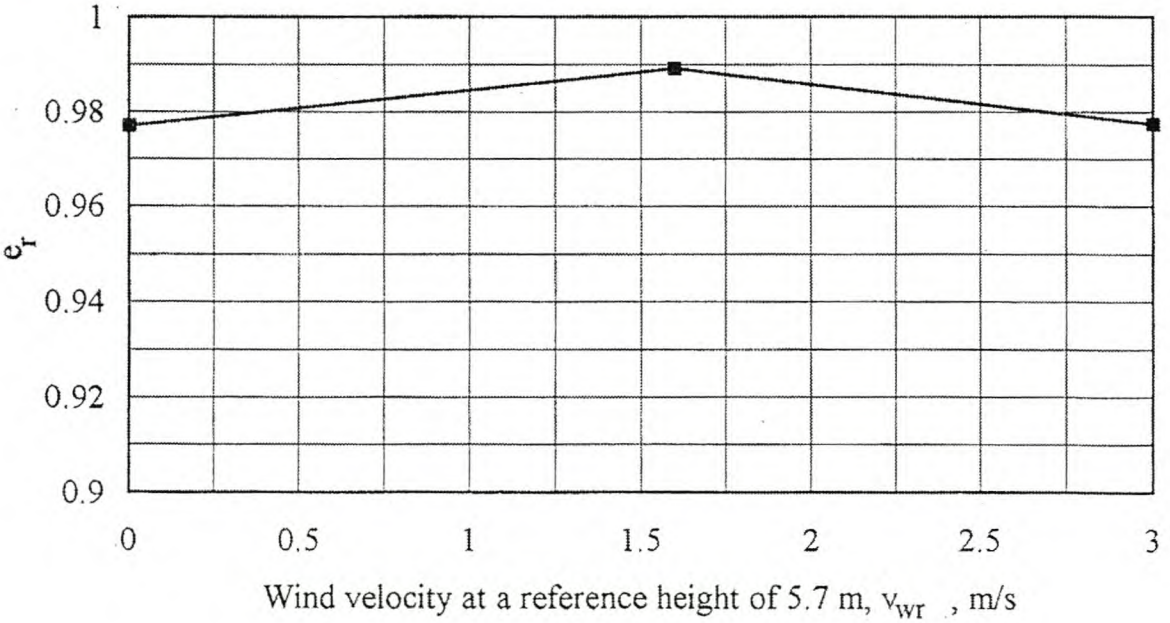

Fig. 9.3.7 Effectiveness due to Recirculation during Crosswinds for an Inlet Height Hi = 5.7 Meters

To evaluate the influence of the inlet height on air flow rate through the particular heat exchanger, H_i was varied in the numerical model. A fixed wind profile was retained with a reference velocity of v_{wr} = 3 m/s at a reference height of z_r = 5.7 m. The changes in fan air-volume flow rate and effectiveness are shown in Figures 9.3.8 and 9.3.9. By increasing the height of the fan platform, the performance of the heat exchanger is improved due to the increasing air-flow rate. The change in recirculation is small.

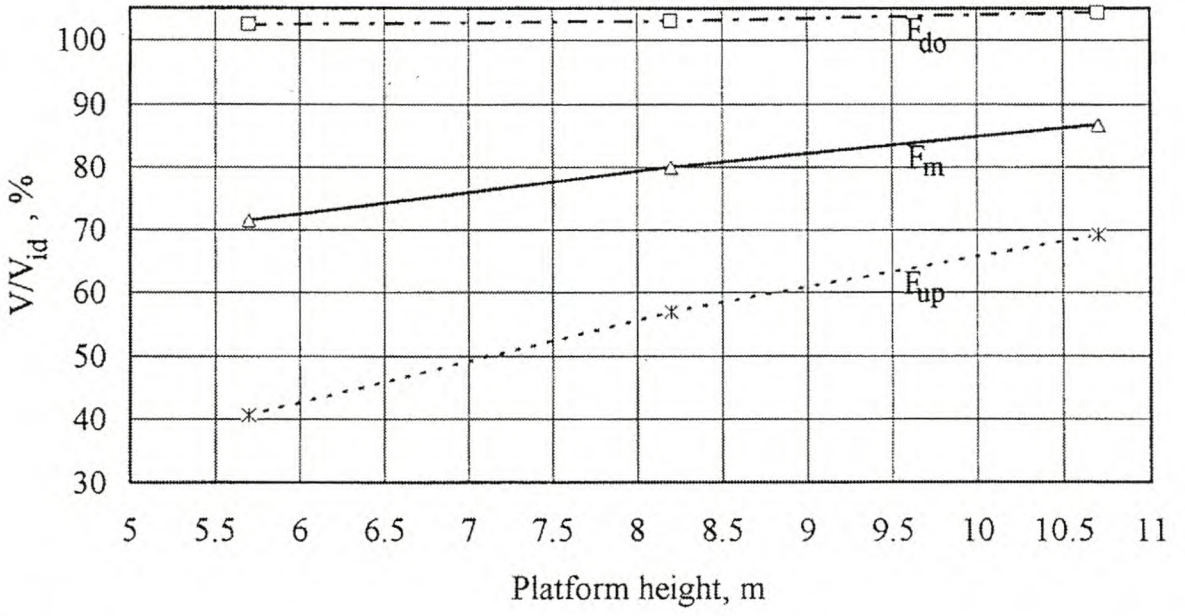

Fig. 9.3.8 Fan Air Flow Rate during Crosswind for Different Fan Platform Heights

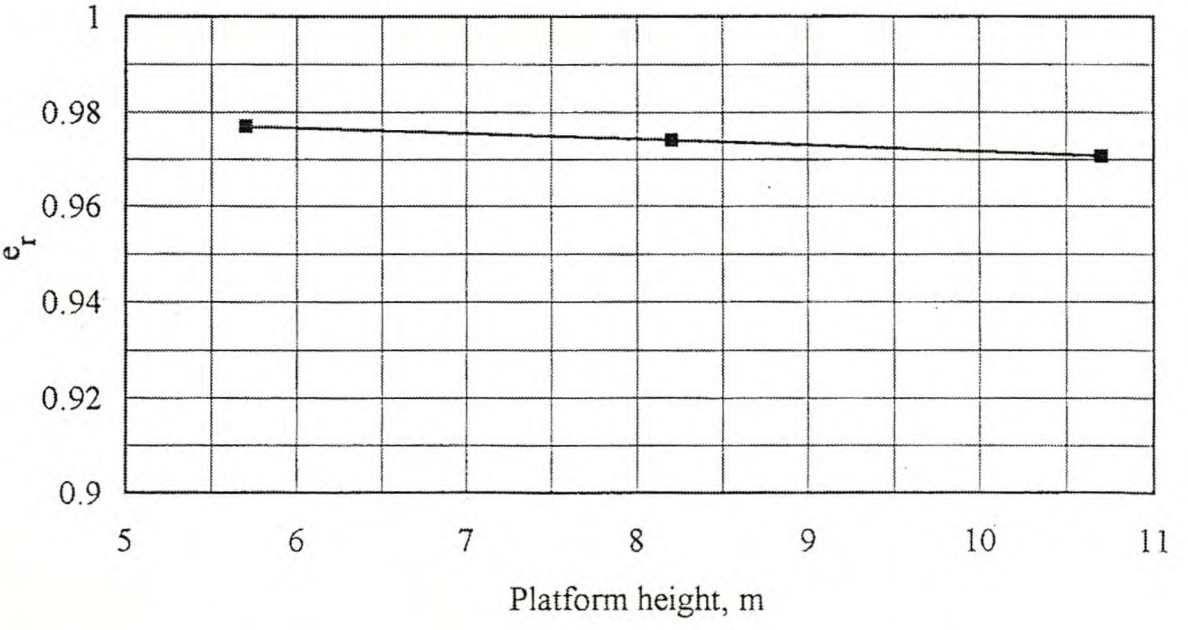

Fig. 9.3.9 Effectiveness due to Recirculation during Crosswinds for Different Fan Platform Heights

The influence on performance of winds blowing in the direction of the longitudinal axis are evaluated numerically for a fan platform height of 10.7 m with wind reference velocities of 3 m/s and 5 m/s at a reference height of 5.7 m. Heat exchanger banks consisting of up to 6 bays are evaluated. In the numerical model, the crosswind solutions are applied to the 2 fans in the first 2 upwind bays, while the remaining fans are assumed to operate ideally. The resultant recirculation is shown in Figure 9.3.10. The corresponding heat exchanger effectiveness is given by $e_r = 1 - r$.

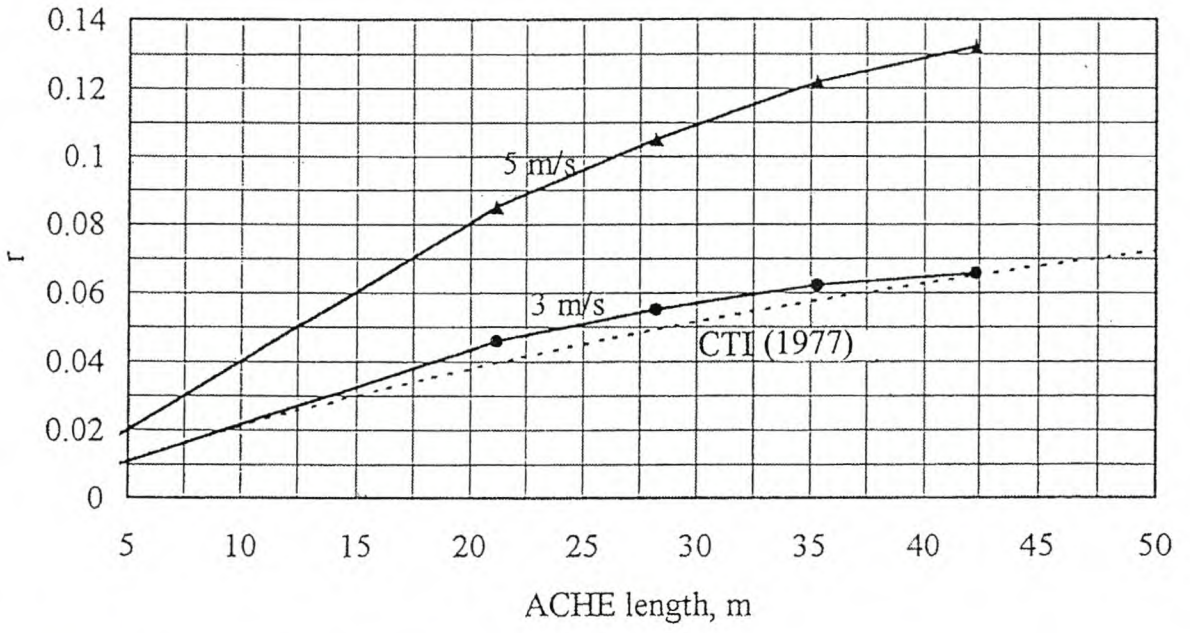

Fig. 9.3.10 Recirculation for Winds Blowing in the Direction of the Longitudinal Axis

Recirculation clearly increases with greater heat exchanger length and wind speed. For purposes of comparing trends, a correlation for recirculation recommended by the CTI is also shown in Figure 9.3.10. This is applicable to induced draft cooling towers although the authors do state they expect the recirculation of a forced draft system to be double the value of the correlation shown.

Duvenhage et al. show the mean flow rate through the fans (Fig. 9.3.11) tends to improve with the addition of a solid walkway along the periphery of the air-cooled heat exchanger at the fan platform elevation.

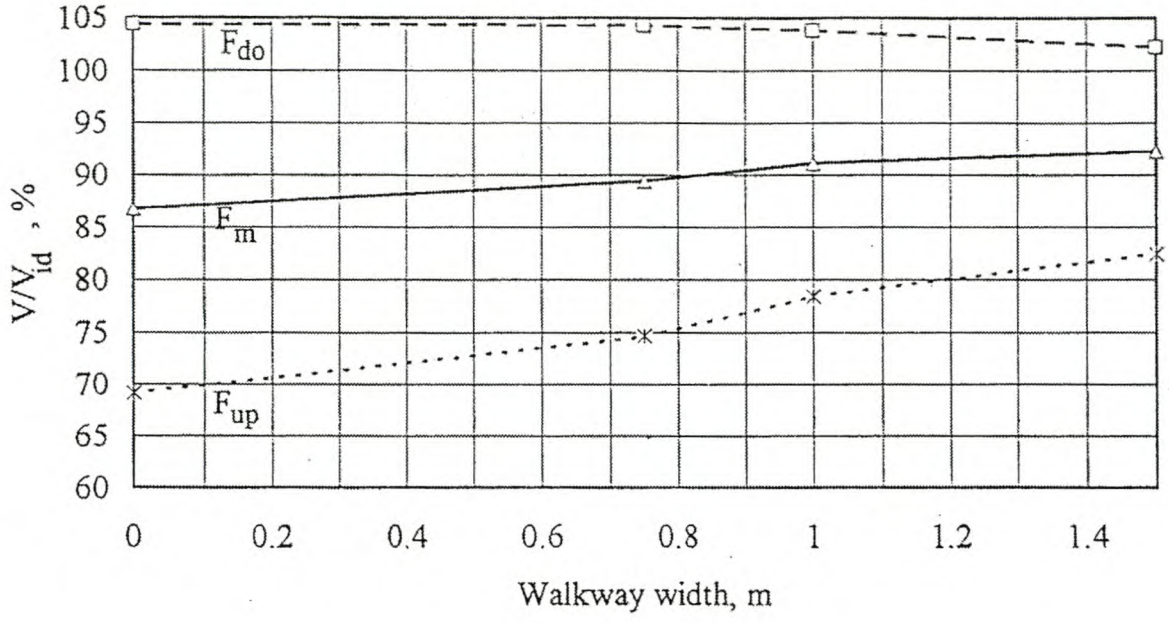

Fig. 9.3.11 Walkway Effect

According to the previous findings, the reduction of performance in a long, forced-draft, air-cooled heat exchanger may be ascribed to a reduction in air flow through the fans along the windward side of the bank when crosswinds prevail (Fig. 9.3.12a). When the winds blow in the direction of the major axis of the heat exchanger, it is attributed to the recirculation of hot plume air (Fig. 9.3.12 b). Fahlsing observed reverse rotation of out-of-service fans on the windward side of a large air-cooled condenser when crosswinds prevailed.

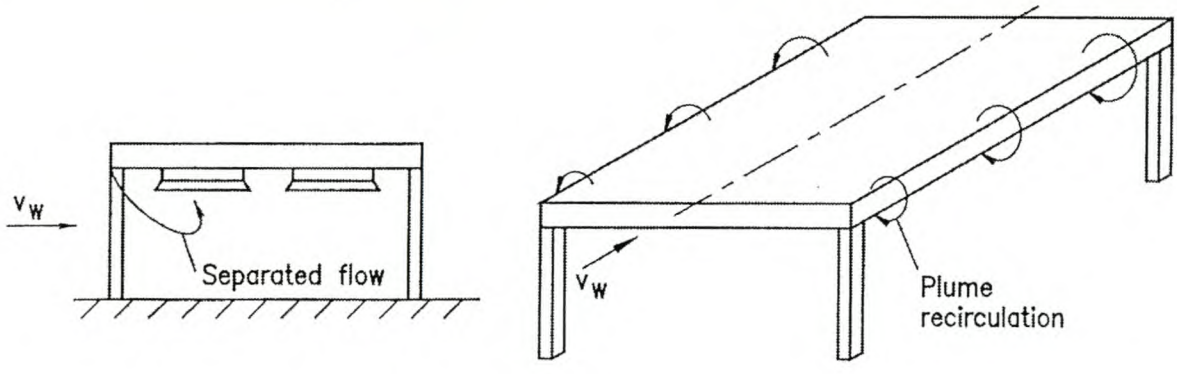

(a) Crosswind (b) Longitudinal wind

Fig. 9.3.12 Flow Patterns Reducing Performance (a) Crosswind (b) Longitudinal Wind

Example 9.3.1

Consider the air-cooled heat exchanger described in Example 8.3.1, and find the approximate heat rejected if a crosswind blows at a speed of 3 m/s at a height of 5.7 m above ground level. The wind velocity distribution is given by

$$v_w/v_{wr} = (z/z_r)^{0.2})$$

Solution

When a wind blows across a long, two-fan-row, air-cooled heat exchanger bank, the air flow rate through the fans, and recirculation is affected (Figs. 9.3.8 and 9.3.9). Although these figures are applicable to a heat exchanger with a plenum 3 m high, they will be used in the present analysis since more appropriate information is unavailable.

Extrapolate a reduction in mean air-volume flow rate through the fans from Figure 9.3.8, i.e., $V/V_{id} \approx 0.9$. Due to some hot plume air recirculation, the effectiveness of the heat exchanger is reduced. By extrapolating the curve in Figure 9.3.9 to a platform height of 12.7 m, find $e_r \approx 0.97$.

The approximate heat rejected under these windy conditions is

$$Q_{6wr} = 6(V/V_{id})e_rQ = 6 \text{ x } 0.9 \text{ x } 0.97 \text{ x } 12.477 = 65.355 \text{ MW}$$

Example 9.3.2

Consider the air-cooled heat exchanger described in Example 8.3.1, and find the approximate heat rejected if a wind blows in the direction of the major axis of the heat exchanger bank at a rate of 3 m/s and a height of 5.7 m above ground level. The wind velocity distribution is given by

$$v_w/v_{wr} = (z/z_r)^{0.2}$$

Solution

To solve this problem, the change in the air volume flow rate through the fans in the first two bays on the upwind side is assumed to be similar to that of the two fan rows under crossflow conditions. Upon extrapolation of the curve, find for F_{up} in Figure 9.3.8 to a 12.7 m platform height that $(V/V_{id})_{up} \approx 0.8$. For F_{do}, and find $(V/V_{id})_{do} \approx 1.05$. In the remaining four fan banks, the reduction in flow may be approximated by the case of no wind, i.e., as determined in Example 8.3.1, $V/V_{id} = 0.985$. Due to the kinetic energy of the wind, this value for V/V_{id} possibly is conservative. The recirculation factor for the 42.3 m long bank is obtained from Figure 9.3.10, i.e., $r = 0.065$. The corresponding effectiveness is $e_r = 1 - r = 0.935$.

The heat rejected is then

$$Q_{6wr} = \left[(V/V_{id})_{up} + (V/V_{id})_{do} + 4\ V/V_{id}\right] e_r\ Q$$

$$= (0.8 + 1.05 + 4 \text{ x } 0.985)\, 0.935 \text{ x } 12.477 = 67.546\ MW$$

9.4 Recirculation and Interference

As in the case of banks of air-cooled heat exchangers, recirculation of hot, moist plume air is known to reduce the performance of rows of cooling tower units or cells according to CTI Bulletin PFM-110 and the British Standards Institution Code BS4485. When several banks of air-cooled heat exchangers or rows of cooling tower cells are located next to each other, the plume of one bank or row may be drawn into an adjacent one. This phenomenon is referred to as *interference*.

Ribier conducted recirculation tests on models of induced draft cooling towers cells similar to the types shown in Figure 1.1.3 but without a diffuser. Initial tests were conducted on a row consisting of three cells with fills in counterflow and crossflow. The results of these tests are shown in Figures 9.4.1(a) and 9.4.1(b) as a function of different wind directions and ratios of wind speed measured 10 m above ground level to plume exhaust speed, v_w/v_p. The percentage recirculation is less for the counterflow arrangement

than for the crossflow arrangement. When a diffuser was added to the counterflow unit, a reduction in recirculation was observed.

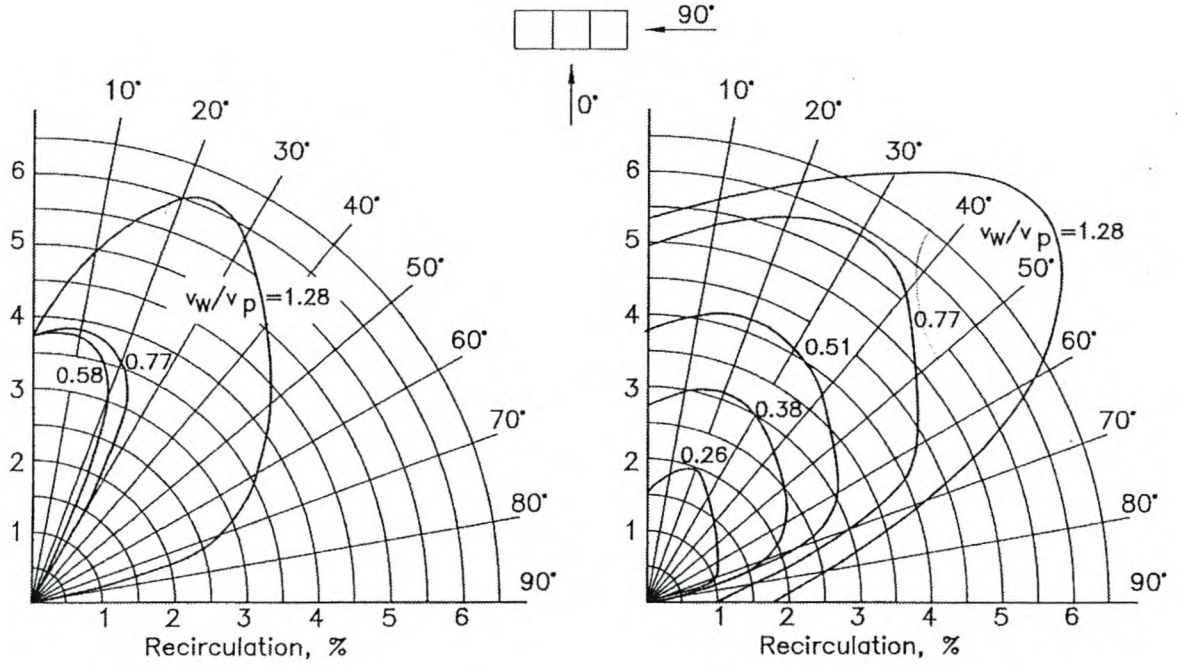

(a) Counterflow (b) Crossflow

Fig. 9.4.1 Recirculation in Three-Cell Counterflow and Crossflow Cooling Tower (a) Counterflow (b) Crossflow

A further set of tests was conducted by Ribier in which two rows of counterflow cooling towers each consisting of three cells were first arranged end to end (six cells) and then systematically spaced one, two, and three cells apart. Of these tests, the continuous row of six cells experienced most recirculation with the results shown in Figure 9.4.2. Recirculation appears to be a maximum at $v_w/v_p \approx 0.9$.

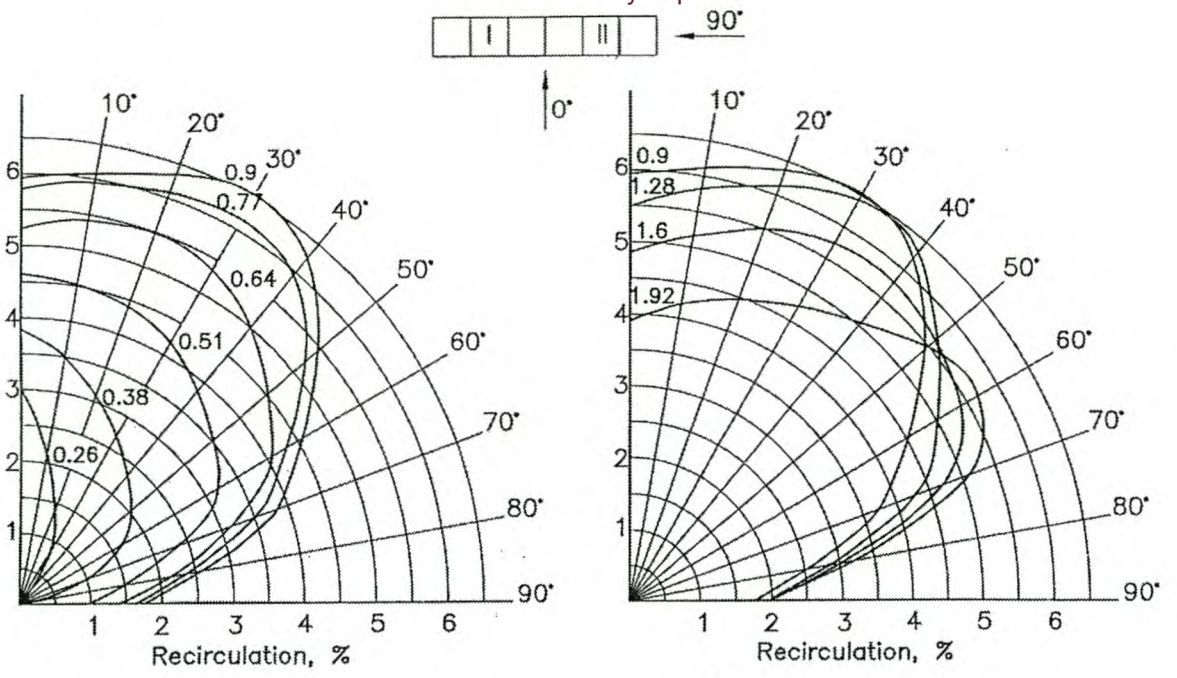

Fig. 9.4.2 Recirculation in Six-Cell Cooling Tower

As shown in Figure 9.4.3, recirculation is considerably reduced when the two rows of three cells each are separated by a distance of two cells. Further separation does not reduce recirculation to any extent.

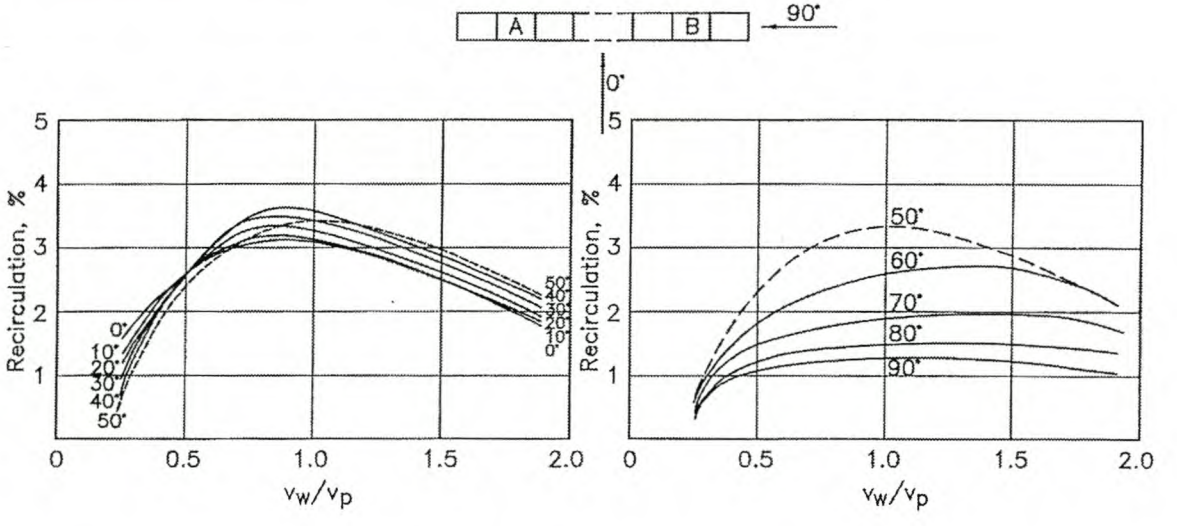

Fig. 9.4.3 Recirculation in a Counterflow Cooling Tower Consisting of Two Three-Cell Rows, Two Cells Apart

By placing two rows of three cells each side by side, recirculation is relatively high (Fig. 9.4.4).

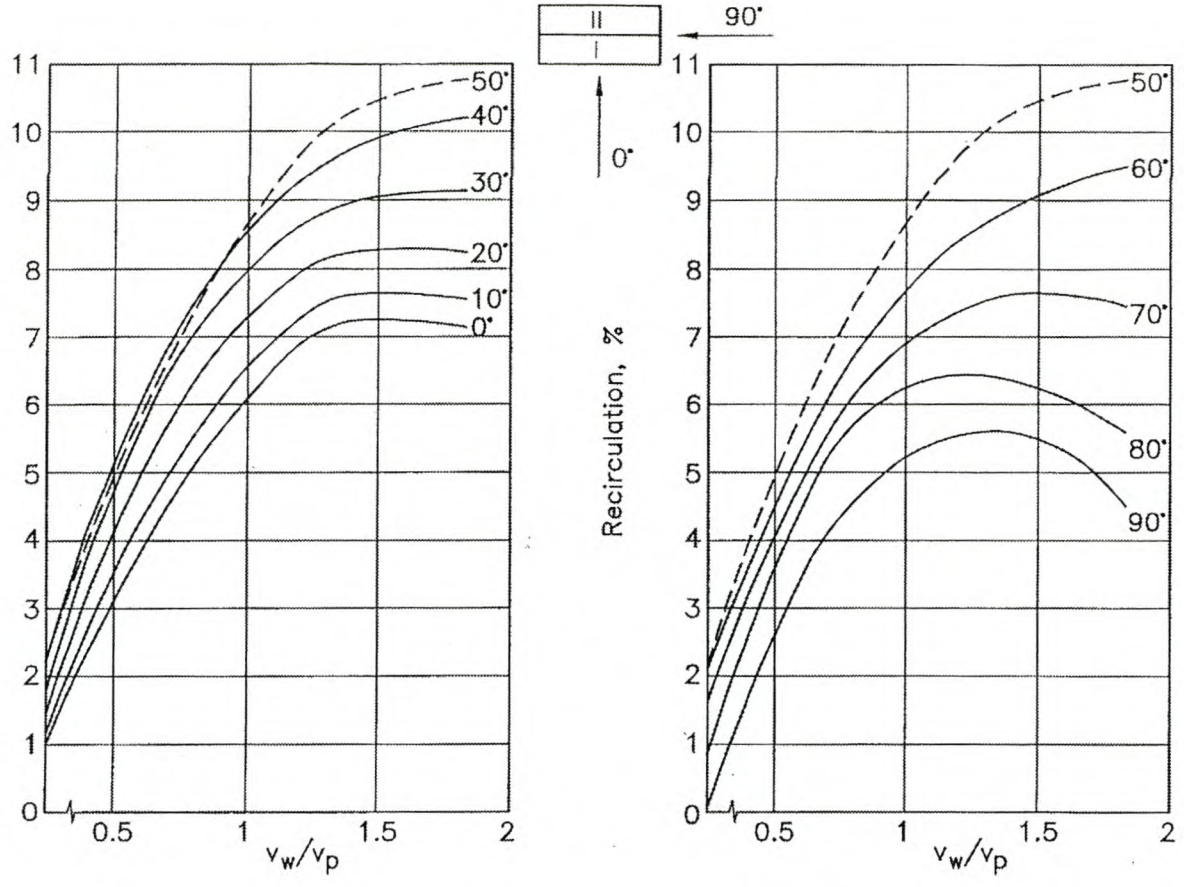

Fig. 9.4.4 Recirculation in Cooling Tower Consisting of Two Rows of Three Cells Located Side by Side

If the two rows of three cells are separated by one cell width, only a relatively small reduction in maximum recirculation is experienced (Fig. 9.4.5).

Based on these results, it may be concluded that a row of induced-draft cooling tower cells should be arranged in-line with the prevailing wind direction. A high air outlet velocity and the addition of a diffuser will tend to reduce recirculation.

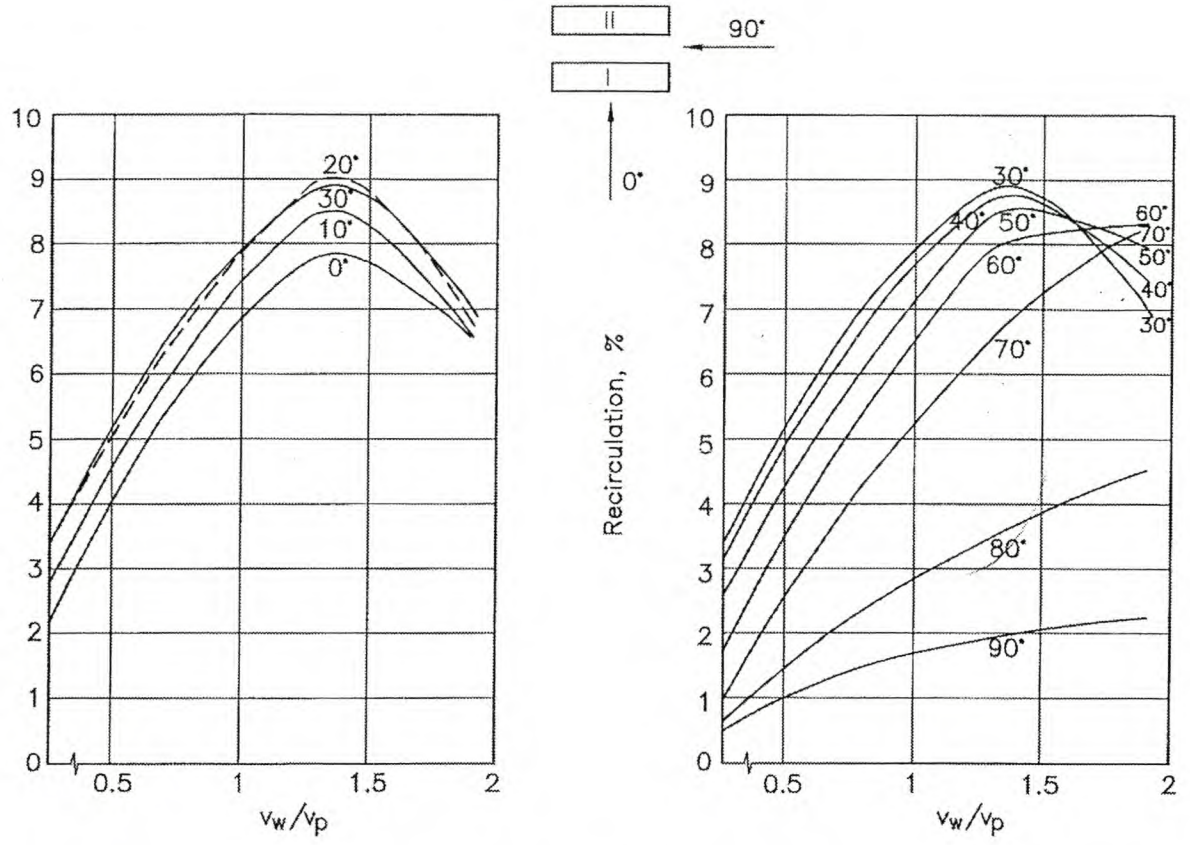

Fig. 9.4.5 Recirculation in Cooling Tower Consisting of Two Rows of Three Cells Separated by One Cell Width

Bender et al. numerically analyzed the air flow into a counterflow induced draft cooling tower consisting of two adjacent cells of the type shown in Figure 1.1.3(b). Their objective was to reduce or eliminate ice formation at the tower inlet during windy periods in winter. The dimensions of the tower they studied were 9.14 m wide, 18.3 m long, and 11.7 m high with an intake height of 2.59 m. The stack or diffuser diameter was 6.1 m, and its height was 3.05 m.

Ice buildup tends to be most prevalent at the windward facing intake where the entering air flow rate is higher than on the leeward intake. By placing a 10% porous wall 2.875 m high in front of the cooling tower inlet at a distance of 1.875 m, the air flow entering on either intake was found to be the same.

Tesche conducted model tests to determine the effect of recirculation and interference on the performance of rows of induced-draft hybrid cooling tower cells similar to the unit or cell shown in Figure 9.4.12. His results are applicable in cases where the wind velocity distribution is given by $v_w/v_{wr} = (z/z_r)^{0.2}$. The recirculation of individual cells in a row consisting of twelve cells varies (Fig. 9.4.6). All wind speeds are specified at 10 m above ground level.

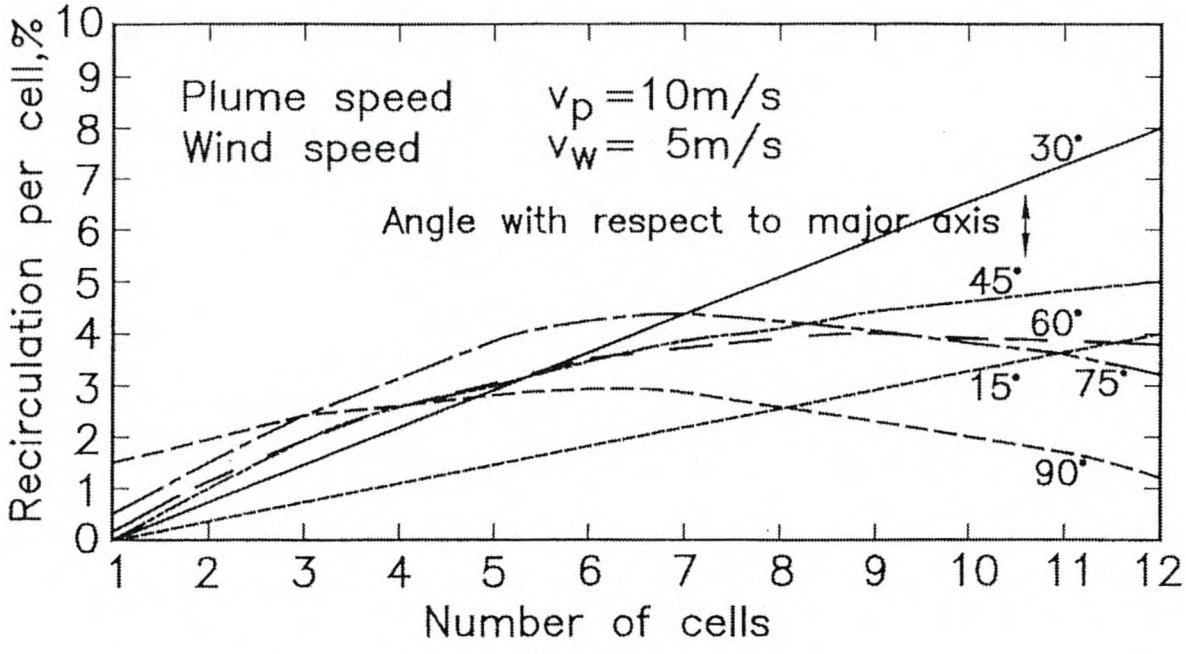

Fig. 9.4.6 Recirculation in a Row Consisting of Twelve Hybrid Cooling Tower Cells

The lowest recirculation is observed when the wind blows in the direction of the major axis of the cell row. The influence of the number of cells under these conditions is shown in Figure 9.4.7.

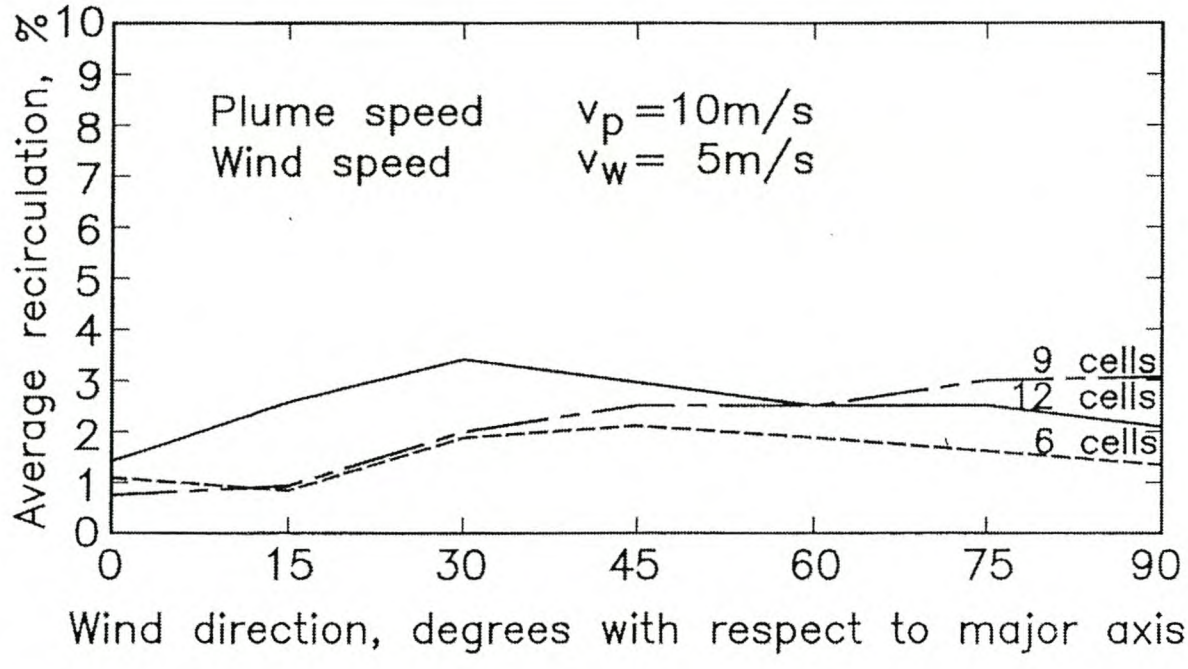

Fig. 9.4.7 Recirculation as a Function of Number of Cells in Row

The influence of the ratio of wind speed to plume exhaust speed, v_w/v_p, on recirculation is shown in Figure 9.4.8. A maximum recirculation occurs at a wind speed of 5 m/s.

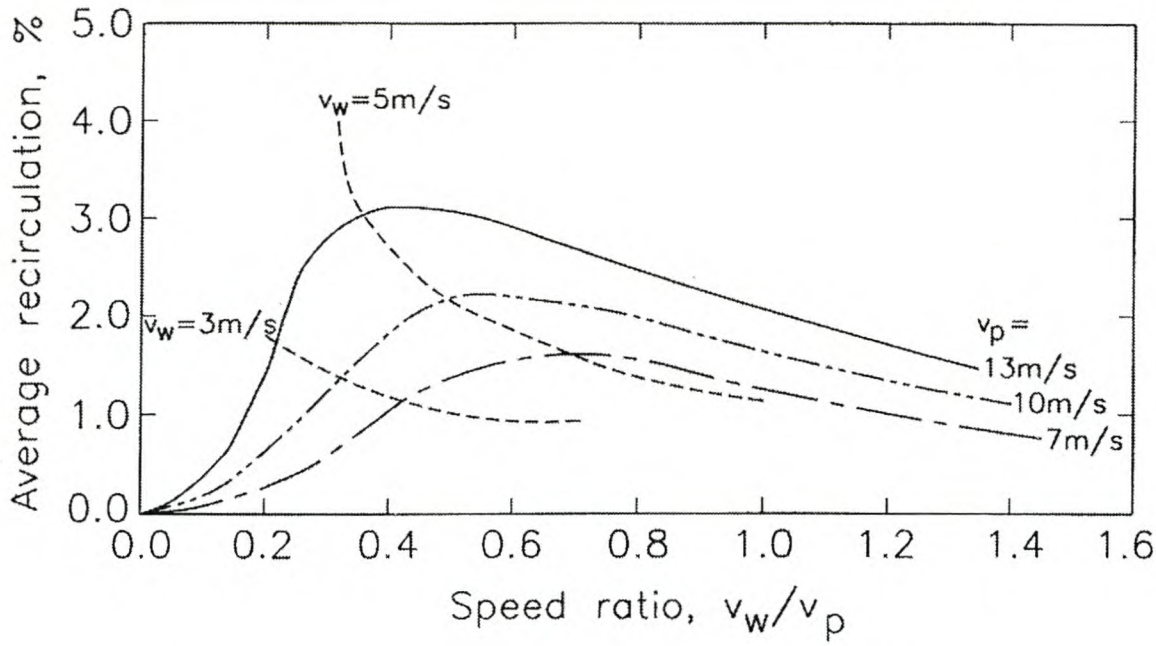

Fig. 9.4.8 Recirculation as a Function of Speed Ratio

When two rows of six cells each are placed next to each other with their major axes in parallel, the resultant average interference for different spacings between them is shown in Figure 9.4.9. The interference for rows of twelve cells is shown in Figure 9.4.10.

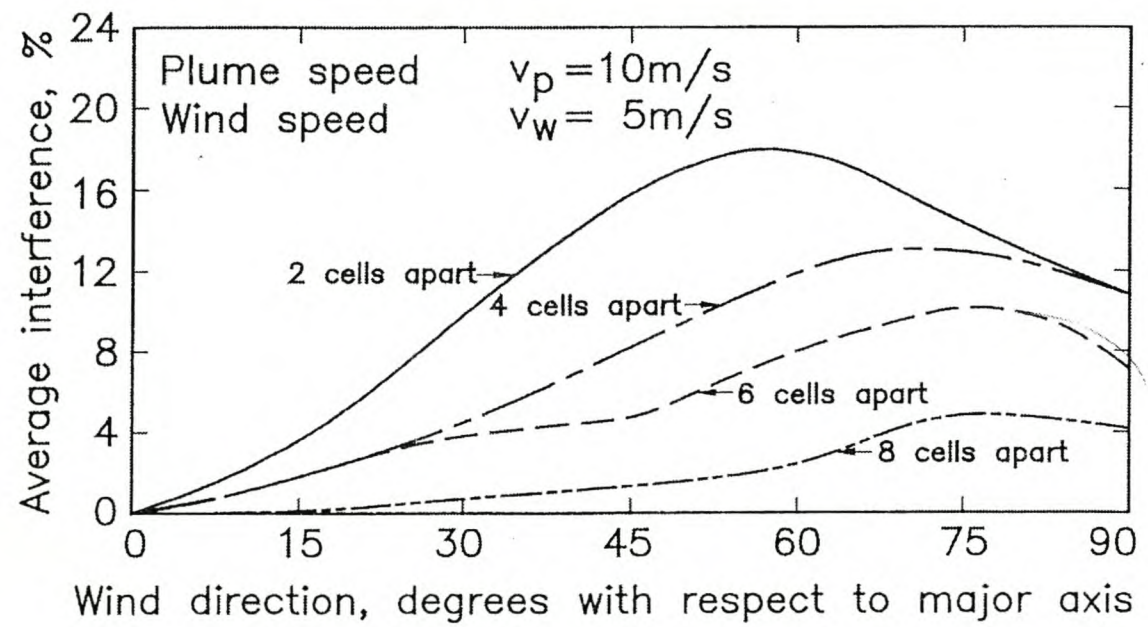

Fig. 9.4.9 Interference for Two Rows of Six Cells at Different Spacings

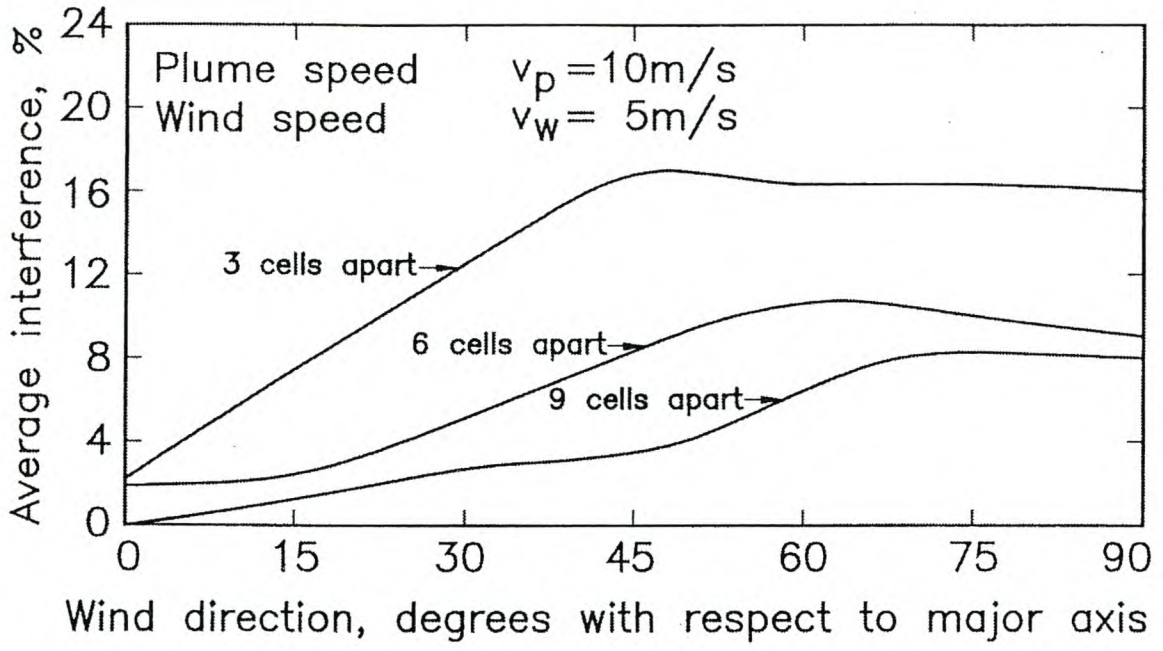

Fig. 9.4.10 Interference for Two Rows of Twelve Cells at Different Spacings

Recirculating plume air increases the effective wetbulb temperature at the inlet to the cooling tower (Fig. 9.4.11). Since this increase is not only a function of the wetbulb temperature of the ambient air but also of the thermodynamic state of the plume air, Figure 9.4.11 is an indication at best of the trend in wetbulb temperature change.

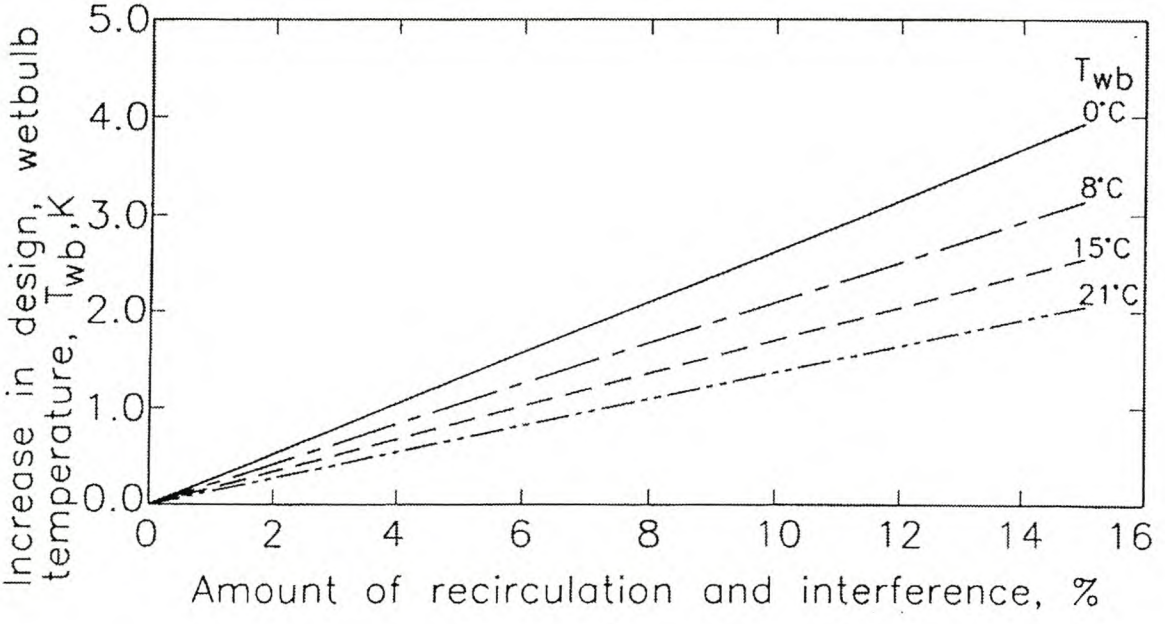

Fig. 9.4.11 Increase in Wetbulb Temperature due to Recirculation

The cells located at the ends of the rows or banks are usually most sensitive to the influence of winds.

Example 9.4.1

Determine the heat rejected and the water lost due to evaporation in the induced-draft hybrid cooling tower shown in Figure 9.4.12, and show that no plume is formed.

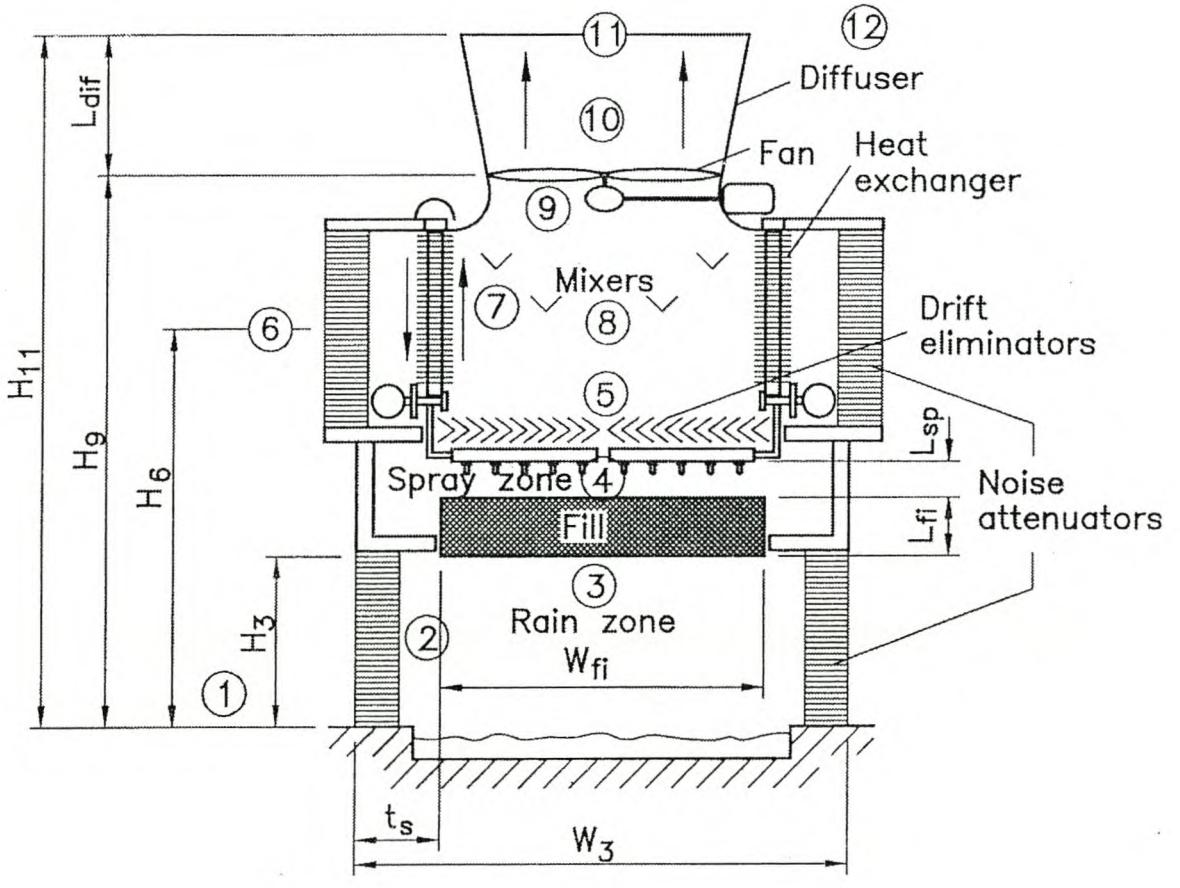

Fig. 9.4.12 Hybrid Cooling Tower

Water enters the dry section of the tower at a rate of

$$m_w = 450 \text{ kg/s}$$

and at a temperature of

$$T_{wi} = 40^\circ\text{C}$$

Ambient conditions:

- Air temperature at ground level: T_{a1} = 15.45 °C (288.6 K)
- Wetbulb temperature at ground level: T_{wb} = 11.05 °C (284.2 K)
- Atmospheric pressure at ground level: p_{a1} = 84100 N/m^2
- The ambient temperature gradient: -0.00975 K/m from ground level

Cooling tower specifications:

- Inlet height to wet section: H_3 = 3.5 m
- Inlet width: W_3 = 18 m
- Inlet breadth or length: B_3 = 12 m
- Height to middle of dry bundles: H_6 = 8.38 m
- Height to fan: H_9 = 12.38 m
- Tower height: H_{11} = 15.38 m

Wet section specification:

The cooling tower is fitted with an expanded metal fill (L_{fi} = 1.878 m) described in Example 4.3.1. The performance characteristic are:

- Transfer coefficient

$$h_{dfi}\, a_{fi} L_{fi} / G_w = 0.2692\, L_{fi}\, G_w^{-0.094}\, G_a^{0.6023} = 0.5061\, G_w^{-0.094}\, G_a^{0.6023}$$

- Loss coefficient

$$K_{fdm} = 1.9277\, L_{fi}\, G_w^{1.2752} G_a^{-1.0356} = 3.62\, G_w^{1.2752} G_a^{-1.0356}$$

- Width of fill: Wfi = 15 m
- Breadth or length of fill: B_{fi} = 12 m
- Depth of spray zone above fill: L_{sp} = 0.3 m
- Height of rain zone: $L_{rz} = H_3$ = 3.5 m
- Mean drop diameter in rain zone: d_d = 0.0035 m
- Fill support and contraction loss coefficient: $K_{fs} + K_{ctc}$ = 0.5
- Loss coefficient for water distribution system: K_{wd} = 0.775
- Noise attenuator pressure loss coefficient: K_{na} = 2.78
- The loss coefficient for the drift eliminator (type c) is given by Equation 4.7.2.

Dry section specification:

- Effective height of finned tube bundles: L_t = 4 m
- Number of heat exchanger bundles: n_b = 8

- Number of tube rows: $n_r = 4$
- Number of tubes per row: $n_{tr} = 50$
- Number of water passes: $n_p = 2$
- Outside diameter of stainless steel core tube: $d_o = 0.0254$ m
- Inside diameter of smooth, stainless steel core tube: $d_i = 0.0216$ m
- Thermal conductivity of stainless steel core tube: $k_t = 17$ W/mK
- Transversal tube pitch: $P_t = 0.058$ m
- Longitudinal tube pitch: $P_\ell = 0.05022$ m
- Fin diameter (extruded aluminum): $d_f = 0.0572$ m
- Fin root diameter: $d_r = 0.0276$ m
- Fin tip thickness: $t_{ft} = 0.00025$ m
- Mean fin thickness: $t_f = 0.0005$ m
- Fin root thickness: $t_{fr} = 0.00075$ m
- Fin pitch: $P_f = 0.0028$ m
- Thermal conductivity of aluminum fin: $k_f = 204$ W/mK
- Thermal contact resistance between the fin root and the core tube is negligible
- Finned tubes are geometrically similar to those described in Example 5.4.2

Mixed section and fan specification:

- Air mixing elements pressure loss coefficient: $K_m = 0.8$, based on frontal area of fill
- Fan upstream loss coefficient: $K_{up} = 0.2$, based on cross-sectional area of casing
- Fan downstream loss coefficient: $K_{do} = 0.2$, based on cross-sectional area of casing
- Fan diameter: $d_F = 9.5$ m
- Fan casing diameter: $d_c = 9.5265$ m
- Rotational speed of fan: $N_F = 118$ rpm
- Fan blade angle: $\alpha_F = 14^\circ$
- Height of diffuser: $L_{dif} = 3$m
- Included diffuser angle: $2\theta = 14^\circ$
- Fan/diffuser performance characteristics determined according to BS 848 installation type A are available for the 9.5 m diameter fan having 14° blade angles with reference conditions at $\rho = 1.2$ kg/m^3 and $N_{F/dif} = 120$ rpm.
- Fan/diffuser static pressure

$$\Delta p_{F/difs} = 299.903 + 40.0071 \times 10^{-3} V_{F/dif} - 96.5087 \times 10^{-6} V_{F/dif}^2$$

$$- 152.2243 \times 10^{-9} V_{F/dif}^3 \text{, N/m}^2$$

- Fan/diffuser power consumption

$$P_{F/difs} = 203302.6779 - 58.3775 V_{F/dif} + 458.7692 \times 10^{-3} V_{F/dif}^2$$

$$- 405.2315 \times 10^{-6} V_{F/dif}^3 \text{, W}$$

Solution

The results of the final iteration in the determination of the performance characteristics of the hybrid cooling tower are presented, and their correctness is confirmed.

Dry section

The draft and energy equations through the dry section are satisfied if:

- Dry air mass flow rate: m_{a67} = 267.8392 kg/s
- Outlet air temperature: T_{a7} = 305.9084 K
- Outlet water temperature: T_{wod} = 310.6171 K
- Outlet air pressure: p_{a7} = 83891.4308 N/m^2

The following calculations confirm these values are correct.

The humidity ratio of the ambient air according to Equation A.3.5 is

$$w_1 = 0.008127 \text{ kg/(kg dry air)}$$

if evaluated at

$$T_{a1} = 288.6 \text{ K}, \; T_{wb} = 284.2 \text{ K}$$

and

$$p_{a1} = 84100 \text{ N/m}^2$$

With this value, it is possible to determine the air-vapor mass flow rate through the dry section if it is assumed the ambient humidity ratio is constant.

$$m_{av67} = m_{a67} (1 + w_1) = 267.8392 (1 + 0.008127) = 270.0159 \text{ kg/s}$$

The mean temperature of the air entering the dry section at elevation H_6 is, according to Equation 9.1.8,

$$T_{a6} = 288.6 - 0.00975 \times 8.38 = 288.5183 \text{ K}$$

The corresponding air pressure at this elevation is, according to Equation 7.2.9,

$$p_{a6} = 84100\left[1 - 0.00975\,(8.38 / 288.6)\right]^{3.5(1+0.008127)[1-0.008127/(0.008127+0.62198)]}$$

$$= 84017.1026 \text{ N/m}^2$$

Other properties of the inlet air to the dry section are evaluated according to the equations given in Appendix A at

$$T_{a6} = 288.5183 \text{ K}$$

and

$$p_{a6} = 84017.1026 \text{ N/m}^2$$

with

$$w_6 = w_1$$

- Air-vapor density: $\eta_{av6} = 1.0094$ kg/m^3 using Equation A.3.1
- Dynamic viscosity: $\mu_{av6} = 1.7853 \times 10^{-5}$ kg/ms using Equation A.3.3
- Enthalpy of entering air: $i_{ma6} = 36031.2296$ J/kg dry air using Equation A.3.6b

The properties at the mean conditions through the heat exchanger, i.e., at

$$T_{a67} = (T_{a6} + T_{a7})/2 = (288.5183 + 305.9084)/2 = 297.2133 \text{ K}$$

and

$$p_{a67} = (84017.1026 + 83891.4308)/2 = 83954.2667 \text{ N/m}^2$$

are:

- Air-vapor density: $\rho_{av67} = 0.97915$ kg/m^3 using Equation A.3.1
- Specific heat: $c_{pav67} = 1013.9222$ J/kg K using Equation A.3.2
- Dynamic viscosity: $\mu_{av67} = 1.8255 \times 10^{-5}$ kg/ms using Equation A.3.3
- Thermal conductivity: $k_{av67} = 0.025923$ W/mK using Equation A.3.4

To find the performance characteristics of the finned surfaces in the dry section, certain geometric parameters are of relevance.

The total frontal area of the dry section is

$$A_{frd} = n_b L_t [P_t (n_{tr} - 0.5) + d_f] = 8 \times 4 [0.058(50 - 0.5) + 0.0572] = 93.7024 \text{ m}^2$$

The minimum free flow area through the heat exchanger is given by

$$A_c = A_{frd} - n_b \; n_{tr} \; L_t \left[d_f \, t_f + (P_f - t_f) \, d_r \right] / P_f$$

$$= 93.7024 - 8 \times 50 \times 4 \left[0.0572 \times 0.0005 + (0.0028 - 0.0005) \, 0.0276 \right] / 0.0028$$

$$= 41.0853 \text{ m}^2$$

The ratio of the air-side area to the root area if no fins were present, is

$$\frac{A_f + A_{re}}{A_r} = \frac{\left(d_f^2 - d_r^2\right)/2 + d_r\left(P_f - t_{fr}\right) + d_f t_{ft}}{d_r P_f}$$

$$= \frac{\left(0.0572^2 - 0.0276^2\right)/2 + 0.0276(0.0028 - 0.00075) + 0.0572 \text{ x } 0.00025}{(0.0276 \text{ x } 0.0028)}$$

$$= 17.1573$$

The ratio of the fin area to the total air-side area is

$$\frac{A_f}{A_f + A_{re}} = \frac{\left(d_f^2 - d_r^2\right)/2 + d_f t_{ft}}{\left(d_f^2 - d_r^2\right)/2 + d_r\left(P_f - t_{fr}\right) + d_f t_{ft}}$$

$$= \frac{\left(0.0572^2 - 0.0276^2\right)/2 + 0.0572 \text{ x } 0.00025}{\left(0.0572^2 - 0.0276^2\right)/2 + 0.0276\left(0.0028 - 0.00075\right) + 0.0572 \text{ x } 0.00025}$$

$$= 0.95733$$

The total air-side area is

$$A_a = A_f + A_{re} = \pi\left[\left(d_f^2 - d_r^2\right)/2 + d_f\, t_{ft} + d_r\left(P_f - t_{fr}\right)\right]\left(L_t\, n_r\, n_{tr}\, n_b / P_f\right)$$

$$= \pi\left[\left(0.0572^2 - 0.0276^2\right)/2 + 0.0572 \text{ x } 0.00025 + 0.0276(0.0028 - 0.00075)\right]$$

$$\text{x } (4 \text{ x } 4 \text{ x } 50 \text{ x } 8 / 0.0028) = 9521.1441 \text{ m}^2$$

The velocity of the air-vapor through the minimum cross-sectional area of the heat exchanger is given by

$$v_{av67c} = m_{av67} / \left(A_c \rho_{av\,67}\right) = 270.0159 / (41.0853 \text{ x } 0.97915) = 6.712 \text{ m/s}$$

To find the air-side heat transfer coefficient according to Equation 5.5.4, the Reynolds number based on the root diameter is required, i.e.,

$$Re_a = m_{av67}\, d_r / (\mu_{av\,67}\, A_c) = 270.0159 \text{ x } 0.0276 / (1.8255 \text{ x } 10^{-5} \text{ x } 41.0853)$$

$$= 9936.5488$$

The Prandtl number of the air is given by

$$Pr_a = \mu_{av\,67}\, c_{pav67} / k_{av\,67} = 1.8255 \text{ x } 10^{-5} \text{ x } 1013.9222 / 0.025923 = 0.714$$

According to Equation 5.5.4, the Nusselt number of the air flowing through the finned tube bundles is

$$Nu_a = 0.38 \text{ x } 9936.5488^{0.6} \text{ x } 0.714^{0.333} \text{ x } 17.1573^{-0.15} = 55.493$$

With this value, find the air-side heat transfer coefficient.

$$h_a = Nu_a \text{ k}_{\text{av67}} / d_r = 55.493 \text{ x } 0.025923 / 0.0276 = 52.1213 \text{ W/ m}^2\text{K}$$

To determine the corresponding efficiency of the fin according to Equation 3.3.12, find

$$b = [2 \text{ x } 52.1213 / (204 \text{ x } 0.0005)]^{0.5} = 31.9685$$

$$\varphi = (0.0572 / 0.0276 - 1)[1 + 0.35\, \ell n\, (0.0572 / 0.0276)] = 1.346$$

Substitute these values into Equation 3.3.12, and find

$$\eta_f = \tanh (31.9685 \text{ x } 0.0276 \text{ x } 1.346 / 2) / (31.9685 \text{ x } 0.0276 \text{ x } 1.346 / 2) = 0.89697$$

Using Equation 3.3.11, the corresponding fin effectiveness is

$$e_f = 1 - 0.95733\, (1 - 0.89697) = 0.90137$$

With this value, find the effective heat transfer coefficient.

$$h_{ae} = h_a e_f = 52.1213 \text{ x } 0.90137 = 46.9804 \text{ W / m}^2\text{K}$$

The mean temperature of the water flowing through the dry section is:

$$T_{wmd} = (T_{wi} + T_{wod}) / 2 = (313.15 + 310.6171) / 2 = 311.8836 \text{ K}$$

The thermophysical properties of the water stream evaluated at this temperature are obtained with the aid of the equations given in Appendix A.

- Specific heat of water: c_{pwm} = 4176.7618 J/kg K using Equation A.4.2
- Dynamic viscosity of water: μ_{wm} = 6.6744 x 10^{-4} kg/ms using Equation A.4.3
- Thermal conductivity of water: k_{wm} = 0.62949 W/m K using Equation A.4.4

The Reynolds number of the water flowing inside the tubes is given by

$$Re_w = \frac{4\, m_w}{(n_{tr}\ n_b\ n_r / n_p)\, \mu_{wm}\, \pi\, d_i} = \frac{4 \text{ x } 450}{(50 \text{ x } 8 \text{ x } 4 / 2)\ 6.6744 \text{ x } 10^{-4} \text{ x } \pi \text{ x } 0.0216}$$

$$= 49678.4373$$

The corresponding Prandtl number is

$$Pr_w = \frac{\mu_{wm}\, c_{pwm}}{k_{wm}} = \frac{6.6744 \text{ x } 10^{-4} \text{ x } 4176.7618}{0.62949} = 4.4285$$

According to Equation 2.2.10, the Darcy friction factor for turbulent flow in a smooth tube is

$$f_D = (1.82 \log 49678.4373 - 1.64)^{-2} = 0.020961$$

With this value, find the Nusselt number on the water-side as given by Equation 3.2.29.

$$Nu_w = \frac{(0.020961/8)(49678.4373 - 1000)4.4285\left[1 + (0.0216/4)^{0.67}\right]}{1 + 12.7(0.020961/8)^{0.5}\left(4.4285^{0.67} - 1\right)} = 275.5662$$

The corresponding heat transfer coefficient is

$$h_w = Nu_w\, k_{wm}/di = 275.5662 \text{ x } 0.62949/0.0216 = 8030.8778 \text{ W/m}^2 \text{ K}$$

The total surface area on the inside of the tubes, water-side, is given by

$$A_i = A_w = \pi\, d_i\, n_b\, n_r\, n_{tr}\, L_t = \pi \text{ x } 0.0216 \text{ x } 8 \text{ x } 4 \text{ x } 50 \text{ x } 4 = 434.2938 \text{ m}^2$$

In the absence of any contact resistance, the overall heat transfer coefficient based on the inside surface area of the finned tubes is given by

$$U_i = \left(\frac{1}{h_w} + \frac{A_w\, \ell n(d_o / d_i)}{2\pi\, k_t\, L_t\, n_r\, n_{tr}\, n_b} + \frac{A_w}{A_a\, h_{ae}} \right)^{-1}$$

$$= \left(\frac{1}{8030.8778} + \frac{434.2938\, \ell n\,(0.0254 / 0.0216)}{2\pi \text{ x } 17 \text{ x } 4 \text{ x } 4 \text{ x } 50 \text{ x } 8} + \frac{434.2938}{9521.1441 \text{ x } 46.9804} \right)^{-1}$$

$$= 834.46 \text{ W/m}^2 \text{ K}$$

The heat rates of the air and water streams are respectively,

$$C_{av} = m_{av67}\, c_{pav67} = 270.0159 \text{ x } 1013.9222 = 273775.1185 \text{ J/Ks}$$

$$C_w = m_w\, c_{pwm} = 450 \text{ x } 4176.7618 = 1879542.801 \text{ J/Ks}$$

The heat capacity ratio is

$$C = C_{\min}/C_{\max} = C_{av}/C_w = 273775.1185/1879542.801 = 0.14566$$

The number of transfer units per pass is

$$NTU_p = N_p = \frac{U_i\ A_i}{C_{\min} n_p} = \frac{834.46 \text{ x } 434.2938}{273775.1185 \text{ x } 2} = 0.66186$$

If both fluids are assumed to be unmixed, the effectiveness per pass is, according to Table 3.5.1,

$$e_p = 1 - \exp\left[0.66186^{0.22}\left\{\exp\left(-0.14566 \text{ x } 0.66186^{0.78}\right) - 1\right\} / 0.14566\right] = 0.46641$$

Substitute this value into Equation 3.5.23, and find

$$e = \left[\{(1 - 0.46641 \times 0.14566) / (1 - 0.46641)\}^2 - 1\right]$$

$$/\left[\{(1 - 0.46641 \times 0.14566) / (1 - 0.46641)\}^2 - 0.14566\right] = 0.70596$$

The maximum theoretical heat transfer rate is

$$Q_{\max} = C_{\min}(T_{wi} - T_a 6) = 273775.1185\,(313.15 - 288.5183) = 6.743547 \times 10^6 \text{ W}$$

The actual heat transferred in the dry section is

$$Q_d = eQ_{\max} = 0.70596 \times 6.743547 \times 10^6 = 4.760678 \times 10^6 \text{ W}$$

With this value, the temperature of the water leaving the dry section can be confirmed

$$T_{wod} = T_{wi} - Q_d / (c_{pwm}\ m_w) = 313.15 - 4.760678 \times 10^6 / (4176.7618 \times 450)$$

$$= 310.6171 \text{ K}$$

The enthalpy of the air leaving the dry section is

$$i_{ma7} = i_{ma6} + Q_d / m_{a67} = 36031.2296 + 4.760678 \times 10^6 / 267.8392$$

$$= 53805.621 \text{ J / kg dry air}$$

With this value for the enthalpy at (7), the correctness of the value of T_{a7} can be confirmed with the aid of Equation A.3.6b. Here the specific heats of dry air and water vapor are evaluated according to Equations A.1.2 and A.2.2 at

$$(T_{a7} + 273.15)/2 = (305.9084 + 273.15)/2 = 289.5292 \text{ K}$$

i.e.,

$$i_{ma7} = 1006.6291(305.9084 - 273.15) + 0.008127\left[25.016 \times 10^{6} + 1876.5184 \times (305.9084 - 273.15)\right] = 53805.621 \text{ J/kg}$$

This value agrees with that obtained previously.

To find the pressure drop through the dry section, determine the density of the air vapor at (7) according to Equation A.3.1.

$$\rho_{av7} = (1 + 0.008127)[1 - 0.008127 / (0.008127 + 0.62198)]\, 83891.4308 / (287.08 \times 305.9084) = 0.95061 \text{ kg/m}^3$$

The air mass velocity through the minimum cross-sectional flow area of the finned tube heat exchanger is

$$G_{avc} = m_{av67}/A_c = 270.0159/41.0853 = 6.5721 \text{ kg/m}^2\text{s}$$

The mean free-stream air velocity through the heat exchanger is

$$v_{av67} = m_{av67} / (\rho_{av67}\, A_{frd}) = 270.0159 / (0.97915 \times 93.7024) = 2.943 \text{ m/s}$$

The velocity of the air at the outlet of the heat exchanger is

$$v_{av7} = m_{av67} / (\rho_{av7}\, A_{frd}) = 270.0159 / (0.95061 \times 93.7024) = 3.0314 \text{ m/s}$$

The Euler number for the four-row, finned-tube heat exchanger can be determined according to Equation 5.5.9.

$$Eu = \frac{\rho_{av67}\, \Delta p}{G_{avc}^2} = 2 \times 4 \left[1 - 2\exp\left\{\frac{0.0572 - 0.058}{4 \times 0.0276}\right\} / \left\{1 + \frac{0.058 - 0.0572}{0.0276}\right\}\right] \times \left[0.021 + \frac{13.6\,(0.0572 - 0.0276)}{9936.5488\,(0.0028 - 0.0005)} + 0.25246\left\{\frac{0.0572 - 0.0276}{9936.5488(0.0028 - 0.0005)}\right\}^{0.2}\right] = 2.4702$$

With this value and taking into consideration the pressure drop through the noise attenuator, find the static pressure at (7) immediately downstream of the heat exchanger.

$$p_{a7} = p_{a6} - \left[\frac{Eu\ G_{avc}^2}{\rho_{av\,67}} + K_{na} \left(\frac{\rho_{av\,67}}{\rho_{av\,6}} \right) \frac{\rho_{av\,67}\, v_{av\,67}^{\ 2}}{2} + \frac{\rho_{av\,7}\, v_{av\,7}^{\ 2}}{2} \right]$$

$$= 84017.1026 - \left[2.4702 \text{ x } \frac{6.5721^2}{0.97915} + \frac{2.78 \text{ x } 0.97915 \text{ x } 0.97915 \text{ x } 2.943^2}{1.0094 \text{ x } 2} \right.$$

$$\left. + \frac{0.95061 \text{ x } 3.0314^2}{2} \right] = 83891.4308 \text{ N/m}^2$$

Wet section

The water leaving the dry section enters the wet section at a temperature

$$T_{wiw} = T_{wod} = 310.6171 \text{ K.}$$

Other conditions through the wet section of the hybrid cooling system are found to be satisfied under the following conditions:

- Dry air mass flow rate: $m_{a34} = 482.345$ kg/s
- Outlet water temperature: $T_{wo} = 296.014$ K
- Mean air velocity through the fill: $v_{av34} = 2.7656$ m/s
- Air pressure after the drift eliminators: $p_{a5} = 83{,}931.5803$ N/m^2

Losses through fill and other losses in its immediate vicinity based on the effective frontal area of the fill are

$$(K_{fs} + K_c) + K_{fi} + K_{sp} + K_{wd} + K_{de} = 11.2404$$

The following calculations show these values satisfy the energy and draft equation.

According to Appendix A, the thermophysical properties of the air entering the wet section at

$$T_{a1} = 288.6 \text{ K}, \ T_{wb} = 284.2 \text{ K}$$

and

$$p_{a1} = 84100 \text{ N/m}^2$$

are as follows:

- Density of air-vapor: ρ_{av1} = 1.0101 kg/m^3 using Equation A.3.1
- Dynamic viscosity: μ_{av1} = 1.7857 x 10^{-5} kg/ms using Equation A.3.3
- Enthalpy: i_{ma1} = 36114.7173 J/kg dry air using Equation A.3.6b

The diffusion coefficient for an air-vapor mixture at this condition can be determined using Equation 4.1.2.

$$D = 0.04357 \text{ x } 288.6^{1.5}\left(\frac{1}{28.97}+\frac{1}{18.016}\right)^{0.5}/\left[84100\left(29.9^{0.333}+18.8^{0.333}\right)^2\right]$$

$$= 2.3 \text{ x } 10^{-5} \text{ m}^2/\text{s}$$

According to Equation 4.1.5, the corresponding Schmidt number is

$$Sc = \mu_{av1}/(\rho_{av1}D) = 1.7857 \text{ x } 10^{-5}/(1.0101 \text{ x } 2.3 \text{ x } 10^{-5}) = 0.7686$$

Since the entrance duct to the wet section is relatively long, it may be assumed that the inlet flow is similar to that obtained with a well-rounded inlet. The approximate effective width of the fill can be determined using Equation 8.3.6.

$$\frac{W_{fie}}{W_{fi}} = 1.0487 - 0.17408\,\ell n\left(\frac{15}{3.5}\right) + 0.09\,\ell n\,11.2404 = 1.0131$$

Since W_{fie} cannot be greater than W_{fi}, let

$$W_{fie} = W_{fi}$$

The frontal area of the fill is given by

$$A_{fr} = B_{fi}W_{fi} = 12 \text{ x } 15 = 180 \text{ m}^2$$

The mass velocity of the dry air through the fill is

$$G_a = m_{a34}/A_{fr} = 482.345/180 = 2.6797 \text{ kg/m}^2\text{s}$$

Similarly, the mass velocity of the water is

$$G_w = m_w/A_{fr} = 450/180 = 2.5 \text{ kg/m}^2\text{s}$$

To find the transfer coefficient in the rain zone, conditions immediately under the fill or at the outlet of the rain zone are required. As a first

approximation, thermophysical properties of the water can be evaluated at the water outlet temperature, which was given as T_{wo} = 296.014 K.

- Density of the water: $\rho_{w3} \approx 997.5455$ kg/m^3 using Equation A.4.1
- Surface tension of water: $\sigma_{w3} \approx 0.072339$ N/m using Equation A.4.7
- Humidity ratio of saturated air: $w_{sw3} \approx 0.021414$ kg/kg dry air using Equation A.3.5

The mean velocity of the water based on the effective frontal area of the fill at (3) is given by

$$v_{w3} = m_w / (\rho_{w3} A_{fr}) = 450 / (997.5455 \text{ x } 180) = 0.0025062 \text{ m/s}$$

The corresponding velocity of the air at (3) is

$$v_{av3} \approx m_{av1} / (\rho_{av1} A_{fr}) = m_{a34}(1 + w_1) / \rho_{av1} A_{fr}$$

$$= 482.345(1 + 0.008127) / (1.0101 \text{ x } 180) = 2.6744 \text{ m/s}$$

To find the transfer coefficient in a rectangular rain zone, Equation 4.6.15 is employed.

$$\frac{h_{drz} a_{rz} H_i}{G_w} = 3.6 \left(\frac{p_{a1}}{R_v T_{a1} \rho_{w3}}\right)\left(\frac{D}{v_{av3} d_d}\right)\left(\frac{H_3}{d_d}\right) \text{Sc}^{0.33} \left[\ell n \left(\frac{w_{sw3} + 0.622}{w_1 + 0.622}\right) / (w_{sw3} - w_1) \right]$$

$$\text{x } [4.68851 \, a_\rho \rho_{av1} - 187128.7 \, a_\mu \mu_{av1} - 2.29322 + 22.4121$$

$$\text{x} \left\{0.350396 (a_v v_{av3})^{1.38046} + 0.09\right\} \left\{1.60934 (a_L H_3)^{-1.12083} + 0.66\right\}$$

$$\text{x} \left\{34.6765 (a_L d_d)^{0.732448} + 0.45\right\} \exp\{7.7389 \exp(-0.399827 \, a_L H_3)$$

$$\text{x } \ell n \left(0.087498 \exp(0.026619 \, a_L W_{fie}) + 0.85\right)\}]$$

where

$$a_\rho = 998/?_{w3} = 998/997.5455 = 1.0004 \text{ m}^3/\text{kg}$$

$$a_\mu = 3.061 \times 10^{-6} \left(\rho_{w3}^{\ 4}\, g^9 / \sigma_{w3}\right)^{0.25} = 3.061 \times 10^{-6} \left(997.5455^4 \times 9.8^9 / 0.072339\right)^{0.25}$$

$$= 1.0004 \text{ s/kgm}$$

$$a_v = 73.298 \left(g^5 \sigma_{w3}^{\ 3} / \rho_{w3}^{\ 3}\right)^{0.25} = 73.298 \left(9.8^5 \times 0.072339^3 / 997.5455^3\right)^{0.25} = 0.99875 \text{ s/m}$$

$$a_L = 6.122\ (g\sigma_{w3}/\rho_{w3})^{0.25} = 6.122(9.8 \times 0.072339/997.5455)0.25 = 0.99956 \text{ m}^{-1}$$

Thus,

$$\frac{h_{drz}\, a_{rz}\, H_i}{G_w} = 3.6 \left(\frac{84100}{461.52 \times 288.6 \times 997.5455}\right)\left(\frac{2.3 \times 10^{-5}}{2.6744 \times 0.0035}\right)\left(\frac{3.5}{0.0035}\right) 0.7686^{0.33}$$

$$\times\ \ell n \left(\frac{0.021414 + 0.622}{0.008127 + 0.622}\right) / (0.021414 - 0.008127)$$

$$\times \left[4.68851 \times 1.0004 \times 1.0101 - 187128.7 \times 1.0004 \times 1.7857 \times 10^{-5} - 2.29322\right.$$

$$+ 22.412\left\{0.350396 (0.99875 \times 2.6744)^{1.38046} + 0.09\right\}$$

$$\times \left\{1.60934\ (0.99956 \times 3.5)^{-1.12083} + 0.66\right\}\left\{34.6765\ (0.99956 \times 0.0035)^{0.732448}\right.$$

$$+ 0.45\left.\right\} \exp\left\{7.7389 \exp\left(-0.399827 \times 0.99956 \times 3.5\right)\right.$$

$$\left.\left.\times\ \ell n\ (0.087498 \exp(0.026619 \times 0.99956 \times 15) + 0.85)\right\}\right] = 0.25924$$

The transfer coefficient for the fill is given as

$$\frac{h_{dfi}\ \ a_{fi}\ \ L_{fi}}{G_w} = 0.5061 G_w^{-0.094} G_a^{0.6023} = 0.5061 \times 2.5^{-0.094} \times 2.6797^{0.6023} = 0.84074$$

Using Equation 7.2.4, the transfer coefficient in the spray zone is calculated as

$$\frac{h_{dsp}\, a_{sp}\, L_{sp}}{G_w} = 0.2 \text{ x } 0.3\left(\frac{2.6797}{2.5}\right)^{0.5} = 0.062118$$

Add the transfer coefficients in the rain, fill, and spray zones and apply the Chebyshev numerical method of integration to the Merkel equation, i.e.,

$$\frac{h_{drz}\, a_{rz}\, H_3}{G_w} + \frac{h_{dfi}\, a_{fi}\, L_{fi}}{G_w} + \frac{h_{dsp}\, a_{sp}\, L_{sp}}{G_w} = 0.25924 + 0.84074 + 0.062118 = 1.1622$$

$$= \int_{T_{wo}}^{T_{wi}} \left(\frac{c_{pw}\, dT}{i_{masw} - i_{ma}}\right) \approx \frac{c_{pwm}\,(T_{wiw} - T_{wo})}{4}\left[\frac{1}{\Delta i_{(1)}} + \frac{1}{\Delta i_{(2)}} + \frac{1}{\Delta i_{(3)}} + \frac{1}{\Delta i_{(4)}}\right]$$

The enthalpy differentials in this equation are evaluated at the following temperatures:

- $T_{w(1)} = T_{wo} + 0.1(T_{wiw} - T_{wo}) = 296.014 + 0.1(310.6171 - 296.014) = 297.4743$ K
- $T_{w(2)} = 296.014 + 0.4(310.6171 - 296.014) = 301.8552$ K
- $T_{w(3)} = 296.014 + 0.6(310.6171 - 296.014) = 304.7758$ K
- $T_{w(4)} = 296.014 + 0.9(310.6171 - 296.014) = 309.1567$ K

To determine the enthalpy of the saturated air at condition (1), i.e.,

$$T_{w(1)} = 297.4743 \text{ K}$$

the humidity ratio for saturated air is evaluated at the mean pressure through the wet section, i.e.,

$$p_{a15} = (p_{a1} + p_{a5})/2 = (84100 + 83931.5803)/2 = 84015.7902 \text{ N/m}^2$$

According to Equation A.3.5,

$$w_{s(1)} = 0.023483 \text{ kg/kg}$$

The required mean specific heats are evaluated at

$$(T_{w(1)} + 273.15)/2 = (297.4743 + 273.15)/2 = 285.3122 \text{ K}$$

- Specific heat of dry air: $c_{pa(1)m} = 1006.528$ J/kg K using Equation A.1.2
- Specific heat of water vapor: $c_{pv(1)m} = 1872.9247$ J/kg K using Equation A.2.2

According to Equation A.3.6b, the enthalpy of the saturated air at condition (1) is,

$$i_{masw(1)} = c_{pa(1)m}(T_{w(1)} - 273.15) + w_{s(1)}\left[i_{fgwo} + c_{pv(1)m}(T_{w(1)} - 273.15)\right]$$

$$= 1006.528(297.4743 - 273.15) + 0.023483\left[2.5016 \times 10^{6} + 1872.9247\right.$$

$$\left. \times (297.4743 - 273.15)\right] = 84297.3326 \text{ J/kg dry air}$$

Find the specific heat of the water at its mean temperature

$$T_{wm} = (T_{wiw} + T_{wo})/2 = (310.6171 + 296.014)/2 = 303.3155 \text{ K}$$

according to Equation A.4.2, i.e.,

$$c_{pwm} = 4178.5265 \text{ J/kg K}$$

With this value, find the enthalpy of the air at condition (1) according to Equation 4.2.21.

$$i_{ma(1)} = m_w c_{pwm} (T_{w(1)} - T_{wo})/m_{a34} + i_{ma1}$$

$$= 450 \times 4178.5265 (297.4743 - 296.014)/482.345 + 36114.7173$$

$$= 41807.4357 \text{ J/kg}$$

With the previous values, find the enthalpy differential at condition (1)

$$\Delta i_{(1)} = (i_{masw(1)} - i_{ma(1)}) = 84297.3326 - 41807.4357 = 42489.8968 \text{ J/kg}$$

Similarly, determine the remaining three enthalpy differentials, i.e.,

$$\Delta i_{(2)} = 107452.3836 - 58885.591 = 48566.7926 \text{ J/kg}$$

$$\Delta i_{(3)} = 125759.1774 - 70271.0278 = 55488.1496 \text{ J/kg}$$

$$\Delta i_{(4)} = 158562.7279 - 87349.183 = 71213.5449 \text{ J/kg}$$

Substitute these values into the Merkel equation given above, to find

$$1.1622 = 4178.5265(310.6171 - T_{wo})(1/42489.8968 + 1/48566.7926 + 1/55488.1496$$

$$+ 1/71213.5449)/4$$

or

$$T_{wo} = 296.014 \text{ K}$$

This temperature is in agreement with the value assumed.

The enthalpy of the saturated air leaving the wet section can be determined with the aid of Equation 4.2.21, i.e.,

$$i_{mas5} = m_w c_{pwm} (T_{wiw} - T_{wo}) / m_{a34} + i_{ma1}$$

$$= 450 \text{ x } 4178.5265(310.6171 - 296.014)/482.345 + 36114.7173$$

$$= 93041.8847 \text{ J/kg K}$$

With this enthalpy, it is possible to determine the air temperature at (5) by following a trial and error method to solve Equation A.3.6b. By following this procedure, find

$$T_{a5} = 299.2212 \text{ K}$$

To confirm this is the correct value, determine the thermophysical properties of saturated air at

$$T_{a5} = 299.2212 \text{ K}$$

and

$$p_{a5} = 83931.5803 \text{ N/m}^2$$

- Density of air-vapor: $\rho_{av5} = 0.96216$ kg/m^3 using Equation A.3.1
- Dynamic viscosity: $\mu_{av5} = 1.8162 \text{ x } 10^{-5}$ kg/ms using Equation A.3.3
- Humidity ratio: $w_5 = 0.026191$ kg/kg using Equation A.3.5
- Specific heats are evaluated at:
  $(T_{a5} + 273.15)/2 = (299.2212 + 273.15)/2 = 286.1856$ K
- Specific heat of air: $c_{pa5m} = 1006.5475$ J/kg K (A.1.2)
- Specific heat of water vapor: $c_{pv5m} = 1873.6637$ J/kg K (A.2.2)
- Specific heat of water: $c_{pw5m} = 4192.8305$ J/kg K (A.4.2)
- The specific heat of the air-vapor mixture is:
  $c_{pav5m} = c_{pa5m} + w_5 c_{pv5m} = 1006.5475 + 0.026191 \text{ x } 1873.6637 = 1055.6215$ J/kg K

Determine i_{mas5} using Equation A.3.6b.

$$i_{mas5} = c_{pa5m}(T_{a5} - 273.15) + w_5\left[i_{fgwo} + c_{pv5m}(T_{av} - 273.15)\right]$$

$$= 1006.5475(299.2212 - 273.15) + 0.026191\left[2.5016 \text{ x } 10^6 + 1873.6637\right.$$

$$\text{x } (299.2212 - 273.15)\left.\right] = 93041.8847 \text{ J/kg}$$

This value is similar to that obtained previously, which confirms the value of T_{a5} is correct.

The approximate harmonic mean air density of the air flowing through the fill is

$$\rho_{av34} \approx \rho_{av15} = 2\left[1/\rho_{av1} + 1/\rho_{av5}\right]^{-1} = 2\left[1/1.0101 + 1/0.96216\right]^{-1}$$

$$= 0.98556 \text{ kg/m}^3$$

The mean air-vapor mass flow rate through the fill is approximately

$$m_{av34} \approx m_{av15} = m_{a34}(2 + w_1 + w_5)/2 = 482.345(2 + 0.008127 + 0.026191)/2$$

$$= 490.6216 \text{ kg/s}$$

The air-vapor mass flow rate at (1) is

$$m_{av1} = m_{a34}(1 + w_1) = 482.345(1 + 0.008127) = 486.2867 \text{ kg/s}$$

while the mean air-vapor mass flow rate at (5) is

$$m_{av5} = m_{a34}(1 + w_5) = 482.345(1 + 0.026191) = 494.9783 \text{ kg/s}$$

The mean air-vapor velocity across the fill is

$$v_{av34} \approx v_{av15} = m_{av15}/(\rho_{av15} A_{fre}) = 490.6216/(0.98556 \text{ x } 180) = 2.7656 \text{ m/s}$$

This value is in agreement with that specified at the beginning of the evaluation.

In further calculations, the loss coefficients in the wet section will be evaluated.

At the inlet to the wet section, a loss is experienced across the noise attenuators, which have a frontal area of

$$A_{na} = 2B_3H_3 = 2 \text{ x } 12 \text{ x } 3.5 = 84 \text{ m}^2$$

Based on mean fill conditions, the resultant loss coefficient is

$$K_{nafi} = K_{na}\left(\frac{\rho_{a34}}{\rho_{av1}}\right)\left(\frac{A_{fr}}{A_{na}}\right)^2\left(\frac{m_{av1}}{m_{av34}}\right)^2 = 2.78\left(\frac{0.98556}{1.0101}\right)\left(\frac{180}{84}\right)^2\left(\frac{486.2867}{490.6216}\right)^2$$

$$= 12.234$$

The loss coefficient for the rain zone is, using Equation 4.6.13,

$$K_{rz} = 1.5\, a_v v_{w3}(H_3/d_d)[0.219164 + 8278.7\, a_\mu \mu_{av1} - 0.30487\, a_\rho \rho_{av1}$$

$$+ 0.954153\{0.328467\exp(135.7638\, a_L d_d) + 0.47\}\{26.28482(a_L H_3)^{-2.95729} + 0.56\}$$

$$\text{x}\exp\{\ell n(0.204814\exp(0.066518\, a_L W_{fi}) + 0.21)(3.9186\exp(-0.3\, a_L H_3))$$

$$\text{x}\,(0.31095\,\ell n\,(a_L d_d) + 2.63745)\}\{2.177546\,(a_v v_{av}3)^{-1.46541} + 0.21\}]$$

Thus,

$$K_{rz} = 1.5\text{ x }0.99875\text{ x }0.0025062\,(3.5/0.0035)\,[0.219164 + 8278.7$$

$$\text{x}\,1.0004\text{ x}\,1.7857\text{ x}\,10^{-5} - 0.30487\text{ x}\,1.0004\text{ x}\,1.0101 + 0.954153$$

$$\{0.328467\exp(135.7638\text{ x }0.99956\text{ x }0.0035) + 0.47\}\text{ x }\{26.28482(0.99956$$

$$\text{x}\,3.5)^{-2.95729} + 0.56\}\exp\{\ell n\,(0.204814\exp(0.066518\text{ x }0.99956\text{ x }15)$$

$$+ 0.21)(3.9186\exp(-0.3\text{ x }0.99956\text{ x }3.5))(0.31095\,\ell n\,(0.99956\text{ x }0.0035)$$

$$+ 2.63745)\}\text{ x }\{2.177546\,(0.99875\text{ x }2.6744)^{-1.46541} + 0.21\}] = 3.922$$

If this loss coefficient is based on fill conditions, find

$$K_{rzfi} = K_{rz}\,(\rho_{av34}/\rho_{av1})(m_{av1}/m_{av34})^2$$

$$= 3.922(0.98556/1.0101)(486.2867/490.6216)^2$$

$$= 3.759$$

If the specified fill support and contraction loss coefficient is referred to conditions through the fill, find

$$(K_{fs} + K_{ctc})_{fi} = 0.5\,(\rho_{av34}/\rho_{av1})(m_{av1}/m_{av34})^2$$

$$= 0.5\,(0.98556/1.0101)(486.2867/490.6216)^2 = 0.47921$$

To find the loss coefficient across the fill, determine the approximate air velocity at its outlet and inlet respectively, i.e.,

$$v_{av4} \approx v_{av5} \approx m_{av5}/(\rho_{av5}\,A_{fr}) = 494.9783/(0.96216 \text{ x } 180) = 2.858 \text{ m/s}$$

and

$$v_{av3} \approx m_{av1}/(\rho_{av1}\,A_{fr}) = 486.2867/(1.0101 \text{ x } 180) = 2.6744 \text{ m/s}$$

According to the note at the end of Example 4.3.1, the actual fill loss coefficient in this case is

$$K_{fi} = K_{fdm} + \frac{(\rho_{av4}\,v_{av4}^{\,2} - \rho_{av3}\,v_{av3}^{\,2})}{\rho_{av34}\,v_{av34}^{\,2}} \approx K_{fdm} + \frac{\rho_{av5}\,v_{av5}^{\,2} - \rho_{av1}\,v_{av3}^{\,2}}{\rho_{av34}\,v_{av34}^{\,2}}$$

$$= 3.62 \text{ x } 2.5^{1.2752}\,2.6797^{-1.0356} + (0.96216 \text{ x } 2.858^2 - 1.0101 \text{ x } 2.6744^2)$$

$$/\,(0.98556 \text{ x } 2.7656^2) = 4.2849$$

The loss coefficient through the spray zone is given by Equation 7.2.19. If this is referred to the fill conditions find, according to Equation 7.2.20,

$$\kappa_{spfi} \approx L_{sp}[0.4\,(G_w/G_a) + 1](\rho_{av34}/\rho_{av5})(m_{av5}/m_{av34})^2$$

$$= 0.3\,[0.4\,(2.5/2.6797) + 1](0.98556/0.96216)(494.9783/490.6216)^2$$

$$= 0.4295$$

For the water distribution system, find

$$K_{wdfi} = K_{wd}(\rho_{av34} / \rho_{av5})(m_{av5} / m_{av34})^2$$

$$= 0.775\,(0.98556 / 0.96216)(494.9783 / 490.6216)^2 = 0.808$$

According to Equation 4.7.2, the loss coefficient for the drift eliminators referred to fill conditions is

$$K_{defi} = 27.4892\,[m_{av5} / (\mu_{av5}\, A_{fr})]^{-0.14247}(\rho_{av34} / \rho_{av5})(m_{av5} / m_{av34})^2$$

$$= 27.4892\,[494.9783 / (1.8162 \times 10^{-5} \times 180)]^{-0.14247}$$

$$\times\,(0.98556 / 0.96216)(494.9783 / 490.6216)^2 = 5.2392$$

Because of the horizontal air inflow into the fill from two sides, it can be assumed the cooling tower inlet loss coefficient for rounded inlets is applicable. For small values of 0.5 W_{fi}/H_i, e.g., 0.5 W_{fi}/H_i = 0.5 x 15/3.5 = 2.14, the loss coefficient hardly deviates from the square-edged inlet loss coefficient for K_{he} = 35, as shown in Figure 8.3.7. Equation 8.3.4 may be employed with

$$K_{he} = (K_{fs} + K_{ctc} + K_{fi} + K_{sp} + K_{wd} + K_{de})_{fi} =$$

$$0.47921 + 4.2849 + 0.4295 + 0.808 + 5.2392 = 11.24$$

to determine the approximate loss coefficient.

$$K_{ct} = \left[1.1 + 1.1(0.5 \times 15 / 3.5)^3 - 0.05(0.5 \times 15 / 3.5)\exp(0.5 \times 15 / 3.5)\right]$$

$$11.24^{[-0.29 + 0.079\cos\{0.5 \times 15 \times 180/(3.5 \times \pi)\} + 0.102\sin\{0.5 \times 15 \times 180/(3.5 \times \pi)\}]}$$

$$= 6.0569$$

Refer to conditions at the fill, and find

$$K_{ctfi} = K_{ct}(\rho_{av34}/\rho_{av1})(m_{av1}/m_{av34})^2 = 6.0569 \times (0.98556/1.0101)$$

$$\times\,(486.2867/490.6216)^2 = 5.806$$

Based on fill conditions, the sum of all the loss coefficients through the effective wet section of the tower is

$$(K_{na} + K_{rz} + K_{ct} + (K_{fs} + K_{ctc}) + K_{fi} + K_{sp} + K_{wd} + K_{de})_{fi}$$

$$= 12.234 + 3.759 + 5.806 + 0.47921 + 4.2849 + 0.4295 + 0.808 + 5.2392 = 33.04$$

The hydrostatic pressure difference between ground level and the middle of the fill is:

$$p_{a1}\left[1-\left\{1-0.00975\left(H_3 + L_{fi}/2\right)/T_{a1}\right\}^{3.5(1+w_1)[1-w_1/(w_1+0.62198)]}\right] = 84100\,[1-$$

$$\left\{1-0.00975(3.5+1.878/2)/288.6\right\}^{3.5(1+0.008127)[1-0.008127/(0.008127+0.62198)]}\Big] = 43.929\ \mathrm{N/m^2}$$

According to Equation 7.2.10, the temperature lapse rate for the air above the fill is:

$$\xi_{Ta5} = -(1+0.026191)\,9.8\Big[1+0.42216\times10^{-11}\times0.026191^2\times83931.5803$$

$$\times\exp(5406.1915/299.2212)\left\{2.5016\times10^6-(4192.8305-1873.6637)(299.2212\right.$$

$$\left.-273.15)\right\}/\left\{(0.026191+0.622)\,287.08\times299.2212\right\}\Big]/\Big[1055.6215+3.6693\times10^{-8}$$

$$\times\,0.026191^2\times83931.5803\times\exp(5406.1915/299.2212)\left\{2.5016\times10^6\right.$$

$$\left.-(4192.8305-1873.6637)(299.2212-273.15)\right\}/(299.2212)^2\Big] = -0.00345\ \mathrm{K/m}$$

With this value, the hydrostatic pressure difference between the middle of the fill and immediately upstream of the mixers can be determined.

$$p_{a5}\left[1-\left\{1+\xi_{Ta5}\left(\frac{H_8-H_3-L_{fi}/2}{T_{a5}}\right)\right\}^{-[(1+w_5)\{1-w_5/(w_5+0.62198)\}g/(R\xi_{Ta}5)]}\right]$$

$$= 83931.5803\left[1-\left\{1-0.00345\left(\frac{8.38-3.5-1.878/2}{299.2212}\right)\right\}^{-[(1+0.026191)}\right.$$

$$\left.\times\left\{1-0.026191/(0.026191+0.62198)\right\}9.8/(-287.08\times0.00345)\right]] = 37.153\ \mathrm{N/m^2}$$

The static pressure immediately upstream of (8) can be determined by taking into consideration the previous hydrostatic pressure differences and pressure drops due to flow resistances, i.e.,

$$p_{a8} = p_{a1} - 43.929 - 37.153 - 33.04\,\rho_{av34} v_{av34}^2 / 2 - \rho_{av8} v_{av8}^2 / 2$$

$$= 84100 - 81.082 - 33.04 \text{ x } 0.98556 \text{ x } 2.7656^2 / 2 - 0.96216 \text{ x } 2.858^2 / 2$$

$$= 83890.46 \text{ N/m}^2$$

where

$\rho_{av8} \approx \rho_{av5}$

$v_{av8} \approx v_{av5}$

This value is in agreement with the static pressure after the dry section, i.e.,

$$p_{a7} = 83891.4308 \text{ N/m}^2$$

The static pressure at (5) can be obtained by subtracting the hydrostatic pressure difference.

Mixed section

If it is assumed that complete mixing of the wet and the dry air streams occurs at (8), the properties of the mixed air at this cross section can be determined as follows:

- The total air-vapor mass flow rate through the mixed region with $w_7 = w_6 = w_1$ is

$$m_{av8} = m_{a34}(1 + w_5) + m_{a67}(1 + w_7)$$

$$= 482.345(1 + 0.026191) + 267.8392(1 + 0.008127) = 764.994 \text{ kg/s}$$

- The corresponding humidity ratio of the mixed air is

$$w_8 = (w_5 m_{a34} + w_7 m_{a67}) / (m_{a34} + m_{a67})$$

$$= (0.026191 \text{ x } 482.345 + 0.008127 \text{ x } 267.8392) / (482.345 + 267.8392)$$

$$= 0.019742 \text{ kg / kg dry air}$$

- The enthalpy of the mixed air stream is given by the following equation:

$$i_{ma8} = (i_{ma5} m_{a34} + i_{ma7} m_{a67}) / (m_{a34} + m_{a67})$$

$$= (93041.8847 \text{ x } 482.345 + 53805.621 \text{ x } 267.8392) / (482.345 + 267.8392)$$

$$= 79033.3124 \text{ J / kg dry air}$$

With this value for the enthalpy at (8) and by following a trial and error procedure, the drybulb temperature T_{a8} = 301.5588 K is found with the aid of Equation A.3.6b. This depends on the relevant specific heats for dry air and water vapor being evaluated according to Equations A.1.2 and A.2.2 respectively at

$$(301.5588 + 273.15)/2 = 287.3544 \text{ K.}$$

Find

$$i_{ma8} = 1006.5748 (301.5588 - 273.15) + 0.019742 [2.5016 \text{ x } 10^6 + 1874.6565$$

$$(301.5588 - 273.15)] = 79033.3124 \text{ J / kg}$$

This value is in agreement with the one obtained previously.

To find the change in total pressure between (8) and the outlet at (11), determine the density of the air-vapor at (8) using Equation A.3.1:

$$\rho_{av8} = (1 + 0.019742)[1 - 0.019742 / (0.019742 + 0.62198)]$$

$$\text{x } 83891.4308 / (287.08 \text{ x } 301.5588) = 0.95777 \text{ kg/ m}^3$$

The air-velocity at (8) follows from

$$v_{av8} = m_{av8} / (\rho_{av8} A_{fr}) = 764.994 / (0.95777 \text{ x } 180) = 4.4373 \text{ m/s}$$

The loss coefficient of the mixing devices based on the cross-sectional area of the fan casing is

$$K_{mc} = K_m (A_c / A_{fr})^2 = 0.8 [\pi \text{ x } 9.5265^2 / (4 \text{ x } 180)]^2 = 0.12545$$

The approximate mean air velocity through the fan assuming $\rho_{av9} \approx \rho_{av8}$ and with $m_{av9} = m_{av8}$ is

$$v_{av9} = 4m_{av9} / (\rho_{av9} \pi d_c^2) = 4 \text{ x } 764.994 / (0.95777 \text{ x } \pi \text{ x } 9.5265^2) = 11.2057 \text{ m/s}$$

Assume the velocity distribution at (8) to be uniform, and take into consideration K_{mc}, K_{up} and K_d as well as the required hydrostatic effect between cross sections (8) and (11). Thus, the fan static pressure differential can be expressed as

$$\Delta p_{Fs} = p_{a12} - p_{a8} - (\rho_{av8} v_{av8}^2) / 2 + (K_{mc} + K_{up} + K_{do})(\rho_{av9} v_{av9}^2) / 2$$

$$+ p_{a8} \left[1 - \{ 1 - 0.00975 (H_{11} - H_6) / T_{a8} \}^{3.5(1+w_8)[1 - w_8/(w_8 + 0.62198)]} \right]$$

where

$p_{a12} = p_{a11}$

$H_8 = H_6$

The atmospheric pressure at (12) can be found using Equation 7.2.9:

$$p_{a12} = 84100 \left[1 - 0.00975 \text{ x } 15.38 / 288.6 \right]^{3.5 (1 + 0.008127) [1 - 0.008127 / (0.008127 + 0.62198)]}$$

$$= 83947.9012 \text{ N/m}^2$$

Substitute the previous values into the equation for Δp_{Fs}, and find with $\rho_{av9} \approx \rho_{av8}$

$$\Delta p_{Fs} = 83947.9012 - 83891.4308 - (0.95777 \text{ x } 4.4373^2) / 2 + (0.12545 + 0.2 + 0.2)$$

$$\text{x } (0.95777 \text{ x } 11.2057^2) / 2 + 83891.4308 \left[1 - \{ 1 - 0.00975 (15.38 - 8.38) \right.$$

$$\left. / 301.5588 \}^{3.5 (1 + 0.019742) [1 - 0.019742 / (0.019742 + 0.62198)]} \right]$$

$$= 144.2997 \text{ N/m}^2$$

The required volume flow rate through the fan with $m_{av9} = m_{av8}$ is

$$V = m_{av8} / ?_{av9} = 764.994 / 0.95777 = 798.7221 \text{ m}^3/\text{s}$$

To confirm that these values for Δp_{Fs} and V are achieved at the specified fan rotational speed of 118 rpm, apply the fan law Equation 6.2.1 to find the air volume flow rate at the fan/diffuser reference speed of 120 rpm, i.e.,

$$V_{F/dif} = V/(N_F/N_{F/dif}) = 798.7221/(118/120) = 812.2598\ \mathrm{m^3/s}$$

For this air volume flow rate, the corresponding fan/diffuser static pressure can be determined from the specified performance equation.

$$\Delta P_{F/difs} = 299.903 + 40.0071 \times 10^{-3} \times 812.2598 - 96.5087 \times 10^{-6} \times 812.2598^2$$

$$- 152.2243 \times 10^{-9} \times 812.2598^3 = 187.1489\ \mathrm{N/m^2}$$

This value can be converted to actual operating conditions with the aid of the relevant fan law Equation 6.2.2, i.e.,

$$\Delta p_{Fs} = (N_F/N_{F/dif})^2(\rho_{av9}/\rho)\Delta p_{F/difs}$$

$$= (118/120)^2(0.95777/1.2)187.1489 = 144.43\ \mathrm{N/m^2}$$

This compares very well with the value of 144.2997 N/m^2 obtained previously.

The fan power at the specified reference condition is

$$P_{F/dif} = 203302.6779 - 58.3775 \times 812.2598 + 458.7692 \times 10^{-3} \times 812.2598^2$$

$$- 405.2315 \times 10^{-6} \times 812.2598^3 = 241.4012\ \mathrm{kW}$$

The actual fan shaft power can be obtained with the aid of Equation 6.2.3, i.e.,

$$P_F = P_{F/dif}(N_F/N_{F/dif})^3(\rho_{av9}/\rho)$$

$$= 241.4012\,(118/120)^3(0.95777/1.2) = 183.1984\ \mathrm{kW}$$

The efficiency of the fan is

$$\eta_F = \Delta p_{Fs} V / P_F = 144.43 \times 798.7221/183198 = 0.63 \text{ or } 63\%$$

The approximate plume characteristics can be determined by assuming the air drybulb temperature at the outlet of the diffuser is

$$T_{a11} \approx T_{a8} = 301.5588\ \mathrm{K}$$

while the humidity ratio

$$w_{11} = w_8 = 0.019742 \text{ kg/kg dry air}$$

If it is also assumed that the dilution of the plume air follows a linear path, the equation for this line can be determined as follows:

$$w = \left(\frac{w_{11} - w_1}{T_{a11} - T_{a1}}\right) T_a + \left(\frac{T_{a11} w_1 - T_{a1} w_{11}}{T_{a11} - T_{a1}}\right)$$

$$= \left(\frac{0.019742 - 0.008127}{301.5588 - 288.6}\right) T_a + \left(\frac{301.5588 \text{ x } 0.008127 - 288.6 \text{ x } 0.019742}{301.5588 - 288.6}\right)$$

$$= 8.963 \text{ x } 10^{-4} T_a - 0.25055$$

The equation for the saturation curve obtained from Equation A.3.5 is

$$w_s = 0.62509 \, p_{vs} / (p_{abs} - 1.005 \, p_{vs})$$

where

p_{vs} is obtained from Equation A.2.1

When the expressions shown in Figure 9.4.13 are plotted, they do not intersect, which means that no plume will be visible at the outlet of the cooling tower.

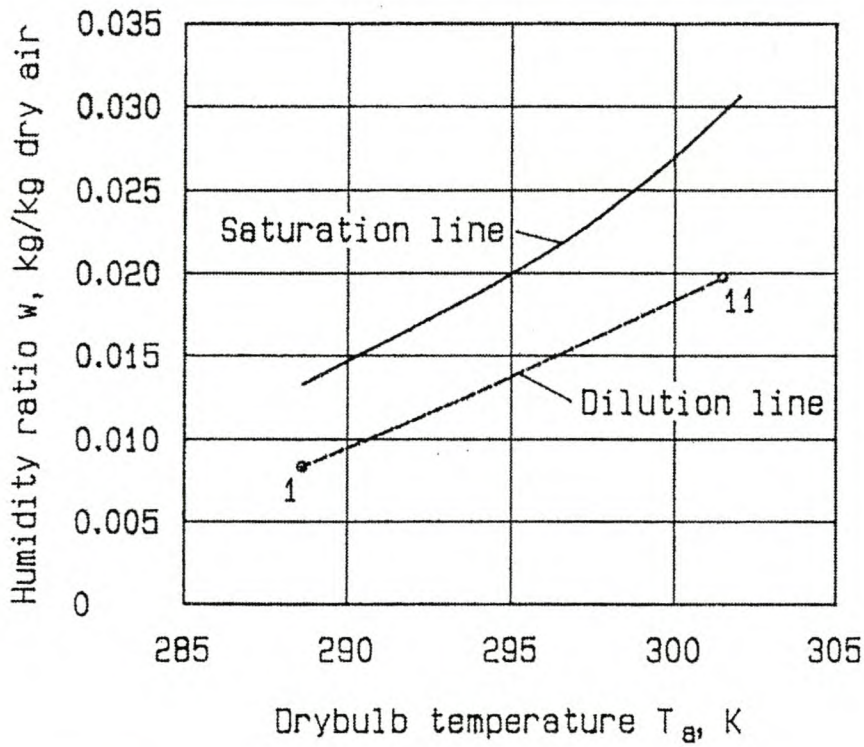

Fig. 9.4.13 Dilution Line for Hybrid Cooling Tower

Example 9.4.2

A wind having a velocity distribution of

$$v_w = v_{wr}\,(z/z_r)^{0.2}$$

- blows at a speed of v_w = 5 m/s
- 10 m above ground level
- at an angle of 45° with respect to the major axis of a hybrid cooling tower
- consisting of a row of six cells

Other ambient conditions and cell details are described in Example 9.4.1. Due to recirculation of the plume under windy conditions, the wetbulb temperature of the air entering the cooling tower will be higher than the value specified in Example 9.4.1. Determine the approximate, average-design, wetbulb temperature of the inlet air.

Solution

The mean velocity of the air leaving the diffuser or plume velocity is

$$v_{av11} = v_p = 4V / \left[\pi \{d_c + 2\,(3 \tan 7°)\}^2\right]$$

$$= 4 \text{ x } 798.7221 / \left[\pi \{9.5265 + 2\,(3 \text{ x } 0.1228)\}^2\right]$$

$$= 9.655 \text{ m/s}$$

With this value, find the ratio

$$v_w/v_p = 5/9.655 = 0.518$$

From Figure 9.4.7, it follows that the average recirculation is approximately 2%. With this recirculation and the ambient wetbulb temperature of T_{wb} = 11.05 °C, find a corresponding increase in wetbulb temperature of 0.375 °C from Figure 9.4.11 giving an average design wetbulb temperature of 11.425 °C.

9.5 Inversions

In the presence of an atmospheric temperature inversion, the performance of an air-cooled heat exchanger and of a cooling tower is reduced. This is because the potential driving force or pressure differential is less and the effective temperature of the air entering the cooling system is higher than during conditions when the adiabatic lapse rate prevails. In 1925, Merkel mentioned that temperature inversions might be the cause of apparent inconsistencies in cooling tower performance predictions.

Normally, cooling tower acceptance tests should not be performed during periods of inversions according to Lauraine, Lemmens, and Monjoie. During a temperature inversion, the moist air in the plume of a wet-cooling tower may be trapped in the inversion, and plume dispersion is greatly reduced. This may lead to fog formation and precipitation. In extreme cases, it can lead to the formation of ice. An indication of the nature and frequency of inversions is presented by Tesche. Exceptionally strong inversions have been observed in arid and desert areas where dry-cooling towers are most likely to be erected.

Buxmann tries to quantify the influence that an inversion has on the performance of a natural-draft, dry-cooling tower. Employing the temperatures measured 1.2 m above ground level and at the tower top, he assumes a linear profile between the two. According to his model, the effective air inlet temperature is the average of the two values. This approach enables him to obtain an improved estimate of the air inlet temperature. It also allows quantifying the effect of the inversion on the effective density difference between the ambient air and the heated air inside the tower. His model is approximate at best since it implies the air entering the tower is effectively drawn from an elevation between ground level and the top of the tower, while adiabatic compression is ignored. As shown in Figure 9.5.1, his analytical method, assuming a linear and a parabolic temperature distribution, predicts the trend of data obtained at the dry-cooling tower Grootvlei 5 according to Van der Walt et al.

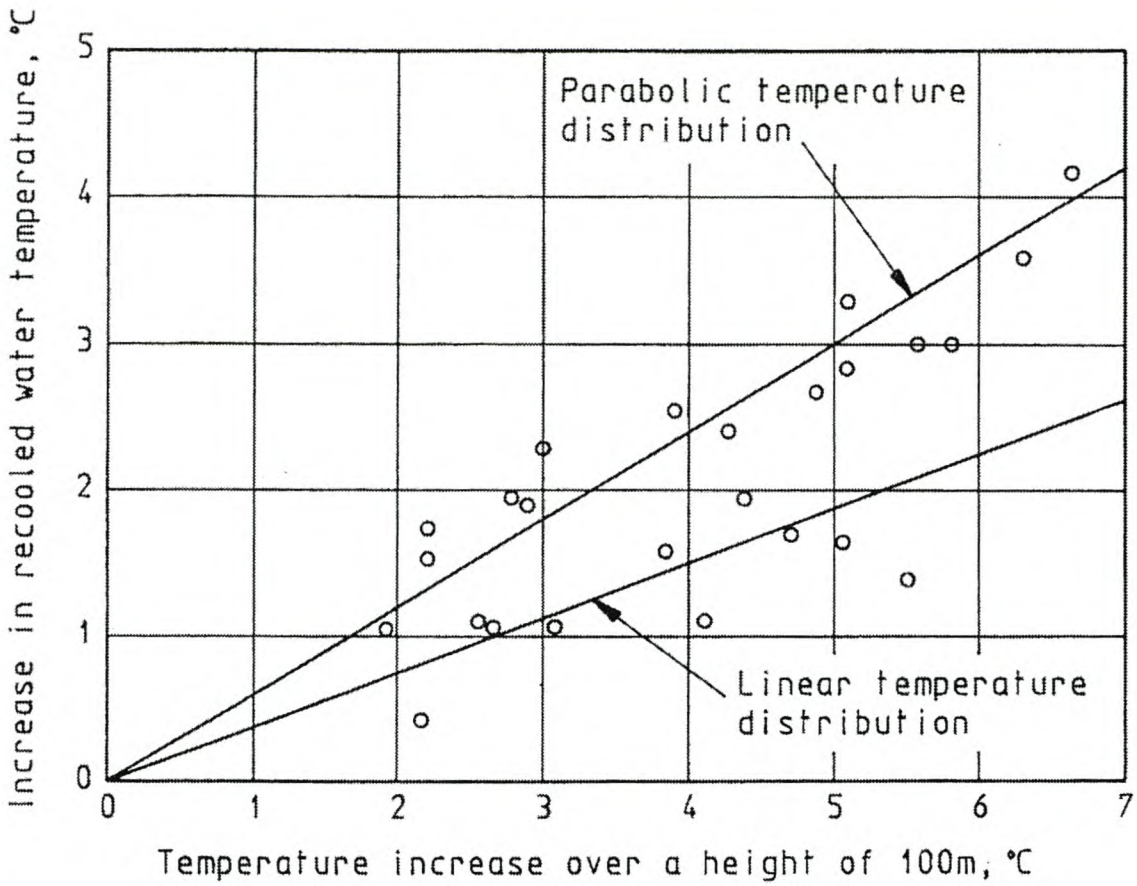

Fig. 9.5.1 Reduction in Performance due to Inversion at Grootvlei 5

The impact of an inversion on the performance of a large natural-draft, wet-cooling tower is quantified experimentally and analytically by Benton and Mirsky. The results of their study on a particular cooling tower are shown in Figure 9.5.2. During an inversion or positive lapse rate, the performance of the tower is measurably reduced due to the lower driving potential and higher effective inlet air temperature compared to conditions measured near ground level.

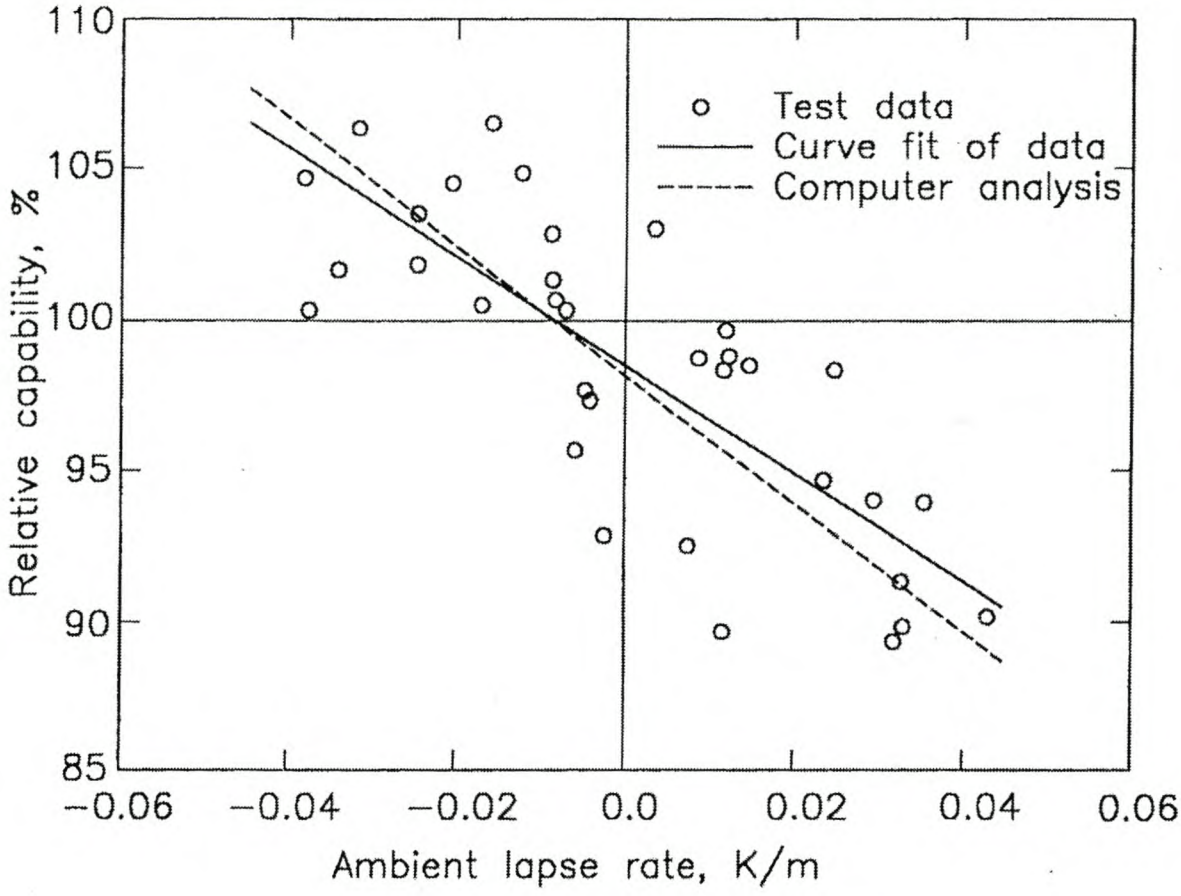

Fig. 9.5.2 Impact of Lapse Rate on Tower Performance

Hoffmann and Kröger numerically analyzed the air temperature and flow fields about and through a large dry-cooling tower during stable adiabatic daytime conditions and during inversions at night. Good agreement was obtained between measured and predicted recooled water temperatures under these conditions. A relatively simple expression was presented relating air inlet temperature of the cooling tower to limited meteorological measurements if the atmospheric stability class was known. Hoffmann employed this expression to determine the performance of a cooling tower under different conditions of ambient air temperature stratification.

References

Azad, R. S., *The Atmospheric Boundary Layer for Engineers,* Kluwer Academic Publishers, Dordrecht, 1993.

Baer, E., "Einfluss des Windes Auf die Strömung im Kamin eines Naturzug-kühlturmes," Doctoral thesis, Universität Karlsruhe, 1978.

Baer, E. et al., "Thermodynamische Untersuchungen am Naturzug-Nasskühlturm C des Kraftwerkes Neurath und Modelle für das Betriebsverhalten und die Schwadenausbreitung," *Fortschritt-Berichte der Verein Deutscher Ingenieure-Zeitschriften,* Reihe 15, no. 7, Verein Deutscher Ingenieure-Verlag, Düsseldorf, 1979.

Barbaud, J., "Cooling Tower of the NPP Civaux Auxiliary Systems: Features of the Function and Requirements Related to Nuclear Safety," Paper, Ninth International Association for Hydraulics Research Cooling Tower and Spraying Pond Symposium, von Karman Institute, Brussels, September 1994.

Bender, T. J., D. J. Bergstrom, and K. S. Rezkallah, "A Study on the Effects of Wind on the Air Intake Flow Rate of a Cooling Tower," *Journal of Wind Engineering and Industrial Aerodynamics,* 64-1:47–59, 61–72, 73–88, 1996.

Benton, D. and G. R. Mirsky, "Impact of Atmospheric Lapse Rate on Power Plant Performance," *Proceedings,* American Power Conference, 55-2:1427–1431, 1993.

Blanquet, J. C., F. Goldwirt, and B. Manas, "Wind Effects on the Aerodynamic Optimization of a Natural Draft Cooling Tower," *Proceedings,* International Association for Hydraulics Research Cooling Tower Workshop, Monterey, 1986.

Bourillot, C., J. L. Grange, and J. M. Lecoeuvre, "Effect of Wind on the Performance of a Natural Wet Cooling Tower," *Proceedings,* Second International Association of Hydraulics Research Cooling Tower Workshop, San Francisco, 1980.

Bouton, F., "Design Studies for Natural Draught Dry Towers," Société Hydrotechnique de France Conference, Paris, 1978.

British Standards Institution, *Water Cooling Towers, Part 3, Code of Practice for Thermal and Functional Design,* BS4485, 1988.

Buchlin, J. M. and D. Olivari, "Experimental Investigation of Flow in Natural Draft Cooling Towers by use of Heated Models," *Proceedings*, Third International Association for Hydraulic Research Cooling Tower Workshop, Budapest, 1982.

Buxmann, J., "Dry Cooling Tower Characteristics Effected by Cooling Circuit and the Top Shape of the Tower," *Proceedings*, Fifth International Association for Hydraulic Research Cooling Tower Workshop, Monterey, 1986.

Buxmann, J., "The Effect of Temperature Layers on the Heat Capacity of a Natural Draft Dry Cooling Tower," *Brennstoff-Wärme-Kraft*, 29-3:90–94, 1977.

Buxmann, J., "Operating Characteristics Influenced by Inversion and Inlet Pressure Losses at Dry Cooling Towers," International Association for Hydraulic Research Cooling Tower Workshop, Budapest, 1982.

Buxmann, J., "Strömungsverteilung und Wärmeübertragung bei unterschiedlichen Elementanordnugen im Trockenkühlturm," *Sonderforschungsbereich* 61, Teilproject E10, Bericht Nr. 54, Universität Hannover, 1983.

Caytan, Y. and Fabre, L., "Wind Effects on the Performance of Natural Draft Wet Cooling Towers Comparison of Constructors Proposals and Realization of Performance Control Tests," *Proceedings*, International Cooling Tower Conference, Electric Power Research Institute Report GS-6317, 1989.

Chaboseau, J., "Calculation of the Characteristics of an Air Cooling Tower Exposed to Wind," *Proceedings*, Third International Association for Hydraulic Research Cooling Tower Workshop, Budapest, 1982.

Christopher, P. J. and V. T. Forster, "Rugeley Dry Cooling Tower System," *Proceedings*, Institution of Mechanical Engineers, London, 184-11:197–211, 1969–1970.

Cooling Tower Institute, *Report on the Study of Recirculation*, CTI Bulletin PFM-110, 1958.

Cooling Tower Institute, *Report on the Study of Recirculation*, CTI Bulletin PFM-110, 1977.

De Bruin, H. A. R. and A. A. M. Holtslag, "A Simple Parameterization of the Surface Fluxes of Sensible and Latent Heat during Daytime Compared with the Penman-Monteith Concept," *Journal of Applied Meteorology*, 21:1610–1621, 1982.

Dibelius, G. and A. Eberhof, "Der Windeinfluss auf den Volumenstrom von Naturzugkühltürmen, *BWK*, 31-8:319–326, August 1979.

Du Preez, A. F., "The Influence of Crosswinds on the Performance of Natural Draft Dry-Cooling Towers," Doctoral thesis, University of Stellenbosch, November 1992.

Du Preez, A. F. and D. G. Kröger, "The Effect of Heat Exchanger Arrangement and Windbreak Walls on the Performance of Natural Draft Dry-Cooling Towers Subjected to Crosswinds," *Journal of Wind Engineering and Industrial Aerodynamics*, 58:293–303, 1995b.

Du Preez, A. F. and D. G. Kröger, "Effect of the Shape of the Tower Supports and Walls on the Performance of a Dry-Cooling Tower Subjected to Crosswinds," *Heat Transfer Engineering*, 16-2:42–49, 1995a.

Du Preez, A. F. and D. G. Kröger, "Effect of Wind on Performance of a Dry-Cooling Tower," *Heat Recovery Systems and CHP*, 13-2:139–146, 1993.

Du Preez, A. F. and D. G. Kröger, "Experimental Investigation into the Influence of Crosswinds on the Performance of Dry-Cooling Towers," *South African Institution of Mechanical Engineers Research and Development Journal*, 9-2:1–11, 1993.

Du Preez, A. F. and D. G. Kröger, "Investigation into the Influence of Crosswinds on the Performance of Dry-Cooling Towers," Paper, Eighth International Association for Hydraulic Research Cooling Tower and Spraying Pond Symposium, Karlsruhe, 1992.

Du Toit, C. G., G. D. Thiart, and D. G. Kröger, "Analysis of Recirculation in Mechanical-draught Heat Exchangers," *Proceedings*, Third World Conference on Experimental Heat Transfer, Fluid Mechanics and Thermodynamics, 377–380, Hawaii, 1993.

Duvenhage, K. and D. G. Kröger, "The Influence of Wind on the Performance of Forced-Draft Air-Cooled Heat Exchangers," *Journal of Wind Engineering and Industrial Aerodynamics*, 62-2/3:259–277, September 1996.

Duvenhage, K., C. G. Du Toit, and D. G. Kröger, "Methods to Combat the Influence of Cross Wind on Fan Performance in Forced Draught Air-cooled Heat Exchangers," *Proceedings*, First South African Conference on Applied Mechanics, Midrand, July 1996.

Eck, B., *Ventilatoren, Entwurf und Betrieb der Radial-, Axial- und Querstromventilatoren,* Springer-Verlag, Berlin, 1972.

Electric Power Research Institute, *Investigation of Numerical Modeling Techniques for Recirculating Flows*, Report CS-1665, Parts 1 and 2, EPRI, 1981.

Fabre, L., "Wet Cooling Towers: The Different Antifreeze Systems, Experience Feedback," Paper, Ninth International Association for Hydraulic Research Cooling Tower and Spraying Pond Symposium, von Karman Institute, Brussels, September 1994.

Fahlsing, P. M., "Benefits of Variable Speed Drives Applied on Dry Condensing at the Wyodak Plant," *Proceedings*, American Society of Mechanical Engineers Joint Power Generation Conference, PWR-28:463–471, October 1995.

Gee, J. H., "An Approximate Treatment of the Effect of Thermal Stability on Turbulent Diffusion," *Quarterly Journal of the Royal Meteorological Society*, 91:301–305, 1965.

Golder, D., "Relations Among Stability Parameters in the Surface Layer," *Boundary-Layer Meteorology*, 3:47–57, 1972.

Goldschagg, H., "Winds of Change at Eskom's Matimba Plant," *Modern Power Systems*, 43–45, January 1999.

Goldschagg, H. B., "Lessons Learned from the World's Largest Forced Draft-Direct Air-Cooled Condenser," Paper, Electric Power Research Institute International Symposium on Improved Technology for Fossil Power Plants—New and Retrofit Applications, Washington, March 1993.

Goldschagg, H. B., F. Vogt, C. G. du Toit, G. D. Thiart, and Kröger, D. G., "Air-Cooled Steam Condenser Performance in the Presence of Crosswinds," EPRI TR-108483 2113, *Proceedings*, International Cooling Tower Technology Conference, 1.61–1.77, July 1997.

Grange, J. L. and J. Y. Simon, "Behaviour of Crossflow and Natural Draft Cooling Towers in the Presence of Wind," *Proceedings*, Third International Association for Hydraulic Research Cooling Tower Workshop, Budapest, 1982.

Gunter, A. Y. and K. V. Shipes, "Hot Air Recirculation by Air Coolers," *Proceedings*, Twelfth National Heat Transfer Conference, American Institute of Chemical Engineers and American Society of Mechanical Engineers, Tulsa, August 1971.

Gunter, A. Y. and K. V. Shipes, "Hot Air Recirculation by Air Coolers," *Chemical Engineering Progress*, 68-2:49–58, February 1972.

Heberholz, P. and S. Schulz, "The Influence of Atmospheric Precipitation on the Operation of a Natural-Draught Indirect-Contact Cooling Tower," *German Chemical Engineering*, 2-1:352–360, 1979.

Hoffmann, J. E., "The Influence of Temperature Stratification in the Lower Atmospheric Boundary Layer on the Operating Point of a Natural Draft Dry-Cooling Tower," Doctoral thesis, University of Stellenbosch, 1997.

Hoffmann, J. E. and D. G. Kröger, "The Response of a Large Natural Draft Dry-Cooling Tower to Ambient Temperature Stratification," EPRI TR-108483 2113, *Proceedings*, International Cooling Tower Technology Conference, 1.79–1.94, July 1997.

Kennedy, J. F. and H. Fordyce, "Plume Recirculation and Interference in Mechanical-Draft Cooling Towers," *Proceedings*, Cooling Tower Environment Symposium, 58–87, University of Maryland, Baltimore, 1974.

Kosten, G. J., J. I. Morgan, J. M. Burns, and Curlett, P. L., "Operating Experience and Performance Testing of the World's Largest Air-cooled Condenser," American Power Conference, Chicago, April 1981.

Lauraine, H., P. Lemmens, and M. Monjoie, "Experimental Data Coupling Atmospheric Temperature Inversions and Cooling Tower Performances," *Proceedings*, Sixth International Association for Hydraulic Research Cooling Tower Workshop, Pisa, 1988.

Leene, J. A., "Draught Reduction of Hyperbolic Natural-Draught Cooling Towers as a Result of Wind," Proceedings, 4th Colloquium on Industrial Aerodynamics, Part 2, Fachhochschule, Aachen, 71–82, 1980.

Lettau, H., *Atmosphärische Turbulenz*, Akademische Verlagsgesellschaft, Leibzig, 1939.

Lowe, H. J. et al., "Aerodynamic Implications of the Ferrybridge Research Investigation," *Proceedings*, Symposium of the International Center for the Environment on Natural Draught Cooling Towers, Paper 9, 1964.

Markòczy, E. and E. Stämpfli, "Experimentelle Untersuchung des Einflusses atmosphärischer Umgebungsbedingungen auf das Betriebsverhalten von Naturzug-Trockenkühltürmen," Eidgenössisches Institut für Reaktorforschung-Bericht, no. 324, Würenlingen, 1977.

Merkel, F., "Verdunstungskühlung", *Verein Deutsche Ingenieure Zeitschrift*, 70:123–128, 1925.

Michell, F. L. and D. H. Drew, "Cold Weather Operating Guidelines and Experience for Natural Draft Cooling Towers on the American Electric Power Systems," EPRI TR-108483 2113, *Proceedings*, Cooling Tower Technology Conference, 4.1–4.10, July 1997.

Monin, A. S. and A. M. Obukhov, "Basic Regularity in Turbulent Mixing in the Surface Layer of the Atmosphere," Trudy Geofiz. Inst. Akkad. Nauk. SSSR, No. 24 (151), 163–187, 1954.

Moore, F. K., "Effects of Aerodynamic Losses on the Performance of Large Dry Cooling Towers," 78-WA/HT-18, American Society of Mechanical Engineers Winter Annual Meeting, 1978.

Nouri-Borujerdi, A., "Effects of Shell Materials and Atmospheric Conditions on Natural Draft Cooling Tower Performance," Paper, Ninth International Association for Hydraulic Research Cooling Tower and Spraying Pond Symposium, von Karman Institute, Brussels, September 1994.

Olivari, D. and F. Thiry, *Report VKI TR 148*, Von Karman Institute for Fluid Dynamics, Brussels, 1978.

Olivari, D. and F. Thiry, *Report VKI TR 165*, Von Karman Institute for Fluid Dynamics, Brussels, 1979.

Onishi, Y. and D. S. Trent, *Mathematical and Experimental Investigations on Dispersion and Recirculation of Plumes from Dry Cooling Towers at Wyodak Power Plant in Wyoming*, BNWL-1982, Battelle Pacific Northwest Laboratories, Richland, 1976.

Panofsky, H. A. and J. A. Dutton, *Atmospheric Turbulence*, John Wiley & Sons, New York, 1983.

Plánky, G. and A. Sztrilich, A., "Experiences of the Performance Measurements on the Dry Cooling Towers of the Shahid Rajai Power Plant," Paper, Tenth International Association for Hydraulic Research Cooling Tower and Spraying Pond Symposium, Tehran, 1996.

Preussag, A. G., "Steinkohlenbergwerke Ibbenbüren, Kraftwerke Ibbenbüren 150 MW Block," Bericht über die am 22 und 23. 8. 1967 durchgeführten Messungen am Kühlturm der luftgekühlten Kondensationsanlage, 6 Nov, 1967.

Radosavljevic, D. and D. Spalding, "The Use of PHOENIX to Simulate Three-Dimensional Effects in Natural-Draught Cooling Towers," *The PHOENIX Journal of Computational Mechanics*, CHAM Ltd, London, 1989.

Radosavljevic, D. and D. B. Spalding, "Simultaneous Prediction of Internal and External Aerodynamic and Thermal Flow Fields of a Natural-Draft Cooling Tower in a Crosswind," *Proceedings*, Sixth International Association for Hydraulic Research Cooling Tower Workshop, Pisa, 1988.

Ribier, J. G., "Evaluation of Recirculation in Induced Draft Cooling Towers," *Proceedings*, Sixth International Association for Hydraulic Research Cooling Tower Workshop, Pisa, October 1988.

Roshko, A., "Experiments on the Flow Past a Circular Cylinder at Very High Reynolds Number," *Journal of Fluid Mechanics*, vol. 10, part 3, no. 17, 1961.

Ruscheweyh, H., "Full-Scale Measurements on a Large Natural Draught Cooling Tower," *Proceedings*, Sixth International Conference on Wind Engineering, Australia, 1983.

Ruscheweyh, H., "Modelluntersuchung zum Einfluss der Kühlturm-kronenform auf das Zugverhalten grosser Naturzugkühltürme unter Querwindeinfluss," *Brennstoff-Wärme-Kraft*, 34-7:361–369, 1982.

Russell, C. M. B., H. R. McChesney, D. W. Holder, T. V. Jones, and M. Verlinden, "Crosswind and Internal Flow Characteristics of Dry Cooling Towers," *Combustion*, 20–24, May 1978.

Sabaton, M., Y. Cayton, and J. Goussebaile, "Numerical and Experimental Studies for the Cooling Tower Optimization," *Proceedings*, Third International Association for Hydraulic Research Cooling Tower Workshop, Budapest, 1982.

Schulenberg, F. J., "Steam Condensation in the Utility Industry Using Air-Cooled Heat Exchangers," Paper, Power Utility Industry, Hiroshima, Japan, 1976.

Seinfeld, J. H., *Air Pollution: Physical and Chemical Fundamentals*, McGraw-Hill Book Co., New York, 1975.

Slawson, P. R. and H. F. Sullivan, "Model Studies on the Design and Arrangement of Forced Draft Cooling Towers to Minimize Recirculation and Interference," *Proceedings*, Conference on Waste Heat Management and Utilization, 235–244, 1981.

Sun, T. F. and Z. F. Gu, "Interference Between Wind Loading on Group of Structures," *Journal of Wind Engineering and Industrial Aerodynamics*, 54/55:213–225, 1995.

Surridge, A. D., "Extrapolation of the Nocturnal Temperature Inversion from Ground-Based Measurements," *Atmospheric Environment*, vol. 20, 1986.

Tesche, W., "The Behaviour of Recirculation and Interference between Rows of Cooling Tower Cells and the Integration of these Effects at the Planning Stage," Paper, Tenth International Association for Hydraulic Research Cooling Tower and Spraying Pond Symposium, Tehran, 1996.

Tesche, W., "Inversionen Häufigkeit und Einflüsse auf natürlich belüftete Kühltürme," *VGB Kraftwerkstechnik 61 Jahrgang*, 7:611–618, 1978.

Tesche, W., "Inversions: Frequency and Influence on Natural-Draught Cooling Towers," *VGB Kraftwerkstechnik*, 7:535–542, 1981.

Trage, B. and F. J. Hintzen, "Design and Construction of Indirect Dry Cooling Units," *Proceedings*, VGB Conference, South Africa 1987, 1:70–79, Johannesburg, 1987.

Van der Walt, N. T., L. A. West, T. J. Sheer, and D. Kuball, "The Design and Operation of a Dry Cooling System for a 200 MW Turbo-generator at Grootvlei, Power Station, South Africa," *The South African Mechanical Engineering Research and Development Journal*, 26-12:498–511, 1976.

Vauzanges, M. and G. Ribier, "Variation of the Head Losses in the Air Inlets of Natural Draft Cooling Towers with the Shape of the Lintel and Shell Supports," *Proceedings*, Fifth International Association for Hydraulic Research Cooling Tower Workshop, Monterey, 1986.

Verein Deutscher Ingenieure, *Thermal Acceptance and Performance Tests on Dry Cooling Towers*, VDI-Guide Lines, VDI 2049, 1978.

Völler, G., "Untersuchungen zum Windeinfluss auf die Strömung im Naturzug-Trockenkühlturm," Doctoral thesis, Universität Hannover, 1985.

Wei, Q., B. Zhang, K. Liu, X. Du, and X. Meng, "A Study of the Unfavourable Effects of Wind on the Cooling Efficiency of Dry Cooling Towers," *Journal of Wind Engineering and Industrial Aerodynamics*, 54/55:633–643, 1995.

Witte, R., *Das Betriebsverhalten atmosphärisch beeinflusster Trockenkühltürme*, Fortschritt-Berichte der VDI-Z, Reihe 6, no. 132, Verein Deutsche Ingenieure-Verlag, Düsseldorf, 1983.

10

Cooling System Selection and Optimization

10.0 Introduction

Although the selection of a cooling system for an industrial plant or process is usually straightforward, this is not always the case. Fairly extensive studies may be required before a final decision is made concerning the choice of a particular cooling system. These studies include:

- process and operating requirements
- existing and changing local cost structures
- environmental concerns
- aesthetic considerations
- legal constraints
- social factors
- other considerations

For example, the relatively expensive GKN hybrid cooling tower shown in Figure 1.3.13 was constructed in an area where less costly alternatives would not have been tolerated by the public because of noise and unsightly cooling towers with visible plumes.

In contrast, the low-cost, wooden, natural-draft cooling tower shown in Figure 10.0.1 was erected at a power plant in the wooded area near Petrozavodsk, Russia. This cooling tower only uses spray nozzles to create a rain zone at its base. No fill or packing is employed. This reduces possible freezing problems during periods of extremely low ambient temperatures. Although the tower is not very sophisticated technically, it was probably the most appropriate choice for the particular plant during the planning stage.

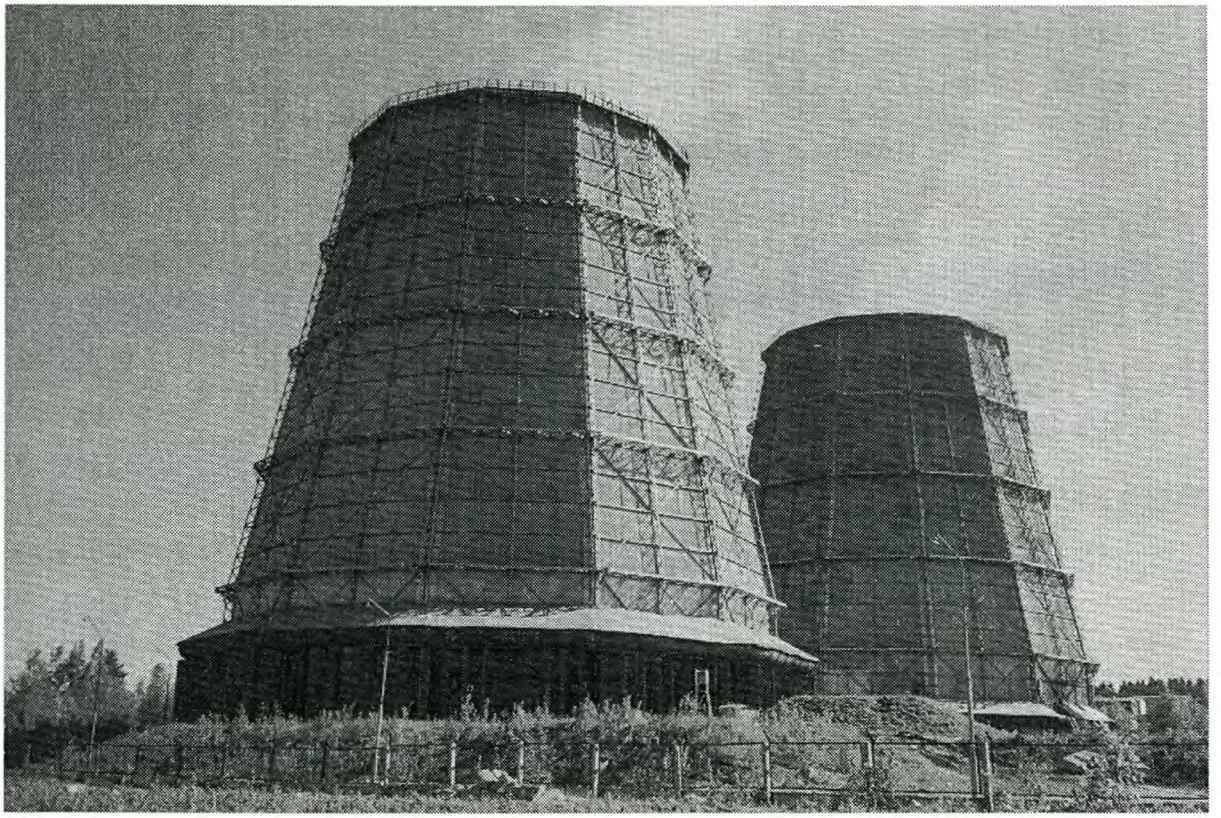

Fig. 10.0.1 Wooden Natural-Draft Cooling Towers

Natural-draft wet-cooling towers are often found where relatively large amounts of heat must be rejected. Mechanical draft units are preferred in smaller installations. Mohiuddin and Kant present a simple but effective selection process, which can be followed to obtain an indication of the most appropriate system for a particular installation.

In many applications where the process outlet temperature is relatively low, air cooling alone may not be feasible. A combination of air cooling followed by trim cooling with water can be considered according to Mukherjee.

Once the most suitable type of cooling system has been identified for application in a particular plant or process, some degree of optimization is

usually required. In certain cases, the choice of cooling system and the optimization process go hand in hand. For example, in a power plant where the cost of water is relatively high, the life-cycle cost of a conventional wet-cooling tower is similar to that of a dry-cooling tower. In such a case, a simple optimization that matches a given turbine with a suitable boiler and cooling system at a specified ambient condition is inadequate. A far more extensive study is required. This should include, among others:

- evaluation of different combinations of plant components
- seasonal weather patterns
- the cost of electricity and its demand pattern
- water availability
- cost of water

No modern plant optimization exercise is complete without considering the immediate and, as far as possible, future environmental and sociological implications. Although aspects of this holistic approach may be subjective and often emotional in nature, an increasing amount of quantitative information is available to incorporate in the optimization process. These inputs are usually obtained from a variety of sources and may involve a wide spectrum of expertise and individuals. Even a drab concrete cooling tower can be made aesthetically more pleasing or interesting if an imaginative artist is involved (Fig. 10.0.2).

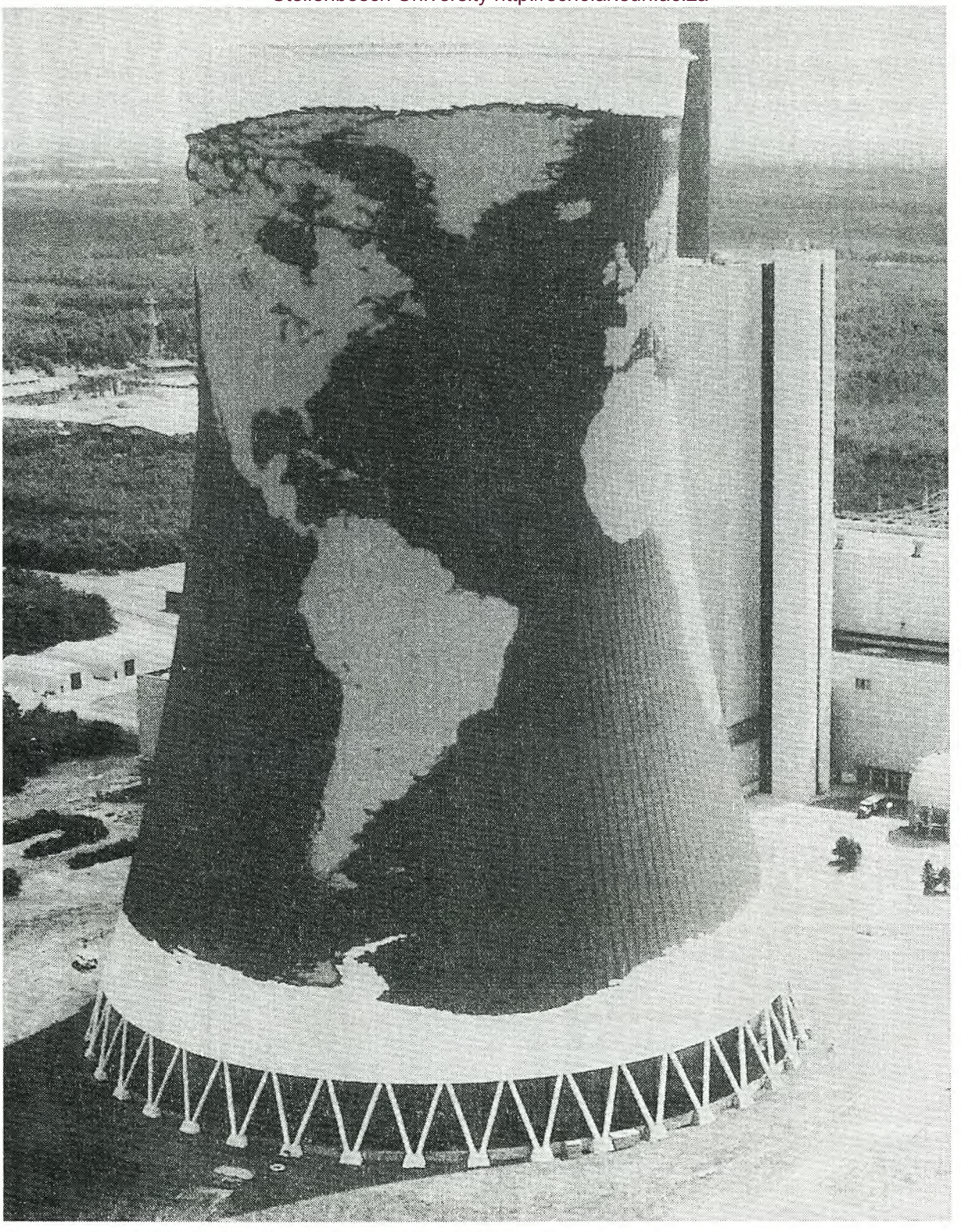

Fig. 10.0.2 Colorful Cooling Tower

10.1 Power Generation

In the design of a base-load power plant, the selection and matching of various components is of utmost importance to achieve effective operation and power output. For a turbo-generator-surface-condenser system, the net power output and the heat to be rejected by the cooling tower may be presented in tabular or graphic format. It is represented as a function of the recooled condenser water temperature, T_{wo}, or the temperature of water at the outlet of the cooling tower and condenser inlet for a specified water-mass flow rate, m_w. Figure 10.1.1 shows the performance characteristics of such a system and incorporates a surface condenser. To obtain the net power output, 1.2 MW, the auxiliary power required to drive the cooling-water recirculating pump and the boiler pump, is subtracted from the gross generator output.

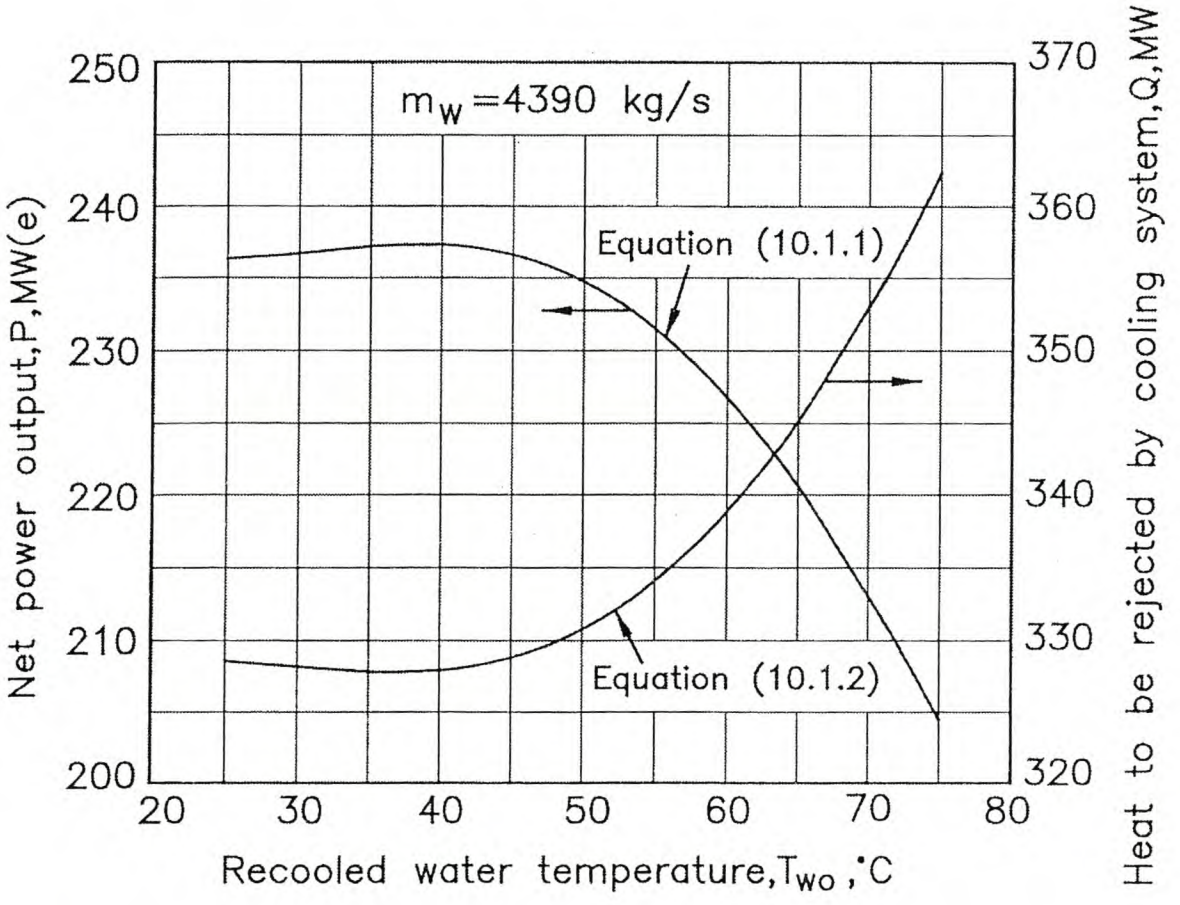

Fig. 10.1.1 Performance Characteristics of Turbo-Generator-Condenser System

Since prevailing atmospheric conditions influence the performance of cooling towers, the recooled water temperature may fluctuate across a relatively wide range, especially in the case of dry-cooling towers. Changes in ambient temperature are the most important reason for this fluctuation, although other effects such as humidity, winds, and inversions must also be considered.

The mean hourly frequency of different temperatures during a period of one year is normally supplied in tabulated or graphical form. An example of the frequency of dry- and wetbulb temperatures two meters above ground level is shown in Figure 10.1.2. Significant temperature gradients exist near ground level. This opens the possibility of considerable deviation of the measured temperatures from the actual mean air temperature entering the cooling tower at a given time. Greater detail in the information about ambient temperature distribution is preferred for a more sophisticated design.

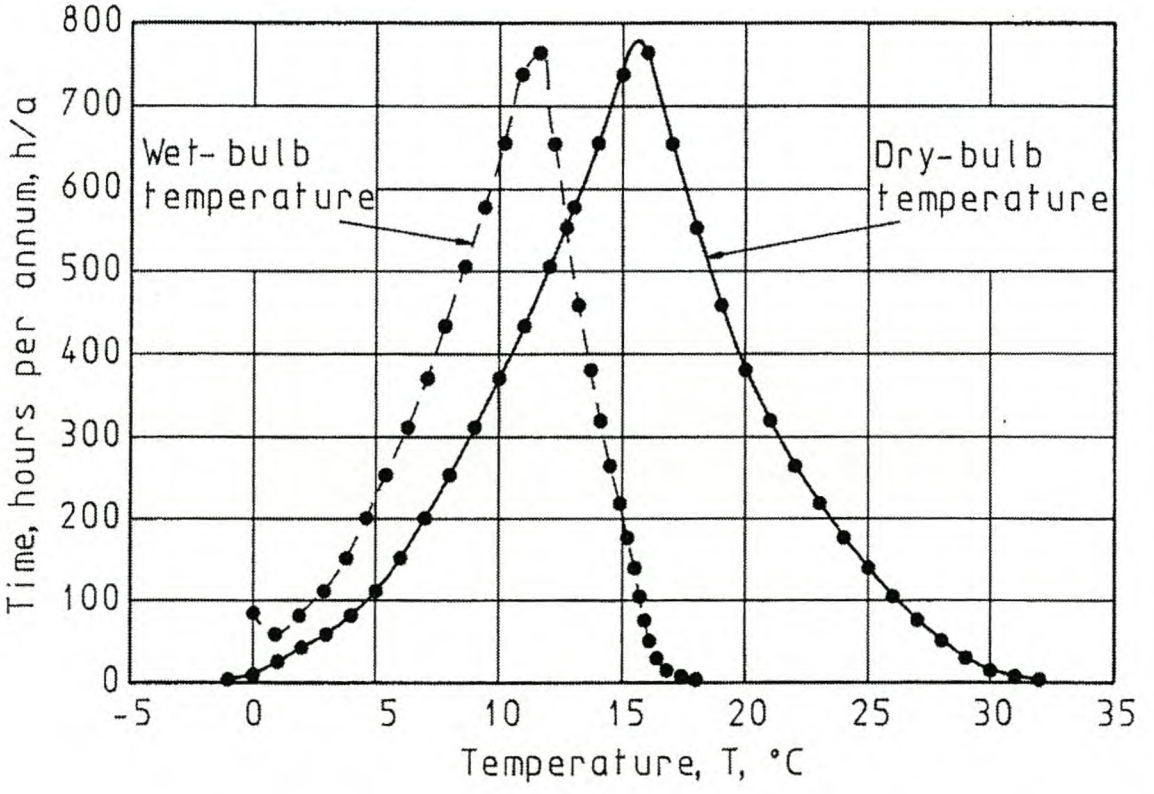

Fig. 10.1.2 Frequency of Ambient Dry- and Wetbulb Temperatures

To find the approximate net annual power output, the output is calculated at each specified ambient temperature for the corresponding number of hours. These outputs are added to give the annual total value according to Trage and Hintzen.

Example 10.1.1

Table 10.1.1 shows data for a dry-cooled power plant to be erected at a location where the atmospheric pressure p_{a1} = 84,600 N/ m^2. The table also shows the drybulb temperature distribution during a year. This distribution corresponds with that shown in Figure 10.1.2. Ignore the wetbulb temperature shown, i.e., assume the air to be dry.

No.	T_{a1}, °C	Time, h/a	No.	T_{a1}, °C	Time, h/a
1	-1	4	18	16	764
2	0	10	19	17	655
3	1	26	20	18	553
4	2	43	21	19	459
5	3	59	22	20	381
6	4	82	23	21	320
7	5	112	24	22	265
8	6	152	25	23	219
9	7	201	26	24	177
10	8	254	27	25	140
11	9	312	28	26	105
12	10	371	29	27	76
13	11	434	30	28	51
14	12	506	31	29	30
15	13	578	32	30	15
16	14	656	33	31	8
17	15	738	34	32	4
					Total 8760 h/a

Table 10.1.1 Ambient Air Temperature Distribution

The performance characteristics of the turbo-generator set are specified in Table 10.1.2 as a function of the recooled water temperature T_{WO} at the inlet to the surface condenser. These values correspond with the values shown in Figure 10.1.1. The condenser surface area is such that the difference in temperature between the steam and the condenser outlet water temperature, *terminal temperature difference*, is 2.5 °C during the operating conditions specified in Example 7.3.1.

No.	Recooled water temp. T_{WO}, °C	Net power output P, MW (e)	Heat dissipated Q, MW
1	23.00	236.15	328.64
2	25.86	236.50	328.43
3	31.01	237.02	328.07
4	36.16	237.32	327.94
5	41.29	237.14	328.10
6	46.33	236.11	329.18
7	51.31	233.93	331.46
8	53.77	232.38	333.09
9	56.20	230.51	335.05
10	58.14	228.76	336.88
11	60.04	226.81	338.89
12	61.96	224.62	341.16
13	63.85	222.23	343.61
14	65.74	219.60	346.24
15	68.55	215.26	350.55
16	71.00	211.44	354.83
17	74.00	206.24	360.28

Table 10.1.2 Turbo-Generator-Condenser Performance Characteristics

A polynomial regression function for the net power output specified in Table 10.1.2 is

$$P = 2.6377194 \times 10^{2} - 3.0377669\, T_{wo} + 0.11534328\, T_{wo}^{2}$$

$$- 1.6951135 \times 10^{-3}\, T_{wo}^{3} + 7.4217464 \times 10^{-6}\, T_{wo}^{4} \qquad (10.1.1)$$

Similarly, a curve fit through the data for the heat to be rejected by the condenser is

$$Q = 3.1151196 \times 10^{2} + 1.9876312\, T_{wo} - 7.8019992 \times 10^{-2}\, T_{wo}^{2}$$

$$+ 1.1440403 \times 10^{-3}\, T_{wo}^{3} - 4.4881617 \times 10^{-6}\, T_{wo}^{4} \qquad (10.1.2)$$

These functions are shown in Figure 10.1.1 with T_{wo} in °C and P and Q in MW.

The water flow rate through the condenser is m_w = 4390 kg/s. The cooling tower described in Example 7.3.1 is connected to the condenser.

Determine the total annual, i.e., 8760 hours, net energy output of the generating unit.

Solution

To solve the problem, start the calculation at the lowest ambient temperature. Assume a cooling tower outlet temperature, T_{wo} is the recooled water temperature, at some value above the ambient temperature specified. With this assumed value, the heat rejected by the condensing steam to the cooling water in the condenser is given by Equation 10.1.2. First, evaluate the specific heat of the water at the assumed temperature, T_{wo}, and the condenser outlet temperature, which is the same as the cooling tower inlet temperature, T_{wi}, using the following relation,

$$T_{wi} = T_{wo} + Q / m_w c_{pw} \qquad (10.1.3)$$

With this temperature and the specified ambient temperature, follow the procedure described in Example 7.3.1, and find the cooling tower operating point. The heat rejected by the tower under these conditions should be in agreement

with the value obtained from Equation 10.1.2. If this is not the case, determine an improved value of T_{wo} from the following relation:

$$T_{wo} = T_{wi} - (T_{ao} - T_{ai})\, m_a\, c_{pa} / (m_w\, c_{pw}) \qquad (10.1.4)$$

By evaluating the fluid properties at the mean temperature, repeat this procedure until equilibrium conditions are attained.

At this stage, evaluate the power output according to Equation 10.1.1, and multiply the value by the corresponding number of operating hours.

Repeat this procedure for other specified ambient temperatures, and by addition, find the total annual net energy output. The results of the calculations are listed in Table 10.1.3. The total net energy output during the year is 2,069,648 MWh while the heat rejected is 2,882,646 MWh if the turbine runs for 8760 hours during the year.

No.	T_{a1} °C	T_{wb} °C	Hours / Annum h/a	T_{wi} °C	T_{wo} °C	Q MW	P MW(e)
1	-1.0	0.0	4.0	43.844	25.955	328.5085	236.3583
2	0.0	0.0	10.0	44.885	27.002	328.4342	236.4169
3	1.0	0.0	26.0	45.936	28.054	328.3486	236.4990
4	2.0	0.0	43.0	46.988	29.110	328.2563	236.5985
5	3.0	0.0	59.0	48.049	30.174	328.1610	236.7103
6	4.0	0.0	82.0	49.087	31.223	328.0694	236.8258
7	5.0	0.0	112.0	50.123	32.269	327.9844	236.9411
8	6.0	0.0	152.0	51.208	33.347	327.9075	237.0543
9	7.0	0.0	201.0	52.233	34.387	327.8476	237.1532
10	8.0	0.0	254.0	53.309	35.460	327.8042	237.2397
11	9.0	0.0	312.0	54.375	36.531	327.7835	237.3054
12	10.0	0.0	371.0	55.452	37.604	327.7891	237.3459
13	11.0	0.0	434.0	56.502	38.657	327.8234	237.3568
14	12.0	0.0	506.0	57.575	39.728	327.8913	237.3344
15	13.0	0.0	578.0	58.624	40.771	327.9921	237.2766
16	14.0	0.0	656.0	59.653	41.776	328.1246	237.1838
17	15.0	0.0	738.0	60.841	42.973	328.3309	237.0222
18	16.0	0.0	764.0	61.924	44.051	328.5650	236.8253
19	17.0	0.0	655.0	63.037	45.142	328.8515	236.5733
20	18.0	0.0	553.0	64.129	46.227	329.1883	236.2674
21	19.0	0.0	459.0	65.271	47.339	329.5902	235.8936
22	20.0	0.0	381.0	66.376	48.425	330.0399	235.4677
23	21.0	0.0	320.0	67.509	49.533	330.5596	234.9688
24	22.0	0.0	265.0	68.647	50.643	331.1442	234.4017
25	23.0	0.0	219.0	69.788	51.753	331.7943	233.7659
26	24.0	0.0	177.0	70.943	52.870	332.5174	233.0545
27	25.0	0.0	140.0	72.086	53.982	333.3067	232.2747
28	26.0	0.0	105.0	73.276	55.125	334.1922	231.3974
29	27.0	0.0	76.0	74.461	56.259	335.1465	230.4503
30	28.0	0.0	51.0	75.655	57.402	336.1861	229.4182
31	29.0	0.0	30.0	76.930	58.607	337.3671	228.2462
32	30.0	0.0	15.0	78.061	59.689	338.5036	227.1200
33	31.0	0.0	8.0	79.294	60.851	339.8053	225.8329
34	32.0	0.0	4.0	80.525	62.011	341.1877	224.4702

Table 10.1.3 Net Power Output and Heat Dissipated

Example 10.1.2

Repeat Example 10.1.1 taking into consideration the wetbulb temperatures shown in Figure 10.1.2. These values are listed in Table 10.1.4 and also shown in Figure 10.1.2.

No.	T_{a1} °C	T_{wb} °C	Hours Annum h/a	T_{wi} °C	T_{wo} °C	Q MW	P MW(e)
1	-1.0	0.0	4.0	43.844	25.955	328.5085	236.3583
2	0.0	0.0	10.0	44.885	27.002	328.4342	236.4169
3	1.0	0.0	26.0	45.936	28.054	328.3486	236.4990
4	2.0	0.0	43.0	46.988	29.11	328.2563	236.5985
5	3.0	0.9	59.0	48.038	30.171	328.1613	236.7099
6	4.0	1.9	82.0	49.075	31.216	328.0701	236.8250
7	5.0	2.9	112.0	50.156	32.295	327.9824	236.9439
8	6.0	3.8	152.0	51.197	33.338	327.9081	237.0535
9	7.0	4.6	201.0	52.249	34.397	327.8470	237.1541
10	8.0	5.4	254.0	53.313	35.466	327.8040	237.2402
11	9.0	6.3	312.0	54.374	36.531	327.7835	237.3054
12	10.0	7.1	371.0	55.436	37.595	327.7888	237.3457
13	11.0	7.8	434.0	56.514	38.668	327.8240	237.3568
14	12.0	8.6	506.0	57.534	39.684	327.8878	237.3361
15	13.0	9.4	578.0	58.653	40.804	327.9960	237.2741
16	14.0	10.2	656.0	59.770	41.903	328.1439	237.1694
17	15.0	10.9	738.0	60.846	42.976	328.3315	237.0216
18	16.0	11.6	764.0	61.924	44.048	328.5643	236.8259
19	17.0	12.2	655.0	63.041	45.147	328.8530	236.5719
20	18.0	12.7	553.0	64.125	46.222	329.1865	236.2690
21	19.0	13.2	459.0	65.241	47.32	329.5828	235.9005
22	20.0	13.7	381.0	66.361	48.421	330.0380	235.4695
23	21.0	14.1	320.0	67.507	49.533	330.5597	234.9687
24	22.0	14.5	265.0	68.660	50.651	331.1483	234.3977
25	23.0	14.9	219.0	69.787	51.753	331.7941	233.7661
26	24.0	15.2	177.0	70.940	52.871	332.5180	233.0540
27	25.0	15.5	140.0	72.087	53.984	333.3076	232.2738
28	26.0	15.7	105.0	73.260	55.11	334.1800	231.4094
29	27.0	15.9	76.0	74.518	56.302	335.1843	230.4128
30	28.0	16.1	51.0	75.642	57.388	336.1721	229.4320
31	29.0	16.4	30.0	76.843	58.535	337.2938	228.3189
32	30.0	16.8	15.0	78.069	59.695	338.5102	227.1135
33	31.0	17.4	8.0	79.289	60.847	339.8003	225.8378
34	32.0	18.0	4.0	80.515	62.002	341.1775	224.4802

Table 10.1.4 Temperature Distribution, Net Power Output, and Heat Rejected

Solution

The results of the analysis are listed in Table 10.1.4. The total energy output during the year is 2,069,643 MWh, while the heat rejected is 2,882,655 MWh if the turbine runs for 8760 hours during the year.

Example 10.1.3

Repeat Example 10.1.1 for the case where the ambient air is saturated. The specified dry- and wetbulb temperatures are listed in Table 10.1.5.

No.	T_{a1} °C	T_{wb} °C	Hours / Annum h/a	T_{wi} °C	T_{wo} °C	Q MW	P MW(e)
1	-1.0	0.0	4.0	43.844	25.955	328.5085	236.3583
2	0.0	0.0	10.0	44.885	27.002	328.4342	236.4169
3	1.0	1.0	26.0	45.952	28.067	328.3475	236.5002
4	2.0	2.0	43.0	46.990	29.112	328.2561	236.5988
5	3.0	3.0	59.0	48.038	30.166	328.1618	236.7094
6	4.0	4.0	82.0	49.088	31.223	328.0694	236.8259
7	5.0	5.0	112.0	50.142	32.286	327.9831	236.9429
8	6.0	6.0	152.0	51.197	33.339	327.9081	237.0535
9	7.0	7.0	201.0	52.236	34.393	327.8472	237.1538
10	8.0	8.0	254.0	53.310	35.463	327.8041	237.2399
11	9.0	9.0	312.0	54.373	36.528	327.7835	237.3053
12	10.0	10.0	371.0	55.431	37.590	327.7888	237.3456
13	11.0	11.0	434.0	56.521	38.670	327.8241	237.3568
14	12.0	12.0	506.0	57.501	39.636	327.8840	237.3378
15	13.0	13.0	578.0	58.670	40.814	327.9970	237.2734
16	14.0	14.0	656.0	59.756	41.897	328.1431	237.1701
17	15.0	15.0	738.0	60.827	42.963	328.3290	237.0236
18	16.0	16.0	764.0	61.923	44.049	328.5646	236.8256
19	17.0	17.0	655.0	63.039	45.146	328.8528	236.5721
20	18.0	18.0	553.0	64.145	46.236	329.1915	236.2644
21	19.0	19.0	459.0	65.257	47.329	329.5861	235.8974
22	20.0	20.0	381.0	66.377	48.425	330.0400	235.4675
23	21.0	21.0	320.0	67.520	49.540	330.5630	234.9654
24	22.0	22.0	265.0	68.641	50.638	331.1411	234.4046
25	23.0	23.0	219.0	69.786	51.752	331.7935	233.7667
26	24.0	24.0	177.0	70.977	52.901	332.5379	233.0343
27	25.0	25.0	140.0	72.111	53.997	333.3176	232.2640
28	26.0	26.0	105.0	73.276	55.120	334.1882	231.4013
29	27.0	27.0	76.0	74.446	56.246	335.1352	230.4615
30	28.0	28.0	51.0	75.613	57.367	336.1530	229.4510
31	29.0	29.0	30.0	76.846	58.534	337.2928	228.3199
32	30.0	30.0	15.0	78.036	59.666	338.4785	227.1448
33	31.0	31.0	8.0	79.256	60.820	339.7691	225.8686
34	32.0	32.0	4.0	80.481	61.976	341.1448	224.5124

Table 10.1.5 Net Power Output and Heat Rejected

Solution

The power output and heat rejected is shown in Table 10.1.5 for different ambient conditions.

The total energy output during the year is 2,069,641 MWh, while the heat rejected is 2,882,655 MWh. Since these values do not deviate measurably from those obtained in Example 10.1.1, it follows that any water vapor in the air can be ignored in the performance evaluation of a generating system coupled to a dry-cooling tower.

Example 10.1.4

Consider the power plant described in Example 10.1.1 with a turbo-generator set having characteristics given by Equations 10.1.1 and 10.1.2. The drybulb and wetbulb temperatures are specified in Table 10.1.4.

Determine the annual energy output of the plant if the cooling tower operates in the dry mode for all ambient drybulb temperatures below 24 °C. At temperatures of 24 °C or higher, a fine spray of water adiabatically precools the ambient inlet air under controlled conditions to a relative humidity of 70%. If the ratio of the total cost of 1 m^3 of spray water to 1 kWh of energy is $C_r = 10$, what is the additional annual income of the plant, expressed in terms of the net effective gain in energy, compared to dry mode operation only?

Solution

While operating in the dry mode only, the power plant generates E_d = 2,070,514 MWh per annum. With adiabatic cooling, the output is E_{ac} = 2,072,231 MWh. The annual amount of spray water required is V_{ws} = 52,880.016 m^3/annum.

To cover the cost of this spray at a cost ratio of $C_r = 10$, the following amount of energy must be sold:

$$E_s = 10 \times V_{ws} = 10 \times 52880.016 = 528{,}800 \text{ kWh}$$

The actual additional annual income of the plant expressed in terms of the net effective energy is,

$$E_{net} = (E_{ac} - E_d) - E_s = (2072231 - 2070514) - 528.8$$

$$= 1188.2 \text{ MWh}$$

Although the efficiency of the turbine is improved at higher ambient air temperatures, the additional annual output is small.

Example 10.1.5

Repeat Example 10.1.4 by starting the adiabatic cooling process at different ambient temperatures ranging from 12 °C to 32 °C and at spray to energy cost ratios varying between 5 and 25 in increments of 5. Present E_{net} and the annual spray water consumption, V_{ws}, graphically in terms of the ambient temperature where adiabatic cooling commences. Also show graphically the improvement in turbine output and the corresponding water consumption at different ambient temperatures according to Conradie and Kröger.

Solution

The results of the analysis are shown in Figures 10.1.3 and 10.1.4.

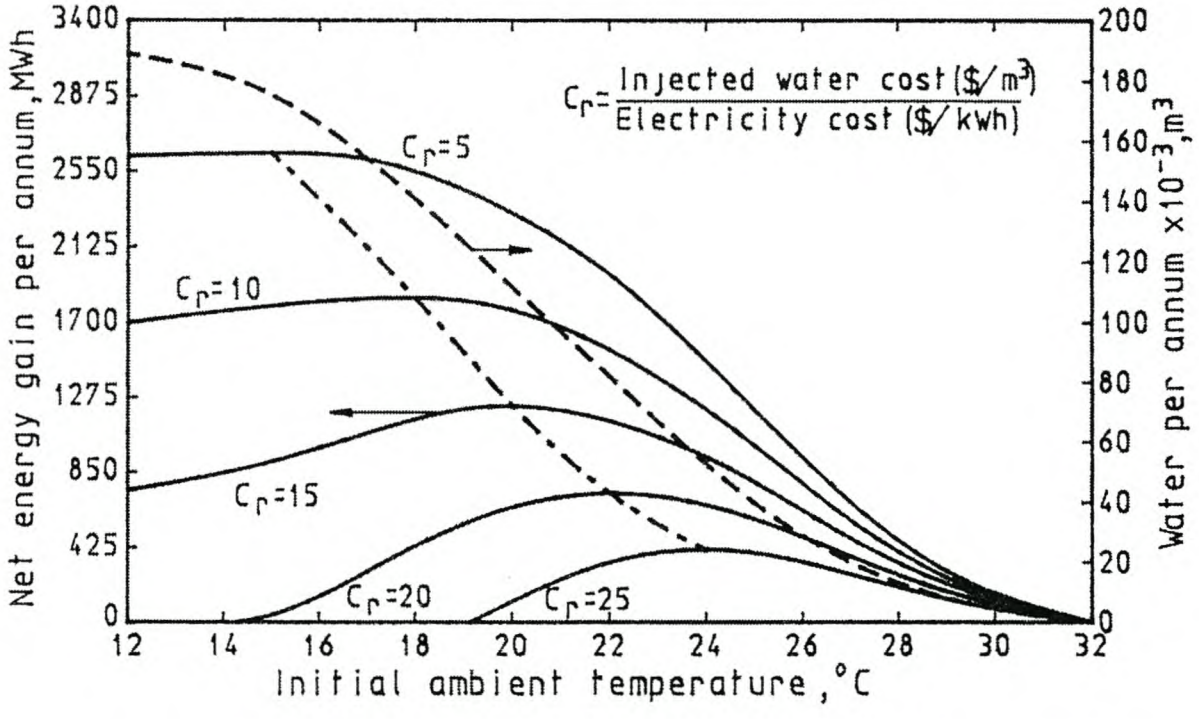

Fig. 10.1.3 Net Energy Gain through Precooling to 70% Relative Humidity

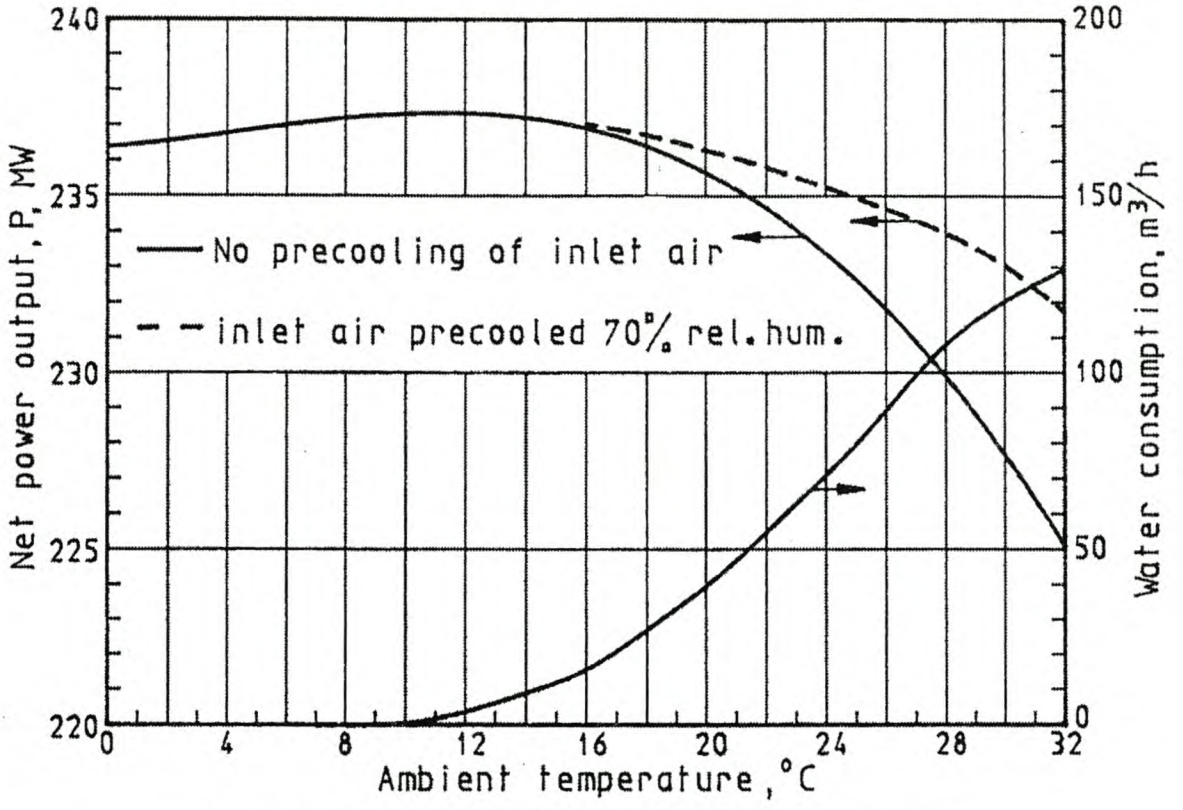

Fig. 10.1.4 Turbo-Generator Performance Characteristics

Example 10.1.6

Consider the power plant described in Example 10.1.1 with the ambient conditions specified in Example 10.1.2. Determine the annual net power output of the particular turbo-generator set if it is connected to a direct air-cooled condenser consisting of the array of 3 x 6 = 18 A-frame units described in Example 8.3.2. The free standing fan platform is 25 m above ground level with an 8.27 m high windwall along its edge to minimize recirculation (Fig. 8.3.8). The influence of plume air recirculation and inlet flow losses can be assumed to be negligible. To obtain the turbo-generator performance characteristics from the turbo-generator-condenser characteristics shown in Figure 10.1.1, it may be assumed that the product of overall heat transfer coefficient and the surface area of the water-cooled condenser are approximately constant.

This applies in the range of plant operation, and its value is $U_{sc}A_{sc}$ = 38,479,756.36 W/K.

Solution

It is preferable to express the relevant turbo-generator performance characteristics for the direct condensing system in terms of the turbine back-pressure or the corresponding vapor temperature, T_v. These may be obtained from the turbo-generator-condenser characteristics specified in Example 10.1.1.

At a particular recooled water temperature, T_{wo}, the net power, P, generated by the indirectly cooled power plant described in Example 10.1.1 is expressed by Equation 10.1.1. By adding the 1.2 MW required by the water recirculating pump to this output, the resultant generator output is obtained. This pump is not required in a direct cooling system.

$$P_{gen} = P + 1.2 = 1.2 + 2.6377194 \times 10^{2} - 3.0377669\, T_{wo} + 0.11534328\, T_{wo}^{2}$$

$$- 1.6951135 \times 10^{-3}\, T_{wo}^{3} + 7.4217464 \times 10^{-6}\, T_{wo}^{4}$$

with

T_{wo} in °C

P_{gen} in MW

For the performance evaluation of the power plant incorporating a direct air-cooled condenser, it is more convenient to express the turbo-generator characteristics in terms of the vapor temperature or pressure at the turbine outlet. To obtain the desired characteristic relations, consider condition 1 listed in Table 10.1.2. To find the water inlet temperature, it follows from the heat transfer relation $Q = m_w c_{pw} (T_{wi} - T_{wo})$ that

$$T_{wi} = Q/m_w c_{pw} + T_{wo}$$

where

c_{pw} is determined according to Equation A.4.2 at $T_{wm} = (T_{wi} + T_{wo})/2$

By following an iterative procedure, find

$$T_{wi} = 38.9545\ ^{\circ}C$$

for

$$m_w = 4390\ kg/s$$

and

$$Q = 328.64 \text{ x } 10^6 \text{ W}$$

At

$$T_{wm} = (38.9545 + 23.00)/2 = 30.977 \text{ °C or } 304.127 \text{ K}$$

find

$$c_{pw} = 4178.22 \text{ J/kg K}$$

The heat transfer from the condensing steam to the cooling water in the surface condenser can also be expressed as

$$Q = \frac{U_{sc} A_{sc} [(T_v - T_{wo}) - (T_v - T_{wi})]}{\ell n [(T_v - T_{wo})/(T_v - T_{wi})]}$$

or

$$T_v = \frac{T_{wo} - T_{wi} \exp [(T_{wi} - T_{wo}) U_{sc} A_{sc} / Q]}{1 - \exp [(T_{wi} - T_{wo}) U_{sc} A_{sc} / Q]}$$

For condition 1, the vapor temperature calculated according to this equation is

$$T_v = \frac{23 - 38.9545 \exp [(38.9545 - 23) 38479756.36 / (328.64 \text{ x } 10^6)]}{1 - \exp [(38.9545 - 23) 38479756.36 / (328.64 \text{ x } 10^6)]} = 41.8681 \text{ °C}$$

The saturation vapor pressure corresponding to this temperature is found to be p_v = 8114.61 N/m^2 according to Equation A.2.1. Conditions corresponding to other cases listed in Table 10.1.2 are given in Table 10.1.6.

No.	T_{wi} °C	T_{wo} °C	T_{wm} °C	c_{pw} J/kgK	T_v °C	p_v N/m^2	P_{gen} MW	Q MW
1	38.9545	23.00	30.9772	4178.22	41.8681	8114.61	237.35	328.64
2	41.8075	25.86	33.8337	4177.38	44.7185	9395.77	237.70	328.43
3	46.9424	31.01	38.9762	4176.76	49.8497	12153.60	238.22	328.07
4	52.0843	36.16	44.1222	4177.20	54.9909	15602.30	238.52	327.94
5	57.2168	41.29	49.2534	4178.60	60.1259	19870.20	238.34	328.10
6	62.3008	46.33	54.3154	4180.80	65.2214	25075.80	237.31	329.18
7	67.3804	51.31	59.3452	4183.68	70.3236	31436.80	235.13	331.46
8	69.9131	53.77	61.8415	4185.32	72.8722	35107.30	233.58	333.09
9	72.4313	56.20	64.3156	4187.07	75.4093	39124.00	231.71	335.05
10	74.4541	58.14	66.2971	4188.56	77.4497	42636.80	229.96	336.88
11	76.4455	60.04	68.2428	4190.07	79.4603	46361.60	228.01	338.89
12	78.4692	61.96	70.2146	4191.66	81.5055	50435.30	225.82	341.16
13	80.4713	63.85	72.1607	4193.27	83.5309	54770.10	223.43	343.61
14	82.4820	65.74	74.1110	4194.92	85.5664	59446.10	220.80	346.24
15	85.4902	68.55	77.0201	4197.44	88.6153	67091.60	216.46	350.55
16	88.1379	71.00	79.5690	4199.67	91.3032	74518.20	212.64	354.83
17	91.3898	74.00	82.6949	4202.41	94.6062	84601.40	207.44	360.28

Table 10.1.6 Turbo-Generator Performance Characteristics

A third-order polynomial can be fitted to the data listed in Table 10.1.6 to give the generator output and the heat to be rejected by the condenser in terms of the vapor temperature.

$$P_{gen} = 225.83 - 0.0043\,T_v + 0.01332\,T_v^2 - 0.000163\,T_v^3$$

and

$$Q = 336.4 + 0.18223\,T_v - 0.01601\,T_v^2 + 0.00018\,T_v^3$$

where

T_v is in °C

P_{gen} is in MW

Q is in MW

Similarly, in terms of the saturation pressure determined using Equation 3.4.65

$$P_{gen} = 234.8942 + 4.76016 \times 10^{-4} p_v - 1.81657 \times 10^{-8} p_v^2 + 1.03341 \times 10^{-13} p_v^3$$

and

$$Q = 330.8352 - 4.25866 \times 10^{-4} p_v + 1.73191 \times 10^{-8} p_v^2 - 9.70383 \times 10^{-14} p_v^3$$

where

p_v is in N/m^2

P_{gen} is in MW

Q is in MW

To find the net power output at a particular temperature, the fan power required must be subtracted from P_{gen}.

To determine the operating point of the turbo-generator, start the calculation at the lowest ambient temperature listed in Table 10.1.3. Assume a vapor temperature at some value above the minimum specified for the turbo-generator, and determine the heat rejected by 18 fan units using the procedure given in Example 8.1.4 for a single fan unit. If this heat transfer rate does not agree with the rate required according to the turbo-generator characteristic given by the previous equations at the particular vapor temperature, a new temperature is chosen. The procedure is repeated until agreement is obtained, i.e., the turbo-generator operating point matches that of the air-cooled condenser.

At this point, the power input to each fan unit is known. Subtract the total power consumed by 18 fan units from the generator power output, P_{gen}, to find the net power output of the plant. The latter quantity is multiplied by the corresponding number of operating hours listed in Table 10.1.4 to give the energy output for this period. By following a similar procedure at all other ambient temperatures listed, the corresponding net energy output and heat rejected are obtained as shown in Table 10.1.7. Add these values to find the total annual net energy output is 2,056,189 MWh and 2,874,207 MWh of heat is rejected.

No	T_{a1} °C	T_{sdbh} °C	T_{swb} °C	Hours h	p_v N/m^2	P_F MW(e)	Q MW	P_{gen} MW(e)	P MW(e)
1	-1.00	-1.00	0.01	4.0	8400	3.83	328.79	237.22	233.39
2	0.00	0.00	0.01	10.0	8720	3.82	328.65	237.40	233.58
3	1.00	1.00	0.01	26.0	9060	3.81	328.51	237.57	233.77
4	2.00	2.00	0.01	43.0	9430	3.79	328.37	237.74	234.95
5	3.00	3.00	0.90	59.0	9810	3.78	328.24	237.91	234.13
6	4.00	4.00	1.90	82.0	10230	3.76	328.12	238.07	234.30
7	5.00	5.00	2.90	112.0	10660	3.75	328.00	238.22	234.47
8	6.00	6.00	3.80	152.0	11130	3.74	327.89	238.35	234.62
9	7.00	7.00	4.60	201.0	11630	3.72	327.80	238.48	234.75
10	8.00	8.00	5.40	254.0	12150	3.71	327.72	238.59	234.88
11	9.00	9.00	6.30	312.0	12710	3.69	327.65	238.68	234.98
12	10.00	10.00	7.10	371.0	13300	3.68	327.60	238.75	235.07
13	11.00	11.00	7.80	434.0	13920	3.67	327.57	238.81	235.14
14	12.00	12.00	8.60	506.0	14570	3.65	327.56	238.84	235.19
15	13.00	13.00	9.40	578.0	15270	3.64	327.57	238.85	235.21
16	14.00	14.00	10.20	656.0	16000	3.63	327.60	238.83	235.20
17	15.00	15.00	10.90	738.0	16770	3.61	327.67	238.79	235.17
18	16.00	16.00	11.60	764.0	17580	3.60	327.76	238.71	235.11
19	17.00	17.00	12.20	655.0	18440	3.59	327.88	238.61	235.02
20	18.00	18.00	12.70	553.0	19350	3.58	328.03	238.47	234.90
21	19.00	19.00	13.20	459.0	20300	3.56	328.21	238.30	234.74
22	20.00	20.00	13.70	381.0	21300	3.55	328.44	238.09	234.54
23	21.00	21.00	14.10	320.0	22360	3.54	328.70	237.84	234.30
24	22.00	22.00	14.50	265.0	23470	3.53	329.00	237.55	234.03
25	23.00	23.00	14.90	219.0	24640	3.51	329.35	237.22	233.70
26	24.00	18.94	15.20	177.0	25880	3.50	329.74	236.84	233.34
27	25.00	19.27	15.50	140.0	27180	3.49	330.18	236.41	232.92
28	26.00	19.49	15.70	105.0	28550	3.48	330.67	235.93	232.45
29	27.00	19.72	15.90	76.0	29990	3.47	331.22	235.40	231.93
30	28.00	19.94	16.10	51.0	31510	3.46	331.82	234.81	231.35
31	29.00	20.27	16.40	30.0	33110	3.45	332.49	234.16	230.71
32	30.00	20.71	16.80	15.0	34800	3.44	333.22	233.45	230.01
33	31.00	21.37	17.40	8.0	36580	3.42	334.02	232.67	229.25
34	32.00	22.04	18.00	4.0	38450	3.41	334.89	231.83	228.42

Table 10.1.7 Performance of Plant with Air-Cooled Condenser

Example 10.1.7

By taking into consideration plume air recirculation and inlet losses, determine operating conditions and output of the plant described in Example 10.1.6.

Solution

Recirculation is relatively small due to the windwall. Considering the recirculation and inlet losses, the net annual energy output is only 2,055,225 MWh, and the heat rejected is 2,875,325 MWh. The heat rejected and energy output of the plant is given in Table 10.1.8.

No	T_{a1} °C	T_{sdbh} °C	T_{swb} °C	Hours h	p_v N/m^2	P_F MW	Q MW	P_{gen} MW(e)	P MW(e)
1	-1.00	-1.00	0.01	4.0	8710	3.83	328.66	237.39	233.56
2	0.00	0.00	0.01	10.0	9050	3.82	328.52	237.57	233.75
3	1.00	1.00	0.01	26.0	9410	3.81	328.38	237.74	233.93
4	2.00	2.00	0.01	43.0	9800	3.79	328.25	237.90	234.11
5	3.00	3.00	0.90	59.0	10210	3.78	328.12	237.06	234.28
6	4.00	4.00	1.90	82.0	10650	3.76	328.00	238.21	234.45
7	5.00	5.00	2.90	112.0	11120	3.75	327.90	238.35	234.60
8	6.00	6.00	3.80	152.0	11610	3.74	327.80	238.47	234.74
9	7.00	7.00	4.60	201.0	12140	3.72	327.72	238.58	234.86
10	8.00	8.00	5.40	254.0	12700	3.71	327.65	238.68	234.97
11	9.00	9.00	6.30	312.0	13280	3.69	327.60	238.75	235.06
12	10.00	10.00	7.10	371.0	13910	3.68	327.57	238.81	235.13
13	11.00	11.00	7.80	434.0	14560	3.67	327.56	238.84	235.17
14	12.00	12.00	8.60	506.0	15260	3.65	327.57	238.85	235.19
15	13.00	13.00	9.40	578.0	15990	3.64	327.60	238.83	235.19
16	14.00	14.00	10.20	656.0	16760	3.63	327.67	238.79	235.16
17	15.00	15.00	10.90	738.0	17580	3.61	327.76	238.72	235.10
18	16.00	16.00	11.60	764.0	18440	3.60	327.87	238.61	235.01
19	17.00	17.00	12.20	655.0	19340	3.59	327.03	238.47	234.89
20	18.00	18.00	12.70	553.0	20300	3.58	328.21	238.30	234.73
21	19.00	19.00	13.20	459.0	21300	3.56	328.44	238.09	234.53
22	20.00	20.00	13.70	381.0	22360	3.55	328.70	237.84	234.29
23	21.00	21.00	14.10	320.0	23470	3.54	329.00	237.55	234.01
24	22.00	22.00	14.50	265.0	24650	3.53	329.35	237.22	233.69
25	23.00	23.00	14.90	219.0	25890	3.51	329.74	236.84	233.32
26	24.00	24.00	15.20	177.0	27190	3.50	330.18	236.41	232.90
27	25.00	25.00	15.50	140.0	28570	3.49	330.68	235.93	232.43
28	26.00	26.00	15.70	105.0	30010	3.48	331.23	235.39	231.91
29	27.00	27.00	15.90	76.0	31540	3.47	331.84	234.80	231.33
30	28.00	28.00	16.10	51.0	33150	3.46	332.51	234.15	230.69
31	29.00	29.00	16.40	30.0	34840	3.45	333.24	233.43	229.98
32	30.00	30.00	16.80	15.0	36630	3.44	334.04	232.65	229.21
33	31.00	31.00	17.40	8.0	38510	3.42	334.92	231.80	228.37
34	32.00	32.00	18.00	4.0	40500	3.41	335.87	230.87	227.46

Table 10.1.8 Performance of Plant with Recirculation and Inlet Losses

Example 10.1.8

Consider the power plant described in Example 10.1.6. Determine the volume of water evaporated and the annual net power output of the particular turbo-generator set if the inlet air is adiabatically cooled to a relative humidity of 70% for ambient temperatures of 24 °C or higher. Take into consideration plume recirculation and inlet flow losses.

Solution

The results of the calculations are listed in Table 10.1.9. With adiabatic cooling, the net power output is increased to 2,056,752 MWh. This is 1527 MWh more than the output obtained in Example 10.1.8 for dry operation only. A total of V_{ws} = 61,169 m^3 of water is evaporated during the year, and the heat rejected by the condensing steam is 2,873,705 MWh.

No	T_{a1} °C	T_{sdbh} °C	T_{swb} °C	V_{ws} m^3/h	Hours h	p_v N/m^2	P_F MW(e)	Q MW	P_{gen} MW(e)	P MW(e)
1	-1.00	-1.00	0.01	0.00	4.0	8710	3.83	328.66	237.39	233.56
2	0.00	0.00	0.01	0.00	10.0	9050	3.82	328.52	237.57	233.75
3	1.00	1.00	0.01	0.00	26.0	9410	3.81	328.38	237.74	233.93
4	2.00	2.00	0.01	0.00	43.0	9800	3.79	328.25	237.90	234.11
5	3.00	3.00	0.90	0.00	59.0	10210	3.78	328.12	238.06	234.28
6	4.00	4.00	1.90	0.00	82.0	10650	3.76	328.00	238.21	234.45
7	5.00	5.00	2.90	0.00	112.0	11120	3.75	327.90	238.35	234.60
8	6.00	6.00	3.80	0.00	152.0	11610	3.74	327.80	238.47	234.74
9	7.00	7.00	4.60	0.00	201.0	12140	3.72	327.72	238.58	234.86
10	8.00	8.00	5.40	0.00	254.0	12700	3.71	327.65	238.68	234.97
11	9.00	9.00	6.30	0.00	312.0	13280	3.69	327.60	238.75	235.06
12	10.00	10.00	7.10	0.00	371.0	13910	3.68	327.57	238.81	235.13
13	11.00	11.00	7.80	0.00	434.0	14560	3.67	327.56	238.84	235.17
14	12.00	12.00	8.60	0.00	506.0	15260	3.65	327.57	238.85	235.19
15	13.00	13.00	9.40	0.00	578.0	15990	3.64	327.60	238.83	235.19
16	14.00	14.00	10.20	0.00	656.0	16760	3.63	327.67	238.79	235.16
17	15.00	15.00	10.90	0.00	738.0	17580	3.61	327.76	238.72	235.10
18	16.00	16.00	11.60	0.00	764.0	18440	3.60	327.87	238.61	235.01
19	17.00	17.00	12.20	0.00	655.0	19340	3.59	328.03	238.47	234.89
20	18.00	18.00	12.70	0.00	553.0	20300	3.58	328.21	238.30	234.73
21	19.00	19.00	13.20	0.00	459.0	21300	3.56	328.44	238.09	234.53
22	20.00	20.00	13.70	0.00	381.0	22360	3.55	328.70	237.84	234.29
23	21.00	21.00	14.10	0.00	320.0	23470	3.54	329.00	237.55	234.01
24	22.00	22.00	14.50	0.00	265.0	24650	3.53	329.35	237.22	233.69
25	23.00	23.00	14.90	0.00	219.0	25890	3.51	329.74	236.84	233.32
26	24.00	18.94	15.20	80.30	177.0	21230	3.56	328.42	238.11	234.55
27	25.00	19.27	15.50	90.79	140.0	21580	3.55	328.50	238.03	234.47
28	26.00	19.49	15.70	103.03	105.0	21810	3.55	328.56	237.98	234.42
29	27.00	19.72	15.90	115.24	76.0	22050	3.55	328.62	237.92	234.37
30	28.00	19.94	16.10	127.44	51.0	22280	3.55	328.68	237.86	234.32
31	29.00	20.27	16.40	137.82	30.0	22640	3.54	328.77	237.77	234.23
32	30.00	20.71	16.80	146.43	15.0	23140	3.53	328.91	237.64	234.11
33	31.00	21.37	17.40	151.49	8.0	23890	3.53	329.12	237.44	233.91
34	32.00	22.04	18.00	156.54	4.0	24680	3.52	329.36	237.21	233.69

Table 10.1.9 Plant Performance with Adiabatic Precooling and Water Evaporated

10.2 Cooling System Optimization

Due to the competitive nature of the industry and the high capital cost of air-cooled heat exchangers and cooling towers, optimizing the design for a given cooling capacity is justified within practical limitations. The degree of optimization ultimately achieved is usually a function of:

- the sophistication of the design program
- computational cost
- quality of available input data including material, labor, and energy cost structures

In general, heat exchangers are designed for many varied applications and may involve many different performance criteria. Some of these criteria are:

- minimum initial cost
- minimum initial and operating costs
- minimum weight or material
- minimum volume or heat transfer surface area
- minimum mean temperature difference
- maximum heat transfer rate
- minimum destruction of exergy, according to Bejan

The design objective of an optimal radiator for a military vehicle described by Eckert, Chiou, and Hawes will be quite different from a cooling tower for a power plant described by Johnson. When a single performance measure has been defined quantitatively and is to be minimized or maximized, it is called an *objective function* in a design optimization. A particular design may be subjected to certain requirements such as required heat transfer, allowable pressure drop, and limitations on height, width, and/or length of the exchanger. These requirements are called *constraints* in a design optimization. A number of different finned surfaces can be incorporated in a specific design problem, and many geometrical parameters can be varied for each surface geometry. In addition, operating flows and

temperatures can be changed. Thus, a large number of design variables are associated with a heat exchanger design. The question arises as to how one can effectively adjust these design variables within imposed constraints and come up with a design having an optimum objective function.

Once the general configuration and surface are selected, an optimized heat exchanger design may be determined if the objective function and constraints can be expressed mathematically. This will be possible if all of the variables are automatically and systematically changed on some statistical or mathematical basis. Engineering judgments based on experience are involved in different stages of the thermal and mechanical design of a heat exchanger. Even during the thermal design, if many constraints are imposed, it may not be possible to satisfy all conditions. It is the designer's responsibility to make judgments on the constraints that can be relaxed to obtain a good design.

Ideally, the optimization exercise should not be limited to the heat exchanger, but should be extended to include the entire system or process according to Veck and Rubbers. Such a thermo-economic analysis combines a second-law or exergy analysis with an economic one according to Tsatsaronis and Valero as well as Moran and Sciubba.

In a multi-dimensional design space, an intuitive approach to optimizing a system becomes a futile exercise. For a limited number of variables, analytic approaches may indicate certain trends according to Moore, but these methods are inadequate in the case of more detailed system optimizations.

Heat exchanger optimization through a package of optimization computer programs has been suggested by Shah. A summary of optimization procedures applicable to air-cooled heat exchangers is presented by Hedderich et al. Mukherjee offers guidance on the selection, design, and optimization of air-cooled heat exchangers employing commercially available components for various applications.

Several papers have addressed the problem of economic optimization of dry-cooled power plants. Some of these include papers by Rossie, Smith and Larinoff, Hauser, Miliaras, Fryer, Choi, Li, Veck, and Lovino. More complex optimization studies have been attempted by other investigators such as Ecker and Wiebking as well as Buys and Kröger.

An example of an optimization exercise applied to retrofitting the finned tubes in an existing dry-cooling tower is presented by Buys and Kröger. They considered an existing natural-draft cooling tower similar to that described in

Example 7.3.1. The finned tubes were replaced by new ones at a minimum cost without affecting plant performance.

For purposes of illustration, it is assumed the total effective cost of a round, extruded, bi-metallic finned tube, as shown in Figure 5.1.4 (b), can be expressed as

$$C_{ft} = \left[C_{wf}\left(C_t + C_f\right) + C_{fix}\right] L_t n_{tb} n_b \tag{10.2.1}$$

where

C_{wf} = a weighting factor

The core tube cost per unit length is

$$C_t = \pi \rho_t \left(d_o^2 - d_i^2\right) C_{tm} / 4 \tag{10.2.2}$$

where

C_{tm} = the total material cost per unit mass

The cost of the fin material per unit tube length is

$$C_f = \frac{\pi \rho_f}{4 P_f}\left[\left(d_f^2 - d_r^2\right) t_f + \left(d_r^2 - d_o^2\right)\left(P_f - t_f\right)\right] C_{fm} \tag{10.2.3}$$

where

C_{fm} = the fin material cost per unit mass

The fixed cost of the tube per unit length, C_{fix}, covers other costs incurred by the manufacturer. The cost of the manifolds may also be included in C_{fix} and C_{wf}.

The following dimensions are specified for a hyperbolic natural-draft cooling tower (Fig. 7.1.1):

- Tower height: H_5 = 120 m
- Inlet height: H_3 = 13.67 m
- Inlet diameter: d_3 = 82.958 m
- Outlet (throat) diameter: d_5 = 58 m

According to the original design, 142 heat exchanger bundles are arranged radially in the form of A-frames in the base of the tower. The particulars of the bundles area are as follows:

- Effective length (finned tube) of bundle: L_t = 15 m
- Effective width of bundle: W_b= 2.262 m
- Apex angle of A-frame: $2\theta = 61.5^\circ$
- Number of water passes: n_{wp}= 2
- Number of tube rows: n_r = 4

A schematic drawing of the heat exchanger geometry is shown in Figure 10.2.1. To minimize cost, the original bundle base support is employed and no changes are made to the water pipe layout to and from the bundles or the water pump. The bundle support structure imposes the restriction that $L_b = W_b \sin\theta$ = 1.157 m. The existing pump provides a water flow rate of 4390 kg/s at a pressure drop of 16,302 N/m^2 through the finned tube. Deviation from these values are not permitted. In effect, this means the pumping power, P_w, remains unchanged.

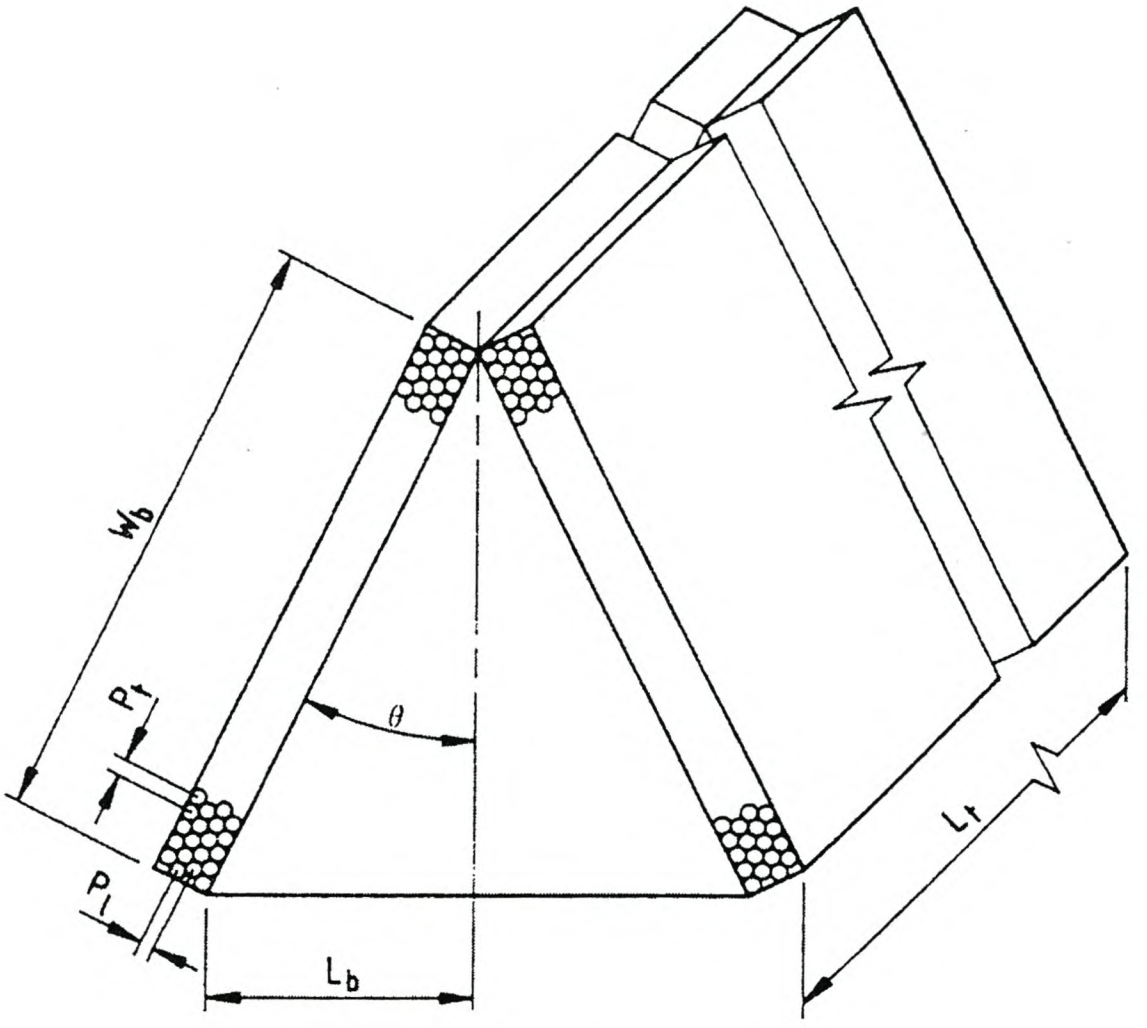

Fig. 10.2.1 Heat Exchanger Bundle Geometry

Due to structural considerations, the tube wall and the fin root thickness are assumed constant at 1.655 mm and 1.08 mm respectively. The contact resistance, R_c, is assumed to be negligible.

The cooling tower is required to remove 365.08 MW at:

- an inlet water temperature of 61.45 °C
- an ambient air pressure at ground level of 84,600 N/m^2
- a corresponding air temperature of 15.6 °C

In order to achieve an optimum design, the independent parameters t_f, d_f, θ, d_i, P_t, P_l, P_f, and n_{wp} may be varied subject to the constraints specified.

A fin pitch of 2.35 mm is arbitrarily chosen as the design reference value. Where fouling is significant, very small fin pitches are avoided. The values are taken as:

- $C_{wf} = 2$
- $C_{tm} = 0.8$ \$/kg
- $C_{fm} = 4.2$ \$/kg
- $C_{fix} = 2$ \$/m

The cost minimization problem may be solved numerically with a general purpose algorithm for non-linear constrained optimization. A *generalized reduced gradient* algorithm according to Lasdon and a *constrained variable metric* algorithm according to Powell were investigated. The variable metric algorithm was very efficient when applied to this problem. All results presented in this paper were obtained using the FORTRAN subroutine called VMCWD according to Powell. Derivatives of the cost function and constraints were calculated numerically. Variables and constraints were carefully scaled since they differed greatly in magnitude. All calculations were performed in double precision in order to obtain reasonably accurate values for the derivatives. On average, the VMCWD subroutine calls other routines, which calculate the cost function, constraints, and gradients 6–10 times for each complete optimization.

The results of the cost minimization are presented in Table 10.2.1. The values of the independent parameters corresponding to the minimum cost are taken as reference values from the first line of Table 10.2.1. In order to investigate the dependence of the minimum cost on each parameter, one parameter is perturbed, and a minimization is performed with respect to the other parameters. The influence of various parameters on the total cost are also shown in Figure 10.2.2.

Parameter	t_f mm	d_f mm	θ °	d_i mm	P_t mm	P_ℓ mm	P_f mm	C $
Optimum	0.0903	61.95	27.08	21.68	61.95	53.65	2.35	2617869
t_f	0.0500	55.67	22.68	19.57	55.67	48.21		2789929
	0.1000	62.79	27.88	22.01	62.79	54.37		2623508
	0.2000	64.71	30.35	23.46	68.86	59.63	2.35	2984172
	0.3000	64.40	30.61	23.70	70.19	60.78		3545850
	0.4000	63.22	30.00	23.48	69.75	60.40		4181762
d_f	0.0768	50.00	25.20	19.85	52.40	45.37		2756065
	0.0831	55.00	26.24	20.17	56.37	48.81		2661283
	0.0878	60.00	27.04	21.41	60.00	51.96	2.35	2621230
	0.0940	65.00	27.08	22.07	65.00	56.29		2625553
	0.0996	70.00	26.90	22.64	70.00	60.62		2668214
θ	0.0734	60.38	21.00	20.60	68.68	59.48		2762512
	0.0793	60.78	24.00	21.13	64.73	56.06		2659733
	0.0895	61.94	27.00	21.65	61.94	53.64	2.35	2617917
	0.1328	64.69	30.00	22.82	64.69	56.02		2702217
	0.2016	72.15	33.00	24.56	72.15	62.48		3044095
d_i	0.0390	44.41	22.16	18.00	45.46	39.37		3080373
	0.0790	58.57	26.26	21.00	58.57	50.73	2.35	2632745
	0.1390	74.33	29.82	24.00	74.33	64.37		2791658
P_t	0.0732	50.00	26.11	19.75	50.00	43.30		2767791
	0.0878	60.00	27.04	21.41	60.00	51.96	2.35	2621230
	0.1011	67.16	26.07	22.40	70.00	60.62		2660119
P_ℓ	0.0763	51.96	26.39	20.12	51.96	45.00		2718706
	0.0922	63.51	27.09	21.88	63.51	55.00	2.35	2619920
$P_\ell = 0.866 P_t$	0.1075	69.86	25.14	22.70	75.06	65.00		2719226
P_ℓ	0.0863	58.89	26.99	21.25	58.89	51.00		2626282
	0.0870	58.89	27.36	21.34	58.89	55.00		2602379
$P_\ell \geq P_{\ell min}$	0.0876	58.77	27.71	21.42	58.77	59.00	2.35	2580370
	0.0881	58.66	28.04	21.50	58.66	63.00		2559978
P_f	0.0828	61.91	28.17	22.22	63.82	55.27	2.10	2482365
	0.0854	62.07	27.83	22.00	62.83	54.41	2.20	2537426
	0.0884	62.09	27.40	21.79	62.09	53.77	2.30	2591074
	0.0922	61.81	26.76	21.57	61.81	53.53	2.40	2644808
	0.0959	61.53	26.14	21.36	61.53	53.29	2.50	2699153
0.5	0.0857	60.66	26.77	21.42	60.66	52.53		2418587
1.0	0.0933	62.78	27.28	21.84	62.78	54.36	2.35	2748466
1.5	0.1005	64.74	27.73	22.22	64.74	56.06		3067823

Table 10.2.1 Optimized Finned Tube Bundles (n_{wp} = 2)

Parameter	t_f mm	d_f mm	θ °	d_i mm	P_t mm	P_ℓ mm	P_f mm	C $
3.0	0.1039	65.64	27.94	22.39	65.66	56.84		2204230
4.0	0.0921	62.45	27.20	21.78	62.45	54.08	2.35	2550819
5.0	0.0843	60.26	26.67	21.34	60.26	52.19		2880734
1.0	0.1118	67.71	28.41	22.79	67.71	58.64		1630395
3.0	0.0818	59.55	26.50	21.20	59.55	51.57	2.35	3571350
5.0	0.0744	57.35	25.95	20.75	57.35	49.67		5449476
1.0	0.0773	58.21	26.17	20.93	58.21	50.41		2256577
3.0	0.1016	65.04	27.81	22.28	65.04	56.33	2.35	2950093
5.0	0.1211	70.07	28.93	23.23	70.07	60.68		3554603
$n_{wp} = 4$								
Optimum	0.0826	77.39	26.72	36.18	83.87	72.63	2.35	2611998
	0.1	78.88	27.63	37.10	86.91	75.27		2629576
	0.2	82.08	29.97	39.42	94.67	81.99	2.35	3051830
t_f	0.3	81.59	30.10	39.61	95.50	82.71		3666459
	0.4	79.70	29.37	39.00	93.77	81.20		4354121

Table 10.2.1 cont.

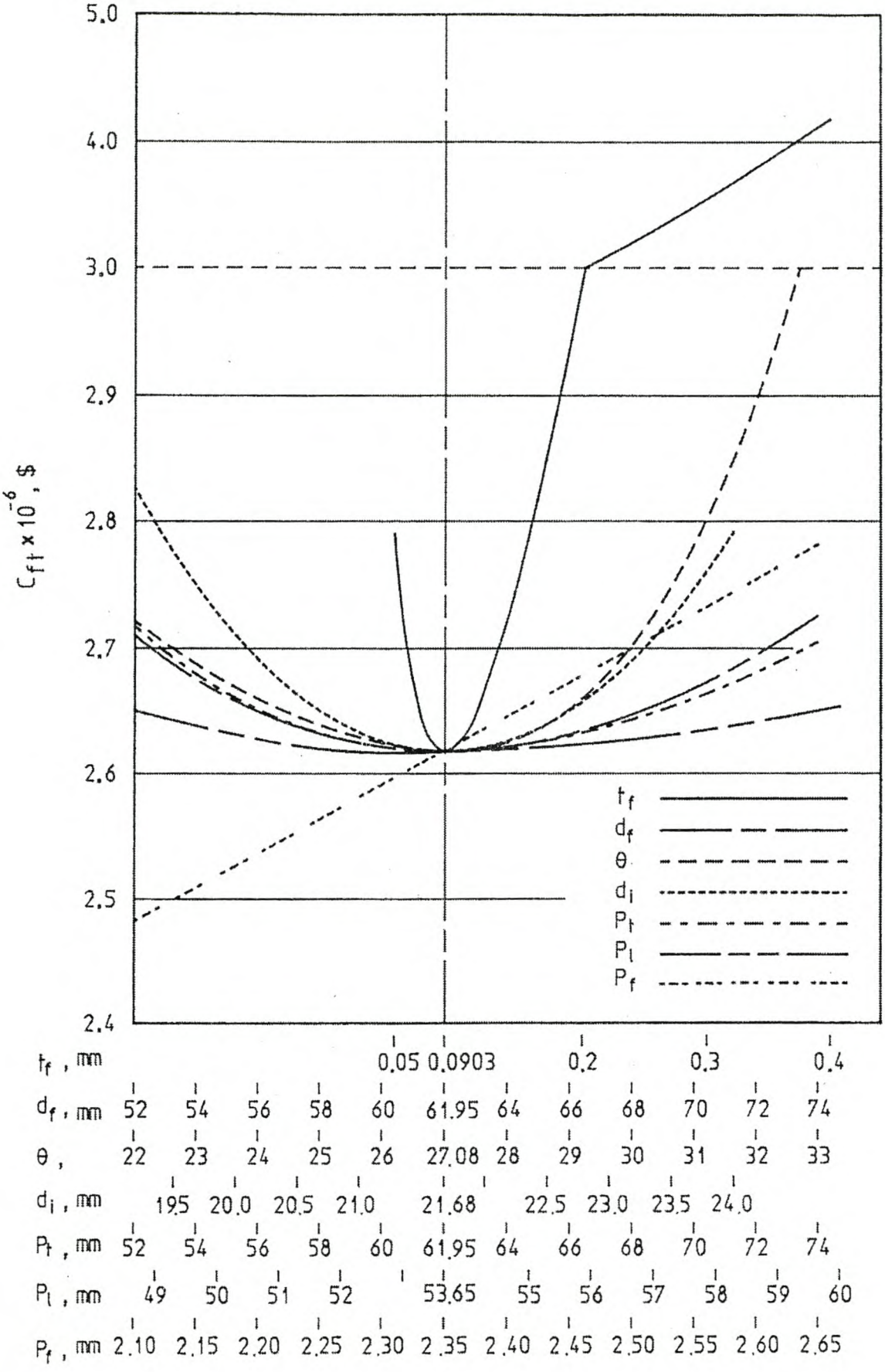

Fig. 10.2.2 Graphical Presentation of Optimum Finned Tube Bundles

According to the results shown in Table 10.2.1, the optimum fin thickness is only 0.0903 mm, and the fin diameter is 61.95 mm. In practice, somewhat thicker fins are preferred and result in a corresponding increase in system cost (Table 10.2.1).

According to the analysis, the finned tubes are closely packed at optimum conditions if a triangular pattern is assumed. For larger fin thicknesses, a more open arrangement is preferable. The influence of the longitudinal pitch is shown for both a triangular tube layout and for the case where P_l is not tied to the transversal pitch. As P_l increases, the system cost is reduced. However, this reduction is only applicable within certain limits in which the finned tube correlations apply.

Where fouling is not serious, a reduction in fin pitch will generally result in a lower cost system. The influence of variations in the cost structure are also shown in Table 10.2.1.

The possibility of installing a four-pass heat exchanger was investigated. This optimum design is only slightly less costly than the two-pass system. For the thicker fin, the converse is true. In addition, the inside diameter of the tubes is considerably larger to ensure a pressure drop on the water side that does not exceed the pressure drop specified for the pump.

In a later publication, Buys and Kröger attempted to improve an existing cooling tower/surface condenser system design. The existing tower design was similar to that described in Example 7.3.1. The main parameters are shown in Table 10.2.2, and the optimum design dimensions are in this table for a surface condenser having a fixed value for UA. The fin is only 0.078 mm thick, but the tube and fin diameters are considerably larger than in the original design. The optimum tower is lower, while the inlet height is considerably larger. If the fin thickness is increased to a more practical value, the tower height also tends to increase while other parameters do not change significantly.

Parameter	t_f mm	d_f mm	d_i mm	θ °	P_t mm	H_5 m	H_3 m	d_5 m	m_w kg/s	C $\frac{\$}{annum}$
Existing tower design	0.500	57.2	22.09	30.75	58.0	120.0	13.67	58.0	4390	863022
Optimum tower	0.078	75.4	33.00	24.50	77.0	101.0	25.10	66.9	5274	548793
t_f	0.100	76.4	33.50	25.70	79.8	101.7	25.10	66.8	5203	552363
	0.300	75.2	33.90	31.30	86.6	118.1	25.00	64.2	5029	674646
	0.500	72.9	31.30	30.60	78.1	135.3	24.80	61.9	5031	811463

Table 10.2.2 Dimensions of Optimized Cooling System

Conradie et al. applied modern optimization techniques to obtain cost optimal design and performance of dry-cooling systems for power plant applications. Their optimization method took into consideration all the parameters that affect the capital and operating cost of the dry-cooling systems. Their method did not prescribe any constraints other than practical limitations and effective system simulation.

The Sequential Quadratic Programming (SQP) method is used as the basis in implementing the constrained, nonlinear, optimization techniques. The equation-based models and the optimization problems are simultaneously solved along an infeasible path. Significant computational advantages are achieved when the special mathematical structure of the equation-based models is exploited by adapting the basic SQP code. An SQP decomposition strategy is introduced to overcome the increase in matrix storage requirements and computational expense for large optimization problems. The performance of the decomposition strategy is superior when compared to the conventional SQP optimization method, and it solves the dry-cooling system optimization problem effectively. Of course, this procedure can be applied in the optimization of any other heat exchanger or cooling tower system.

Castro et al. developed an optimization model for a cooling water system that incorporates a wet-cooling tower. The model considered the thermal and hydraulic interactions in the process and was applied to the study and analysis of typical operational cases. The objective function was the minimization of the overall operating cost.

References

Bejan, A., "The Thermodynamic Design of Heat and Mass Transfer Processes and Devices," *International Journal of Heat and Fluid Flow*, 8-4:258–276, 1987.

Buys, J. D. and D. G. Kröger, "Cost-optimal Design of Dry Cooling Towers through Mathematical Programming Techniques," *American Society of Mechanical Engineers Journal of Heat Transfer*, 111:322–327, 1989a.

Buys, J. D. and D. G. Kröger, "Dimensioning Heat Exchangers for Existing Dry Cooling Towers," *Energy Conversion Management*, 29-1:63–71, 1989b.

Castro, M. M., T. W. Song, and J. M. Pinto, "Minimization of Operational Costs in Cooling Water Systems," *Transactions International Chemical Engineering*, vol. 78, part A, March 2000.

Chiou, J. P., *Optimization of Liquid-to-air Heat Exchanger in the Cooling System of Military Combat/Tactical Vehicle*, SAE 760851, Society of Automotive Engineers, 1976.

Choi, M. and L. R. Glicksman, *Computer Optimization of Dry and Wet/dry Cooling Tower Systems for Large Fossil and Nuclear Power Plants*, MIT Energy Laboratory Report No. MIT-EL 79-034, Massachusetts Institute of Technology, Cambridge, Massachusetts, 1979.

Conradie, A. E., J. D. Buys, and D. G. Kröger, "Performance Optimization of Dry-cooling Systems for Power Plants through SQP Methods," *Applied Thermal Engineering*, 18-1:25–40, 1998.

Conradie, T. A. and D. G. Kröger, "Enhanced Performance of a Dry-Cooled Power Plant Through Air Precooling," Paper 91-JPGC-Pwr-6, American Society of Mechanical Engineers Fluids International Joint Power Conference, San Diego, October 1991.

Ecker, J. G. and R. D. Wiebking, "Optimal Design of a Dry-Type Natural-Draft Cooling Tower by Geometric Programming," *Journal of Optimization Theory and Applications*, 26-2:305–323, 1978.

Eckert, B., "Aufgaben bei der Gestaltung der Kühlanlage des Kraftwagens," *Automobiltechnische Zeitschrift*, 8–10 Heft, May 1942.

Fryer, B. C., *A Review and Assessment of Engineering Economic Studies of Dry Cooled Electrical Generating Plants*, BNWL, 1976.

Hauser, L. G., K. A. Oleson, and R. J. Budenholzer, "An Advanced Optimization Technique for Turbine, Condenser, Cooling System Combinations," *Proceedings*, American Power Conference, 33:427–445, 1971.

Hawes, S. P., "Improved Passenger Car Cooling Systems," Society of Automotive Engineers Automotive Engineering Congress, Detroit, February 1976.

Hedderich, C. P., M. D. Kelleher, and G. N. Van der Plaats, "Design and Optimization of Air-Cooled Heat Exchangers," Transactions of the American Society of Mechanical Engineers, *Journal of Heat Transfer*, 104:683–690, 1982.

Johnson, B. M., ed., *Cooling Tower Performance Prediction and Improvement, Vol. 1, Applications Guide*, Electric Power Research Institute Report, GS-6370, Palo Alto, 1989.

Lasdon, L. S., A. D. Waren, A. Jain, and M. Ratner, "Design and Testing of a Generalized Reduced Gradient Code for Nonlinear Programming," *Transactions on Mathematical Software 4*, Association for Computing Machinery, 34–50, 1978.

Li, K. W. and W. Sadiq, "Computer-aided Optimization of Cooling Systems," American Society of Mechanical Engineers International Computers in Engineering Conference, 3: 165–171, 1985.

Lovino, G., H. Hattoni, L. Hazzocchi, R. Senis, and R. Vanzan, "Optimal Sizing of Natural Draft Dry Cooling Towers for ENEL Combined Cycle Power Plants, A Future for Energy," *Proceedings*, Florence World Energy Research Symposium, Firenze, ed. S. S. Stecco and M. J. Moran, Pergamon Press, New York, 1990.

Miliaras, E. S., *Power Plants with Air-cooled Condensing Systems*, MIT Press, Cambridge, Massachusetts, 1974.

Mohiuddin, A. K. M. and K. Kant, "Knowledge Base for the Systematic Design of Wet Cooling Towers, Part 1: Selection and Tower Characteristics," *International Journal of Refrigeration*, 19-1:43-51, 1996.

Moore, F. K., "The Minimization of Air Heat-Exchange Surface Areas of Dry Cooling Towers for Large Power Plants," *Heat Transfer Digest*, 6:13–22, 1973.

Moore, F. K., "On the Minimum Size of Natural-Draft Dry Cooling Towers for Large Power Plants," Paper 72-WA/HT-60, American Society of Mechanical Engineers Winter Annual Meeting, November 1972.

Moran, M. J. and E. Sciubba, "Exergy Analysis: Principles and Practice," Transactions of the American Society of Mechanical Engineers, *Journal of Engineering for Gas Turbines and Power*, 116:285–290, April 1994.

Mukherjee, R., "Effectively Design Air-Cooled Heat Exchangers," *Chemical Engineering Progress*, 26–47, February 1997.

Powell, M. J. D., "A Fast Algorithm for Nonlinearly Constrained Optimization Calculation, in Numerical Analysis," *Proceedings Dundee, Springer Lecture Notes in Mathematics 630*, ed. G. A. Watson, 114–157, 1977.

Powell, M. J. D., "VMCWD: A Fortran Subroutine for Constrained Optimization," SIGMAP *Bulletin*, no. 32, 1983.

Rossie, J. P. and E. A. Cecil, *Research on Dry-Type Cooling Towers for Thermal Electric Generation. Part I and II*, EPA Report, Water Pollution Control Research Series 16130 EES, 1970.

Shah, R. K., *Compact Heat Exchanger Surface Selection, Optimization, and Computer-aided Thermal Design, Low Reynolds Number Flow Heat Exchangers*, ed. S. Kakac, R. K. Shah, and A. E. Bergles, Hemisphere Publishing Corp., Washington, 1983.

Shah, R. K., K. A. Afimiwala, and R. W. Mayne, *Heat Exchanger Optimization, Heat Transfer 1978*, 4:193–199, Hemisphere Publishing Corp., Washington, 1987.

Smith, E. C. and M. W. Larinoff, "Power Plant Siting, Performance and Economics with Dry Cooling Tower Systems," *Proceedings*, American Power Conference, 32:544–572, 1970.

Trage, B. and F. J. Hintzen, "Design and Construction of Indirect Dry Cooling Units," *Proceedings*, Verein Grosskraftwerksbetreiber Conference, 1:70–79, Johannesburg, 1987.

Tsatsaronis, G. and A. Valero, "Thermodynamics Meets Economics," *Mechanical Engineering*, 111-8:84–86, August 1989.

Veck, G. A. and P. J. E. Rubbers, "Economic Evaluation of Dry Cooling: The Options," *Proceedings,* Verein Grosskraftwerksbetreiber Conference, 1:80–89, Johannesburg, November 1987.

Appendix A

Properties of Fluids

A.1 The Thermophysical Properties of Dry Air from 220K to 380K at Standard Atmospheric Pressure (101325 N/m2)

Density

$$\rho_a = p_a/(287.08\ T),\ \text{kg/m}^3 \tag{A.1.1}$$

Specific heat from General Electric *Heat Transfer and Fluid Flow Data Book*

$$c_{pa} = 1.045356 \times 10^3 - 3.161783 \times 10^{-1}\ T + 7.083814 \times 10^{-4}\ T^2 - 2.705209 \times 10^{-7}\ T^3,\ \text{J/kgK} \tag{A.1.2}$$

Dynamic viscosity from General Electric *Heat Transfer and Fluid Flow Data Book*

$$\mu_a = 2.287973 \times 10^{-6} + 6.259793 \times 10^{-8}\ T - 3.131956 \times 10^{-11}\ T^2 + 8.15038 \times 10^{-15}\ T^3,\ \text{kg/sm} \tag{A.1.3}$$

Thermal conductivity

$$k_a = -4.937787 \times 10^{-4} + 1.018087 \times 10^{-4}\, T - 4.627937 \times 10^{-8}\, T^2 + 1.250603 \times 10^{-11}\, T^3, \text{ W/mK} \quad \text{(A.1.4)}$$

Table A.1 The Thermophysical Properties of Dry Air at Standard Atmospheric Pressure

T	ρ_a	c_{pa}	$\mu_a \times 10^5$	k_a	$\alpha_a \times 10^5$	Pr_a
K	kg/m^3	J/kgK	kg/ms	W/mK	m^2/s	
220	1.60432	1007.20	1.46304	0.0197973	1.22518	0.744330
225	1.56866	1006.99	1.48797	0.0202127	1.27957	0.741309
230	1.53456	1006.81	1.51278	0.0206262	1.33500	0.738428
235	1.50191	1006.66	1.53746	0.0210378	1.39145	0.735680
240	1.47062	1006.53	1.56201	0.0214475	1.44892	0.733056
245	1.44061	1006.43	1.58643	0.0218553	1.50738	0.730550
250	1.41180	1006.35	1.61073	0.0222613	1.56684	0.728156
255	1.38411	1006.30	1.63490	0.0226655	1.62727	0.725867
260	1.35750	1006.28	1.65894	0.0230678	1.68867	0.723678
265	1.33188	1006.28	1.68286	0.0234683	1.75103	0.721585
270	1.30722	1006.30	1.70666	0.0238669	1.81433	0.719581
275	1.28345	1006.35	1.73033	0.0242638	1.87857	0.717663
280	1.26053	1006.42	1.75388	0.0246589	1.94373	0.715828
285	1.23842	1006.52	1.77731	0.0250521	2.00980	0.714070
290	1.21707	1006.64	1.80061	0.0254436	2.07677	0.712387
295	1.19644	1006.78	1.82380	0.0258334	2.14463	0.710776
300	1.17650	1006.95	1.84686	0.0262213	2.21336	0.709233
305	1.15721	1007.14	1.86980	0.0266075	2.28297	0.707755
310	1.13854	1007.35	1.89263	0.0269920	2.35342	0.706340
315	1.12047	1007.59	1.91533	0.0273747	2.42472	0.704985
320	1.10297	1007.85	1.93792	0.0277558	2.49685	0.703688
325	1.08600	1008.13	1.96039	0.0281351	2.56980	0.702446
330	1.06954	1008.43	1.98274	0.0285127	2.64356	0.701258
335	1.05358	1008.76	2.00498	0.0288886	2.71811	0.700122
340	1.03808	1009.11	2.02710	0.0292628	2.79345	0.699035
345	1.02304	1009.48	2.04911	0.0296353	2.86957	0.697997
350	1.00842	1009.87	2.07100	0.0300062	2.94645	0.697004
355	0.99422	1010.28	2.09278	0.0303754	3.02408	0.696056
360	0.98041	1010.71	2.11444	0.0307430	3.10246	0.695151
365	0.96698	1011.17	2.13599	0.0311098	3.18156	0.694288
370	0.95392	1011.64	2.15743	0.0314732	3.26138	0.693465
375	0.94120	1012.13	2.17876	0.0318359	3.34191	0.692681
380	0.92881	1012.65	2.19998	0.0321970	3.42313	0.691935

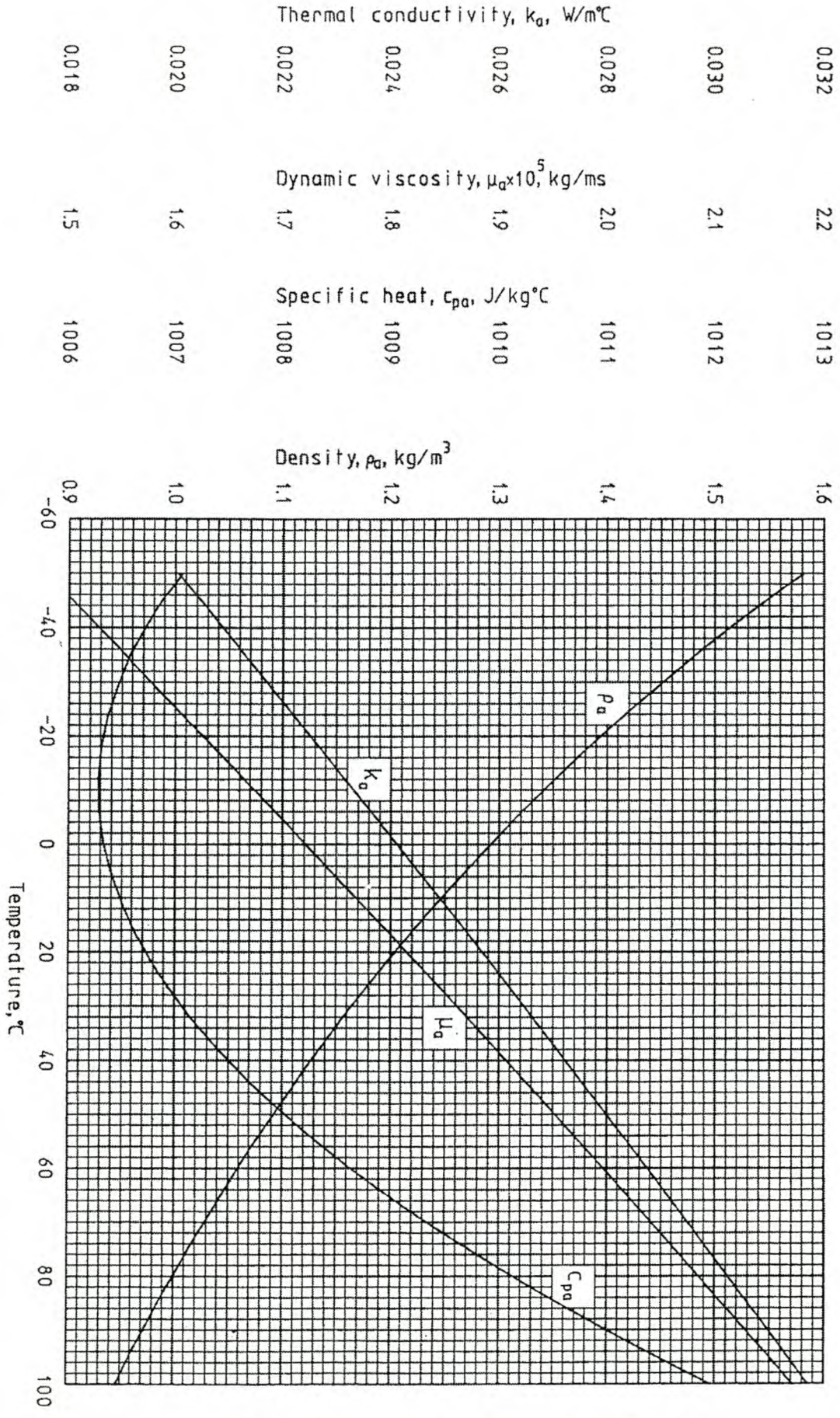

Figure A.1 The Thermophysical Properties of Dry Air at Standard Atmospheric Pressure (101325 N/m^2)

A.2 The Thermophysical Properties of Saturated Water Vapor from 273.15K to 380K

Vapor pressure according to Goff

$$p_v = 10^z, \text{ N/m}^2 \tag{A.2.1}$$

$$z = 10.79586(1 - 273.16/T) + 5.02808 \log_{10}(273.16/T)$$

$$+ 1.50474 \times 10^{-4} [1 - 10^{-8.29692\{(T/273.16) - 1\}}]$$

$$+ 4.2873 \times 10^{-4}[10^{4.76955(1 - 273.16/T)} - 1] + 2.786118312$$

Specific heat

$$c_{pv} = 1.3605 \times 10^3 + 2.31334T - 2.46784 \times 10^{-10}T^5 + 5.91332 \times 10^{-13}T^6, \text{ J/kgK} \tag{A.2.2}$$

Dynamic viscosity

$$\mu_v = 2.562435 \times 10^{-6} + 1.816683 \times 10^{-8}T + 2.579066 \times 10^{-11}T^2 - 1.067299 \times 10^{-14}T^3, \text{ kg/ms} \tag{A.2.3}$$

Thermal conductivity from General Electric *Heat Transfer and Fluid Flow Data Book*

$$k_v = 1.3046 \times 10^{-2} - 3.756191 \times 10^{-5}T + 2.217964 \times 10^{-7}T^2 - 1.111562 \times 10^{-10}T^3, \text{ W/mK} \tag{A.2.4}$$

Vapor density from the *U.K. Steam Tables in SI Units 1970*

$$\rho_v = -4.062329056 + 0.10277044T - 9.76300388 \times 10^{-4}T^2 + 4.475240795 \times 10^{-6}T^3 - 1.004596894 \times 10^{-8}T^4 + 8.9154895 \times 10^{-12}T^5, \text{ kg/m}^3 \quad \text{(A.2.5)}$$

Temperature

$$T = 164.630366 + 1.832295 \times 10^{-3}p_v + 4.27215 \times 10^{-10}p_v^2 + 3.738954 \times 10^{3}p_v^{-1} - 7.01204 \times 10^{5}p_v^{-2} + 16.161488\ \ell n p_v - 1.437169 \times 10^{-4}p_v\ \ell n p_v, \text{K} \quad \text{(A.2.6)}$$

Table A.2 The Thermophysical Properties of Saturated Water Vapor

T	p_v	ρ_v	c_{pv}	$\mu_v \times 10^6$	k_v	$\alpha_v \times 10^5$	Pr_v
K	N/m^2	kg/m^3	J/kgK	kg/ms	W/mK	m^2/s	
275	697.820	0.00550	1864.29	9.28676	0.0171781	167.602	1.00786
280	990.897	0.00767	1868.46	9.4368	0.0174774	121.992	1.00887
285	1387.70	0.01056	1872.66	9.58775	0.0177831	90.0091	1.00964
290	1918.11	0.01436	1876.92	9.73950	0.0180951	67.2777	1.01023
295	2618.61	0.01928	1881.31	9.89208	0.0184134	50.8805	1.01068
300	3533.19	0.02557	1885.89	10.0454	0.0187378	38.9260	1.01103
305	4714.45	0.03355	1890.74	10.1996	0.0190684	30.1011	1.01135
310	6224.58	0.04360	1895.92	10.3546	0.0194049	23.5132	1.01168
315	8136.44	0.05611	1901.52	10.5104	0.0197474	18.5427	1.01207
320	10534.7	0.07155	1907.63	10.6670	0.0200957	14.7547	1.01259
325	13516.9	0.09045	1914.35	10.8244	0.0204498	11.8400	1.01329
330	17194.7	0.11341	1921.79	10.9825	0.0208095	9.57698	1.01425
335	21694.5	0.14108	1930.04	11.1414	0.0211749	7.80452	1.01551
340	27158.9	0.17418	1939.25	11.3010	0.0215457	6.40488	1.01716
345	33747.7	0.21352	1949.63	11.4614	0.0219219	5.29095	1.01927
350	41638.4	0.26000	1961.03	11.6225	0.0223035	4.39779	1.02191
355	51027.6	0.31455	1973.90	11.7844	0.0226904	3.67653	1.02516
360	62131.3	0.37821	1988.29	11.9470	0.0230824	3.09016	1.02910
365	75186.3	0.45213	2004.37	12.1102	0.0234795	2.61037	1.03382
370	90450.0	0.53750	2022.33	12.2742	0.0238816	2.21538	1.03940
375	108201	0.63568	2042.35	12.4389	0.0242886	1.888304	1.04595
380	128743	0.74799	2064.63	12.6043	0.0247005	1.615964	1.05355

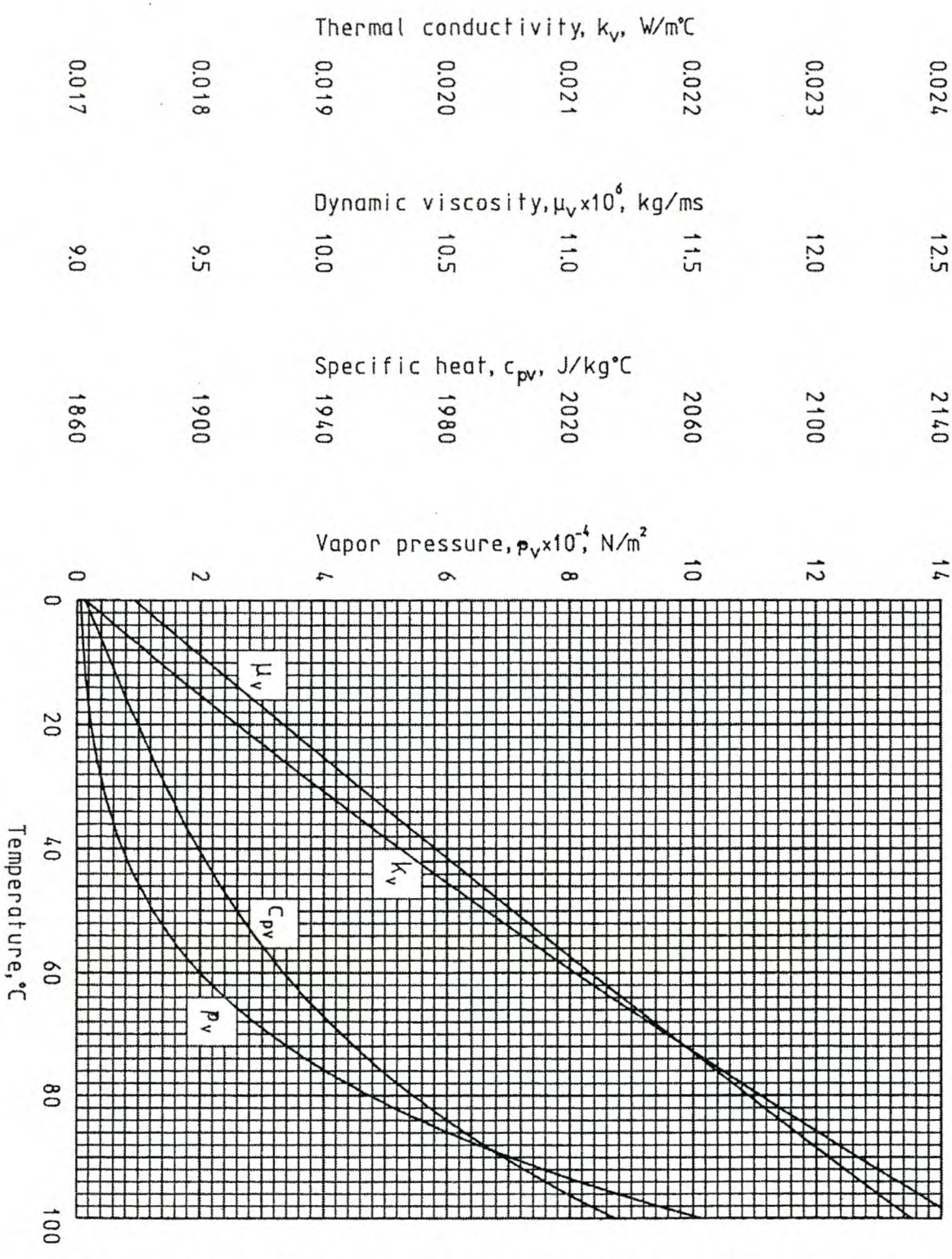

Figure A.2 The Thermophysical Properties of Saturated Water Vapor

A.3 The Thermophysical Properties of Mixtures of Air and Water Vapor

Density from ASHRAE *Handbook of Fundamentals*

$$\rho_{av} = (1+w)\,[1 - w/(w + 0.62198)]\,p_{abs}/(287.08\,T),\ \text{kg air- vapor/m}^3 \qquad \text{(A.3.1)}$$

Specific heat according to Faires

$$c_{pav} = (c_{pa} + wc_{pv})/(1 + w),\ \text{J/K kg air-vapor} \qquad \text{(A.3.2a)}$$

or the specific heat of the air-vapor mixture per unit mass of dry air

$$c_{pma} = (c_{pa} + wc_{pv}),\ \text{J/K kg dry air} \qquad \text{(A.3.2b)}$$

Dynamic viscosity according to Godridge

$$\mu_{av} = (X_a \mu_a M_a^{0.5} + X_v \mu_v M_v^{0.5})\,/(X_a M_a^{0.5} + X_v M_v^{0.5}),\ \text{kg/ms} \qquad \text{(A.3.3)}$$

where

M_a = 28.97 kg/mole

M_v = 18.016 kg/mole

$X_a = 1/(1 + 1.608\ w)$

$X_v = w/(w + 0.622)$

Thermal conductivity according to Lehmann

$$k_{av} = (X_a k_a M_a^{0.33} + X_v k_v M_v^{0.33})\,/(X_a M_a^{0.33} + X_v M_v^{0.33}),\ \text{W/mK}_1 \qquad \text{(A.3.4)}$$

Humidity ratio according to Johannsen

$$w = \left(\frac{2501.6 - 2.3263(T_{wb} - 273.15)}{2501.6 + 1.8577(T - 273.15) - 4.184(T_{wb} - 273.15)}\right)\left(\frac{0.62509\,p_{vwb}}{p_{abs} - 1.005\,p_{vwb}}\right) - \left(\frac{1.00416\,(T - T_{wb})}{2501.6 + 1.8577(T - 273.15) - 4.184(T_{wb} - 273.15)}\right), \text{ kg/kg dry air} \quad \text{(A.3.5)}$$

Enthalpy

(A.3.6a)

$i_{av} = [c_{pa}\,(T - 273.15) + w\{i_{fgwo} + c_{pv}\,(T - 273.15)\}]/(1+w)$, J/kg air-vapor

or the enthalpy of the air-vapor mixture per unit mass of dry air

$$i_{ma} = c_{pa}(T - 273.15) + w\left[i_{fgwo} + c_{pv}(T - 273.15)\right], \text{ J/kg dry air} \quad \text{(A.3.6b)}$$

where the specific heats are evaluated at (T + 273.15)/2 and the latent heat, i_{fgwo}, is evaluated at 273.15 K according to equation (A.4.5), i.e., i_{fgwo} = 2.5016 x 10^6 J/kg

A.4 The Thermophysical Properties of Saturated Water Liquid from 273.15k to 380k

Density

$$\rho_w = (1.49343 \times 10^{-3} - 3.7164 \times 10^{-6}T + 7.09782 \times 10^{-9}T^2 - 1.90321 \times 10^{-20}T^6)^{-1}, \text{ kg/m}^3 \quad \text{(A.4.1)}$$

Specific heat

$$c_{pw} = 8.15599 \times 10^{3} - 2.80627 \times 10T + 5.11283 \times 10^{-2}T^{2} - 2.17582 \times 10^{-13}T^{6}, \text{ J/kgK} \quad \text{(A.4.2)}$$

Dynamic viscosity from General Electric *Heat Transfer and Fluid Flow Data Book*

$$\mu_{w} = 2.414 \times 10^{-5} \times 10^{247.8/(T-140)}, \text{ kg/ms} \quad \text{(A.4.3)}$$

Thermal conductivity

$$k_{w} = -6.14255 \times 10^{-1} + 6.9962 \times 10^{-3}T - 1.01075 \times 10^{-5}T^{2} + 4.74737 \times 10^{-12}T^{4}, \text{ W/mK} \quad \text{(A.4.4)}$$

Latent heat of vaporization

$$i_{fgw} = 3.4831814 \times 10^{6} - 5.8627703 \times 10^{3}T + 12.139568T^{2} - 1.40290431 \times 10^{-2}T^{3}, \text{ J/kg} \quad \text{(A.4.5)}$$

Critical pressure

$$p_{wc} = 22.09 \times 10^{6}, \text{ N/m}^{2} \quad \text{(A.4.6)}$$

Surface tension from *U.K. Steam Tables in SI Units 1970*

$$\sigma_{w} = 5.148103 \times 10^{-2} + 3.998714 \times 10^{-4}T - 1.4721869 \times 10^{-6}T^{2} + 1.21405335 \times 10^{-9}T^{3}, \text{ N/m} \quad \text{(A.4.7)}$$

Table A.3 The Thermophysical Properties of Saturated Water Liquid

T	ρ_w	c_{pw}	$\mu_w \times 10^4$	k_w	$\beta_w \times 10^5$	Pr_w
K	kg/m^3	J/kgK	kg/ms	W/mK	1/K	
275	1000.03	4211.21	16.5307	0.572471	0.780333	12.1603
280	999.864	4202.04	14.2146	0.581432	6.184114	10.2730
285	999.422	4194.41	12.3510	0.590001	11.45765	8.78055
290	998.721	4188.27	10.8327	0.598179	16.59011	7.58474
295	997.768	4183.53	9.58179	0.605972	21.57093	6.61511
300	996.572	4180.10	8.54057	0.613383	26.38963	5.82026
305	995.141	4177.92	7.66576	0.620417	31.03593	5.16215
310	993.487	4176.87	6.92443	0.627079	35.49975	4.61225
315	991.618	4176.88	6.29125	0.633372	39.77122	4.14887
320	989.547	4177.83	5.74650	0.639300	43.84070	3.75534
325	987.284	4179.63	5.27468	0.644870	47.69877	3.41871
330	984.842	4182.17	4.86348	0.650084	51.33626	3.12881
335	982.232	4185.32	4.50304	0.654948	54.74422	2.87758
340	979.469	4188.98	4.18540	0.659466	57.91392	2.65859
345	976.564	4193.01	3.90407	0.663644	60.83688	2.46665
350	973.532	4197.28	3.65373	0.667486	63.50480	2.29754
355	970.386	4201.67	3.43001	0.670997	65.90961	2.14781
360	976.141	4206.01	3.22924	0.674182	68.04338	2.01462
365	963.811	4210.17	3.04839	0.677046	69.89838	1.89562
370	960.409	4213.99	2.88488	0.679595	71.46697	1.78884
375	956.952	4217.31	2.73656	0.681833	72.74164	1.69263
380	953.453	4219.96	2.60158	0.683767	73.71494	1.60560

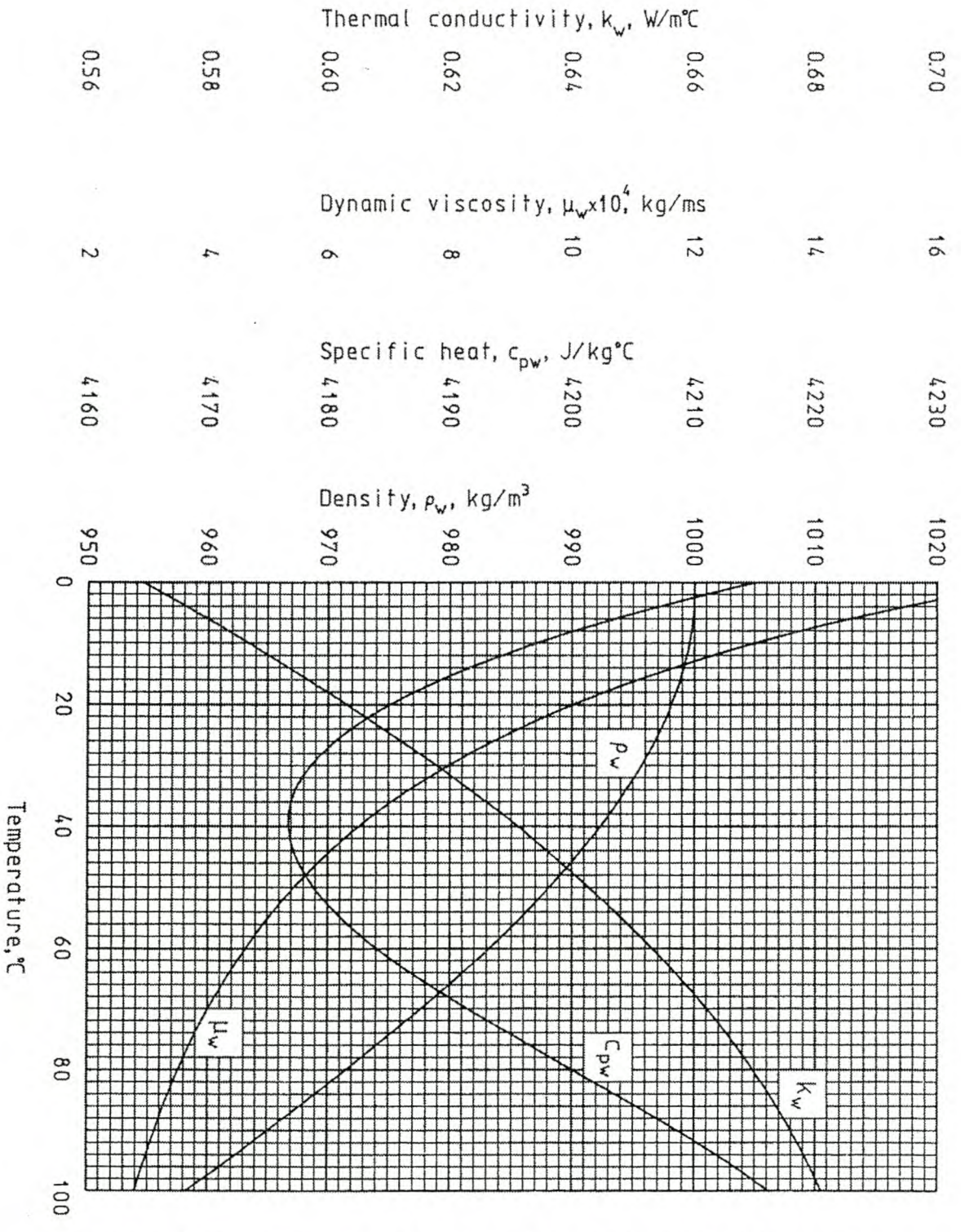

Figure A.3 The Thermophysical Properties of Saturated Water Liquid

A.5 The Thermophysical Properties of Saturated Ammonia Vapor

Vapor pressure (230K to 395K) according to Raznjevic

$$p_{ammv} = 1.992448 \times 10^6 - 57.56814 \times 10^3 T + 0.5640265 \times 10^3 T^2 - 2.337352 T^3 + 3.54143 \times 10^{-3} T^4, \text{ N/m}^2 \quad \text{(A.5.1)}$$

Density (260K to 390K) according to Raznjevic

$$\rho_{ammv} = -6.018936 \times 10^2 + 5.361048 T - 1.187296 \times 10^{-2} T^2 - 1.161479 \times 10^{-5} T^3 + 4.739058 \times 10^{-8} T^4, \text{ kg/m}^3 \quad \text{(A.5.2)}$$

Specific heat (230K to 325K) from ASHRAE *Handbook of Fundamentals*

$$c_{pammv} = -2.7761190256 \times 10^4 + 3.39116449 \times 10^2 T - 1.3055687 T^2 - 1.728649 \times 10^{-3} T^3; \text{ J/kgK} \quad \text{(A.5.3)}$$

Dynamic viscosity (240K to 370K) from ASHRAE *Handbook of Fundamentals*

$$\mu_{ammv} = -2.748011 \times 10^{-5} + 2.82526 \times 10^{-7} T - 5.201831 \times 10^{-10} T^2 - 6.061761 \times 10^{-13} T^3 + 2.12607 \times 10^{-15} T^4, \text{ kg/sm} \quad \text{(A.5.4)}$$

Thermal conductivity (245K to 395K) from ASHRAE *Handbook of Fundamentals*

$$k_{ammv} = -0.1390216 + 1.35238 \times 10^{-3} T - 2.532035 \times 10^{-6} T^2 - 4.884341 \times 10^{-9} T^3 + 1.418657 \times 10^{-11} T^4, \text{ W/mK} \quad \text{(A.5.6)}$$

Table A.4 The Thermophysical Properties of Saturated Ammonia Vapor

T K	$p_{ammv} \times 10^{-3}$ N/m^2	ρ_{ammv} kg/m^3	c_{pammv} J/kgK	$\mu_{ammv} \times 10^{6}$ kg/sm	k_{ammv} W/mK	Pr_{ammv}
230	60.58		2230.48			
235	79.09		2265.33			
240	102.08		2322.84	9.0376		
245	130.32		2377.30	9.2605	0.019611	1.12261
250	164.65		2430.01	9.4734	0.019920	1.15567
255	205.93		2482.27	9.6774	0.020185	1.19009
260	255.10	1.78881	2535.37	9.8737	0.020414	1.22632
265	313.14	2.56766	2590.61	10.0635	0.020613	1.26477
270	381.09	3.28963	2649.29	10.2480	0.020790	1.30588
275	460.03	3.98405	2712.69	10.4284	0.020954	1.35007
280	551.10	4.68094	2782.13	10.6060	0.021111	1.39774
285	655.51	5.41106	2858.89	10.7822	0.021270	1.44924
290	774.50	6.20583	2944.27	10.9583	0.021439	1.50491
295	909.36	7.09745	3039.57	11.1356	0.021627	1.56503
300	1061.74	8.11876	3146.08	11.3156	0.021843	1.62979
305	1232.21	9.30337	3265.10	11.4997	0.022096	1.69932
310	1423.06	10.68557	3397.93	11.6894	0.022394	1.77368
315	1635.53	12.30036	3545.87	11.8862	0.022748	1.85280
320	1871.19	14.18346	3710.20	12.0917	0.023166	1.93654
325	2131.65	16.37130	3892.24	12.3074	0.023660	2.02466
330	2418.59	18.90102		12.5349	0.024238	
335	2733.73	21.81047		12.7758	0.024911	
340	3078.86	25.13821		13.0318	0.025690	
345	3455.81	28.92352		13.3047	0.026586	
350	3866.46	33.20637		13.5961	0.027608	
355	4312.75	38.02745		13.9078	0.028769	
360	4796.68	43.42818		14.24159	0.030080	
365	5320.28	49.45067		14.5993	0.031551	
370	5885.67	56.13774		14.9827	0.033196	
375	6494.98	63.53294			0.035026	
385	7854.27	80.62539			0.039289	
395	9416.42				0.044441	

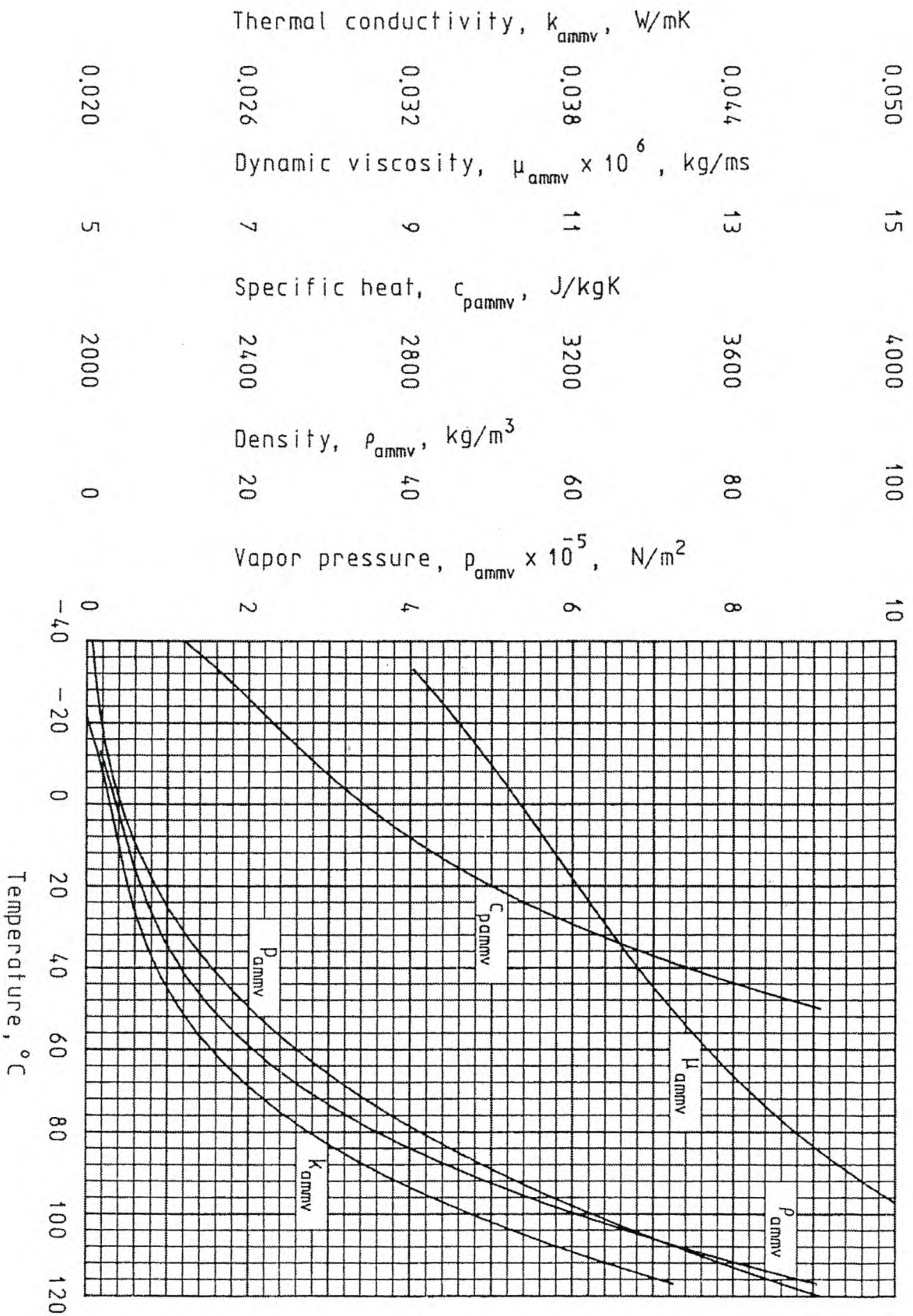

Figure A.4 The Thermophysical Properties of Saturated Ammonia Vapor

A.6 The Thermophysical Properties of Saturated Ammonia Liquid from 200K to 405K

Density according to Yaws

$$\rho_{amm} = 2.312 \times 10^2 \times 0.2471^{[-(1 - T/405.5)^{0.285714}]}, \text{kg/m}^3 \qquad \text{(A.6.1)}$$

Specific heat (200K to 375K) according to Yaws

$$c_{pamm} = -2.497276939 \times 10^3 + 7.7813907 \times 10T - 3.006252 \times 10^{-1}T^2 + 4.06714 \times 10^{-4}T^3, \text{J/kgK} \qquad \text{(A.6.2)}$$

Dynamic viscosity according to Yaws

$$\mu_{amm} = 0.001 \times 10^{(-8.591+876.4/T0.02681+T-3.612\times10^{-5}T^2)}, \text{kg/sm} \qquad \text{(A.6.3)}$$

Thermal conductivity (200K to 375K) according to Yaws

$$k_{amm} = 1.068229 - 1.576908 \times 10^{-3}T - 1.228884 \times 10^{-6}T^2, \text{W/mK} \qquad \text{(A.6.4)}$$

Latent heat of vaporization according to Yaws

$$i_{fgamm} = 1.370758 \times 10^6[(405.55 - T)/(165.83)]^{0.38}, \text{J/kg}_2 \qquad \text{(A.6.5)}$$

Critical pressure

$$p_{ammc} = 11.28 \times 10^6, \text{N/m}^2 \qquad \text{(A.6.6)}$$

Surface tension according to Yaws

$$\sigma = 0.0366[(405.55 - T)/177.4]^{1.1548}, \text{N/m} \qquad \text{(A.6.7)}$$

Table A.5 The Thermophysical Properties of Saturated Ammonia Liquid

T	ρ_{pamm}	c_{pamm}	$\mu_{amm} \times 10^5$	k_{amm}	Pr_{amm}	$i_{fgamm} \times 10^{-3}$
K	kg/m^3	J/kgK	kg/sm	W/mK		J/kg
200	731.094	4294.20	51.0740	0.703692	3.11673	1487.29
205	725.217	4324.69	45.9440	0.693319	2.86583	1473.44
210	719.282	4352.65	41.6429	0.682885	2.65428	1459.37
215	713.288	4378.38	37.9998	0.672389	2.47443	1445.08
220	707.232	4402.21	34.8841	0.661832	2.32034	1430.55
225	701.111	4424.42	32.1948	0.651213	2.18736	1415.78
230	694.923	4445.33	29.8529	0.640532	2.07181	1400.75
235	688.663	4465.24	27.7961	0.629791	1.97076	1385.45
240	682.329	4484.46	25.9749	0.618988	1.88184	1369.87
245	675.918	4503.28	24.3494	0.608123	1.80313	1354.00
250	669.424	4522.03	22.8875	0.597197	1.73306	1337.82
255	662.844	4540.99	21.5630	0.586210	1.67035	1321.31
260	656.173	4550.48	20.3543	0.575161	1.61390	1304.46
265	649.406	4580.79	19.2438	0.564050	1.56284	1287.25
270	642.537	4602.25	18.2170	0.552878	1.51641	1269.65
275	635.560	4625.14	17.2617	0.541645	1.47399	1251.65
280	628.469	4649.78	16.3678	0.530351	1.43503	1233.21
285	621.255	4676.47	15.5271	0.518994	1.39909	1214.31
290	613.912	4705.52	14.7325	0.507577	1.36578	1194.92
295	606.428	4737.23	13.9783	0.496098	1.33478	1175.01
300	598.794	4771.90	13.2596	0.484557	1.30581	1154.52
305	590.999	4809.85	12.5727	0.472955	1.27861	1133.42
310	583.029	4851.37	11.9141	0.461292	1.25300	1111.67
315	574.868	4896.77	11.2814	0.449567	1.22879	1089.19
320	566.500	4946.35	10.6723	0.437781	1.20584	1065.93
325	557.905	5000.43	10.0853	0.425933	1.18401	1041.82
330	549.060	5059.31	9.5189	0.414024	1.16320	1016.75
335	539.936	5123.28	8.9722	0.402054	1.14331	990.644
340	530.501	51.92.66	8.4445	0.390022	1.12428	963.355
345	520.717	5267.75	7.9351	0.377928	1.10604	934.743
350	510.534	5348.86	7.4438	0.365773	1.08855	904.625
355	499.893	5436.29	6.9704	0.353557	1.07177	872.776
360	488.718	5530.35	6.5146	0.341279	1.05568	838.908
365	476.910	5631.34	6.0765	0.328940	1.04028	802.648
370	464.337	5739.56	5.6561	0.316539	1.02558	763.498
375	450.814	5855.32	5.2534	0.304077	1.01160	720.764
380	436.074		4.8684			673.437
385	419.697		4.5011			619.951
395	378.461		3.8199			481.199
405	285.772		3.2093			156.612

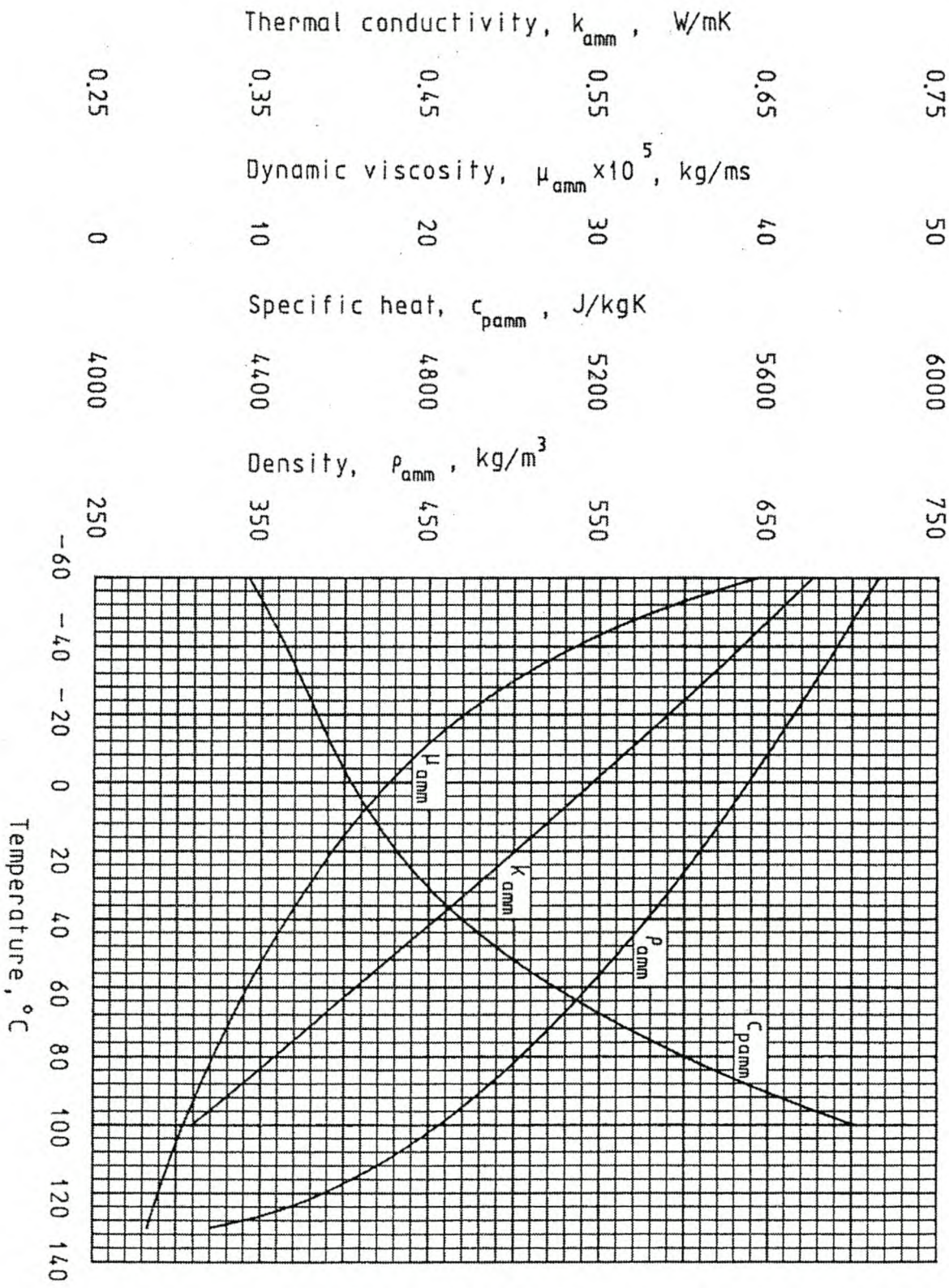

Figure A.5 The Thermophysical Properties of Saturated Ammonia Liquid

References

ASHRAE, *Handbook of Fundamentals*, American Society of Heating, Refrigeration and Air Conditioning Engineers, Inc., 1972.

Faires, V. M., and C. M. Simmang, *Thermodynamics*, 6th ed., Macmillan Publishing Co. Inc., 1978.

General Electric, *Heat Transfer and Fluid Flow Data Book*, General Electric Co., Corporate Research Division, New York, 1982.

Godridge, A.M., *British Coal Utilisation Research Association Monthly*, vol. 18 no. 1, 1954.

Goff, J.A., *Saturation Pressure of Water on the New Kelvin Scale, Humidity and Moisture Measurement and Control in Science and Industry*, ed., A. Wexler and W. H. Wildhack, Reinhold Publishing Co., New York, 1965.

Johannsen, A., "Plotting Psychrometric Charts by Computer," *The South African Mechanical Engineer*, 32:154–162, July 1982.

Lehmann, H., *Chemical Technology*, 9:530, 1957.

Popiel, C. O. and J. Wojtkowiak, "Simple Formulas for Thermophysical Properties of Liquid Water for Heat Transfer Calculations (from 0°C to 150°C)," *Heat Transfer Engineering*, 19-3:87–101, 1998.

Raznjevic, K., *Handbook of Thermodynamic Tables and Charts*, McGraw-Hill Book Co., New York, 1976.

United Kingdom Committee on the Properties of Steam, *U.K. Steam Tables in SI Units 1970*, Edward Arnold Ltd., London, 1970.

Yaws, C. L., *Physical Properties*, Chemical Engineering Publ., McGraw-Hill Book Co., New York, 1977.

Appendix B

Temperature Correction Factor

To determine the performance characteristics of heat exchangers, it is essential to determine the mean temperature difference between fluids accurately. Since this difference depends on the geometry and the flow pattern through the heat exchanger, simple analytic solutions are not always possible. For computational purposes, the method proposed by Roetzel is of value.

Consider the heat exchanger shown in Figure B.1.

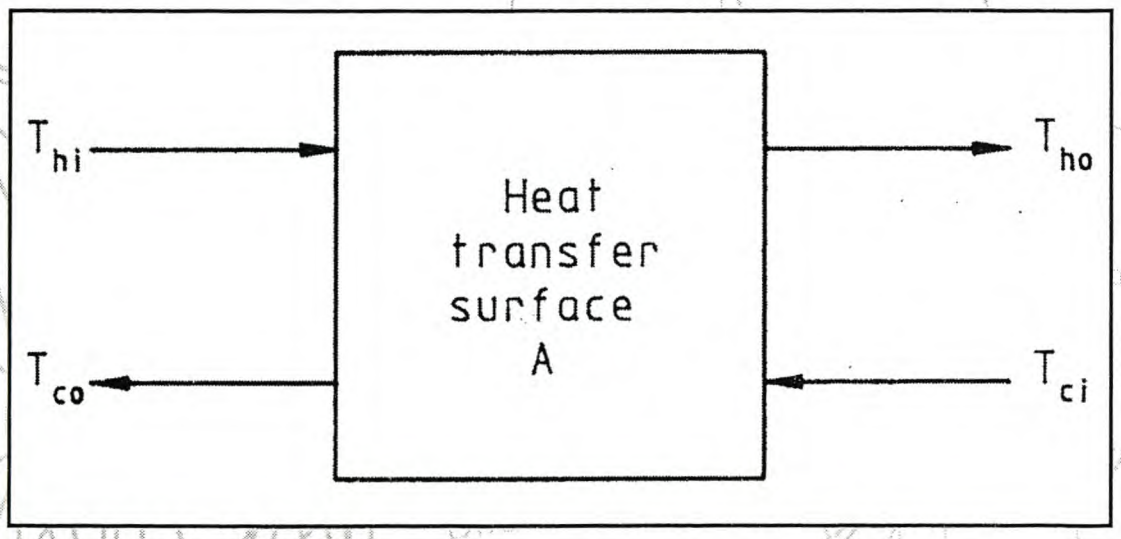

Figure B.1 Schematic of Heat Exchanger

In such an exchanger, the heat transfer rate is given by

$$Q = UA\Delta T_m \tag{B.1}$$

where

UA is the conductance of the exchanger

U is the overall heat transfer coefficient and is assumed to be constant

Q is the heat and flows from the hot fluid, subscript $_h$, to the cold fluid, subscript $_c$

According to Equation B.1, the mean temperature difference between the two streams, ΔT_m, may be expressed as

$$\Delta T_m = Q/UA$$

or, if made dimensionless with respect to the largest temperature difference,

$$\varphi = \frac{\Delta T_m}{T_{hi} - T_{ci}} = \frac{Q}{UA(T_{hi} - T_{ci})} \tag{B.2}$$

Dimensionless temperature changes of the two streams may be defined as

$$\varphi_h = \frac{T_{hi} - T_{ho}}{T_{hi} - T_{ci}} = \frac{Q}{m_h c_{ph}(T_{hi} - T_{ci})} \tag{B.3}$$

and

$$\varphi_c = \frac{T_{co} - T_{ci}}{T_{hi} - T_{ci}} = \frac{Q}{m_c c_{pc}(T_{hi} - T_{ci})} \tag{B.4}$$

where

m = the mass flow rate

c_p = the specific heat of the fluid

In the case of counterflow, a dimensionless mean temperature difference can be expressed in terms of the logarithmic mean temperature difference, i.e.,

$$\varphi_{cf} = \frac{\Delta T_{\ell m}}{(T_{hi} - T_{ci})} = \frac{\varphi_h - \varphi_c}{\ell n[(1-\varphi_c)/(1-\varphi_h)]} \tag{B.5}$$

According to Roetzel, a temperature correction factor can be expressed as

$$F_T = \frac{\varphi}{\varphi_{cf}} = 1 - \sum_{i=1}^{4} \sum_{k=1}^{4} a_{i,k} (1-\varphi_{cf})^k \sin\left(2i \arctan \frac{\varphi_h}{\varphi_c}\right) \tag{B.6}$$

Tables B.1 to B.10 present the sixteen values of the empirical constant $a_{i,k}$ for ten different heat exchanger geometries.

Table B.1 Crossflow with One Tube Row

$a_{i,k}$	i = 1	2	3	4
k = 1	-4.62×10^{-1}	-3.13×10^{-2}	-1.74×10^{-1}	-4.20×10^{-2}
2	5.08×10^{0}	5.29×10^{-1}	1.32×10^{0}	3.47×10^{-1}
3	-1.57×10^{1}	-2.37×10^{0}	-2.93×10^{0}	-8.53×10^{-1}
4	1.72×10^{1}	3.18×10^{0}	1.99×10^{0}	6.49×10^{-1}

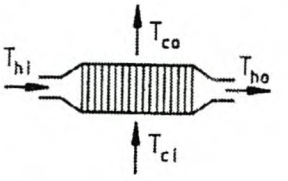

Table B.2 Crossflow with Two Tube Rows and One Pass

$a_{i,k}$	i = 1	2	3	4
k = 1	-3.34×10^{-1}	-1.54×10^{-1}	-8.65×10^{-2}	5.53×10^{-2}
2	3.30×10^{0}	1.28×10^{0}	5.46×10^{-1}	-4.05×10^{-1}
3	-8.70×10^{0}	-3.35×10^{0}	-9.29×10^{-1}	9.53×10^{-1}
4	8.70×10^{0}	2.83×10^{0}	4.71×10^{-1}	-7.17×10^{-1}

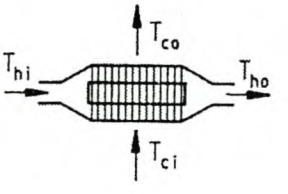

Table B.3 Crossflow with Three Tube Rows and One Pass

$a_{i,k}$	i = 1	2	3	4
k = 1	-8.74×10^{-2}	-3.18×10^{-2}	-1.83×10^{-2}	7.10×10^{-3}
2	1.05×10^{0}	2.74×10^{-1}	1.23×10^{-1}	-4.99×10^{-2}
3	-2.45×10^{0}	-7.46×10^{-1}	-1.56×10^{-1}	1.09×10^{-1}
4	3.21×10^{0}	6.68×10^{-1}	6.17×10^{-2}	-7.46×10^{-2}

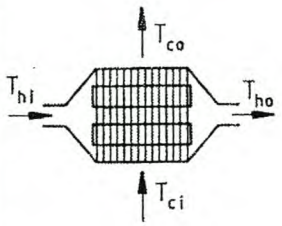

Table B.4 Crossflow with Four Tube Rows and One Pass

$a_{i,k}$	i = 1	2	3	4
k = 1	-4.14×10^{-2}	-1.39×10^{-2}	-7.23×10^{-3}	6.10×10^{-3}
2	6.15×10^{-1}	1.23×10^{-1}	5.66×10^{-2}	-4.68×10^{-2}
3	-1.20×10^{0}	-3.45×10^{-1}	-4.37×10^{-2}	1.07×10^{-1}
4	2.06×10^{0}	3.18×10^{-1}	1.11×10^{-2}	-7.57×10^{-2}

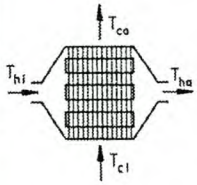

Table B.5 Crossflow with Two Tube Rows and Two Tube Passes

$a_{i,k}$	i = 1	2	3	4
k = 1	-2.35×10^{-1}	-7.73×10^{-2}	-5.98×10^{-2}	5.25×10^{-3}
2	2.28×10^{0}	6.32×10^{-1}	3.64×10^{-1}	-1.27×10^{-2}
3	-6.44×10^{0}	-1.63×10^{0}	-6.13×10^{-1}	-1.14×10^{-2}
4	6.24×10^{0}	1.35×10^{0}	2.76×10^{-1}	2.72×10^{-2}

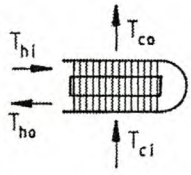

Table B.6 Crossflow with Three Tube Rows and Three Tube Passes

$a_{i,k}$	i = 1	2	3	4
k = 1	-8.43×10^{-1}	3.02×10^{-2}	4.80×10^{-1}	8.12×10^{-2}
2	5.85×10^{0}	-9.64×10^{-3}	-3.28×10^{0}	-8.34×10^{-1}
3	-1.28×10^{1}	-2.28×10^{-1}	7.11×10^{0}	2.19×10^{0}
4	9.24×10^{0}	2.66×10^{-1}	-4.90×10^{0}	-1.69×10^{0}

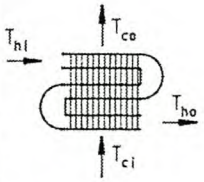

Table B.7 Crossflow with Four Tube Rows and Four Tube Passes

$a_{i,k}$	i = 1	2	3	4
k = 1	-3.39×10^{-1}	2.77×10^{-2}	1.79×10^{-1}	-1.99×10^{-2}
2	2.38×10^{0}	-9.99×10^{-2}	-1.21×10^{0}	4.00×10^{-2}
3	-5.26×10^{0}	9.04×10^{-2}	2.62×10^{0}	4.94×10^{-2}
4	3.90×10^{0}	-8.45×10^{-4}	-1.81×10^{0}	-9.81×10^{-2}

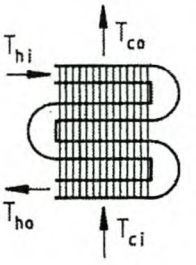

Table B.8 Crossflow with Four Tubes and Two Passes Through Two Tubes

$a_{i,k}$	i = 1	2	3	4
k = 1	-6.05×10^{-1}	2.31×10^{-1}	2.94×10^{-1}	1.98×10^{-2}
2	4.34×10^{0}	5.90×10^{-3}	-1.99×10^{0}	-3.05×10^{-1}
3	-9.72×10^{0}	-2.48×10^{-1}	4.32×10^{0}	8.97×10^{-1}
4	7.54×10^{0}	2.87×10^{-1}	-3.00×10^{0}	-7.31×10^{-1}

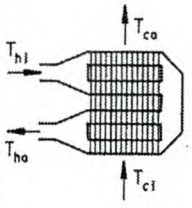

Table B.9 Crossflow with Both Streams Unmixed

$a_{i,k}$	i = 1	2	3	4
k = 1	6.69×10^{-2}	0.0	3.95×10^{-2}	0.0
2	-2.78×10^{-1}	0.0	-2.20×10^{-1}	0.0
3	1.11×10^{0}	0.0	4.54×10^{-1}	0.0
4	1.36×10^{-1}	0.0	-2.58×10^{-1}	0.0

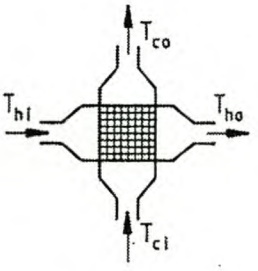

Table B.10 Crossflow with Both Streams Mixed

$a_{i,k}$	i = 1	2	3	4
k = 1	-4.775×10^{-1}	0.0	-1.292×10^{-1}	0.0
2	6.097×10^{0}	0.0	1.349×10^{0}	0.0
3	-2.153×10^{1}	0.0	-3.986×10^{0}	0.0
4	2.596×10^{1}	0.0	3.593×10^{0}	0.0

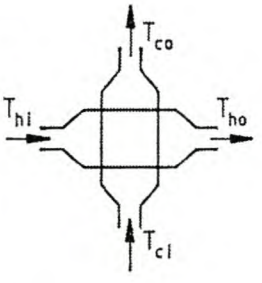

References

Roetzel, W., "Berechnung von Wärmeübertragern," *Verein Deutscher Ingenieure-Wärmeatlas*, Ca1–Ca31, VDI-Verlag GmbH, Düsseldorf, 1984.

Roetzel, W., and J. Neubert, "Calculation of Mean Temperature Difference in Air-Cooled Cross-Flow Heat Exchangers," *Journal of Heat Transfer*, Transactions of the American Society of Mechanical Engineers, 101:511–513, August 1979.

Roetzel, W., and J. Fürst, "Schnelle Berechnung der mittleren Temperaturdifferenz in luftgekühlten Kreuzstrom Wärmeaustauschern," *Wärme und Stoffübertragung*, 14:131–136, 190.

Spang, B., and W. Roetzel, "Neue Näherungsgleichung zur einheitlichen Berechnung von Wärmeübertragern," *Heat and Mass Transfer*, 30:415–422, Springer Verlag, 1995.

Appendix C

Conversion Factors

Acceleration

1 cm/s^2 = 1.000 x 10^{-2} m/s^2

1 m/h^2 = 7.716 x 10^{-8} m/s^2

1 ft/s^2 = 0.3048 m/s^2

1 ft/h^2 = 2.352 x 10^{-8} m/s^2

Area

1 ha = 10^4 m^2

1 acre = 4.047 x 10^3 m^2

1 cm^2 = 1.000 x 10^{-4} m^2

1 ft^2 = 9.290 x 10^{-2} m^2

1 in^2 = 6.452 x 10^{-4} m^2

1 yard^2 = 0.8361 m^2

1 square mile = 2.59 x 10^6 m^2

Density

1 g/cm^3 = 1000 kg/m^3

1 1b/ft^3 = 16.02 kg/m^3

1 kg/ft^3 = 35.31 kg/m^3

Energy, work, heat

1 cal = 4.187 J

1 kcal = 4187 J

1 Btu = 1055 J

1 erg = 1.000 x 10^{-7} J

1 kWh = 3.600 x 10^6 J

1 ft pdl = 4.214 x 10^{-2} J

1 ft lbf = 1.356 J

1 Chu = 1899 J

1 therm = 1.055 x 10^8 J

Force

1 dyne = 1.000 x 10^{-5} N

1 kgf = 9.807 N

1 pdl = 0.1383 N

1 lbf = 4.448 N

Heat flux

1 cal/s cm^2 = 4.187 x 10^4 W/m^2

1 kcal/h m^2 = 1.163 W/m^2

1 Btu/h ft^2 = 3.155 W/m^2

1 Chu/h ft^2 = 5.678 W/m^2

1 kcal/h ft^2 = 12.52 W/m^2

Heat transfer coefficient

1 cal/s cm^2 °C = 4.187×10^4 W/m^2 K

1 kcal/h m^2 °C = 1.163 W/m^2 K

1 Btu/h ft^2 °F = 5.678 W/m^2 K

1 Chu/h ft^2 °C = 5.678 W/m^2 K

1 kcal/h ft^2 °C = 12.52 W/m^2 K

Length

1 cm = 1.000×10^{-2} m

1 ft = 0.3048 m

1 micron = 1.000×10^{-6} m

1 in = 2.540×10^{-2} m

1 yard = 0.9144 m

1 mile = 1609 m

Mass

1 g = 1.000×10^{-3} kg

1 lb = 0.4536 kg

1 tonne = 1000 kg

1 grain = 6.480×10^{-5} kg

1 oz = 2.835×10^{-2} kg

1 ton (long) = 1016 kg

1 ton (short) = 907 kg

Mass flow rate

1 g/s = 1.000×10^{-3} kg/s

1 kg/h = 2.778×10^{-4} kg/s

1 lb/s = 0.4536 kg/s

1 tonne/h = 0.2778 kg/s

1 lb/h = 1.260×10^{-4} kg/s

1 ton (long)/h = 0.2822 kg/s

Mass flux

1 g/s cm^2 = 10.00 kg/s m^2

1 kg/h m^2 = 2.778×10^{-4} kg/s m^2

1 lb/s ft^2 = 4.882 kg/s m^2

1 lb/h ft^2 = 1.356×10^{-3} kg/s m^2

1 kg/h ft^2 = 2.990×10^{-3} kg/s m^2

Mass transfer coefficient

1 lb/h ft^2 = 1.3385×10^{8} kg/sm^2

1 g/s cm^2 = 9.869×10^{-5} kg/sm^2

1 kg/h m^2 = 2.7415×10^{-9} kg/sm^2

Power

1 cal/s = 4.187 W

1 kcal/h = 1.163 W

1 Btu/s = 1055 W

1 erg/s = 1.000×10^{-7} W

1 hp (metric) = 735.5 W

1 hp (British) = 745.7 W

1 ft pdl/s = 4.214×10^{-2} W

1 ft lbf/s = 1.356 W

1 Btu/h = 0.2931 W

1 Chu/h = 0.5275 W

1 ton refrigeration = 3517 W

Pressure

1 dyne/cm^2 = 0.100 N/m^2

1 kgf/m^2 = 9.807 N/m^2

1 pdl/ft^2 = 1.488 N/m^2

1 standard atm = 1.0133 x 10^5 N/m^2

1 bar = 1.000 x 10^5 N/m^2

1 kgf/cm^2 (1 at) = 9.807 x 10^4 N/m^2

1 lbf/ft^2 = 47.88 N/m^2

1 lbf/in^2 = 6895 N/m^2

1 mm water = 9.807 N/m^2

1 in water = 249.1 N/m^2

1 ft water = 2989 N/m^2

1 mm Hg = 133.3 N/m^2

1 in Hg = 3387 N/m^2

Specific enthalpy or latent heat

1 cal/g = 4187 J/kg

1 Btu/lb = 2326 J/kg

1 Chu/lb = 4187 J/kg

1 kcal/kg = 4187 J/kg

Specific heat capacity

1 cal/g °C = 4187 J/kgK

1 Btu/lb °F = 4187 J/kgK

Specific volume

1 cm^3/g = 1.000 x 10^{-3} m^3/kg

1 ft^3/lb = 6.243 x 10^{-2} m^3/kg

1 ft^3/kg = 2.832 x 10^{-2} m^3/kg

Surface tension

1 dyne/cm = 1.000×10^{-3} N/m

1 pdl/ft = 0.4536 N/m

1 lbf/ft = 14.59 N/m

Temperature difference

1 deg F = 0.556 K

Thermal conductivity

1 cal/s cm °C = 4187 W/m K

1 kcal/h m °C = 1.163 W/m K

1 Btu/h ft °F = 1.731 W/m K

Time

1 h = 3600 s

1 day = 8.640×10^{4} s

1 year = 3.156×10^{7} s

Velocity

1 cm/s = 1.000×10^{-2} m/s

1 m/h = 2.778×10^{-4} m/s

1 ft/s = 0.3048 m/s

1 ft/h = 8.467×10^{-5} m/s

1 mile/h = 0.4470 m/s

1 knot = 0.5148 m/s

Viscosity (dynamic)

1 g/cm s (poise) = 0.1000 kg/m s (N s/m^2)

1 kg/m h = 2.778 x 10^{-4} kg/ms

1 lb/ft s = 1.488 kg/m s

1 lb/ft h = 4.134 x 10^{-4} kg/m s

Viscosity (kinematic)

1 cm^2/s (stoke) = 1.000 x $10^{-4}m^2$/s

1 ft^2/s = 0.0929 m^2/s

Volume

1 $yard^3$ = 0.7646 m^3

1 cm^3 = 1.000 x 10^{-6} m^3

1 ft^3 = 2.832 x 10^{-2} m^3

1 litre = 1.000 x 10^{-3} m^3

1 in^3 = 1.639 x 10^{-5} m^3

1 UK gal = 4.546 x 10^{-3} m^3

1 US gal = 3.785 x 10^{-3} m^3

Volumetric flow

1 cm^3/s = 1.000 x 10^{-6} m^3/s

1 m^3/h = 2.778 x 10^{-4} m^3/s

1 ft^3/s = 2.832 x 10^{-2} m^3/s

1 ft^3/h = 7.866 x 10^{-6} m^3/s

1 UK gal/min = 7.577 x 10^{-5} m^3/s

1 US gal/min = 6.309 x 10^{-5} m^3/s

Appendix D

This is the Table of Contents for Volume I.

Index

A

B

C

D

G

H

I

J

K

L

M

N

O

P–Q

R

S

T

U

V

W–Z